

Aptamers for Analytical Applications

Aptamers for Analytical Applications

Affinity Acquisition and Method Design

Edited by Yiyang Dong

WILEY-VCH

Editor**Prof. Yiyang Dong**

Beijing University of Chemical
Technology
College of Life Science and Technology
No.15 Beisanhuan East Road
Chaoyang District
100029 Beijing
PR China

Cover Image:

Courtesy of Sai Wang, Yiyang Dong;
background © Toria/Shutterstock;
mesh © ktsdesign/Shutterstock

■ All books published by **Wiley-VCH** are carefully produced. Nevertheless, authors, editors, and publisher do not warrant the information contained in these books, including this book, to be free of errors. Readers are advised to keep in mind that statements, data, illustrations, procedural details or other items may inadvertently be inaccurate.

Library of Congress Card No.: applied for

British Library Cataloguing-in-Publication Data

A catalogue record for this book is available from the British Library.

Bibliographic information published by the Deutsche Nationalbibliothek

The Deutsche Nationalbibliothek lists this publication in the Deutsche Nationalbibliografie; detailed bibliographic data are available on the Internet at <<http://dnb.d-nb.de>>.

© 2018 Wiley-VCH Verlag GmbH & Co. KGaA, Boschstr. 12, 69469 Weinheim, Germany

All rights reserved (including those of translation into other languages). No part of this book may be reproduced in any form – by photoprinting, microfilm, or any other means – nor transmitted or translated into a machine language without written permission from the publishers. Registered names, trademarks, etc. used in this book, even when not specifically marked as such, are not to be considered unprotected by law.

Print ISBN: 978-3-527-34267-9

ePDF ISBN: 978-3-527-80682-9

ePub ISBN: 978-3-527-80680-5

oBook ISBN: 978-3-527-80679-9

Typesetting SPi Global, Chennai, India
Printing and Binding

Printed on acid-free paper

10 9 8 7 6 5 4 3 2 1

I dedicate this book to my beloved daughter, Yumeng Dong. She has passed the college entrance examination and becomes a medical student of Capital Medical University this summer, I hope she will begin her college life with joy and fun.



Photograph in the year 2005, Tuanjiehu Park, Beijing

Contents

	About the Author	<i>xv</i>
	Foreword	<i>xvii</i>
	Preface	<i>xix</i>
1	Introduction of SELEX and Important SELEX Variants	1
	<i>Yiyang Dong, Zhuo Wang, Sai Wang, Yehui Wu, Yufan Ma, and Jiahui Liu</i>	
1.1	SELEX	1
1.2	Negative SELEX and Its Analogs	3
1.3	One-Round SELEX	5
1.4	CE-SELEX	6
1.5	Microfluidic SELEX	8
1.6	Cell-SELEX	10
1.7	<i>In Silico</i> -SELEX	12
1.8	Post-SELEX and <i>In Chemico</i> -SELEX	14
1.9	Auto-SELEX	17
1.10	Primer-Free SELEX	17
1.11	Genomic SELEX	18
1.12	Photo-SELEX	19
1.13	qPCR-SELEX	19
1.14	Perspectives	20
	References	21
2	<i>In Chemico</i> Modification of Nucleotides for Better Recognition	27
	<i>Przemyslaw Jurek, Marta Matusiewicz, Maciej Mazurek, and Filip Jelen</i>	
2.1	Introduction	27
2.1.1	Beyond ATGC	27
2.1.2	The Scope of This Chapter	29
2.2	Modified Functional Nucleic Acids	30
2.2.1	The “Hows”	30
2.2.1.1	Post-SELEX Optimization	30
2.2.1.2	In-line Modifications	30
2.2.2	The “Whys”	31
2.2.2.1	The Hurdles	31

2.2.2.2	The Gains	32
2.2.3	The “Ifs”	33
2.3	Backbone Modifications	35
2.3.1	2'-OH Modifications	36
2.3.2	Phosphodiester Bond Modifications	36
2.3.3	Xeno Nucleic Acids	38
2.3.3.1	TNA	39
2.3.3.2	FANAs	39
2.3.3.3	HNA, CeNA, LNA, ANA	39
2.3.3.4	Other Modifications	40
2.4	Nucleobase Modifications	40
2.4.1	General Information	40
2.4.2	Modified Aptamers and Catalysts	42
2.4.2.1	Introduction of Cationic Moieties	42
2.4.2.2	Catalysts with Protein-like Sidechains	43
2.4.2.3	Nucleobase-linked Nucleobases	44
2.4.2.4	Glycans Targeting with Boronic Acids	44
2.4.2.5	“Click Chemistry”-Based Versatile Approach	45
2.4.2.6	Nonenzymatic Selection – X-aptamers	45
2.4.2.7	Slow Off-rate Modified Aptamers	46
2.5	Aptamers with Expanded Genetic Alphabet	48
2.5.1	GACTZP Aptamers	48
2.5.2	Aptamers with a Hydrophobic Fifth Base	50
2.6	Summary	52
2.A	Appendix	52
	References	68
3	Immobilization of Aptamers on Substrates	85
	<i>Annalisa De Girolamo, Maureen McKeague, Michelangelo Pascale, Marina Cortese, and Maria C. DeRosa</i>	
3.1	Introduction	85
3.2	Methods for Immobilization of Aptamers	87
3.2.1	Physical Adsorption	87
3.2.2	Covalent Binding	88
3.2.2.1	Covalent Immobilization of Activated Aptamers on a Functionalized Surface	88
3.2.2.2	Covalent Immobilization of Modified Aptamers on Activated Surfaces	92
3.2.2.3	Covalent Immobilization by Entrapment	95
3.2.2.4	Covalent Immobilization by Electrografting	97
3.2.3	Self-assembled Monolayers	98
3.2.4	Avidin–Biotin Binding (Affinity Coupling)	100
3.2.5	Electrochemical Adsorption	101
3.2.6	Hybridization	101
3.3	Immobilization of Aptamers on Substrates for Diagnostic Applications	102
3.3.1	Flat Gold	102
3.3.1.1	Surface Plasmon Resonance Detection	109

3.3.1.2	Electrochemical Detection	109
3.3.2	Solid Phase	111
3.3.2.1	Optical Detection	112
3.3.2.2	Sample Cleanup	114
3.3.3	Nanomaterials	115
3.4	Future Perspectives on New Substrates and New Immobilization Chemistries	116
3.5	Conclusions	117
	References	119
4	Characterization of Aptamer–Ligand Complexes	127
	<i>Rebeca Miranda-Castro, Noemí de-los-Santos-Álvarez, and María J. Lobo-Castañón</i>	
4.1	Introduction	127
4.2	Equilibrium Characterization: Thermodynamics	128
4.2.1	Basic Principles	128
4.2.2	Separation-Based Methods	133
4.2.2.1	Equilibrium Dialysis and Related Techniques	133
4.2.2.2	High-Performance Liquid Chromatography	135
4.2.2.3	Electrophoresis	136
4.2.3	Direct Methods	137
4.2.3.1	Isothermal Titration Calorimetry	138
4.2.3.2	Fluorescence-Based Methods	140
4.3	Kinetic Characterization	146
4.3.1	Heterogeneous Methods	148
4.3.1.1	Surface Plasmon Resonance	148
4.3.1.2	Electrochemical Impedance Spectroscopy	152
4.3.2	Homogeneous Methods	154
4.3.2.1	Rotating Droplet Electrochemistry	154
4.3.2.2	Capillary Electrophoresis	157
4.3.2.3	Nanopore-Based Studies	159
4.4	Concluding Remarks	162
	Acknowledgments	163
	References	164
5	Utilization of Aptamers for Sample Preparation in Analytical Methods	173
	<i>Zhiyong Yan and Yang Liu</i>	
5.1	Introduction	173
5.2	Substrate Materials Developed for Immobilization of Aptamers	175
5.3	Utilization of Aptamers for Sample Preparation in SPE	177
5.3.1	Aptamers Utilized in Affinity Column for SPE	181
5.3.2	Aptamers Utilized in Other SPE	182
5.4	Aptamers Utilized in SPME	182
5.4.1	Aptamers Utilized in Fiber SPME	183
5.4.2	Aptamers Utilized in SBSE	184
5.4.3	Aptamers Utilized in Other Formats of SPME	185

5.5	Aptamers Utilized in Other Affinity Chromatography	185
5.6	Aptamers Utilized in Microfluidic Separation System	187
5.7	Aptamers Utilized in Magnetic Separation System	189
5.7.1	Aptamers Utilized in Magnetic Solid-Phase Extraction (MSPE)	190
5.7.2	Aptamers Utilized in Other Magnetic Separation Formats	190
5.8	Aptamers Utilized in CE	191
5.9	Aptamers Utilized in Other Sample Separation Methods	192
5.10	Conclusion and Outlook	192
	References	192
6	Development of Aptamer-Based Colorimetric Analytical Methods	205
	<i>Subash C.B. Gopinath, Thangavel Lakshmi Priya, M.K. Md Arshad, and Chun Hong Voon</i>	
6.1	Introduction	205
6.2	Aptamer Generation for Colorimetric Assay	206
6.3	Aptasensor	206
6.4	Aptamer-AuNP-Based Colorimetric Assays	207
6.5	Applications of AuNP-Aptamer-Based Colorimetric Assays	211
6.6	Conclusions	213
	References	213
7	Enzyme-Linked Aptamer Assay (ELAA)	219
	<i>Yiyang Dong and Sai Wang</i>	
7.1	Introduction	219
7.2	Enzyme-Linked Immunosorbent Assay	219
7.3	Analytical Merits of Aptamer vs Antibody	221
7.4	Enzyme-Linked Aptamer Assay (ELAA)	223
7.5	Comparison of Direct-Competitive ELAA (<i>dc</i> -ELAA), Indirect-Competitive ELAA (<i>ic</i> -ELAA), and ELISA	225
7.6	Conclusion	226
	References	227
8	Development of Aptamer-Based Fluorescence Sensors	229
	<i>Seyed M. Taghdisi, Rezvan Yazdian-Robati, Mona Alibolandi, Mohammad Ramezani, and Khalil Abnous</i>	
8.1	Introduction	229
8.2	Fluorescent-Dye-Based Aptasensors	230
8.3	Nanoparticle-Based Aptasensors	231
8.3.1	Fluorescent Aptasensors Based on Gold Nanoparticles	231
8.3.2	Fluorescent Aptasensors Based on Carbon Nanomaterials	234
8.3.3	Fluorescent Aptasensors Based on Silica Nanoparticles	236
8.3.4	Fluorescent Aptasensors Based on Silver Nanoparticles	238
8.3.5	Fluorescent Aptasensors Based on DNA Structures	239
8.3.5.1	Fluorescent Aptasensors Based on DNA Nanostructures	239
8.3.5.2	Fluorescent Aptasensors Based on Triple-Helix Molecular Switch (THMS)	240

8.4	Conclusion	241
	Acknowledgment	241
	Suggested Websites	242
	References	242
9	Development of Aptamer-Based Electrochemical Methods	247
	<i>Jian-guo Xu, Li Yao, Lin Cheng, Chao Yan, and Wei Chen</i>	
9.1	Introduction	247
9.2	Classification of Electrochemical Aptasensors	247
9.3	Amperometric Aptasensors	248
9.3.1	Covalent Labels	248
9.3.1.1	Enzyme Labels	248
9.3.1.2	Other Covalently Linked Redox Species	250
9.3.2	Non-covalent Labels	256
9.3.2.1	Intercalated Redox Species	256
9.3.2.2	Cationic Redox Species	260
9.3.3	Label-Free Aptasensors	263
9.4	Potentiometric Aptasensors	265
9.5	Impedimetric Aptasensors	266
9.6	Electrochemiluminescence Aptasensors	268
9.7	Conclusion	268
	References	269
10	Development of Aptamer-Based Lateral Flow Assay Methods	273
	<i>Miriam Jauset-Rubio, Mohammad S. El-Shahawi, Abdulaziz S. Bashammakh, Abdulrahman O. Alyoubi, and Ciara K. O'Sullivan</i>	
10.1	Introduction	273
10.2	Development of Aptamer-Based Lateral Flow Assay – Strategy	275
10.2.1	Analogies and Differences Compared to Lateral flow Immunoassays (LFIA) s)	275
10.2.2	Fundamental Assay Considerations	276
10.2.3	Fundamental Analytical Considerations	277
10.3	Lateral Flow Aptamer Assays	278
10.3.1	Sandwich Assay	278
10.3.2	Competitive Assay	281
10.3.3	Signal Amplification	283
10.4	Summary and Perspectives	291
	References	294
11	Development of Aptamer-Based Non-labeling Methods	301
	<i>Huajie Gu, Liling Hao, and Zhouping Wang</i>	
11.1	Introduction	301
11.2	Surface Plasmon Resonance (SPR)-Based Aptasensor	302
11.2.1	Introduction	302

11.2.2	The Principle of SPR Technique	302
11.2.3	The Classification of SPR Biosensors	303
11.2.3.1	SPR Biosensors Based on Angular Modulation	303
11.2.3.2	SPR Biosensors Based on Wavelength Modulation	304
11.2.3.3	SPR Biosensors Based on Amplitude Modulation	304
11.2.3.4	SPR Biosensors Based on Phase Modulation	304
11.2.4	The Application of Aptamer-Based SPR Technique	304
11.2.4.1	Determination of the Affinity of Aptamers	305
11.2.4.2	Detection Analyte Concentrations	305
11.2.5	Summary and Prospects of SPR Aptasensors	310
11.3	Quartz Crystal Microbalance (QCM)-Based Aptasensor	311
11.3.1	Introduction	311
11.3.2	The Principle of QCM Technique	311
11.3.3	The Application of Aptamer-Based QCM Technique	312
11.3.3.1	Determination of the Affinity of Aptamers	312
11.3.3.2	Detection of Analyte Concentrations	313
11.3.4	Summary and Prospect of QCM Aptasensors	318
11.4	Isothermal Titration Calorimetry (ITC)	319
11.4.1	Introduction	319
11.4.2	The Principle of ITC Technique	319
11.4.3	Thermodynamic Parameters Obtained from ITC Experiment	320
11.4.4	Application of ITC in Association Between Aptamer and Target	322
11.4.4.1	Interaction Between the Aptamer Domain of the Purine Riboswitch and Ligands	322
11.4.4.2	Interaction Between the Cocaine-Binding Aptamer and Quinine	324
11.4.4.3	Affinity Test by ITC After Systemic Evolution of Ligands by EXponential Enrichment (SELEX)	327
11.4.5	Summary	329
11.5	MicroScale Thermophoresis (MST)	329
11.5.1	Introduction	329
11.5.2	The Principle of MST Technique	330
11.5.3	Application of MST in Association Between Aptamer and Target	332
11.5.3.1	Interaction Between Steroid Hormones and Aptamers	332
11.5.3.2	Affinity Test by MST After Systemic Evolution of Ligands by EXponential Enrichment (SELEX)	333
11.5.4	Summary	335
	References	335
12	Challenges of SELEX and Demerits of Aptamer-Based Methods	345
	<i>Haiyun Liu and Jinghua Yu</i>	
12.1	Introduction	345
12.2	Challenges of SELEX	347
12.2.1	Aptamer Degradation	347
12.2.2	Purification	348
12.2.3	Binding Affinity (K_d)	348
12.2.4	Target Immobilization	349

12.2.5	Cross-Reactivity	350
12.2.6	Time and Cost	350
12.2.7	Interaction of Aptamers with Intracellular Targets	351
12.2.8	Bioinformatics Tools	352
12.3	Demerits of Aptamer-Based Methods	352
12.3.1	Sensitivity	352
12.3.2	Selectivity and Specificity	354
12.3.3	Reproducibility	355
12.3.4	Calibration and Uncertainty	355
12.3.5	Regeneration	355
12.3.6	Immobilization of Aptamers	356
12.4	Summary and Perspectives	356
	References	357
13	State of the Art and Emerging Applications	365
	<i>Lin-Chi Chen, Jui-Hong Weng, and Pei-Wei Lee</i>	
13.1	Introduction	365
13.2	Frontiers of Analytical Aptamer Selection and Probe Design	368
13.2.1	Biochip-Based Aptamer Selection	368
13.2.2	SELEX with Next-Generation Sequencing (NGS)	372
13.2.3	Aptamer Optimization and Specialized Selection	373
13.2.4	<i>In Silico</i> Aptamer Design	376
13.3	Novel Aptasensing Platforms – From Assays and Sensors to Instrumental Analyses	378
13.3.1	Aptamer Assays	378
13.3.2	Aptasensors	380
13.3.3	Aptamer Chips	382
13.3.4	Cell-Based Aptasensing	384
13.4	Emerging Applications of Aptamer Diagnostics	385
13.4.1	Human Disease Diagnosis	386
13.4.2	Food/Environmental Monitoring – Mycotoxins, Pesticides, Heavy Metal Ions	387
13.4.3	Therapeutic Drug Assessment – Organ-on-a-Chip	387
13.4.4	New Molecular Biology Applications – CRISPR/Cas9, Stem Cells, IHC	388
13.5	Concluding Remarks – Frontiers of Frontiers	389
	Acknowledgments	389
	References	390
	Index	397

About the Author



Yiyang Dong obtained his bachelor's degree in chemistry in 1989 from East China Normal University, where he got fundamental analytical chemistry knowledge. He then went on to pursue his postgraduate study in Nankai University and got his master's degree in liquid chromatography. In 1995, he went to Peking University to investigate capillary electrophoresis for chiral separation and obtained a doctorate of philosophy in separation science in 1998. He also carried out a post-doctoral research

at Prof. Kitamori's Lab in the University of Tokyo, Japan to study microfluidics and related miniaturized bioanalytical techniques, and try to hyphenate these frontier techniques for various analytical applications later.

In early 2012, he joined Beijing University of Chemical Technology (BUCT) as a full professor of chemistry by a talent program and set up a research laboratory for food safety analysis and risk assessment, where he developed several aptamer-based biosensing and facile bioanalytical methodologies for fast identification of small molecular adulterants, mycotoxins, and antibiotics in various food matrices.

This research interest continued when his graduate students Sai Wang, Xueting Yin, Yali Tang, Ji Li, Shuai Zhao, Shanshan Zhang, and Yan Yang began to participate in relevant research projects. Recent years have witnessed a broad utilization of aptamer-based researches in various analytical fields, to introduce aptamers with method developments and representative analytical applications, he is therefore pleased to be the editor of this book, and feels happy to share with the audience the state of the art.

Foreword

Modern analytical chemistry with intellectual separation, unbiased identification, and precise quantitation strategies were well studied and utilized to meet scientific, technical, and, sometimes, engineering needs. However, in the twenty-first century, accompanying mass industrialization, business globalization, and rapid urbanization, there are many serious problems, e.g. resource shortage, climate change, environment deterioration, and disease transmission facing the world, contemporary analytical chemistry with cutting-edge methodologies needs to go further to deal with eco-environmental, social public, macro-economic, human health, or even individual ethical needs, accordingly.

The discovery of target/analyte amenable aptamers, or single-stranded functional DNA/RNA oligonucleotides, endowed with superior molecular recognition capability, was developed independently by SELEX (Systematic Evolution of Ligands by EXponential Enrichment) strategy in two laboratories led by Larry Gold and Jack William Szostak in 1990. In contrast to antibody, the aptamer selected by such an *in vitro* combinatorial chemistry process is more advantageous in terms of production ease, conformational adaptability, target affinity, analytical selectivity, structural tenability, and storage stability. Development of aptamer-based methods to address the aforementioned issues became frontier analytical field of hot investigation in recent years thereof.

Aptamers for Analytical Applications: Affinity Acquisition and Method Design edited by Professor Yiyang Dong with 13 chapters containing insightful contents is an analytical monograph not only for experienced aptamer analysts venturing into the critical analytical endpoint but also for researchers from diverse analytical/bioanalytical fields who are novices to aptamer applications. Furthermore, this book represents an essential tool for academic research or compliance accredited laboratories involved in the development of high performance aptamer-based analytical methods.

Gainesville, February 2018

Weihong Tan
Academician of the Chinese Academy of Sciences
Distinguished Professor, Vestus Twiggs and
Louise Jackson Professor of Chemistry
Department of Chemistry
The University of Florida

Preface

In this book, my chapter authors and I have tried to illustrate that aptamers, as novel molecular recognition elements with affinity acquisition and method design, have been successfully developed into promising analytical tools for various applications.

In Chapter 1, the selection of aptamers based on conventional SELEX (Systematic Evolution of Ligands by EXponential enrichment) strategies and important SELEX variants is systematically introduced. In order to get better recognition or affinity toward target analytes for aptamers, mainstream *in chemico* rather than *in silico* modification methods of nucleotides are well depicted in Chapter 2.

In Chapter 3, different schemes to efficiently immobilize aptamers on substrates are described. In Chapter 4, characterization methods for aptamer-ligand complexes are summarized. Because of the necessity of pretreatment steps in analytical methods, aptamers utilized for sample preparation are presented in Chapter 5.

Aptamer-based colorimetric, enzyme-linked, fluorescent, electrochemical, lateral flow, and non-labeling analytical methods are comprehensively presented in Chapters 6–11, respectively. In Chapter 12, challenges of SELEX and demerits of aptamer-based methods are drafted. To conclude, Chapter 13 reflects state-of-the-art and emerging applications of aptamer-based methods.

I hope both aptamer experts and novice analytical investigators will find this book very useful, and acknowledge my chapter authors with great appreciations thereof.

Yiyang Dong
Beijing University of Chemical Technology
PR China

Introduction of SELEX and Important SELEX Variants

Yiyang Dong¹, Zhuo Wang², Sai Wang³, Yehui Wu², Yufan Ma², and Jiahui Liu¹

¹Beijing University of Chemical Technology, College of Life Science and Technology, Beijing, 100029, PR China

²Beijing University of Chemical Technology, State Key Laboratory of Chemical Resource Engineering, Beijing Advanced Innovation Center for Soft Matter Science and Engineering, College of Science, Beijing, 100029, PR China

³Ocean University of China, College of Food Science and Engineering, Qingdao 266003, PR China

1.1 SELEX

In 1990, from a randomly synthesized nucleic acid library composed of more than 10^{15} different sequences [1, 2], two laboratories led by Larry Gold and Jack William Szostak invented independently a technique for selection of aptamers or single-stranded functional oligonucleotides (DNA or RNA), which shows high affinity to their respective targets. As shown in Figure 1.1, the aptamers are developed by repeated selection and amplification processes [3]. This *in vitro* oligonucleotides selection scheme is termed as SELEX (Systematic Evolution of Ligands by EXponential Enrichment), and has become a general and powerful method for the discovery and isolation of nucleic acid aptamers for a rich variety of analytical applications.

Mechanistically, the SELEX process starts with a single-stranded deoxyribonucleic acid (ssDNA) library generated by solid-phase synthesis using traditional phosphoramidite method, the library comprised of random sequences at the center flanked by defined primer binding sites at each 5' and 3' termini. The variety of the ssDNA library relies on the length of the random region. Around 10^{15} different sequences are contained in an initial ssDNA pool, which makes it appropriate for the existence of sequences specific for a target. Actually, the entire aptamer sequence library has only a short fraction that binds effectively to the target, which suggests that aptamer screening can be eventually accomplished within a short period of time [4]. It is noteworthy that long random sequences can provide higher structural complexity, which is vital in isolating aptamers with high affinity [5]. In an early stage of aptamer selection, RNA libraries are widely used due to the fact that RNA can easily fold into complex 3D structures which show higher affinity to the targets. However, RNA aptamers are much more expensive than DNA aptamers, and they are relatively difficult to be modified in SELEX cycles [6]. Furthermore, stems and loops can be generated when ssDNA folds into a 3D configuration [7]. So DNA libraries are used more frequently now.

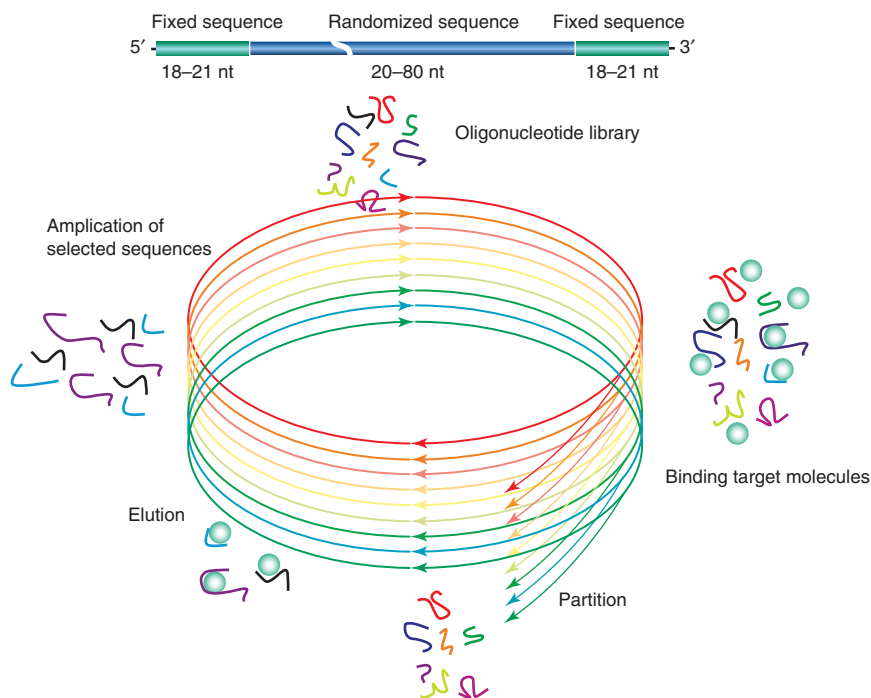


Figure 1.1 Schematic drawing of SELEX procedures. Source: Dong et al. 2013 [3]. Reprinted with permission of Taylor and Francis.

The essential steps of a typical SELEX process include binding, partitioning/ eluting, amplification, and identification. Normally, due to limited resolution and efficiency, many cycles of SELEX rounds need to be carried out to obtain a good result. In the first step, a random DNA or RNA library is incubated with the target to ensure definite binding of some oligonucleotides with the target, while others will be removed in the following steps. In the partitioning/ eluting step, unbound oligonucleotides can be removed on the basis of the different molecular weights of nucleotide-target complexes and nucleic acids. For example, a chromatographic column packed with the target-immobilized beads can be applied for the separation of oligonucleotides binding with the target molecules. Besides chromatography, other methods can also be used to separate unbound, weakly bound, or elute bound oligonucleotides, for example, filtration, heating, the change of ionic strength or pH, the addition of denaturing substances such as urea, sodium dodecyl sulfate (SDS), or ethylenediaminetetraacetic acid [8–10]. In this step, target molecules are interacted with either free nucleic acid or separable nucleic acid immobilized on a certain substrate [11]. However, it is difficult to elute strongly bound oligonucleotides from targets, which may restrict the isolation of the aptamers with extremely high affinity. Because of this, high affinity of aptamers are commonly obtained by SELEX with free-form target molecules [12, 13]. In some cases, it is difficult to remove unbound oligonucleotides from the free target-oligonucleotide

complex. So, low-affinity targets are appropriate for SELEX with free-form target molecules. After partitioning/eluting, the next step is to amplify the bound oligonucleotides by PCR (polymerase chain reaction) with primers for aptamer screening. The amplification will generate a new population of oligonucleotides for the next round of SELEX. Commonly, 10–20 amplifications are needed [14]. After repeated cycles of selection and amplification, the nucleotide pool becomes enriched, while the affinity between nucleotide and aptamers becomes higher because low- or no-affinity oligonucleotides are removed in previous cycles. The progress of SELEX can be monitored by the quantification of target-bound oligonucleotides among the pools of incubated nucleotides at each round of SELEX [15]. The selection is stopped when oligonucleotides bound to the target are fully dominant in the pool of oligonucleotides or significant enhancement of target-bound oligonucleotides cannot be observed during two or three successive SELEX rounds. These selected oligonucleotides are subject to amplification. Subsequently, the sequences of individually selected oligonucleotides are identified by cloning and sequencing of the selected clones, and the number of different aptamer sequences screened by the SELEX process depends on the stringency of the selection conditions and target characteristics thereof.

For the discovery of aptamer as a novel molecular recognition biochemical element, conventional SELEX is inherently an *in vitro* screening protocol of elegant simplicity, independent of animal or cell lines, which applies three principles of evolution – heredity, variation, and selection pressure [16]. Various aptamers, e.g. tetracycline aptamer [17] and thrombin aptamer [4], were successfully developed with iterative experimental rounds of incubation with ssDNA or RNA library, partitioning from the unbound, amplification of the binders, affinity characterization, and sequence identification, respectively.

However, the efficiency of conventional SELEX in the discovery of aptamers is somewhat low in terms of its cost-effectiveness, unsatisfactory specificity, limited partition capability, the necessity of a foreknowable targetability, difficult predictability, and inadequate stability or cross-linking capability, etc. Hence, different upgraded SELEX variants, i.e. negative SELEX (counter SELEX, subtractive SELEX), one-round SELEX, capillary electrophoresis (CE)-SELEX, microfluidic-SELEX, cell-SELEX, HTS-SELEX or *in silico*-SELEX, post-SELEX or *in chemico*-SELEX, auto-SELEX, primer-free SELEX, genomic SELEX, photo-SELEX, qPCR-SELEX, and so on were developed to further enhance the selection efficiency or analytical functionality, accordingly.

1.2 Negative SELEX and Its Analogs

In order to ensure the specificity of the aptamer recognition with target analytes solely, negative SELEX (counter SELEX, or subtractive SELEX), was frequently applied to remove nonspecific binding or erroneous recognition with structurally similar compounds of target analytes, and this is especially the case when target molecules of low abundance are in complex matrices, such as cell lysates, whole blood, or other body fluids.

To our knowledge, the first negative SELEX practice was reported by Ellington and Szostak in 1992, when they successfully developed DNA aptamers against small organic dye molecules. To specifically enrich the DNA pool with aptamer candidates, a non-cognate dye precolumn was suspended over a cognate dye column, then a chemically synthesized DNA pool with an estimated complexity of $2-3 \times 10^{13}$ different sequences were loaded onto the precolumn, and the precolumn retained most nonspecific bound sequences when washed with one column volume buffer. The selectivity in percent DNA bound after negative selection can be improved from 2.2, 1.5, 0.8 to 19.0, 7.0, 4.8, using affinity resin cibacron blue (CB), reactive green 19 (GR), and reactive blue 4 (B4) coupled to cross-linked agarose beads, respectively [18].

On the basis of a similar scheme, Takahashi et al. [19] successfully developed an isogenic cell-SELEX with a counterselection strategy to generate RNA aptamers toward cell surface protein, say, integrin α -V (ITGAV), a major transmembrane receptor widely expressed in almost all the cells and closely associated with human diseases such as cancers and pulmonary fibrosis. As illustrated in Figure 1.2, gene of interest (GOI) overexpressed human cell line HEK293 cells were used for positive selection, while GOI knockdown cells as mock cells by microRNA-mediated silencing were used for counterselection, a 100-fold difference in the expressing level of ITGAV between these two isogenic cells gives rise to several RNA aptamers toward ITGAV with dissociation constants ranging from 300 to 400 nM. Thus, the impediment of endogenous expression of target proteins in mocked cells or the heterogeneity of surface proteins between selection and counterselection cells was successfully overcome, as expected.

In addition, in order to discover aptamers to specific biomarkers that identify cells of interest from their homologous counterparts, SELEX with subtractive selection (subtractive SELEX) was frequently applied. Wang et al. reported a subtractive SELEX method to distinguish differentiated PC12 cells from normal PC12 cells. To subtract, randomized ssDNAs were incubated first with regular

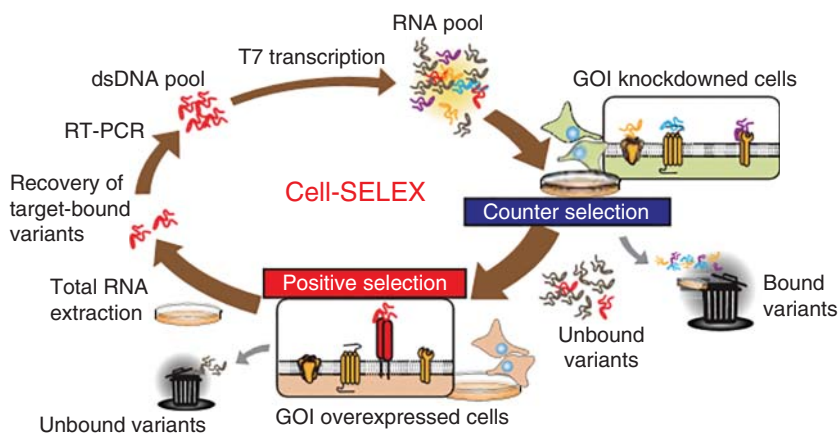


Figure 1.2 Schematic drawing of the isogenic cell-SELEX procedure. Source: Takahashi et al. 2016 [19]. Reprinted with permission of Elsevier.

PC12 cells eliminating those that recognize the common cellular components of both differentiated and undifferentiated PC12 cells; and after six rounds of cell-based selection, aptamers were found binding to differentiated PC12 cells, but not to the parental PC12 cells [20]. The subtractive SELEX presented herein is so potential that it is envisaged that the scheme can be further applied to tumor cell or stem cell research someday.

Nowadays, the negative SELEX and its analogs as aforementioned have become widely available and are rather potential for highly selective isolations of aptamers toward assorted analytes, e.g. human fatty acid-binding protein (FABP3) [21], aflatoxin (B1) [22], and prostate-specific membrane antigen (PSMA) [23], etc.

1.3 One-Round SELEX

The conventional SELEX protocol for a successful aptamer discovery generally necessitates 10+ iterative rounds of incubation, partition, PCR amplification, and sequence identification. The procedure is time-consuming and labor-intensive; hence, minimizing selection rounds to one round with different schemes can obviously enhance selection efficiency and save experimental cost.

In 2007, Nitsche et al. proposed a MonoLEX strategy to acquire high-affinity DNA aptamers binding Vaccinia virus used as a model organism for complex target structures. The approach combined a single affinity chromatography step with subsequent physical segmentation of the affinity resin and one single final exponential amplification step of bound aptamers, and binding specificity was evaluated using an aptamer-based blot assay [24].

Similarly, Arnold et al. identified two DNA aptamers with nanomolar dissociation constants using the one-round SELEX process in 2012 [25]. Kallikrein-related peptidase 6 (KLK6), an active serine protease that has been implicated in neurodegenerative disorders such as Parkinson and Alzheimer disease and certain types of cancer, was immobilized in a 96-well ELISA plate and incubated with the aptamer library overnight. Afterwards, unbound and nonspecifically bound aptamers were separated by salt solutions in a step elution gradient. The most tightly bound specific aptamers were eluted by the highest salt concentration. This fraction was then collected and characterized by competitive ELISA, fluorescence spectroscopy, and quartz crystal microbalance methods, and the specificity of the aptamers was tested on serum albumin.

Interestingly, one-round SELEX can be further applied for the generation of aptamer pairs for “sandwich” assays as in antibody- and antigen-based immunoassays. Using lysozyme as a target, a single-round SELEX based on the proximity ligation selection scheme was successfully developed by Chumphukam et al. [26] As shown in Figure 1.3, a sequence from the forward (F) library and another sequence from the reverse (R) library bind simultaneously to target molecule, allowing hybridization of the connector to both F- and R-sequences. Therefore, the 3'-end of the F-library is sufficiently close to the 5' phosphate of the R-library, ligation of these two sequences can occur, and the aptamer pairs with nanomolar affinities can be generated after two partitioning steps thereof.

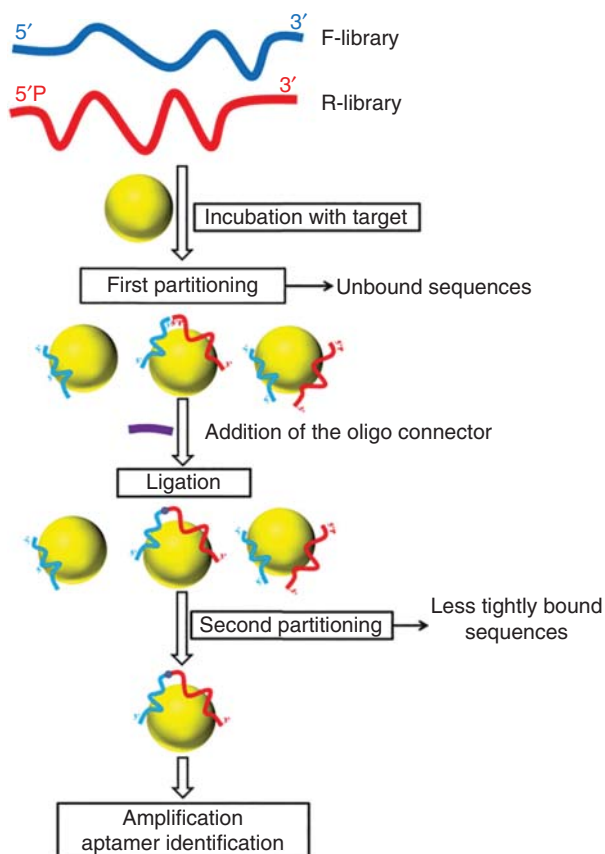


Figure 1.3 A schematic diagram of one-round proximity ligation selection (PLS). Source: Chumphukam et al. 2015 [26]. Reprinted with permission of Royal Society of Chemistry.

Although one-round SELEX can greatly enhance selection efficiency, it is commonly deemed to be inherently a violation of the basic variation principle of evolution. In addition, the selection stringency for the success of aptamer discovery cannot be easily acquired with just a single-round practice in most cases; hence, one-round SELEX for the development of highly affine aptamers still needs to extend its real-world applicability.

1.4 CE-SELEX

CE-SELEX takes advantage of CE and SELEX technology for screening aptamers efficiently. The different charge/mass ratios of the separated materials in the capillary result in different apparent migrations under high voltage, and CE-SELEX uses this mechanism to differentiate effectively between target-aptamer complexes and unbound oligonucleotides in the electric field.

CE-SELEX can greatly improve aptamer screening efficiency, and 2–4 rounds can get the targeting aptamer successfully [27]. The efficiency of the enrichment is attributed to (i) the screening is in a homogeneous solution, can eliminate disadvantages from the interaction of the stationary phase and the mobile phase, and improve the binding specificity thereof; (ii) the separation efficiency of CE is far better than the affinity chromatography or filtration method, the specific recognition sequence and nonspecific sequence can be separated completely, eliminating the elution step in the traditional SELEX method.

As shown in Figure 1.4, in a typical CE-SELEX process, the randomized nucleic acid library is firstly incubated with the target in the free solution; then the incubation mixture is injected into CE capillaries and separated under the high voltage. Nucleic acids that bind to the target show different apparent mobility compared with unbound sequences, and can be collected as different fractions. In the following steps, the binding sequences are amplified and purified for further round selection [28].

Normally, CE-SELEX with rounds of selections can achieve higher affinity aptamers, especially aptamers for relevant proteins than those using conventional selection methods. The combination of strong binding and substantial heterogeneity suggests that CE-SELEX is more successful in retaining very strong binders while eliminating weak ones [28]. The CE can separate a sample regardless of the size or sequence length of the target because binding and nonbinding sequences have obviously different migration behaviors in the capillary [29]. CE-SELEX was used to generate ssDNA aptamers for human immunodeficiency virus reverse transcriptase (HIVRT) in 2005. The ssDNA library was initially incubated with HIVRT, and cycles of HIVRT binding, PCR amplification, and purification were repeatedly performed using CE to procure enriched ssDNA libraries suitable for further rounds of selection [28].

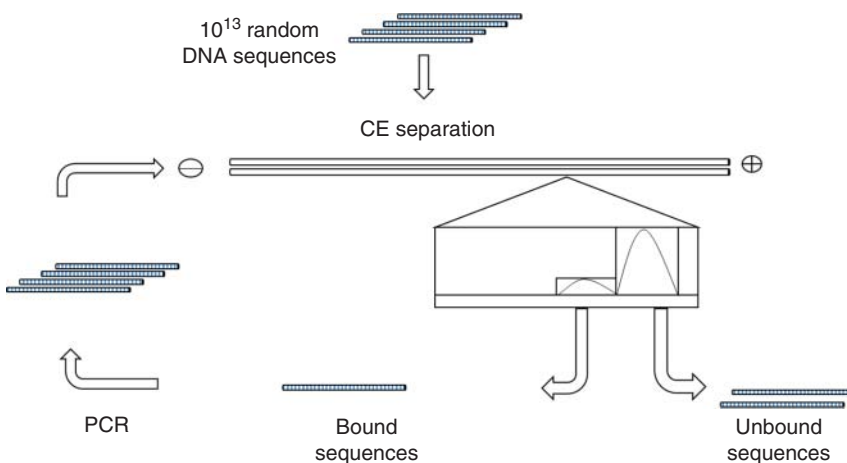


Figure 1.4 Schematic of CE-SELEX. Source: Mosing et al. 2005 [28]. Reprinted with permission of American Chemical Society.

In addition, specific aptamers against IgE [27], neuropeptide, and ricin [30] with low nanomolar dissociation constants had also been achieved successfully.

1.5 Microfluidic SELEX

Microfluidic SELEX or M-SELEX, which generally integrates magnetic microspheres with microfluidic chips, can be an extensive, efficient, and even fully automated nucleic acid aptamer screening platform. Compared to traditional SELEX processing equipment, microfluidic systems are more compact and consume less sample. Typically, a single-cycle SELEX process using a microfluidic chip takes about one hour, which is faster than the traditional SELEX process. In addition, the total sample volume consumed in each operation is only 40 μl , which is significantly less than the required sample volume in the large system (100 μl) [31]. The detailed steps about microfluidic SELEX are summarized in Figure 1.5: (a) the starting ssDNA library consists of 10^{14} unique sequences, each containing a 60-base internal randomized region flanked by two 20-base PCR primer-specific sequences; (b) the target protein is conjugated to the magnetic beads through carbodiimide coupling; (c) target-conjugated beads are incubated with the heat-treated ssDNA library; (d) aptamers that bind to the target protein are separated in the continuous-flow magnetic-activated chip-based separation (CMACS) device; (e and f) the aptamers bound on the target-coated beads are amplified via PCR and single-stranded products are generated; (g) the binding kinetics is measured for resulting aptamers.

Microfluidics technology has some unique advantages in improving the screening efficiency of conventional SELEX with the aid of magnetic beads. The microchannel device with laminar flow minimizes the negative influence of molecular diffusion on separation, and the screening process can be finished within a few rounds. Qian et al. developed a disposable micromagnetic separation (MMS) microfluidic chip and integrated ferromagnetic structures to

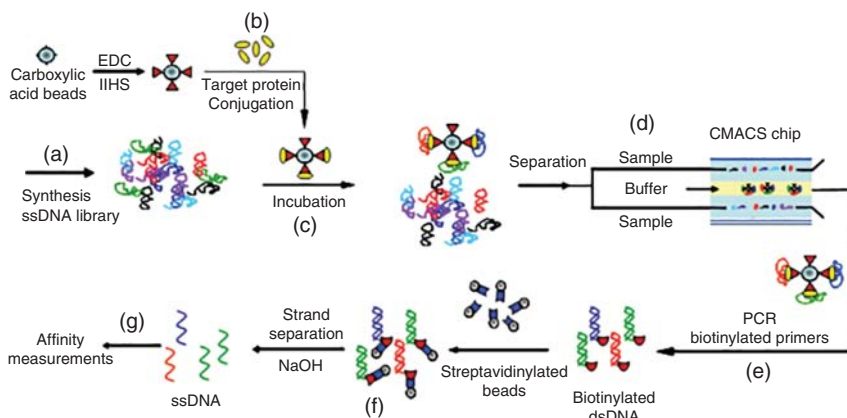


Figure 1.5 Overview of a microfluidic-SELEX process. Source: Lou et al. 2009 [31]. Reproduced with permission from PNAS.

reproducibly generate large magnetic field gradients within the microchannel to trap magnetic bead-bound aptamers efficiently [32]. The DNA aptamer for streptavidin demonstrating good affinity with nanomolar dissociation constant was obtained by three rounds of positive screening, and the specificity of nucleic acid aptamer was improved by negative selection against bovine serum albumin (BSA).

During the microfluidic SELEX process, magnetic beads play an important role. Normally, the target is fixed on the magnetic beads through covalent bonding or non-covalent coupling. Oligonucleotide molecules in the solution diffuse to the surface of the magnetic beads, and interact with the target. Then the non-bound and weak bound oligonucleotide molecules are removed by the elution. The nucleotide molecules bound to the target are separated from the magnetic beads, and the next round of screening library is obtained until good affinities are met.

An integrated microfluidic system with magnetic beads can provide a rapid automated screening approach. The scheme not only improves the efficiency of the SELEX greatly but also is effective for any type of molecular targets, and experimental data show that aptamers screened using an integrated microfluidic system are found to have an excellent affinities. The screening process firstly incubates the magnetic beads coupled to the target in the random nucleic acid library to find specific oligonucleotides; then the bead-bound oligonucleotides are captured and purified for further aptamer extraction by applying a magnetic field in the microchannel. The integrated microfluidic system generally consists of three modules: a microfluidic control module for sample incubation and transport, a bead-based ssDNA extraction module for aptamer screening, and a rapid nucleic acid amplification module. For example, C-reactive protein (CRP)-specific aptamers screened by this method are compared to those performed using laboratory-scale equipment and manual manipulations. Using a combination of magnetic beads and microfluidic transport technique, the CRP-specific aptamer from a complete random ssDNA library is successfully purified and enriched in an automated process [33].

Recently, an acousto-microfluidic SELEX method was suggested by Park et al. to obtain a prostate-specific antigen (PSA)-binding aptamer based on an acoustophoresis technique with simultaneous washing and separation in a continuous flow mode to improve selection efficiency. In addition, next-generation sequencing (NGS) was applied to accelerate the identification of the screened ssDNA pool. After eight rounds of acousto-microfluidic SELEX and following sequence analysis with NGS, seven PSA-binding ssDNA aptamer candidates were obtained and characterized with surface plasmon resonance (SPR) for affinity and specificity. The best PSA-binding aptamer showed specific binding to PSA with a dissociation constant (K_d) of 0.7 nM [34].

In summary, M-SELEX can greatly accelerate the aptamer separation using a very small number of target molecules to achieve highly stringent selection conditions. M-SELEX has become a versatile and automated method for rapid generation of aptamers nowadays, and can utilize many unique microfluidic phenomena such as laminar flow and electroosmosis to achieve unparalleled selection efficiency.

1.6 Cell-SELEX

The SELEX process is universally applicable to different classes of targets. Besides defined single targets, complex target structures or mixtures without proper knowledge of their composition are suitable for a successful aptamer selection. Using complete living cells as target molecules, cell-SELEX can be utilized to screen specific aptamers to identify potential or discover novel biomarkers on the cell surface. Generally, cell-SELEX includes two steps: firstly, the target cells are incubated with oligonucleotides and applied for positive screening; secondly, non-target cells are subject to negative screening. The advantages of cell-SELEX are listed as follows: (i) multiple aptamers targeting different receptor molecules on the target cell surface can be screened simultaneously; (ii) targeting aptamers can effectively recognize the receptor molecules on the cell surface under normal cellular growth condition; (iii) the targeting aptamers can be directly used for cell identification and cell binding studies; (iv) the targeting aptamers can identify the cell surface binding sites, which can be used as potential cell surface biomarkers [35]. Figure 1.6 illustrates the process of cell-SELEX screening.

Recently, Ara et al. successfully screened tumor cell surface antigen aptamers [36]. The results show that the relevant aptamers can be used

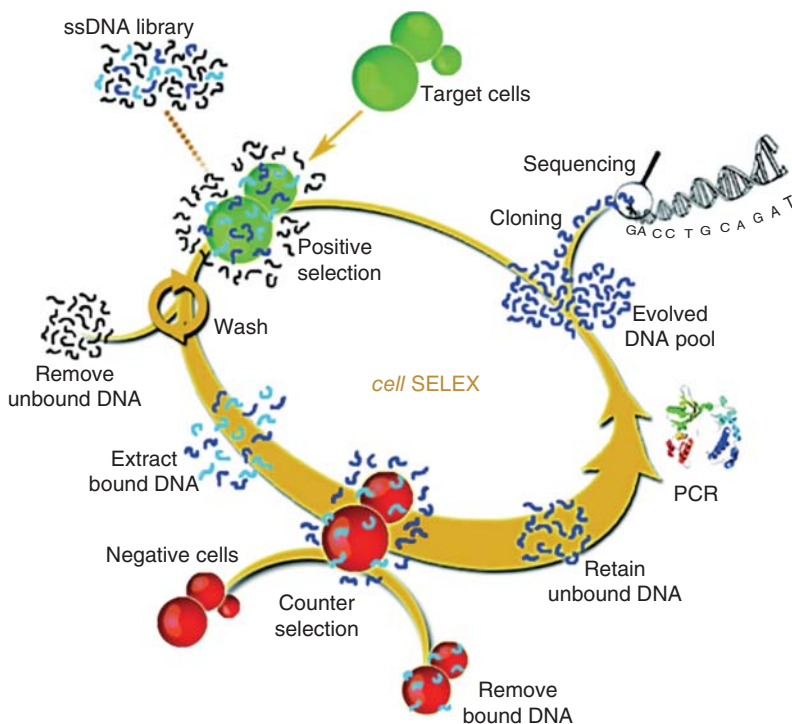


Figure 1.6 Mechanism of cell-SELEX [35]. Source: Fang and Tan 2010 [35]. Reprinted with permission of American Chemical Society.

not only for tumor molecular markers and diagnosis but also for the treatment of cancer. This technique avoids the purification process of the antigen and maintains the antigenic conformation of the cell surface. It is well known that the cell surface contains a plurality of antigens, which are all target substances. So it is particularly necessary to remove nonspecific nucleic acid strands to obtain the desired aptamers. The current cell-SELEX technique uses cells that possess no or low expression aim at target substances for negative screening, and applies control cells to remove nonspecific nucleic acid fragments from the selected secondary library [37].

Cancer-related biomarkers such as platelet-derived growth factor (PDGF), human epidermal growth factor 3 (HER3), vascular endothelial cell growth factor (VEGF), nuclear factor kappa B (NFkB), PMSA, and tenascin-C have been developed to identify cancerous cells [35]. Most of them use purified proteins as targets. Recently, it has been proved that more and more aptamers can be selected for complex targets, especially for whole cells. The selection of aptamers for living cells vs target protein-expressing cells is straightforward: cell surface proteins are endowed with their natural conformation, which is crucial for biological functions [38]. Recognition of human aptamer receptor tyrosine kinase RET is obtained with RET expression cells as targets as well. Compared with protein-based SELEX, cell-based selection can be performed on molecular signature without prior knowledge of the whole cell. When molecular recognition of cancer cells is needed, it is not necessary to know about the amount or type of proteins on the cell membrane. The selection process itself can distinguish between different types of cells, resulting in a specific type of cancer cells that can only bind to the aptamer, rather than normal cells or other types of cancer cells [39]. Moreover, it is feasible to perform whole cell selection in the presence of many receptor proteins on the surface of the cell membrane, so we can select a set of aptamer probes which can reveal the molecular characteristics of the target cancer type. This is the main advantage of cell-SELEX for cancer diagnosis and clinical analysis.

Currently, cell-SELEX is commonly utilized in aptamer selection for cancer study. A cultured precursor T-cell acute lymphoblastic leukemia (ALL) cell line, CCRF-CEM, has been used as the target. Negative selection is performed with a B-cell line derived from human Burkitt's lymphoma as a negative control by adding a Ramos selection process to exclude possible binding of DNA sequences to common molecules on the surface of leukemic cells [40]. In this work, CCRF-CEM cells are incubated with ssDNAs. The cell surface-binding sequences are eluted by heating after they are washed, and interact with excess Ramos cells afterwards. The sequences still free in the supernatant were amplified by PCR to form the starting pool and can be selected for the next round.

Several types of cancer cells have been successfully used in the cell-SELEX process to filter out novel aptamer probes. These aptamers show superior affinity and excellent specificity. However, it should be noted that the number and duration of cell-SELEX selection is longer than conventional SELEX, and cell-SELEX usually takes the risk of failure to damage fragile cells [40].

1.7 *In Silico*-SELEX

Conventional SELEX strategies after multiple *in vitro* selection rounds for the generation of aptamers are not always successful. Rationalizing random single-stranded oligonucleotide libraries via molecular simulation and tuning structural complexities by algorithm filtering are prevailing computational aptamer selection schemes which can be termed as *in silico*-SELEX, consequently.

Probably the first *in silico*-SELEX was reported by Chushak and Stone [41] when they proposed a computational method to develop RNA aptamers for codeine, gentamicin, theophylline, etc. Firstly, RNA sequences were selected from randomly generated RNA pools based on the criteria that limited the presence of sequences with abundant simple structural motifs and maximized the presence of stable low-energy structures. The Rosetta package was used for the prediction of tertiary structures of these selected RNA sequences, the structures were minimized using the AMBER force field and generalized Born implicit solvent, and then ensemble docking with a modified DOVIS package having AutoDock4 software as the docking engine and run in parallel on Linux clusters for a library of RNA molecules with lowest energy structures. RNA aptamers against codeine, gentamicin, theophylline, and other analyte molecules were selected by this high-throughput virtual screening scheme and experimentally validated, respectively.

Inherently, *in vitro* random RNA/DNA pools are not structurally diverse and heavily favor simple topological structures such as stem-loop structures; and increasing the structural diversity of the starting oligonucleotide pool can enhance the possibility of finding novel aptamers with improved affinity thereof. In 2011, Luo et al. [42] developed two computational algorithms of random filtering and genetic filtering to generate sequences that exhibit higher structural complexity and can be used to increase the overall structural diversity of initial pools for *in vitro* selection experiments.

Nowadays, *in silico*-SELEX has found its practical utilization in biomarker analysis for tumor diagnosis and treatment. Ahirwar et al. [43] reported an *in silico* selection strategy to select a candidate RNA ERaptR4 as human estrogen receptor α (ER α) aptamer. RNA analogs of human estrogen response elements (EREs) were used to obtain aptamer-like sequences. AutoDockVina, HADDOCK, and PatchDock docking were applied to examine the likelihood of near-native RNA analogs of selected single-stranded EREs emerge as ER α aptamer. In addition, isothermal titration calorimetry (ITC) was used to validate *in silico* prediction results by thermodynamic characteristics of ER α -RNA complex. After careful analysis of the predicted intermolecular interactions in the selected ER α -RNA complex, as shown in Figure 1.7, ERaptR4 was finally identified as ER α aptamer with a binding constant of $1.02 \pm 0.1 \times 10^8 \text{ M}^{-1}$. The aptamer had a good specificity confirmed through cytochemistry and solid-phase immunoassays as well. Furthermore, the aptamer could resist serum and RNase degradation in the presence of ER α , and the stability will enable

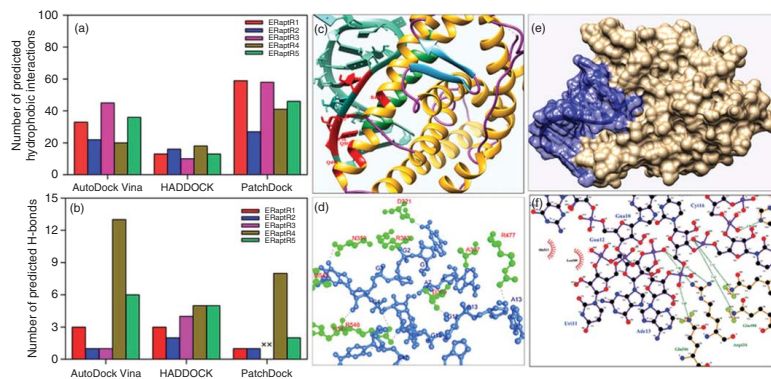


Figure 1.7 Analysis of the predicted intermolecular interactions in the selected ER α -RNA complex. (a) and (b) Numbers of the predicted hydrophobic interactions and H-bonds in complex of ER α with ERapR1–ERapR5. These interactions are predicted using Ligplot and Nucplot. (c) Ribbon view of the HADDOCK predicted ER α (1530)-ERapR4 complex, depicting the interacting residues and the spatial arrangement of protein chains in the vicinity of aptamer molecule. (d) H-bonding residues in the AutoDock Vina generated complex of ER α -ERapR4. The dark gray color represents the aptamer bases while the light gray color indicates the amino acids. (e) Surface view of the PatchDock-generated ER α -ERapR4 complex showing the relative orientations of interacting bases and amino acid chain. (f) Structural representation of H-bond and hydrophobic interactions in the ER α -ERapR4 complex as predicted using Ligplot. H-bonds are represented by dashed lines between H-bonding atoms, whereas the hydrophobic interactions are shown by an arc with spokes radiating toward the interacting ligand atoms. Source: Ahirwar et al. 2016 [43]. Reprinted with permission of Springer Nature.

future applications of this aptamer for the detection of ER α in breast cancer and related diseases as expected.

In summary, although *in silico*-SELEX can facilitate pool rationalization and the subsequent aptamer generation, a good command of molecular simulation and algorithm implementation, and a facile accessibility to computing resources, are generally required.

1.8 Post-SELEX and *In Chemico*-SELEX

To further enhance conformational adaptability and improve *in vivo* stability to degradation and binding affinity of the selected aptamer with analyte molecule, a good command of nucleotide chemistry and organic syntheses is a must. Some frontier SELEX strategies, which can be termed as post-SELEX or *in chemico*-SELEX, were developed successfully in recent years based on either modifying nucleotides or using non-natural nucleotides.

Chemically, the 2' hydroxyl of ribose in RNA molecule is rather reactive, especially at alkaline pH and particularly in the presence of ubiquitous endonuclease. The 2' hydroxyl will attack and break the phosphodiester backbone, resulting in a 2', 3' cyclic phosphate; hence, aptamer can be modified to bridged nucleic acid (BNA)/locked nucleic acid (LNA) at the 2', 4'-position, or substituted with $-F$, $-OCH_3$ or $-NH_2$ groups for hydroxyl at the 2' position of the ribose. In addition, the phosphodiester backbone of the aptamer can be derivatized as well.

2',4'-BNA/LNA with high nuclease resistance and low cytotoxicity were independently developed by Imanishi et al. [44] at Osaka University and Wengel et al. [45] at the University of Southern Denmark in the late 1990s, and *in vitro* selection of BNA/LNA aptamers is feasible owing to the discovery of polymerases available for BNA/LNA-containing oligonucleotide syntheses and genetic engineering of these polymerases in recent years. Using CE-SELEX, high-affinity thrombin-binding aptamers (TBAs) were obtained from DNA-based libraries containing 2'-O,4'-C-methylene-bridged/linked ribonucleotides in the 5'-primer region. After around 10 rounds of selection, as shown in Figure 1.8, 40 sequences were identified, and the binding affinity (K_d) of the best aptamer was 18 nM [46].

Oncostatin M (OSM) is a multifunctional member of the interleukin-6 cytokine family and has been implicated as a powerful proinflammatory mediator and may represent a potentially important, novel therapeutic opportunity for treatment of established rheumatoid arthritis. Andrew Rhodes et al. [47] isolated an RNA aptamer ADR58 for human OSM with a high affinity of 8 nM successfully, the pyrimidine positions in ADR58 all contain a 2' fluoro group on the ribose ring, and this modification stabilizes the aptamer with respect to ribonuclease activity. To better ensure aptamer stability, each individual purine position was sequentially substituted with a 2' O-methyl purine residue. In addition, truncated ADR58 from 71 bases in length to 33 bases with the same OSM affinity was terminated at the 3' end with a 3'-3' thymidine cap to further increase resistance to nuclease attack.

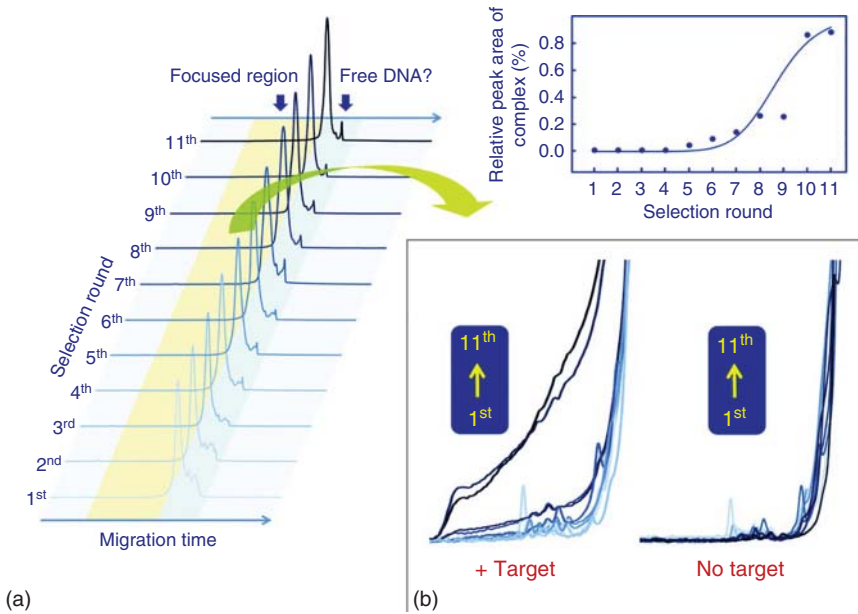


Figure 1.8 Process of active species enrichment in selection rounds. (a) Capillary electropherograms for library E of each round with human thrombin (left graphic). All electropherograms recorded fluorescent intensity of 5'-labeled 6-FAM vs migration time. Saturation curve of library enrichment for TBA acquisition (right graphic). (b) Enlarged and overlapped view of each round of capillary electropherograms with or without human thrombin. Source: Kuwahara and Obika 2013 [46]. Reprinted with permission of Taylor and Francis.

An oligonucleotide library with phosphorothioate backbone thio-substituted at dA positions was synthesized and used for the selection of enhanced nuclease-resistant DNA aptamer to target NF-IL6, a basic leucine zipper transcription factor involved in the induction of acute-phase responsive and cytokine gene promoters in response to inflammation. An individual monothiophosphate 66-mer cloned from the 10th selection round gave an observed binding constant of <2 nM, and, as shown in Figure 1.9, thiophosphorylation of the family A 66-mer at only the dA sites (except for the primers) results in a duplex that is more resistant to DNase I degradation than the unmodified 66-mer [48].

In order to increase both chemical and structural diversity of the DNA molecules for aptamer selection, non-natural nucleotides as developed by Benner [49] and Hirao [50] were introduced into various SELEX protocols. The potential of this genetic alphabet expansion becomes a powerful tool for creating highly functional nucleic acids such as analytical aptamers and medicinal pharmaceuticals.

Zhang et al. [51] developed aptamers against cells overexpressing glypican 3 (GPC3), a probable biomarker of hepatocellular carcinoma (HCC), from an artificially expanded six-letter genetic information system (AEGIS) with two non-natural nucleobases (2-amino-8H-imidazo[1,2-*a*]-[1,3,5]triazin-4-one, Z and 6-amino-5-nitropyridin-2-one, P) as shown in Figure 1.10. With counterselection against non-engineered cells, eight AEGIS-containing

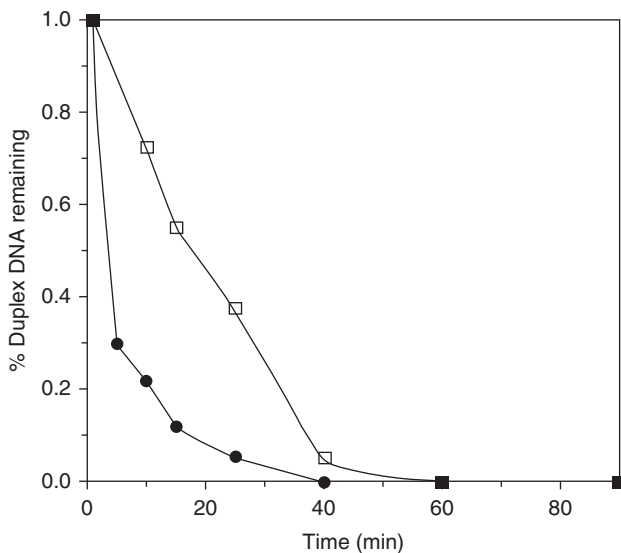


Figure 1.9 Relative sensitivity value of family A 66-mers to degradation by DNase I. Unmodified, phosphoryl duplex (●) and monothiophosphorylated at nonprime dA sites only (□) with 0.0 and 1.0 at time 0 and after 60 minutes, respectively (■). Source: King et al. 1998 [48]. Reprinted with permission of American Chemical Society.

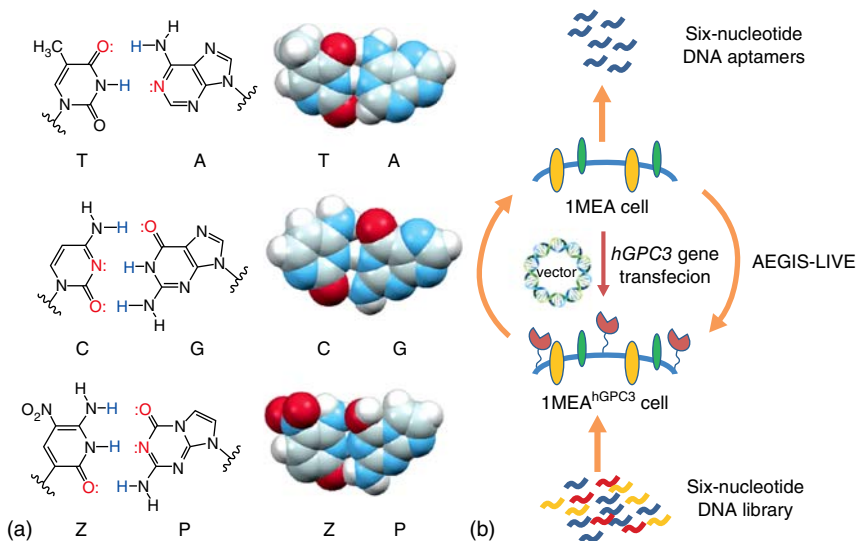


Figure 1.10 Chemical structures of the six nucleotides and AEGIS-LIVE (laboratory *in vitro* evolution). (a) Molecular structures (left) and space-filling models (right) of C:G, T:A, and Z:P pairs showing their similarity (PDB ID: 4RHD). (b) Engineering hGPC3-overexpressing cells and AEGIS-LIVE procedure. Source: Zhang et al. 2016 [51]. Reprinted with permission of John Wiley and Sons.

aptamers were recovered, among which five bound selectively to GPC3-overexpressing cells.

Similarly, Kimoto et al. [52] generated high-affinity DNA aptamers using an expanded genetic alphabet of four natural nucleotides and an unpaired artificial nucleotide with the hydrophobic base 7-(2-thienyl)imidazo[4,5-b]pyridine(Ds). Selection experiments against two human target proteins, VEGF-165 and interferon- γ (IFN- γ), yielded DNA aptamers that bind with K_d values of 0.65 pM and 0.038 nM, respectively, affinities that are >100-fold improved over those of aptamers containing only natural bases.

1.9 Auto-SELEX

The automated SELEX process refers to the selection cycles without any direct manual intervention steps, and is designed to provide high flexibility and versatility in the selection of buffers, reagents to meet rigorous selection criteria [53].

In 2001, the Beckman-Coulter Biomek 2000 automated workstation was used to screen aptamers of lysozyme. The workstation included a mechanical control station, thermal cycler, magnetic bead automatic separator, multiscreen vacuum filter, enzyme cooler, and an automatic pipetting tool. The screening process involved immobilizing the biotinylated target protein on the magnetic beads by the interaction of streptavidin with biotin. The specific binding sequence of separation, reverse transcription polymerase chain reaction (RT-PCR) amplification and transcription were all automated by the programmed procedure. The final sequence was cloned into the vector for sequencing and identification. By this automated screening workbench, the author only needs less than two days to complete 12 rounds of screening [54]. Automated selection saves time and gets good results [55]. Using the automated SELEX method, RNA aptamers to the mirror-image configuration (d-peptide) of substance P have been identified [53]. The anti-lysozyme aptamer is also selected [55]. To date, the auto-SELEX method has been applied for various targets, ranging from small organic molecules to supramolecular structures [1, 6, 56] and organisms [57, 58].

1.10 Primer-Free SELEX

Standard phylogenetic evolution of ligands by SELEX schemes requires libraries containing two primers on both sides of the central random domain, which amplifies the target binding sequence by PCR or RT-PCR. However, these primer sequences may cause nonspecific binding, and result in a large number of binding sequences or interfering with specifically binding random sequences.

The scientists started to develop the primer-free SELEX method that eliminates the primer sequence from the target binding process, thereby eliminating the interference caused by the primer sequence. The method allows the primers to be regenerated and eliminated after selection. It is fast, simple, and does not require any chemical modification [59].

Wen et al. develop a primer-free genome SELEX method to avoid the interference from the interaction of the primer and the oligomers during the amplification process [60]. The method removes the primer from the genomic library before screening, and incubates the library with the target molecule. The gene fragments are screened by hybridization-extension thermal cycling reaction to carry out PCR amplification. This primer-free genomic SELEX is a new platform technology. The primer-free SELEX significantly simplifies SELEX procedures and eliminates the primitive interference problem, and becomes a good method for identifying potentially bio-important nucleic acid sequences of target molecules while reducing human workload [58].

1.11 Genomic SELEX

Genomic SELEX is based on the generation of RNA species that are derived from a library of an organism's entire genomic DNA *in vitro*. The generated RNA pool will undergo successive rounds of association with a given RNA-binding protein, partitioning, and reamplification. This method does not require isolation of non-coding RNAs (ncRNAs) from an organism or cell.

RNA sequences that are stringently bound by the protein partner will be enriched. Once the sequence of the bound RNAs is determined, this method will be used to search for matches in the genome, and predicted genomic regions that can be tested for the expression of unknown ncRNAs. Genomic SELEX has been successfully applied to select mRNA (messenger RNA)-binding protein partners [61, 62].

Valentin-Hansen et al. applied genomic SELEX to identify new Hfq-binding RNAs from *Escherichia coli*. A representative library of the *E. coli* genome is constructed from random 50–500 bp genomic DNA fragments to which defined linkers, one of these containing a T7 RNA polymerase promoter, is attached in the course of the initial library generation step [63]. These fragments are *in vitro* transcribed with T7 RNA polymerase, incubated with Hfq, and selected for Hfq binding on filters. Taking the standard SELEX procedure [64], the retained RNA is converted to complementary DNA (cDNA) and subjected to additional reamplification and selection rounds, which finally result in a pool of RNAs that bind Hfq with K_d values of 5–50 nM. Subsequently, specific Hfq interaction of the enriched RNAs is determined *in vivo* using a yeast three-hybrid screen [65]. Preliminary results suggest that these experiments identified a number of novel Hfq-binding RNAs, including antisense RNAs and candidate ncRNAs from intergenic regions.

However, the studies that focused on ncRNAs have not been published for any organism yet. The combination of genomic-SELEX technology and computer-aided design (CAD) will be used to select ncRNAs in future. Genomic-SELEX would clearly have its strength in finding ncRNAs that are overlooked by methods that require ncRNA genes to be expressed at a certain level. This method can be used in prokaryotes because of their small genome sizes. Since functional ncRNAs are mostly encoded by intergenic regions in

microbes, the DNA original fragments will be loaded by amplifying this portion of the genome specifically, which constitutes below 10% of the entire genome in microbes.

1.12 Photo-SELEX

In photo-SELEX, base moiety in a library oligonucleotide sequence can be replaced by an optically active compound, such as 5-iodouracil and 5-bromouracil; then the sequence is incubated with the target molecule. Induction of target molecule by light irradiation increases the specificity of its covalent cross-linking, which can increase the specificity and affinity of the selected aptamers. The 5-bromouracil chromophore has absorption at 310 nm, while native chromophores of nucleic acids and proteins show very weak or no absorption [66].

Bromodeoxyuridine (BrdU) photoaptamers are rapidly emerging as specific protein capture reagents in protein microarray technologies. A mathematical model for the kinetic analysis of photoaptamer-protein reaction has been presented by Koch et al. [67]. The model is based on specific aptamer/protein binding followed by laser excitation that can lead to either covalent cross-linking of the photoaptamer and protein in the complex or irreversible photodamage to the aptamer. The models are used to characterize the photocross-linking between three photoaptamers and their cognate protein targets (human basic fibroblast growth factor and HIV MN envelope glycoprotein). The cross-linking reaction yields, laser energy dose, and target protein concentration are used to analyze the affinity constants and cross-link reaction rates. The binding dissociation constants derived from the cross-linking data are in good accordance with independent measurements.

Photo-SELEX can obtain an aptamer with higher affinity compared to conventional SELEX. If a good photo-SELEX result is expected, the target molecule must be a protein molecule with photocross-linking functional groups such as aromatic or sulfur-containing amino acid residues.

1.13 qPCR-SELEX

With the development of PCR instruments, aptamers can be quantified by quantitative PCR techniques in real time with aptamer-specific primers after screening with SELEX. This quantitation scheme, which is termed as qPCR-SELEX, can not only be used as an additional monitoring tool to determine the enrichment of bound aptamers for sequence selection but also detect the presence of the corresponding target substance and its amount indirectly. Furthermore, the contamination of the amplified aptamer pool with by-products can be prevented by prior determination of bound aptamers during SELEX rounds.

qPCR-SELEX combines the affinity of the aptamers with the amplification of the PCR reaction, and can obtain a significant increase in the detection capability

for target substance. Besides, due to the high specificity of the aptamers binding to the target substance, the accuracy of the testing can be ensured. In 2013, on the basis of a SYBR Green I real-time PCR technology and cell-SELEX, Avci-Adali et al. used a qPCR-SELEX strategy to determine the accurate aptamer amount on cells after the incubations. The method is highly sensitive and allows the detection of very small quantities of aptamers in cell lysate samples. The lower detection limit is 20 fg [68].

1.14 Perspectives

SELEX and its assorted updates are now evolved rapidly for various analytical or medicinal applications. Aptamers with comparable or even superior affinities of antibodies and improved stabilities are successfully developed on the basis of frontier technologies of random library rationalizing, unbound fractionating, affinity characterization, and sequence identification, accordingly. For instance, Xianbin Yang et al. successfully developed phosphorothioate (PS-) or phosphorodithioate (PS2-) oligonucleotide thioaptamers as potential diagnostic reagents or therapeutics in recent years [69–71].

However, the effort for a successful SELEX is still painstaking. In an effort to overcome conventional SELEX limitations, AM Biotech (see www.am-biotech.com) developed a patented selection technology that eliminates the need to enzymatically replicate the binding aptamer sequences during selection. This exponentially expands the chemical diversity available for target interaction and also enables the X-Aptamer Selection Kit (Figure 1.11), which significantly



Figure 1.11 X-aptamer selection kit developed by AM Biotech. Source: With permission from AM Biotech.

eases the work required for selection. In addition, a universal tool (FCE-SELEX) for the development of aptamers was recently reported by Luo et al. [72], by integrating fraction collection with facile oil sealing to avoid contamination while amplifying the bound DNA–target complex. In a single CE-SELEX round of selection, a streptavidin-binding aptamer with an affinity of 30.8 nM was generated.

It is noteworthy that high-throughput sequencing with bioinformatics is becoming a routine tool for aptamer discovery nowadays [73], and aptamer microarrays [74] have been incorporated into traditional SELEX protocols for unparalleledly efficient sequence characterization and identification as well. The readers are suggested to read Chapter 13 for more information on SELEX with NGS and microarray-based SELEX thereof.

Although aptamers are mostly *in vitro* selected for a definite target, their analytical utilization for non-target profiling and broad-spectrum or class-specific determination remain very limited. Antibodies with good affinities and specificities are still predominant recognition elements for analysis. More theoretical investigations and experimental practices are therefore needed to foresee or interpret aptamer configuration and adaptive folding mechanism at the molecular level, which will necessitate the evolution of SELEX and its variants in the future.

References

- 1 Ellington, A.D. and Szostak, J.W. (1990). In vitro selection of RNA molecules that bind specific ligands. *Nature* 346: 818–822.
- 2 Tuerk, C. and Gold, L. (1990). Systematic evolution of ligands by exponential enrichment: RNA ligands to bacteriophage T4 DNA polymerase. *Science* 249: 505–510.
- 3 Dong, Y.Y., Xu, Y., Yong, W. et al. (2013). Aptamer and its potential applications for food safety. *Crit. Rev. Food Sci. Nutr.* 54: 1548–1561.
- 4 Bock, L.C., Griffin, L.C., Latham, J. et al. (1992). Selection of single-stranded DNA molecules that bind and inhibit human thrombin. *Nature* 355: 564–566.
- 5 Marshall, K.A. and Ellington, A.D. (2000). In vitro selection of RNA aptamers. *Methods Enzymol.* 318: 193–214.
- 6 Jenison, R., Gill, S., Pardi, A., and Polisky, B. (1994). High-resolution molecular discrimination by RNA. *Science* 263: 1425–1429.
- 7 Harada, K. and Frankel, A.D. (1995). Identification of two novel arginine binding DNAs. *EMBO J.* 14: 5798–5811.
- 8 Stoltenburg, R., Reinemann, C., and Strehlitz, B. (2005). FluMag-SELEX as an advantageous method for DNA aptamer selection. *Anal. Bioanal. Chem.* 383: 83–91.
- 9 Weiss, S., Proske, D., Neumann, M. et al. (1997). RNA aptamers specifically interact with the prion protein PrP. *J. Virol.* 71: 8790–8797.
- 10 Bridonneau, P., Chang, Y., Buvoli, A. et al. (1999). Site-directed selection of oligonucleotide antagonists by competitive elution. *Antisense Nucleic Acid Drug Dev.* 9: 1–11.

- 11 Shimada, T., Fujita, N., Maeda, M., and Ishihama, A. (2005). Systematic search for the Cra-binding promoters using genomic SELEX system. *Genes Cells* 10: 907–918.
- 12 Berezovski, M., Drabovich, A., Krylova, S.M. et al. (2005). Nonequilibrium capillary electrophoresis of equilibrium mixtures: a universal tool for development of aptamers. *J. Am. Chem. Soc.* 127: 3165–3171.
- 13 White, R., Rusconi, C.P., Scardino, E. et al. (2001). Generation of species cross-reactive aptamers using toggle SELEX. *Mol. Ther.* 4: 567–573.
- 14 Kim, Y.S. and Gu, M.B. (2014). Advances in aptamer screening and small molecule aptasensors. *Adv. Biochem. Eng./Biotechnol.* 140: 29–67.
- 15 Conrad, R.C., Baskerville, S., and Ellington, A.D. (1995). In vitro selection methodologies to probe RNA function and structure. *Mol. Diversity* 1: 69–78.
- 16 Gotrik, M.R., Feagin, T.A., Csordas, A.T. et al. (2016). Advancements in aptamer discovery technologies. *Acc. Chem. Res.* 49: 1903–1910.
- 17 Niazi, J.H., Lee, S.J., and Gu, M.B. (2008). Single-stranded DNA aptamers specific for antibiotics tetracyclines. *Bioorg. Med. Chem.* 16: 7245–7253.
- 18 Ellington, A.D. and Szostak, J.W. (1992). Selection in vitro of single-stranded DNA molecules that fold into specific ligand-binding structures. *Nature* 355: 850–852.
- 19 Takahashi, M., Sakota, E., and Nakamura, Y. (2016). The efficient cell-SELEX strategy, Icell-SELEX, using isogenic cell lines for selection and counter-selection to generate RNA aptamers to cell surface proteins. *Biochimie* 131: 77–84.
- 20 Wang, C.L., Zhang, M., Yang, G. et al. (2003). Single-stranded DNA aptamers that bind differentiated but not parental cells: subtractive systematic evolution of ligands by exponential enrichment. *J. Biotechnol.* 102: 15–22.
- 21 Kakoti, A. and Goswami, P. (2016). Multifaceted analyses of the interactions between human heart type fatty acid binding protein and its specific aptamers. *Biochim. Biophys. Acta* 1861 (1): 3289–3299.
- 22 Setlem, K., Monde, B., Ramlal, S., and Kingston, J. (2016). Immuno affinity SELEX for simple, rapid, and cost-effective aptamer enrichment and identification against aflatoxin B1. *Front. Microbiol.* 7: 1–14.
- 23 Almasi, F., Gargari, S.L.M., Bitaraf, F., and Rasoulinejad, S. (2016). Development of a single stranded DNA aptamer as a molecular probe for LNCap cells using cell-SELEX. *Avicenna J. Med. Biotechnol.* 8: 104–111.
- 24 Nitsche, A., Kurth, A., Dunkhorst, A. et al. (2007). One-step selection of Vaccinia virus-binding DNA aptamers by MonoLEX. *BMC Biotech.* 7: 48–48.
- 25 Arnold, S., Pampalakis, G., Kantiotou, K. et al. (2012). One round of SELEX for the generation of DNA aptamers directed against KLK6. *Biol. Chem.* 393 (5): 343–353.
- 26 Chumphukam, O., Le, T.T., Piletsky, S.A., and Cass, A.E.G. (2015). Generation of a pair of independently binding DNA aptamers in a single round of selection using proximity ligation. *Chem. Commun.* 51: 9050–9053.
- 27 Mendonsa, S.D. and Bowser, M.T. (2004). In vitro evolution of functional DNA using capillary electrophoresis. *J. Am. Chem. Soc.* 126: 20–21.

- 28 Mosing, R.K., Mendonsa, S.D., and Bowser, M.T. (2005). Capillary electrophoresis-SELEX selection of aptamers with affinity for HIV-1 reverse transcriptase. *Anal. Chem.* 77: 6107–6112.
- 29 Yang, Y., Yang, D.L., Schluesener, H.J., and Zhang, Z.R. (2007). Advances in SELEX and application of aptamers in the central nervous system. *Biomol. Eng.* 24: 583–592.
- 30 Tang, J.J., Xie, J.W., Shao, N.S., and Yan, Y. (2006). The DNA aptamers that specifically recognize ricin toxin are selected by two in vitro selection methods. *Electrophoresis* 27: 1303–1311.
- 31 Lou, X.H., Qian, J.R., Xiao, Y. et al. (2009). Micromagnetic selection of aptamers in microfluidic channels. *Proc. Natl. Acad. Sci. U. S. A.* 106 (9): 2989–2994.
- 32 Qian, J., Lou, X., Zhang, Y. et al. (2009). Generation of highly specific aptamers via micromagnetic selection. *Anal. Chem.* 81: 5490–5495.
- 33 Huang, C.J., Lin, H.I., Shiesh, S.C., and Lee, G.B. (2010). Integrated microfluidic system for rapid screening of CRP aptamers utilizing systematic evolution of ligands by exponential enrichment (SELEX). *Biosens. Bioelectron.* 25: 1761–1766.
- 34 Park, J.W., Lee, S.J., Ren, S. et al. (2016). Acousto-microfluidics for screening of ssDNA aptamer. *Sci. Rep.* 6: 27121.
- 35 Fang, X. and Tan, W. (2010). Aptamers generated from cell-SELEX for molecular medicine: a chemical biology approach. *Acc. Chem. Res.* 43: 48–57.
- 36 Ara, M.N., Hyodo, M., Ohga, N. et al. (2012). Development of a novel DNA aptamer ligand targeting to primary cultured tumor endothelial cells by a cell-based SELEX method. *PLoS One* 7 (12): e50174.
- 37 Daniels, D.A., Chen, H., Hicke, B.J. et al. (2003). A tenascin-C aptamer identified by tumor cell SELEX: systematic evolution of ligands by exponential enrichment. *Proc. Natl. Acad. Sci. U. S. A.* 100: 15416–15421.
- 38 Cerchia, L., Duconge, F., Pestourie, C. et al. (2005). Neutralizing aptamers from whole-cell SELEX inhibit the RET receptor tyrosine kinase. *PLoS Biol.* 3 (4): 697–704.
- 39 Shamah, S.M., Healy, J., and Cloud, S.T. (2008). Complex target SELEX. *Acc. Chem. Res.* 41: 130–138.
- 40 Blank, M., Weinschenk, T., Priemer, M., and Schluesener, H. (2001). Systematic evolution of a DNA aptamer binding to rat brain tumor microvessels: selective targeting of endothelial regulatory protein p19. *J. Biol. Chem.* 276: 16464–16468.
- 41 Chushak, Y. and Stone, M.O. (2009). In silico selection of RNA aptamers. *Nucleic Acids Res.* 37 (12): 87–95.
- 42 Luo, X., Mckeague, M., Pitre, S. et al. (2010). Computational approaches toward the design of pools for the in vitro selection of complex aptamers. *RNA* 16: 2252–2262.
- 43 Ahirwar, R., Nahar, S., Aggarwal, S. et al. (2016). In silico selection of an aptamer to estrogen receptor alpha using computational docking employing estrogen response elements as aptamer-alike molecules. *Sci. Rep.* 6: 21285.

- 44 Obika, S., Nanbu, D., Hari, Y. et al. (1997). Synthesis of 2-O,4'-C-methyleneuridine and -cytidine. Novel bicyclic nucleosides having a fixed C3, -endo sugar pucker. *Tetrahedron Lett.* 38 (50): 8735–8738.
- 45 Alexei, A.K., Sanjay, K.S., Poul, N. et al. (1998). LNA (locked nucleic acids): synthesis of the adenine, cytosine, guanine, 5-methylcytosine, thymine and uracil bicyclonucleoside monomers, oligomerisation, and unprecedented nucleic acid recognition. *Tetrahedron* 54 (14): 3607–3630.
- 46 Kuwahara, M. and Obika, S. (2013). In vitro selection of BNA (LNA) aptamers. *Artif. DNA PNA XNA* 4: 39–48.
- 47 Rhodes, A., Deakin, A., Spaul, J. et al. (2000). The generation and characterization of antagonist RNA aptamers to human oncostatin M. *J. Biol. Chem.* 275: 28555–28561.
- 48 King, D.J., Ventura, D.A., Brasier, A.R., and Gorenstein, D.G. (1998). Novel combinatorial selection of phosphorothioate oligonucleotide aptamers. *Biochemistry* 37: 16489–16493.
- 49 Yang, Z., Hutter, D., Sheng, P. et al. (2006). Artificially expanded genetic information system: a new base pair with an alternative hydrogen bonding pattern. *Nucleic Acids Res.* 34: 6095–6101.
- 50 Hirao, I., Kimoto, M., Mitsui, T. et al. (2006). An unnatural hydrophobic base pair system: site-specific incorporation of nucleotide analogs into DNA and RNA. *Nat. Methods* 3: 729–735.
- 51 Zhang, L.Q., Yang, Z.Y., Trinh, T.L. et al. (2016). Aptamers against cells overexpressing glypican 3 from expanded genetic systems combined with cell engineering and laboratory evolution. *Angew. Chem. Int. Ed. Engl.* 55: 12372–12375.
- 52 Kimoto, M., Yamashige, R., Matsunaga, K. et al. (2013). Generation of high-affinity DNA aptamers using an expanded genetic alphabet. *Nat. Biotechnol.* 31: 453–457.
- 53 Eulberg, D., Buchner, K., Maasch, C., and Klussmann, S. (2005). Development of an automated in vitro selection protocol to obtain RNA-based aptamers: identification of a biostable substance P antagonist. *Nucleic Acids Res.* 33 (4): 45–54.
- 54 Cox, J.C. and Ellington, A.D. (2001). Automated selection of anti-protein aptamers. *Bioorg. Med. Chem.* 9: 2525–2531.
- 55 Drolet, D.W., Jenison, R.D., Smith, D.E. et al. (1999). A high throughput platform for systematic evolution of ligands by exponential enrichment (SELEX). *Comb. Chem. High Throughput Screening* 2: 271–278.
- 56 Famulok, M. (1999). Oligonucleotide aptamers that recognize small molecules. *Curr. Opin. Struct. Biol.* 9: 324–329.
- 57 Homann, M. and Goring, H.U. (1999). Combinatorial selection of high affinity RNA ligands to live African trypanosomes. *Nucleic Acids Res.* 27: 2006–2014.
- 58 Morris, K.N., Jensen, K.B., Julin, C.M. et al. (1998). High affinity ligands from in vitro selection: complex targets. *Proc. Natl. Acad. Sci. U. S. A.* 95: 2902–2907.

- 59 Pan, W., Xin, P., and Clawson, G.A. (2008). Minimal primer and primer-free SELEX protocols for selection of aptamers from random DNA libraries. *BioTechniques* 44: 351–360.
- 60 Wen, J. and Gray, D.M. (2004). Selection of genomic sequences that bind tightly to Ff gene 5 protein: primer-free genomic SELEX. *Nucleic Acids Res.* 32 (22): 182–191.
- 61 Stoughton, R.B. (2005). Applications of DNA microarrays in biology. *Annu. Rev. Biochem.* 74: 53–82.
- 62 Zhang, A., Wassarman, K.M., Rosenow, C. et al. (2003). Global analysis of small RNA and mRNA targets of Hfq. *Mol. Microbiol.* 50: 1111–1124.
- 63 Valentinhanen, P., Erikse, M., and Udesen, C. (2004). The bacterial Sm-like protein Hfq: a key player in RNA transactions. *Mol. Microbiol.* 51: 1525–1533.
- 64 Barad, O., Meiri, E., Avniel, A. et al. (2004). MicroRNA expression detected by oligonucleotide microarrays: system establishment and expression profiling in human tissues. *Genome Res.* 14: 2486–2494.
- 65 Iyer, V.R., Horak, C.E., Scafe, C.S. et al. (2001). Genomic binding sites of the yeast cell-cycle transcription factors SBF and MBF. *Nature* 409: 533–538.
- 66 Golden, M.C., Collins, B.D., Willis, M.C., and Koch, T.H. (2000). Diagnostic potential of PhotoSELEX-evolved ssDNA aptamers. *J. Biotechnol.* 81: 167–178.
- 67 Koch, T.D., Smith, D., Tabacman, E., and Zichi, D.A. (2004). Kinetic analysis of site-specific photoaptamer–protein cross-linking. *J. Mol. Biol.* 336 (5): 1159–1173.
- 68 Avci-Adali, M., Wilhelm, N., Perle, N. et al. (2013). Absolute quantification of cell-bound DNA aptamers during SELEX. *Nucleic Acid Ther.* 23: 125–130.
- 69 Yang, X. and Gorenstein, D.G. (2004). Progress in thioaptamer development. *Curr. Drug Targets* 5: 705–715.
- 70 Yang, X., Bassett, S.E., Li, X. et al. (2002). Construction and selection of bead-bound combinatorial oligonucleoside phosphorothioate and phosphorodithioate aptamer libraries designed for rapid PCR-based sequencing. *Nucleic Acids Res.* 30: e132.
- 71 Yang, X., Wang, H., David, W.C. et al. (2006). Selection of thioaptamers for diagnostics and therapeutics. *Ann. N. Y. Acad. Sci.* 1082: 116–119.
- 72 Luo, Z.F., Zhou, H.M., Jiang, H. et al. (2015). Development of a fraction collection approach in capillary electrophoresis SELEX for aptamer selection. *Analyst* 140: 2664–2670.
- 73 Hoon, S., Zhou, B., Janda, K.D. et al. (2011). Aptamer selection by high-throughput sequencing and informatic analysis. *BioTechniques* 51: 413.
- 74 Chen, L., Tzeng, S., and Peck, K. (2013). Aptamer microarray as a novel bioassay for protein-protein interaction discovery and analysis. *Biosens. Bioelectron.* 42: 248–255.

2

***In Chemico* Modification of Nucleotides for Better Recognition**

Przemyslaw Jurek, Marta Matusiewicz, Maciej Mazurek, and Filip Jelen

Pure Biologics Inc., R&D Department, Dunska 11, 54-427 Wroclaw, Poland

2.1 Introduction

Nucleic acids play a role not only in storing and passing the hereditary information but also take part in other important biological processes such as gene expression (mRNA, tRNA), gene expression regulation (microRNA, siRNA, riboswitches) or catalysis of enzymatic reactions (ribozymes, DNAzymes, aptazymes).

With the advent of *in vitro* selection methods such as SELEX (Systematic Evolution of Ligands by EXponential enrichment), the development of new active oligonucleotides called aptamers became possible. Nowadays, aptamers are widely used in laboratory research, in diagnostic tool development, and even as therapeutic/theranostic agents. The activity of aptamers is strictly related to their 2D and 3D structure and therefore strongly depends on their building components, i.e. nucleobases, sugars, and linkers (e.g. phosphate groups). Many excellent reviews discussing functional nucleic acids in their different aspects are available in the literature [1–9].

2.1.1 Beyond ATGC

Although it has been shown that nucleic acids can be built by more than five standard nucleobases (i.e. adenine, cytosine, guanine, thymine, and uracil), the natural diversity of aptamer building blocks is still rather limited compared to proteins, consisting of 20 natural aminoacids (Figure 2.1). The following six natural nucleobase modifications have been identified in the mRNA: N6-methyladenosine (m⁶A), 5-methylcytidine (m⁵C), 5-hydroxymethylcytidine (hm⁵C), N1-methyladenosine (m¹A), inosine, and pseudouridine. Apart from the nucleobase modifications, sugar moieties can also be altered naturally, i.e. 2'-O-methylation of the ribose [10].

Nevertheless, the true power of aptamers lies in the possibility of introduction of a whole range of various chemical modifications into their nucleic acid structure by substitution of standard atoms or chemical groups with artificial ones. This leads to the acquisition of new desirable features (e.g. resistance

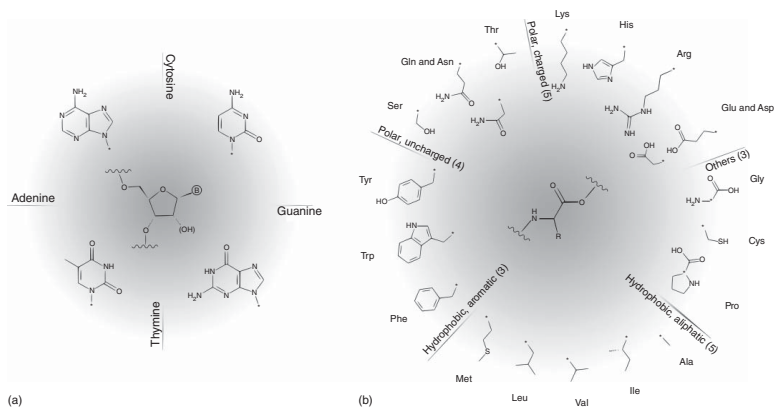


Figure 2.1 The natural diversity possible for polynucleotide (a) and polypeptide (b) chains.

to nucleolytic degradation; enhanced thermal stability; increased variety of interacting moieties such as hydrophobic, positively charged, metal chelating residues; or introduction of functional groups such as fluorophores, haptens, etc.) The modifications can pertain to every structural element of a nucleic acid, i.e. sugar–phosphate backbone or nucleobases. Changes to the backbone (i.e. sugar analogs, phosphodiester bond modifications) affect not only the nucleolytic stability of nucleic acids but also their morphological traits, while the changes pertaining to the nucleobases alter and broaden the spectrum of chemical entities available to natural oligonucleotides. This in turn affects the ability of aptamers to specifically interact with their molecular targets and significantly broaden the set of potential binding partners. The alterations in the nucleobase region may also change the 2D and 3D structure of aptamers, as they may influence Watson–Crick base-pair formation in complementary regions or even allow designing unnatural base pairs (UBPs), directly affecting the thermal stability and enlarging the information storage capacity of nucleic acids [11–22].

The idea of modifying nucleotides, and, in consequence, oligonucleotides, can date back to the early 1960s, when its main purposes were basic nucleic acid and nucleic-acid processing enzymes research, as well as early nucleotide-based therapeutics development. Initial analogous base pairs and various modifications to nucleobases emerged during the 1980s [23–25], but it was not until 1994 when the first modified aptamers were communicated, taking advantage of *in vitro* selection methods (such as, still young at that time, the SELEX methodology) and favorable nucleic acid properties [26, 27]. Nowadays, modified nucleotides are used commonly in many routine applications, which include cellular imaging [28–30] or next-generation sequencing (NGS) techniques [31, 32].

But there are two sides to every story, and the usability of numerous modifications in currently available aptamer *in vitro* selection approaches is restricted due to at least a few technological and non-technological reasons. One technical hurdle is an issue of polymerase compatibility toward modified nucleotides, which is required for successful amplification of interacting variants during PCR-based selection approaches. Another concern is the analytical limitation in the reconstruction of modified aptamer nucleotide sequence (deconvolution of aptamers structure) after the end of the selection. In addition, the possible theoretical chemical space that can be generated with randomized chemically modified oligonucleotides (i.e. the theoretical number of different aptamer variants that can be generated) is much greater than current chemical synthesis and material handling possibilities, restraining the practical maximum size of a library that can be generated and successfully screened. Finally, the chemical modifications introduced into the aptamers may make them immunogenic or/and toxic *in vivo*, greatly limiting their therapeutic and *in vivo* diagnostic potential.

2.1.2 The Scope of This Chapter

All the information contained within this chapter is presented in the context of aptamer/aptazyme selection. The general idea and the rationale for nucleotide and oligonucleotide modifications are discussed. Backbone alterations are mentioned more concisely, while nucleobases modifications and UBPs, more

important from the recognition aspect point of view, are elaborated on and supported by figures. The polymerase compatibility issue is also raised with a few working examples. Due to a very broad array of existing literature on this subject, in this chapter we concentrate on more recent advancements in the field, while a comprehensive set of examples of modified nucleotides used for oligonucleotide synthesis and aptamer selection is presented in detailed structures in additional tables in Appendix 2.A.

2.2 Modified Functional Nucleic Acids

2.2.1 The “Hows”

To obtain chemically endowed functional nucleic acids, two main strategies were proposed – post-SELEX optimization of selected aptamers to enhance the binding properties and nuclease resistance, and on the other hand – incorporation of modified nucleotides during the selection procedure. It should be noted that even though these two approaches seem to lie in opposition, they are in fact not mutually exclusive, and combining them could produce even better results.

2.2.1.1 Post-SELEX Optimization

Post-SELEX optimization is advantageous in the sense that it has almost no constraints – one could introduce almost any conceivable modification to the aptamers (of known sequence and activity) being synthesized, as long as it is of course accessible and feasible to introduce it during solid-phase synthesis, which is the major way of obtaining single aptamer clones for activity testing [33, 34]. What is more, post-SELEX procedures are almost always performed after every selection in order to shorten the obtained sequences to their minimal binding elements (which lowers the price of future synthesis and might reduce potential unspecific reactions). Nevertheless, post-SELEX optimization is a very tedious process which comprises testing dozens, if not hundreds, of individual mutated aptamers in order to choose those with improved desired properties [33, 35]. For instance, if one seeks to evaluate three different mutations (e.g. introducing nuclease-resistant nucleotides) in five different positions of the aptamer, which would not be considered a very broad array, a full spectrum of combinations would include as many as 243 clones (3^5). Structure prediction tools help to reduce the number of sequence positions to be tested and infer potential changes to the structure, but the calculations are far from accurate. It has been proved that even small differences in the structure induced by introducing modified nucleotides can lead to significant changes in the structure – either stabilizing or disrupting it, and therefore influence the binding of the aptamer [36, 37].

2.2.1.2 In-line Modifications

Introducing modified nucleotides during the enzymatic steps in the whole SELEX process reduces the tremendous amount of work needed for a meticulous post-SELEX optimization with multiple different modifications. In fact, it exploits the very same idea as does the classical *in vitro* selection – relying

on the physical forces to perform all the “hard work” and to drive the choice of the optimal ligand out of billions of possible sequences. However, it comes with a price. While post-SELEX allows introducing virtually any modification to the chosen sequence positions, introducing a modified nucleotide into the selection usually means deciding on one out of four natural nucleotides being wholly replaced in all the positions (optionally excluding the primer region) in the library being screened. It limits the number of different modifications in the library to four – and that is an optimistic setup, where all four natural nucleotides can be replaced with their modified counterparts without losing intrinsic nucleic acid properties, that is – being recognized and processed by polymerases, and forming stable and specific base pairs with their cognate nucleotides. This issue is partially solved by introduction of new UBPs, which enlarge the nucleic acid alphabet – it is discussed in more detail later on in this work. Nevertheless, incorporation of four modified nucleotides in PCR, where each of the natural nucleobases carries a different modification, was shown to be feasible [38, 39].

On the other hand, using a blend of natural/modified nucleotide or a blend of multiple modified nucleotides replacing the one chosen natural nucleobase imposes greatly increased selection bias (some nucleotides are better substrates than others) and utterly difficult deconvolution of selected sequences after the last round of selection – to the point that to the authors’ best knowledge there were no attempts to perform aptamer selection with blended modified nucleotides up to now.

2.2.2 The “Whys”

2.2.2.1 The Hurdles

Despite all that, the major obstacle for successfully employing modified nucleotides during aptamer selection remains the polymerase compatibility. SELEX in its core relies on the polymerase-driven exponential amplification of nucleic acids in between the consecutive rounds of selection, which allows for reconstruction of an aptamer-enriched oligonucleotide pool [6, 40, 41]. Replacing one of the natural nucleotides in enzymatic reactions with its modified analog requires this analog to be at least (i) accepted by one polymerase during the synthesis of a single-stranded modified oligonucleotide from a single-stranded unmodified template, and at the same time (ii) being accepted as a template nucleotide during the reverse transcription (RT) which converts modified nucleotide-bearing aptamers after elution into natural dsDNA. These steps have to obviously retain the principality and specificity of Watson–Crick base pairing [11, 42, 43]. PCR compatibility is not compulsory, but it greatly reduces the effort needed for each selection round, and therefore is a highly sought property of new modified nucleotides.

The ability of a modified nucleotide to serve as a good substrate for polymerase-mediated reactions depends both on the modification structure as well as on the polymerase itself. Several nucleobase-modified nucleotides have been studied extensively along with different polymerases in this context. It has been noted that family B polymerases have a broader substrate variability than family A polymerases, and that the best substrate properties are obtained via modification

of C5 position of pyrimidines and 7-deaza-position of purines [14, 38, 44–59]. Structural data reveals that it is due to the major groove of DNA duplex being less sterically hindered when in complex with family B polymerases than with family A polymerases [60–64]. Minor groove-oriented modifications are acceptable to a lesser extent [56]. On the other hand, while nucleobase-modifications seem to be quite acceptable by various enzymes, modifications to sugar or phosphate moiety seem to impose an even bigger challenge, to the extent that it requires engineering new mutated polymerases by means of directed evolution [42, 65–73]. Nevertheless, despite the well-acknowledged fact that the increased mutation rate and substrate preference due to the modified nucleotides introduce undesired and hard-to-assess selection bias, both nucleobase- and backbone-modified nucleotides gain increasingly more space in the aptamer landscape. This, however, often raises the question posed in the next paragraph.

2.2.2.2 The Gains

Is the modification actually worth it?

Hundreds, if not thousands, native DNA and RNA aptamers and aptazymes have been reported since the conception of the SELEX idea more than 25 years ago, displaying various binding and catalytic properties. Over these years, at least a few attempts have been made to provide a comprehensive catalogue of selected and disclosed aptamers in the form of a database, preferentially also containing the data on selection method and conditions [74–76], but surprisingly neither of these stood the test of time. As of June 2017, the only publicly accessible database on aptamers (both nucleic acids and peptides) and aptazymes is Apta-Index™ supported by Aptagen LLC, covering over 500 indexes with sequence, reported affinity and binding conditions, predicted secondary structure, and publication reference [77]. However, with several thousand search results in PubMed database since 1992 (and a panel of modified aptamers toward more than 3000 human proteins prepared solely by SomaLogic [78, 79]), this does not seem to make the cut. The functional nucleic acids field is also still missing proper large meta-analysis research, which could shed more light into the so called “black box of SELEX” [80] and visualize trends that are yet concealed, possibly providing guidance to more effective aptamer acquisition. The very well-known publication bias further aggravates this shortfall – as in most of the fields and subfields of biomedicine (with some prominent exceptions), the failed experiment reports usually tend not to leave the laboratory, which leads to the lack of data concerning failed selections. As a result, the real success rate of SELEX in all its sophisticated forms and attempts is close to unknown, but is claimed to oscillate from around 50% [81] to even below 30% for unmodified nucleic acid aptamer selections [82, 83]. These estimations are however based mostly on isolated in-house datasets and personal experiences.

Probably the biggest and most comprehensive view on the efficiency of SELEX belongs to the SomaLogic research team, who over the years have selected aptamers (called SOMAmers – Slow Off-rate Modified Aptamers) toward thousands of proteins, using natural or hydrophobic group-modified DNA [82]. When selection “success” was defined as pool $K_d < \sim 30$ nM, their overall success rate rose to 84% with modified nucleotides even for “difficult” protein targets.

Structural analysis of SOMAmers also revealed that hydrophobic-enabled nucleic acids adopt new structural conformations, not accessible for all-natural oligonucleotides, which could possibly lead to better target recognition [37, 84, 85]. The tremendous amount of work performed by SomaLogic team is probably the biggest knowledge base on modified aptamers available to date, and represents one of the best practical diagnostic applications of functional nucleic acids. It is discussed in more detail later in this chapter.

In order to answer the question of usefulness of modified aptamers, another group recently reported a parallel selection using native DNA or a library with modified nucleotides, in which aptamers modified with linker-attached adenine performed more than 1 order of magnitude better in terms of K_d toward the cognate small molecular target camptothecin than their natural counterparts [86]. In spite of the fact that first nucleobase-modified aptamers were selected over 20 years ago [26], such “direct comparison” proofs, however, are still scarce. Usually, if at all, modified aptamers or aptazymes are compared to their natural predecessors selected by other researchers, often with different aims, conditions, reagents, and different binding assessment methods, which renders such comparisons rather unavailing. On the other hand, at least a few times it has been reported that the modifications employed during the selection are not essential for selected binders or catalysts, or even perform worse [58, 87–89]. Another argument that can be procured against introducing modifications to the oligonucleotide is their unknown toxicity (in contrast to low or null toxicity and immunogenicity of unmodified nucleic acids [90]) – this aspect is still hardly explored, with very limited amount of data available for selected modified residues [91–94].

Thus, the question persists: are chemical modifications applied to the natural set of four nucleotides really indispensable, or even at all favorable, for attaining new or ameliorated functions (i.e. binding or catalysis)? Even though the scarce amount of data collected so far and the lack of wider perspective-enabling analysis makes it impossible to answer the question directly and with confidence, more and more examples indeed support the hypothesis that only endowing nucleic acids with new chemical groups allow to accomplish some particular tasks, however often for the price of increased time and labor consumption, as well as higher costs [82, 85, 95–99]. The authors of this chapter readily disclose their personal endorsement of the said assumption, and as such will try to justify their belief by presenting recent advancements, reports of successful selections employing modified residues, and a comprehensive review of selection-ready nucleotide modifications.

2.2.3 The “Iifs”

Before attempting aptamer selection with a new modified nucleotide, the feasibility of all the steps required for a successful experiment must be evaluated. Stovall et al. have concisely presented a decision and conditions scheme along with detailed protocols for validation and optimization of the successful incorporation of modified nucleotides into oligonucleotide library prepared for selection [43]. To constitute a promising candidate, a novel nucleotide should demonstrate a set of properties which can be presented in the form of a checklist:

- Are triphosphates and phosphoramidites available?

While triphosphates are used during the selection of aptamers or aptazymes, screening of single clones is usually performed after it finishes and the sequences are collected. Enzymatic synthesis of single aptamers for testing is possible when single clones with known sequence are physically available. In recent years, however, the deconvolution of selected oligonucleotide pool after the selection is often performed with NGS techniques, which provide orders of magnitude more data than classical sequencing of single clones, but the process does not allow for retrieval of single selected sequences. Therefore, phosphoramidites of the modified nucleotide (or analogous solid-phase synthesis-enabled residues) enable acquisition of single clone samples for further testing. It might also be possible to employ an intermediate which will allow for introduction of modified residues after the solid-phase synthesis [100, 101].

- Is the modification stable in required conditions?

When employing new modified nucleotides into the selection, it has to be assured that the conditions (such as temperature, pH, reactive moieties, etc.) during the binding, washing, elution, or following enzymatic steps do not interfere with the modification. The decomposition or undesired reactivity of modified nucleotides has been observed at certain occasions [102, 103].

- Is the modified nucleotide accepted by a polymerase as a substrate?

- Can the modification-bearing oligonucleotide serve as a template for a polymerase?

Either with RNA or DNA, a selection-round scheme similar to that of RNA-based SELEX can be employed, which requires the modified nucleotide to be compatible with polymerase- or transcriptase-mediated polymerization of nucleotides into an oligo(deoxy)ribonucleotide on an unmodified (natural) template, and with a RT (or rather “RT” in the case of DNA), which enables reconstruction of all-natural dsDNA from the modified aptamer pool after elution from the target [97, 104, 105]. It is also indispensable to be able to reconstruct the natural DNA for cloning and reliable sequencing after the selection – this is indeed a substantial problem for expanded genetic alphabet nucleotides [106–108].

- Is the replication fidelity retained when the modified nucleotide is used?

Despite millions of years of evolution, nucleic acid polymerases still commit errors while catalyzing templated polymerization with their native substrates – standard (deoxy)ribonucleotides [109, 110]. It is not surprising, therefore, that the introduction of modified nucleotides, replacing their natural counterparts in the reaction, can lead to an increased mutation rate during transcription, primer extension, and PCRs. While a reasonably small mutation rate is considered even beneficial to the selection, too high a rate might lead to delayed or abrupt sequence convergence [111–113].

- Is it possible to obtain satisfactory yields?

In order to proceed to the next round, the pool of oligonucleotides being selected has to be amplified and regenerated in the amounts sufficient to withstand the selection pressure. In most cases, modified nucleotides exhibit decreased yield in enzymatic synthesis reactions compared to the natural substrates [49, 52, 56, 57, 78, 114, 115], with a few notable exceptions [49, 78].

Positive answers to all these questions provide a reasonable rationale for introduction of the modified nucleotide in question into aptamer selection process. Optionally, examining some further properties might prove beneficial as well and may weigh in to the decision of pursuing with the use of the nucleotide:

- Can the modified nucleotide be used in PCR?
- Does it infer nuclease resistance?
- Is it proved to be nontoxic (if theranostic development is planned)?

The applicability to PCR renders possible a selection scheme omitting “transcription” and “RT” steps (if DNA aptamers are sought). The other two properties are not universal, but often desired, especially for diagnostics in bodily fluids or theranostic applications.

In a broader perspective, one additional property of a novel modified nucleotide can be of use – a versatility of modification chemistry. It has been shown by the SomaLogic team that certain protein targets are reluctant to generate aptamer ligands with one modification, whereas aptamers with another type of modification produce binders of high quality [57, 82]. Therefore, if a larger aptamer-generating platform employing modified residues is being developed, it would be of great value to design a panel of modifying moieties favorably based on the same attachment chemistry for the coupling to a nucleotide, thus obtaining a versatile “toolbox.” Besides SOMAmer technology, where the carboxyamide linker is exploited, such an approach was also presented by Tolle et al. [116], who utilized alkyne-bearing deoxyuridine triphosphate in enzymatic steps, which was later modified prior to target binding by robust and specific copper-catalyzed “click” chemistry [117–119].

2.3 Backbone Modifications

The polymeric structure of natural nucleic acids can be described as composed of a backbone providing linear scaffold – comprising the ribose or deoxyribose residue and a phosphate group bridging the adjacent nucleotides – and nucleobases responsible for base-pair association. Functional nucleic acids are single-stranded oligonucleotides, whose secondary and tertiary structure, guided by intramolecular base-pair formation and supported by the backbone arrangement, confers on them the recognition and/or catalytic function. Therefore, chemical modifications to the backbone influence aptamer recognition ability not only by providing additional chemical groups which can come in direct contact with a molecular target but also by altering the general structure-adopting properties and possibly granting the oligonucleotides new shapes and conformations [17, 120–122]. However, the main feature for which nucleotides modified in the backbone region are used is that they provide nuclease resistance, a property highly desired in aptamers, especially for diagnostic and therapeutic applications [36, 121, 123, 124]. The backbone-modified oligonucleotides are generally referred to as xeno nucleic acids, or XNAs, with “X” often being replaced by a specific letter(s) disclosing the type of modification. Herein we briefly review possible variants of backbone modifications along with reporting most recent advancements.

2.3.1 2'-OH Modifications

The 2'-OH group of the ribose is the target of cleavage by ribonuclease enzymes such as RNase A [125]. It has been therefore a subject of intensive efforts aiming to improve RNA stability and its nuclease resistance. Several modifications to 2'-OH have been found which confer to RNA those desired properties, and thus became very popular – notably replacing the hydroxyl group with fluorine atom (2'-F), amine group (2'-NH₂), or methoxy group (2'-OMe) (Figure 2.2a). They have been employed both as post-SELEX modifications [33, 35, 126, 127] or directly during the selection [27, 36, 128–130] (not exclusively [126]).

Probably the best known example of 2'-OH-modified aptamer is the only U. S. Food and Drug Administration (FDA)-approved aptameric drug Macugen (pegaptanib), which specifically binds the VEGF₁₆₅ in the intraocular space to prevent aggravation of age-related macular degeneration – its sequence comprises numerous 2'-F and 2'-OMe modifications which grant it improved nuclease resistance [121, 126, 131]. Recent advances disclose not only the ability to perform RNA transcription using four modified nucleotides by developing an engineered mutant polymerase variants [67, 71, 73, 132] but also the ability to select highly resistant aptamers fully substituted with 2'-OH modifications (2'-F-dG and 2'-OMe-dA/dC/U) binding a bacterial protein with dissociation constant as low as 67 nM [123]. It is also worth mentioning that several DNA polymerases were found to be compatible with 2'-F-modified dNTPs [133, 134].

2.3.2 Phosphodiester Bond Modifications

Phosphodiester bond between subsequent (deoxy)ribose units has also been a target of modifications inclined toward increasing nuclease resistance, or has even been fully replaced by a nonenzymatically formed triazole linkage, which however was not explored in the context of functional nucleic acids [135–137] (Figure 2.2b). The most common modification applied to aptamers is phosphorothioate linkage attained using α S-dNTPs, which replaces one of the oxygens of the phosphate with sulfur atom (with Sp-stereoisomers being preferred over Rp-stereoisomers due to their compatibility with polymerases and stronger nuclease resistance [138–142]). Several phosphorothioate aptamers have been recovered exhibiting significant nuclease resistance, including a fully thio-modified species [143], albeit apart from their exceptional stability neither study showed their other potential advantages over unmodified aptamers [144–149].

Another interesting yet largely unexplored modification to the standard phosphodiester bond is a boranophosphate in which an oxygen atom is replaced with a —BH₃ group. Useful changes induced in the electronic effects of the bond provoke high resistance to enzymatic hydrolysis and increase in lipophilicity, while not influencing the polymerase and reverse transcriptase compatibility [150]. These claimed properties however do not find strong confirmation in reported evidence, as only one selected aptamer comprising boranophosphates and targeting ATP has been reported [151].

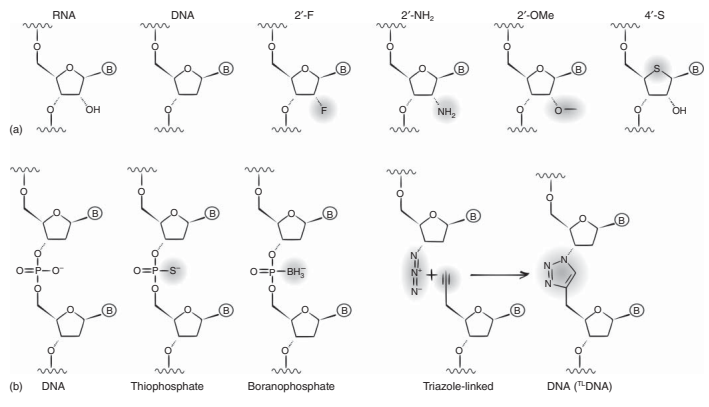


Figure 2.2 Possible modifications of (a) 2'-OH functional group in the sugar moieties of oligonucleotide backbone and (b) phosphodiester bond in the oligonucleotide backbone.

2.3.3 Xeno Nucleic Acids

Proper “xeno” nucleic acids replace the (deoxy)ribose sugar moiety with structurally diverse carbohydrate analogs (Figure 2.3) retaining their nascent property of self-assembling into antiparallel Watson–Crick duplexes [12, 13]. The nuclease resistance gain was long considered the main profit of XNA research [152] in the aptamer field, but as more data is being generated and analyzed, the perspective broadens. In a recent scrupulous comparative review by Anosova et al., the authors compared structural data available for over a dozen different homo- and heteroduplexes formed by both natural nucleic acids and XNA [17]. Features of the helix morphology regarding its torsion and phase angles which are directly dependable on the sugar (or sugar replacement) pucker-conformation revealed XNA helix geometries are distinctively different from those of DNA and RNA [17]. As already mentioned, for the aptamers new 3D structures and shapes mean possible new or ameliorated recognition or catalytic properties [36, 37, 85] – this represents therefore a strong rationale for employing XNAs in new aptamers and aptazymes selections. However, post-SELEX modification is quite a challenging and labor-intensive process [120], and does not allow to apply the selection pressure directly onto diverse XNA-reserved structures. On the other hand, enzymatic synthesis of XNA with largely or fully substituted backbone had not been possible until recently, when both naturally occurring and mutated polymerases were identified, which can encode and decode (RT) XNA from and to DNA [53, 59, 129, 153–159]. While some aptamers employing

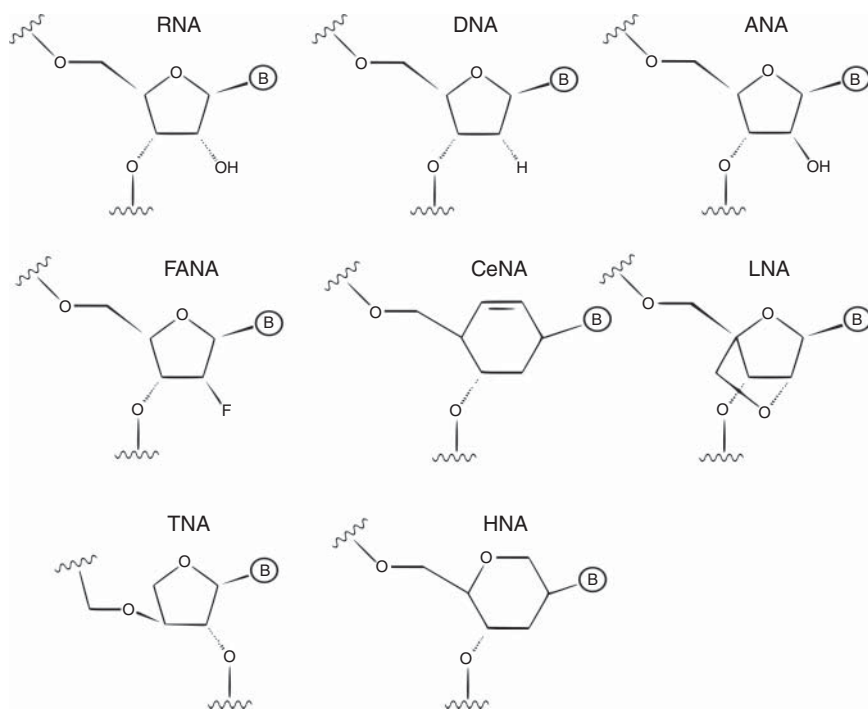


Figure 2.3 Xeno nucleic acids – building blocks with their ribose or deoxyribose exchanged to different sugar moiety, retaining ability to form double helix.

modified nucleotides in the primer regions or incorporated post-selection were selected earlier [127, 160–162], these recent advancements were leveraged for selection of several aptamers heavily or even fully modified in the random region.

2.3.3.1 TNA

One of the first groups that managed to produce an aptamer with fully substituted backbone was Chaput and colleagues, who in 2012 devised a way to overcome the lack of an enzyme capable of reverse transcribing threose nucleic acid (α -L-threofuranosyl; TNA) back into replicable DNA [163, 164]. The technique of “DNA display” employs a covalent link between the DNA genotype and TNA-based phenotype (obtained by intramolecular primer extension of DNA hairpin with threose nucleotides triphosphates-accepting Terminator DNA polymerase) and applies *in vitro* selection principles upon the latter. The amplification of the genetic material is achieved by providing a DNA primer and performing a standard PCR on the DNA template. This strategy enabled selection of a thrombin-binding all-TNA aptamer using capillary electrophoresis system [163]. About a year later, the very same group announced an efficient replication system for TNA using Terminator DNA polymerase as a transcription enzyme, and SuperScript II DNA polymerase functioning as a reverse transcriptase for TNA under optimized conditions [165]. The feasibility of exploiting this setup for aptamer selection, its replication fidelity, and nuclease resistance were also evaluated with positive results – single-stranded TNA oligonucleotide was found intact against RQ1 DNase and RNase A even after 72 hours, whereas DNA and RNA oligonucleotides exhibited half-life of 30 minutes and <10 seconds, respectively. Its exceptional resistance was also proved as an antisense oligonucleotide – while DNA:RNA duplex is rapidly degraded by RNase H in less than 1 minute, the TNA:RNA hybrid remained undegraded even after 16 hours of incubation with the enzyme [165].

2.3.3.2 FANAs

2'-Deoxy-2'-fluoroarabinonucleotides (FANAs) are yet another example of highly nuclease resistant XNA. They differ from 2'-F-ribonucleotides in that the sugar pucker in FANA favorably adopts a C2'/O4'-endo conformation, in contrast to C3'-endo conformation adopted by 2'-F-RNA [166, 167]. D4K polymerase was used to successfully select HIV-1 reverse transcriptase-binding aptamers with all four FANA residues by gel-shift-aided SELEX in just five rounds [128]. The best selected clone exhibited an apparent K_d of ~4 pM, similar to that of a minimal G-quadruplex DNA aptamer selected previously [168].

2.3.3.3 HNA, CeNA, LNA, ANA

Holliger's group focused for several years on synthetic genetic polymers with great success. First, they reported a handful of mutated polymerases capable of transcription and/or RT of six chosen XNAs: HNA (1,5-anhydrohexitol nucleic acids), CeNA (cyclohexenyl nucleic acids), LNA (2'-O,4'-C-methylene- β -D-ribonucleic acids; locked nucleic acids), ANA (arabinonucleic acids), FANA, and TNA [157]. They also proved the feasibility of this system for aptamer selection by providing an example of two all-HNA aptamers toward HIV trans-activating response RNA and hen egg lysozyme with confirmed

binding activity in a cellular setup [157]. Subsequent work disclosed catalytic XNA polymers exhibiting (i) RNA endonuclease activity (both trans- and cis-molecular) derived from four different XNAs: ANA, FANA, HNA, and CeNA; (ii) RNA–RNA ligase activity from FANA framework; and finally (iii) a FANA–FANA metalloligase also composed entirely of FANA [129]. Even though the obtained catalytic rates are equal or lower than those of DNA or RNA enzymes, the results show a first set of enzymes derived from unnatural nucleic acid polymers. As the authors state, as the technology of XNA handling is still young, factors such as fidelity and sensitivity of the transcription/RT, as well as XNA-specific sequence biases add up to suboptimal conditions for functional species selection (e.g. precludes high stringency [169]). This in turn may lead to undersampling of possible sequence space and reduced directed evolution efficiency and thus production of suboptimal binders and catalysts. Nevertheless, the diverse structural landscape of XNAs which surpasses that of DNA and RNA might still hide much more effective functional species [129, 169].

2.3.3.4 Other Modifications

Other backbone modifications of nucleic acids which are usually not classified as XNAs are 4'-thioribose and spiegelmers. 4'-Thioribose uses a sulfur atom–replacing oxygen atom in the ribose ring, leading to high nuclease resistance. Model aptamer to thrombin was successfully selected employing 4'-thio UTP and CTP, as well as mixtures of ATP + 4'-thioATP and GTP + 4'-thioGTP [170, 171].

Spiegelmers are mirror-image oligonucleotides. They are composed of L-ribose units instead of naturally occurring D-ribose, which makes them highly resistant to nuclease degradation. The drawback is however on the side of the selection – if one wishes to obtain a spiegelmer, an enantiomer version of the target is needed to perform the selection, of which a natural-RNA aptamer is obtained which binds the mirror-imaged version of the real target. As the L-ribose is not substrate for any natural polymerases, the L-ribose-aptamer is chemically synthesized, which in turn binds the real target. Due to their biological inactivity (in terms of enzyme compatibility and any other potential biological functions apart from the recognition properties), spiegelmers are considered promising clinical candidates [172–174].

2.4 Nucleobase Modifications

2.4.1 General Information

While interesting and useful, modifications imposed on the sugar and phosphate moieties of nucleic acids generally do not broaden the spectrum of chemical entities available to oligonucleotides. This aim is most often reached by modifying, changing or replacing purine and pyrimidine bases which form the Watson–Crick base pairs in natural nucleic acids. In the context of aptamers and aptazymes they allow to create new molecular interactions with their cognate targets, as well as to adopt new structural features, shapes, and conformations, which can also ameliorate target recognition. Post-SELEX modification methodology is hardly adequate here – the true power of *in vitro*

evolution is unleashed by introducing new chemical groups directly into the selection. This in turn requires at least partial polymerase compatibility, i.e. ability to synthesize and reverse transcribe the modified oligonucleotides. Since the first attempt by Latham et al. [26], when a single-stranded DNA (ssDNA) thrombin aptamer (alas with K_d inferior to its natural counterparts) bearing in its sequence 5-(1-pentynyl)-modified 2'-deoxyuridines had been isolated, numerous nucleotide analogs displaying various types of chemical groups were reported (reviewed vigilantly over the years [11–14, 16, 18, 19, 42, 43, 47]). In spite of this fact, not many of them have been employed in successful and reported aptamer selection, and even fewer have shown evident improvement in binding or catalysis when compared with natural nucleic acids. It has to be admitted with regret that too few studies have dwelled into the “ifs” and “hows” of this alleged phenomenon. Nevertheless, judging from successful examples, clear aims and carefully planned strategy seem to be able to generate exceptional new binders and catalysts.

As the portfolio of reported modified nucleotides is very broad, a comprehensive list of those substrates which are claimed to be at least accepted by a chosen polymerase into ssDNA formation in primer extension experiment is provided in Appendix 2.A. If further research toward their SELEX compatibility is available, it is also referenced. In the section to follow, we provide examples of outstanding recent research reporting successful selections of nucleobase-modified functional nucleic acids.

To successfully introduce a modified moiety into the SELEX process, the proposed modified nucleotide has to fulfill the postulates enlisted earlier, i.e. it has to be accepted by a polymerase at least during a primer extension and RT reactions and it cannot significantly disrupt the base pair formation fidelity. Extensive research has produced a consensus of certain positions of natural nucleobases to which attaching additional chemical cargo is accepted more easily than to others. It is directly associated with the double-helix geometry with its major and minor grooves, and the topology of polymerase-DNA or polymerase-RNA complex formed during enzymatic reactions.

Studies of the structure of the double helix reveal that the C5 position of pyrimidine heterocycle and N6, N7, and C8 positions of purines point toward the major groove, where a potential modification is expected to meet less steric hindrance. The minor groove, on the other hand, is created by the cavity toward which the C2 position of purines is exposed the most (Figure 2.4). Indeed, it has been proved numerous times that modifications to C5 of pyrimidines and N7 (usually with the nitrogen atom replaced by carbon to form N7-deazapurines) of purines are best tolerated by various polymerases. The N6, C2, and C8 position of purines were reported to accept modifications too, but to a lesser extent, and no reports have been found on modifications of N4 of cytosine in the context of aptamers. It was also shown that the unnatural substrate tolerance differs from enzyme to enzyme, with certain polymerases and polymerase families being more “forgiving” than others; and on the other hand, a great influence of the linker geometry and rigidity was shown [45, 48–51, 54, 57, 61]. However, concerning the plethora of available linkers and modifications, there are no general rules that can be applied for the selection of an enzyme suitable to the nucleotide in question.

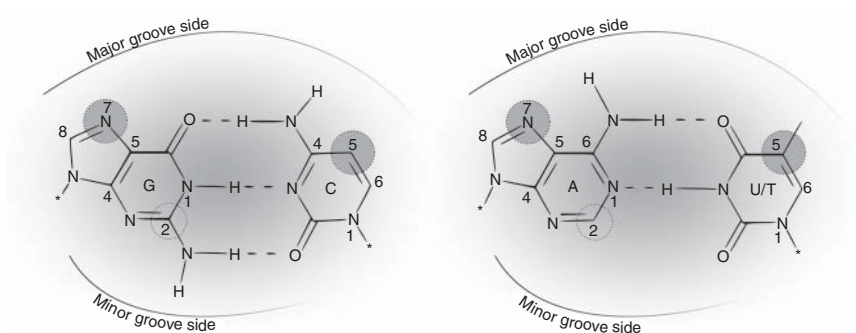


Figure 2.4 Hydrogen Interactions and a spatial organization of nucleotides in the minor and the major groove of double helix.

A significant bias in the development of new modified nucleotides is evident. It occurs due to the aforementioned fact that certain positions of nucleobase molecules are better suited to accept modifications than others and compatible polymerase partners are identified more easily, and due to the various aspects of organic synthesis. While uracil/thymine analogs are reported numerously and a considerable number of aptamers and catalysts has been selected, communications concerning modified adenines and cytosines appear much less frequently, and guanine modifications are scarce (Appendix 2.A). Fortunately, this aspect has also been constantly ameliorated in recent years.

2.4.2 Modified Aptamers and Catalysts

2.4.2.1 Introduction of Cationic Moieties

Cationic residues were amongst the first to draw scientists' attention as a potentially useful modification to be introduced to nucleic acids, as the natural polymers lack this functionality [175]. In 1999, Battersby et al. presented a direct comparison of unmodified vs modified nucleotides in a selection experiment [58]. Two parallel SELEX campaigns were run to isolate ATP-binding aptamers, one employing only four standard bases, and the other with thymidine replaced with a 5-(3'-aminopropynyl)-2'-deoxyuridine – a primary amine-bearing nucleotide exposing a positively charged ammonium ion in physiological pH, and compatible with PCR when using Vent polymerase. Identified cationic binders surprisingly presented sequences analogous to those selected from natural nucleotides, which in turn contained previously identified ATP-binding motifs, and with similar modest binding affinity. The authors explain this phenomenon by the fact that the selection pressure and SELEX setup (column-bound target) did not allow to fully exploit the cationic functionality [58]. Similar results and conclusions were presented by Vaish et al., when 5-(3'-aminopropyl)-uridine was used to select RNA aptamers to bind ATP. However, the selected clone did not bear any sequence resemblance to previously identified natural nucleotide binders [89].

Other research groups soon followed with successful selections encompassing cationic modifications in different forms. Teramoto et al. used an aminohexyl

modified and located on N6 of adenosine residues to select for a ligase ribozyme, and they also showed that removal of the modification significantly reduced the catalysis rate [104]. It is worth noting that the authors had failed to identify such a ribozyme before with all-natural RNA. Shoji et al. reported a modified DNA aptamer that binds the small-molecular-weight drug thalidomide derivative displaying high enantioselectivity for its (*R*)-isomer [176]. The selection involved a cationic modified in the form of 5-*N*-(6-aminohexyl)carbamoylmethyl-2'-deoxyuridine triphosphate introduced into the library by primer extension with KOD Dash DNA polymerase [176]. The same group also reported two DNA aptamers bearing arginine-modified uridines (5-((2-(6-(arginamido)hexylamino)-2-oxoethyl))-dU) recognizing enantiomers of glutamic acid, obtained in a similar way to the previous thalidomide-binding aptamer [177].

2.4.2.2 Catalysts with Protein-like Sidechains

Even though many chemical reactions were found to be catalyzed by nucleic acid enzymes, some were elusive. Silverman's group sought to identify species hydrolyzing the aliphatic amide bond; however, they initially failed to do so, and isolated DNA-hydrolyzing catalyst instead [178]. Therefore, they later reached for modified nucleotides with the same aim and successfully screened for the catalysts from three different libraries – one with amine-, one with carboxyl-, and one with hydroxyl-bearing uridines. For amine and carboxyl libraries, the authors showed that the modifications were indispensable for the catalysis. However, surprisingly and contrarily to their previous research, some of the deoxyribozymes identified from hydroxyl libraries turned out not to require the modifications to retain their function – the authors declared further investigation of this intriguing fact [96].

A nucleic acid enzyme studied probably the most is an RNase mimic which cleaves a phosphodiester bond between two subsequent ribose monomers in an RNA molecule. The lack of diverse functional groups in (deoxy)ribozymes has been often complemented by the presence of metal ions or a histidine cofactor in the reaction buffer [179]. However, it has soon been shown that the enhanced functionality can be gained by the very same imidazole group embedded in the (deoxy)ribozyme by means of a nucleotide modification. The first successful attempt of such an unnatural nucleic acid enzyme was presented in 1999 in the form of a metal-dependent DNAzyme comprising imidazole-bearing uridines [180]. Not much later, the metal ion catalytic function was also transferred to the nucleic acids by the simultaneous use of two modified residues – amine-bearing uridine and imidazole-bearing adenosine [87]. The resulting DNAzyme selected by Perrin's group cleaved the RNA substrate with rather a low rate constant, but in the absence of any divalent metal ions, and was the first reported deoxyribozyme with two modified bases. It was later shortened and further improved to provide trans-cleaving functionality, and its kinetics and substrate specificity studied more rigorously [181–183]. A similar catalyst carrying an “inversed” modifications set (amino-adenosine and imidazolyl-uridine) with comparable characteristics was also isolated by another group [184]. However, Perrin's group took it a step further – in order to produce an even better catalyst, they introduced three modifications resembling the side chains of the

amino acids histidine, lysine, and arginine (attached to adenosine, cytidine, and uridine, respectively), which are often found in the active sites of protein enzymes. This self-cleaving divalent metal-independent DNAzyme operating at physiological conditions is only 19 nucleotides long and is strictly dependent on the presence of the modified groups, with the rate constant improved with regard to previously identified catalysts [95]. A few years later, the same group presented another deoxyribozyme with the same modifications and an even better rate constant [185].

Parallely, Perrin's group also reported a divalent metal-dependent RNA-cleaving DNAzyme carrying phenol residues in the form of 5-(4-hydroxybenzoyl-aminomethyl)-2'-deoxyuridine [186]. This tyrosine-resembling modification was later used to run bacterial cell-SELEX screening for binders toward a selected *Escherichia coli* strain DH5 α [105]. Despite the fact that no significant convergence was found among the clones tested after the selection, the over-representation of phenol-modified uridine was evident – for the best binder, it reached almost 50% (19 out of 40 nucleotides in the random region) – and DNA aptamers selectively binding the target strain with high affinity ($K_d < 30$ nM) were identified. Several tested ligands were found to also recognize the K12 strain of *E. coli*, which is a parental strain to DH5 α , but other strains and other bacterial or yeast species were discriminated [105].

2.4.2.3 Nucleobase-linked Nucleobases

It is known that aptamers are superior binders of small molecules when compared to, e.g. antibodies. Routinely, low micromolar dissociation constants are reported for small-molecular-weight targets (summed up in several review articles [9, 187–190]). Imaizumi et al. described an attempt to obtain improved aptamers to an anticancer drug camptothecin in parallel from an all-natural DNA library and a library comprising deoxyuridine modified with linker-attached adenine residue [86]. Highly specific and strong binders were isolated, with modified aptamers showing K_d as low as 39 nM, compared to unmodified ligand with K_d of 1100 nM [86]. This work is one of the strong arguments for the introduction of base-modified nucleotides into SELEX methodology. Another one, employing the same modification, is described by Minagawa et al. who recently selected tightly binding modified aptamers toward salivary α -amylase, a stress biomarker [191]. The authors claim to have failed to select an unmodified DNA ligand toward this target a few times before, and only reaching for a modified nucleotide provided satisfying results. Indeed, the identified aptamer displayed a subnanomolar dissociation constant even after significant minimization (most of the primer regions were removed), with uridine modifications being required for the binding [191].

2.4.2.4 Glycans Targeting with Boronic Acids

Li et al. proposed an interesting tailored approach to nucleobase modifications to screen for desired binders to the glycan part of fibrinogen [98]. With the help of click chemistry they synthesized an analog of uridine bearing a boronic acid moiety – boronic acids display intrinsic affinity toward hydroxyl groups and diols – used for library construction for SELEX. The authors managed to isolate strong and specific binders, with K_d as low as 6 nM, and binding activity

confirmed to involve the modified residues, and both the glycan and the protein part of the target. Indeed, when the selected clones were prepared with natural thymidines instead of boronic acid–modified residues, the dissociation constant was about 20-fold higher, ranging from 100 to 200 nM depending on the clone. However, this still represents a decent binder, which suggests that the boronic moiety does indeed improve the binding but, in spite of authors' claims, it is not indispensable for the binding. A confirmatory selection performed with natural nucleotides led to the isolation of much weaker binders, with best K_d s above 450 nM, which again supports the rationale for introducing modified bases into the selection process [98].

2.4.2.5 “Click Chemistry”–Based Versatile Approach

Preparation of modified nucleotides by means of organic chemistry can sometimes be challenging and often requires resources not available to a more biology- or biochemistry-oriented laboratory. Tolle et al. leveraged the robustness of click chemistry (notably copper-catalyzed alkyne-azide cycloaddition – CuAAC) to overcome this drawback and proposed utilizing a commercially available uridine analog – 5'-ethynyl(deoxy)uridine triphosphate (EdU) – to introduce modifications into the oligonucleotide library [116]. EdU is easily compatible with PCR regardless of the polymerase used and is thought not to introduce any undesired amplification bias. After ssDNA generation, the chosen modifying azide compound (a great number of which is readily available from different vendors) is “clicked” onto the oligonucleotides and the target binding step is performed, after which the eluted aptamers are amplified in a regular PCR. This methodology – termed click-SELEX – is surely robust and appealing but has at least two caveats. First, performing the click reaction with oligonucleotides as substrates with no purification step (for none is possible due to the degeneration of the library sequences) does not ensure full conversion of all the EdU residues in all the sequences into the click-modified residues – some species with a defined 3D structure might impose steric hindrance for the reaction by “hiding” the ethynyl groups in the confines not accessible to other reaction substrates. Secondly, as the authors pinpoint that issue themselves, even after the introduction of the modification passed PCR, there is still the need for a polymerase that can “read” the modified strands and use it as a template in subsequent PCRs. Therefore, large modifying residues might not be fully compatible with this approach. Nevertheless, Tolle et al. proved its feasibility by selecting an imidazole-modified aptamer toward GFP with K_d of about 18 nM. The binding was confirmed to be fully dependent on the imidazole modification; and when other chemical groups were tested using the same selected sequence, no observable binding was detected [116]. The versatile approach of click-SELEX is further supported by an improved method of solid-phase synthesis of click-modified residues overcoming the issue of by-product formation due to alkaline workup conditions, also described recently by the same group [100].

2.4.2.6 Nonenzymatic Selection – X-aptamers

Another adjustable approach to generate nucleic acid binders was presented by He et al. in the form of X-aptamers, and it was later introduced in the market by AMBiotec [192, 193]. The technique employs synthesis of a pseudo-random

library with $\sim 10^6$ sequence diversity via a bead-based split-and-pool protocol using short (2–4 nts) oligonucleotides. Each bead carries oligonucleotides of different sequence with about 10^{12} copies per bead. As the formation of the library is purely chemical, X-aptamers could accommodate various modifications on the same base simultaneously (and on different bases as well) without the need for polymerase compatibility, because only one *in vitro* selection round is performed, and backbone modifications are also possible. However, after the target partitioning using magnetic beads and collection of the bound fraction, selected binders are subjected to PCR to recover the sequence information (the identity of the modification, if multiple were used, can be deduced from the surrounding sequences and the original library design). Therefore, each implemented modification, either of the backbone or the nucleobases, has to be accepted as a template in a RT reaction, which somewhat limits the scope of the technique. The authors have proved the feasibility of X-aptamer selection by identifying a binder toward CD44-HABD (hyaluronic acid-binding domain of CD44) [192]. During the fully phosphorothioated library synthesis, amino-uridines were introduced at selected positions along the four other natural nucleotides. Next, a small molecular drug called ADDA (or NADNA; *N*-acetyl-2,3-dehydro-2-deoxyneuraminic acid) was attached to those residues via standard carboxyl-amine condensation chemistry. Surprisingly, out of over a dozen selected sequences (with K_{ds} from low to high nanomolar) the addition of ADDA decreased the apparent binding [192], as did the use of fully thioated clones. On the other hand, shortened motifs derived from one of the clones showed decreased dissociation constant when ADDA was conjugated, but still exhibited substantial binding (as low as ~ 7 nM) with only amino-uridines in the sequence [192]. This suggests that the X-aptamer approach suffers from the same drawback as the click-SELEX technique referenced herein – there is no certainty that all the residues to be modified were actually modified, which is not an issue when purified modified nucleotides are used directly for library generation.

2.4.2.7 Slow Off-rate Modified Aptamers

The last, but surely not least, example of modified aptamers provided here are the SOMAmers – developed by SomaLogic, which harbors a team of scientists engaged in the aptamer field for many years, including Larry Gold, one of the inventors of SELEX. Their broad experience led them to the conception of SOMAmers, which employ protein-like side chains to better address difficult protein targets (Figure 2.5) [82]. By introducing hydrophobic residues located on uridines and an improved SELEX protocol promoting slow off-rate binders, they managed to obtain aptamers to targets that eluded successful ligand identification before, with the dissociation constant routinely reaching low- and sub-nanomolar range [82, 85, 194]. The goal of the SOMAmer idea was to set up an aptamer-based proteomic tool – termed SOMAscan – which can measure the levels of hundreds of different human serum proteins in a single assay and enable proteomic profiling for biomarker discovery and diagnostics [195]. Indeed, SOMAscan array proved to be a valuable tool with multiple examples of successful implementation for diagnostics [82, 196–205], and distinctive SOMAmers were also trialed with bacteria detection [206] and potential therapeutic use [37, 205, 207]. What is more, the panel of aptamers

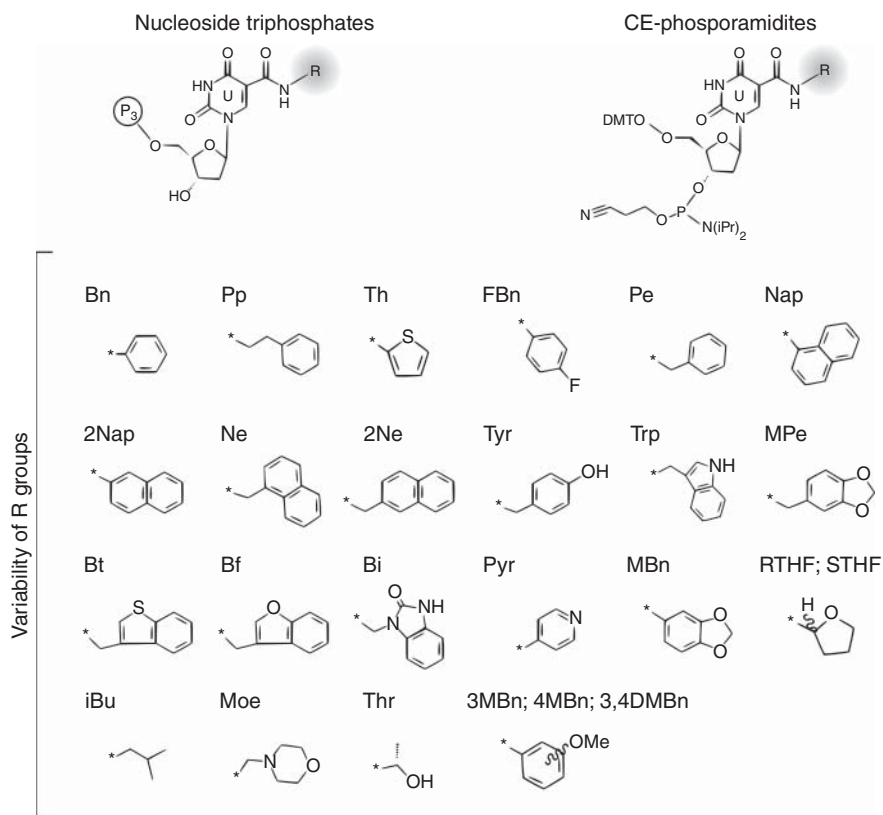


Figure 2.5 An overview of SOMAmers employing protein-like side chains, developed by SomaLogic research group.

is still being broadened by the SomaLogic research team, with the number of different targets which can be measured reaching now over 5000 distinct proteins [78, 79, 194, 195, 208]. Exhaustive structural analysis and post-SELEX optimization experiments provided valuable insight into new structural features enabled by the introduction of modified residues [37, 84, 85, 194, 208–210]. The SOMAscan platform with its SOMAmers is without a doubt the most important and most pronounced argument backing up the idea of chemical modifications to improve the outcomes of aptamer selection.

In addition, the SomaLogic team very recently further developed their idea by introducing modified cytidines into the selection process alongside modified uridines [78, 79]. Thorough research indicates that some combinations of modifications, such as phenol, phenyl, or naphthalene moiety, lead to identification of better binders than others. They also observed anticipated differences in the efficiency of polymerase reactions using two modified bases, but it seems that the benefit of the enrichment of chemical repertoire offsets the drawbacks of compromised sequence-dependent polymerization efficiency. Interestingly, introducing only one modification was often not enough to identify binding ligands in the presented study. Another benefit of using two modified residues was also an increased nuclease resistance not requiring nucleic acid backbone alteration [78].

These multiple examples show that when employed properly, modified nucleotides can significantly improve SELEX outcome. Nevertheless, the path is not straightforward, and many times the said modifications do not bring any profits while almost exclusively leading to undesired bias, e.g. during polymerase reactions. Despite the fact that the literature offers many selection-ready nucleotides and even more chemical approaches that can fairly easily produce tailored residues, the proof-of-concept studies presenting successful binders and catalysts selections are still underrepresented.

2.5 Aptamers with Expanded Genetic Alphabet

The concept of introducing novel groups and structures into nucleic acids was also realized in a way distinctive from modifying the canonical nucleobases, namely, by devising UBPs. Throughout the years at least several structural concepts were proposed, expanded, evolved, and refined, albeit with different efficacy, toward a common end, which was to obtain a synthetic base pair capable of replication with high fidelity by polymerases (Figure 2.6) [106, 211–219]. They exploited both alternative hydrogen bonding patterns (alternative to canonical A–T and C–G base pairs) as well as hydrophobic and packaging forces. The applications of an expanded genetic alphabet are numerous, with the creation of a semisynthetic organism capable of storing and executing extended genetic information as the ultimate goal. Detailed and broad reviews of the subject matter, including the history of the development of the field and the description of applications already in the research pipeline and those only conceptualized, are readily available to the interested reader [16, 20–22, 220–222].

What is interesting, the extensive research surrounding these efforts – in a sense as a by-product – yielded a lot of information regarding the natural nucleic acids and forces driving the hybridization and double-helix formation. Another “side effect” of the UBP research was the ability to select functional nucleic acids employing the expanded genetic alphabet and thus composed of five or six different nucleobases.

Roughly about the same time, in 2013, two separate groups presented results proving that obtaining aptamers using an expanded genetic alphabet is indeed possible. Hirao’s group reported three distinct protein-binding aptamers comprising a hydrophobic thiophene-carrying pyrimidine analog termed “Ds” (Figure 2.6) [107, 108]. The second group led by Steven Benner introduced into the *in vitro* selection a base pair trivially named Z–P, which exploits an alternate hydrogen bonding pattern, and isolated four novel aptamers binding either to different cell lines or selected proteins [223–226]. These examples are discussed here in more detail.

2.5.1 GACTZP Aptamers

Benner’s group for years exploited alternative hydrogen bonding patterns in noncanonical nucleic acid base pairs [24, 227–230]. One of the caveats to

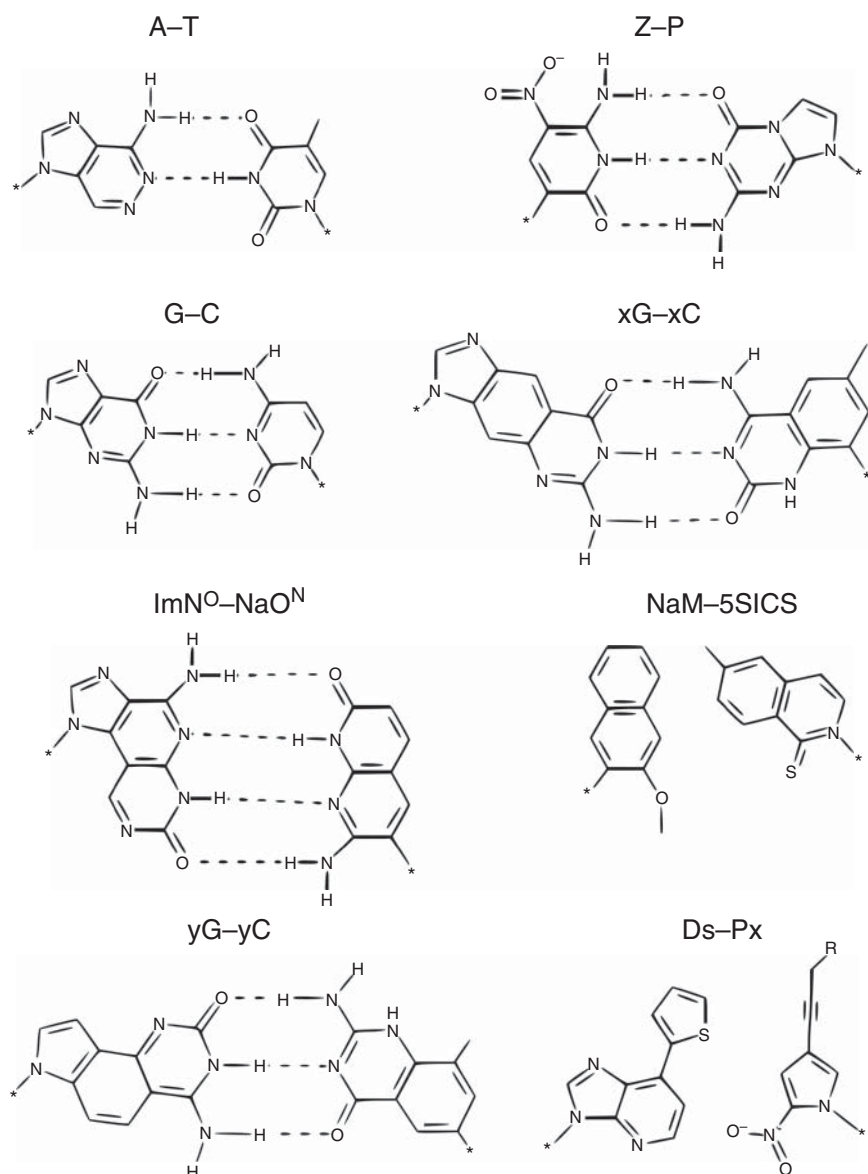


Figure 2.6 An overview of unnatural base pairs capable of being replicated by high-fidelity polymerase.

overcome was also the sequencing strategy – in order to deconvolute putative aptamers sequences after the selection, the researchers invented a “conversion” strategy which employs parallel conversion of the fully PCR-compatible Z–P base pairs either to C–Gs or A–Ts from the same subset of sequences. Deep sequencing of those two samples and comparative analysis reveals positions

within each sequence which differ between the samples and are therefore results of Z–P base pairs of two conversion regimes [231]. Thanks to this, it was possible to engage Z–P in an *in vitro* selection process, termed by the authors AEGIS-SELEX – Artificially Expanded Genetic Information System SELEX.

Next, Benner's group presented a first example of AEGIS-Cell-SELEX to obtain binders toward a breast cancer cell line MDA-MB-231 [223]. The initial library contained a region of 20 randomized nucleotides; but due to the differences in solid-phase synthesis-coupling efficiency, the real ratios obtained by high-performance liquid chromatography (HPLC) analysis were not equal and showed T/G/A/C/Z/P ~ 1.5/1.2/1.0/1.0/1.0/0.5. Despite that the researchers went through with the selection.

The obtained aptamer contained one Z and one P and was shown to bind the target cells with ~30 nM apparent dissociation constant in a flow cytometry assay. Exchanging either Z or P to a different nucleobase led to either significant decrease or elimination of the binding, proving that the AEGIS bases are necessary for the target recognition. Even though no direct comparison to natural binders was presented, the selected aptamer exhibits binding strength at levels similar to all-natural DNA aptamers identified by cell-SELEX. The authors also noted that their AEGIS-Cell-SELEX produced a good binder in only 12 rounds, whereas classical cell-SELEX often requires as many as 15–20 selection rounds to obtain similar results [223].

Another cell-binding GACTZP aptamer was identified by Zhang et al. from a slightly larger (25 randomized GACTZP nucleotides) library, again in 13 rounds of AEGIS-Cell-SELEX. The dissociation constant among selected specific binders was in the range of 14 to ~300 nM for clones comprising at least one Z or P, and in the range of ~234 to ~700 nM for those sequences which contained only four natural nucleotides. The best aptamer identified had two Ps and one Z in its sequence which were needed for the binding, and it represented only 0.4% of the deep-sequenced pool after the 13th round. The emergence of natural sequences with weaker binding properties from the same AEGIS-SELEX supports the rationale for the expanded alphabet introduction [224]. Two more successful selections were reported, identifying GACTZP aptamers toward an isolated protein from anthrax [225] and a glypican 3 protein overexpressed on a cell surface [226]. Identified binders comprised multiple Z–P nucleotides required for binding of the target and exhibited mid- to low-nanomolar dissociation constants. In the most recent study, library synthesis was improved – it contained a longer random region of 35 nucleotides and during the synthesis the ratios of GACTZP phosphoramidites were adjusted to compensate for previously noted inequality in coupling efficiencies [226]. Interestingly, it was this study that produced an aptamer with strongest binding properties ($K_d \sim 6$ nM); but without rigorous direct selection comparisons, it is not possible to indicate the reasons [226].

2.5.2 Aptamers with a Hydrophobic Fifth Base

Contrary to the Benner group's decision to focus on hydrogen bonds already exploited by nucleic acid base pairing, Ichiro Hirao's group proposed that the phenomenon of specific base pairing and double-helix formation might be driven

by other factors as well – namely, hydrophobic interactions and packaging forces. By numerous iterations of subsequent generations of unnatural nucleobases, they designed a Ds–Px base pair (Figure 2.6), with hydrophobic thienyl group of Ds preventing non-cognate base pairing, and pyrrole-2-carbaldehyde Pa base, later evolved into Px base when one of the substituents could be derivatized into various groups [232]. It was several years later that the group reported highly specific aptamers toward two protein targets (VEGF-165 and IFN- γ) by SELEX employing a library composed of a set of barcoded sublibraries with Ds in 1–3 fixed positions within the otherwise randomized region [107]. Selection from a fully randomized library was not yet possible at that point due to the problems associated with sequencing of the selected clones. The authors compared the identified binders to previously known aptamers and aptamers selected parallelly from an all-natural DNA library with the same conditions; they also used those known aptamers as competitors in the later rounds of selection. As a result, they obtained a very good aptamer toward IFN- γ and an exceptional aptamer toward VEGF-165, with K_d s at ~ 124 and ~ 1.7 pM, respectively. These values are more than 2 orders of magnitude lower than both previously reported and parallelly selected natural aptamers. A subsequent doped selection (using a library of partially randomized best binder's sequence) was performed along with post-SELEX optimization, which allowed to even further decrease the dissociation constants down to ~ 38 and 0.65 pM. Interestingly, replacing all the Ds bases with adenines reduces the binding, alas to an extent that still retains low- and sub-nanomolar dissociation constants, which are generally considered to still represent “good binders” [107]. The results reveal that Ds-containing aptamers can produce aptamers with improved binding characteristics compared to natural nucleotides containing oligonucleotides, but this last fact suggests that it was not only due to the presence of the additional nucleobase but rather to a well-performed and stringent selection procedure. The selected expanded alphabet aptamers were further characterized and optimized to enhance their pharmaceutical properties such as stability [34, 233].

A new version of ExSELEX (alphabet expansion SELEX) by Hirao's group allowed the use of a fully randomized library composed of five bases; and in a direct comparative experiment with a library comprising Ds-predetermined positions, it displayed superior binder generating properties toward Willebrand factor A1-domain [108]. The exact sequences were determined by a three-step approach: (i) Ds base conversion to A/T and deep sequencing; (ii) isolation of single Ds-bearing clones with probe hybridization; and (iii) dye-terminator DNA sequencing with UBP. It allowed deconvoluting the randomly positioned Ds bases. Selected clones comprising multiple Ds residues were tested for binding affinity to reveal that the Ds-predetermined library generated binders with best K_d at ~ 1 nM, whereas the fully randomized library-derived aptamers exhibited K_d at ~ 75 pM at the lowest. A known reference aptamer's dissociation constant was at ~ 325 pM. However, when harsh binding conditions were applied in an EMSA test (electrophoresis at 37°C with 3 M urea), the reference aptamer and Ds-predetermined aptamer showed reduced to no binding, while randomized library-derived aptamer retained its recognition properties [108].

2.6 Summary

The opportunity to obtain diversity significantly larger than in the case of polypeptides, along with other nucleic acid properties including the ease of synthesis, the direct relationship between the genotype and the phenotype (and thus the function), the reproducibility between production batches or their low immunogenicity, has made aptamers the apple of the researchers' eye worldwide and a (possibly superior) alternative to polypeptides and proteins. A natural chemical repertoire of aptamers is limited by four standard nucleobases, compared to the 20 natural amino acids that constitute polypeptide chains. This limit worked to the disadvantage of aptamers selected from natural nucleotides. Nowadays, the true potential of nucleic acid-based aptamers is recognized, as a broad range of chemical modifications becomes available. Not only do modified aptamers show improved properties in the context of resistance to nucleolytic degradation and stability but there is also quite a lot of data suggesting that chemical modifications, especially providing new interacting groups or even whole new base pairs, can greatly enhance binding characteristics and thus increase the efficiency of *in vitro* selection procedures.

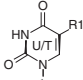
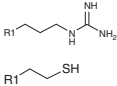
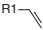
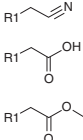
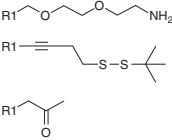
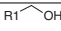
Although the opportunities brought by modified aptamers are encouraging, one should keep in mind current limitations. Modified nucleotides to be employed into the selection procedure still need to exhibit properties such as being accepted by polymerase(s) as a substrate and/or in template, being replicated with required fidelity, and favorably being chemically synthesized easily and with satisfactory yields. In the case of therapeutic candidates, little to no toxicity is also sought for. Those limiting issues were discussed earlier, and recent advancements show that many of them have been approached with promising results, such as by genetic engineering of new mutated polymerases with broader substrate specificity.

Surely more research and functional examples are still needed to provide more insight, but the presented cases – especially when compared even with the best aptamers obtained from natural nucleic acids – give a strong rationale in support of the pursuit of an extended chemical repertoire and expanded genetic alphabets toward the selection of new binders. The idea of nucleic acid modification should be, and inevitably will be, further explored to develop versatile, easier, and more efficient strategies which will overcome current limitations, and thus will hopefully allow increasing the presence of modified aptamers and aptazymes in the scientific research landscape.

2.A Appendix

The appendix contains tables listing modified nucleotides structures. All the nucleotides listed have been at least incorporated into an oligonucleotide by a polymerase-mediated Primer Extension Reaction. If PCR compatibility was proved, or functional nucleic acids were isolated (i.e. aptamers or aptazymes), it is also denoted (Tables 2.A.1–2.A.4).

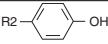
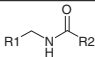
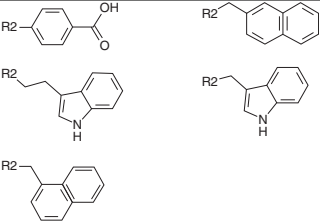
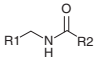
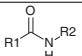
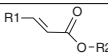
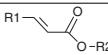
Table 2.A.1 Modified nucleotides derived from thymine/uracil nucleobase.

Modified position/modifying group	Linker	PCR	Functional nucleic acids	References
				
		—	n.d.	[38, 45, 234]
		—	+	[51, 235–237]
	—	+	Amide bond-hydrolyzing DNAzyme	[96]

(Continued)

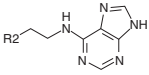
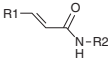
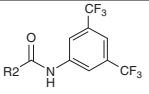
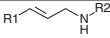
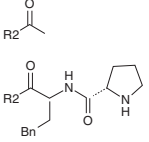
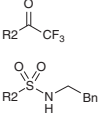
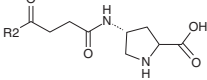
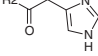
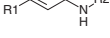
Table 2.A.1 (Continued)

Modified position/modifying group	Linker	PCR	Functional nucleic acids	References	
R1 <chem>CCCCN</chem>	—	n.d.	Aptamer to ATP	[89, 234]	
R2 <chem>CCCCCCCCN</chem>	R1 <chem>CC(=O)NR2</chem>	+	Aptamer to thalidomide	[51, 176, 235, 236]	
R2 <chem>CCCCCCCCNC(=O)N1CCN(C1)N</chem>	R1 <chem>CC(=O)NR2</chem>	n.d.	Aptamer to glutamic acid	[177]	
R2 <chem>CCN(CCN)CCN</chem>	R2 <chem>CCCCN</chem>				
R2 <chem>CCCCCCCCNC(=O)C(F)(F)F</chem>	R2 <chem>CCCCCCCCNC(=N)N</chem>				
R2 <chem>CCCCCCCCNC(=O)C(F)(F)F</chem>	R2 <chem>CCN</chem>	R1 <chem>CC(=O)NR2</chem>	+	—	[51, 235, 236]

		+	RNA cleaving DNAzyme; aptamer to <i>Escherichia coli</i> DH5α	[105, 186]
		+	—	[238]
Please refer to Figure 2.5		+	Various aptamers (SOMAmers)	[57, 78, 79, 82, 85, 194, 195, 199, 200, 202–204, 207, 208, 210, 239–244]
R2-H		+	Amide bond-hydrolyzing DNAzyme	[38, 96]
R2—		n.d.	—	[38]

(Continued)

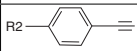
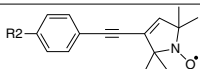
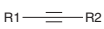
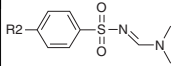
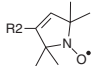
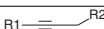
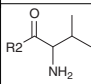
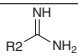
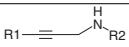
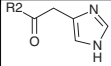
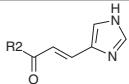
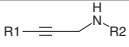
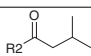
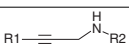
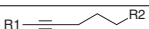
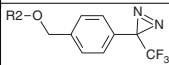
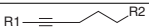
Table 2.A.1 (Continued)

Modified position/modifying group	Linker	PCR	Functional nucleic acids	References
		n.d.	Aptamer to camptothecin; aptamer to amylase	[86, 191, 245]
		—	—	[48]
   		+	—	[48, 51, 54]

		+	-	[175]
		+	RNA cleaving DNAzymes; amide bond-hydrolyzing DNAzyme	[51, 54, 87, 95, 96, 175, 180-182, 236, 246-248]
		+	-	[45, 46, 116, 249, 250]

(Continued)

Table 2.A.1 (Continued)

Modified position/modifying group		Linker	PCR	Functional nucleic acids	References
			n.d.	-	[251–253]
					
R2-H	R2-OH		+	-	[51]
			n.d.	-	[38]
			+	-	[38, 54, 247]
R2-H			+	Aptamers to ATP, ADP, AMP	[38, 51, 54, 58, 247]
R2-H			+	Aptamer to thrombin	[26]
R2-O			n.d.	-	[254]


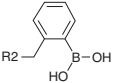
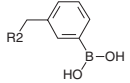
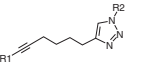
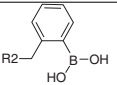
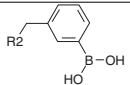
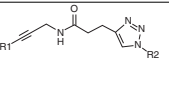
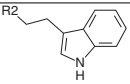
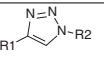
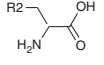
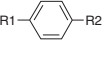
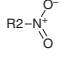
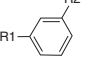
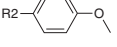
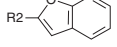
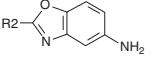
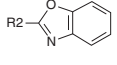
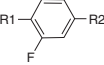
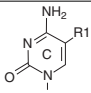
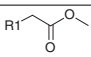
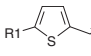
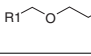
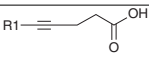
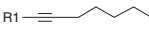
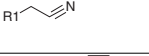
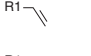
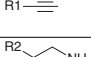
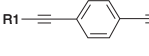
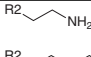
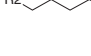
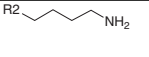
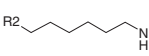
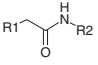
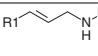
R2-OH		R1  R2	+	-	[115]
			+	-	[255]
			+	-	[255]
			n.d.	Aptamer to GFP	[116]
R2-H		R1  R2	+	-	[45, 46, 250]
R2-NH ₂		R1 	n.d.	-	[250, 256]
					
		R1 	n.d.	-	[257]

Table 2.A.2 Modified nucleotides derived from cytosine nucleobase.

Modified position/modifying group	Linker	PCR	Functional nucleic acids	References	
					
  	  	-	+	-	[51, 101, 115, 249, 258]
 		-	n.d.	-	[45, 250, 252]
 	 		+	-	[51]
R2-H		+	RNA cleaving DNAzyme	[95, 185, 248]	

			+	—	[51]
			—	Aptamer to PCSK9 (SOMAmer)	[78, 79, 259]
			n.d.	—	[38]
R2-H	R2 — Bile acid		+	—	[38, 203, 260]
R2-H	R2-NH ₂		n.d.	—	[45, 250, 256]
R2-S—			n.d.	—	[103]
			+	—	[101]
			n.d.	—	[101]

Table 2.A.3 Modified nucleotides derived from guanine nucleobase.

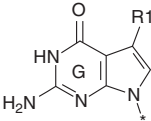
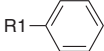
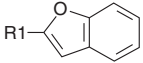
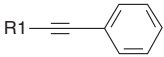
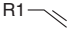
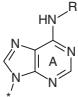
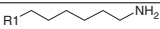
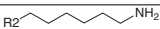
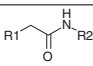
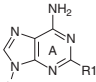
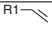
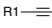
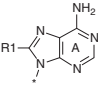
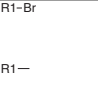
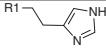
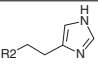
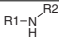
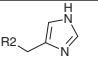
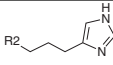
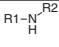



Modified position/modifying group	Linker	PCR	Functional nucleic acids	References
				
R2-H  R1 ≡  R1—  R1 ≡ 				
	—	+	—	[38, 45, 55]

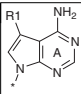

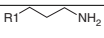
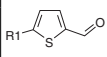
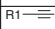
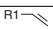
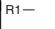
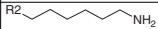
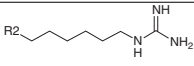
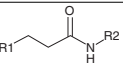
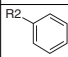
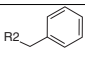
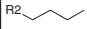
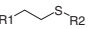
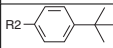
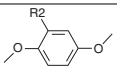
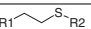
Table 2.A.4 Modified nucleotides derived from adenine nucleobase.

Modified position/modifying group	Linker	PCR	Functional nucleic acids	References
				
R1- 	—	n.d.	Ligase RNAzyme	[104]
R2- 	R1- 	n.d.	—	[246]
				
R1- 	R1-NH ₂			
R1- 	R1—			
R1-Cl	—	n.d.	—	[56]

(Continued)

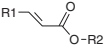

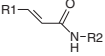
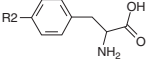
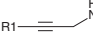
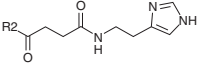
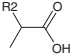
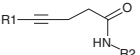
Table 2.A.4 (Continued)

Modified position/modifying group	Linker	PCR	Functional nucleic acids	References
				
R1-Br 				
		n.d.	—	[44, 52]
			RNA cleaving DNAzyme	[52, 87, 95, 102, 181, 182, 248]
			n.d.	—

					
					
		-	+	-	[247, 258]
					
		-	n.d.	-	[45]
			+	-	[50]
					
			+	-	[114]
			n.d.	-	[114]

(Continued)

Table 2.A.4 (Continued)

Modified position/modifying group	Linker	PCR	Functional nucleic acids	References
R2—		+	—	[50]
		+	—	[50]
	R2—H	+	—	[46, 49, 261]
R2—H		+	RNA cleaving DNazyme	[38, 184, 247]
	R2—Bile acid	+	—	[115, 260]
		n.d.	—	[38]

References

- 1 Bunka, D.H.J. and Stockley, P.G. (2006). Aptamers come of age – at last. *Nat. Rev. Microbiol.* 4 (8): 588–596.
- 2 Famulok, M., Hartig, J.S., and Mayer, G. (2007). Functional aptamers and aptazymes in biotechnology, diagnostics, and therapy. *Chem. Rev.* 107 (9): 3715–3743.
- 3 Radom, F., Jurek, P.M., Mazurek, M.P. et al. (2013). Aptamers: molecules of great potential. *Biotechnol. Adv.* 31 (8): 1260–1274.
- 4 Lee, J.H., Yigit, M.V., Mazumdar, D., and Lu, Y. (2010). Molecular diagnostic and drug delivery agents based on aptamer–nanomaterial conjugates. *Adv. Drug Delivery Rev.* 62 (6): 592–605.
- 5 Zhou, J. and Rossi, J. (2016). Aptamers as targeted therapeutics: current potential and challenges. *Nat. Rev. Drug Discovery* 16 (3): 181–202.
- 6 Tan, S.Y., Acquah, C., Sidhu, A. et al. (2016). SELEX modifications and bio-analytical techniques for aptamer–target binding characterisation. *Crit. Rev. Anal. Chem.* 46 (6): 521–537.
- 7 Wolter, O. and Mayer, G. (2017). Aptamers as valuable molecular tools in neurosciences. *J. Neurosci.* 37 (10): 2517–2523.
- 8 Sharma, T.K., Bruno, J.G., and Dhiman, A. (2017). ABCs of DNA aptamer and related assay development. *Biotechnol. Adv.* 35 (2): 275–301.
- 9 Pfeiffer, F. and Mayer, G. (2016). Selection and biosensor application of aptamers for small molecules. *Front. Chem.* 4: 25.
- 10 Harcourt, E.M., Kietrys, A.M., and Kool, E.T. (2017). Chemical and structural effects of base modifications in messenger RNA. *Nature* 541 (7637): 339–346.
- 11 Pfeiffer, F., Rosenthal, M., Siegl, J. et al. (2017). Customised nucleic acid libraries for enhanced aptamer selection and performance. *Curr. Opin. Biotechnol.* 48: 111–118.
- 12 Meek, K.N., Rangel, A.E., and Heemstra, J.M. (2016). Enhancing aptamer function and stability via in vitro selection using modified nucleic acids. *Methods* 106: 29–36.
- 13 Lipi, F., Chen, S., Chakravarthy, M. et al. (2016). In vitro evolution of chemically-modified nucleic acid aptamers: pros and cons, and comprehensive selection strategies. *RNA Biol.* 13 (12): 1232–1245.
- 14 Lapa, S.A., Chudinov, A.V., and Timofeev, E.N. (2016). The toolbox for modified aptamers. *Mol. Biotechnol.* 58 (2): 79–92.
- 15 Hasegawa, H., Savory, N., Abe, K., and Ikebukuro, K. (2016). Methods for improving aptamer binding affinity. *Molecules* 21 (4): 421.
- 16 Chen, T., Hongdilokkul, N., Liu, Z. et al. (2016). The expanding world of DNA and RNA. *Curr. Opin. Chem. Biol.* 34: 80–87.
- 17 Anosova, I., Kowal, E.A., Dunn, M.R. et al. (2016). The structural diversity of artificial genetic polymers. *Nucleic Acids Res.* 44 (3): 1007–1021.
- 18 Diafa, S. and Hollenstein, M. (2015). Generation of aptamers with an expanded chemical repertoire. *Molecules* 20 (9): 16643–16671.

- 19 Tolle, F. and Mayer, G. (2013). Dressed for success – applying chemistry to modulate aptamer functionality. *Chem. Sci.* 4 (1): 60.
- 20 Malyshev, D.A. and Romesberg, F.E. (2015). The expanded genetic alphabet. *Angew. Chem. Int. Ed. Engl.* 54 (41): 11930–11944.
- 21 Hirao, I. and Kimoto, M. (2012). Unnatural base pair systems toward the expansion of the genetic alphabet in the central dogma. *Proc. Jpn. Acad. Ser. B, Phys. Biol. Sci.* 88 (7): 345–367.
- 22 Wojciechowski, F. and Leumann, C.J. (2011). Alternative DNA base-pairs: from efforts to expand the genetic code to potential material applications. *Chem. Soc. Rev.* 40 (12): 5669.
- 23 Rappaport, H.P. (1988). The 6-thioguanine/5-methyl-2-pyrimidinone base pair. *Nucleic Acids Res.* 16 (15): 7253–7267.
- 24 Switzer, C., Moroney, S.E., and Benner, S.A. (1989). Enzymatic incorporation of a new base pair into DNA and RNA. *J. Am. Chem. Soc.* 111 (21): 8322–8323.
- 25 Piccirilli, J.A., Krauch, T., Moroney, S.E., and Benner, S.A. (1990). Enzymatic incorporation of a new base pair into DNA and RNA extends the genetic alphabet. *Nature* 343 (6253): 33–37.
- 26 Latham, J.A., Johnson, R., and Toole, J.J. (1994). The application of a modified nucleotide in aptamer selection: novel thrombin aptamers containing-(1-pentynyl)-2'-deoxyuridine. *Nucleic Acids Res.* 22 (14): 2817–2822.
- 27 Lin, Y., Qiu, Q., Gill, S.C., and Jayasena, S.D. (1994). Modified RNA sequence pools for in vitro selection. *Nucleic Acids Res.* 22 (24): 5229–5234.
- 28 Baker, M. (2012). RNA imaging in situ. *Nat. Methods* 9 (8): 787–790.
- 29 Okamoto, A. (2013). Application of caged fluorescent nucleotides to live-cell RNA imaging. *Methods Mol. Biol. (Clifton, NJ)* 1039: 303–318.
- 30 Sawant, A.A., Tanpure, A.A., Mukherjee, P.P. et al. (2016). A versatile toolbox for posttranscriptional chemical labeling and imaging of RNA. *Nucleic Acids Res.* 44 (2): e16.
- 31 Bentley, D.R., Balasubramanian, S., Swerdlow, H.P. et al. (2008). Accurate whole human genome sequencing using reversible terminator chemistry. *Nature* 456 (7218): 53–59.
- 32 Harris, T.D., Buzby, P.R., Babcock, H. et al. (2008). Single-molecule DNA sequencing of a viral genome. *Science* 320 (5872): 106–109.
- 33 Gao, S., Zheng, X., Jiao, B., and Wang, L. (2016). Post-SELEX optimization of aptamers. *Anal. Bioanal. Chem.* 408 (17): 4567–4573.
- 34 Kimoto, M., Nakamura, M., and Hirao, I. (2016). Post-ExSELEX stabilization of an unnatural-base DNA aptamer targeting VEGF165 toward pharmaceutical applications. *Nucleic Acids Res.* 44 (15): 7487–7494.
- 35 Eaton, B.E., Gold, L., Hicke, B.J. et al. (1997). Post-SELEX combinatorial optimization of aptamers. *Bioorg. Med. Chem.* 5 (6): 100–200.
- 36 Green, L.S., Jellinek, D., Bell, C. et al. (1995). Nuclease-resistant nucleic acid ligands to vascular permeability factor/vascular endothelial growth factor. *Chem. Biol.* 2 (10): 683–695.

- 37 Gupta, S., Hirota, M., Waugh, S.M. et al. (2014). Chemically modified DNA aptamers bind interleukin-6 with high affinity and inhibit signaling by blocking its interaction with interleukin-6 receptor. *J. Biol. Chem.* 289 (12): 8706–8719.
- 38 Jäger, S., Rasched, G., Kornreich-Leshem, H. et al. (2005). A versatile toolbox for variable DNA functionalization at high density. *J. Am. Chem. Soc.* 127 (43): 15071–15082.
- 39 Jäger, S. and Famulok, M. (2004). Generation and enzymatic amplification of high-density functionalized DNA double strands. *Angew. Chem. Int. Ed. Engl.* 43 (25): 3337–3340.
- 40 Ellington, A.D. and Szostak, J.W. (1990). In vitro selection of RNA molecules that bind specific ligands. *Nature* 346 (6287): 818–822.
- 41 Tuerk, C. and Gold, L. (1990). Systematic evolution of ligands by exponential enrichment: RNA ligands to bacteriophage T4 DNA polymerase. *Science* 249 (4968): 505–510.
- 42 Dellafiore, M.A., Montserrat, J.M., and Iribarren, A.M. (2016). Modified nucleoside triphosphates for in-vitro selection techniques. *Front. Chem.* 4.
- 43 Stovall, G.M., Bedenbaugh, R.S., Singh, S. et al. (2014). In vitro selection using modified or unnatural nucleotides. *Curr. Protoc. Nucleic Acid Chem.* 56 (1): 9.6.1–9.6.33.
- 44 Cahová, H., Pohl, R., Bednářová, L. et al. (2008). Synthesis of 8-bromo-, 8-methyl- and 8-phenyl-dATP and their polymerase incorporation into DNA. *Org. Biomol. Chem.* 6 (20): 3657.
- 45 Cahová, H., Panattoni, A., Kielkowski, P. et al. (2016). 5-Substituted pyrimidine and 7-substituted 7-deazapurine dNTPs as substrates for DNA polymerases in competitive primer extension in the presence of natural dNTPs. *ACS Chem. Biol.* 11 (11): 3165–3171.
- 46 Capek, P., Cahová, H., Pohl, R. et al. (2007). An efficient method for the construction of functionalized DNA bearing amino acid groups through cross-coupling reactions of nucleoside triphosphates followed by primer extension or PCR. *Chem. Weinh. Bergstr. Ger.* 13 (21): 6196–6203.
- 47 Hollenstein, M. (2012). Nucleoside triphosphates — building blocks for the modification of nucleic acids. *Molecules* 17 (11): 13569–13591.
- 48 Hollenstein, M. (2012). Synthesis of deoxynucleoside triphosphates that include proline, urea, or sulfonamide groups and their polymerase incorporation into DNA. *Chem. Weinh. Bergstr. Ger.* 18 (42): 13320–13330.
- 49 Kielkowski, P., Fanfrlík, J., and Hocek, M. (2014). 7-Aryl-7-deazaadenine 2'-deoxyribonucleoside triphosphates (dNTPs): better substrates for DNA polymerases than dATP in competitive incorporations. *Angew. Chem. Int. Ed. Engl.* 53 (29): 7552–7555.
- 50 Kuwahara, M., Suto, Y., Minezaki, S. et al. (2006). Substrate property and incorporation accuracy of various dATP analogs during enzymatic polymerization using thermostable DNA polymerases. *Nucleic Acids Symp. Ser.* 50 (1): 31–32.
- 51 Kuwahara, M., Nagashima, J.-I., Hasegawa, M. et al. (2006). Systematic characterization of 2'-deoxynucleoside-5'-triphosphate analogs as substrates for DNA polymerases by polymerase chain reaction and kinetic studies

- on enzymatic production of modified DNA. *Nucleic Acids Res.* 34 (19): 5383–5394.
- 52 Lam, C., Hipolito, C., and Perrin, D.M. (2008). Synthesis and enzymatic incorporation of modified deoxyadenosine triphosphates. *Eur. J. Org. Chem.* 2008 (29): 4915–4923.
- 53 Lauridsen, L.H., Rothnagel, J.A., and Veedu, R.N. (2012). Enzymatic recognition of 2'-modified ribonucleoside 5'-triphosphates: towards the evolution of versatile aptamers. *ChemBioChem* 13 (1): 19–25.
- 54 Lee, S.E., Sidorov, A., Gourlain, T. et al. (2001). Enhancing the catalytic repertoire of nucleotides: a systematic study of linker length and rigidity. *Nucleic Acids Res.* 29 (7): 1565–1573.
- 55 Mačková, M., Boháčová, S., Perlíková, P. et al. (2015). Polymerase synthesis and restriction enzyme cleavage of DNA containing 7-substituted 7-deazaguanine nucleobases. *ChemBioChem* 16 (15): 2225–2236.
- 56 Matyašovský, J., Perlíková, P., Malnuit, V. et al. (2016). 2-Substituted dATP derivatives as building blocks for polymerase-catalyzed synthesis of DNA modified in the minor groove. *Angew. Chem. Int. Ed. Engl.* 128 (51): 16088–16091.
- 57 Vaught, J.D., Bock, C., Carter, J. et al. (2010). Expanding the chemistry of DNA for in vitro selection. *J. Am. Chem. Soc.* 132 (12): 4141–4151.
- 58 Battersby, T.R., Ang, D.N., Burgstaller, P. et al. (1999). Quantitative analysis of receptors for adenosine nucleotides obtained via in vitro selection from a library incorporating a cationic nucleotide analog. *J. Am. Chem. Soc.* 121 (42): 9781–9789.
- 59 Veedu, R.N. and Wengel, J. (2009). Locked nucleic acid nucleoside triphosphates and polymerases: on the way towards evolution of LNA aptamers. *Mol. Biosyst.* 5 (8): 787–792.
- 60 Bergen, K., Steck, A.-L., Strütt, S. et al. (2012). Structures of KlenTaq DNA polymerase caught while incorporating C5-modified pyrimidine and C7-modified 7-deazapurine nucleoside triphosphates. *J. Am. Chem. Soc.* 134 (29): 11840–11843.
- 61 Hottin, A. and Marx, A. (2016). Structural insights into the processing of nucleobase-modified nucleotides by DNA polymerases. *Acc. Chem. Res.* 49 (3): 418–427.
- 62 Hottin, A., Betz, K., Diederichs, K., and Marx, A. (2017). Structural basis for the KlenTaq DNA polymerase catalysed incorporation of alkene- versus alkyne-modified nucleotides. *Chemistry* 23 (9): 2109–2118.
- 63 Obeid, S., Baccaro, A., Welte, W. et al. (2010). Structural basis for the synthesis of nucleobase modified DNA by *Thermus aquaticus* DNA polymerase. *Proc. Natl. Acad. Sci. U. S. A.* 107 (50): 21327–21331.
- 64 Obeid, S., Bußkamp, H., Welte, W. et al. (2013). Snapshot of a DNA polymerase while incorporating two consecutive C5-modified nucleotides. *J. Am. Chem. Soc.* 135 (42): 15667–15669.
- 65 Chelliserrykattil, J. and Ellington, A.D. (2004). Evolution of a T7 RNA polymerase variant that transcribes 2'-O-methyl RNA. *Nat. Biotechnol.* 22 (9): 1155–1160.

- 66 Ghadessy, F.J., Ramsay, N., Boudsocq, F. et al. (2004). Generic expansion of the substrate spectrum of a DNA polymerase by directed evolution. *Nat. Biotechnol.* 22 (6): 755–759.
- 67 Ibach, J., Dietrich, L., Koopmans, K.R.M. et al. (2013). Identification of a T7 RNA polymerase variant that permits the enzymatic synthesis of fully 2'-O-methyl-modified RNA. *J. Biotechnol.* 167 (3): 287–295.
- 68 Laos, R., Shaw, R., Leal, N.A. et al. (2013). Directed evolution of polymerases to accept nucleotides with nonstandard hydrogen bond patterns. *Biochemistry (Mosc.)* 52 (31): 5288–5294.
- 69 Loakes, D. and Holliger, P. (2009). Polymerase engineering: towards the encoded synthesis of unnatural biopolymers. *Chem. Commun.* 31: 4619–4631.
- 70 Padilla, R. and Sousa, R. (2002). A Y639F/H784A T7 RNA polymerase double mutant displays superior properties for synthesizing RNAs with non-canonical NTPs. *Nucleic Acids Res.* 30 (24): e138.
- 71 Rosenblum, S.L., Weiden, A.G., Lewis, E.L. et al. (2017). Design and discovery of new combinations of mutant DNA polymerases and modified DNA substrates. *ChemBioChem* 18 (8): 816–823.
- 72 Staiger, N. and Marx, A. (2010). A DNA polymerase with increased reactivity for ribonucleotides and C5-modified deoxyribonucleotides. *ChemBioChem* 11 (14): 1963–1966.
- 73 Meyer, A.J., Garry, D.J., Hall, B. et al. (2015). Transcription yield of fully 2'-modified RNA can be increased by the addition of thermostabilizing mutations to T7 RNA polymerase mutants. *Nucleic Acids Res.* 43 (15): 7480–7488.
- 74 Cruz-Toledo, J., McKeague, M., Zhang, X. et al. (2012). Aptamer base: a collaborative knowledge base to describe aptamers and SELEX experiments. *Database J. Biol. Databases Curation* 2012: bas006.
- 75 Lee, J.F., Hesselberth, J.R., Meyers, L.A., and Ellington, A.D. (2004). Aptamer database. *Nucleic Acids Res.* 32 (Database issue): D95–D100.
- 76 Thodima, V., Pirooznia, M., and Deng, Y. (2006). RiboaptDB: a comprehensive database of ribozymes and aptamers. *BMC Bioinf.* 7 (Suppl 2): S6.
- 77 Apta-Index(TM).
- 78 Gawande, B.N., Rohloff, J.C., Carter, J.D. et al. (2017). Selection of DNA aptamers with two modified bases. *Proc. Natl. Acad. Sci. U. S. A.* 114 (11): 2898–2903.
- 79 Veedu, R.N. and AlShamaileh, H. (2017). Next generation nucleic acid aptamers with two base modified nucleotides improve the binding affinity and potency. *ChemBioChem* 18 (16): 1565–1567.
- 80 Blank, M. (2016). Next-generation analysis of deep sequencing data: bringing light into the black box of SELEX experiments. In: *Nucleic Acid Aptamers* (ed. G. Mayer), 85–95. New York: Springer.
- 81 Mayer, G., Ahmed, M.-S.L., Dolf, A. et al. (2010). Fluorescence-activated cell sorting for aptamer SELEX with cell mixtures. *Nat. Protoc.* 5 (12): 1993–2004.
- 82 Gold, L., Ayers, D., Bertino, J. et al. (2010). Aptamer-based multiplexed proteomic technology for biomarker discovery. *PLoS One* 5 (12): e15004.

- 83 Famulok, M. and Mayer, G. (2014). Aptamers and SELEX in chemistry & biology. *Chem. Biol.* 21 (9): 1055–1058.
- 84 Gelinas, A.D., Davies, D.R., Edwards, T.E. et al. (2014). Crystal structure of interleukin-6 in complex with a modified nucleic acid ligand. *J. Biol. Chem.* 289 (12): 8720–8734.
- 85 Davies, D.R., Gelinas, A.D., Zhang, C. et al. (2012). Unique motifs and hydrophobic interactions shape the binding of modified DNA ligands to protein targets. *Proc. Natl. Acad. Sci. U. S. A.* 109 (49): 19971–19976.
- 86 Imaizumi, Y., Kasahara, Y., Fujita, H. et al. (2013). Efficacy of base-modification on target binding of small molecule DNA aptamers. *J. Am. Chem. Soc.* 135 (25): 9412–9419.
- 87 Perrin, D.M., Garestier, T., and Hélène, C. (2001). Bridging the gap between proteins and nucleotides: a metal-independent RNaseA mimic with two protein-like functionalities. *J. Am. Chem. Soc.* 123 (8): 1556–1563.
- 88 Zinnen, S.P., Domenico, K., Wilson, M. et al. (2002). Selection, design, and characterization of a new potentially therapeutic ribozyme. *RNA* 8 (2): 214–228.
- 89 Vaish, N.K., Larralde, R., Fraley, A.W. et al. (2003). A novel, modification-dependent ATP-binding aptamer selected from an RNA library incorporating a cationic functionality. *Biochemistry (Mosc.)* 42 (29): 8842–8851.
- 90 Bouchard, P.R., Hutabarat, R.M., and Thompson, K.M. (2010). Discovery and development of therapeutic aptamers. *Annu. Rev. Pharmacol. Toxicol.* 50 (1): 237–257.
- 91 Iannitti, T., Morales-Medina, J.C., and Palmieri, B. (2014). Phosphorothioate oligonucleotides: effectiveness and toxicity. *Curr. Drug Targets* 15 (7): 663–673.
- 92 Janas, M.M., Jiang, Y., Schlegel, M.K. et al. (2017). Impact of oligonucleotide structure, chemistry, and delivery method on in vitro cytotoxicity. *Nucleic Acid Ther.* 27 (1): 11–22.
- 93 Lorenz, P., Baker, B.F., Bennett, C.F., and Spector, D.L. (1998). Phosphorothioate antisense oligonucleotides induce the formation of nuclear bodies. *Mol. Biol. Cell* 9 (5): 1007–1023.
- 94 Shen, W., Liang, X., Sun, H., and Crooke, S.T. (2015). 2'-Fluoro-modified phosphorothioate oligonucleotide can cause rapid degradation of P54nrb and PSF. *Nucleic Acids Res.* 43 (9): 4569–4578.
- 95 Hollenstein, M., Hipolito, C.J., Lam, C.H., and Perrin, D.M. (2009). A self-cleaving DNA enzyme modified with amines, guanidines and imidazoles operates independently of divalent metal cations (M^{2+}). *Nucleic Acids Res.* 37 (5): 1638–1649.
- 96 Zhou, C., Avins, J.L., Klauser, P.C. et al. (2016). DNA-catalyzed amide hydrolysis. *J. Am. Chem. Soc.* 138 (7): 2106–2109.
- 97 Nieuwlandt, D., West, M., Cheng, X. et al. (2003). The first example of an RNA urea synthase: selection through the enzyme active site of human neutrophil elastase. *ChemBioChem* 4 (7): 651–654.
- 98 Li, M., Lin, N., Huang, Z. et al. (2008). Selecting aptamers for a glycoprotein through the incorporation of the boronic acid moiety. *J. Am. Chem. Soc.* 130 (38): 12636–12638.

- 99 Wiegand, T.W., Janssen, R.C., and Eaton, B.E. (1997). Selection of RNA amide synthases. *Chem. Biol.* 4 (9): 675–683.
- 100 Tolle, F., Rosenthal, M., Pfeiffer, F., and Mayer, G. (2016). Click reaction on solid phase enables high fidelity synthesis of nucleobase-modified DNA. *Bioconjugate Chem.* 27 (3): 500–503.
- 101 Raindlová, V., Pohl, R., and Hocek, M. (2012). Synthesis of aldehyde-linked nucleotides and DNA and their bioconjugations with lysine and peptides through reductive amination. *Chemistry* 18 (13): 4080–4087.
- 102 Lermer, L., Hobbs, J., and Perrin, D.M. (2002). Incorporation of 8-histaminyl-deoxyadenosine [8-(2-(4-imidazolyl)ethylamino)-2'-deoxyriboadenosine] into oligodeoxyribonucleotides by solid phase phosphoramidite coupling. *Nucleosides Nucleotides Nucleic Acids* 21 (10): 651–664.
- 103 Macíčková-Cahová, H., Pohl, R., Horáková, P. et al. (2011). Alkylsulfanylphenyl derivatives of cytosine and 7-deazaadenine nucleosides, nucleotides and nucleoside triphosphates: synthesis, polymerase incorporation to DNA and electrochemical study. *Chemistry* 17 (21): 5833–5841.
- 104 Teramoto, N., Imanishi, Y., and Ito, Y. (2000). In vitro selection of a ligase ribozyme carrying alkylamino groups in the side chains. *Bioconjugate Chem.* 11 (6): 744–748.
- 105 Renders, M., Miller, E., Lam, C.H., and Perrin, D.M. (2016). Whole cell-SELEX of aptamers with a tyrosine-like side chain against live bacteria. *Org. Biomol. Chem.* 15 (9): 1980–1989.
- 106 Malyshev, D.A., Dhama, K., Quach, H.T. et al. (2012). Efficient and sequence-independent replication of DNA containing a third base pair establishes a functional six-letter genetic alphabet. *Proc. Natl. Acad. Sci. U. S. A.* 109 (30): 12005–12010.
- 107 Kimoto, M., Yamashige, R., Matsunaga, K. et al. (2013). Generation of high-affinity DNA aptamers using an expanded genetic alphabet. *Nat. Biotechnol.* 31 (5): 453–457.
- 108 Matsunaga, K., Kimoto, M., and Hirao, I. (2016). High-affinity DNA aptamer generation targeting von Willebrand factor A1-domain by genetic alphabet expansion for systematic evolution of ligands by exponential enrichment using two types of libraries composed of five different bases. *J. Am. Chem. Soc.* 139 (1): 324–334.
- 109 McInerney, P., Adams, P., and Hadi, M.Z. (2014). Error rate comparison during polymerase chain reaction by DNA polymerase. *Mol. Biol. Int.* 2014: e287430.
- 110 Marx, V. (2016). PCR: the price of infidelity. *Nat. Methods* 13 (6): 475–479.
- 111 Hoinka, J., Berezhnoy, A., Dao, P. et al. (2015). Large scale analysis of the mutational landscape in HT-SELEX improves aptamer discovery. *Nucleic Acids Res.* 43 (12): 5699–5707.
- 112 Stoltenburg, R., Reinemann, C., and Strehlitz, B. (2007). SELEX – a (r)evolutionary method to generate high-affinity nucleic acid ligands. *Biomol. Eng.* 24 (4): 381–403.
- 113 Nieuwlandt, D., Wecker, M., and Gold, L. (1995). In vitro selection of RNA ligands to substance P. *Biochemistry (Mosc.)* 34 (16): 5651–5659.

- 114 Slavičková, M., Pohl, R., and Hocek, M. (2016). Additions of thiols to 7-vinyl-7-deazaadenine nucleosides and nucleotides. Synthesis of hydrophobic derivatives of 2'-deoxyadenosine, dATP and DNA. *J. Org. Chem.* 81 (22): 11115–11125.
- 115 Hollenstein, M. (2013). Deoxynucleoside triphosphates bearing histamine, carboxylic acid, and hydroxyl residues – synthesis and biochemical characterization. *Org. Biomol. Chem.* 11 (31): 5162–5172.
- 116 Tolle, F., Brändle, G.M., Matzner, D., and Mayer, G. (2015). A versatile approach towards nucleobase-modified aptamers. *Angew. Chem. Int. Ed. Engl.* 54 (37): 10971–10974.
- 117 Besanceney-Webler, C., Jiang, H., Zheng, T. et al. (2011). Increasing the efficacy of bioorthogonal click reactions for bioconjugation: a comparative study. *Angew. Chem. Int. Ed. Engl.* 50 (35): 8051–8056.
- 118 El-Sagheer, A.H. and Brown, T. (2010). Click chemistry with DNA. *Chem. Soc. Rev.* 39 (4): 1388–1405.
- 119 Horisawa, K. (2014). Specific and quantitative labeling of biomolecules using click chemistry. *Front. Physiol.* 5: 457.
- 120 Schmidt, K.S., Borkowski, S., Kurreck, J. et al. (2004). Application of locked nucleic acids to improve aptamer in vivo stability and targeting function. *Nucleic Acids Res.* 32 (19): 5757–5765.
- 121 Ng, E.W.M., Shima, D.T., Calias, P. et al. (2006). Pegaptanib, a targeted anti-VEGF aptamer for ocular vascular disease. *Nat. Rev. Drug Discovery* 5 (2): 123–132.
- 122 Campbell, M.A. and Wengel, J. (2011). Locked vs. unlocked nucleic acids (LNA vs. UNA): contrasting structures work towards common therapeutic goals. *Chem. Soc. Rev.* 40 (12): 5680.
- 123 Friedman, A.D., Kim, D., and Liu, R. (2015). Highly stable aptamers selected from a 2'-fully modified fGmH RNA library for targeting biomaterials. *Biomaterials* 36: 110–123.
- 124 Wang, R.E., Wu, H., Niu, Y., and Cai, J. (2011). Improving the stability of aptamers by chemical modification. *Curr. Med. Chem.* 18 (27): 4126–4138.
- 125 Elliott, D. and Lodomery, M. (2015). *Molecular Biology of RNA*. Oxford, New York: Oxford University Press.
- 126 Ruckman, J. (1998). 2'-Fluoropyrimidine RNA-based aptamers to the 165-amino acid form of vascular endothelial growth factor (VEGF165). Inhibition of receptor binding and VEGF-induced vascular permeability through interactions requiring the exon 7-encoded domain. *J. Biol. Chem.* 273 (32): 20556–20567.
- 127 Hernandez, F.J., Kalra, N., Wengel, J., and Vester, B. (2009). Aptamers as a model for functional evaluation of LNA and 2'-amino LNA. *Bioorg. Med. Chem. Lett.* 19 (23): 6585–6587.
- 128 Alves, Ferreira-Bravo, I., Cozens, C., Holliger, P., and DeStefano, J.J. (2015). Selection of 2'-deoxy-2'-fluoroarabinonucleotide (FANA) aptamers that bind HIV-1 reverse transcriptase with picomolar affinity. *Nucleic Acids Res.* 43 (20): 9587–9599.
- 129 Taylor, A.I., Pinheiro, V.B., Smola, M.J. et al. (2015). Catalysts from synthetic genetic polymers. *Nature* 518 (7539): 427–430.

- 130 Thirunavukarasu, D., Chen, T., Liu, Z. et al. (2017). Selection of 2'-fluoro-modified aptamers with optimized properties. *J. Am. Chem. Soc.* 139 (8): 2892–2895.
- 131 Fraunfelder, F.W. (2005). Pegaptanib for wet macular degeneration. *Drugs Today (Barc. Spain 1998)* 41 (11): 703–709.
- 132 Zhu, B., Hernandez, A., Tan, M. et al. (2015). Synthesis of 2'-fluoro RNA by Syn5 RNA polymerase. *Nucleic Acids Res.* 43 (14): e94.
- 133 Richardson, F.C., Kuchta, R.D., Mazurkiewicz, A., and Richardson, K.A. (2000). Polymerization of 2'-fluoro- and 2'-O-methyl-dNTPs by human DNA polymerase alpha, polymerase gamma, and primase. *Biochem. Pharmacol.* 59 (9): 1045–1052.
- 134 Ono, T., Scalf, M., and Smith, L.M. (1997). 2'-Fluoro modified nucleotides: polymerase-directed synthesis, properties and stability to analysis by matrix-assisted laser desorption/ionization mass spectrometry. *Nucleic Acids Res.* 25 (22): 4581–4588.
- 135 Isobe, H., Fujino, T., Yamazaki, N. et al. (2008). Triazole-linked analogue of deoxyribonucleic acid (^{TL} DNA): design, synthesis, and double-strand formation with natural DNA. *Org. Lett.* 10 (17): 3729–3732.
- 136 Birts, C.N., Sanzone, A.P., El-Sagheer, A.H. et al. (2014). Transcription of click-linked DNA in human cells. *Angew. Chem. Int. Ed.* 53 (9): 2362–2365.
- 137 Sanzone, A.P., El-Sagheer, A.H., Brown, T., and Tavassoli, A. (2012). Assessing the biocompatibility of click-linked DNA in *Escherichia coli*. *Nucleic Acids Res.* 40 (20): 10567–10575.
- 138 Yang, Z., Sismour, A.M., and Benner, S.A. (2007). Nucleoside alpha-thiotriphosphates, polymerases and the exonuclease III analysis of oligonucleotides containing phosphorothioate linkages. *Nucleic Acids Res.* 35 (9): 3118–3127.
- 139 Romaniuk, P.J. and Eckstein, F. (1982). A study of the mechanism of T4 DNA polymerase with diastereomeric phosphorothioate analogues of deoxyadenosine triphosphate. *J. Biol. Chem.* 257 (13): 7684–7688.
- 140 Brautigam, C.A. and Steitz, T.A. (1998). Structural principles for the inhibition of the 3'-5' exonuclease activity of *Escherichia coli* DNA polymerase I by phosphorothioates. *J. Mol. Biol.* 277 (2): 363–377.
- 141 Di Giusto, D. and King, G.C. (2003). Single base extension (SBE) with proof-reading polymerases and phosphorothioate primers: improved fidelity in single-substrate assays. *Nucleic Acids Res.* 31 (3): e7.
- 142 Yu, D., Kandimalla, E.R., Roskey, A. et al. (2000). Stereo-enriched phosphorothioate oligodeoxynucleotides: synthesis, biophysical and biological properties. *Bioorg. Med. Chem.* 8 (1): 275–284.
- 143 Gandham, S.H.A., Volk, D.E., Rao, L.G.L. et al. (2014). Thioaptamers targeting dengue virus type-2 envelope protein domain III. *Biochem. Biophys. Res. Commun.* 453 (3): 309–315.
- 144 Somasunderam, A., Thiviyanathan, V., Tanaka, T. et al. (2010). Combinatorial selection of DNA thioaptamers targeted to the HA binding domain of human CD44. *Biochemistry (Mosc.)* 49 (42): 9106–9112.
- 145 Thiviyanathan, V., Somasunderam, A.D., and Gorenstein, D.G. (2007). Combinatorial selection and delivery of thioaptamers. *Biochem. Soc. Trans.* 35 (1): 50.

- 146 Kang, J., Lee, M.S., Copland, J.A. III et al. (2008). Combinatorial selection of a single stranded DNA thioaptamer targeting TGF- β 1 protein. *Bioorg. Med. Chem. Lett.* 18 (6): 1835–1839.
- 147 Somasunderam, A., Ferguson, M.R., Rojo, D.R. et al. (2005). Combinatorial selection, inhibition, and antiviral activity of DNA thioaptamers targeting the RNase H domain of HIV-1 reverse transcriptase. *Biochemistry (Mosc.)* 44 (30): 10388–10395.
- 148 Higashimoto, Y., Matsui, T., Nishino, Y. et al. (2013). Blockade by phosphorothioate aptamers of advanced glycation end products-induced damage in cultured pericytes and endothelial cells. *Microvasc. Res.* 90: 64–70.
- 149 Jhaveri, S., Olwin, B., and Ellington, A.D. (1998). In vitro selection of phosphorothiolated aptamers. *Bioorg. Med. Chem. Lett.* 8 (17): 2285–2290.
- 150 Shaw, B.R. (2007). Versatility of borane nucleic acids mimics for coding, decoding and modulating genetic information. *Nucleic Acids Symp. Ser.* 51 (1): 117.
- 151 Lato, S.M., Ozerova, N.D.S., He, K. et al. (2002). Boron-containing aptamers to ATP. *Nucleic Acids Res.* 30 (6): 1401–1407.
- 152 Morihira, K., Kasahara, Y., and Obika, S. (2017). Biological applications of xeno nucleic acids. *Mol. Biosyst.* 13 (2): 235–245.
- 153 Dunn, M.R. and Chaput, J.C. (2016). Reverse transcription of threose nucleic acid by a naturally occurring DNA polymerase. *ChemBioChem* 17 (19): 1804–1808.
- 154 Kuwahara, M., Obika, S., Nagashima, J. et al. (2008). Systematic analysis of enzymatic DNA polymerization using oligo-DNA templates and triphosphate analogs involving 2',4'-bridged nucleosides. *Nucleic Acids Res.* 36 (13): 4257–4265.
- 155 Crouzier, L., Dubois, C., Edwards, S.L. et al. (2012). Efficient reverse transcription using locked nucleic acid nucleotides towards the evolution of nuclease resistant RNA aptamers. *PLoS One* 7 (4): e35990.
- 156 Dunn, M.R., Larsen, A.C., Zahurancik, W.J. et al. (2015). DNA polymerase-mediated synthesis of unbiased threose nucleic acid (TNA) polymers requires 7-deazaguanine to suppress G:G mispairing during TNA transcription. *J. Am. Chem. Soc.* 137 (12): 4014–4017.
- 157 Pinheiro, V.B., Taylor, A.I., Cozens, C. et al. (2012). Synthetic genetic polymers capable of heredity and evolution. *Science* 336 (6079): 341–344.
- 158 Houlihan, G., Arangundy-Franklin, S., and Holliger, P. (2017). Engineering and application of polymerases for synthetic genetics. *Curr. Opin. Biotechnol.* 48: 168–179.
- 159 Houlihan, G., Arangundy-Franklin, S., and Holliger, P. (2017). Exploring the chemistry of genetic information storage and propagation through polymerase engineering. *Acc. Chem. Res.* 50 (4): 1079–1087.
- 160 Elle, I.C., Karlsen, K.K., Terp, M.G. et al. (2015). Selection of LNA-containing DNA aptamers against recombinant human CD73. *Mol. Biosyst.* 11 (5): 1260–1270.
- 161 Kuwahara, M. and Obika, S. (2013). In vitro selection of BNA (LNA) aptamers. *Artif. DNA PNA XNA* 4 (2): 39–48.
- 162 Hagiwara, K., Fujita, H., Kasahara, Y. et al. (2014). In vitro selection of DNA-based aptamers that exhibit RNA-like conformations using a chimeric

- oligonucleotide library that contains two different xeno-nucleic acids. *Mol. Biosyst.* 11 (1): 71–76.
- 163 Yu, H., Zhang, S., and Chaput, J.C. (2012). Darwinian evolution of an alternative genetic system provides support for TNA as an RNA progenitor. *Nat. Chem.* 4 (3): 183–187.
- 164 Dunn, M.R. and Chaput, J.C. (2014). An in vitro selection protocol for threose nucleic acid (TNA) using DNA display: an in vitro selection protocol for threose nucleic acid (TNA) using DNA display. In: *Current Protocols in Nucleic Acid Chemistry* (ed. M. Egli, P. Herdewijn, A. Matusda and Y.S. Sanghvi), 9.8.1–9.8.19. Hoboken, NJ, USA: Wiley.
- 165 Yu, H., Zhang, S., Dunn, M.R., and Chaput, J.C. (2013). An efficient and faithful in vitro replication system for threose nucleic acid. *J. Am. Chem. Soc.* 135 (9): 3583–3591.
- 166 Berger, I., Tereshko, V., Ikeda, H. et al. (1998). Crystal structures of B-DNA with incorporated 2'-deoxy-2'-fluoro-arabino-furanosyl thymines: implications of conformational preorganization for duplex stability. *Nucleic Acids Res.* 26 (10): 2473–2480.
- 167 Damha, M.J., Noronha, A.M., Wilds, C.J. et al. (2001). Properties of arabinonucleic acids (ANA & 2'F-ANA): implications for the design of antisense therapeutics that invoke RNase H cleavage of RNA. *Nucleosides Nucleotides Nucleic Acids* 20 (4–7): 429–440.
- 168 Michalowski, D., Chitima-Matsiga, R., Held, D.M., and Burke, D.H. (2008). Novel bimodular DNA aptamers with guanosine quadruplexes inhibit phylogenetically diverse HIV-1 reverse transcriptases. *Nucleic Acids Res.* 36 (22): 7124–7135.
- 169 Taylor, A.I. and Holliger, P. (2015). Directed evolution of artificial enzymes (XNAzymes) from diverse repertoires of synthetic genetic polymers. *Nat. Protoc.* 10 (10): 1625–1642.
- 170 Minakawa, N., Sanji, M., Kato, Y., and Matsuda, A. (2008). Investigations toward the selection of fully-modified 4'-thioRNA aptamers: optimization of in vitro transcription steps in the presence of 4'-thioNTPs. *Bioorg. Med. Chem.* 16 (21): 9450–9456.
- 171 Takahashi, M., Minakawa, N., and Matsuda, A. (2009). Synthesis and characterization of 2'-modified-4'-thioRNA: a comprehensive comparison of nuclease stability. *Nucleic Acids Res.* 37 (4): 1353–1362.
- 172 Eulberg, D. and Klussmann, S. (2003). Spiegelmers: biostable aptamers. *ChemBioChem* 4 (10): 979–983.
- 173 Leva, S., Lichte, A., Burmeister, J. et al. (2002). GnRH binding RNA and DNA Spiegelmers: a novel approach toward GnRH antagonism. *Chem. Biol.* 9 (3): 351–359.
- 174 Purschke, W.G. (2003). A DNA Spiegelmer to staphylococcal enterotoxin B. *Nucleic Acids Res.* 31 (12): 3027–3032.
- 175 Sakthivel, K. and Barbas, C.F. III (1998). Expanding the potential of DNA for binding and catalysis: highly functionalized dUTP derivatives that are substrates for thermostable DNA polymerases. *Angew. Chem. Int. Ed. Engl.* 37 (20): 2872–2875.

- 176 Shoji, A., Kuwahara, M., Ozaki, H., and Sawai, H. (2007). Modified DNA aptamer that binds the (*R*)-isomer of a thalidomide derivative with high enantioselectivity. *J. Am. Chem. Soc.* 129 (5): 1456–1464.
- 177 Ohsawa, K., Kasamatsu, T., Nagashima, J. et al. (2008). Arginine-modified DNA aptamers that show enantioselective recognition of the dicarboxylic acid moiety of glutamic acid. *Anal. Sci.* 24 (1): 167–172.
- 178 Chandra, M., Sachdeva, A., and Silverman, S.K. (2009). DNA-catalyzed sequence-specific hydrolysis of DNA. *Nat. Chem. Biol.* 5 (10): 718–720.
- 179 Joyce, G.F. (1998). Nucleic acid enzymes: playing with a fuller deck. *Proc. Natl. Acad. Sci. U. S. A.* 95 (11): 5845–5847.
- 180 Santoro, S.W., Joyce, G.F., Sakthivel, K. et al. (2000). RNA cleavage by a DNA enzyme with extended chemical functionality. *J. Am. Chem. Soc.* 122 (11): 2433–2439.
- 181 Lermer, L., Roupioz, Y., Ting, R., and Perrin, D.M. (2002). Toward an RNaseA mimic: a DNAzyme with imidazoles and cationic amines. *J. Am. Chem. Soc.* 124 (34): 9960–9961.
- 182 Ting, R., Thomas, J.M., Lermer, L., and Perrin, D.M. (2004). Substrate specificity and kinetic framework of a DNAzyme with an expanded chemical repertoire: a putative RNaseA mimic that catalyzes RNA hydrolysis independent of a divalent metal cation. *Nucleic Acids Res.* 32 (22): 6660–6672.
- 183 Ting, R., Thomas, J.M., and Perrin, D.M. (2007). Kinetic characterization of a *cis*- and *trans*-acting M²⁺-independent DNAzyme that depends on synthetic RNaseA-like functionality – BURST-phase kinetics from the coalescence of two active DNAzyme folds. *Can. J. Chem.* 85 (4): 313–329.
- 184 Sidorov, A.V., Grasby, J.A., and Williams, D.M. (2004). Sequence-specific cleavage of RNA in the absence of divalent metal ions by a DNAzyme incorporating imidazolyl and amino functionalities. *Nucleic Acids Res.* 32 (4): 1591–1601.
- 185 Hollenstein, M., Hipolito, C.J., Lam, C.H., and Perrin, D.M. (2013). Toward the combinatorial selection of chemically modified DNAzyme RNase A mimics active against all-RNA substrates. *ACS Comb. Sci.* 15 (4): 174–182.
- 186 Lam, C.H., Hipolito, C.J., Hollenstein, M., and Perrin, D.M. (2011). A divalent metal-dependent self-cleaving DNAzyme with a tyrosine side chain. *Org. Biomol. Chem.* 9 (20): 6949.
- 187 Famulok, M. (1999). Oligonucleotide aptamers that recognize small molecules. *Curr. Opin. Struct. Biol.* 9 (3): 324–329.
- 188 McKeague, M. and DeRosa, M.C. (2012). Challenges and opportunities for small molecule aptamer development. *J. Nucleic Acids* 2012: 1–20.
- 189 McKeague, M., De Girolamo, A., Valenzano, S. et al. (2015). Comprehensive analytical comparison of strategies used for small molecule aptamer evaluation. *Anal. Chem.* 87 (17): 8608–8612.
- 190 Ruscito, A. and DeRosa, M.C. (2016). Small-molecule binding aptamers: selection strategies, characterization, and applications. *Front. Chem.* 4: 14.
- 191 Minagawa, H., Onodera, K., Fujita, H. et al. (2017). Selection, characterization and application of artificial DNA aptamer containing appended bases with sub-nanomolar affinity for a salivary biomarker. *Sci. Rep.* 7: 42716.

- 192 He, W., Elizondo-Riojas, M.-A., Li, X. et al. (2012). X-aptamers: a bead-based selection method for random incorporation of druglike moieties onto next-generation aptamers for enhanced binding. *Biochemistry (Mosc.)* 51 (42): 8321–8323.
- 193 AMBiotech | Next generation aptamers.
- 194 Rohloff, J.C., Gelinas, A.D., Jarvis, T.C. et al. (2014). Nucleic acid ligands with protein-like side chains: modified aptamers and their use as diagnostic and therapeutic agents. *Mol. Ther. Acids* 3 (10): e201.
- 195 Kraemer, S., Vaught, J.D., Bock, C. et al. (2011). From SOMAmer-based biomarker discovery to diagnostic and clinical applications: a SOMAmer-based, streamlined multiplex proteomic assay. *PLoS One* 6 (10): e26332.
- 196 Gupta, S., Thirstrup, D., Jarvis, T.C. et al. (2011). Rapid histochemistry using slow off-rate modified aptamers with anionic competition. *Appl. Immunohistochem. Mol. Morphol.* 19 (3): 273–278.
- 197 Ochsner, U.A., Green, L.S., Gold, L., and Janjic, N. (2014). Systematic selection of modified aptamer pairs for diagnostic sandwich assays. *BioTechniques* 56 (3): 125–128, 130, 132–133.
- 198 Nahid, P., Bliven-Sizemore, E., Jarlsberg, L.G. et al. (2014). Aptamer-based proteomic signature of intensive phase treatment response in pulmonary tuberculosis. *Tuberculosis (Edinburgh, Scotland)* 94 (3): 187–196.
- 199 Trausch, J.J., Shank-Retzlaff, M., and Verch, T. (2017). Replacing antibodies with modified DNA aptamers in vaccine potency assays. *Vaccine* 35 (41): 5495–5502.
- 200 Wu, D., Katilius, E., Olivas, E. et al. (2016). Incorporation of slow off-rate modified aptamers reagents in single molecule array assays for cytokine detection with ultrahigh sensitivity. *Anal. Chem.* 88 (17): 8385–8389.
- 201 Qiao, Z., Pan, X., Parlayan, C. et al. (2016). Proteomic study of hepatocellular carcinoma using a novel modified aptamer-based array (SOMAscan™) platform. *Biochim. Biophys. Acta* 1865 (4): 434–443.
- 202 Ashley, S.L., Xia, M., Murray, S. et al. (2016). Six-SOMAmer index relating to immune, protease and angiogenic functions predicts progression in IPF. *PLoS One* 11 (8): e0159878.
- 203 Park, N.J., Wang, X., Diaz, A. et al. (2013). Measurement of cetuximab and panitumumab-unbound serum EGFR extracellular domain using an assay based on slow off-rate modified aptamer (SOMAmer) reagents. *PLoS One* 8 (8): e71703.
- 204 Baird, G.S., Nelson, S.K., Keeney, T.R. et al. (2012). Age-dependent changes in the cerebrospinal fluid proteome by slow off-rate modified aptamer array. *Am. J. Pathol.* 180 (2): 446–456.
- 205 Ganz, P., Heidecker, B., Hveem, K. et al. (2016). Development and validation of a protein-based risk score for cardiovascular outcomes among patients with stable coronary heart disease. *JAMA* 315 (23): 2532–2541.
- 206 Baumstummeler, A., Lehmann, D., Janjic, N., and Ochsner, U. (2014). Specific capture and detection of *Staphylococcus aureus* with high-affinity modified aptamers to cell surface components. *Lett. Appl. Microbiol.* 59 (4): 422–431.

- 207 Hirota, M., Murakami, I., Ishikawa, Y. et al. (2016). Chemically modified interleukin-6 aptamer inhibits development of collagen-induced arthritis in cynomolgus monkeys. *Nucleic Acid Ther.* 26 (1): 10–19.
- 208 Gelinas, A.D., Davies, D.R., and Janjic, N. (2016). Embracing proteins: structural themes in aptamer–protein complexes. *Curr. Opin. Struct. Biol.* 36: 122–132.
- 209 Jarvis, T.C., Davies, D.R., Hisaminato, A. et al. (2015). Non-helical DNA triplex forms a unique aptamer scaffold for high affinity recognition of nerve growth factor. *Structure* 23 (7): 1293–1304.
- 210 Wolk, S.K., Shoemaker, R.K., Mayfield, W.S. et al. (2015). Influence of 5-N-carboxamide modifications on the thermodynamic stability of oligonucleotides. *Nucleic Acids Res.* 43 (19): 9107–9122.
- 211 Benner, S.A., Karalkar, N.B., Hoshika, S. et al. (2016). Alternative Watson–Crick synthetic genetic systems. *Cold Spring Harbor Perspect. Biol.* 8 (11): a023770.
- 212 Winnacker, M. and Kool, E.T. (2013). Artificial genetic sets composed of size-expanded base pairs. *Angew. Chem. Int. Ed. Engl.* 52 (48): 12498–12508.
- 213 Tarashima, N., Komatsu, Y., Furukawa, K., and Minakawa, N. (2015). Faithful PCR amplification of an unnatural base-pair analogue with four hydrogen bonds. *Chem. Weinh. Bergstr. Ger.* 21 (30): 10688–10695.
- 214 Yamashige, R., Kimoto, M., Takezawa, Y. et al. (2012). Highly specific unnatural base pair systems as a third base pair for PCR amplification. *Nucleic Acids Res.* 40 (6): 2793–2806.
- 215 Hirao, I., Mitsui, T., Kimoto, M., and Yokoyama, S. (2007). An efficient unnatural base pair for PCR amplification. *J. Am. Chem. Soc.* 129 (50): 15549–15555.
- 216 Li, L., Degardin, M., Lavergne, T. et al. (2014). Natural-LIKE replication of an unnatural base pair for the expansion of the genetic alphabet and biotechnology applications. *J. Am. Chem. Soc.* 136 (3): 826–829.
- 217 Seo, Y.J., Hwang, G.T., Ordoukhanian, P., and Romesberg, F.E. (2009). Optimization of an unnatural base pair toward natural-like replication. *J. Am. Chem. Soc.* 131 (9): 3246–3252.
- 218 Kim, T.W. and Kool, E.T. (2005). A series of nonpolar thymidine analogues of increasing size: DNA base pairing and stacking properties. *J. Org. Chem.* 70 (6): 2048–2053.
- 219 Lee, A.H.F. and Kool, E.T. (2005). A new four-base genetic helix, γ DNA, composed of widened benzopyrimidine–purine pairs. *J. Am. Chem. Soc.* 127 (10): 3332–3338.
- 220 Henry, A. (2003). Beyond A, C, G and T: augmenting nature’s alphabet. *Curr. Opin. Chem. Biol.* 7 (6): 727–733.
- 221 Hocek, M. (2009). C-Nucleosides: synthetic strategies and biological applications. *Chem. Rev.* 109 (12): 6729–6764.
- 222 Kimoto, M., Cox, R.S. 3rd, and Hirao, I. (2011). Unnatural base pair systems for sensing and diagnostic applications. *Expert Rev. Mol. Diagn.* 11 (3): 321–331.

- 223 Sefah, K., Yang, Z., Bradley, K.M. et al. (2014). In vitro selection with artificial expanded genetic information systems. *Proc. Natl. Acad. Sci. U. S. A.* 111 (4): 1449–1454.
- 224 Zhang, L., Yang, Z., Sefah, K. et al. (2015). Evolution of functional six-nucleotide DNA. *J. Am. Chem. Soc.* 137 (21): 6734–6737.
- 225 Biondi, E., Lane, J.D., Das, D. et al. (2016). Laboratory evolution of artificially expanded DNA gives redesignable aptamers that target the toxic form of anthrax protective antigen. *Nucleic Acids Res.* 44 (20): 9565–9577, gkw890.
- 226 Zhang, L., Yang, Z., Le Trinh, T. et al. (2016). Aptamers against cells over-expressing glypican 3 from expanded genetic systems combined with cell engineering and laboratory evolution. *Angew. Chem. Int. Ed. Engl.* 128 (40): 12560–12563.
- 227 Switzer, C.Y., Moroney, S.E., and Benner, S.A. (1993). Enzymic recognition of the base pair between isocytidine and isoguanosine. *Biochemistry (Mosc.)* 32 (39): 10489–10496.
- 228 Geyer, C.R., Battersby, T.R., and Benner, S.A. (2003). Nucleobase pairing in expanded Watson–Crick-like genetic information systems. *Structure* 11 (12): 1485–1498.
- 229 Yang, Z., Sismour, A.M., Sheng, P. et al. (2007). Enzymatic incorporation of a third nucleobase pair. *Nucleic Acids Res.* 35 (13): 4238–4249.
- 230 Georgiadis, M.M., Singh, I., Kellett, W.F. et al. (2015). Structural basis for a six nucleotide genetic alphabet. *J. Am. Chem. Soc.* 137 (21): 6947–6955.
- 231 Yang, Z., Chen, F., Alvarado, J.B., and Benner, S.A. (2011). Amplification, mutation, and sequencing of a six-letter synthetic genetic system. *J. Am. Chem. Soc.* 133 (38): 15105–15112.
- 232 Hirao, I., Kimoto, M., Mitsui, T. et al. (2006). An unnatural hydrophobic base pair system: site-specific incorporation of nucleotide analogs into DNA and RNA. *Nat. Methods* 3 (9): 729–735.
- 233 Matsunaga, K., Kimoto, M., Hanson, C. et al. (2015). Architecture of high-affinity unnatural-base DNA aptamers toward pharmaceutical applications. *Sci. Rep.* 5: 18478.
- 234 Vaish, N.K., Fraley, A.W., Szostak, J.W., and McLaughlin, L.W. (2000). Expanding the structural and functional diversity of RNA: analog uridine triphosphates as candidates for in vitro selection of nucleic acids. *Nucleic Acids Res.* 28 (17): 3316–3322.
- 235 Masud, M.M., Ozaki-Nakamura, A., Satou, F. et al. (2001). Enzymatic synthesis of modified DNA by PCR. *Nucleic Acids Res. Suppl.* 2001 (1): 21–22.
- 236 Sawai, H., Ozaki-Nakamura, A., Mine, M., and Ozaki, H. (2002). Synthesis of new modified DNAs by hyperthermophilic DNA polymerase: substrate and template specificity of functionalized thymidine analogues bearing an sp³-hybridized carbon at the C5 alpha-position for several DNA polymerases. *Bioconjug. Chem.* 13 (2): 309–316.
- 237 Held, H.A. and Benner, S.A. (2002). Challenging artificial genetic systems: thymidine analogs with 5-position sulfur functionality. *Nucleic Acids Res.* 30 (17): 3857–3869.

- 238 Liu, E., Lam, C.H., and Perrin, D.M. (2015). Synthesis and enzymatic incorporation of modified deoxyuridine triphosphates. *Molecules* 20 (8): 13591–13602.
- 239 Vaught, J.D., Dewey, T., and Eaton, B.E. (2004). T7 RNA polymerase transcription with 5-position modified UTP derivatives. *J. Am. Chem. Soc.* 126 (36): 11231–11237.
- 240 Gold, L., Walker, J.J., Wilcox, S.K., and Williams, S. (2012). Advances in human proteomics at high scale with the SOMAscan proteomics platform. *N. Biotechnol.* 29 (5): 543–549.
- 241 Ostroff, R.M., Bigbee, W.L., Franklin, W. et al. (2010). Unlocking biomarker discovery: large scale application of aptamer proteomic technology for early detection of lung cancer. *PLoS One* 5 (12): e15003.
- 242 Mehan, M.R., Ayers, D., Thirstrup, D. et al. (2012). Protein signature of lung cancer tissues. *PLoS One* 7 (4): e35157.
- 243 Ostroff, R.M., Mehan, M.R., Stewart, A. et al. (2012). Early detection of malignant pleural mesothelioma in asbestos-exposed individuals with a noninvasive proteomics-based surveillance tool. *PLoS One* 7 (10): e46091.
- 244 Trausch, J.J., Shank-Retzlaff, M., and Verch, T. (2017). Development and characterization of an HPV type-16 specific modified DNA aptamer for the improvement of potency assays. *Anal. Chem.* 89 (6): 3554–3561.
- 245 Fujita, H. and Kuwahara, M. (2016). Selection of natural and base-modified DNA aptamers for a camptothecin derivative: selection of DNA aptamers for a camptothecin derivative. In: *Current Protocols in Nucleic Acid Chemistry* (ed. M. Egli, P. Herdewijn, A. Matusda and Y.S. Sanghvi), 9.10.1–9.10.19. Hoboken, NJ, USA: Wiley.
- 246 Schoetzau, T., Langner, J., Moyroud, E. et al. (2003). Aminomodified nucleobases: functionalized nucleoside triphosphates applicable for SELEX. *Bioconjug. Chem.* 14 (5): 919–926.
- 247 Goullain, T., Sidorov, A., Mignet, N. et al. (2001). Enhancing the catalytic repertoire of nucleic acids. II. Simultaneous incorporation of amino and imidazolyl functionalities by two modified triphosphates during PCR. *Nucleic Acids Res.* 29 (9): 1898–1905.
- 248 Wang, Y., Ng, N., Liu, E. et al. (2017). Systematic study of constraints imposed by modified nucleoside triphosphates with protein-like side chains for use in in vitro selection. *Org. Biomol. Chem.* 15 (3): 610–618.
- 249 Gierlich, J., Gutmiedl, K., Gramlich, P.M.E. et al. (2007). Synthesis of highly modified DNA by a combination of PCR with alkyne-bearing triphosphates and click chemistry. *Chemistry* 13 (34): 9486–9494.
- 250 Macíčková-Cahová, H., Pohl, R., and Hocek, M. (2011). Cleavage of functionalized DNA containing 5-modified pyrimidines by type II restriction endonucleases. *ChemBioChem* 12 (3): 431–438.
- 251 Goubet, A., Chardon, A., Kumar, P. et al. (2013). Synthesis of DNA oligonucleotides containing C5-ethynylbenzenesulfonamide-modified nucleotides (EBNA) by polymerases towards the construction of base functionalized nucleic acids. *Bioorg. Med. Chem. Lett.* 23 (3): 761–763.

- 252 Obeid, S., Buřkamp, H., Welte, W. et al. (2012). Interactions of non-polar and “Click-able” nucleotides in the confines of a DNA polymerase active site. *Chem. Commun.* 48 (67): 8320.
- 253 Obeid, S., Yulikov, M., Jeschke, G., and Marx, A. (2008). Enzymatic synthesis of multi spin-labeled DNA. *Nucleic Acids Symp. Ser.* 52 (1): 373–374.
- 254 Smith, C.C., Hollenstein, M., and Leumann, C.J. (2014). The synthesis and application of a diazirine-modified uridine analogue for investigating RNA–protein interactions. *RSC Adv.* 4 (89): 48228–48235.
- 255 Cheng, Y., Dai, C., Peng, H. et al. (2011). Design, synthesis, and polymerase-catalyzed incorporation of click-modified boronic acid-TTP analogues. *Chemistry* 6 (10): 2747–2752.
- 256 Cahová, H., Havran, L., Brázdilová, P. et al. (2008). Aminophenyl- and nitrophenyl-labeled nucleoside triphosphates: synthesis, enzymatic incorporation, and electrochemical detection. *Angew. Chem. Int. Ed. Engl.* 47 (11): 2059–2062.
- 257 Riedl, J., Pohl, R., Rulíšek, L., and Hocek, M. (2012). Synthesis and photo-physical properties of biaryl-substituted nucleos(t)ides. Polymerase synthesis of DNA probes bearing solvatochromic and pH-sensitive dual fluorescent and ¹⁹F NMR labels. *J. Org. Chem.* 77 (2): 1026–1044.
- 258 Raindlová, V., Pohl, R., Šanda, M., and Hocek, M. (2010). Direct polymerase synthesis of reactive aldehyde-functionalized DNA and its conjugation and staining with hydrazines. *Angew. Chem. Int. Ed. Engl.* 49 (6): 1064–1066.
- 259 Rohloff, J.C., Fowler, C., Ream, B. et al. (2015). Practical synthesis of cytidine-5-carboxamide-modified nucleotide reagents. *Nucleosides Nucleotides Nucleic Acids* 34 (3): 180–198.
- 260 Ikonen, S., Macíčková-Cahová, H., Pohl, R. et al. (2010). Synthesis of nucleoside and nucleotide conjugates of bile acids, and polymerase construction of bile acid-functionalized DNA. *Org. Biomol. Chem.* 8 (5): 1194.
- 261 Kielkowski, P., Macíčková-Cahová, H., Pohl, R., and Hocek, M. (2011). Transient and switchable (triethylsilyl)ethynyl protection of DNA against cleavage by restriction endonucleases. *Angew. Chem. Int. Ed. Engl.* 50 (37): 8727–8730.

3

Immobilization of Aptamers on Substrates

Annalisa De Girolamo¹, Maureen McKeague², Michelangelo Pascale¹,
Marina Cortese¹, and Maria C. DeRosa³

¹National Research Council of Italy, Institute of Sciences of Food Production, viale G. Amendola 122/O,
Bari, 70126, Italy

²ETH Zürich, Department of Health Sciences and Technology, Schmelzbergstrasse 9, Zürich, 8092, Switzerland

³Carleton University, Chemistry Department, 1125 Colonel By Drive, Ottawa, ON K1S 5B6, Canada

3.1 Introduction

Aptamers are a new generation of receptors, composed of single-stranded DNA (ssDNA) or RNA that are selected *in vitro* by the Systematic Evolution of Ligands by EXponential Enrichment (SELEX). Selected aptamers are usually in the region of 35–100 nucleotides in length and have the ability to recognize different classes of targets (such as protein, toxin, drug, or cell) [1] with high specificity and affinity. Despite having functions similar to that of antibodies, aptamers have several advantages in terms of selection and production, costs, stability, shelf life, modification, and oriented immobilization. Furthermore, unlike antibodies, aptamers can be reversibly denatured, which facilitates capture and release of target compounds in reusable applications. Notably, based on their nucleic acid composition, aptamers have the inherent ability to bind to their complementary sequence in addition to their cognate target, which can be exploited for immobilization or signaling strategies. Because of all these features, various applications using aptamers as biorecognition elements in biosensor design or in homogeneous assays have been reported in the literature [2–7].

According to the IUPAC definition, “A biosensor is a self-contained integrated device which is capable of providing specific quantitative or semi-quantitative analytical information using a biological recognition element (biochemical receptor) which is in direct spatial contact with a transducer element” [8]. Biosensors that use DNA or RNA aptamers as bioreceptors are named “aptasensors” [9].

Aptamer–target interactions are based on affinity binding between an aptamer and its target; the high affinity of aptamers is attributed to the remarkable dissociation constants (K_d), often ranging from picomolar to low micromolar levels. An important step in the development of aptasensors is the immobilization of the aptamer, which plays a major role in the overall biosensor performance.

In particular, the stability, affinity, and specificity of the aptamer toward the target molecule depend on the technique used to immobilize it onto the transducer surface. The binding conditions used during the immobilization step could affect the structural characteristics of the aptamers, thus inducing a conformational change of the fixed aptamers, which, in turn, could alter the binding strength. In particular, the K_d value may be different from that of the same aptamer in free solution. For example, under immobilized conditions, the K_d might increase because of restricted mobility due to the formation of unique secondary structures leading to limited access to active sites on the aptamer. Alternatively, the K_d might decrease as a result of enhanced molecular interaction between the aptamer and the target in this altered configuration [2]. In this framework, a parallel comparison of the biorecognition properties of five different aptamers specific to the small-molecule target ochratoxin A (OTA) using conventional affinity binding assays was recently performed. In particular, free (both aptamer and target) in-solution assays (i.e. micro equilibrium dialysis, ultrafiltration, fluorescence polarization, microscale thermophoresis, DNase I gel, SYBR Green I), and aptamer immobilized assays (i.e. surface plasmon resonance (SPR), gold nanoparticles) were compared. From the analytical comparison of these assays, it was observed that aptamer binding varied when the aptamer was used in solution or immobilized, and that the sensitivity of each technique affected the apparent affinity. Results highlighted the importance of measuring aptamer affinity using multiple binding assays prior to aptamer integration into a platform [10, 11]. Similarly, Centi et al. [12] compared different assay formats for the detection of thrombin by immobilizing the aptamer or thrombin onto magnetic beads. The comparison demonstrated the variability of optimal assay conditions when using aptamers in different assay formats. Therefore, when possible, different assay formats for the detection of the same target should be performed to compare the analytical performances of each and to choose the approach that is the best compromise in terms of sensitivity, specificity, analysis time, and costs [12]. This is because immobilized aptamers are susceptible to conformational changes as a response to the nature of the charge of the surface and of the surrounding environment (pH, temperature, ionic strength, etc.). In particular, the conformation of the aptamer tends to be random coil (unfolded) thanks to the strong repulsion between the negative charges of the phosphate moieties. When negative charges of an aptamer interact with charged surfaces, negative charges are neutralized and the aptamer forms intramolecular hydrogen bonds to assume a folded conformation such as hairpin, G-quadruplex, or pseudoknot structures [13].

Various methods of immobilizing aptamers on solid supports have been reported. The choice of the immobilization method depends on a few factors, such as the nature of the bioreceptor and surface, the physicochemical properties of the target molecule, and the operating conditions of the aptasensor. Furthermore, the control of surface chemistry is essential for assuring high reactivity, orientation/accessibility, and stability of the surface-bound aptamer, as well as for minimizing nonspecific binding/adsorption events [9, 14, 15].

This chapter describes different aptamer immobilization chemistries used in the production of aptasensors, providing key examples of the most applied technologies. In addition, some recent diagnostic applications in relation to the immobilization method are reviewed. As the number of literature contributions

on aptasensors is constantly expanding, this chapter highlights developments in aptasensors over a period between 2010 and mid-2017.

3.2 Methods for Immobilization of Aptamers

According to the IUPAC definition, in biotechnology the term “immobilization” indicates “the technique used for the physical or chemical fixation of cells, organelles, enzymes, or other proteins (e.g. monoclonal antibodies) onto a solid support, into a solid matrix or retained by a membrane, in order to increase their stability and make possible their repeated or continued use” [16].

Generally, the choice of a suitable immobilization strategy is determined by the physicochemical properties of both the surface and the aptamer. An ideal material for aptasensor development should allow the effective immobilization of the DNA on its surface, guarantee a robust interaction between the target and the DNA, as well as exhibit a negligible nonspecific adsorption of the label and a sensitive detection of the biological event.

Several immobilization techniques have been developed in the past years. These include (i) physical adsorption, (ii) covalent binding, (iii) self-assembly, (iv) avidin–biotin immobilization, and (v) hybridization. These immobilization chemistries are chiefly achieved through modifications of the 3'-and/or 5'-ends of the aptamer with an appropriate functional group (e.g. thiol, amine, or biotin). In general, the 3'-end seems to be more suitable, since it is the primary target for exonucleases, and, thus, its coupling to the solid support would simultaneously confer resistance to nucleases [9, 14, 15, 17]. Nevertheless, the nature of solid-phase oligonucleotide synthesis is such that addition of a modifier at the 5'-end of a sequence is the terminal step, generally improving yield and simplifying purification. Sometimes an oligonucleotide spacer is added to the terminal functional groups to create flexibility in between the aptamer and functional group. Thymidine (in general, from 1 to 20) is the nucleotide of choice for the spacer because, compared to the other DNA bases, it has a lower chance of binding nonspecifically to various immobilization surfaces [18]. In some cases, spacers can also incorporate an alkyl group $[-(\text{CH}_2)_n]$ that is directly attached from one side to the functional group and from the other side to the nucleotide spacer. The inclusion of a spacer can affect, to different extents, the affinity of the aptamer for the target molecule by altering the aptamer secondary structure and, consequently, the K_d [14]. Different surfaces could be used for aptamer immobilization depending on the kind of aptasensors; these include bulk metals, such as gold, or other solid phases, such as resins, polymers, silicates, or nanomaterials. Figure 3.1 shows a schematic representation of aptamer immobilization onto a sensor surface, while Table 3.1 summarizes the different aptamer immobilization methods in relation to the sensing surface and the relative advantages and challenges.

3.2.1 Physical Adsorption

The immobilization method based on physical adsorption of DNA is the easiest way to immobilize an aptamer to surfaces without using reagents or modified

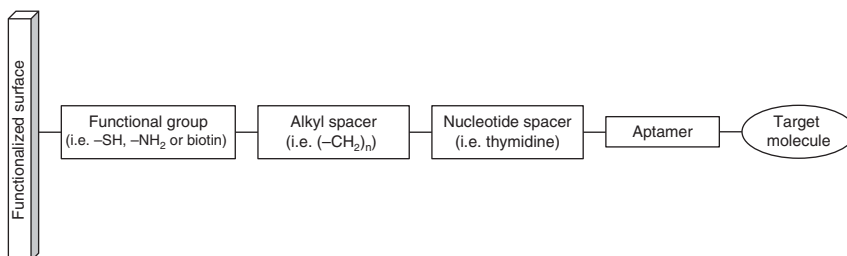


Figure 3.1 Schematic representation of aptamer immobilization onto sensor surface. The aptamer could be functionalized with biotin, amine, or thiol group. A spacer group (alkyl and/or nucleotides) could also be required for improving the aptamer–ligand binding.

DNA sequences. This binding strategy is based on electrostatic, van der Waals interactions, hydrogen bonds, and hydrophobic interactions of the reactants. The adsorption is a complex interplay between the chemical properties, structure, and porosity of the surface with the aptamer to be adsorbed. Aptamers are negatively charged due to the anionic phosphate group contained in each base. Thanks to these negative charges and to hydrophobic effect, DNA can bind several positively charged surfaces, including gels, carbon, metal oxide, polymers, and membranes or functionalized surfaces, in a simple and fast way (Figure 3.2) [17, 19].

The resulting immobilized aptamers are likely to be heterogeneous and randomly oriented on the surface because each molecule can form many contacts in different orientations to minimize repulsive interactions with the substrate and previously adsorbed DNA probes. The limitation of physical adsorption is the poor stability, the weak attachment of aptamer to the surface and random orientation of aptamers, poor reproducibility, and easy desorption (i.e. by detergent) [20, 21].

3.2.2 Covalent Binding

The sharing of electrons between two atoms forms a covalent bond. The dissociation constant for a typical covalent bond is the strongest one in biochemistry. The immobilization of aptamers onto sensor surfaces through covalent binding can be performed by the immobilization of activated aptamers (typically at its 5'- or 3'-end) on functionalized surfaces or in the immobilization of modified aptamer on activated surfaces. In the last case, both the aptamer and the surface present a reactive pair of functional groups. Details on the relevant reaction chemistries have been reviewed elsewhere [14, 19, 22].

3.2.2.1 Covalent Immobilization of Activated Aptamers on a Functionalized Surface

The covalent immobilization of activated aptamer on a surface is characterized by the activation of the phosphate group of aptamer to allow it to react with the modified surface. Three activation methods can be used [19] and are shown in Figure 3.3:

Table 3.1 Summary of different aptamer immobilizing methods in relation to the surface.

Immobilizing methods	Surface	Aptamer modifications	Principle	Advantages	Drawbacks/challenges
Physical adsorption	<ul style="list-style-type: none"> Positively charged surfaces 	<ul style="list-style-type: none"> None 	Direct immobilization of aptamer on surfaces by electrostatic forces or van der Waals forces	<ul style="list-style-type: none"> Simple and rapid Direct method (no linkers are required) 	<ul style="list-style-type: none"> Weak attachment Random orientation of aptamers Poor reproducibility Desorption by detergent
Covalent binding of activated aptamer on functionalized surfaces	<ul style="list-style-type: none"> Silicon and silicates Gold Carbon nanomaterials Cellulose Quantum dots Magnetic beads Agarose Sepharose 	<ul style="list-style-type: none"> None 	Activation of aptamer followed by chemical binding to the surface's functional group	<ul style="list-style-type: none"> Increased specificity of aptasensors Good stability High binding strength Decreased interference signal due to nonspecific adsorption Wide range of flexibility 	<ul style="list-style-type: none"> Chemical modifications are required Use of linker molecules Slow and irreversible Possible interference factors such as surfactants, cross-linking agents, could be present The optimum reaction conditions of chemical reagents, aptamers, and targets must be considered
Covalent binding of modified aptamer on activated surfaces		<ul style="list-style-type: none"> Thiols (—SH) Amines (—NH₂) 	Chemical binding between the surface's functional groups and the aptamer's modified group		

(Continued)

Table 3.1 (Continued)

Immobilizing methods	Surface	Aptamer modifications	Principle	Advantages	Drawbacks/challenges
Covalent binding by entrapment	<ul style="list-style-type: none"> • Polymers • Polymeric gel • Hydrogels • Dendrimeric structures 	<ul style="list-style-type: none"> • None • Amines ($-NH_2$) 	Chemical binding between the surface's functional groups and the aptamer's modified group	<ul style="list-style-type: none"> • Increased amount of aptamer on the surface • Higher coupling density • Flexibility for chemical modification • Can be used as coating on other substrates 	<ul style="list-style-type: none"> • Cost-effective • Complexity of the procedure for entrapped matrix synthesis
Covalent binding by electrografting	<ul style="list-style-type: none"> • Carbon • Graphene • Silicon • Copper • Gold 	<ul style="list-style-type: none"> • Amines ($-NH_2$) 	Chemical binding between the surface's functional groups and the aptamer's modified group	<ul style="list-style-type: none"> • Uniform, controlled, and efficient immobilization of aptamer • Improved sensitivity • Reduced nonspecific signals 	<ul style="list-style-type: none"> • Long incubation times for the reaction • Requirement for complex equipment for immobilization
Self-assembly	<ul style="list-style-type: none"> • Gold-coated plane surfaces • Gold nanoparticles • Gold nanorods • Glass • Silicon 	<ul style="list-style-type: none"> • Thiols ($-SH$) • Amines ($-NH_2$) 	Specific adsorption of the aptamer's modified group to the surface	<ul style="list-style-type: none"> • Stability • Oriented recognition • Prevention of nonspecific adsorption • Easy to be produced 	<ul style="list-style-type: none"> • Possible leaching of biomolecules from the support and possible denaturation

Avidin–biotin binding (affinity coupling)	<ul style="list-style-type: none"> • Avidin and its derivatives (such as neutravidin or streptavidin) 	<ul style="list-style-type: none"> • Biotin 	Interaction between the biotin group of the aptamer and amine group of the avidine	<ul style="list-style-type: none"> • High specificity and functionality • Potential to be reversible • Increased amount of aptamers on the sensor surface • Reduced incidence of nonspecific adsorption • Improved sensor signal-to-noise ratio 	<ul style="list-style-type: none"> • Great influence of pH values on avidin • Poor reproducibility • Problem of crowding effect
Electrochemical adsorption	<ul style="list-style-type: none"> • Positively charged surfaces 	<ul style="list-style-type: none"> • None 	Adsorption controlled by a potential	<ul style="list-style-type: none"> • Rapid and efficient 	<ul style="list-style-type: none"> • Great influence of the pH • Unpredictable arrangement of the aptamer on the surface
Hybridization	<ul style="list-style-type: none"> • (Partially) complementary oligonucleotides 	<ul style="list-style-type: none"> • None 	Hybridization between an aptamer and a complementary region of its reverse	<ul style="list-style-type: none"> • Highly efficient and specificity 	<ul style="list-style-type: none"> • Large dependence on salt concentration and composition as well as pH • Large electrostatic repulsion and steric hindrance

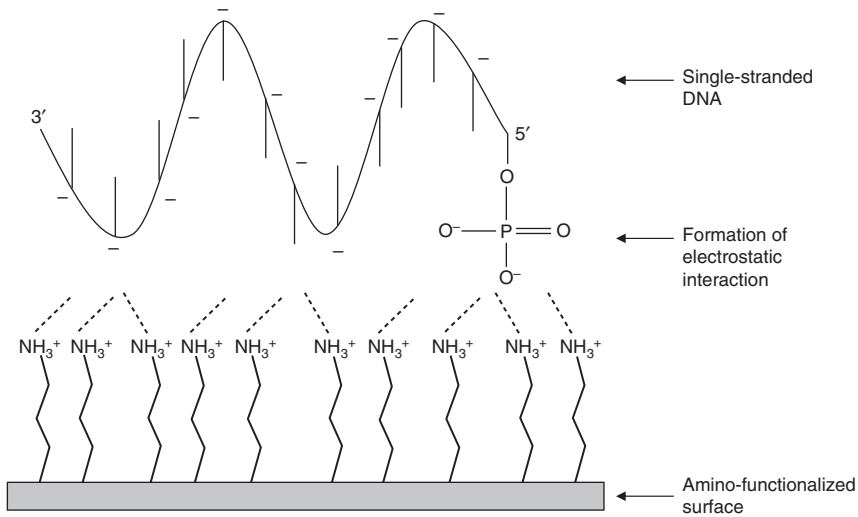


Figure 3.2 Electrostatic interactions on charged surfaces. Source: Heise and Bier 2006 [19]. © Springer-Verlag Berlin Heidelberg 2005. Reproduced with permission of Springer.

1. The *carbodiimide method* uses the carbodiimide to mediate the formation of phosphoramidate linkages between phosphates and amines, and *N*-hydroxysuccinimide (NHS) or imidazole, to stabilize the active phosphodiester intermediate. This reaction leads to the formation of a phosphorimidazolide or reactive NHS ester. The positively charged phosphorus atom reacts with the nucleophilic agents (such as amines) on the modified surface to form stable covalent bonds (phosphoramides).
2. The *reactive anhydrides method* uses the chloroformic butyric acid ester for the formation of a phosphor-carboxy anhydride. The positively charged phosphorus atom reacts covalently with nucleophils (such as amines) on the modified surface.
3. The *activated ester method* uses 1-chloro-4-nitrobenzene or chloroacetonitrile to form a reactive ester that polarizes the 5'-phosphate group to a partially positive charge. Then the positively charged phosphorus atom reacts with the nucleophilic agents of the surface to form covalent bonds (phosphoramides).

3.2.2.2 Covalent Immobilization of Modified Aptamers on Activated Surfaces

The use of activated surfaces for immobilization of the modified aptamer increases the specificity of the aptasensors and decreases nonspecific adsorption. The kind of surface activation strategy depends on the type of terminal functional groups linked to the aptamer. Surfaces can be activated using zero-length cross-linkers or bifunctional cross-linkers. Zero-length cross-linkers are reactive molecules that activate functional groups on surfaces without any chain elongation or incorporation in molecules that have to be attached and are used for the “direct coupling” of the aptamers to the surface. The most common functional groups of zero-length cross-linkers include hydroxyl

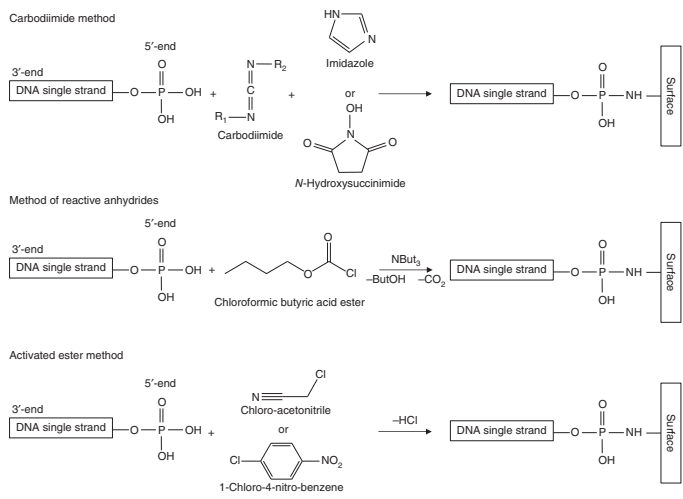


Figure 3.3 DNA activation and covalent coupling on amino-functionalized surfaces. Source: Heise and Bier 2006 [19]. © Springer-Verlag Berlin Heidelberg 2005. Reproduced with permission of Springer.

(—OH), amine (—NH₂), carboxyl (—COOH), and aldehyde (—CHO) that react with modified aptamers containing an amine group [19, 20]. A typical surface activation is the silanization that is used to functionalize glass, silica, silicon, and metal oxide surfaces. The reaction requires the presence of hydroxyl groups on the surface (typical of glassy and silica surfaces) which react with silanol (Si—OH), thus forming a covalent —Si—O—Si— bond to which aptamers can be immobilized covalently. Organosilanes have a general structure of (RO₃)Si(CH₂)_n-X and the reactive group (X) for covalent immobilization of aptamers include aldehyde, amino, mercapto, and epoxy groups. Some of the common silanes used for glass modification are 3-aminopropyltrimethoxysilane, 3-mercaptopropyltrimethoxysilane, 3-glycidoxypropyltrimethoxysilane, and 4-trimethoxysilylbenzaldehyde [19] (Figure 3.4). The result of the silanization is the formation of a self-assembled silane monolayer whose structure depends on the chemical structure of the reagent used for the silanization, the density of silanol groups on the surface monolayer, and the physical structure of the surface at the nanoscale level. Further information on surface activation by silanization can be found elsewhere [20].

Thionyl chloride is another zero-length cross-linker that can be used for the activation of surfaces containing hydroxyl groups. In particular, in the presence of thionyl chloride and a catalyst, the hydroxyl group is chlorinated with the release of sulfur dioxide and hydrogen chloride. Then, the chlorinated surface can covalently react with functionalized aptamers by hydrogen atom transfer reaction [20].

In the case of indirect coupling, homobifunctional cross-linkers are used. This class of linkers has the same reactive group to both sides. Prior to

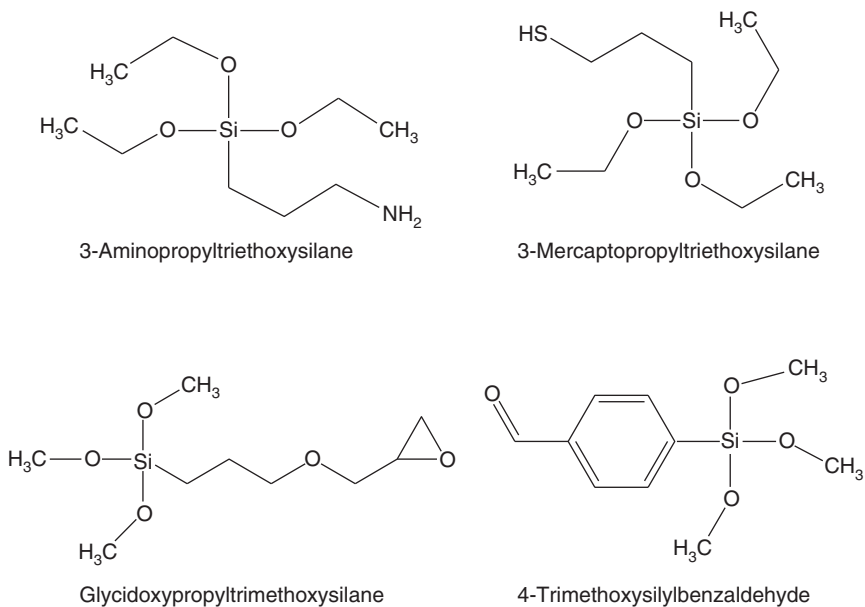


Figure 3.4 Some organosilanes used for glass modification.

coupling aptamer probes, bifunctional linkers must be reacted with the surface to inhibit the formation of aptamer dimers. The most often employed bifunctional cross-linkers are 1,4-phenylene diisothiocyanate, glutaraldehyde, 1,4-butanediol diglycidylether, disuccinimidyl carbonate, dimethylsuberimide, and carbonyldiimidazole (CDI) [19, 22]. In the case of CDI, hydroxylated surfaces are first modified with CDI to form a reactive intermediate which forms a carbamate bond to an amino-terminated aptamer group (Figure 3.5). In the case of the glutaraldehyde, the surface modified with an amine group can be modified with glutaraldehyde, which forms an imine bond with an aldehyde and leaves the other aldehyde free for bonding with an amino-terminated aptamer group (Figure 3.5).

Carbonaceous materials, like graphite, graphite fiber, carbon monoliths, and glassy carbon, are widely used as solid support for covalent immobilization of aptamers and for the development of electrochemical biosensors. In particular, carbon nanotubes (CNTs) have attracted a great deal of interest for the development of aptasensors thanks to their main characteristic of large surface-to-volume ratio. CNTs are micro-structured carbon materials with a novel design and improved sensing compared to traditional carbon materials. They have a closed topology and tubular structure that are typically several nanometers in diameter and many micrometers in length. Two classes of CNTs can be synthesized: single-walled carbon nanotubes (SWCNTs) or multiwalled carbon nanotubes (MWCNTs). SWCNTs consist of a single rolled-up graphene sheet, while two or more concentric tubes form MWCNTs. Aminated or carboxylated aptamer can be immobilized on the respective carboxylated or aminated SWCNTs using 1-ethyl-3-(3-dimethylaminopropyl)carbodiimide hydrochloride (EDC) coupling. SWCNTs have abundant accessible surface area for biological immobilization and their high electron mobility, low electrical resistance, and favorable biocompatibility make them excellent candidates for biosensing. Several aptasensors have been reported using DNA aptamers immobilized onto SWCNTs or MWCNTs [17, 23].

The power of covalent binding of the aptamer to the sensor surface lies in the increase of the specificity of the aptasensors and decrease of the interference signal of nonspecific adsorption. Furthermore, the variety of ways in which aptamers can be fixed onto the sensor surfaces allows for their integration into a wide range of platforms. However, this method requires chemical modification of the surface, as well as the use of linkers. Furthermore, possible interference factors like surfactants or cross-linking agents could be present and affect the performance of the aptasensor.

3.2.2.3 Covalent Immobilization by Entrapment

Another approach used for aptamer immobilization includes the covalent entrapment of the aptamer into three-dimensional matrices, thus allowing the use of a higher aptamer concentration and then an increase of the overall assay sensitivity. Conducting polymers represent an excellent support for the preparation of these matrices. Among them, polypyrrole (Ppy) is the most commonly used polymer to immobilize aptamers for electrochemical aptasensors because it has good electrical conductivity, environmental stability to air and water, and can be synthesized

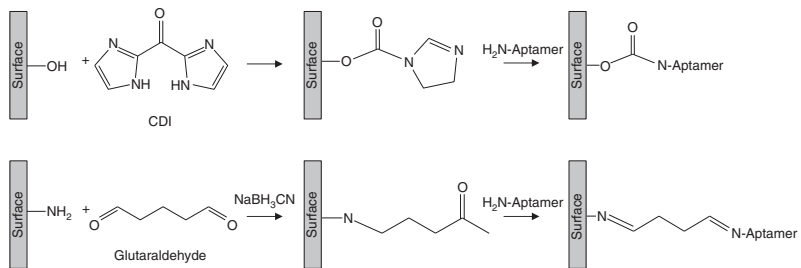


Figure 3.5 Typical reaction sequences reported for covalent attachment of aptamers to hydroxyl ($-\text{OH}$) and amine ($-\text{NH}_2$)-modified surfaces using carbonyldiimidazole (CDI) or glutaraldehyde, respectively, as bifunctional cross-linkers.

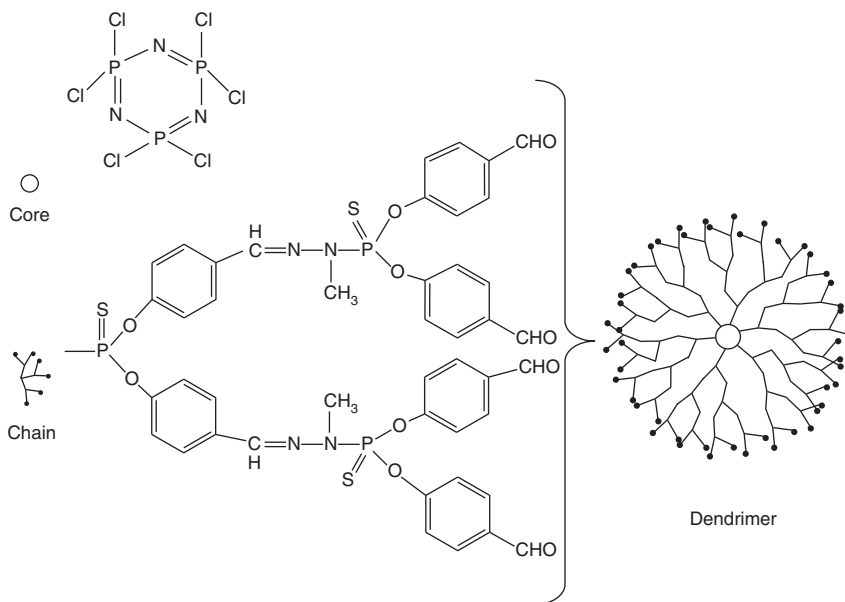


Figure 3.6 Homobifunctional cross-linker dendrimer: an initiatory core is extended through a number of branching reactions to form a dendrimer. Source: Luderer and Walschus 2005 [25]. © Springer-Verlag Berlin Heidelberg 2005. Reproduced with permission of Springer.

easily through electropolymerization or copolymerization with other pyrroles. An aptamer can be covalently immobilized (entrapped) onto a Ppy film by its conjugation to a pyrrole monomer followed by electropolymerization, or, alternatively, by direct incorporation of the aptamer into the Ppy backbone during electropolymerization, thus obtaining aptamer polypyrrole [20, 24].

Other materials used for the formation of three-dimensional matrices and the entrapment of aptamers include polymeric gels (such as polyacrylamide and polysaccharides), hydrogels, and dendrimeric structures. Dendrimers are nanospherical structures with an initial core that is extended through a number of branching reactions to form numerous polymer arms. The exact size depends on the number of branching points (Figure 3.6) [25]. The dendron-modified substrate provides lateral spacing between the immobilized aptamer by reducing the nonspecific interactions.

Trifunctional cross-linkers are commonly used to create dendrimers or dendritic layers on a sensor surface and then react with modified aptamers. Although these dendrimeric structures offer an increased amount of aptamer on the surface and then a higher coupling density and a good flexibility for chemical modification, they have some drawbacks like the complexity and the costs related to the procedure for their synthesis [15, 20].

3.2.2.4 Covalent Immobilization by Electrografting

Another method for covalent immobilization of modified DNA onto modified surfaces is electrografting, which is based on aryl diazonium electrochemical

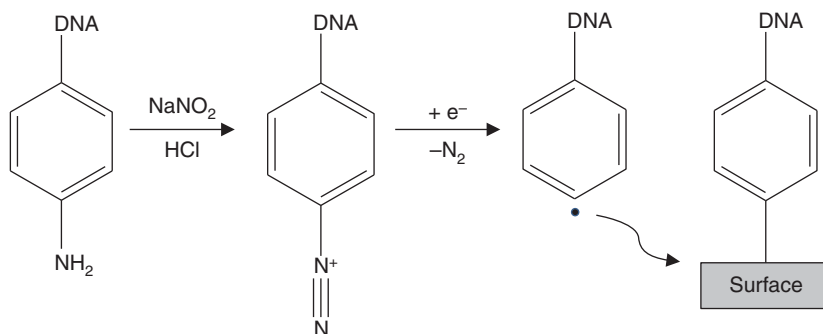


Figure 3.7 Immobilization of aptamers by electrografting using aryl diazonium electroreduction.

reduction. Aryl diazonium salts are promising candidates for surface modifications. This approach is mainly used to immobilize modified DNA onto carbon electrodes. More detailed information on diazonium reduction chemistry has been reported by Downard [26]. Briefly, the reaction involves the diazotization of an arylamine residue in the presence of sodium nitrite (NaNO_2) and hydrochloric acid (HCl) to produce an aryl diazonium. This is electroreduced to an aryl radical before reacting with the electrode surface material. The modified electrodes can be then covalently bound to the aptamer (Figure 3.7) [20, 26, 27]. Materials like carbon, graphene, silicon, copper, and gold have been reported as surfaces for the formation of aryl film by reduction of diazonium salts.

3.2.3 Self-assembled Monolayers

Self-assembled monolayers (SAMs) are ordered monolayers formed spontaneously by chemisorption and self-organization of long-chain molecules on the surface of appropriate substrates. Then, the densely packed and organized molecular layer extends the hydrocarbon chains approximately orthogonally to the surface, and the thickness depends on the length and orientation of the hydrocarbon chain (Figure 3.8). Factors like good control at the molecular level, easy preparation in the laboratory, and the very small amount of chemicals

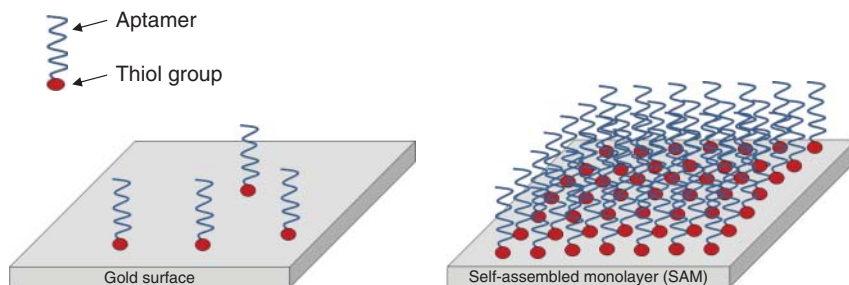


Figure 3.8 Representative immobilization of thiolated aptamers on gold surface. Large-scale immobilization of the thiolated aptamers forms a self-assembled monolayer (SAM).

needed for their preparation make SAMs an excellent platform for biosensor development [28].

Molecules that form SAMs have a “head group” with a specific affinity for a substrate. Types of substrates range from planar surfaces (glass or silicon slabs supporting thin films of metal, metal foils, single crystals) to highly curved nanostructures (colloids, nanocrystals, nanorods). Some examples of SAMs include monolayers of long-chain alcohols on glass, long-chain amines on platinum, alkyl trichlorosilane on silicon, long-chain thiols, thioesters, thiones, and alkyldisulfides on gold surface. The formation of SAMs on surfaces can be easily characterized by several methods, such as contact angle measurement, SPR, ellipsometry, UV–vis absorption, infrared spectroscopy, atomic force microscopy (AFM), scanning electron microscopy (SEM), and X-ray photoelectron spectroscopy (XPS) [28, 29].

The most extensively studied class of SAMs is derived from the adsorption of alkanethiols on metals, including gold, silver, copper, and palladium [29], with SAMs based on the strong adsorption of sulfur compounds on gold as one of the most important class. Gold is the standard surface used for SAM production for many reasons: it is easy to obtain, it is an inert metal that does not react with most chemicals, and thin gold films can be easily integrated into several technologies [29].

Chemisorption is a simple and effective method that is based on the strong affinity of thiol groups ($-\text{SH}$) of modified aptamer for gold atoms. The interaction leads to the formation of a bond with an energy that is one-fourth of that obtained with a pure covalent bond, providing a stronger and more stable surface anchoring as compared to that achieved by most physical absorption processes [9, 17, 22]. Protocols for preparing SAMs of organosulfur compounds on gold are very easy and mainly consist in the immersion of the clean gold surface into the aptamer–thiol solution followed by a blocking step to reduce the nonspecific interaction of the aptamers with the gold surface [29], even though several other studies have been performed to optimize their preparations [14, 28, 30]. Some of the experimental factors that can affect the structure of the resulting SAM and the rate of formation include solvent, temperature, concentration and purity of aptamer, immersion time, and cleanliness of the substrate [29]. Furthermore, the density of the aptamer on the surface can be tuned by a number of factors such as linker length [18] and the addition of divalent cations to reduce interstrand repulsion [31].

Advantages of using SAM surfaces with aptamers include uniformity of the monolayer, resistance to nonspecific adsorption of interfering molecules, the ability to include multiple aptamers or other moieties (mixed SAMs), and ease of preparation and integration into techniques such as quartz crystal microbalance (QCM) and SPR. However, long aptamers with larger numbers of amine groups (in their base unit) have a greater probability of nonspecific binding to the gold surface; furthermore, the cost of the thiol-modified aptamers is higher than the non-modified or amine-modified aptamers. Some external factors, such as surface impurities, single-atom vacancies that nucleate into large vacancy “islands,” purity of the aptamer solution, etc. can also be responsible for some defects in SAMs [28, 29]. SAM-functionalized surfaces can also be

used to couple avidin (or its derivatives) on the gold surface for conjugation to biotin-terminated aptamers [14].

3.2.4 Avidin–Biotin Binding (Affinity Coupling)

One of the most widely employed techniques for aptamer immobilization is biotin–avidin (or a related derivative such as streptavidin or neutravidin) affinity coupling binding. It is considered one of the strongest interactions in nature, with a K_d value of 10^{-15} M for avidin and 10^{-13} M for streptavidin. Avidin and streptavidin are tetrameric proteins that have four identical binding sites for biotin and high affinity for this molecule due to conserved amino acid sequences and structure. Among them, only avidin has one disulfide bond and a carbohydrate chain.

Streptavidin is preferably used over avidin because it leads to fewer nonspecific interactions associated with the lower isoelectric point ($pI = 5$ vs 10.5 , respectively) [17, 29]. Avidin (or its derivatives) can be either physisorbed or covalently immobilized onto the appropriate substrate. Numerous avidin-, streptavidin-, and neutravidin-coated substrates have been reported in the literature, including silica surfaces, magnetic beads, gold, quartz crystal chips, metal electrodes, quantum dots, and glass or microtiter plates [14, 17, 32]. Avidin is chemically linked to the organic layer by 3,3'-dithiopropionic acid di(*N*-succinimidylester) (DSP), while neutravidin can be directly chemisorbed on gold and does not require additional chemical modification of the surface. Some coated surfaces, like magnetic beads or glass slides, as well as biotin-conjugated aptamers, are commercially available. The immobilization of biotinylated aptamer on avidin mainly requires incubation of the biotinylated aptamer with the avidin-coated substrate at room temperature in a buffer solution to give efficient immobilization of biotin to avidin (Figure 3.9).

Some of the advantages of immobilization of biotinylated aptamers onto avidin-coated surfaces include high specificity and functionality, increased amount of aptamers on the sensor surface, and improved signal-to-noise ratio of the sensor. However, although (strept)avidin is easily immobilized on various surfaces, the binding capacity decreases over time. Furthermore, the

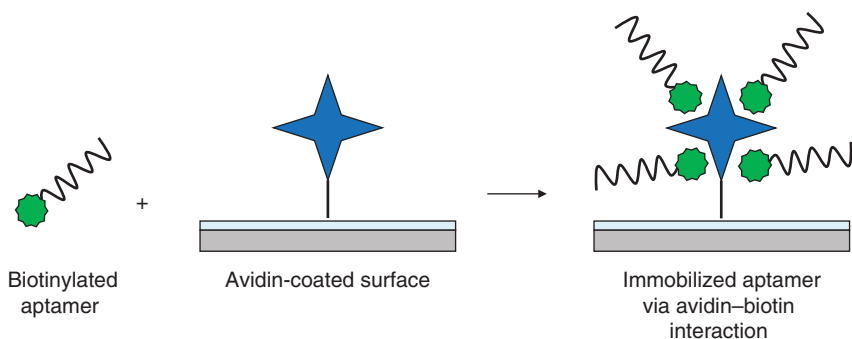


Figure 3.9 Immobilization of biotinylated aptamers to avidin-coated surfaces.

immobilization of (strept)avidin suffers from drawbacks like the instability of the immobilized aptamers and nonspecific interactions, thus resulting in the low sensitivity and specificity [14, 21, 33]. Other drawbacks include influence of pH values on avidin, poor reproducibility, and crowding effect.

3.2.5 Electrochemical Adsorption

The electrochemical adsorption is an adsorption controlled by a potential to an electrode. This method is mainly used to immobilize nucleic acids on screen-printed carbon transducers and is based on the electrostatic binding of oligonucleotides to positively charged carbon electrodes. In particular, the positive charge applied to the electrodes generates a potential that enhances the stability of the aptamer through the electrostatic attraction between the positively charged surface and the negatively charged sugar-phosphate backbone of DNA (Figure 3.10). This immobilization method is widely used for immobilizing rapidly and efficiently nucleic acids on screen-printed carbon transducers since the electrostatic binding of aptamer to positively charged carbon electrodes is sufficiently strong [34].

3.2.6 Hybridization

Another immobilizing method is the hybridization of aptamers to partially complementary sequences, which are themselves immobilized onto a surface. This approach is widely used to develop aptasensors, where the aptamer is hybridized to a short partially complementary sequence, immobilized on surfaces, such as nanoparticles or planar gold, SPR chips or glassy carbon electrodes. The added target may lead to the dissociation of the aptamer from the complementary sequence, thus generating a signal [33], or may lead to a target-binding signal that can be detected without the removal of the aptamer sequence [35]. Several aptasensors and microarrays for DNA detection by hybridization have been reported [17] (Figure 3.11), although several aptamer-based assays using competition between partially complementary sequence and target molecule toward the aptamer probe have also been reported [33, 36]. The limitations of this binding method are related to the large electrostatic repulsion and steric hindrance that require stringent control of experimental conditions [17, 20].

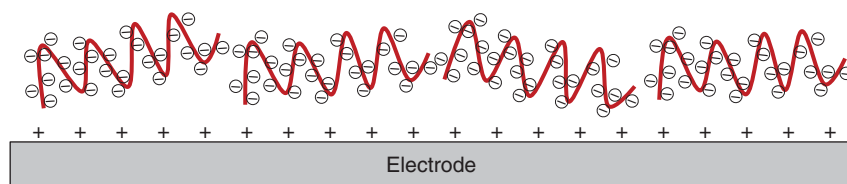


Figure 3.10 Example of electrochemical adsorption between the negatively charged sugar-phosphate backbone of aptamer and a positively charged electrode.

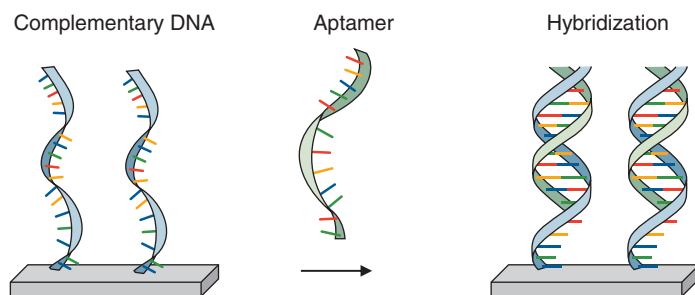


Figure 3.11 Hybridization of aptamers to partially complementary DNA sequences immobilized onto surfaces.

3.3 Immobilization of Aptamers on Substrates for Diagnostic Applications

Analytical and diagnostic applications of aptamers typically require immobilization to a surface for integration into a device. The number and diversity of substrates (or surfaces) incorporated for aptamer-based analytical applications are increasing each year. Typically, the requirements of the desired analytical methods for aptasensor development determine the choice of substrate and chemistry for aptamer immobilization. Here, we have categorized the immobilization based on substrate type: (i) planar or flat gold; (ii) solid phase; and (iii) nanomaterials (Tables 3.2–3.4). To date, these three surfaces have been the focus in aptamer analytical and diagnostic applications. A short discussion on new substrate materials is also provided subsequently.

3.3.1 Flat Gold

Due in part to its broad applicability to biosensor designs, bulk gold surfaces modified by SAMs with thiol-derivatized DNA have been an intensely studied area for more than 20 years [86]. While early work focused on the immobilization of duplex DNA on gold electrodes for the study of DNA damage and repair [87, 88] or ssDNA for the detection of complementary nucleic acid sequences [89], more recently, the detection of a wide variety of non-nucleic acid targets has been examined through aptamer-modified gold electrode surfaces [90]. In parallel, optical systems employing DNA-modified flat gold surfaces, like SPR and ellipsometry systems, have also emerged and are now being applied more routinely to aptamer–target detection [91–94]. Notably, the resistance of these SAM-coated gold surfaces, coupled with the inertness of gold, in general, and the specificity of aptamers as molecular recognition elements, makes these systems uniquely suited for the selective detection of targets in complex matrices, such as blood or food samples. Table 3.2 highlights select examples of applications where aptamer immobilization on a flat, bulk gold substrate, either by gold–thiol interaction or by other approaches, was used as a component of a biosensor or an assay. Gold substrates are almost exclusively used for SPR and electrochemical measurements.

Table 3.2 Some examples of flat gold surfaces for immobilization of aptamers.

Gold surface	Aptamer modification/spacer	Analytical technique	Application	References
SAMs	NH ₂ /C ₆	SPR	Thrombin detection	Zheng et al. [37]
Streptavidin-gold slides	Biotin	SPR	Bovine catalase in milk	Ashley and Li [38]
Streptavidin-sensor chip	Biotin	SPR	Ochratoxin A in wine and peanut oil	Zhu et al. [39]
Neutravidin-gold chip	Biotin	SPR	Exosomes	Zhou et al. [40]
SAMs on nanostructured gold surface	HS/C ₆	SPR polarization	Ochratoxin A in solution	Bianco et al. [41]
Streptavidin-gold electrode	Biotin/T ₅	Electrochemical	Tetracycline	Kim et al. [42]
Mixed SAMs	HS/C ₆ /TTT	Electrochemical field-effect transistor	Lysozyme and thrombin in serum	Goda and Miyahara [43]
AuNP-modified screen-printed carbon electrodes	HS/C ₆	Electrochemical	Lysozyme in eggs	Xie et al. [44]
AuNP-dotted graphene nanocomposite film on a glass carbon electrode	HS/C ₆	Electrochemical	Bisphenol A in milk	Zhou et al. [45]
Poly(amidoamine) dendrimers immobilized on gold electrodes	NH ₂	Electrochemical impedance spectroscopy	Aflatoxin B1 in peanuts	Castillo et al. [46]
Poly(amidoamine) dendrimers of the fourth generation immobilized on gold electrodes	NH ₂ /C ₆	Electrochemical impedance spectroscopy	Ochratoxin A in solution	Mejri-Omrani et al. [47]

(Continued)

Table 3.2 (Continued)

Gold surface	Aptamer modification/spacer	Analytical technique	Application	References
Mixed SAMs	HS/C ₆	Electrochemical field-effect transistor	Tenofovir in plasma	Aliakbarinodahi et al.[48]
Gold electrodes	SS/C ₆	Electrochemical impedance spectroscopy	<i>Ara h1</i>	Trashin et al. [49]
Gold electrode	HS/C ₆	QCM	Mercury ions	Dong and Zhao [1]
SAMs and mixed SAMs on gold electrode	HS/C ₆ (5'-termination) HS/T ₁₅ (5'-termination) HS/C ₃ (3'-termination) HS/C ₁₅ (3'-termination)	QCM	Screening of aptamers specific for ochratoxin A	Bianco et al. [41]
Two-dimensional nanoarray interface	HS/T ₁₅	QCM in combination with SERS	Thrombin in solution	Deng et al. [50]
Nanowell gold electrode	NH ₂ /C ₆	QCM	Avian influenza virus	Wang et al. [51]
Gold-coated silicon cantilevers	HS/C ₆	Optical beam deflection	Kanamycin in solution	Bai et al. [52]
Gold-coated silicon cantilevers	HS/C ₆	Optical beam deflection	Fumonisin B1 in solution	Chen et al. [53]
Gold/silver/gold multilayer array	HS	Raman spectroscopy	Vasopressin	Huh and Erikson [54]

HS, thiol group; NH₂, amine group; EG, ethylene oxide; SAMs, self-assembled monolayers; AuNPs, gold nanoparticles; SPR, surface plasmon resonance; QCM, quartz crystal microbalance; SERS, surface enhancement Raman spectroscopy.

Table 3.3 Selected examples of solid phases for immobilization of aptamers.

Solid-phase surface	Aptamer modification/spacer	Analytical technique	Application	References
Glass conical nanopore tip	NH ₂ /C ₆	Capture and detection by linear sweep voltammetry	Lysozyme	Cai et al. [55]
Silicon micro ring	NH ₂ /C ₇	Capture and detection by optical measurement	Thrombin	Park et al. [56]
Polystyrene resin	NH ₂	Solid-phase hybridization and detection by colorimetric measurement	DNA	Kannoujia et al. [57]
Polypeptide polymer	NH ₂ /C ₆	Capture and detection by electrochemical	Cocaine	Bozokalfa et al. [58]
Avidin-poly-dimethylsiloxane layer	Biotin	Capture and counting by image analysis	Tumor cells	Chen et al. [59]
Streptavidin-nitrocellulose membrane	Biotin	Lateral flow assay	Trypanosoma mRNA	Wang et al. [60]
Streptavidin-nitrocellulose membrane	Biotin/poly A	Lateral flow assay	Aflatoxin B1 in corn	Shim et al. [61]
Streptavidin-nitrocellulose membrane	Biotin SH	Lateral flow assay	Thrombin	Qin et al. [62]
Streptavidin-nitrocellulose membrane	Biotin	Lateral flow assay	Ochratoxin A in <i>Astragalus membranaceus</i>	Zhou et al. [40]
CNBr-activated sepharose	NH ₂ /C ₆ ,	Solid-phase extraction	Cocaine in blood	Madru et al. [63]
Thiol-sepharose	NH ₂ /C ₁₂			
Streptavidin-agarose	Biotin/C ₆ ,			
Glutaraldehyde silica	Biotin/C ₁₂			

(Continued)

Table 3.3 (Continued)

Solid-phase surface	Aptamer modification/spacer	Analytical technique	Application	References
Streptavidin-agarose	Biotin	Solid-phase extraction	Ochratoxin A in wine	Chapuis-Hugon et al. [64]
Cross-linked beaded agarose derivatized with DAADPA	None	Solid-phase extraction	Ochratoxin A in wheat	De Girolamo et al. [65, 66]
Hybrid silica monolithic capillary column	NH ₂ /C ₆	Solid-phase extraction	Thrombin	Deng et al. [67]
CNBr-activated sepharose	NH ₂ /C ₆	Solid-phase extraction	Tetracycline in human urine and plasma samples	Aslipashaki et al. [68]
Silica gel	NH ₂	Solid-phase extraction	Ergot alkaloids in rye feed	Rouah-Martin et al. [69]
Amino-modified silica beads	NH ₂	Solid-phase extraction	Chymotripsin	Xiao and Huang, [70]

HS, thiol group; NH₂, amine group.

Table 3.4 Selected examples of nanomaterials for immobilization of aptamers.

Nanomaterial surface	Aptamer modification/spacer	Analytical technique	Application	References
Gold nanoparticles	None	Capture and colorimetric detection	Kanamycin	Song et al. [71]
Graphene-oxide-coated gold chip	None	SPR	Lysozyme	Subramanian et al. [72]
Flat graphite on a silicon atomic force microscope probe	NH ₂ /C ₆	Capture and detection by single-molecule force spectroscopy	Hg ²⁺ molecules	Li et al. [73]
Streptavidin-silica nanoparticles	Biotin	Capture and detection by fluorescence	Digoxin	Emrani et al. [74]
Avidin-magnetic nanoparticles	Biotin	Capture and detection by fluorescence	Oxytetracycline and kanamycin in pork, milk, and honey	Liu et al. [75]
Magnetic nanoparticles/polyaniline-coated electrode	Not described	Capture and electrochemical detection	Aflatoxin M ₁	Nguyen et al. [76]
Gold nanoparticles	HS	Capture and fluorescence detection	Ochratoxin A in wheat	Velu et al. [77]
Gold nanorods	NH ₂			
Carboxyl quantum dots				
UIO-66-NH ₂ -membrane-coated magnetic beads	NH ₂ /C ₆	Solid-phase extraction	Poly-chlorinated biphenyls (PCBs) from oil samples	Lin et al. [78]

(Continued)

Table 3.4 (Continued)

Nanomaterial surface	Aptamer modification/spacer	Analytical technique	Application	References
Gold nanoparticles	HS/None	Capture and detection by fluorescence	Ochratoxin A in grape juice and serum	Taghdisi et al. [79]
Graphene-oxide-functionalized gold nanoparticles	HS/C ₆	Capture and detection by gel electrophoresis	α-Thrombin	Deng et al. [80]
Platinum-nanoparticle-coated electrode	HS	Capture and electrochemical detection	Cocaine	Roushani and Shahdost-fard [81]
Silver-gold core-shell-coated carbon paste electrode	HS/C ₆	Capture and electrochemical detection	<i>Escherichia coli</i>	Hamidi-Asl et al. [82]
Quantum dots	HS/C ₅	Capture and fluorescence detection	Ochratoxin A	Lu et al. [83]
Single-walled carbon nanotubes	None	Capture and electrochemical detection	Cocaine	Taghdisi et al. [84]
Reduced graphene oxide-chitosan film	NH ₂ via a glutaraldehyde linker/C ₆	Electrochemical	Human epidermal growth factor receptor 2 protein	Tabasi et al. [85]

3.3.1.1 Surface Plasmon Resonance Detection

SPR is an optical phenomenon that can be used to measure changes in refractive index near the surface of a metal (typically gold) sensor. When plane-polarized light interacts with a metal film under total internal reflection conditions, there is a specific incidence angle (depending on thickness and dielectric constant of metal and interface) where intensity of the reflected light is attenuated. If all the other conditions are constant, the binding of molecules to the metal surface will modify the dielectric constant of the interface region, thus changing that resonance angle. SPR experiments involve immobilizing one partner in a binding reaction (e.g. the aptamer) and flowing the other partner (e.g. the target) over the surface. The technique is label-free and is useful for examining equilibrium and kinetic constants. Once again, a number of immobilization strategies are feasible, including thiol–gold, or streptavidin biotin (see Table 3.2). In one example, an SPR aptasensor for the detection of the mycotoxin ochratoxin A in spiked red wine and peanut oil employed a sensor chip premodified with streptavidin via an amine coupling reaction, followed by incubation with biotin-modified aptamer [39]. An advantage to this approach was that the immobilization steps could be monitored *in situ* using the SPR platform (Figure 3.12)

3.3.1.2 Electrochemical Detection

Among the many electrochemical transducers that can be employed in aptasensor design (including amperometric, potentiometric, and conductometric), two of most promising approaches are impedimetric and semiconductor field-effect sensors [95]. Both approaches are relatively simple and low-cost, and are label-free, other than any necessary immobilization chemistry. Electrochemical impedance spectroscopy (EIS) aptasensors are based on the monitoring of changes in the electron transfer resistance at the electrodes as a result of target binding. An increase in resistance can signal the formation of an insulating layer due to the target blocking the electrode surface, while a decrease in resistance can be due to screening of the negative charge of the aptamers by a positively charged target. A variety of immobilization techniques have been used to prepare the aptamer-modified electrodes for these experiments, including gold–thiol and biotin–streptavidin (see Table 3.2). For example, a label-free impedance aptasensor for the food allergen trimeric protein, Ara h1, was recently developed [49]. Mixed monolayers of 2-mercaptoethanol and thiol-modified Ara h1 aptamers were deposited on flat gold electrodes. The insulation effect of the bulky protein captured by the immobilized aptamer allowed for effective detection of the protein in the sub-micromolar range. Biosensors based on field-effect transistors (FETs) are devices whereby the conductivity between two electrodes (source and drain) is gated by the changes in the surface potential that are elicited by receptor (aptamer)–target binding. These devices offer advantages such as excellent sensitivity and capacity for real-time monitoring. Recently, a 10-microelectrode array was prepared, and was connected to the gate of the FET aptasensor to enable multi-parallel detections of lysozyme and thrombin in serum (Figure 3.13) [43]. The aptamer-based FET biosensor was able to detect the targets with a lysozyme dynamic range from 34 to 2090 nM and a thrombin dynamic range from 40 to 403 nM [43].

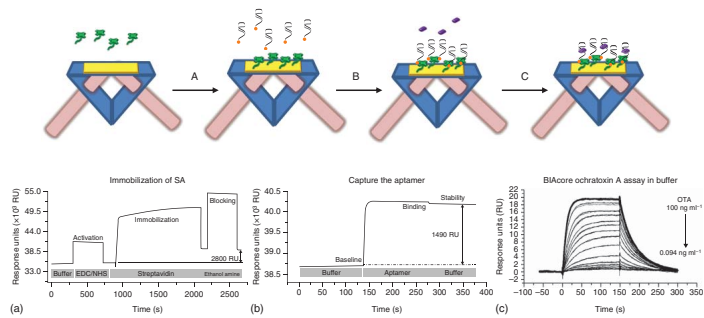


Figure 3.12 Illustration of an SPR aptasensor for ochratoxin A (OTA). The immobilization of a streptavidin layer (a) as well as the capture of a biotin-labeled OTA aptamer (b) can be tracked in real time to prepare a functional sensor that can detect the presence of the OTA in buffer, wine, or peanut oil (c). Source: Zhu et al. 2015 [39]. © 2015. Reproduced with permission of Elsevier.

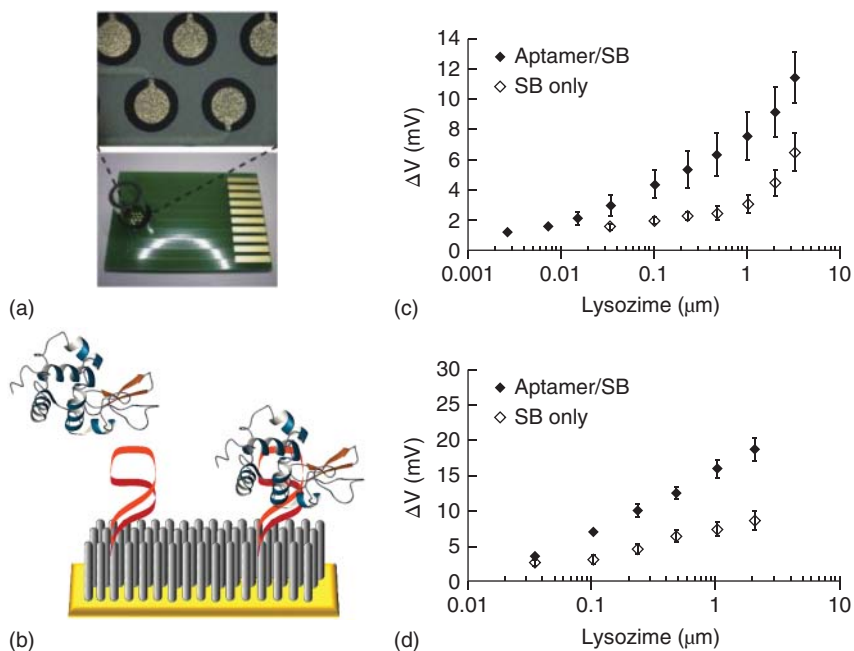


Figure 3.13 (a) Microelectrode array on a chip. (b) A schematic representation of aptamer-induced target binding in an electrical double layer at the gate-solution interface. Specific lysozyme detection (c) and thrombin detection (d) using the appropriate aptamer-immobilized SB SAM on the extended gate-FET in 10% fetal bovine serum (FBS). Source: Goda and Miyahara 2013 [43]. © 2013. Reproduced with permission of Elsevier.

Ideally, a number of complementary approaches to aptamer immobilization and characterization should be combined to ensure complete optimization, and thus the maximum applicability, of an aptasensor system. One recent example involved aptamer immobilization on flat gold for real-time drug monitoring [48]. In this system, the aptamer for the drug tenofovir was immobilized on a variety of gold surfaces for characterization before implementation on a gold electrode FET biosensor system. Aptamer-modified gold electrodes for EIS experiments were used to optimize immobilization conditions, such as ratio of aptamer to blocking thiol. A gold SPR chip was used to optimize target binding conditions, such as buffers and washing steps (Figure 3.14). With these conditions optimized, the FET system showed an excellent, specific dose-response, even in human plasma, with a limit of detection (LOD) that falls within the therapeutic range of the drug [48]. This example underscores a significant advantage of using flat gold as the aptamer immobilization substrate and broad applicability where conditions can be transferred across a variety of sensor platforms.

3.3.2 Solid Phase

Two main analytical applications utilize immobilization of aptamers onto solid-phase substrates. The first is optical-based biosensing that either reports

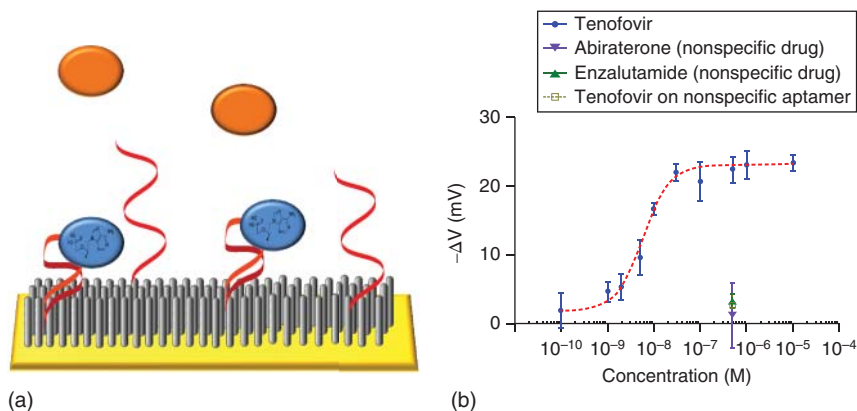


Figure 3.14 (a) Mixed SAM of tenofovir-aptamer and 6-mercaptohexanol as the sensing surface of biosensor. (b) Dose–response curve of AptaFET biosensor. Specific response (circle) fitted to Hill function with linear range between 1 nM and 100 nM, and EC_{50} of 5.8 ± 0.5 nM and responses related to non-specific drugs and non-specific aptamers as negative controls (triangles and dashed line). Source: Aliakbarinodehi et al. 2017 [48]. © 2017. Reproduced with permission of Nature Publishing Group.

on or allows the quantification of the aptamer target through fluorescence or colorimetry. The second application is the sample preparation or cleanup prior to employing a sensitive analytical measurement such as mass spectrometry or fluorescence. Table 3.3 lists selected examples of solid-phase substrates that have been coupled to aptamers for a variety of analytical applications.

3.3.2.1 Optical Detection

For optical measurements, such as UV–vis and fluorescence, glass or polymer substrates are typically employed to allow for signal transduction. These substrates have the additional benefit of avoiding spectroscopic quenching that may occur with other surfaces, such as gold [14].

While there have been many previous examples of optical aptasensors [3], most recent applications employ lateral-flow assays (or dipsticks), which have the benefit of permitting rapid on-site detection [4] (see Table 3.3). As one exciting example, Shim et al. [61] immobilized a biotin-labeled aptamer that recognized the mycotoxin target, aflatoxin B₁ (AFB₁) to streptavidin coated on a nitrocellulose substrate. The detection assay was based on the competitive reaction of the biotin-modified aptamer between the target (AFB₁) and a fluorescent dye (cy5)-modified DNA probe. In the presence of the target, the non-immobilized cy5-DNA probe was released from the test line, and subsequently captured and detected by an anti-cy5 antibody at the control line. In the absence of the target, the cy5-DNA probe remained hybridized to the immobilized aptamer and was detected at the test line. A detection limit of 0.3 ng g^{-1} AFB₁ in artificially spiked corn samples was obtained (Figure 3.15).

Beyond detection of a single molecular target, aptamers have recently been incorporated into microarrays for “multiplexing,” allowing detection and quantification of many targets in parallel. Aptamers may be covalently immobilized

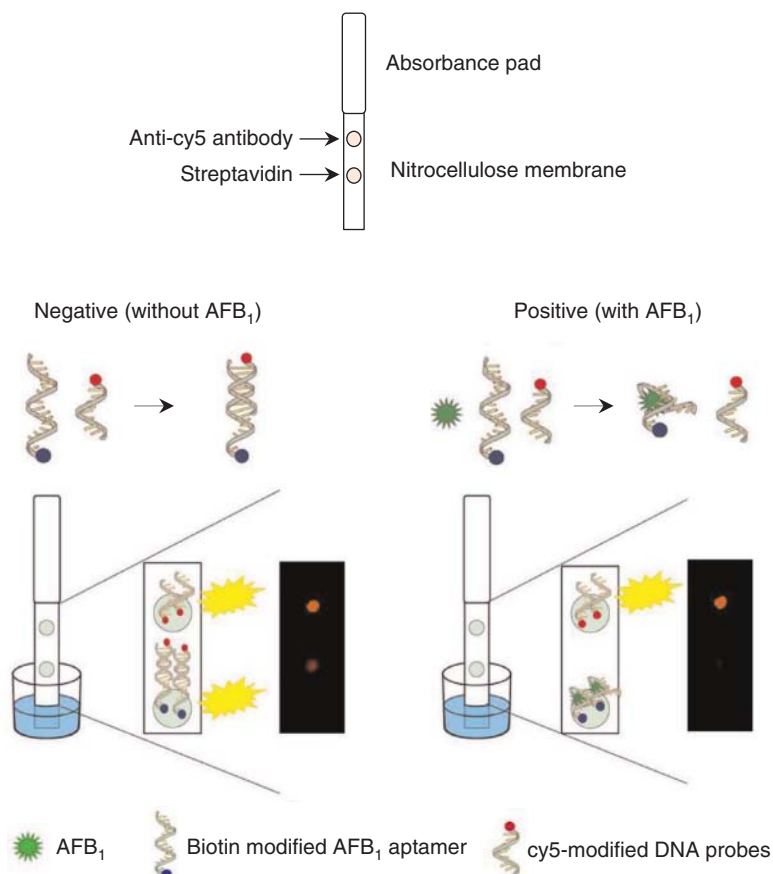


Figure 3.15 Schematic illustration of the dipstick assay for the simple and rapid detection of AFB₁. A construction of dipstick assay is shown on the upper part. The procedures and results of the dipstick assay for negative (bottom left) and positive tests are presented at the bottom of the schematic illustration. Source: Shim et al. 2014 [61]. © 2014. Reproduced with permission of Elsevier.

onto a microarray surface, but, more typically, streptavidin-coated glass slides are used, allowing easy capture of biotinylated aptamers [96]. The most prominent example of this multiplexing technique is the SOMAscan[®] assay which allows for the simultaneous detection of human proteins using approximately 1000 unique SOMAmers (slow off-rate-modified aptamers) [97]. The SOMAscan platform permits the simultaneous measurement and quantification of over 1000 proteins. The dynamic range covers eight orders of magnitude and measures molecules with high sensitivity (limits of detection in the femtomolar range) [98]. Due to the flexibility, sensitivity, and specificity imparted by the dual capture/immobilization strategy [99] (see Figure 3.16), the SOMAscan has been used to analyze clinical samples, including serum, plasma, and cerebrospinal fluid; as well as to study protein signatures in cell extracts and exosomes. As a result, new protein biomarkers related to hepatocellular carcinoma, asthma,

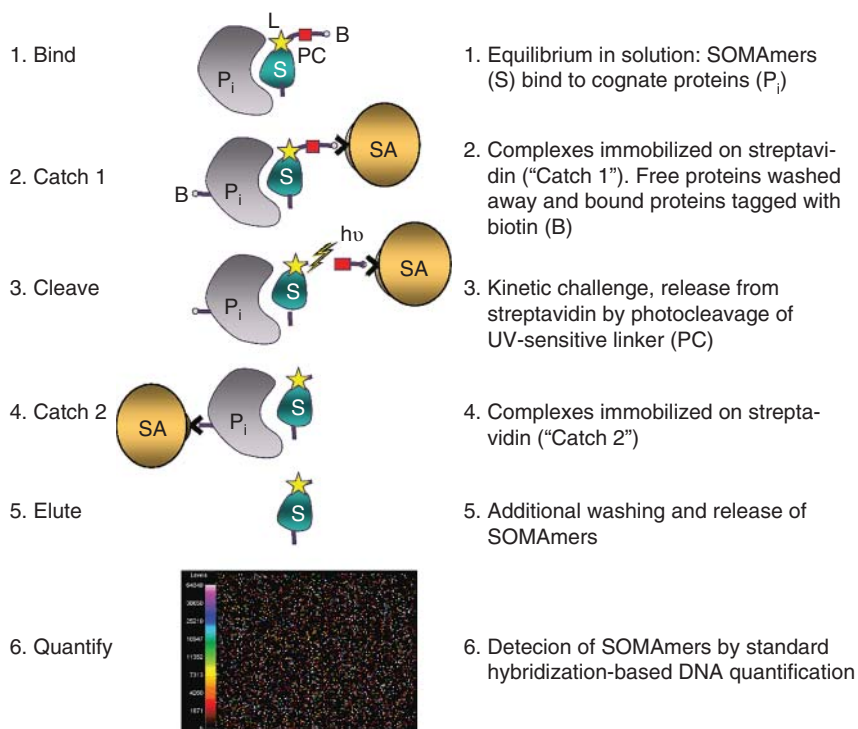


Figure 3.16 SOMAmers are modified with a photocleavable linker and biotin. Following binding, SOMAmers are immobilized on a streptavidin-substituted solid support. Proteins immobilized through interaction with bound SOMAmers are biotinylated. After washing, the entire SOMAmer population is released into solution via long-wave ultraviolet light-catalyzed cleavage of the photocleavable linker. The biotinylated analyte–SOMAmer complexes are then selectively captured on another streptavidin support. Finally, analyte-bound SOMAmers are eluted by disrupting the affinity interaction and can be quantified by hybridization to microarrays. Source: Kraemer et al. 2011 [99]. <http://journals.plos.org/plosone/article?id=10.1371/journal.pone.0026332>. Licensed under CC BY 4.0.

cystic fibrosis, nonalcoholic fatty liver disease, tuberculosis, and others have been discovered [100–104].

3.3.2.2 Sample Cleanup

Despite the advances in sensitive analytical instrumentation for quantifying analytes in environmental samples, biological samples, and food, presample treatment is usually necessary to extract the compounds of interest from complex matrixes. In particular, solid-phase extraction (SPE) is the common method for sample preparation. However, most analyte retention is based on hydrophobic interactions that are not sufficiently selective for most matrixes and applications [105]. As a result, aptamers are increasingly being immobilized onto column materials, most frequently onto silica particles, to develop highly selective SPE-based methods [6]. The workflow for a sample cleanup, using

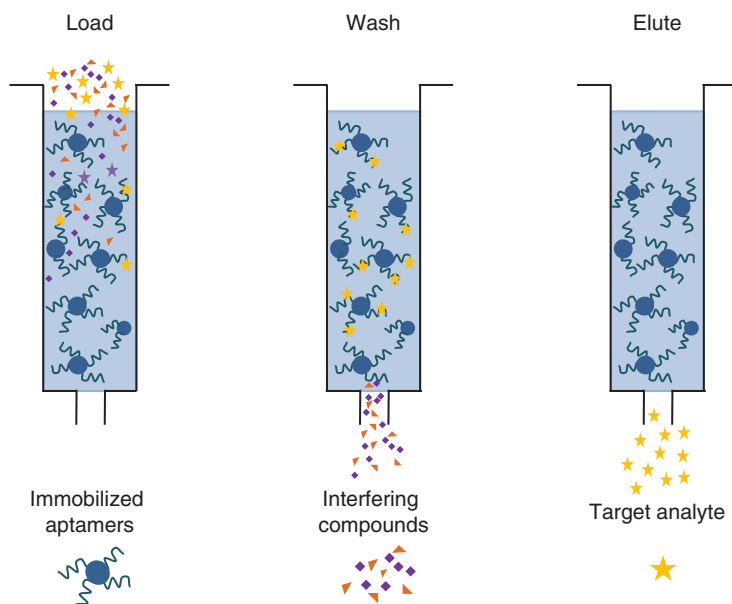


Figure 3.17 A sample is incubated with an aptamer-immobilized column material. The target analyte becomes immobilized to the column through the specific interaction with the aptamer. Thus, washing steps permit the efficient removal of interfering compounds. The target analyte (star) can be eluted from the column using denaturing conditions and quantified by a variety of techniques (e.g. LC–MS, fluorescence, etc.).

aptamer-based SPE columns is similar to most hydrophobic SPE methods and is shown in Figure 3.17.

In one study, tetracycline-binding aptamers were immobilized to CNBr-activated sepharose to develop an aptamer sorbent. The aptamer sorbent was employed to clean up both urine and plasma samples prior to tetracycline detection using electrospray ionization-ion mobility spectrometry (ESI-IMS). The authors showed that the extraction efficiency was 86.5% for urine and 82.8% for plasma samples; and under optimized conditions, the LOD for tetracycline in urine and plasma samples were found to be 0.019 and 0.037 $\mu\text{g ml}^{-1}$, respectively [68]. This strategy has been effectively used by other groups to clean up other molecules, including, for example, cocaine in human blood and ochratoxin A in wheat [63, 65, 66] (see Table 3.3).

3.3.3 Nanomaterials

Over the past several decades, nanotechnology has resulted in significant advancements in many fields, including materials science, manufacturing, medical treatment, and fundamental research. Therefore, it is not surprising that the combination of nanomaterials and biomolecules, including aptamers, has several analytical and therapeutic applications. One reason for immobilizing aptamers to nanomaterial surfaces may be to increase the aptamer density on the material due to higher surface area. Another important reason, however, is that

many nanomaterials possess a variety of desired intrinsic properties. There is a wealth of recent reviews that cover aptamers immobilized onto nanomaterials for applications in imaging and therapy, as well as in diagnostics and analytical applications [106–108]. Here, we present recent selected analytical applications (Table 3.4).

Compared to immobilization of aptamers onto similar material planar surfaces (for example, flat gold), there are several factors to take into consideration when immobilizing aptamers onto nanomaterials [109]. First, the increased immobilization density [110], while beneficial in some cases, also presents the risk of higher steric hindrance effects. Second, most nanomaterials have nanoscale surface features, including groves and pores that may make controlling surface density and steric hindrance challenging. Furthermore, these surface features may also render the nanobiosensor prone to nonspecific adsorption.

As evidenced in Table 3.4, there are several examples of aptamers immobilized onto a variety of nanomaterials for detection of a wide range of target samples. Just as there are several types of available aptamers, there are several different nanomaterials including quantum dots; carbon materials (e.g. carbon nanotubes, graphene); and nanoparticles (e.g. gold, silica, magnetic). However, gold nanoparticles are the most popular nanomaterial for aptasensing due to their intrinsic properties and well-characterized immobilization strategies. Specifically, gold nanostructures exhibit plasmonic, absorbance, and scattering properties that make them excellent signal transducers. However, graphene, a single layer of graphite that possesses a large specific surface area, as well as the more solution processable graphene oxide (GO), has recently become a popular nanomaterial choice for aptasensor development [111, 112]. GO permits the adsorption of many different molecules via π -stacking and hydrogen bonding, and is able to quench fluorescence through Förster resonance energy transfer (FRET).

In a novel example of aptamers immobilized to GO, Tabasi et al. [85] developed reduced GO-chitosan-coated nanosheets. Next, an amino-functionalized aptamer, recognizing human epidermal growth factor receptor 2 (HER2) protein, was immobilized on the nanosurface via glutaraldehyde. By incorporating methylene blue as an electrochemical probe and performing differential pulse voltammetry, the result of this unique combination was extremely sensitive and specific detection of HER2 in human serum, with limits of detection lower than the clinical cutoff.

3.4 Future Perspectives on New Substrates and New Immobilization Chemistries

As the availability of aptamer–target systems grows, so does the list of possible suitable substrates for aptamer immobilization. Among these, cloth and paper are substrates worthy of increased attention [113, 114]. The low-cost, portable, robust, and abundant nature of these substrates has led to their consideration as platforms for biosensing and diagnostic assays, particularly for point-of-care

(POC) diagnostics in remote locations. In particular, a variety of approaches have been used to immobilize DNA on paper, ranging from encapsulation into gels deposited onto the paper, to covalent modification of the cellulose using bifunctional cross-linking agents [70, 115]. Expanding these approaches for the immobilization of aptamers should be a priority. Indeed, recent work using the simple adsorption of aptamers onto paper has yielded very promising results [114]. An aptamer signaling system (prepared from a long sequence consisting of multiple repeats of the ATP aptamer and hybridized fluorophore and quencher strands) was deposited onto a paper substrate using an ink-jet printer. Fluorescence detection of the target was achieved and it was found that the large size of the polymeric system was required for efficient immobilization and signaling.

New immobilization approaches for the preparation of robust aptamer-modified surfaces are also emerging. For example, “click chemistry,” a class of biocompatible, one-pot, high-yielding coupling reactions, holds a great deal of promise for effective aptamer immobilization. Already in use in the preparation of DNA microarrays [116], the Cu(I)-catalyzed azide-alkyne Huisgen cycloaddition (CuAAC) could be very useful for aptamer tethering. The highly selective reaction is tolerant to solvent, pH, and temperatures and can be carried out under mild reaction conditions. Another click alternative that avoids the potential degradation of DNA in the presence of Cu(I) and oxygen is strain-promoted azide-alkyne [3+2] cycloaddition (SPAAC). In this reaction, a strained alkyne, typically a cyclooctane derivative, reacts with an azide to form the triazole. While these approaches have been used for target detection [117] and preparation of fluorescent aptamer conjugates [118], they are still underrepresented in aptamer immobilization studies [44, 119, 120]. An electrochemical lysozyme aptasensor was recently prepared by depositing an azido-modified thiol onto the gold-nanoparticle-coated electrode, and then coupling an alkynyl-modified aptamer in the presence of Cu(I) [44]. In a second example, a 5'-alkyne-modified aptamer for a cancer biomarker (ErbB2) was immobilized on an azido-modified SPR sensor chip that had been prepared in a multistep reaction (Figure 3.18). A 10% COOH-(PEG)₆-alkanethiol/90% (PEG)₃-alkanethiol SAM was deposited onto the gold chip, and was then activated using EDC/NHS chemistry. The activated surface was then reacted with an azidoamine (11-azido-3,6,9-trioxaundecan-1-amine). Sensitive detection of the ErbB2 biomarker was achieved with this approach, with an apparent dissociation constant value in the low nanomolar level [119].

3.5 Conclusions

Aptamer-based biosensors, assays, and diagnostics hold great potential for applications in medical, food safety, and environmental analyses. A critical parameter in the successful development of these new analytical tools is the efficient immobilization of aptamers on the appropriate substrate for the method of interest. The choice of surface and immobilization chemistry is predicated on the desired application and should have a view to minimize challenges such as

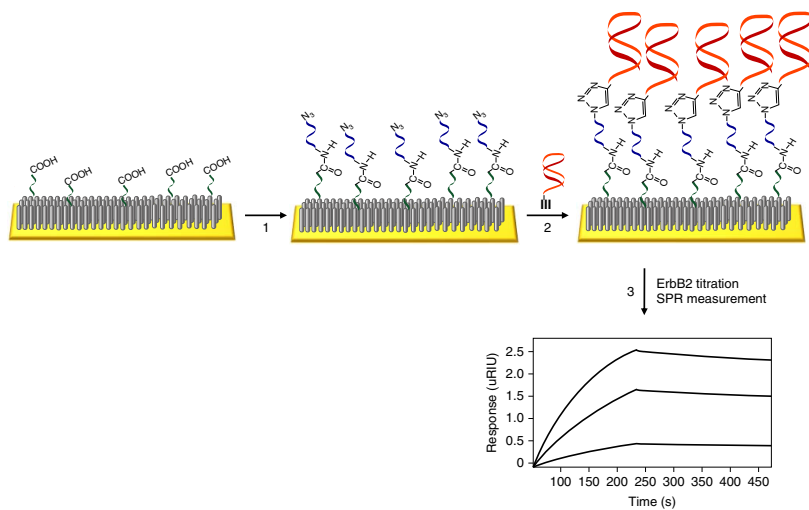


Figure 3.18 Scheme illustrating click immobilization of 5'-alkyne-modified ErbB2 aptamer. (1) Carboxy-functionalization, activation, and azido-functionalization, (2) 5'-terminal-alkyne-modified DNA aptamer immobilization, and (3) SPR measurement. Source: Kim et al. 2015 [119], © 2015. Reproduced with permission of John Wiley and Sons.

nonspecific binding and changes in affinity due to modification of the aptamer. Strategies for immobilization must be reliable, simple, and must allow the aptamers to retain their biophysical characteristics and binding abilities. Here, an overview of the standard approaches for aptamer immobilization on an array of materials including the relevant advantages and limitations has been provided. New trends in immobilization chemistry and substrate choice were highlighted. Future work should focus on the development of multianalyte systems for the concurrent detection of different targets, such as multiple biomarkers, food contaminants, and pathogens. In this regard, the limiting factor is the paucity of well-characterized aptamers for various targets of interest.

References

- 1 Dong, Z.M. and Zhao, G.C. (2012). Quartz crystal microbalance aptasensor for sensitive detection of mercury(II) based on signal amplification with gold nanoparticles. *Sensors* 12: 7080–7094.
- 2 Acquah, C., Danquah, M.K., Yon, J.L.S. et al. (2015). A review on immobilised aptamers for high throughput biomolecular detection and screening. *Anal. Chim. Acta* 888: 10–18.
- 3 Feng, C., Dai, S., and Wang, L. (2014). Optical aptasensors for quantitative detection of small biomolecules: a review. *Biosens. Bioelectron.* 59: 64–74.
- 4 Chen, A. and Yang, S. (2015). Replacing antibodies with aptamers in lateral flow immunoassay. *Biosens. Bioelectron.* 71: 230–242.
- 5 Citartan, M., Gopinath, S.C.B., Tominaga, J. et al. (2012). Assays for aptamer-based platforms. *Biosens. Bioelectron.* 34: 1–11.
- 6 Zhao, Q., Wu, M., Chris Le, X., and Li, X.F. (2012). Applications of aptamer affinity chromatography. *TrAC, Trends Anal. Chem.* 41: 46–57.
- 7 Toh, S.Y., Citartan, M., Gopinath, S.C., and Tang, T.H. (2015). Aptamers as a replacement for antibodies in enzyme-linked immunosorbent assay. *Biosens. Bioelectron.* 64: 392–403.
- 8 Thevenot, D.R., Toth, K., Durst, R., and Wilson, G. (1999). Electrochemical biosensors: recommended definitions and classification (technical report). *Pure Appl. Chem.* 71: 2333–2348.
- 9 Meirinho, S.G., Dias, L.G., Peres, A.M., and Rodrigues, L.R. (2016). Voltammetric aptasensors for protein disease biomarkers detection: a review. *Biotechnol. Adv.* 34: 941–953.
- 10 McKeague, M., De Girolamo, A., Valenzano, S. et al. (2015). Comprehensive analytical comparison of strategies used for small molecule aptamer evaluation. *Anal. Chem.* 87: 8608–8612.
- 11 McKeague, M., Velu, R., De Girolamo, A. et al. (2016). Comparison of in-solution biorecognition properties of aptamers against ochratoxin A. *Toxins (Basel)* 8: 336.
- 12 Centi, S., Messina, G., Tombelli, S. et al. (2008). Different approaches for the detection of thrombin by an electrochemical aptamer-based assay coupled to magnetic beads. *Biosens. Bioelectron.* 23: 1602–1609.

- 13 Tello, A., Cao, R., Marchant, M.J., and Gomez, H. (2016). Conformational changes of enzymes and aptamers immobilized on electrodes. *Bioconjug. Chem.* 27: 2581–2591.
- 14 Balamurugan, S., Obubuafo, A., Soper, S.A., and Spivak, D.A. (2008). Surface immobilization methods for aptamer diagnostic applications. *Anal. Bioanal. Chem.* 390: 1009–1021.
- 15 Hianik, T. and Wang, J. (2009). Electrochemical aptasensors – recent achievements and perspectives. *Electroanalysis* 21: 1223–1235.
- 16 Nagel, B., Dellweg, H., and Giera, L.M. (1992). Glossary for chemists of terms used in biotechnology. *Pure Appl. Chem.* 64: 143–168.
- 17 Sassolas, A., Leca-Bouvier, B.D., and Blum, L.J. (2008). DNA biosensors and microarrays. *Chem. Rev.* 108: 109–139.
- 18 Balamurugan, S., Obubuafo, A., McCarley, R. et al. (2008). Effect of linker structure on surface density of aptamer monolayers and their corresponding protein binding efficiency. *Anal. Chem.* 80: 9630–9634.
- 19 Heise, C. and Bier, F.F. (2006). Immobilization of DNA on microarrays. In: *Topics in Current Chemistry* (ed. C. Wittmann), 1–25. Berlin, Heidelberg: Springer-Verlag.
- 20 Marquette, C. and Wittmann, C. (2012). DNA immobilization. In: *Encyclopedia of Analytical Chemistry* (ed. R.A. Meyers), 1–34. Wiley.
- 21 Nimse, S.B., Song, K., Sonawane, M.D. et al. (2014). Immobilization techniques for microarray: challenges and applications. *Sensors (Switzerland)* 14: 22208–22229.
- 22 Tjong, V., Tang, L., Zauscher, S., and Chilkoti, A. (2014). “Smart” DNA interfaces. *Chem. Soc. Rev.* 43: 1612–1626.
- 23 Hernandez, F.J. and Ozalp, V.C. (2012). Graphene and other nanomaterial-based electrochemical aptasensors. *Biosensors* 2: 1–14.
- 24 Ramanavičius, A., Ramanavičiene, A., and Malinauskas, A. (2006). Electrochemical sensors based on conducting polymer-polypyrrole. *Electrochim. Acta* 51: 6025–6037.
- 25 Luderer, F. and Walschus, U. (2005). Immobilization of oligonucleotides for biochemical sensing by self-assembled monolayers: thiol-organic bonding on gold and silanization on silica surfaces. In: *Topics in Current Chemistry*, vol. 260 (ed. C. Wittmann), 37–56. Berlin, Heidelberg: Springer-Verlag.
- 26 Downard, A.J. (2000). Electrochemically assisted covalent modification of carbon electrodes. *Electroanalysis* 12: 1085–1096.
- 27 Walsh, R.W., Ho, U., Wang, X.L., and DeRosa, M.C. (2015). Selective dopamine detection using aptamer-functionalized glassy carbon electrodes. *Can. J. Chem.* 93: 572–577.
- 28 Samanta, D. and Sarkar, A. (2011). Immobilization of bio-macromolecules on self-assembled monolayers: methods and sensor applications. *Chem. Soc. Rev.* 40: 2567–2592.
- 29 Love, J.C., Estroff, L.A., Kriebel, J.K. et al. (2005). Self-assembled monolayers of thiolates on metals as a form of nanotechnology. *Chem. Rev.* 105: 1103–1169.

- 30 Petrovykh, D.Y., Kimura-Suda, H., Whitman, L.J., and Tarlov, M.J. (2003). Quantitative analysis and characterization of DNA immobilized on gold. *J. Am. Chem. Soc.* 125: 5219–5226.
- 31 Tom, S., Jin, H.E., and Lee, S.W. (2016). Aptamers as functional bionanomaterials for sensor applications. In: *Engineering of Nanobiomaterials* (ed. A. Grumezescu), 181–226. Elsevier Inc.
- 32 Citartan, M., Ch'ng, E.-S., Rozhdestvensky, T.S., and Tang, T.H. (2016). Aptamers as the “capturing” agents in aptamer-based capture assays. *Microchem. J.* 128: 187–197.
- 33 Zhou, L., Wang, M.H., Wang, J.P., and Ye, Z.Z. (2011). Application of biosensor surface immobilization methods for aptamer. *FenxiHuaxue/Chinese J. Anal. Chem.* 39: 432–438.
- 34 Palchetti, I. and Mascini, M. (2006). Electrochemical adsorption technique for immobilization of single-stranded oligonucleotides onto carbon screen-printed electrodes. *Anion Sens.* 261: 27–43.
- 35 Chang, A.L., McKeague, M., Liang, J.C., and Smolke, C.D. (2014). Kinetic and equilibrium binding characterization of aptamers to small molecules using a label-free, sensitive, and scalable platform. *Anal. Chem.* 86: 3273–3278.
- 36 Rhouati, A., Catanante, G., Nunes, G. et al. (2016). Label-free aptasensors for the detection of mycotoxins. *Sensors (Switzerland)* 16: 1–21.
- 37 Zheng, R., Park, B., Kim, D., and Cameron, B.D. (2011). Development of a highly specific amine-terminated aptamer functionalized surface plasmon resonance biosensor for blood protein detection. *Biomed. Opt. Express* 2: 90–96.
- 38 Ashley, J. and Li, S.F.Y. (2013). An aptamer based surface plasmon resonance biosensor for the detection of bovine catalase in milk. *Biosens. Bioelectron.* 48: 126–131.
- 39 Zhu, Z., Feng, M., Zuo, L. et al. (2015). An aptamer based surface plasmon resonance biosensor for the detection of ochratoxin A in wine and peanut oil. *Biosens. Bioelectron.* 65: 320–326.
- 40 Zhou, Q., Rahimian, A., Son, K. et al. (2016). Development of an aptasensor for electrochemical detection of exosomes. *Methods* 97: 88–93.
- 41 Bianco, M., Sonato, A., De Girolamo, A. et al. (2017). An aptamer-based SPR-polarization platform for high sensitive OTA detection. *Sens. Actuators, B* 241: 314–320.
- 42 Kim, Y.J., Kim, Y.S., Niazi, J.H., and Gu, M.B. (2010). Electrochemical aptasensor for tetracycline detection. *Bioprocess Biosyst. Eng.* 33: 31–37.
- 43 Goda, T. and Miyahara, Y. (2013). Label-free and reagent-less protein biosensing using aptamer-modified extended-gate field-effect transistors. *Biosens. Bioelectron.* 45: 89–94.
- 44 Xie, D., Li, C., Shangguan, L. et al. (2014). Click chemistry-assisted self-assembly of DNA aptamer on gold nanoparticles-modified screen-printed carbon electrodes for label-free electrochemical aptasensor. *Sens. Actuators, B* 192: 558–564.

- 45 Zhou, L., Wang, J., Li, D., and Li, Y. (2014). An electrochemical aptasensor based on gold nanoparticles dotted graphene modified glassy carbon electrode for label-free detection of bisphenol A in milk samples. *Food Chem.* 162: 34–40.
- 46 Castillo, G., Spinella, K., Poturnayová, A. et al. (2015). Detection of aflatoxin B1 by aptamer-based biosensor using PAMAM dendrimers as immobilization platform. *Food Control* 52: 9–18.
- 47 Mejri-Omrani, N., Miodek, A., Zribi, B. et al. (2016). Direct detection of OTA by impedimetric aptasensor based on modified polypyrrole-dendrimers. *Anal. Chim. Acta* 920: 37–46.
- 48 Aliakbarinodehi, N., Jolly, P., Bhalla, N. et al. (2017). Aptamer-based field-effect biosensor for tenofovir detection. *Sci. Rep.* 7: 44409.
- 49 Trashin, S., de Jong, M., Breugelmans, T. et al. (2015). Label-free impedance aptasensor for major peanut allergen Ara h 1. *Electroanalysis* 27: 32–37.
- 50 Deng, Y., Yue, X., Hu, H., and Zhou, X. (2017). A new analytical experimental setup combining quartz crystal microbalance with surface enhancement Raman spectroscopy and its application in determination of thrombin. *Microchem. J.* 132: 385–390.
- 51 Wang, R., Wang, L., Callaway, Z.T. et al. (2017). A nanowell-based QCM aptasensor for rapid and sensitive detection of avian influenza virus. *Sens. Actuators, B* 240: 934–940.
- 52 Bai, X., Hou, H., Zhang, B., and Tang, J. (2014). Label-free detection of kanamycin using aptamer-based cantilever array sensor. *Biosens. Bioelectron.* 56: 112–116.
- 53 Chen, X., Bai, X., Li, H., and Zhang, B. (2015). Aptamer-based microcantilever array biosensor for detection of fumonisin B1. *RSC Adv.* 5: 35448–35452.
- 54 Huh, Y. and Erikson, D. (2010). Aptamer based surface enhanced Raman scattering detection of vasopressin using multilayer nanotube arrays. *Biosens. Bioelectron.* 25: 1240–1243.
- 55 Cai, S.L., Cao, S.H., Zheng, Y.B. et al. (2015). Surface charge modulated aptasensor in a single glass conical nanopore. *Biosens. Bioelectron.* 71: 37–43.
- 56 Park, J.-W., Tatavarty, R., Kim, D.W. et al. (2012). Immobilization-free screening of aptamers assisted by graphene oxide. *Chem. Commun.* 48: 2071–2073.
- 57 Kannoujia, D.K., Ali, S., and Nahar, P. (2010). Single-step covalent immobilization of oligonucleotides onto solid surface. *Anal. Methods* 2: 212–216.
- 58 Bozokalfa, G., Akbulut, H., Demir, B. et al. (2016). Polypeptide functional surface for the aptamer immobilization: electrochemical cocaine biosensing. *Anal. Chem.* 88: 4161–4167.
- 59 Chen, Q., Wu, J., Zhang, Y. et al. (2012). Targeted isolation and analysis of single tumor cells with aptamer-encoded microwell array on microfluidic device. *Lab Chip* 12: 5180.
- 60 Wang, Y., Fill, C., and Nugen, S.R. (2012). Development of chemiluminescent lateral flow assay for the detection of nucleic acids. *Biosensors* 2: 32–42.

- 61 Shim, W.B., Kim, M.J., Mun, H., and Kim, M.G. (2014). An aptamer-based dipstick assay for the rapid and simple detection of aflatoxin B1. *Biosens. Bioelectron.* 62: 288–294.
- 62 Qin, C., Wen, W., Zhang, X. et al. (2015). Visual detection of thrombin using a strip biosensor through aptamer-cleavage reaction with enzyme catalytic amplification. *Analyst* 140: 7710–7717.
- 63 Madru, B., Chapuis-Hugon, F., and Pichon, V. (2011). Novel extraction supports based on immobilised aptamers: evaluation for the selective extraction of cocaine. *Talanta* 85: 616–624.
- 64 Chapuis-Hugon, F., Du Boisbaudry, A., Madru, B., and Pichon, V. (2011). New extraction sorbent based on aptamers for the determination of ochratoxin A in red wine. *Anal. Bioanal. Chem.* 400: 1199–1207.
- 65 De Girolamo, A., McKeague, M., Miller, J.D. et al. (2011). Determination of ochratoxin A in wheat after clean-up through a DNA aptamer-based solid phase extraction column. *Food Chem.* 127: 1378–1384.
- 66 De Girolamo, A., Le, L., Penner, G. et al. (2012). Analytical performances of a DNA–ligand system using time-resolved fluorescence for the determination of ochratoxin A in wheat. *Anal. Bioanal. Chem.* 403: 2627–2634.
- 67 Deng, N., Liang, Z., Liang, Y. et al. (2012). Aptamer modified organic – inorganic hybrid silica monolithic capillary columns for highly selective recognition of thrombin. *Anal. Chem.* 84: 10186–10190.
- 68 Aslipashaki, S.N., Khayamian, T., and Hashemian, Z. (2013). Aptamer based extraction followed by electrospray ionization-ion mobility spectrometry for analysis of tetracycline in biological fluids. *J. Chromatogr. B* 925: 26–32.
- 69 Rouah-Martin, E., Maho, W., Mehta, J. et al. (2014). Aptamer-based extraction of ergot alkaloids from ergot contaminated rye feed. *Adv. Biosci. Biotechnol.* 5: 692–698.
- 70 Xiao, W. and Huang, J. (2011). Immobilization of oligonucleotides onto cellulose nanofibers and the specific molecular recognition. *Langmuir* 27: 12284–12288.
- 71 Song, K.M., Lee, S., and Ban, C. (2012). Aptamers and their biological applications. *Sensors* 12: 612–631.
- 72 Subramanian, N., Sreemanthula, J.B., Balaji, B. et al. (2014). A strain-promoted alkyne–azide cycloaddition (SPAAC) reaction of a novel EpCAM aptamer–fluorescent conjugate for imaging of cancer cells. *Chem. Commun.* 50: 11810–11813.
- 73 Li, Q., Michaelis, M., Wei, G., and ColombiCiacchi, L. (2015). A novel aptasensor based on single-molecule force spectroscopy for highly sensitive detection of mercury ions. *Analyst* 140: 5243–5250.
- 74 Emrani, A.S., Taghdisi, S.M., Danesh, N.M. et al. (2015). A novel fluorescent aptasensor for selective and sensitive detection of digoxin based on silica nanoparticles. *Anal. Methods* 7: 3814–3818.
- 75 Liu, C., Lu, C., Tang, Z. et al. (2015). Aptamer-functionalized magnetic nanoparticles for simultaneous fluorometric determination of oxytetracycline and kanamycin. *Microchim. Acta* 182: 2567–2575.

- 76 Nguyen, B.H., Tran, L.D., Do, Q.P. et al. (2013). Label-free detection of aflatoxin M1 with electrochemical Fe₃O₄/polyaniline-based aptasensor. *Mater. Sci. Eng. C* 33: 2229–2234.
- 77 Velu, R., Frost, N., and DeRosa, M.C. (2015). Linkage inversion assembled nano-aptasensors (LIANAs) for turn-on fluorescence detection. *Chem. Commun.* 51: 14346–14349.
- 78 Lin, S., Gan, N., Cao, Y. et al. (2016). Selective dispersive solid phase extraction-chromatography tandem mass spectrometry based on aptamer-functionalized UiO-66-NH₂ for determination of polychlorinated biphenyls. *J. Chromatogr. A* 1446: 34–40.
- 79 Taghdisi, S.M., Danesh, N.M., Emrani, A.S. et al. (2015). A novel electrochemical aptasensor based on single-walled carbon nanotubes, gold electrode and complimentary strand of aptamer for ultrasensitive detection of cocaine. *Biosens. Bioelectron.* 73: 245–250.
- 80 Deng, N., Jiang, B., Chen, Y. et al. (2016). Aptamer-conjugated gold functionalized graphene oxide nanocomposites for human α -thrombin specific recognition. *J. Chromatogr. A* 1427: 16–21.
- 81 Roushani, M. and Shahdost-fard, F. (2016). An aptasensor for voltammetric and impedimetric determination of cocaine based on a glassy carbon electrode modified with platinum nanoparticles and using rutin as a redox probe. *Microchim. Acta* 183: 185–193.
- 82 Hamidi-Asl, E., Dardenne, F., Pilehvar, S. et al. (2016). Unique properties of core shell Ag@Au nanoparticles for the aptasensing of bacterial cells. *Chemosensors* 4: S1–S8.
- 83 Lu, Z., Chen, X., and Hu, W. (2017). A fluorescence aptasensor based on semiconductor quantum dots and MoS₂ nanosheets for ochratoxin A detection. *Sens. Actuators, B* 246: 61–67.
- 84 Taghdisi, S.M., Danesh, N.M., Beheshti, H.R. et al. (2016). A novel fluorescent aptasensor based on gold and silica nanoparticles for the ultrasensitive detection of ochratoxin A. *Nanoscale* 8: 3439–3446.
- 85 Tabasi, A., Noorbakhsh, A., and Sharifi, E. (2017). Reduced graphene oxide–chitosan–aptamer interface as new platform for ultrasensitive detection of human epidermal growth factor receptor 2. *Biosens. Bioelectron.* 95: 117–123.
- 86 Herne, T. and Tarlov, M. (1997). Characterization of DNA probes immobilized on gold surfaces. *J. Am. Chem. Soc.* 7863: 8916–8920.
- 87 Boon, E.M., Ceres, D.M., Drummond, T.G. et al. (2000). Mutation detection by electrocatalysis at DNA-modified electrodes. *Nat. Biotechnol.* 18: 1096–1100.
- 88 DeRosa, M.C., Sancar, A., and Barton, J.K. (2005). Electrically monitoring DNA repair by photolyase. *Proc. Natl. Acad. Sci. U. S. A.* 102: 10788–10792.
- 89 Drummond, T.G., Hill, M.G., and Barton, J.K. (2003). Electrochemical DNA sensors. *Nat. Biotechnol.* 21: 1192–1199.
- 90 Sassolas, A., Blum, L.J., and Leca-Bouvier, B.D. (2009). Electrochemical aptasensors. *Electroanalysis* 21: 1237–1250.

- 91 Nelson, B., Grimsrud, T., Liles, M. et al. (2001). Surface plasmon resonance imaging measurements of DNA and RNA hybridization adsorption onto DNA microarrays. *Anal. Chem.* 73: 1–7.
- 92 Gray, D.E., Case-Green, S.C., Fell, T.S. et al. (1997). Ellipsometric and interferometric characterization of DNA probes immobilized on a combinatorial array. *Langmuir* 13: 2833–2842.
- 93 D'Agata, R. and Spoto, G. (2012). Artificial DNA and surface plasmon resonance. *Artif. DNA PNA XNA* 3: 45–52.
- 94 Balamurugan, S., Obubuafo, A., Soper, S.A. et al. (2006). Designing highly specific biosensing surfaces using aptamer monolayers on gold. *Langmuir* 22: 6446–6453.
- 95 Jarczewska, M., Górski, Ł., and Malinowska, E. (2016). Electrochemical aptamer-based biosensors as potential tools for clinical diagnostics. *Anal. Methods* 8: 3861–3877.
- 96 Witt, M., Walter, J.-G., and Stahl, F. (2015). Aptamer microarrays—current status and future prospects. *Microarrays* 4: 115–132.
- 97 Gold, L., Ayers, D., Bertino, J. et al. (2010). Aptamer-based multiplexed proteomic technology for biomarker discovery. *PLoS One* 5: 1–17.
- 98 Billing, A.M., Ben Hamidane, H., Bhagwat, A.M. et al. (2017). Complementarity of SOMAscan to LC–MS/MS and RNA-seq for quantitative profiling of human embryonic and mesenchymal stem cells. *J. Proteomics* 150: 86–97.
- 99 Kraemer, S., Vaught, J.D., Bock, C. et al. (2011). From SOMAmer-based biomarker discovery to diagnostic and clinical applications: a SOMAmer-based, streamlined multiplex proteomic assay. *PLoS One* 6: 1–13.
- 100 Qiao, Z., Pan, X., Parlayan, C. et al. (2017). Proteomic study of hepatocellular carcinoma using a novel modified aptamer-based array (SOMAscan™) platform. *Biochim. Biophys. Acta, Proteins Proteomics* 1865: 434–443.
- 101 Rossios, C., Pavlidis, S., Hoda, U. et al. (2018). Sputum transcriptomics reveal upregulation of IL-1 receptor family members in patients with severe asthma. *J. Allergy Clin. Immunol.* 141: 560–570.
- 102 Wood, G.C., Chu, X., Argyropoulos, G. et al. (2017). A multi-component classifier for nonalcoholic fatty liver disease (NAFLD) based on genomic, proteomic, and phenomic data domains. *Sci. Rep.* 7: 43238.
- 103 DeBoer, E.M., Kroehl, M., Wagner, B.D. et al. (2017). Proteomic profiling identifies novel circulating markers associated with bronchiectasis in cystic fibrosis. *Proteomics Clin. Appl.* 11: 1–9.
- 104 De Groot, M.A., Higgins, M., Hraha, T. et al. (2017). Highly multiplexed proteomic analysis of quantiferon supernatants to identify biomarkers of latent tuberculosis infection. *J. Clin. Microbiol.* 55: 391–402.
- 105 Du, F., Guo, L., Qin, Q. et al. (2015). Recent advances in aptamer-functionalized materials in sample preparation. *TrAC, Trends Anal. Chem.* 67: 134–146.
- 106 Urmann, K., Modrejewski, J., Scheper, T., and Walter, J.-G. (2017). Aptamer-modified nanomaterials: principles and applications. *BioNano-Materials* 18: 1–17.

- 107 Jo, H. and Ban, C. (2016). Aptamer–nanoparticle complexes as powerful diagnostic and therapeutic tools. *Exp. Mol. Med.* 48: e230.
- 108 Kim, Y.S., Raston, N.H.A., and Gu, M.B. (2016). Aptamer-based nanobiosensors. *Biosens. Bioelectron.* 76: 2–19.
- 109 Oliveira, O.N., Iost, R.M., Siqueira, J.R. et al. (2014). Nanomaterials for diagnosis: challenges and applications in smart devices based on molecular recognition. *ACS Appl. Mater. Interfaces* 6: 14745–14766.
- 110 Hill, H.D., Millstone, J.E., Banholzer, M.J., and Mirkin, C.A. (2009). The role radius of curvature plays in thiolated oligonucleotide loading on gold nanoparticles. *ACS Nano* 3: 418–424.
- 111 Alsaafin, A. and McKeague, M. (2017). Functional nucleic acids as in vivo metabolite and ion biosensors. *Biosens. Bioelectron.* 94: 94–106.
- 112 Zhang, X., Zhang, Y., and DeRosa, M.C. (2016). *Progress in Graphene-Based Optical and Electrochemical Aptasensors* (ed. A. Grumezescu), 393–431. Elsevier Inc.
- 113 Smiley, S., Derosa, M., and Blais, B. (2013). Immobilization of DNA aptamers on polyester cloth for antigen detection by dot blot immunoenzymatic assay (aptablot). *J. Nucleic Acids* 2013: 3–8.
- 114 Carrasquilla, C., Little, J.R.L., Li, Y., and Brennan, J.D. (2015). Patterned paper sensors printed with long-chain DNA aptamers. *Chem. Eur. J.* 21: 7369–7373.
- 115 Araújo, A., Song, Y., Lundeberg, J. et al. (2012). Through capillary transport. *Anal. Chem.* 84: 3311–3317.
- 116 Uszczyńska, B., Ratajczak, T., Frydrych, E. et al. (2012). Application of click chemistry to the production of DNA microarrays. *Lab Chip* 12: 1151–1156.
- 117 Sharma, A.K. and Heemstra, J.M. (2011). Small-molecule-dependent split aptamer ligation. *J. Am. Chem. Soc.* 133: 12426–12429.
- 118 Subramanian, P., Lesniewski, A., Kaminska, I. et al. (2013). Lysozyme detection on aptamer functionalized graphene-coated SPR interfaces. *Biosens. Bioelectron.* 50: 239–243.
- 119 Kim, N.H., Le, H.T., Yang, Y. et al. (2015). Modified DNA aptamer immobilization via Cu(I)-stabilizing ligand-assisted azide-alkyne cycloaddition for surface plasmon resonance measurement. *Bull. Korean Chem. Soc.* 36: 2601–2608.
- 120 Feng, L., Lyu, Z., Offenhäusser, A., and Mayer, D. (2016). Electrochemically triggered aptamer immobilization via click reaction for vascular endothelial growth factor detection. *Eng. Life Sci.* 16: 550–559.

4

Characterization of Aptamer–Ligand Complexes

Rebeca Miranda-Castro, Noemí de-los-Santos-Álvarez, and María J. Lobo-Castañón

Universidad de Oviedo, Departamento de Química Física y Analítica, Julián Clavería, 8, 33006 Oviedo, Spain

4.1 Introduction

Nucleic acid aptamers are synthetic receptors originated from an *in vitro* combinatorial process, referred to as SELEX: systematic evolution of ligands by exponential enrichment [1, 2], for recognizing and binding with high affinity and selectivity a broad range of targets. Such binding provides an alternative to antibodies in a wide range of functions, such as analytical applications, clinical diagnosis, and therapeutics. The chemical reaction between an aptamer and its corresponding target (ligand or analyte) can be seen as resulting from the folding of the nucleic acid around a specific part of the target [3], which provides multiple and reversible intermolecular interactions conferring specificity to the ligand recognition. These are many weak, non-covalent interactions, which working in concert provide high affinity, and include three-dimensional arrangement of the bases, electrostatic interactions, hydrogen bonding, or hydrophobic effect. A complete description of this interaction will provide insights into the fundamental mechanism of molecular recognition and opportunities for the rational design or improvement of the aptamer structures.

This chapter is devoted to the description of common and emerging methods for understanding the interaction between nucleic acid aptamers and their targets. The characterization of this reaction begins with ligand binding studies under equilibrium conditions, which provides reliable estimates of the affinities of the aptamers for their cognate ligands. Besides knowledge of the affinity constants, binding assays can provide a description of the thermodynamics of the binding event. Complementing the static and thermodynamic information available from equilibrium binding studies, a kinetic characterization for unraveling the dynamics of the interaction is indispensable, and the second part of this chapter describes some techniques used with this aim.

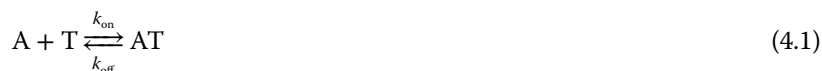
4.2 Equilibrium Characterization: Thermodynamics

The formation of the aptamer–target (AT) complex, qualitatively described as the process of molecular recognition, is realized by specific interactions between both solutes. Understanding and improving these interactions requires a quantitative description of the energetics of complex formation, which can be obtained by analyzing the data from binding assays under equilibrium conditions. From an experimental point of view, binding assays are easy to do; they involve the incubation of the two partners at a defined temperature in a defined buffer, fixing the concentration of one of them in the presence of an incrementing series of concentrations of the other. Once the equilibrium is attained, the concentration of the free target, or the concentration of the complex AT (bound target) is determined while maintaining equilibrium. From these data, it is possible to obtain a reliable estimation of the affinity constant. Extensive binding studies require the evaluation of the temperature dependence of the affinity constant, from which the thermodynamic signature for the AT interaction can be obtained. Such information provides a deep understanding of the enthalpy and entropic interplay between the aptamer and the target, and thus an indication of the forces that drive the binding.

In this section, we first outline the theoretical foundations of these binding studies, and then the methods available for their experimental evaluation. These methods can be classified into two broad categories. The first one encompasses those methods that involve the separation, upon binding, of the bound and free binding partner in excess, and they are referred to as separation-based methods. The feasibility of these methods is conditioned by the strength of the interaction; more specifically, the complex dissociation rate should be slow enough not to alter the binding equilibrium during the separation step. The second category embraces those methods capable of measuring the molecular complex directly, without a previous separation step. In this group, it is possible to distinguish homogeneous methods that allow the binding reaction to be directly monitored in solution and heterogeneous assays in which one of the partners is immobilized.

4.2.1 Basic Principles

The binding of a ligand or target T to an aptamer A can be formulated by the reaction:



where AT represents the aptamer–target complex, and k_{on} (in units of $M^{-1} s^{-1}$) and k_{off} (in units of s^{-1}) the kinetic rate constants that govern the forward binding and reverse dissociation, respectively. At equilibrium, the rate of association is equal to the rate of dissociation, and thus:

$$k_{\text{on}}[A][T] = k_{\text{off}}[AT] \quad (4.2)$$

$[A]$, $[T]$, and $[AT]$ represent the equilibrium concentrations of free aptamer, free target, and aptamer–target complex, respectively. The affinity constant,

K_A (in unit of M^{-1}) for the equilibrium between the aptamer and the receptor, obeying the law of mass action, is defined by

$$K_A = \frac{k_{\text{on}}}{k_{\text{off}}} = \frac{[AT]}{[A][T]} = \frac{1}{K_D} \quad (4.3)$$

K_D (in unit of M) defines the equilibrium dissociation constant, which is a measure of the tendency of the AT complex to dissociate. Therefore, a high-affinity interaction usually involves a fast association rate and a slow dissociation rate. Equation (4.3) shows the relationship between equilibrium and kinetic constants, although the equilibrium constants can be measured independently, without needing to know the kinetic constants.

Provided that the total concentration of the aptamer, $[A]_t$, is fixed and conserved in the experiment, for a 1 : 1 stoichiometry the affinity constant is calculated as

$$K_A = \frac{[AT]}{([A]_t - [AT])[T]} = \frac{1}{K_D} \quad (4.4)$$

Equation (4.4) can be arranged to

$$f = \frac{[AT]}{[A]_t} = \frac{[T]}{[T] + K_D} \quad (4.5)$$

where f represents the fraction of bound aptamer at equilibrium, and it can also be considered as the fraction of bound ligand to the maximal AT complex, which is that corresponding to the saturation value (theoretically achieved when all the aptamer is bound). Equation (4.5) is an expression of the Langmuir isotherm, with the form of a rectangular hyperbola (Figure 4.1); it is a general equation describing the equilibrium binding between a ligand and a receptor with a 1 : 1 stoichiometry [4]. From this expression, K_D represents the ligand concentration that results in 50% of occupancy of the aptamer binding sites. Plotting the data of the binding assays in the form of this equation, i.e. the bound fraction of the

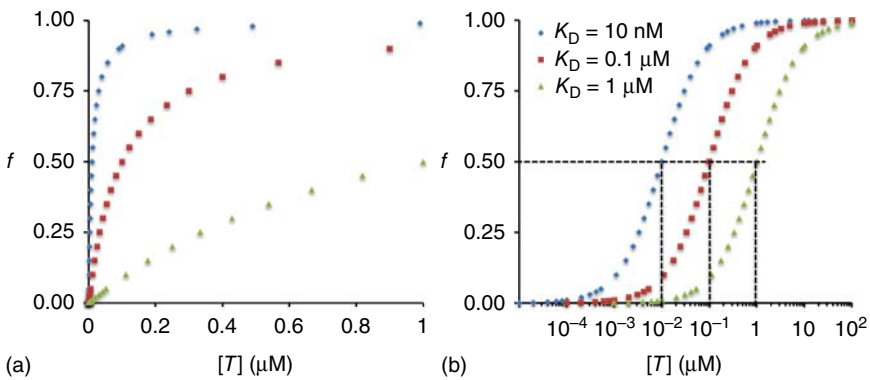


Figure 4.1 Simulated binding curves for aptamer–target interaction with different affinity constants plotted on a linear scale (a), and a semi-logarithmic scale revealing the characteristic sigmoid plot (b).

aptamer, f , on the Y axis, and the free target concentration on the X axis, it is possible to obtain K_D using a nonlinear regression analysis or linear regression with plots that linearize Eq. (4.5), such as the double reciprocal plot ($1/f$ vs $1/[T]$), the Y -reciprocal plot ($[T]/f$ vs $[T]$) and the X -reciprocal plot or Scatchard plot ($f/[T]$ vs $1/[T]$). These plots lead to different errors in the estimation of K_D [5], and the direct fitting of the untransformed data is nowadays the preferred method for evaluating the affinity constant. The saturation binding curves are also frequently plotted using a logarithmic scale for target concentration, giving rise to characteristic sigmoidal binding curves. The semi-logarithmic plots for different values of K_D are parallel, with the same sigmoid shape but occupying different positions on the log concentration axis, with the midpoint located at $\log_{10} K_D$ (Figure 4.1). Note that $[T]$ represents the concentration of free target in equilibrium, which has to be measured or estimated, together with the concentration of the aptamer–ligand complex. In the experiment, it is imperative that the method used for measuring bound and free fractions of the target does not perturb the equilibrium, and this must be subjected to close scrutiny. A simplification is achieved when the experiment is performed fixing the initial concentration of aptamer, $[A]_t$, well below K_D . Under these conditions, the complex concentration, limited by the aptamer, will be much lower than the concentration of target in the whole target concentration window, and hence free target concentration can be approximated by the total target concentration. To maximize the accuracy with which the affinity may be estimated from these measurements, it is very important to study a wide range of target concentrations.

In principle, it is also possible to titrate a fixed amount of target with increasing amounts of aptamer to obtain the affinity constant, using similar expressions for calculation. In practice, the choice is often forced by the availability and solubility of both reagents and by the suitability of properties for the experimental measurement.

The binding equations presented hitherto are based on the assumption that the target is univalent in its interaction with the aptamer. This is entirely reasonable for systems in which the target is a small molecule, but not in the cases, for example, of whole cells or viruses [6, 7]. On the other hand, it is also possible to engineer polyvalent aptamers [8], for example, by using suitable linkers [9] or by coupling aptamers to nanoparticles [10]. With any of these approaches, multiple copies of a selected aptamer interact with target molecules in the same scaffold, resulting in higher binding affinity [11]. In these cases, the aptamer scaffold comprises several identical (or similar) subunits, and the binding of a univalent target to any of the subunits has the potential to induce conformational changes in the adjacent subunits and thereby alter their intrinsic affinities for ligand (cooperativity). Under these conditions, the binding curves do not follow the simple hyperbolic function represented by Eq. (4.5), showing significant deviations. The general expression of what is called the Hill model is more general, highly flexible, and effective in fitting these experimental data.

The Hill model is a descriptive-deterministic model to analyze the binding equilibrium in the case of multiple ligand binding, according to the following

reaction scheme:



From this scheme, the Hill equation is readily derived (Eq. (4.7)) relating the ratio of bound aptamer at equilibrium to total aptamer, f , with the total target employed in the experiment:

$$f = \frac{[AT_n]}{[A] + [AT_n]} = \frac{[T]^n}{K_D + [T]^n} = \frac{[T]^n}{(K_{1/2})^n + [T]^n} \quad (4.7)$$

n is called the Hill coefficient, ideally representing the number of binding sites. In practice, the application of this model typically results in a noninteger Hill coefficient [12], which provides a minimum estimate of the number of binding sites involved [13], and it is more appropriately described as an interaction coefficient reflecting cooperativity. This parameter and $K_{1/2}$ are obtained by nonlinear curve fitting of binding experiments. $K_{1/2}$ represents the ligand concentration at which one-half of the aptamers are bound, and is equivalent to the n th root of the dissociation constant (with M^n units). The Hill equation has proved to be of general use, even in the case of single binding with no cooperativity for which n equals 1 [14]. In order to tune the aptamer's binding affinity, it is possible to rationally introduce cooperativity into aptamer interaction [15–17]. This may be achieved, for example, by incorporating the aptamer sequence in stem-loop structures at different placements [15], designing an aptamer-complementary sequence which results in a duplexed aptamer [16] or using a tandem repeat of the aptamer, splitting the secondary structure by means of a long unstructured loop [17]. In all cases, it is possible to tune the binding affinity as well as the cooperative index (Hill coefficients between 0.5 and 2).

From a thermodynamic perspective, the binding of the aptamer with its target involves enthalpy (ΔH) and entropy (ΔS) changes that can be defined by the change in free energy of binding (ΔG), the main driving force of the formation of the AT complex.

$$\Delta G = \Delta H - T\Delta S \quad (4.8)$$

As is the case for other spontaneous processes, aptamer binding occurs only when the change in ΔG is negative when the system reaches the equilibrium state at constant pressure and temperature. The temperature is an important factor affecting the binding affinity; and to obtain the thermodynamic signature for the AT interaction, as defined by the Gibbs equation, affinity constants are determined over a range of temperatures. The temperature dependence of the standard Gibbs free energy of binding (ΔG°), which refers to the free energy change measured under standard conditions (10^5 Pa pressure and a temperature of 298.15 K) is given by the Gibbs–Helmholtz equation as

$$\Delta G^\circ = -RT \ln K_A \quad (4.9)$$

where T is the temperature in Kelvin and R the ideal gas constant. Equation (4.9) can thus be arranged to

$$\ln K_A = \frac{-\Delta H^\circ}{R} \left(\frac{1}{T} \right) + \frac{\Delta S^\circ}{R} \quad (4.10)$$

which is the integrated form of the van't Hoff equation, assuming ΔH and ΔS are not temperature dependent. Equation (4.10) indicates that by constructing a van't Hoff plot ($\ln K_A$ vs $1/T$) a linear relationship is obtained, from which slope and intercept it is possible to obtain ΔH° and ΔS° , respectively.

Binding enthalpy reflects the energy change taking place when the aptamer binds to the target; it is negative in the case of the exothermic process, implying the formation of energetically favorable non-covalent interactions between both partners, while it is positive for endothermic interactions leading to disruption of energetically favorable bonds. Note that this is a global property of the whole system, including contributions from the solutes and the solvent. Therefore, it will be the result of forming and disrupting many individual interactions between the aptamer and the solvent and the target and the solvent, the formation of non-covalent interactions between aptamer and target, and solvent reorganization near the complex surface [18]. The net enthalpy change is the result of all these contributions, which can be favorable or unfavorable.

Binding entropy is another important global thermodynamic property of the system, which indicates the overall increase ($\Delta S > 0$) or decrease ($\Delta S < 0$) in its degrees of freedom. The overall change in entropy for the AT binding can be decomposed into three contributions:

$$\Delta S = \Delta S_{\text{solv}} + \Delta S_{\text{conf}} + \Delta S_{\text{r/t}} \quad (4.11)$$

ΔS_{solv} corresponds to the entropic changes associated with solvation/desolvation of aptamer and target upon binding, which often has a large positive value, and thus a favorable contribution, because of the solvent release in the binding process. The conformational entropy change (ΔS_{conf}) represents the change in both the aptamer and target conformational freedom, which may be positive or negative as complex degrees of freedom may increase or decrease regarded to those of free target and aptamer. Certainly, the complex formation leads to a reduction in the number of units in solution, implying a loss of translational and rotational degrees of freedom of the target and the aptamer ($\Delta S_{\text{r/t}} < 0$) and contributing unfavorably to the binding entropy [18].

The dominant driving force for the aptamer–ligand interaction, depending on the system under investigation, may be either a favorable enthalpy change, with unfavorable binding entropy (enthalpically driven) [19–22], or a favorable entropic contribution accompanied by an enthalpy penalty (entropically driven) [23]. In any case, a complementary change between enthalpy and entropy, which is called the enthalpy–entropy compensation [18] occurs, since only when the change of the system free energy is negative can the aptamer–ligand binding occur spontaneously; and the higher the magnitude of the free energy change upon binding, the greater the stability of the complex. But because of this enthalpy–entropy compensation, a great change in binding free energy is not usually observed, and it is very important to identify if the recognition process is entropically or enthalpically driven in order to rationally optimize it by looking for experimental modifications that maximize the favorable enthalpy or entropic contribution while minimizing the entropic or enthalpy penalty.

The thermodynamic signature for the binding allows having an in-depth understanding of the mechanism by which the binding reaction occurs, and

could help improve binding affinity by modifying the aptamer. There are two different models that can be used to explain the AT binding mechanism: induced fit and conformational selection [24]. The induced-fit model assumes that the presence of the ligand induces in the aptamer, with a flexible structure, a conformational change such that the new conformation accommodates the ligand more effectively. The conformational selection model (also known as population selection, fluctuation selection, or selected fit) postulates that the native unbound aptamer does not exist in a single conformation but as a large set of conformations states/substates in equilibrium. The ligand selects, among these different dynamically fluctuating states, the one which is compatible with binding, and shifts the initial equilibrium toward this state, resulting in the formation of the AT complex. The distinction between the two models is not absolute; both assume that the recognition process implies a switch of the aptamer from one preferential conformation in the unbound state to another in the bound state, but the difference strives in knowing when this conformational transition occurs [25]. In fact, induced fit can be seen as an extremity of the conformational selection model, which seems a more general model for explaining the formation of aptamer–ligand complexes [26].

4.2.2 Separation-Based Methods

Different separation techniques have been employed to isolate free and bound target once the equilibrium of the aptamer binding interaction has been reached. The following sections consider in detail the most used. In all cases, after separation, an instrumental technique must be used to quantitate the isolated free partner. The choice of this technique depends on the physical properties of the species being measured; and in many cases, one of the two reagents is labeled to make the quantitation possible. In such a case, the label should have a minimal effect on the binding behavior, that is, the labeled and unlabeled reagents should behave identically with respect to the AT binding. In addition, the labels should be easily detected, with high sensitivity, and ideally using readily automated instrumentation.

4.2.2.1 Equilibrium Dialysis and Related Techniques

Separation in equilibrium dialysis and related techniques such as diafiltration and ultrafiltration are based on differences in molecular size. Consequently, these techniques can be used when the aptamer (molecular size higher than 10 000 Da for a 40-nucleotide aptamer) and the target differ greatly in size. A membrane that is selectively permeable to either the target or the aptamer, depending on their relative sizes, but not to the other partner and the AT complex, is used to create a two-phase system in which one phase comprises the complex in equilibrium and the other the free partner in equilibrium.

In dialysis, the semipermeable membrane is used to divide the dialysis cell in two compartments (Figure 4.2). A solution of each partner is introduced into each compartment, or, alternatively, a mixture of aptamer and target is placed in one chamber and the buffer in the other. The system is allowed to equilibrate at constant temperature until the thermodynamic equilibrium is attained. Since

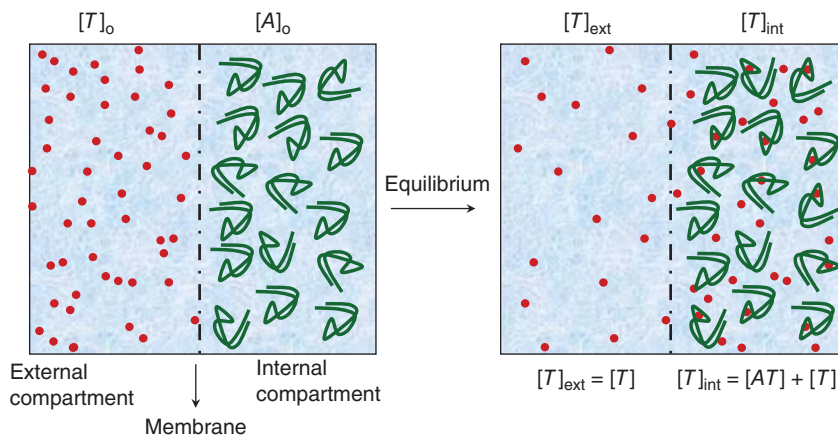


Figure 4.2 Experimental setup used in equilibrium dialysis. Dots represent the target molecules (T) and the folded structure is the aptamer (A).

only the smallest component will pass through the membrane (the target in Figure 4.2), the analysis of the total amount of this component in the two phases provides the required information for the study of binding. The concentration of the free (unbound) component able to pass through the membrane is identical in the two compartments at equilibrium, so the concentration of this component in the chamber where there is no big partner yields its equilibrium concentration in the mixture. The bound fraction is obtained by difference.

Equilibrium dialysis is simple, inexpensive, and easy to perform. It requires a small amount of sample (25–500 μl with microdialyzers commercially available), and generally yields satisfactory results. However, it is tedious, requiring long times to achieve equilibrium (typically in the range 12–48 hours). Another complication is the possibility of dilution errors. Since the membrane is impermeable to the largest partner, there is an osmotic pressure between the two compartments, which may lead to a net solvent flow into the chamber containing the largest reagent. This will change the volumes of the solutions in the two compartments; although if the concentration of the largest component is very low, this volume change will be unimportant. Problems may also arise from adsorption of the reagents to the membrane, and control experiments should be carried out to take into account this effect. In practice, dialysis equilibrium has been mainly applied to study the binding of small molecules such as ochratoxin A [27, 28], cortisol [29], tyramine [30], and glycine [31].

Much faster acquisition of binding data may be achieved by ultrafiltration. In this case, the binding equilibrium between aptamer and target is established, and then the equilibrium mixture is passed through the ultrafiltration membrane under an applied hydrostatic pressure, which may be obtained using pressure, vacuum, or centrifugal force. Solutes larger than the largest pores in the membrane are retained, while those smaller than the smallest pores pass the membrane, and the concentration of the smallest unbound component is measured to calculate the affinity constant. Adsorption of the free component to the membrane and filtration assembly can be a serious problem, and again

proper control experiments must be performed. Another cause of error is the incomplete retention of the AT complex by the membrane due to retention efficiency lower than one. Nitrocellulose filter binding has been extensively used to investigate binding properties of protein–aptamer complexes. In this case, protein and protein–aptamer complexes will be retained, but not free aptamer. In combination with ^{32}P -labelled aptamers and high sensitive radioactive measurements, this method can be employed for obtaining dissociation constants in the low pM range [32–34]. Improvements in accuracy and precision are achieved by placing an anion exchange membrane directly beneath the nitrocellulose membrane as a trap for the aptamer not retained by nitrocellulose. In this way, the radioactivity retained in both the nitrocellulose membrane (bound aptamer) and the anion exchange membrane (free aptamer) is measured, improving the quality of data [35].

4.2.2.2 High-Performance Liquid Chromatography

Liquid chromatography can be used for the separation of free and bound aptamer based on their differential migration through a chromatographic bed (stationary phase) carried by a flowing liquid (mobile phase). Size exclusion chromatography (SEC), also called gel filtration, is one of the possible separation mechanisms for obtaining binding data. It is based on differences in molecular size, with small molecules being retained and large species eluting first. A stationary phase that excludes the largest interacting component is usually selected. In this way, AT complex and the free fraction of this component is analyzed in the void volume (V_0), whereas the free fraction of the other component is analyzed from the corresponding chromatographic peak.

The most common in aptamer binding assays is the use of affinity chromatography in combination with frontal elution [36, 37]. The aptamer is immobilized to a solid support to form the stationary phase, and a solution of the target is applied continuously at constant concentration, $[T]_0$, to the column, giving rise to an elution front and a plateau. Once dynamic equilibrium is reached in the column, the concentration of free target, $[T]$, is constant and equal to the initial concentration since T is continuously supplied. The elution front will be retarded to an extent corresponding to the amount of immobilized target, and thus the volume, V , of the target solution needed to saturate the column is used to determine the bound fraction, equal to $[T]_0(V - V_0)$. V_0 is the volume required to elute a nonretained molecule. The dissociation constant can be related to the chromatographic parameters as follows:

$$K_D = \frac{[T]_0\{[A]_0 - [T]_0(V - V_0)/\nu\}}{[T]_0(V - V_0)/\nu} = \frac{A_t}{V - V_0} - [T]_0 \quad (4.12)$$

where $[A]_0$ is the amount of immobilized aptamer per unit of volume of affinity adsorbent, ν is the bed volume of the column, and A_t the total amount of aptamer ($[A]_0\nu$). Equation (4.12) can be rearranged to

$$\frac{1}{[T]_0(V - V_0)} = \frac{K_D}{A_t} \frac{1}{[T]_0} + \frac{1}{A_t} \quad (4.13)$$

Therefore, by obtaining V values for different initial target concentrations, the reciprocal of $[T]_0(V - V_0)$ is a linear function of the reciprocal of $[T]_0$, and the

dissociation constant and the amount of active aptamer can be obtained from the slope and intercept of the corresponding plot [38]. This method has been applied to the estimation of the affinity constant for small targets such as adenosine [36, 37] but also proteins [39], although a relatively large amount of target is required to complete the experiment.

4.2.2.3 Electrophoresis

Electrophoresis is a particularly versatile technique for the separation of biomolecules, based on the differential migration of the species under the effect of an electric field. Since aptamers are polyanions and the formation of the AT complex may influence its electrophoretic mobility, the migration pattern of the interacting mixture under an electrical field can be used to quantitate and identify specific AT binding and estimate the binding constants.

The classic electrophoretic technique uses a small slab or strip of plastic material covered by a porous substance (a gel), which is impregnated with an electrolyte buffer. The strip is immersed by its extremities into the reservoirs containing the same electrolyte and linked to the two electrodes of a continuous voltage supply. This technique has been used for decades to evaluate strong interactions between proteins and DNA [40]. The preincubated mixture of DNA and protein (at different ratios) is deposited in the form of a band on the gel, and under the external electrical field unbound DNA is separated from complexed DNA because of differences in their electrophoretic mobility. Amounts of both fractions are estimated by densitometry or radioactive counting of the bands (using radiolabeled DNA in the assay), and used for the affinity constant estimation. This classical method is useful for the study of aptamer binding provided that the AT interaction alters the electrophoretic mobility of the aptamer. In addition, the AT complex has to be stable enough to ensure there are no significant changes in free and bound aptamer during the course of the electrophoresis experiment (30–60 minutes). An implicit assumption is that the binding constants are not influenced by the electrical field. The high resolution of contemporary gel electrophoresis methods are however detrimental to the survival of most aptamer binding interactions and thus this technique is not frequently used in aptamer characterization.

Capillary electrophoresis (CE), an adaptation of the general electrophoresis methodology carried out inside capillaries that connect anodic and cathodic buffer reservoirs, is a preferable technique for the study of molecular interaction with aptamers. CE is a rapid, high-resolution technique that has been used as the separation technique during the SELEX process, shortening the selection procedure and allowing aptamers with high affinity and specificity to be generated with a much higher rate of enrichment [41–43]. In addition, various CE modes have been used for quantitative binding studies [44]. Among them, three are the particular modes of what is called affinity capillary electrophoresis (ACE), a CE separation where the separation patterns are influenced by reversible molecular binding interactions taking place during the separation process in free solution [45], which have been used in aptamer characterization: dynamic equilibrium ACE, pre-equilibrium ACE, and kinetic ACE [46].

Estimation of binding constants by dynamic equilibrium ACE involves adding the target in the running buffer (in varying concentrations) and measuring the change in the electrophoretic mobility of the injected aptamer. For 1 : 1 interactions, the electrophoretic mobility shift of the aptamer with changing target concentrations can be used to obtain the affinity constant using Eq. (4.14):

$$\mu_i = \frac{\mu_f + \mu_c K_A [T]}{1 + K_A [T]} \quad (4.14)$$

where μ_i is the electrophoretic mobility of the aptamer with the different target concentrations in running buffer, μ_f the electrophoretic mobility of free aptamer (in the absence of target), and μ_c the electrophoretic mobility of the AT complex. The experimental data are fitted using nonlinear regression to obtain the affinity constant or alternatively linear plots, similar to that used in other techniques (see Section 4.2.1) can be employed [47]. This method assumes that the equilibrium between the aptamer and the target is established very quickly in the capillary; therefore, it is valid for the study of rapid interactions, where the binding-equilibrium relaxation time is short with respect to the separation time [46].

For slow interaction kinetics, preequilibrium ACE is recommended. In this ACE mode, aptamer and target are preequilibrated together before injecting into the capillary. The bound and free aptamer will appear as separate peaks in the corresponding electropherogram when a small volume of the equilibrated solution is injected, and the binding constant is obtained from some of the plots explained in Section 4.2.1. It is important that the AT complex is long-lived compared to the separation time. This separation mode has been frequently used in combination with laser-induced fluorescence detection for characterizing aptamers specifically recognizing proteins, such as IgE [48], thrombin [49], vascular endothelial growth factor (VEGF) [50], and HE4 protein (an ovarian cancer biomarker) [51].

Kinetic methods are useful for intermediate situations, when the timescales for separation and chemical interaction are more similar, and, in consequence, they provide information about the association and dissociation rate constants. This ACE mode is explained in Section 4.3.

4.2.3 Direct Methods

As discussed, direct methods for thermodynamic characterization of the aptamer–target binding do not require a physical separation of the complex from the free partners for quantifying the affinity constant, thus enabling the measurement of even low-affinity interactions (particularly those with fast dissociation rates) with no risk of perturbing equilibrium, and, of course, the procedure is less cumbersome and, in turn, faster and simpler. This section reviews the homogeneous approaches most frequently used over the recent years for measuring AT interactions. The most common heterogeneous approaches provide information not only about thermodynamics but also about binding kinetics, and they are dealt with in Section 4.3.

4.2.3.1 Isothermal Titration Calorimetry

In general, a molecular binding event between an aptamer and its cognate target causes heat to be released or absorbed; and this heat transfer, which is proportional to the extent of binding, can be directly measured by isothermal titration calorimetry (ITC). Unlike other techniques, ITC provides a detailed thermodynamic picture of the molecular interaction, i.e. binding constant (K_A), reaction stoichiometry (n), enthalpy change (ΔH), entropy change (ΔS), and Gibbs free energy change (ΔG). All this information is obtained by titration or stepwise addition of one partner (titrant) into a sample solution containing the other partner involved in the binding process (titrand); both partners are therefore free in solution, with no need to be labeled [52].

ITC analysis requires a heat-flow calorimeter (Figure 4.3a) that works following the principle of dynamic power compensation, that is, it measures the thermal power ($\mu\text{cal s}^{-1}$) needed to maintain constant the temperature difference between the sample cell and the reference cell, this one being close to zero ($\Delta T < 10^{-6} \text{ }^\circ\text{C}$). Initially, the system applies a small power to the sample cell where the titrand is placed, which determines the baseline level. Then, each injection of the titrant from the syringe triggers the molecular recognition reaction and, depending on the affinity and concentration of the reactants in the cell, a certain amount of affinity complex is formed. It is accompanied by a release or absorption of heat that causes a temperature difference between the two cells, and this is compensated for in the calorimeter by applying a

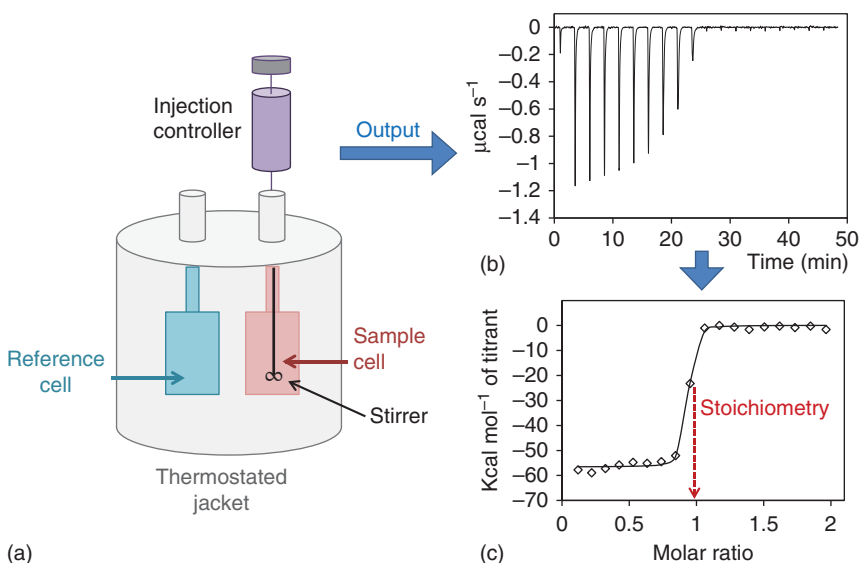


Figure 4.3 (a) Schematic setup of ITC. Sample and reference cells are placed into an adiabatic jacket and set at the same temperature ($\Delta T < 10^{-6} \text{ }^\circ\text{C}$). An injection device allows addition of titrant to the sample cell and mixing the solution. (b) Example of a raw ITC thermogram for an exothermic reaction. (c) The binding isotherm from the integrated thermogram fitted to a single-site binding model. Source: Amano et al. 2016 [53]. Copyright (2016). Adapted with permission of American Chemical Society.

heating power (feedback mechanism). After each injection, the system returns to equilibrium [54].

The signal, heat power, in each injection takes the form of a peak. By integrating the area under the peak and assuming the baseline as a reference, the amount of heat associated with the injection is obtained. Since the experiment constitutes a closed thermodynamic system, for each addition of titrant the heat absorbed or released is given by

$$q = V\Delta H \Delta[T_B] \quad (4.15)$$

where V is the reaction volume, ΔH is the enthalpy change in kcal (mol ligand)⁻¹, and $\Delta[T_B]$ is the change in bound titrand concentration that, assuming a 1 : 1 stoichiometry, corresponds to $\Delta[A-T]$. And the total cumulative heat absorbed or released (Q) is

$$Q = V\Delta H \sum \Delta[AT] = V\Delta H[AT] \quad (4.16)$$

In Figure 4.3b, an exothermic binding reaction is depicted, which means the sample cell becomes warmer than the reference cell, thus giving rise to a downward peak per each injection plotted vs time. The binding isotherm (Figure 4.3c) is obtained by integrating the area of each peak and plotted vs the molar ratio of aptamer/target (provided that the aptamer is the titrant dosed from the syringe). It can be fitted to a binding model from which n (also estimated from the titration equivalence point), ΔH , and K_A are determined; whereas ΔG and ΔS are calculated using Eqs. (4.8) and (4.9), from just a single titration experiment.

Data analysis in ITC could seem somewhat cumbersome, but recent improvements in software have made this technique increasingly user-friendly. Likewise, a detailed protocol including a video with tips on how to avoid potential issues in ITC experiments can be found in Ref. [55].

Traditional ITC allows precise determination of binding constants (K_A) between 10^3 and 10^9 M⁻¹. However, extension of the upper limit of this affinity window becomes particularly interesting for quantifying high-affinity aptamer–macromolecule interactions, and several approaches have accordingly been proposed. Sigurskjold [56] developed a displacement titration methodology where a weaker ligand, whose affinity is in the accessible window of ITC, is prebound to the target with the aim of decreasing the apparent affinity of the high-affinity ligand of interest. A previous standard titration of the target with the weak ligand is required; therefore, two separate titrations are performed in total. The new range of affinities measurable by ITC will depend exclusively on the weak ligands available. The application of the displacement method is limited when one wants to study high-affinity interactions involving hydrophobic ligands due to solubility limitations at the high ligand concentrations required filling the injection device. In that case, an ITC competition strategy has been reported, where a mixture of high-affinity and moderate-affinity ligands is titrated with the binding macromolecule for which the two ligands compete. A single titration resulting in a biphasic isotherm allows characterizing both ligands [57]. Alternatively, if the solubility problems affect the target macromolecule, a single-experiment displacement assay where titration of the high-affinity ligand into a solution containing the target bound to the moderate-affinity ligand, as

well as an excess of the latter, has been proposed [58]. The previous approaches, even if not yet applied to the characterization of AT binding, have been used, for example, to quantify the binding of nucleotide inhibitors [59] to protein targets; therefore, straight adaptation to quantify AT interactions could be expected.

ITC goes beyond the affinity measurement and allows studying the mechanism of the molecular interaction, particularly the nature (hydrophilic or hydrophobic) as well as the driving force. With proteins, both thermodynamic signatures were reported. The binding of thrombin [60, 61], VEGF₁₆₅ [62], and acute myeloid leukemia 1 (AML1) protein [53] aptamers was found to be controlled by a favorable enthalpy change ($\Delta H < 0$) accompanied by an unfavorable but compensated entropy contribution ($\Delta S < 0$). Conversely, lysozyme [63] and 33-mer gliadin peptide [23] interact with their respective DNA aptamers in accordance with an entropic driving force, that is, large positive entropy together with small but positive enthalpy. This energetic pattern is usually associated with the release of ordered water molecules upon complex formation between the aptamer and a hydrophobic target [64], as is the case for 33-mer gliadin peptide. The case of lysozyme is rather bizarre since its DNA aptamer has not been SELEX-selected but transcribed from the *in vitro* evolved RNA analog, and directly applied in analytical assays with modest results. This quick fix to avoid RNA manipulation is not necessarily feasible as demonstrated for anti-dopamine RNA and DNA aptamers [65]. The entropy-driven binding between lysozyme and its DNA aptamer has been attributed to electrostatic interactions rather than to sequence specificity.

The interaction of aptamers with small molecules such as antibiotics [22], organic dyes [19], L-tyrosinamide [20], adenosine [21], flavin [66], and 2'-deoxyguanosine [67] has been proved to be an enthalpy-driven process. Strikingly, recent ITC experiments have demonstrated that cocaine-binding aptamer is capable of switching from one- to two-site ligand binding by decreasing the concentration of NaCl [68]. The two ligand-binding sites are independent, with different affinity and enthalpy. Indeed, ΔH becomes more negative after the occupancy of the second low-affinity site, supporting the crucial role of electrostatic interactions in ligand binding at the second binding site.

Hence, ITC is a powerful, label-free, homogeneous technique that allows a thermodynamic in-depth analysis of aptamer–small molecule and aptamer–macromolecule interactions, as well as accurate quantification of binding constants around 10^9 M^{-1} or even higher by implementing displacement or competition assays. Moreover, it is also worth mentioning that Burnouf et al. [69] have developed a new method named kinetic isothermal titration calorimetry (KinITC) that, from a classical ITC experiment, provides not only thermodynamic but also kinetic data about binding processes. This promising tool paves the way for more complete information about the recognition and binding of an aptamer and its cognate target. Currently, consolidated kinetic methods are discussed further in this chapter.

4.2.3.2 Fluorescence-Based Methods

Alternative to the label-free homogeneous method explained earlier, in-solution fluorescence-based methods exploit the outstanding sensitivity of fluorescence

techniques, capable of detecting fluorophore concentrations down to the low picomolar range, for AT binding characterization. In a fluorescent mix-and-measure assay without separation or washing steps, the AT complex formation equilibrium remains undisturbed, but it requires distinguishing between bound and free fluorescent partners, and this entails the modulation of the fluorophore signal by the binding event. This can be achieved by detecting a change in the local environment surrounding the fluorescent dye (fluorescent quantum yield) [70, 71], a molecular rearrangement (fluorescence quenching [72], particularly stressing aptamer beacons [73], as well as Förster resonance energy transfer or FRET [74]), by measuring the increase in size of the AT complex (fluorescence polarization, FP), or a change in molecular properties as a consequence of a thermal gradient (MicroScale Thermophoresis, MST). Obviously, labeling one or both binding partners with a fluorophore or a quencher may affect the binding process; and with a view to exclude this possibility, suitable controls should be performed.

Fluorescence Anisotropy/Polarization FP measures the capability of a fluorophore to emit depolarized radiation when excited with plane-polarized light, being the main cause of depolarization of its rotational diffusion [75]. Generally, after excitation of the fluorescent molecules present in a sample with plane-polarized light, the light emitted in the parallel (I_{\parallel}) and perpendicular (I_{\perp}) planes with respect to the incoming light can be detected with the help of a polarizer, and such intensities are related to the polarization, P , as follows:

$$P = \frac{I_{\parallel} - I_{\perp}}{I_{\parallel} + I_{\perp}} \quad (4.17)$$

Another term frequently used in the context of polarized emission is anisotropy, r , defined as

$$r = \frac{I_{\parallel} - I_{\perp}}{I_{\parallel} + 2I_{\perp}} \quad (4.18)$$

The information provided for the polarization and the anisotropy is equivalent. If there is no rotation of the fluorophore during the lifetime of its excited state (ns), the fluorophore keeps its original orientation and P reaches its maximum value. However, if the fluorescent molecule rotates, the emitted light aligned with the source decreases to some extent; therefore, P decreases.

The Perrin equation [76] reflects the dependence of the observed polarization with the rotational rate as well as with the excited state lifetime of the fluorescent probe.

$$\frac{1}{P} - \frac{1}{3} = \left(\frac{1}{P_0} - \frac{1}{3} \right) \left(1 - \frac{3\tau}{\rho} \right) \quad (4.19)$$

where P is the observed polarization, P_0 is the limiting polarization when there is no rotation and it can be considered as a constant, τ is the excited state lifetime (the interval between absorbing and emitting a photon, typically several nanoseconds), and ρ is the rotational relaxation time. For a spherical molecule, this is defined as $\rho = 3\eta V/RT$; with V molecular volume, η viscosity, T temperature,

and R the universal gas constant. For a spherical protein, however, the rotational relaxation time is $\rho = [3\eta M(\nu + h)]/RT$, with M molecular weight, ν partial specific volume, and h degree of hydration.

Therefore, polarization increases with the rotational rate, whereas it decreases as the excited state lifetime of the dye increases. Moreover, keeping other conditions constant, rotational rate is inversely related to molecular volume or molecular weight of the fluorescent molecule; and hence a large molecule is prone to keep the same orientation, while a small molecule tends to tumble and disorient.

FP can be used for quantifying the strength of a binding event, provided that this one triggers a change in the rotational rate of a fluorescent binding partner. If the fluorescent dye is attached to a small molecule, the rate at which it rotates can diminish dramatically when it is bound to a large molecule, passing from low FP values in the unbound state to high FP values when included in the complex. Conversely, if the fluorophore is anchored to a large molecule, this one rotates too slowly for recording a significant variation in polarization after binding to its partner. In consequence, less accurate results will be obtained with the second approach, thus being preferable to the fluorescent labeling of the smaller binding partner (Figure 4.4a).

In the context of investigating AT interactions, the binding of an aptamer to a large molecule such as thrombin [77], human heat shock factors [78], norovirus [79], VEGF₁₆₅ [50], and lactoferrin [80] has been tackled by labeling the nucleic acid partner, i.e. the DNA or RNA aptamer, with a fluorescent dye for maximizing the variation in the FP signal. Likewise, an insightful study of the aptamer–thrombin interactions has been carried out using fluorescence anisotropy [77].

In contrast, when the cognate target of the aptamer is a small molecule, the fluorescent probe is usually attached to the target [81], although the reverse labeling configuration has been also reported [82]. Affinity binding of small molecules to their aptamers often results in modest FP changes, which leads to less accurate determination of binding constants. To circumvent this limitation, several strategies based on increasing the differences in size of bound and unbound fluorescent binding have been proposed. These amplification strategies use aptamers with dual binding affinity [83], anchor protein modules [84], or nanomaterials [85]. These methods, however, introduce a certain degree of complexity in the procedure; and in the particular case of nanomaterials, fluorescence quenching phenomena could interfere.

Two different assay formats have been employed for thermodynamic characterization by FP: saturation and competition binding analyses; therefore, affinities of both fluorescent partners and unlabeled competing partners can be reliably measured. These studies are performed in a conventional fluorometer additionally equipped with polarizers, and the procedure is easily automated (Figure 4.4b).

MicroScale Thermophoresis Besides a heat flow, a thermal gradient in an aqueous solution of (bio)molecules induces the movement thereof, i.e. a molecular flow. This phenomenon, called thermophoresis, thermodiffusion, or Soret effect, was first described by Ludwig in 1856, but its theoretical foundation is still under debate [86]. In general, thermophoresis is depicted as a molecular flow that

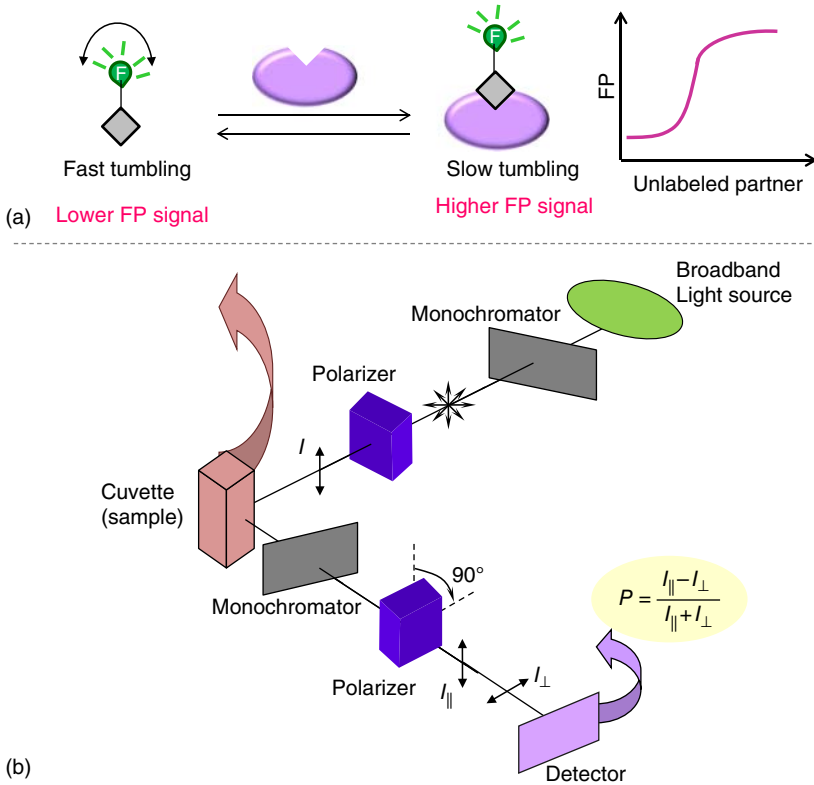


Figure 4.4 (a) Typical fluorescence polarization assay (saturation binding analysis). Under equilibrium conditions, the fluorescent smaller partner has much lower polarization value compared to that of the fluorescent binding complex. (b) Scheme of a spectrofluorometer for FP measurements (L-format or single channel). The second polarizer, located in the emission light path, is rotated along parallel and orthogonal directions to record I_{\parallel} and I_{\perp} , respectively.

linearly depends on the temperature gradient, with a proportionality constant, D_T , called the thermal diffusion coefficient. This mass flow overlaps to ordinary mass diffusion described by Fick's law. As a result, the total mass flow rate under the application of a nonuniform temperature can be written as

$$j = -cD_T \nabla T - D \nabla c \quad (4.20)$$

where D is the diffusion coefficient, c the molecule concentration, and T the temperature. This means that if a temperature gradient is applied to a dilute solution, in the absence of convection, the system will reach a steady-state concentration gradient ($j = 0$):

$$\nabla c = -cS_T \nabla T \quad (4.21)$$

where $S_T = D_T/D$ is the Soret coefficient, representing the degree of separation of the molecules or strength of the thermophoretic effect. Therefore, if a temperature difference ΔT is applied across a capillary, where convective effects

are expected to be negligible, and provided that S_T can be taken as temperature independent within the range of temperature studied, the integration of Eq. (4.21) provides the steady-state concentration of the molecule in the hot area, c_{hot} , related to its value in the cold area according to

$$c_{\text{hot}}/c_{\text{cold}} = \exp(-S_T \Delta T) \quad (4.22)$$

Molecules typically move out of regions with enhanced temperature ($c_{\text{hot}} < c_{\text{cold}}$) and this thermophoretic depletion depends on the size and charge of the molecule as well as the hydration shell. The binding event between the molecule and its partner induces a change in one or more of these parameters, which can be monitored by the MST technique using fluorescence detection, allowing the analysis of the affinity interaction.

In an MST experiment, a temperature gradient (typically 2–6 °C) is induced by an infrared laser, and the resulting movement of molecules is detected and quantified by fluorescence. MST is measured in glass capillaries of 4 μl (total volume) containing both binding partners, one of them either intrinsically fluorescent or turned into that by covalent attachment of a fluorophore. The sample in the capillary is locally heated with an infrared (IR) laser arranged in the same optical device used for fluorescence excitation/emission (Figure 4.5a). Changes in the thermophoretic mobility of the fluorescent partner are monitored in several capillaries with increasing concentration of the nonfluorescent binding partner. A maximum of 16 capillaries can be scanned in a single experiment [87].

The typical signal of an MST experiment is shown in Figure 4.5b. Prior to switching on the IR laser, molecules are homogeneously distributed at room temperature and constant fluorescence intensity is recorded. As soon as the IR laser is switched on, the sample is heated and, just before thermophoretic motion of the molecules starts, a sharp decrease in fluorescence takes place during less than a second (temperature jump or T-jump). This is due to a change in the fluorescence yield of the fluorophore as a result of the change in temperature. Immediately afterwards, thermophoresis occurs for several seconds, and fluorescence intensity slowly decreases before leveling off (steady state). Then, the IR laser is switched off, the sample cools down, and an inverse T-jump is observed. Finally, the initial fluorescence intensity is recovered, which is only related to mass diffusion. Thermophoretic depletion profiles for the fluorescent partner unbound and bound to different concentrations of its partner are illustrated in Figure 4.5c. For each profile, the change in the normalized fluorescence $F_{\text{norm}} = F_{\text{hot}}/F_{\text{cold}}$ (values marked in Figure 4.5c) is determined.

Taking into account that for small temperature and concentration changes, as is the case in MST experiments, Eq. (4.22) can be approximated to a lineal variation:

$$c_{\text{hot}}/c_{\text{cold}} \approx 1 - S_T \Delta T \quad (4.23)$$

The normalized fluorescence is a measure of S_T , which changes for free and bound partners. Therefore, F_{norm} values are plotted vs the concentration of the nonfluorescent ligand and fitted to a suitable binding model in order to infer K_A .

Regarding MST strengths, since molecule migration is mainly limited by diffusion, the temperature gradient generated with the IR laser is constrained to a micrometric region of the sample; this way, changes in thermophoretic mobility

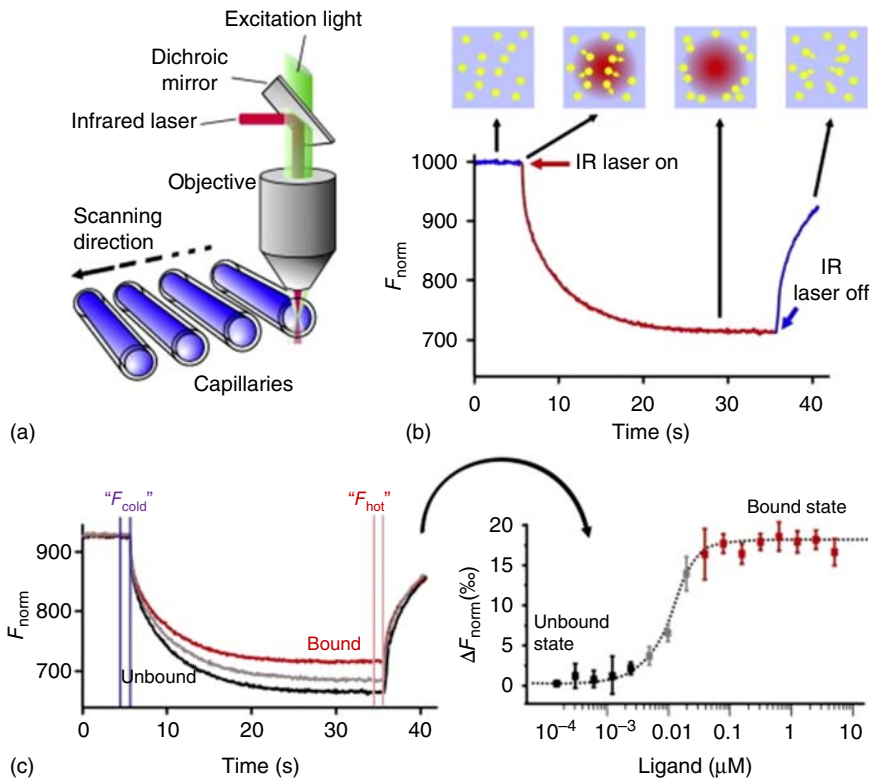


Figure 4.5 (a) Schematic representation of the experimental setup for MST measurements. (b) Typical MST signal – fluorescence intensity over time – for a single capillary. (c) Binding experiment based on MST measurements. See the main text for details. Source: Entzian and Schubert 2016 [87]. Copyright (2016). Reprinted with permission of Elsevier.

can be observed and quantified in less than one minute, and thereby fast MST analyses are performed.

Recently, sample consumption in MST measurements was significantly reduced by performing the experiments in nanodroplets instead of glass capillaries [88]. Droplets are reproducibly generated with a commercially available system by acoustic droplet ejection into multiple-well plates. Its applicability in quantifying biomolecule interactions was evaluated with the system adenosine-binding aptamer and its cognate target, and compared to previous results recorded by capillary-based MST. Clear concordance between both setups was obtained. This new approach represents an important step forward for automation of the MST technique.

Unlike FP based on large size changes of the fluorescent binding partner, which imposes the titration of the bigger partner with the fluorescently modified smaller one, MST possesses a more flexible assay design because of its sensitivity to more than one molecular properties; namely, size, charge, and hydration shell. Therefore, in the absence of intrinsic fluorescence, any of the two partners can be labeled for its further titration with the other partner, thus circumventing

possible effects on the binding behavior (labeling of small binding partners tends to be detrimental).

This freedom of design widens the applicability of MST to virtually any molecular interaction. For example, it has been reported that the use of MST for the measurement of the binding affinity of aptamers for proteins, such as thrombin [89], protein A [90], β -conglutin [91], and HIV-1 integrase [92]. In the latter case, MST has been applied to gain insight into the interaction between the viral enzyme HIV-1 integrase and its inhibitor aptamer d(GGGT)₄, a 16-mer DNA adopting a G-quadruplex structure, by introduction of point abasic sites in the aptamer sequence. By recording the thermophoretic profiles of the mutants with the fluorescently labeled protein and comparing their binding constants with that for the natural counterpart, important residues in the molecular interaction have been identified. Although not universal, this strategy could be extended to other G-quadruplex aptamers in combination with traditional structural studies.

Likewise, MST has been employed for characterizing the interaction of aptamers with small molecules, not only model targets such as ATP [87] and ochratoxin A [93] but also estereoids [94, 95]. Thermophoretic results for 17 β -estradiol and progesterone exhibited large variation (modest reproducibility), which may be attributed to their poor solvation in aqueous solutions, even when a small percentage of ethanol was included in the binding solution.

For all these systems, the affinity constants derived from MST experiments were in the 10^9 – 10^5 M⁻¹ range. Although stronger interactions as the binding of single-strand binding protein from *Escherichia coli* to a single-stranded DNA d(T)₇₀ with K_a 10^{12} M⁻¹ have been also determined with this homogeneous technique [96]. Moreover, aptamer binding affinity has been characterized in complex media (serum [89] and food samples [93]) by MST. An abrupt decrease (6000 times) in ochratoxin A (OTA)-binding aptamer affinity in food samples (beer) has been ascertained by conventional MST experiments. This loss in affinity turned out to be significantly dependent on the pH of the sample, 4 pH units lower than that in the SELEX medium; while a more subtle effect of composition (e.g. ethanol content) was found. From these results it is clear that, to keep aptamers functional, they should be evolved under conditions as close as possible to their application.

To sum up, although the phenomenon on which it is based was already described in the nineteenth century, MST is a newly developed and highly promising technique. Apart from its immobilization-free nature, its versatility in assay design (even if a fluorophore is required) and in measurement media, as well as the low sample consumption are remarkable.

4.3 Kinetic Characterization

The extent to which an aptamer is bound to its ligand at equilibrium (the binding affinity) is the main criterion employed for the aptamer selection, assuming that affinity is an appropriate surrogate for the efficiency of the aptamer in the different applications. But kinetics of aptamer–ligand binding could be as important as affinity in determining its efficacy.

The rates at which AT association and dissociation occur, as reflected by the rate constants k_{on} and k_{off} defined in Eqs. (4.1) and (4.2), provide additional information about the mechanism of the interaction. As stated earlier, binding affinity depends on the change of Gibbs free energy of binding according to Eq. (4.9), i.e. the difference in free energy between the bound and unbound states (Figure 4.6a). Conversely, on- and off-rates depend on the local free energy maximum that separates both states, called the transition state. Therefore, K_{D} is determined by stable molecular interactions between the aptamer, target, and solvent, whereas the rate constants k_{on} and k_{off} depend upon transient interactions along the binding pathway, much more difficult to observe. In fact, very different kinetics can result in the same affinity as is shown in Figure 4.6b, where iso-affinity lines are defined in the space spanned by association and dissociation rate constants. Destabilizing only the transition state decreases both rates without altering affinity; on the contrary, stabilizing, for example, the bound state will decrease the off-rate without altering the on-rate and increasing the affinity. This has been achieved with the new class of aptamers called SOMAmers (slow off-rate-modified aptamers) that employ nucleotides modified with different functional groups to expand their chemical diversity for selecting protein-binding receptors. The majority of SOMAmers selected bind their target proteins with high affinity ($K_{\text{D}} < 1$ nM), due primarily to slow complex dissociation rates, on the order of 10^{-4} – 10^{-5} s $^{-1}$ [97]. The rational modulation of aptamer binding kinetics is thus another way of optimizing aptamers.

Measuring the change in concentration of a reagent (disappearance) or a product (accumulation) as a function of time once the binding partners have been

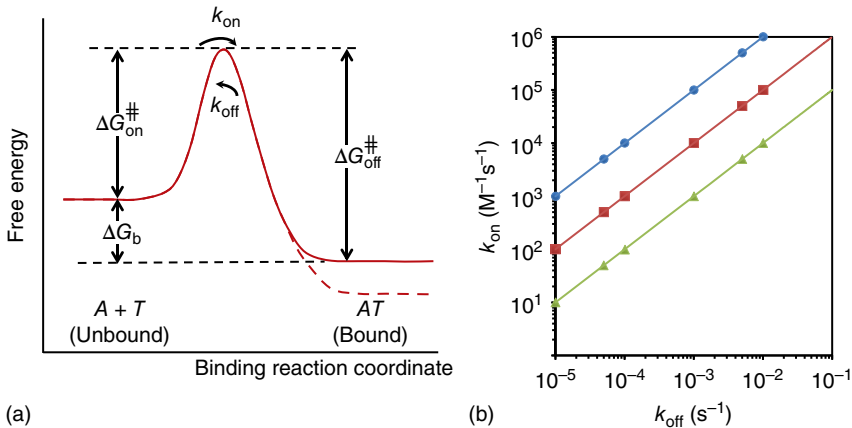


Figure 4.6 (a) Free energy profile of binding of aptamer, A, to target, T, to form the AT complex. Binding affinity depends on the free energy difference between the unbound and bound states, ΔG_{b} . The free energy difference between these states and the transition state, $\Delta G_{\text{on}}^{\ddagger}$ and $\Delta G_{\text{off}}^{\ddagger}$, determines the association and dissociation rate constants. The dashed profile shows modulation leading to an increase in affinity constant by slowing the dissociation process. (b) Simulated kinetic profiles showing that the same binding affinity (iso-affinity lines) may be achieved with different association and dissociation rates.

mixing underpins most analytical methods used for kinetic studies of AT interactions. They can be clustered in two main groups, i.e. heterogeneous methods, those involving a immobilized binding partner (such as surface plasmon resonance (SPR), and electrochemical impedance spectroscopy (EIS)) and homogeneous, those used with in-solution interactions (stopped-flow analysis, rotating droplet electrochemistry (RD), kinetic CE, and nanopore-based studies). Both types of methods are discussed here by paying special attention to their general principles and applications, as well as comparative advantages and limitations.

4.3.1 Heterogeneous Methods

4.3.1.1 Surface Plasmon Resonance

SPR spectroscopy is an optical, surface-sensitive, label-free, and real-time technique that enables to measure the binding kinetics as well as the affinity between an aptamer and its cognate target; and because of its high performance, it has become an established technique for characterizing biomolecular recognition events. Generally, one of the interacting partners is immobilized on a metal surface, typically a gold film, and its interaction with the other partner in solution is monitored in real time by making use of the change in refractive index, n , in the near vicinity of the metal surface as a result of the complex formation [98].

Surface plasmons occur as a consequence of collective oscillations of the free electrons in the conduction band of a metal that, when the metal layer is very thin, take place only on the surface. They are charge density waves generated at the interface between a metal and a dielectric medium, by application of an electromagnetic field with certain characteristics, and propagate longitudinally along the interface. SPR, for its part, is an optical phenomenon arising from the interaction of an electromagnetic evanescent wave generated by total internal reflection of a light beam at the interface between a metal and a dielectric, and mobile electrons on the metal surface. If, and only if, its energy coincides with that of the plasmons, the SPR or energy coupling occurs. In that case, an energy transfer takes place to each other, resulting in a minimum in the reflected radiation, since part of the energy of the incident beam is transmitted to the electrons, that is, it is not reflected and therefore does not reach the detector. In short, when the resonance occurs, a minimum in reflectivity, also known as *dip*, is observed. Besides, for each incident wavelength, SPR appears only at a certain angle of incidence, which depends strongly on the refractive index near the metal surface. This angle is referred to as SPR angle. A more detailed explanation of the basis of SPR can be found in specialized handbooks [99].

To reproduce the phenomenon of SPR, SPR instruments consist of an optically dense (high n) prism on which a sensor is positioned (optically coupled to the prism by means of an index-matching oil). The sensor comprises a thin metal layer, typically gold, in contact with a dielectric of lower refractive index than that of the prism, usually an aqueous medium (Figure 4.7a). One of the interacting partners, aptamer or target, is anchored to the metal film, while the other one remains in the aqueous solution in contact with the sensor. When p-polarized monochromatic light is directed to the metal–dielectric interface with an angle of incidence superior to the critic angle, an evanescent wave is generated and

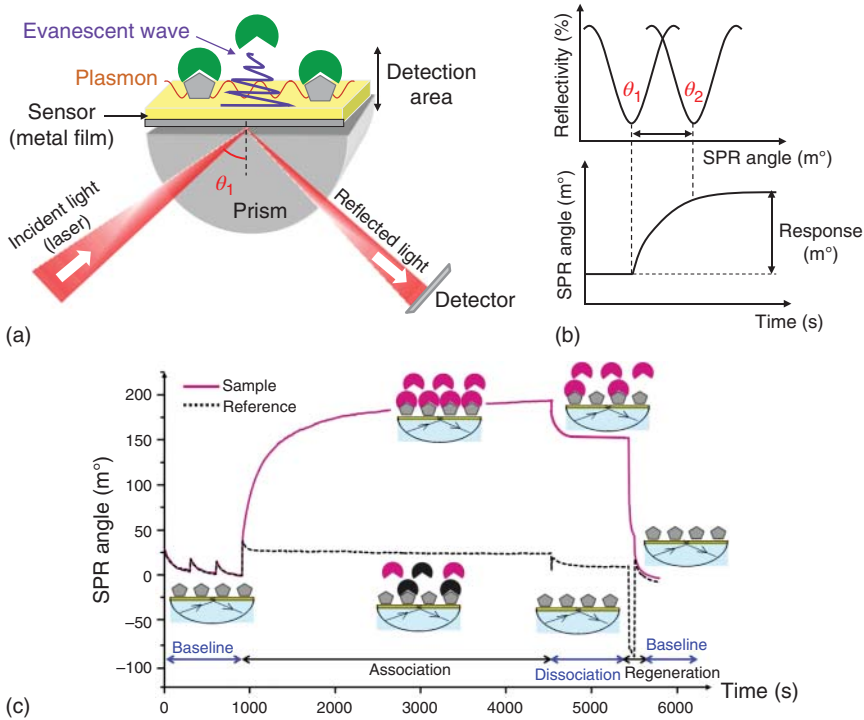


Figure 4.7 (a) Typical setup for SPR measurements (Kretschmann configuration). (b) Reflectivity vs. angle of incidence depicts a drop in reflected light or dip, as a result of SPR. The angular position of the SPR dip is measured over time. (c) Variation of SPR angle as a function of time or *sensorgram* for a typical SPR experiment involving association, dissociation and regeneration steps.

interacts with the surface plasmons, transferring energy to thereof only at the SPR angle. As the interacting partner in solution binds to the anchored partner, the SPR resonant conditions change and the shift in the SPR angle can be monitored over time, providing information on the biomolecular binding (Figure 4.7a,b).

The generated evanescent wave decays exponentially with the distance from the sensor surface and its penetration depth depends on the wavelength of the incident light (λ) being around $\lambda/2$. This value determines the distance to which the technique is sensitive, meaning that the instrument becomes blind to variations in the refractive index far away from such a limiting distance. Thus, particles larger than $\lambda/2$ could only be studied qualitatively. By way of example, in order to excite surface plasmons at a gold thin film, radiation around 670 nm should be used; as a result, instrument sensitivity is constrained to 300–400 nm from the metal surface.

According to the optical system configuration, SPR instruments can be classified into three groups: (i) those monitoring the SPR angle over time (they are the most widely used for AT characterization studies), (ii) instruments recording the wavelength vs time, and (iii) those measuring the reflectivity at a fixed angle with time. On the other hand, depending on the way to administer the sample

to the sensor, two options are possible: flow cell systems and cuvette systems. The latter are particularly suitable when limited sample volumes are available for the analyses. In any case, due to its physical principle, this technique lacks intrinsic selectivity since any change in the refractive index that occurs on the metal surface generates a signal variation. Therefore, with the aim of ensuring the specificity of the observed signal variations, an additional channel acting as a blank (reference channel) is indispensable.

Figure 4.7c shows a typical analysis cycle including baseline, association, dissociation, regeneration, and back to baseline steps for both sample and reference channels. Initially, binding buffer is applied to both channels (i.e. sample and reference channels with and without the immobilized partner, respectively) to stabilize the baseline SPR signal. Next, the in-solution binding partner is placed in contact with both channels and a progressive angle variation is recorded in the sample channel, while a negligible angle variation is expected in the reference channel. That is indicative of the fact that a specific interaction (i.e. AT binding) is being monitored in the sample channel (association phase). When the binding process reaches the steady state, binding buffer alone is passed through the channels removing the weakly bound material as well as the previously bound partner to a certain extent (dissociation phase). Eventually, surface regeneration is carried out to completely destroy the complex, followed by binding buffer application to restore baseline. Notice that each step starts with a sharp shift in signal as a result of the change in solution composition.

Characterization of AT binding process (affinity and kinetic constants) can be achieved by two different approaches and, as a way to test the consistency of the estimated values, it is recommended to perform both of them. According to the equilibrium approach, the signal at the equilibrium or the steady-state angle shift, R_{eq} , at different concentrations of the in-solution binding partner, P , can be used to determine binding fractions and obtain K_D from Langmuir binding isotherm:

$$R_{eq} = R_{max} \frac{[P]_{free}}{[P]_{free} + K_D} \quad (4.24)$$

where R_{max} is the maximum angle shift, that is, it represents the maximum capacity of the sensor surface. R_{eq} values are obtained from nonlinear fitting to Eq. (4.25), which considers the exponential nature of association and dissociation processes.

$$R_t = R_0 + E(1 - e^{-k_s t}) \quad (4.25)$$

where R_t is the angle shift with time, R_0 is the angle shift at $t = 0$, $R_{eq} = R_0 + E$, and the apparent rate constant k_s is $k_s = k_{on}[P] + k_{off}$.

The second approach, the kinetic model, implies the estimation of k_s by fitting the association phase for all tested P concentrations to Eq. (4.25). Then, considering the linear relationship between k_s and $[P]_{free}$ rate constants k_{on} and k_{off} can be determined from the slope and the intercept, respectively. And the ratio k_{on}/k_{off} provides the binding affinity K_A . Nevertheless, the uncertainty associated with k_{off} estimation is significant; for this reason, to obtain more reliable k_{off} values, nonlinear fitting of the dissociation phase to a typical first-order exponential decay is recommended. For cuvette-based SPR

instruments, incomplete dissociation is not surprising because this configuration promotes certain rebinding. For such SPR instruments, an extra term, R_∞ , should be included; hence, the equation to be used for fitting becomes

$$R_t = R_0 e^{-k_{\text{off}}t} + R_\infty \quad (4.26)$$

For this heterogeneous kinetic technique, when choosing the partner to immobilize onto the sensor surface, some parameters such as functional groups available, stability, solubility, and size should be borne in mind. Since SPR response is directly related to the mass variation on the sensor surface, immobilization of the smaller binding partner seems to be the most suitable choice to maximize the SPR response. However, the slower diffusion coefficient of the larger partner promotes mass transport limitation (MTL). This physical phenomenon appears when the diffusion velocity of the partner in solution toward the diffusion layer within the binding occurs is slower than the speed at which the binding proceeds. Therefore, it will be a temporary depletion of the free partner in solution, which will delay the binding process and, in consequence, the measured kinetics does not correspond to that for the heterogeneous biomolecular interaction. To minimize this issue, the solution is agitated (mixing system) during the measurement in cuvette-based instruments, whereas a high flow rate is employed in those instruments involving a flow cell system. Moreover, MTL is mitigated by working with low-capacity binding surfaces, but its absence must be verified to obtain valid kinetic measurements.

Detailed SPR-based studies of the interaction between a large target and its aptamer are generally tackled by attachment of the easily modifiable oligonucleotide receptor on the sensor chip using different strategies [53, 100–102]. Among them, hybridization capture strategy deserves a special mention. It entails the annealing or hybridization of the aptamer modified with a poly(A) tail to a biotinylated poly(T) oligonucleotide attached to a streptavidin-coated chip. This non-covalent strategy, first reported by Gopinath et al. [103], allows evaluation of different targets and even different aptamers using the same sensor chip. A variation of this approach is now commercially available, the Biotin CAPture kit, which uses a universal covalently linked oligonucleotide on the carboxymethylated dextran sensor chip. This surface is reversibly modified with a complementary strand-streptavidin conjugate to further bind the oligonucleotide receptor, yielding a regenerated sensor. A few examples involving the opposite approach, binding of the aptamer to a protein-modified surface, have been described [104, 105].

On the other hand, measuring small-molecule–aptamer interactions by SPR spectroscopy remains challenging due to the shift in refractive index triggered by molecules smaller than 1000 Da on a surface with restricted binding sites is insufficient. Even if this lack of sensitivity has been circumvented via aptamer immobilization at higher densities [106], this strategy is not suitable for obtaining kinetic information, unless a fitting model taking account of MTL is used provided that this is not totally limiting. Alternatively, the measurable signal can be increased by immobilization of the small molecule at low density to mitigate mass transport effects [107–110]. Following this idea, immobilization of tobramycin to carboxyl-terminated self-assembled monolayers via carbodiimide

chemistry has been successfully applied to analyze kinetic and binding properties of 2'-O-methylated endonuclease-resistant RNA aptamers to be implemented in real complex samples for antibiotic control. For this particular system, the slight decrease in affinity observed with respect to the natural receptor was fully compatible with its practical application in serum [108].

Summarizing, SPR spectroscopy has proved to be a convenient technique for real-time monitoring of the heterogeneous binding between an aptamer and its cognate target, for a wide range of molecular sizes of the latter. It is well suited to determine dissociation constants from 10^{-12} to 10^{-5} M; likewise, association and dissociation rate constants 10^3 – 10^7 $M^{-1} s^{-1}$ and 0.1 – 5×10^{-6} s^{-1} , respectively, have been quantified for AT complexes. It is worth mentioning that K_D values obtained by SPR spectroscopy smaller than those estimated by solution-phase FP or ITC measurements (with or without labeling) have been reported [53, 62], even though negative surface effects on the binding process have been described when either aptamer or ligand is immobilized, especially in the absence of appropriate linkers. It has been attributed to binding processes with unfavorable entropy changes, whose absolute value is smaller when one of the binding partners is attached to the solid support, thus resulting in a more negative change in Gibbs energy and stronger binding.

In addition to its use for kinetic and equilibrium characterization of aptamer candidates evolved from SELEX as well as upon post-SELEX modifications (truncation and mutations) [111], SPR methodology has been used for monitoring the progress of SELEX enrichment [112]. Particularly, the partitioning step used to separate the target from nonbinding candidates is carried out during the dissociation phase of the sensorgram, albeit flow cell systems are only suitable.

4.3.1.2 Electrochemical Impedance Spectroscopy

EIS has great potential for the analysis of interfacial properties of electrode surfaces, and it is able to provide information about resistance/capacitance changes occurring on conductive or semiconductive surfaces. These changes in the electrical properties of the electrode–solution interface may occur as a consequence of a molecular recognition event; therefore, this technique can be used for kinetic and thermodynamic characterization of AT binding onto an electrode surface on which one of the binding partners is attached.

Impedance, Z , is a measure of the ability of a circuit to resist the flow of electrical current, but in a more general sense than resistance. Electrochemical impedance is usually measured by first polarizing the electrochemical cell at a fixed potential, and then applying an alternating current voltage to perturb the system. Generally, the applied excitation potential is sinusoidal, with small amplitude, and radial frequency ω ; whereas the response to this potential is an alternating current at the same frequency but shifted in phase (φ) [113, 114]. The impedance of the system can be calculated by an expression similar to Ohm's law:

$$Z = \frac{V(t)}{I(t)} = \frac{E_0 \sin(\omega t)}{I_0 \sin(\omega t + \varphi)} = Z_0 \frac{\sin(\omega t)}{\sin(\omega t + \varphi)} \quad (4.27)$$

and with Euler's relationship, it can be expressed as a complex function composed of a real and an imaginary part:

$$Z = Z_0 \exp(j\varphi) = Z_0(\cos \varphi + j \sin \varphi) = Z_{\text{re}}(\omega) + jZ_{\text{im}}(\omega) \quad (4.28)$$

Impedance is typically analyzed in the form of a spectrum, normally with a Nyquist plot (Figure 4.8a). This one represents the imaginary part of impedance vs the real part, and each point corresponds to the impedance at one different frequency, f , whose relationship with radial frequency is $\omega = 2\pi f$. Although frequency values are not explicitly shown in this plot, its values increase toward the left. EIS experiments are usually interpreted using an equivalent circuit of capacitors, resistors, and inductors. Randles circuit is widely used for studying the heterogeneous AT interactions on an electrode surface and models a cell where polarization results from a combination of kinetic and diffusion processes.

We were pioneers in applying Faradaic impedance spectroscopy (FIS), a variant of EIS which informs about changes in the electrode surface that produce a modification in charge-transfer resistance (R_{ct}) in the presence of an electroactive species in the medium (often the redox probe $[\text{Fe}(\text{CN})_6]^{3-/4-}$), for assessing the association and dissociation kinetics of an AT complex [107]. Note that the value of R_{ct} matches the diameter of the semicircle in the Nyquist plot. The method consists in recording the R_{ct} with a working electrode surface modified with one of the binding partners (P1) as a function of time, after incubation with a saturating concentration of the other partner (P2) in solution until the signal is leveled off (association phase) (Figure 4.8b). Once saturation of the surface is reached, this one is immersed in another solution containing a high amount of the immobilized binding partner (P1) to displace P2 from the surface, and R_{ct} measurements are conducted over time (dissociation phase). The experimental results for association and dissociation phases were fitted to a first-order exponential growth [$S(\%) = A_0(1 - \exp(-k_s t))$] and to a first-order exponential decay [$S(\%) = B_0 \exp(-k_{\text{off}} t) + \gamma_0$], respectively. Kinetic parameters, i.e. the dissociation

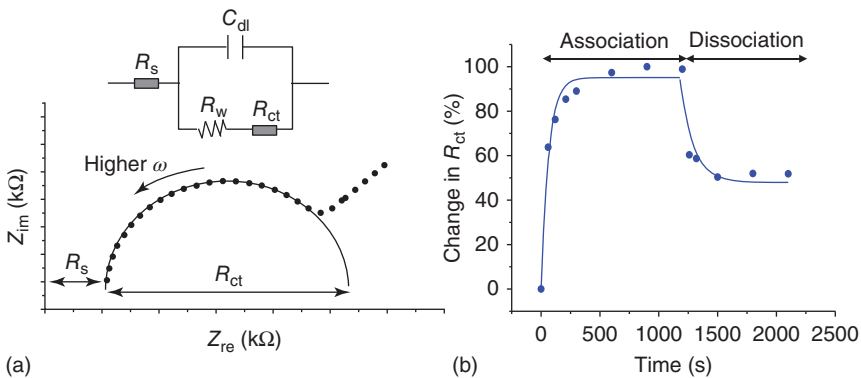


Figure 4.8 (a) Nyquist plot of impedance spectrum for mixed kinetic and charge-transfer control circuit. Inset: Randles circuit applied to fit the FIS experimental data. (b) Aptamer–target binding kinetics. R_{ct} values are obtained from impedance spectrum fitting. Source: de-los-Santos-Álvarez et al. 2009 [107]. Copyright (2009). Adapted with permission of Elsevier.

rate constant, k_{off} , and the association rate constant, k_{on} , with $k_s = k_{\text{on}}[\text{P2}] + k_{\text{off}}$, were obtained accordingly. Likewise, the affinity constant K_A can be estimated.

This methodology has been employed for evaluating the interaction of aptamers with antibiotics, such as neomycin B [107] and tobramycin [115]. Both targets are small molecules, a factor restricting the use of FIS as a feasible kinetic method, since performing measurements without labels, it is expected that the greater the molecular size of the binding partner in solution, the higher the changes in impedance are. In consequence, covalent immobilization of the antibiotic onto the electrode surface was carried out and subsequently challenged with the negatively charged oligonucleotide receptor, which repels and decelerates the electron transfer of the redox probe $[\text{Fe}(\text{CN})_6]^{3-/4-}$ to the electrode surface. This approach led to the maximum signal variation (ΔR_{ct}). Using the same immobilization strategy of the antibiotic onto gold surfaces, k_{on} and k_{off} values were estimated by FIS and SPR and found to be in good agreement [107]. Such results encourage the use of the FIS-based kinetic method for reliable, fast, and affordable analysis of AT interactions, with no requirement for labeling the binding partners.

FIS measurements allow a thermodynamic glimpse through not only the previous kinetic approach but also from titration experiments where equilibrium R_{ct} values are determined as a function of the concentration of one of the binding partners free in solution. These values represent the amount of AT complex formed that, expressed as a relative increase, provides a measure of the bound ligand. The Langmuir equation, which describes a rectangular hyperbola, relates the fraction of bound ligand to that of the free ligand; therefore, by nonlinear fitting, it is possible to obtain the value of K_D (see Eq. (4.5)) and consequently the affinity constant, K_A . This strategy has been applied to characterize the heterogeneous interaction between the most important celiac disease-immunogenic peptide within gluten, the so-called 33-mer peptide, and the immobilized anti-peptide aptamer [23], as well as the recognition between the steroid hormone progesterone anchored to the electrode surface and the handful of aptamers resulting from the SELEX process [116].

As general advice for EIS implementation, it should be said that since this technique detects changes in the surface of the electrode, unspecific interactions therein would provide measurable signals. Hence, control experiments to check the specificity of the measurements have to be performed. Besides, even taking careful precautions in electrode surface modification, the starting R_{ct} values vary significantly. These variations can be properly addressed by normalizing the signal.

4.3.2 Homogeneous Methods

4.3.2.1 Rotating Droplet Electrochemistry

Although some reactions can be monitored manually at low reactant concentration in order to slow down the reaction, the study of fast reactions (timescale <1 s) in solution requires rapid mechanical mixing of the reactants for subsequent monitorization of the reaction progress. For that goal, three different options have been reported, namely, stopped-flow, quenched-flow,

and continuous-flow techniques, the most common among them being the stopped-flow analysis [117].

In stopped-flow methods, small volumes of the aptamer and its cognate target are mixed by means of a syringe device, and the mixture is driven to an observation chamber coupled to a detection system, where the flow is stopped for signal acquisition. The interval time between the mixing and the signal monitorization, known as dead time, is as short as 2 ms, thereby allowing the study of interactions occurring within microseconds. These methods carry out optical detection, typically intrinsic or extrinsic (by incorporating a tag) fluorescence spectroscopy due to its better sensitivity [118, 119].

The development of an equivalent system with electrochemical transduction requires hydrodynamic conditions to improve the mass transport of the species toward the electrode surface, thus avoiding signal limitations derived from slow diffusion. The rotating disk electrode (RDE) is the standard electrochemical device for obtaining hydrodynamic conditions, recording stationary current intensity with high accuracy and reproducibility; however, large sample volumes (several milliliters) are required, so experiments become expensive, especially when involving biomolecules, and there are some limitations in terms of electrode materials and geometries.

To address these drawbacks, Limoges and coworkers have proposed an electrochemical kinetic method easily implementable in a rotating droplet covering a disposable and miniaturized electrochemical cell of flexible design [120]. Specifically, this method, referred to by the authors as kinetic rotating droplet electrochemistry, combines electrochemical real-time monitoring in a rotating microliter droplet with rapid mixing after reactant injection. The experimental setup is shown schematically in Figure 4.9a. A drop of $\sim 50\ \mu\text{l}$ is sandwiched between a screen-printed electrochemical cell, which includes in a circle of 5 mm of diameter the typical three-electrode configuration, and a rotating cylinder just to impose a rotation to the droplet over the surface of the static electrode. The rotating cylinder is indeed a standard RDE previously disconnected from the potentiostat to avoid any electric noise. Therefore, the setup is readily constructed from standard equipment in electrochemical laboratories. Under these conditions, a controlled hydrodynamic regime is rapidly established. The injection of a reactant in the rotating droplet is carried out manually with a micropipette.

This methodology has been successfully applied to the kinetic study of the binding between an aptamer and its electroactive target, *L*-tyrosinamide, taking advantage of the difference in diffusion rates of the bound and free forms of the redox partner. Figure 4.9b shows typical amperometric kinetic plots recorded for this biorecognition reaction. A microdroplet containing the redox binding partner is confined between the screen-printed electrochemical cell and the rotating cylinder. The working electrode is then polarized at a fixed potential, which is suitable for the reaction under consideration, and a stationary current intensity is obtained whose magnitude is proportional to the transport kinetics of the redox partner and, in turn, to its diffusion coefficient. Fast injection of the nonelectroactive partner gives rise to a transient current decrease to subsequently reach a steady state, as a result of the formation of the AT complex, whose transport kinetics is significantly slower than that for the free redox

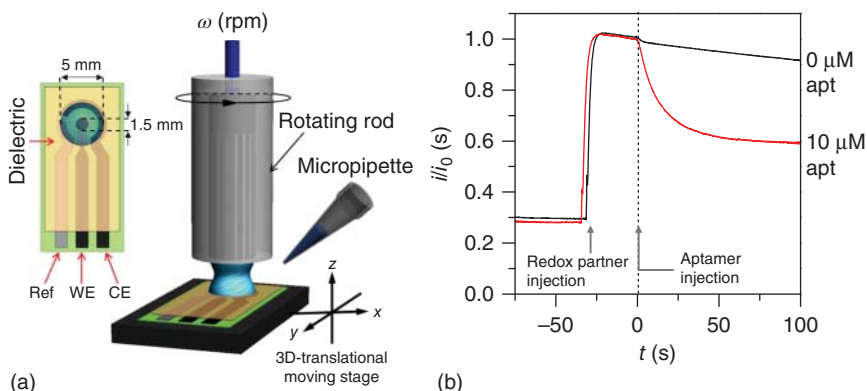


Figure 4.9 (a) Schematic representation of the rotating droplet system with a detailed view of an individual screen-printed electrochemical cell. (b) Normalized amperometric kinetic plot recorded at the rotated droplet for the recognition binding between L-tyrosinamide and its DNA aptamer. Source: Challier et al. 2013 [120]. Copyright (2013). Adapted with permission of American Chemical Society.

binding partner. An increasing amount of the nonelectroactive partner is added to a fixed concentration of the redox partner with the concomitant decrease in current intensity. Then, using free software, a global analysis is performed, considering the entire set of time-course amperometric responses.

Kinetics and thermodynamics of the aptamer-L-tyrosinamide binding have been characterized in detail with the rotating droplet electrochemical method, allowing to identify the minimal sequence for binding of the aptamer. Interestingly, the truncated form of the oligonucleotide receptor exhibits better affinity (K_A value about one order of magnitude higher) than the SELEX-selected counterpart. Such an enhanced affinity is attributed to an increase in the second-order binding rate constant (k_{on}), while the dissociation rate constant (k_{off}) remains practically unchanged [121].

The versatility of this method, even if not yet demonstrated to its full extent due to its recent onset, can be easily anticipated. Although implemented for a redox small molecule and its aptamer to date, this method could be extended to nonelectroactive molecules by labeling with a redox probe or even by means of a displacement assay using a displaceable redox surrogate partner. This latter strategy has been recently applied to thermodynamic studies of the binding between an aminoglycoside and its RNA aptamer in the microdroplet configuration [122]; however, kinetic information could be also extracted, provided that the dissociation rate constants of both competitors are small. On the other hand, if the difference in diffusion coefficients between the complex and the free form of the redox partner is narrow, monitoring of changes in formal potential or redox state, also electrochemically detected, related to the binding could be envisaged.

Temporal resolution of this electrochemical kinetic method depends on four characteristic times: the injection time, the mixing time, the dead time that in this particular case is the time required for a molecule to cross the diffusion layer established in the vicinity of the working electrode, whose thickness is

determined by the cylinder rotating rate, and the instrument response time. After carefully evaluating all of them, the authors conclude that the mixing time (approximately one second) is the determining factor of the kinetic time resolution; therefore, with the ability to determine bimolecular rate constants up to $10^6 \text{ M}^{-1} \text{ s}^{-1}$. Improvements in this direction are under active investigation.

4.3.2.2 Capillary Electrophoresis

CE methods are useful to study not only the thermodynamics but also the kinetics of interactions between aptamers and their binding partners in free solution. Kinetic capillary electrophoresis (KCE) is based on the CE of species that interact during the separation, thus allowing for the estimation of the kinetic parameters characterizing such an interaction. Different KCE methods have been described, depending on how the interaction is arranged, including nonequilibrium capillary electrophoresis of equilibrium mixtures (NECEEM), continuous NECEEM, sweeping CE and plug-plug KCE [123]. Among them, NECEEM is the most versatile and most useful method for aptamer characterization, and its principle is presented later.

Generally, KCE methods for aptamer binding characterization are based on the separation of the aptamer, target, and AT complex according to the differences in their electrophoretic velocities, represented by v_A , v_T , and v_{AT} , respectively. The following system of partial differential equations describes the separation process [124]:

$$\frac{\partial[A]_{t,x}}{\partial t} + v_A \frac{\partial[A]_{t,x}}{\partial x} = -k_{\text{on}}[A]_{t,x}[T]_{t,x} + k_{\text{off}}[AT]_{t,x} \quad (4.29)$$

$$\frac{\partial[T]_{t,x}}{\partial t} + v_T \frac{\partial[T]_{t,x}}{\partial x} = -k_{\text{on}}[A]_{t,x}[T]_{t,x} + k_{\text{off}}[AT]_{t,x} \quad (4.30)$$

$$\frac{\partial[AT]_{t,x}}{\partial t} + v_{AT} \frac{\partial[AT]_{t,x}}{\partial x} = -k_{\text{off}}[AT]_{t,x} + k_{\text{on}}[A]_{t,x}[T]_{t,x} \quad (4.31)$$

In these equations, t represents the time elapsed since the beginning of the separation, x the distance from the injection end of the capillary, whereas $[A]_{t,x}$, $[T]_{t,x}$, and $[AT]_{t,x}$ are the concentration of aptamer, target, and complex in the different steps of the separation. The solution of this system changes depending on the initial and boundary conditions, which are different for the different KCE types.

In NECEEM, the capillary and the reservoirs for the separation are filled with a buffer in which the AT reaction will be evaluated. This buffer must be compatible with CE separations [125]. An equilibrium mixture containing aptamer, target, and AT complex is then injected into the capillary (Figure 4.10a), and the equilibrium fractions of the three components of the mixture are separated under the external electric field. There are two different phases in the separation; in the first phase, whereas AT is separated from A and T, the dissociation of AT must be negligible (slow dissociation), so the amounts of each component in the corresponding equilibrium fraction can be used to obtain K_D . As a result of the separation, A and T are removed from the AT zone, which is no longer at equilibrium and starts to dissociate (second phase). The recombination of A and T must be negligible in this phase (slow recombination), in such a

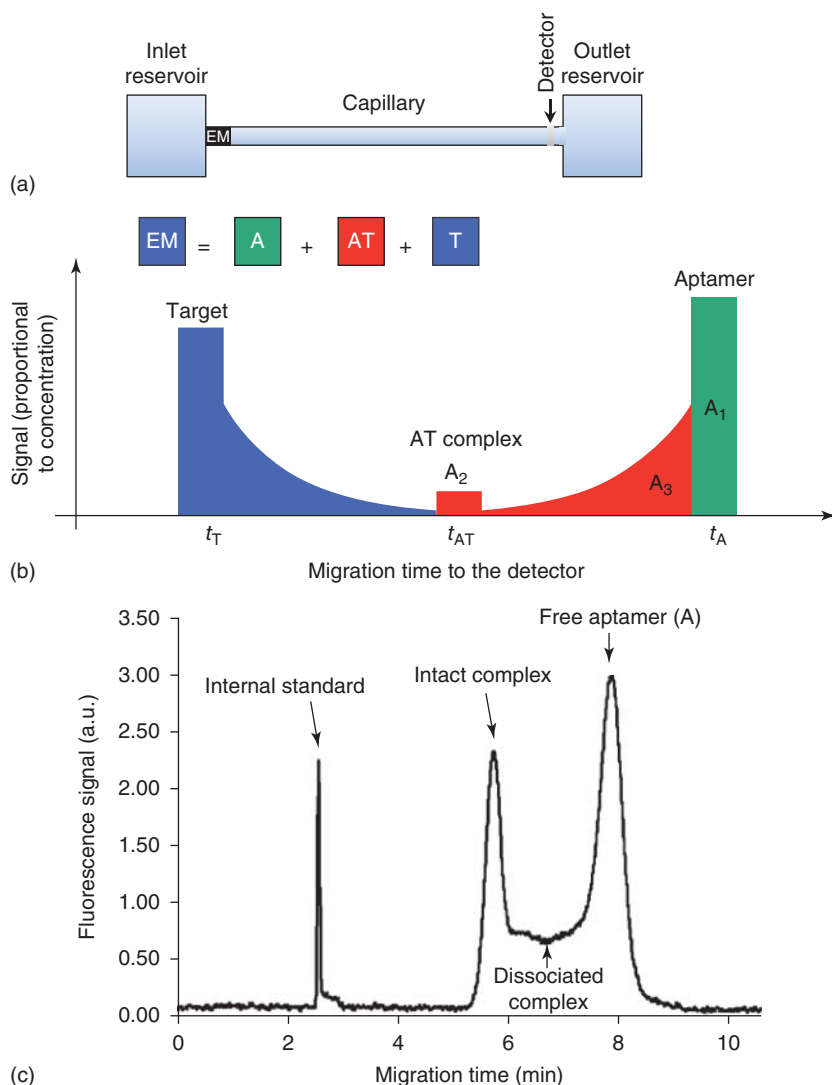


Figure 4.10 (a) Scheme showing the initial and boundary conditions in NECEEM, (b) simulated electropherogram, and (c) a typical signal obtained in the NECEEM method for aptamer characterization. Source: Adapted from Krylova et al. 2011 [126] and Berezovski et al. 2006 [127].

way that the amount of A (or T) released over a known period of time is used to obtain k_{off} [126]. Figure 4.10b shows a simulated electropherogram where it is possible to distinguish three peaks, representing A, AT, and T, and two exponential decay lines (“smears”) corresponding to A and T dissociated from AT during the separation [127].

The solution to Eqs (4.29)–(4.31) considering the initial and boundary conditions (the initial distribution of A, T, and AT along the capillary, and the way these components are injected and eluted during the separation) gives algebraic

equations describing the dependence of A, T, and AT concentrations on the migration time. By fitting the experimental data to the predicted electropherogram, it is possible to obtain the binding parameters by nonlinear regression [123]. Nevertheless, in NECEEM, a single electropherogram, as that shown in Figure 4.10c for the interaction between AlkB protein and its fluorescently labeled DNA aptamer, contains the information needed to find K_D and k_{off} . These constants can be calculated using the following equations [124]:

$$K_D = \frac{[T]_0 \left(1 + \frac{A_1}{A_2 + A_3}\right) - [A]_0}{1 + (A_2 + A_3)/A_1} \quad (4.32)$$

$$k_{\text{off}} = \ln \left(\frac{A_2 + A_3}{A_2} \right) / t_{\text{AT}} \quad (4.33)$$

where A_1 is the area of the peak corresponding to the free aptamer in the equilibrium mixture, A_2 is the peak area corresponding to AT still complexed at the detection time, and A_3 is the area of the exponential smear that appears because the dissociation of the aptamer from the complex. $[A]_0$ and $[T]_0$ are the total concentrations of both partners in the equilibrium mixture, and t_{AT} is the migration time of the AT complex. It is very important to find the proper conditions for good-quality separation of aptamer from the AT complex. In addition, the correct definition of the boundaries of the peaks is critical for the accurate estimation of the constants. This can be achieved by control experiments, comparing the peaks of the free aptamer in the presence and absence of the target [124] or by a mathematical approach, fitting the experimental data to the equations that define the model using nonlinear regression analysis [128]. The first approach, albeit simple, leads to experimental errors in the range of 10% [124].

This method has been used for the characterization of aptamers recognizing proteins. It should be noted that although only one electropherogram is required for obtaining K_D and k_{off} , it is important to select the concentration of the target (if the aptamer is the detectable species, as is usual using fluorescently labeled aptamers), which should be an order of magnitude from the K_D value. In practice, this means that it will be necessary to titrate the aptamer with increasing amounts of target to find the proper conditions. NECEEM has been used to measure dissociation constants in the range 10^{-4} – 1 s^{-1} [124].

4.3.2.3 Nanopore-Based Studies

All the methodologies discussed so far are bulky or ensemble technologies, devoted to explore AT bindings. However, single-molecule studies can provide complementary information about these recognition interactions, while at the same time they are not limited by steric hindrance derived from crowding of the binding sites. Nanopore-based studies belong to this appealing category.

Nanopores occur naturally in cells and they act as traffic lights that control the movement of ions and molecules in and out of cells, as well as among subcellular compartments. Among their many applications in biotechnology and biophysics, nanopores have demonstrated to be suitable single-molecule tools for studying molecular processes such as protein–DNA interactions [129], and they have recently started to be used to investigate the binding process

between an aptamer and its cognate target [130–132]. The basic principle of these nanopore-based analyses is to monitor the ion current fluctuation through the nanopore as a binding process takes place either inside or in the near vicinity of the nanopore.

Biological nanopores, also known as transmembrane protein channels, are usually embedded in a lipid bilayer membrane and their size and structure are perfectly defined and reproducible. A scheme of the most commonly used biological nanopore, α -hemolysin (α -HL), is shown in Figure 4.11a. In nanopore-based studies, the membrane with the nanopore inserted is placed between two chambers, cis and trans, containing an electrolyte solution. Using a pair of electrodes, anode and cathode, a constant voltage is applied across the membrane, triggering a steady ion flow through the nanopore and, as a result, an electric current is generated and measured, i.e. the baseline current (Figure 4.11b). When an individual molecule interacts with the nanopore, current flowing through thereof is blocked, causing an interruption or resistive pulse in the baseline current (Figure 4.11c). Three important parameters allow characterizing the electrical signature of a general event: the dwell time of the molecule in the pore (t_{dwell}), the current amplitude (ΔI), and the time between successive events (Δt). The first two are related to the identity of the molecule, while the third one reports the molecule concentration in solution [133].

Bayley and coworkers [130] have developed a nanopore-based approach for kinetic and equilibrium characterization of the binding of thrombin to its aptamer using the mushroom-shaped α -hemolysin pore. Since thrombin is too large to enter this biological pore, this one was chemically engineered with a cysteine residue near the cis entry to covalently bind a poly(A) oligonucleotide

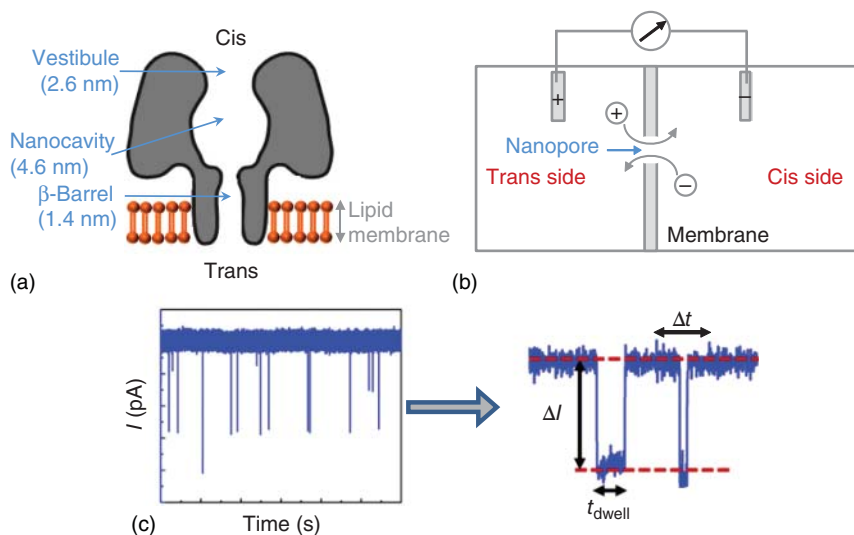


Figure 4.11 (a) Schematic representation of the α -hemolysin (α HL) nanopore. (b) Typical setup for nanopore-based measurements. (c) Current traces from a single nanopore showing characteristic signature blocks. Source: Wanunu 2012 [133]. Adapted with permission of Elsevier.

and, by hybridization, to immobilize the aptamer via a poly(T) tail. The electrical profile of the aptamer attached to the pore is significantly modified after addition of thrombin to the cis chamber and subsequent complex formation, namely, the frequency of current blockades is reduced and a new current level is observed. The rates of the transition between both current levels are determined for different thrombin concentrations, obtaining $k_{\text{on}} = (1.97 \pm 0.01) \times 10^7 \text{ M}^{-1} \text{ s}^{-1}$ and $k_{\text{off}} = 1.5 \pm 0.1 \text{ s}^{-1}$. The resulting K_{D} value was found to be in accordance with those previously obtained with bulky approaches.

Afterwards, the possibility of internalizing proteins inside the cytolysin A (ClyA) biological nanopore was demonstrated, maintaining their 3D structure. This finding was applied for revisiting the model thrombin–aptamer interaction by a different single-molecule approach. It consists in trapping the protein thrombin inside the ClyA nanopore, by applying a certain potential, and subsequently incorporating the antithrombin aptamer in the cis chamber for complex formation inside the nanopore [131]. The dissociation constant, K_{D} , of thrombin–aptamer complex was calculated from titration experiments by plotting, for each tested aptamer concentration, the complex concentration vs the unbound aptamer concentration, and fitting to the one-site binding isotherm. These variables are mathematically related to the total thrombin concentration, the added aptamer concentration, and the unbound thrombin concentration in each case. The first two are known by the experimenter, whereas the unbound thrombin concentration can be measured as the capture frequency of unbound thrombin by the nanopore. This latter decreases when increasing the aptamer concentration. Dissociation rate constant, k_{off} , can be also estimated taking into account that the inverse of t_{dwell} is a measure of k_{off} , whose value depends on the applied potential. Such dependence might be described by a van't Hoff Arrhenius-like expression as follows:

$$k_{\text{off}} = k_{\text{off},0\text{mV}} e^{-(|V|\Delta U/RT)} \quad (4.34)$$

where $k_{\text{off},0\text{mV}}$ is the dissociation rate constant at zero voltage and ΔU is the decrease in the energy barrier due to the application of a potential V . By adjusting the experimental data to the expression resulting from taking the natural logarithms in Eq. (4.34), the extrapolated $k_{\text{off},0\text{mV}}$ value would provide the dissociation rate constant for thrombin–aptamer binding; although the authors noticed that this value could be affected by the confinement of the complex inside the nanopore.

Biological α -hemolysin nanopores have been also employed for investigation of the affinity between a small molecule, ATP, and its aptamer by means of an approach involving the backward translocation of an aptamer construct [132]. The movement of DNA through the α -HL nanopore, or translocation, is possible for single-stranded oligonucleotides but not for structured DNA, just due to geometric issues. Considering this limitation, the aptamer was elongated with an unstructured poly(T) spacer followed by a hairpin-like structured sequence acting as a stopper. This way, by application of a suitable transmembrane potential, the aptamer sequence is unfolded and passes through the nanopore in the cis–trans direction, while the stable hairpin prevents the complete translocation of the DNA construct. Then, the voltage is decreased to allow

the aptamer refolding and ATP binding on the trans side. After a fixed time, the potential was linearly increased; triggering the complex dissociation and the DNA construct is translocated to the cis side. A different unfolding voltage histogram is obtained for each ATP concentration, whose distribution is related to the bound and unbound aptamer concentrations, and thus the K_D value can be calculated. This strategy of anchoring an aptamer construct for subsequent backward translocation is not functional for highly structured aptamers (e.g. G-quadruplex) because the potential necessary to unfold the aptamer structure would also unzip the stopper.

Importantly, when performing nanopore-based studies, the requirement of using high salt concentrations, typically 1 M KCl, should be borne in mind to be able to distinguish specific events from current noise. Such experimental conditions could pose a problem for those interactions particularly sensitive to the ionic strength.

Nanopore-based studies constitute a label-free and real-time methodology that allows characterizing AT bindings operating at a single-molecule level and with low reagent consumption. Because of its recent inception, it is still in its infancy but exciting progress is expected in the near future.

4.4 Concluding Remarks

Understanding how an aptamer selectively recognizes its target is currently mainly based on the study of the thermodynamics and kinetics of the AT interaction. The plethora of methods described in this chapter cover both aspects, also showing that such evaluation is difficult to be accessed experimentally. There is no method that may be applied as universal for aptamer characterization. In fact, it is highly recommended to use more than one method, based on a different principle. This will allow to circumvent discrepancies between different methods as a consequence of their differences in sensitivity or nature of the assay. It would be also desirable to have high-throughput aptamer characterization assays, which coupled to advances in SELEX and the use of high-throughput sequencing methods for the final analysis, would allow a rapid and efficient identification of high-affinity aptamers [134]. Fluorescence-based methods in combination with *in situ* synthesized aptamers are particularly suitable with this aim, enabling the simultaneous measurement of affinity for thousands of candidate aptamers in parallel [135, 136].

This is only one side of the coin. Techniques useful for the characterization of the three-dimensional structure of the aptamer–ligand complexes need to be employed to give a complete description of the structural bases of highly specific ligand discrimination by aptamers. Despite the multiple aptamers evolved and reported in the literature over the past 25 years to selectively, in theory specifically, bind an intended target, only a handful of these bioaffinity pairs have been structurally characterized so far. Identifying the key molecular contacts between an aptamer and its cognate target is crucial to understand the binding interaction itself as well as to tune it in the desired direction (e.g. design of therapeutic

drugs, improvement of biosensing devices) and, in consequence, to optimize their practical applications. AT interactions mainly depend on the nature of the target, the aptamer primary structure (the linear sequence of nucleotides), and the aptamer 3D structure, which can take part in a set of conformations preexisting in equilibrium before target addition (conformational search mechanism) [26], or be promoted by the presence of the target (induced-fit process) [120].

Structural information about AT complexes with atomic resolution can be achieved by means of nuclear magnetic resonance (NMR) spectroscopy, although, because of the complexity of the data, it is more appropriate for complexes of small dimensions [137]. Instead, X-ray crystallography can provide high-resolution structural information independently of the molecular size [138, 139] as long as crystals allow for suited quality diffraction data. Although this challenging issue is typically addressed via an empiric approach using commercial crystallization screening kits in combination with liquid handling robots, some consensus parameters have been reported [140]. In particular, the purity of both binding partners becomes essential for crystallization process. In this sense, polyacrylamide gel electrophoresis (PAGE) and anion-exchange chromatography are recommended as aptamer purification strategies, without excluding a late dialysis step. Moreover, long oligonucleotide sequences can disturb crystallization; therefore, determination of the minimal binding sequence for target binding is required. Most of the biophysical techniques described in the previous sections could assist in this context too. For protein targets, polydispersity and suitable folding should be also controlled by dynamic light scattering and circular dichroism spectroscopy, respectively. Besides carrying out the crystallization process at room temperature, 4 °C is also a good choice since it slows the degradation rate and reduces conformational heterogeneity.

While X-ray crystallography supplies a fixed picture of the AT complex, time-dependent changes in the atomic structure leading to the complex formation can be addressed by computational methods such as molecular dynamic (MD) simulations [141, 142]. This way, transient conformers not observed by other experiment can be revealed. Likewise, other theoretical methods such as molecular docking and free energy calculations enable us to complement the data obtained by experimental methods in a less laborious and rapid manner [18].

The characterization of the AT interaction study is currently getting more attention as evidenced by the number of methods revised in this chapter. A greater understanding of this interaction may create opportunities for more efficient optimization of aptamers, giving rise to high-affinity aptamers for a wide range of analytes, useful for implementing new diagnostics, therapeutics, and analytical applications.

Acknowledgments

This work was sponsored by Principado de Asturias government under the project FC15-GRUPIN14-025. Financial support from the Spanish Ministerio de Economía y Competitividad (Project CTQ2015-63567-R) and FEDER funds is also acknowledged.

References

- 1 Tuerk, C. and Gold, L. (1990). Systematic evolution of ligands by exponential enrichment: RNA ligands to bacteriophage T4 DNA polymerase. *Science* 249: 505–519.
- 2 Ellington, A.D. and Szostak, J.W. (1990). In vitro selection of RNA molecules that bind specific ligands. *Nature* 346: 818–822.
- 3 Hermann, T. and Dinshaw, J.P. (2000). Adaptive recognition by nucleic acid aptamers. *Science* 287: 820–825.
- 4 Hulme, E.C. and Trevethick, M.A. (2010). Ligand binding assays at equilibrium: validation and interpretation. *Br. J. Pharmacol.* 161: 1219–1237.
- 5 Jing, M. and Bowser, M.T. (2011). Methods for measuring aptamer–protein equilibria: a review. *Anal. Chim. Acta* 686: 9–18.
- 6 Pu, Y., Zhu, Z., Liu, H. et al. (2010). Using aptamers to visualize and capture cancer cells. *Anal. Bioanal. Chem.* 397: 3225–3233.
- 7 Tang, Z., Parekh, P., Turner, P. et al. (2009). Generating aptamers for recognition of virus-infected cells. *Clin. Chem.* 55: 813–822.
- 8 Musumeci, D. and Montesarchio, D. (2012). Polyvalent nucleic acid aptamers and modulation of their activity: a focus on the thrombin binding aptamer. *Pharmacol. Ther.* 136: 202–215.
- 9 Mallikaratchy, P.R., Ruggiero, A., Gardner, J.R. et al. (2011). A multivalent DNA aptamer specific for the B-cell receptor on human lymphoma and leukemia. *Nucleic Acids Res.* 39: 2458–2469.
- 10 Pavlov, V., Xiao, Y., Shlyahovsky, B., and Willner, I. (2004). Aptamer-functionalized Au nanoparticles for the amplified optical detection of thrombin. *J. Am. Chem. Soc.* 126: 11768–11769.
- 11 Tan, S.Y., Acquah, C., Sidhu, A. et al. (2016). SELEX modifications and bio-analytical techniques for aptamer-binding characterization. *Crit. Rev. Anal. Chem.* 46: 521–537.
- 12 Prinz, H. (2010). Hill coefficients, dose–response curves and allosteric mechanisms. *J. Chem. Biol.* 3: 37–44.
- 13 Weiss, J.N. (1997). The Hill equation revisited: uses and misuses. *FASEB J.* 11: 835–841.
- 14 Xia, Y., Gan, S., Xu, Q. et al. (2013). A three-way junction aptasensor for lysozyme detection. *Biosens. Bioelectron.* 39: 250–254.
- 15 Armstrong, R.E. and Strouse, G.F. (2014). Rationally manipulating aptamer binding affinities in a stem-loop molecular beacon. *Bioconjugate Chem.* 25: 1769–1776.
- 16 Munzar, J., Ng, A., Corrado, M., and Juncker, D. (2017). Complementary oligonucleotides regulate induced fit ligand binding in duplexes aptamers. *Chem. Sci.* 8: 2251–2256.
- 17 Simon, A.J., Vallée-Bélisle, A., Ricci, E., and Plaxco, K.W. (2014). Intrinsic disorder as a generalizable strategy for the rational design of highly responsive, allosterically cooperative receptors. *Proc. Natl. Acad. Sci. U. S. A.* 111: 15048–15053.

- 18 Du, X., Li, Y., Xia, Y.L. et al. (2016). Insights into protein–ligand interactions: mechanisms, models and methods. *Int. J. Mol. Sci.* 17: 144.
- 19 Sokoloski, J.E., Drombrowski, S.E., and Bevilacqua, P.C. (2012). Thermodynamics of ligand binding to a heterogeneous RNA population in the malachite green aptamer. *Biochemistry* 51: 565–572.
- 20 Lin, P.H., Yen, S.L., Lin, M.S. et al. (2008). Microcalorimetric studies of the thermodynamics and binding mechanisms between L-tyrosinamide and aptamer. *J. Phys. Chem. B* 112: 6665–6673.
- 21 Pang, Y.F., Xu, Z.A., Sato, Y. et al. (2012). Base pairing at the abasic site in DNA duplexes and its applications in adenosine aptasensors. *ChemBioChem* 13: 436–442.
- 22 Ilgu, M., Fulton, D.B., Yennamalli, R.M. et al. (2014). An adaptable pentaloop defines a robust neomycin-B RNA aptamer with conditional ligand bound structures. *RNA* 20: 815–824.
- 23 Amaya-González, S., López-López, L., Miranda-Castro, R. et al. (2015). Affinity of aptamers binding 33-mer gliadin peptide and gluten proteins: influence of immobilization and labelling tags. *Anal. Chim. Acta* 873: 63–70.
- 24 Csermely, P., Palotai, R., and Nussinov, R. (2010). Induced fit, conformational selection and independent dynamic segments: an extended view of binding events. *Trends Biochem. Sci.* 35: 539–546.
- 25 Zhou, H.X. (2010). From induced fit to conformational selection: a continuum of binding mechanism controlled by the timescale of conformational transitions. *Biophys. J.* 98: L15–L17.
- 26 Xia, T., Yuan, J., and Fang, X. (2013). Conformational dynamics of an ATP-binding DNA aptamer: a single-molecule study. *J. Phys. Chem. B* 117: 14994–15003.
- 27 Cruz-Aguado, J.A. and Penner, G. (2008). Determination of ochratoxin A with a DNA aptamer. *J. Agric. Food Chem.* 56: 10456–10461.
- 28 McKeague, M., De Girolamo, A., Valenzano, S. et al. (2015). Comprehensive analytical comparison of strategies used for small molecule aptamer evaluation. *Anal. Chem.* 87: 8608–8612.
- 29 Martin, J.A., Chávez, J.L., Chushak, Y. et al. (2014). Tunable stringency aptamer selection and gold nanoparticle assay for detection of cortisol. *Anal. Bioanal. Chem.* 406: 4637–4647.
- 30 Valenzano, S., De Girolamo, A., DeRosa, M.C. et al. (2016). Screening and identification of DNA aptamers to tyramine using *in vitro* selection and high-throughput sequencing. *ACS Comb. Sci.* 18: 302–313.
- 31 Ruff, K.M. and Strobel, S.A. (2014). Ligand binding by the tandem glycine riboswitch depends on aptamer dimerization but not double ligand occupancy. *RNA* 20: 1775–1788.
- 32 Daniels, D.A., Sohal, A.K., Rees, S., and Grisshammer, R. (2002). Generation of RNA aptamers to the G-protein-coupled receptor for neurotensin, NTS-1. *Anal. Biochem.* 305: 214–226.
- 33 Lim, F. and Peabody, D.S. (2002). RNA recognition site of PP7 coat protein. *Nucleic Acids Res.* 30: 4138–4144.

- 34 Kwon, H.M., Lee, K.H., Han, B.W. et al. (2014). An RNA aptamer that specifically binds to the glycosylated hemagglutinin of avian influenza virus and suppresses viral infection in cells. *PLoS One* 9: e97574/1–e97574/9.
- 35 Wong, I. and Lohman, T.M. (1993). A double filter method for nitrocellulose-filter binding: application to protein–nucleic acid interactions. *Proc. Natl. Acad. Sci. U. S. A.* 90: 5428–5432.
- 36 Deng, Q., German, I., Buchana, D., and Kennedy, R.T. (2001). Retention and separation of adenosine and analogues by affinity chromatography with an aptamer stationary phase. *Anal. Chem.* 73: 5415–5421.
- 37 Ruta, J., Ravelet, C., Désiré, J. et al. (2008). Covalently bonded DNA aptamer chiral stationary phase for the chromatographic resolution of adenosine. *Anal. Bioanal. Chem.* 390: 1051–1057.
- 38 Kasai, K.I. and Oda, Y. (1986). Frontal affinity chromatography: theory for its application to studies on specific interactions of biomolecules. *J. Chromatogr.* 376: 33–47.
- 39 Zhao, Q., Li, X.F., and Li, C. (2008). Aptamer-modified monolithic capillary chromatography for protein separation and detection. *Anal. Chem.* 80: 3915–3920.
- 40 Heegaard, N.N. (2002). A history of the use and measurement of affinity interaction in electrophoresis. In: *A Century of Separation Science* (ed. H.J. Issaq), 527–554. New York: Marcel Dekker.
- 41 Mendonsa, S.D. and Bowser, M.T. (2004). In vitro evolution of functional DNA using capillary electrophoresis. *J. Am. Chem. Soc.* 126: 20–21.
- 42 Mendonsa, S.D. and Bowser, M.T. (2004). In vitro selection of high-affinity DNA ligands for human IgE using capillary electrophoresis. *Anal. Chem.* 76: 5387–5392.
- 43 Mendonsa, S.D. and Bowser, M.T. (2005). In vitro selection of aptamers with affinity for neuropeptide Y using capillary electrophoresis. *J. Am. Chem. Soc.* 127: 9382–9383.
- 44 Rundlett, K.L. and Armstrong, D.W. (2001). Methods for the determination of binding constants by capillary electrophoresis. *Electrophoresis* 22: 1419–1427.
- 45 Heegaard, N.H.H. (2003). Applications of affinity interactions in capillary electrophoresis. *Electrophoresis* 24: 3879–3891.
- 46 Chen, Z. and Weber, S.G. (2008). Determination of binding constants by affinity capillary electrophoresis, electrospray ionization mass spectrometry and phase-distribution methods. *Trends Anal. Chem.* 27: 738–748.
- 47 Meng, C., Zhao, X., Qu, F. et al. (2014). Interaction evaluation of bacteria and protoplasts with single-stranded deoxyribonucleic acid library based on capillary electrophoresis. *J. Chromatogr. A* 1358: 269–276.
- 48 German, I., Buchanan, D.D., and Kennedy, R.T. (1998). Aptamers as ligands in affinity probe capillary electrophoresis. *Anal. Chem.* 70: 4540–4545.
- 49 Kasahara, Y., Irisawa, Y., Fujita, H. et al. (2013). Capillary electrophoresis – systematic evolution of ligands by exponential enrichment selection of base- and sugar-modified DNA aptamers: target binding dominated by 2'-O,4'-C-methylene-bridged/locked nucleic acid primer. *Anal. Chem.* 85: 4961–4967.

- 50 Jing, M. and Bowser, M.T. (2013). Tracking the emergence of high affinity aptamers for rhVEGF₁₆₅ during capillary electrophoresis – systematic evolution of ligands by exponential enrichment using high throughput sequencing. *Anal. Chem.* 85: 10761–10770.
- 51 Eaton, R.M., Shallcross, J.A., Mael, L.E. et al. (2015). Selection of DNA aptamers for ovarian cancer biomarker HE4 using CE-SELEX and high-throughput sequencing. *Anal. Bioanal. Chem.* 407: 6965–6973.
- 52 Wiseman, T., Williston, S., Brandts, J.F., and Lin, L.N. (1989). Rapid measurement of binding constants and heats of binding using a new titration calorimeter. *Anal. Biochem.* 179: 131–137.
- 53 Amano, R., Takada, K., Tanaka, Y. et al. (2016). Kinetic and thermodynamic analyses of interaction between a high-affinity RNA aptamer and its target protein. *Biochemistry* 55: 6221–6229.
- 54 Freire, E., Mayorga, O.L., and Straume, M. (1990). Isothermal titration calorimetry. *Anal. Chem.* 62 (18): 950A–959A.
- 55 Duff, M.R. Jr., Grubbs, J., and Howell, E.E. (2011). Isothermal titration calorimetry for measuring macromolecule–ligand affinity. *J. Vis. Exp.* 55: e2796.
- 56 Sigurskjold, B.W. (2000). Exact analysis of competition ligand binding by displacement isothermal titration calorimetry. *Anal. Biochem.* 277: 260–266.
- 57 Krainer, G., Broecker, J., Vargas, C. et al. (2012). Quantifying high-affinity binding of hydrophobic ligands by isothermal titration calorimetry. *Anal. Chem.* 84: 10715–10722.
- 58 Krainer, G. and Keller, S. (2015). Single-experiment displacement assay for quantifying high-affinity binding by isothermal titration calorimetry. *Methods* 76: 116–123.
- 59 Velázquez-Campoy, A. and Freire, E. (2005). ITC in the post-genomic era...? Priceless. *Biophys. Chem.* 115: 115–124.
- 60 Pagano, B., Martino, L., Randazzo, A., and Giancola, C. (2008). Stability and binding properties of a modified thrombin binding aptamer. *Biophys. J.* 94: 562–569.
- 61 Lin, P.-H., Chen, R.-H., Lee, C.-H. et al. (2011). Studies of the binding mechanism between aptamers and thrombin by circular dichroism, surface plasmon resonance and isothermal titration calorimetry. *Colloids Surf. B* 88: 552–558.
- 62 Potty, A.S.R., Kourentzi, K., Fang, H. et al. (2009). Biophysical characterization of DNA aptamer interactions with vascular endothelial growth factor. *Biopolymers* 91 (2): 145–156.
- 63 Potty, A.S.R., Kourentzi, K., Fang, H. et al. (2011). Biophysical characterization of DNA and RNA aptamer interactions with hen egg lysozyme. *Int. J. Biol. Macromol.* 48: 392–397.
- 64 Homans, S.W. (2007). Dynamics and thermodynamics of ligand–protein interactions. *Top. Curr. Chem.* 272: 51–82.
- 65 Álvarez-Martos, I. and Ferapontova, E. (2017). A DNA sequence obtained by replacement of the dopamine RNA aptamer bases is not an aptamer. *Biochem. Biophys. Res. Commun.* 489 (4): 381–385.

- 66 Sengupta, A., Gavvala, K., Koninti, R.K., and Hazra, P. (2014). Role of Mg²⁺ ions in flavin recognition by RNA aptamer. *J. Photochem. Photobiol. B* 140: 240–248.
- 67 Kim, Y.-B., Wacker, A., von Laer, K. et al. (2017). Ligand binding to 2'-deoxyguanosine sensing riboswitch in metabolic context. *Nucleic Acids Res.* 45 (9): 5375–5386.
- 68 Neves, M.A.D., Slavkovic, S., Churcher, Z.R., and Johnson, P.E. (2017). Salt-mediated two-site ligand binding by the cocaine-binding aptamer. *Nucleic Acids Res.* 45 (3): 1041–1048.
- 69 Burnouf, D., Ennifar, E., Guedich, S. et al. (2012). kinITC: a new method for obtaining joint thermodynamic and kinetic data by isothermal titration calorimetry. *J. Am. Chem. Soc.* 134: 559–565.
- 70 Wang, H., Wang, J., Sun, N. et al. (2016). Selection and characterization of malachite green aptamers for the development of light-up probes. *ChemistrySelect* 1: 1571–1574.
- 71 Lautner, G., Balogh, Z., Gyurkovics, A. et al. (2012). Homogenous assay for evaluation of aptamer–protein interaction. *Analyst* 137: 3929–3931.
- 72 Yu, H., Canoura, J., Guntupalli, B. et al. (2017). A cooperative-binding split aptamer assay for rapid, specific and ultra-sensitive fluorescence detection of cocaine in saliva. *Chem. Sci.* 8: 131–141.
- 73 Porchetta, A., Vallée-Bélisle, A., Plaxco, K.W., and Ricci, F. (2012). Using distal-site mutations and allosteric inhibition to tune, extend, and narrow the useful dynamic range of aptamer-based sensors. *J. Am. Chem. Soc.* 134: 20601–20604.
- 74 Xiang, L. and Tang, J. (2017). QD-aptamer as a donor for a FRET-based chemosensor and evaluation of affinity between acetamiprid and its aptamer. *RSC Adv.* 7: 8332–8337.
- 75 Jameson, D.M. and Ross, J.A. (2010). Fluorescence polarization/anisotropy in diagnostics and imaging. *Chem. Rev.* 101 (5): 2685–2708.
- 76 Perrin, F. (1926). Polarisation de la lumière de fluorescence. Vie moyenne des molécules dans l'état excité. *J. Phys. Radium* 7: 390–401.
- 77 Zhang, D., Lu, M., and Wang, H. (2011). Fluorescence anisotropy analysis for mapping aptamer–protein interaction at the single nucleotide level. *J. Am. Chem. Soc.* 133: 9188–9191.
- 78 Latulippe, D.R., Szeto, K., Ozer, A. et al. (2013). Multiplexed microcolumn-based processes for efficient selection of RNA aptamers. *Anal. Chem.* 85: 3417–3424.
- 79 Giamberardino, A., Labib, M., Hassan, E.M. et al. (2013). Ultrasensitive norovirus detection using DNA aptasensor technology. *PLoS One* 8 (11): e79087.
- 80 Liu, X., Li, H., Jia, W. et al. (2017). Selection of aptamers based on protein microarray integrated with microfluidic chip. *Lab Chip* 17 (1): 178–185.
- 81 Geng, X., Zhang, D., Wang, H., and Zhao, Q. (2013). Screening interaction between ochratoxin A and aptamers by fluorescence anisotropy approach. *Anal. Bioanal. Chem.* 405: 2443–2449.

- 82 Zhao, Q., Geng, X., and Wang, H. (2013). Fluorescent sensing ochratoxin A with single fluorophore-labeled aptamer. *Anal. Bioanal. Chem.* 405: 6281–6286.
- 83 Zhu, Z., Ravelet, C., Perrier, S. et al. (2012). Single-stranded DNA binding protein-assisted fluorescence polarization aptamer assay for detection of small molecules. *Anal. Chem.* 84: 7203–7211.
- 84 Samokhvalov, A.V., Safenkova, I.V., Eremin, S.A. et al. (2017). Use of anchor protein modules in fluorescence polarization aptamer assay for ochratoxin A determination. *Anal. Chim. Acta* 962: 80–87.
- 85 Liu, J., Wang, C., Jiang, Y. et al. (2013). Graphene signal amplification for sensitive and real-time fluorescence anisotropy detection of small molecules. *Anal. Chem.* 85: 1424–1430.
- 86 Duhr, S. and Braun, D. (2006). Why molecules move along a temperature gradient. *Proc. Natl. Acad. Sci. U. S. A.* 103: 19678–19682.
- 87 Entzian, C. and Schubert, T. (2016). Studying small molecule–aptamer interactions using MicroScale Thermophoresis (MST). *Methods* 97: 27–34.
- 88 Seidel, S.A.I., Markwardt, N.A., Lanzmich, S.A., and Braun, D. (2014). Thermophoresis in nanoliter droplets to quantify aptamer binding. *Angew. Chem. Int. Ed.* 53: 7948–7951.
- 89 Breitsprecher, D., Schlinck, N., Witte, D. et al. (2016). Chapter 8: Aptamer binding studies using MicroScale Thermophoresis. In: *Nucleic Acid Aptamers: Selection, Characterization, and Application*, Methods in Molecular Biology (ed. G. Meyer). New York: Springer.
- 90 Stoltenburg, R., Schubert, T., and Strehlitz, B. (2015). In vitro selection and interaction studies of a DNA aptamer targeting protein A. *PLoS One* 10 (7): e0134403.
- 91 Jauset-Rubio, M., Svobodová, M., Mairal, T. et al. (2016). β -Conglutin dual aptamers binding distinct aptatopes. *Anal. Bioanal. Chem.* 408: 875–884.
- 92 Esposito, V., Pirone, L., Mayol, L. et al. (2016). Exploring the binding of d(GGGT)₄ to the HIV-1 integrase: an approach to investigate G-quadruplex aptamer/target protein interactions. *Biochimie* 127: 19–22.
- 93 Schax, E., Lönne, M., Scheper, T. et al. (2015). Aptamer-based depletion of small molecular contaminants: a case study using ochratoxin A. *Biotechnol. Bioprocess Eng.* 20: 1016–1025.
- 94 Svobodová, M., Skouridou, V., Botero, M.L. et al. (2017). The characterization and validation of 17 β -estradiol binding aptamers. *J. Steroid Biochem. Mol. Biol.* 157: 14–22.
- 95 Skouridou, V., Schubert, T., Bashammakh, A.S. et al. (2017). Aptatope mapping of the binding site of a progesterone aptamer on the steroid ring structure. *Anal. Biochem.* 531: 8–11.
- 96 Jerabek-Willemsen, M., André, T., Wanner, R. et al. (2014). MicroScale Thermophoresis: interaction analysis and beyond. *J. Mol. Struct.* 1077: 101–113.
- 97 Gold, L., Ayers, D., Bertino, J. et al. (2010). Aptamer-based multiplexed proteomic technology for biomarker discovery. *PLoS One* 5: e15004.

- 98 Wijaya, E., Lenaerts, C., Maricot, S. et al. (2011). Surface plasmon resonance-based biosensors: from the development of different SPR structures to novel surface functionalization strategies. *Curr. Opin. Solid State Mater. Sci.* 15: 208–224.
- 99 Schasfoort, R.B.M. and Tudos, A.J. (eds.) (2008). *Handbook of Surface Plasmon Resonance*. RSC Publishing.
- 100 Chang, T.-W., Janardhanan, P., Mello, C.M. et al. (2016). Selection of RNA aptamers against botulinum neurotoxin type A light chain through a non-radioactive approach. *Appl. Biochem. Biotechnol.* 180: 10–25.
- 101 Trapaidze, A., Hérault, J.-P., Herbert, J.-M. et al. (2016). Investigation of the selectivity of thrombin-binding aptamers for thrombin titration in murine plasma. *Biosens. Bioelectron.* 78: 58–66.
- 102 Miodek, A., Poturnayová, A., Šnejdárková, M. et al. (2013). Binding kinetics of human cellular prion detection by DNA aptamers immobilized on a conducting polypyrrole. *Anal. Bioanal. Chem.* 405: 2505–2514.
- 103 Gopinath, S.C.B., Sakamaki, Y., Kawasaki, K., and Kumar, P.K.R. (2006). An efficient RNA aptamer against human influenza B virus hemagglutinin. *J. Biochem.* 139: 837–846.
- 104 Ruigrok, V.J.B., van Duijn, E., Barendregt, A. et al. (2012). Kinetic and stoichiometric characterization of streptavidin-binding aptamers. *ChemBioChem* 13: 829–836.
- 105 Hwang, J. and Nishikawa, S. (2006). Novel approach to analyzing RNA aptamer–protein interactions: toward further applications of aptamers. *J. Biomol. Screen.* 11 (6): 599–605.
- 106 Smolke, C.D. (2014). Kinetic and equilibrium binding characterization of aptamers to small molecules using a label-free, sensitive, and scalable platform. *Anal. Chem.* 86: 3273–3278.
- 107 de-los-Santos-Álvarez, N., Lobo-Castañón, M.J., Miranda-Ordieres, A.J., and Tuñón-Blanco, P. (2009). SPR sensing of small molecules with modified RNA aptamers: detection of neomycin B. *Biosens. Bioelectron.* 24: 2547–2553.
- 108 González-Fernández, E., de-los-Santos-Álvarez, N., Miranda-Ordieres, A.J., and Lobo-Castañón, M.J. (2012). SPR evaluation of binding kinetics and affinity study of modified RNA aptamers towards small molecules. *Talanta* 99: 767–773.
- 109 Win, M.N., Klein, J.S., and Smolke, C.D. (2006). Codeine-binding RNA aptamers and rapid determination of their binding constants using a direct coupling surface plasmon resonance assay. *Nucleic Acids Res.* 34 (19): 5670–5682.
- 110 Bala, J., Bhaskar, A., Varshney, A. et al. (2011). In vitro selected RNA aptamer recognizing glutathione induces ROS-mediated apoptosis in the human breast cancer cell line MCF7. *RNA Biol.* 8 (1): 101–111.
- 111 He, X., Guo, L., He, J. et al. (2017). Stepping library-based post-SELEX strategy approaching to the minimized aptamer in SPR. *Anal. Chem.* 89: 6559–6566.
- 112 Dausse, E., Barré, A., Aimé, A. et al. (2016). Aptamer selection by direct microfluidic recovery and surface plasmon resonance evaluation. *Biosens. Bioelectron.* 80: 418–425.

- 113 Bard, A.J. and Faulkner, L.R. (2000). *Electrochemical Methods; Fundamentals and Applications*. Wiley Interscience Publications.
- 114 Barsonkov, E. and Macdonald, I.R. (eds.) (2005). *Impedance Spectroscopy: Theory, Experiment, and Applications*, 2e. Wiley Interscience Publications.
- 115 González-Fernández, E., de-los-Santos-Álvarez, N., Lobo-Castañón, M.J. et al. (2011). Impedimetric aptasensor for tobramycin detection in human serum. *Biosens. Bioelectron.* 26: 2354–2360.
- 116 Contreras-Jiménez, G., Eissa, S., Ng, A. et al. (2015). Aptamer-based label-free impedimetric biosensor for detection of progesterone. *Anal. Chem.* 87: 1075–1082.
- 117 Martin, S.R. and Schilstra, M.J. (2013). Rapid mixing kinetic techniques. In: *Protein–Ligand Interactions, Methods and Applications* (ed. M.A. Williams and T. Daviter), 119–138. New York: Springer.
- 118 Da Costa, J.B., Andreiev, A.I., and Dieckmann, T. (2013). Thermodynamics and kinetics of adaptative binding in the malachite green RNA aptamer. *Biochemistry* 52: 6575–6583.
- 119 Förster, U., Weigand, J.E., Trojanowski, P. et al. (2012). Conformational dynamics of the tetracycline-binding aptamer. *Nucleic Acids Res.* 40 (4): 1807–1847.
- 120 Challier, L., Miranda-Castro, R., Marchal, D. et al. (2013). Kinetic rotating droplet electrochemistry: a simple and versatile method for reaction progress kinetic analysis in microliter volumes. *J. Am. Chem. Soc.* 135: 14215–14228.
- 121 Challier, L., Miranda-Castro, R., Barbe, B. et al. (2016). Multianalytical study of the binding between a small chiral molecule and a DNA aptamer: evidence for asymmetric steric effect upon 3'- versus 5'-end modification. *Anal. Chem.* 88: 11963–11971.
- 122 Guyon, H., Mavré, F., Catala, M. et al. (2017). Use of a redox probe for an electrochemical RNA–ligand binding assay in microliter droplets. *Chem. Commun.* 53: 1140–1143.
- 123 Petrov, A., Okhonin, V., Berezovski, M., and Krylov, S.N. (2005). Kinetic capillary electrophoresis (KCE): a conceptual platform for kinetic homogeneous affinity methods. *J. Am. Chem. Soc.* 127: 17104–17110.
- 124 Krylov, S.N. (2007). Kinetic CE: foundation for homogeneous kinetic affinity methods. *Electrophoresis* 28: 69–88.
- 125 Kanatov, M. and Krylov, S.N. (2016). Analysis of DNA phosphate buffered saline using kinetic capillary electrophoresis. *Anal. Chem.* 88: 7421–7428.
- 126 Krylova, S.M., Dove, P.M., Kanoatov, M., and Krylov, S.N. (2011). Slow-dissociation and slow-recombination assumptions in nonequilibrium capillary electrophoresis of equilibrium mixtures. *Anal. Chem.* 83: 7582–7585.
- 127 Berezovski, M.V., Musheev, M.U., Drabovich, A.P. et al. (2006). Non-SELEX: selection of aptamers without intermediate amplification of candidate oligonucleotides. *Nat. Protoc.* 1: 1359–1369.
- 128 Okhonin, V., Krylova, S.M., and Krylov, S.N. (2004). Nonequilibrium capillary electrophoresis of equilibrium mixtures, mathematical model. *Anal. Chem.* 76: 1507–1512.

- 129 Hornblower, B., Coombs, A., Whitaker, R.D. et al. (2007). Single-molecule analysis of DNA–protein complexes using nanopores. *Nat. Methods* 4: 315–317.
- 130 Rotem, D., Jayasinghe, L., Salichou, M., and Bayley, H. (2012). Protein detection by nanopores equipped with aptamers. *J. Am. Chem. Soc.* 134: 2781–2787.
- 131 Van Meervelt, V., Soskine, M., and Maglia, G. (2014). Detection of two isomeric binding configurations in a protein–aptamer complex with a biological nanopore. *ACS Nano* 8 (12): 12826–12835.
- 132 Arnaut, V., Langecker, M., and Simmel, F.C. (2013). Nanopore force spectroscopy of aptamer–ligand complexes. *Biophys. J.* 105: 1199–1207.
- 133 Wanunu, M. (2012). Nanopores: a journey towards DNA sequencing. *Phys. Life Rev.* 9: 125–158.
- 134 Ozer, A., Pagano, J.M., and Lis, J.T. (2014). New technologies provide quantum changes in the scale, speed, and success of SELEX methods and aptamer characterization. *Mol. Ther. Nucleic Acids* 3: e183.
- 135 Cho, M., Soo Oh, S., Nie, J. et al. (2013). Quantitative selection and parallel characterization of aptamers. *Proc. Natl. Acad. Sci. U. S. A.* 110: 18460–18465.
- 136 Nutiu, R., Friedman, R.C., Luo, S. et al. (2011). Direct visualization of DNA affinity landscapes using a high-throughput sequencing instrument. *Nat. Biotechnol.* 29: 659–664.
- 137 Lin, C.H. and Patel, D.J. (1997). Structural basis of DNA folding and recognition in an AMP–DNA aptamer complex: distinct architectures but common recognition motifs for DNA and RNA aptamers complexed to AMP. *Chem. Biol.* 4 (11): 817–832.
- 138 Sussman, D., Nix, J., and Wilson, C. (2000). The structural basis for molecular recognition by the vitamin B12 RNA aptamer. *Nat. Struct. Mol. Biol.* 7: 53–57.
- 139 Krauss, I.R., Merlino, A., Giancola, C. et al. (2011). Thrombin–aptamer recognition: a revealed ambiguity. *Nucleic Acids Res.* 39: 7858–7867.
- 140 Ruigrok, V.J.B., Levisson, M., Hekelarr, J. et al. (2012). Characterization of aptamer–protein complexes by X-ray crystallography and alternative approaches. *Int. J. Mol. Sci.* 13: 10537–10552.
- 141 Xiao, J. and Salsbury, F.R. (2016). Molecular dynamics simulations of aptamer-binding reveal generalized allostery in thrombin. *J. Biomol. Struct. Dyn.* 35 (15): 3354–3369.
- 142 Ruan, M., Seydon, M., Noel, V. et al. (2017). Molecular dynamics simulation of a RNA aptasensor. *J. Phys. Chem. B* 121 (16): 4071–4080.

5

Utilization of Aptamers for Sample Preparation in Analytical Methods

Zhiyong Yan and Yang Liu

Tsinghua University, Department of Chemistry, Tsinghua Yuan, Beijing, 100084, PR China

5.1 Introduction

A complete sample analysis process comprises sample collection, preparation, and analysis, with data process and result reports as the last step. Samples, particularly those collected from environment, food, clinical specimens, or biological fluids, usually consist of complex chemical compositions and have a multiphase (gas, liquid, or solid) physical system. When analyzed directly, the low-abundance target analytes of interest may not be detected accurately. On the other hand, the impurities in the sample could influence the detective results or even damage the analytical instruments. Therefore, sample preparation techniques are critically necessary in the sample analytical process. Sample preparation can isolate or enrich the targets of interest from the matrix, as well as eliminate unwanted interferences and components. Subsequently, the analytic accuracy and precision are improved. Effective sample preparation can significantly improve the efficiency and accuracy of detective results. It is considered as the most time-consuming and labor-intensive step in the sample analysis process, which accounts for up to 80% of the whole analysis time [1]. During sample preparation, indispensable sample preparation protocols are commonly utilized to protect the analytical apparatus from possible damage and to prolong their service life-time, which makes efficient sample preparation very critical.

Traditional methods for sample preparation include solid-phase extraction (SPE)-based approaches such as SPE, solid-phase microextraction (SPME), monolith spin extraction (MSE), stir-bar sorptive extraction (SBSE), microextraction by packed sorbents (MEPS), and so on. On the other hand, liquid-liquid extraction (LLE)-based approaches consist of LLE, liquid-phase microextraction (LPME), extrelut liquid-liquid extraction (ELLE), and so on. In addition, some common sample preparation methods such as magnetic- and microfluidic-based separations are also used. Most of these sample preparation techniques rely on the trap of analytes of interest from complex samples by sorbent materials, followed by desorption and analysis. Hence, the core of these sample preparation methods lies in the choice of selective sorbents. Sorbents play key roles in the sample preparation methods since they can separate or enrich trace analytes in

complicated matrices. For the purpose of improving selectivity, sensitivity, and accuracy in sample preparation, selective tools such as sol-gel porous silica, molecular imprinted polymers (MIPs), restricted access materials (RAMs), antibodies, and aptamers have been introduced in these sample preparation techniques [2–5]. Molecular imprinting is a technique which creates selective binding sites in synthetic polymers using a molecular template. The resulting MIPs are made up of specific cavities, which are complementary to the target analytes since the size, shape, and position of functional groups fit to each other [6]. MIPs are considered as highly selective tools in sample preparation, and have been widely utilized over the past decade due to their low cost, high selectivity, and stability in a broad range of pH and solvents [7, 8]. RAMs are designed for removing macromolecules based on the size-exclusion mechanism, and RAM-based sorbents can significantly extract small analytes out of large molecules (e.g. proteins) [9, 10]. Despite the great progress, the application of MIPs in complex sample analysis requires solving the following problems, such as inevitable nonspecific binding sites, possible template bleeding, tedious searching for optimal conditions, and the limitation to aqueous biosamples.

The immunoaffinity chromatography based on antibody and antigen interaction makes great contributions to the development of life sciences, especially in analytical chemistry. Antibodies can exclusively bind to the target analytes with high affinity and specificity, which enables the extraction of specific antigens by immobilization of antibody molecules to a solid state. Immunoaffinity chromatography is an efficient selection and purification technique and has been applied in the detection of enzymes, viruses, proteins, and so on [11–13]. However, the inherent nature of antibodies obstructs their wide usage as protein receptors in selective extractions. Antibodies are sensitive to pH value, temperature, and some components of solvents, which make the antibody-binding sites unstable and nonreusable in real samples [14]. On the other hand, steric hindrances will be generated in designing closely packed capture probes, attributed to the relatively large size of antibodies compared with other biomolecules. Furthermore, it usually takes time to obtain antibodies, which might influence the progress of experiments.

Aptamers are a class of single-stranded DNA/RNA molecules with high specificity and sensitivity toward specific targets. And they can be selected by the systematic evolution of ligands by exponential enrichment (SELEX). Aptamers exhibit their superiority, being selective elements in sample preparation techniques when compared with other selective tools. They are nontoxic, chemically stable, and cost-effective. Besides, it is convenient and expeditious to obtain the aptamers once their sequence is determined. Moreover, aptamers functionalized with certain groups can immobilize on various solid supports, and they afford remarkable specificity and high binding affinity to proteins, drugs, metal ions, mycotoxins, cells, and other organic or inorganic materials [15–18]. Compared with antibodies, aptamers with small size ($M_w \sim 3000\text{--}20\,000$) show better performance in separation devices, because the reduced steric hindrance allows more loading amounts of aptamers. Being the competitive candidate as selective tools in sample preparation methods, aptamers have attracted the attention of many research groups. Immobilized aptamers for high-throughput biomolecular

detection and screening have been reviewed [19]. Du et al. discussed the application of aptamer-functionalized materials in sample preparation. They mainly focused on the application of aptamer-functionalized materials in sample preparation techniques such as SPE, SPME, and so on [20]. Pichon et al. reviewed the aptamer-based sorbents for sample treatment. They mainly focused on the properties of the oligosorbents, principles of oligoextraction, and parameters when the potential of aptamer-based extraction sorbents were characterized [21]. Zhao et al. reviewed the advances of aptamer-functionalized nano/micro-materials, especially in the clinical diagnosis field. And they mainly focused on the isolation of the rare circulating tumor cell (CTC) and release from aptamer-functionalized surfaces [22].

Herein, this chapter summarizes the recent representative works to highlight the applications of aptamers in different sample preparation methods. First, the common solid supports for aptamer immobilization are introduced. Different immobilization methods and mechanisms have been discussed and illustrated. Next, we review the utilization of aptamer-based supports in various sample preparation methods, including SPE, SPME, microfluidic, capillary electrophoresis (CE), magnetic separation system, and so on. It is shown that the efficiency of the conventional sorptive extraction methods can be largely improved, attributing it to the advantages of aptamer-target recognition-based techniques. Lastly, we highlight the major challenges and perspectives of aptamers being utilized for sample preparation in analytical methods.

5.2 Substrate Materials Developed for Immobilization of Aptamers

Extraction and preconcentration of target analytes with high selectivity are important for successful analysis. Aptamers modified on solid supports form the affinity sorbents (oligosorbents), and they have been investigated in sample preparation techniques to probe the target analytes and ultimately achieve the purpose of separation and selection. Different strategies for aptamer immobilization have been reported, including physical-based adsorption, covalent bonding, self-assembly, affinity reactions, and so on. The most common way for aptamer immobilization on solid support is aptamer-based affinity assays. It is obtained by the non-covalent biotin–streptavidin or biotin–avidin bridge in most cases. Another common way for aptamer immobilization is covalent binding, because aptamers can be modified with specific functional groups (amino, thiol, and carbonyl groups) [23]. In recent years, benefiting from the rapid development of nanomaterials, various kinds of substrate materials for aptamer immobilization have been developed. The most common ones are carbon-based materials (e.g. carbon nanotubes (CNTs), graphene (G), graphene oxide (GO), and fullerene C60), gold nanoparticles (AuNPs), silicon nanomaterials, metal-organic frameworks (MOFs), magnetic nanoparticles (MNPs), and so on.

CNTs are rolled up sheets of graphite with a wide range of diameters. They possess interesting properties when served as substrate materials. The high

surface areas and high ability for π - π interactions provide abundant reactive sites for aptamers to immobilize. For instance, soft single-stranded DNA (ssDNA) can be immobilized on CNTs by π - π stacking interactions between nucleotide bases and the CNT sidewalls [24–26]. On the other hand, CNTs can be synthesized easily with relatively lower cost. GO is usually regarded as one graphite sheet which contains a variety of functional groups, including carboxyl, hydroxyl, ketone, epoxy, and so on. In recent researches, GO gained much attention than CNTs being solid supports for aptamer immobilization, owing to its improved water solubility, high mechanical strength, and versatile surface modification methods. ssDNA can bind GO via hydrophobic or π - π stacking interactions between the nucleobases and GO. For instance, Gulbakan et al. reported the usage of aptamer-conjugated GO in selective enrichment and detection of cocaine and adenosine in human plasma. During which, the carboxyl groups on thiol-functionalized cocaine and adenosine aptamers were activated by ethyl (dimethylaminopropyl) carbodiimide/*N*-hydroxysuccinimide (EDC/NHS) at first. Then a bifunctional poly(ethylene glycol) (PEG) molecule (NH_2 -PEG-SH) was utilized as the spacer reagent, whose amine groups served as linkers to connect the carboxyl groups on GO, while the thiol groups acted as anchors to join the thiol-functionalized cocaine and adenosine aptamers [27]. Apart from DNA, RNA-functionalized carbon nanomaterials have also been investigated in sample preparation techniques. For example, Hu et al. developed polydispersed RNA-GO nanosheets and utilized them to specifically recognize and absorb trace peptide toxins existing in drinking water. In their study, oxygen and hydroxyl groups were located on the surface of GO randomly (above and/or below), while the vast majority of carboxyl groups were designed to exist on the edge of GO. With the help of the amide between the carboxyl groups on GO and the amine groups at the end of the designed RNA sequence, the RNA aptamers could be covalently immobilized on GO nanosheets [28].

Due to the excellent conductivity, unique optical properties, and good biocompatibility, AuNPs have been widely studied in many fields, including biosensors, catalysis, solar cells, separation techniques, and so on [29–32]. Lin et al. summarized the recent advances in application of AuNPs for the specific extraction and enrichment of biomolecules and environmental pollutants [31]. As is well known, AuNPs possess the specific interaction with thiol-containing compound features. Aptamers containing thiol or amino groups can be adsorbed spontaneously onto AuNPs to generate well-organized and self-assembled monolayers [33, 34]. Compared with individual AuNPs, aptamer-functionalized AuNPs increase the specificity and sensitivity of the sorbent toward a specific target. Thus, they have been widely utilized in sample preparation methods such as CE and SPME [35, 36].

Silicon nanomaterials with huge surface-to-volume ratios are facile to synthesize, the surface of silicon nanomaterials can be modified by various functional groups, and widen their applications in sensors, carriers, and adsorbent-related researches. The core-shell form of silicon nanomaterials has the particular function of protecting nanoparticles and grafting organic ligands, which makes them more suitable in designing aptamer-based sorbents. For instance, Ruta et al.

designed a target-specific aptamer chiral stationary phase for the chromatographic resolution of adenosine. During their research, the 5'-aminomodified aptamer was covalently bonded to macrosphere carboxylic-acid-based silica particles through an amide bond. Furthermore, the separation of adenosine enantiomers could be achieved by changing the eluent's ionic strength, proportion of organic modifiers, or the column temperatures [37].

MOFs are a class of hybrid organic–inorganic materials, constructed by strong coordination bond formation using metal ions as nodes while organic linkers act as rods. MOFs feature super large surface areas; and, more importantly, their pore apertures are controllable [38]. Aptamers can be immobilized on the surface or interior structure of MOFs; integration of aptamer with MOFs endows specific molecular recognition properties and affinity surfaces to MOFs, which widen their potential applications [39, 40]. In recent years, MOFs have been studied as sorbents for extraction of a wide range of analytes from small ions to high-molecular-weight proteins [41–43]. For instance, MIL-53, MIL-100, and MIL-101 have demonstrated efficient enrichment effect of peptides; they can exclude proteins from human plasma simultaneously [44]. Zeolitic imidazolate framework-8 (ZIF-8) were utilized as the pseudostationary phase for capillary electrokinetic chromatography; they improved the separation of the phenolic isomers efficiently [45].

In addition to the common materials mentioned, other new and advanced substrates for aptamer immobilization have been investigated. Table 5.1 shows the recent applications of substrate materials developed for immobilization of aptamers.

5.3 Utilization of Aptamers for Sample Preparation in SPE

Nowadays, SPE is widely accepted in sample preparation for chromatographic analysis [46–48]. It can remove the contaminants/interfering substances and enrich the wanted compositions at the trace amount. In SPE, the sorbent can be packed inside various vessels such as cartridges, syringe barrels, microcolumns, or disks. A solid adsorbent is chosen in SPE to absorb the target analytes in the liquid samples, separate them with interfering substances in the sample matrix, and then elute or heat the desorption solution to achieve the purpose of separation and enrichment of the target analytes. Solid adsorbents in the SPE method have great influences on extraction efficiency, enrichment ratio, and sensitivity. Thus, suitable adsorbents with high selectivity are necessary for a successful sample preparation procedure. Traditionally, sorbent materials for SPE with selectivity include MIPs [49], immunosorbents [50], RAMs [51], oligosorbents, and so on [52–55]. Among them, the aptamer ligands combine the advantages of MIPs, antibodies, and RAMs; and possess several advantages, such as specific targeting capability, good stability, and excellent biocompatibility, showing a broad application prospect in SPE.

Table 5.1 Recent applications of substrate materials developed for immobilization of aptamers.

Aptamers	Substrate materials	Type of modification	Sample preparation technique	Analyte	Matrix	Detection method	The limit of detection/ advantages	References
Carcino-embryonic antigen (CEA) aptamer	GO	π - π stacking interactions	CE	CEA	Serums	Chemiluminescence	A detection limit of 4.8 pg ml ⁻¹	[141]
Thiol-functionalized aptamers	GO	Disulfide bond formation	Affinity extraction	Cocaine and adenosine	Human plasma	Mass spectrometry (MS)	Improved signal-to-noise ratios	[27]
Arginine vasopressin (AVP)-specific aptamer	Bis-acrylamide beads, modified by azlactone and coated with streptavidin	Biotin-streptavidin interaction	Microfluidic platform	AVP	Conditioned samples	MS	Prolonged stability	[146]
5'-C6-amino-modified anti-ochratoxin (OTA) aptamer	CNBr-activated sepharose	Covalent binding	SPE	OTA	Wheat extracts	HPLC/fluorescence	A detection limit of 2.2 μ g kg ⁻¹ A recovery close to 90%.	[147]
Amino-functionalized aptamers which recognize polychlorinated biphenyls (PCBs)	MOFs	Amine, covalent binding	dSPE	PCBs	Soil sample	Gas chromatography tandem MS (GC-MS)	0.010–0.015 ng ml ⁻¹ Replicate for 60 extraction cycles with recovery over 80%.	[39]
Antitetracycline aptamers	CNBr-activated sepharose	Covalent binding	Selective SPE	Tetracycline	Human urine and plasma samples	Electrospray ionization-ion mobility spectrometry (ESI-IMS)	A detection limit of 0.019 g ml ⁻¹ for urine and 0.037 g ml ⁻¹ for plasma	[148]

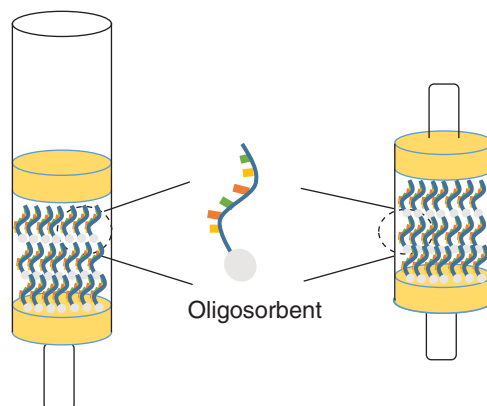
5'-amino-modified DNA aptamer	Hybrid organic-inorganic monolith	Amine, covalent binding	SPE	OTA	Beer samples	On-line to nanoLC	Coverage density of aptamers on the capillaries $6.27 \text{ nmol } \mu\text{l}^{-1}$	[58]
DNA aptamer 1.12.2	CarboxyLink coupling gel (immobilized diaminodipropylamine)	Bonds to the internal phosphate groups	SPE	OTA	Wheat samples	HPLC/fluorescence	A detection limit of 23 pg g^{-1}	[56]
Anti-thrombin DNA aptamer with an amine terminal group	Carboxy-functionalized electrospun microfibers made with the hydrophilic polymer poly (acrylonitrile-co-maleic acid) (PANCMA) on stainless steel rods	Covalent binding between amine functional group and reactive carboxyl moieties	SPME	Thrombin	Diluted human plasma	Liquid chromatography/tandem MS (LC-MS/MS)	A detection limit of 0.30 nM	[73]
Anti-lysozyme DNA aptamer	Poly (glycidyl methacrylate-co-ethylene dimethacrylate) monolithic column	Covalently immobilized through 16-atom spacer arm	Aptamer affinity chromatography	Lysozyme	Chicken egg white	HPLC	Coverage density of immobilized aptamers on monolith: 290 pmol l^{-1}	[149]
Blood glycosylated hemoglobin (HbA1c) -specific aptamers	Magnetic beads	Biotin-streptavidin interaction	Integrated microfluidic system	HbA1c	Blood samples	CL	Automatic detection time 25 min	[150]

(Continued)

Table 5.1 (Continued)

Aptamers	Substrate materials	Type of modification	Sample preparation technique	Analyte	Matrix	Detection method	The limit of detection/ advantages	References
5'-biotin aptamers	Quantum dots	Biotin-streptavidin interaction	Microfluidic	Peanut allergen Ara h1	Food samples	Fluorescence	A detection limit of 56 ng ml ⁻¹	[151]
Human immunoglobulin E (IgE) aptamer	AuNPs	Au-S bonding	CE	IgE	Human serum samples	CL	A detection limit of 7.6 fM	[35]
3'-aminated aptamer	Silica gel	Dichlorodimethylsilane as silane-coupling agent	SPE	Ergot alkaloids	Ergot contaminated flour	Quadrupole-time-of-flight MS (LC-MS-QTOF)	Extract three main ergot alkaloids	[152]
Thrombin-specific aptamer	pH-responsive hydrogel	pH-sensitive contraction and expansion	Microfluidic	Thrombin	Mixture of proteins	ELISA and Polyacrylamide gel electrophoresis	Multiple recycling	[153]
Salmonella binding aptamer containing pendant-NH ₂	P (Hydroxypropyl-methacrylate/ ethyleneglycol dimethacrylate)-g-p (glycidyl methacrylate) beads with functional epoxy groups	Epoxy-amino groups interaction	Magnetic separation	Almonella enterica serovar typhimurium cells	Model food	Quartz crystal microbalance (QCM)	A detection limit of 100 CFU ml ⁻¹	[154]

Figure 5.1 The schematic representation of SPE with an oligosorbent.



5.3.1 Aptamers Utilized in Affinity Column for SPE

There are a variety of aptamer-affinity-based columns which are utilized in selective SPE to target analytes from complicated samples, including aptamer-packed column, aptamer-open column tubular capillary column, aptamer-monolithic column, and aptamer-spin column. The general schematic representation of aptamers being applied in SPE is shown in Figure 5.1.

Aptamer-packed column is prepared by packing aptamer-based sorbents into an empty SPE column. Aptamer-based sorbents are critical in enhancing the separation performance of SPE. Any changes in the sorbents, including the character of the solid support, the immobilization method, or the length of the spacer arm will affect the efficiency of extraction greatly. An aptamer-packed column features the advantages of the high density of the aptamer ligand and high adsorption capacity. Girolamo et al. developed SPE columns packed with aptamer with high affinity and specificity to ochratoxin A (OTA) for the purpose of cleanup of OTA from wheat [56].

Aptamer-open-column tubular capillary column is prepared by immobilizing aptamers on the inner surface of the capillary through covalent binding. However, restricted by the surface area of the inner wall in the capillary and the loading capacity of the sample, the loading amount of immobilized aptamers is usually limited, thus reducing the affinity-capture efficiency.

An aptamer-monolithic column consists of an aptamer-immobilized rigid porous monolith inside the column. With the help of continuous interconnected skeleton structures, the monolithic can enlarge the loading capacity of analytes as well as enhance the permeability, resulting in excellent separation efficiency [57]. Brothier and Pichon designed a miniaturized selective DNA aptamer-based extraction sorbent and utilized them to extract OTA from beer samples. Tetraethoxysilane and 3-aminopropyltriethoxysilane were chosen as precursors during their research; then, the aptamers were covalently immobilized on the hybrid organic–inorganic monolith. The high specific surface area of the synthesized silica-based monolith contributed to the large coverage density of DNA aptamers with $6.27 \text{ nmol } \mu\text{l}^{-1}$. The capacity of OTA is above 5 ng and showed better performance compared with aptamer-based open tubular capillaries or

packed columns [58]. In addition, Deng et al. developed an aptamer-modified organic–inorganic hybrid silica monolithic capillary column and utilized it for human- α thrombin detection. According to their study, the average coverage density of aptamer on the monolithic reached about $568 \text{ pmol } \mu\text{l}^{-1}$. Besides, the binding capacity of thrombin was $1.15 \text{ } \mu\text{g } \mu\text{l}^{-1}$, 14 times compared with the aptamer-modified open tubular capillaries, indicating the great potential of aptamer-monolithic columns in SPE applications [59].

5.3.2 Aptamers Utilized in Other SPE

Dispersive solid-phase extraction (dSPE) features the SPE methodology with a different adsorbent preparation strategy. The adsorbent of dSPE is added in the sample solution straightforward, then extraction and centrifugation will be adopted successively. Lin et al. developed a dSPE adsorbent based on aptamer-functionalized magnetic MOFs, and then they were utilized for enriching trace polychlorinated biphenyls (PCBs) from soil samples. In their strategy, with the aid of polydopamine and glutaraldehyde, amino-functionalized aptamers with specific recognition abilities to PCBs were immobilized on the surface of magnetic amino-functionalized UiO-66 ($\text{Fe}_3\text{O}_4@\text{PDA}@ \text{UiO-66-NH}_2$) MOFs. Due to the specific affinity of aptamers toward PCBs, the obtained aptamer-functionalized MOF adsorbent showed high adsorption capacity in extracting PCBs from complex matrices. Finally, with the assistance of the magnetic separation technique, the MOF adsorbent was separated from the sample matrices efficiently. The dSPE coupled with aptamer-functionalized MOF adsorbent present high selectivity, good reusability, and stability for the extraction of target analytes [39].

5.4 Aptamers Utilized in SPME

SPME is the most popular microextraction technique. It was introduced by Arthur and Pawliszyn in the early 1990s, made up of a fused-silica fiber coated on the outside and an appropriate stationary phase [60]. When the fiber is immersed into the sample, it would absorb or adsorb target analytes (determined by the nature of the coating) until the equilibrium is reached. The total content of the target analytes extracted by the fiber depend on the partition coefficient of the target between the modified fiber and sample matrix. When the extraction step is finished, with the assistance of a syringe-like handling device, the fiber is transferred to an analytical instrument for the next procedures. SPME is a kind of simple, fast, and effective sampling and sample preparation method which combines the sampling, extraction, and enrichment operation in one step. In addition, it can reduce or avoid solvent consumption. These merits of SPME allow it to be an attractive alternative to SPE and LLE. Furthermore, coupling SPME with chromatographic and MS methods has attracted much attention in various applications, especially environmental monitoring (e.g. food, fragrance, biological fluids, and components) [61–63].

The chemistry and physical properties of the SPME sorbent coatings on the fiber play significant roles in the extraction performance of SPME. The extraction

efficiency of previous commercial fiber coatings, such as poly (dimethylsiloxane) (PDMS), polyacrylate (PA), carboxen/PDMS (CAR/PDMS), and polyacrylonitrile (PAN), are largely influenced by the polarity of the target compound. Moreover, several disadvantages limit their further application, such as instability, frangibility, and high cost. Recently, different new SPME coatings have been developed, such as octadecyl-bonded silica (C_{18}), sorptive phase [64], MOFs [65], polymeric ionic liquid-based sorbent coatings [66], electroconductive polymers [67, 68], functionalized ZnO nanorods [69, 70], siloxane-modified polyurethane acrylic resin [71], and so on. In order to further improve the biocompatibility, selectivity, and sensitivity of SPME, many research works are reported on the basis of aptamer-functionalized sorbents. Figure 5.2 is the general representation of the aptamer-based SPME.

5.4.1 Aptamers Utilized in Fiber SPME

As one of the convenient sample preparation techniques, fiber SPME uses the fiber-coated polymeric stationary phase as its extraction device. The absorption of the analyte process takes place on the outer surface of the fiber. When the fiber is inserted into the sample, the target analytes will separate from the sample matrix, and then be absorbed into the polymeric stationary phase which is coated on the surface of the fiber. The separation process will stop when equilibrium is reached. Figure 5.3 shows the extraction procedure of aptamer-based fiber SPME. Fiber SPME integrates all the steps of sample preparation and is more convenient compared with the conventional SPE, which is equipped with packed-bed columns, micro, or non-micro columns.

The core factor in fiber SPME lies in the affinity between the fiber coating and the target analytes. Liquid polymer and porous solid sorbents are usually utilized in functionalized SPME fibers. The polarity of the solvents could affect their absorption performances greatly [72]. In addition to the abovementioned, several kinds of fiber coatings have been developed, including polymer, immunosorbent, RAM, MIP, ion liquid, etc. Among these materials,

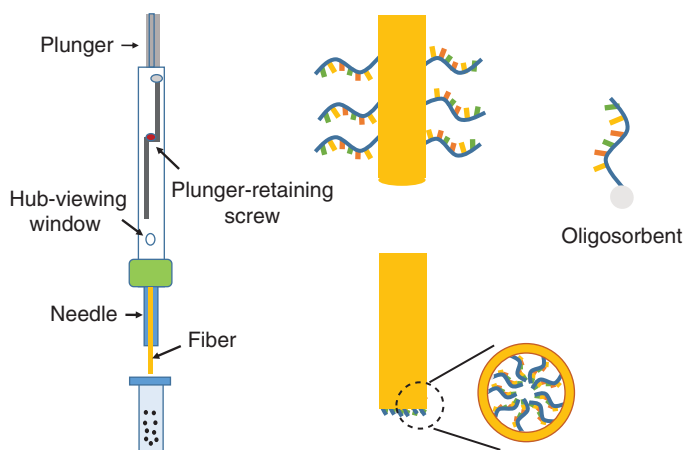


Figure 5.2 The schematic representation of SPME with an oligosorbent.

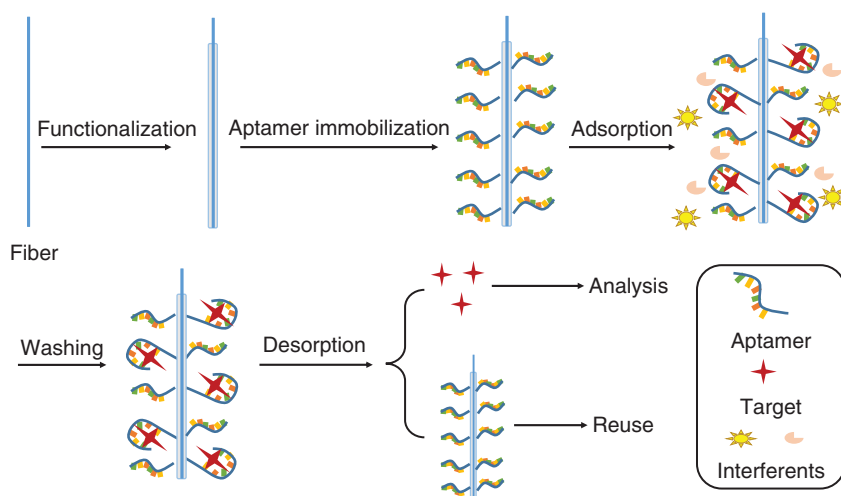


Figure 5.3 The general extraction procedure of aptamer-based fiber SPME.

aptamer-functionalized fibers exhibit good affinity and selectivity. Guo et al. designed an aptamer-functionalized porous-polymer-coated SPME fiber and utilized it for selecting adenosine phosphates. The aptamer-modified fibers showed high stability as well as good reusability [70]. An aptamer-based SPME probe was developed for human α -thrombin extraction and detection in plasma samples with the aid of the LC-MS/MS technique. During which, a 29-mer DNA aptamer specific to the heparin binding site of the thrombin was modified with a 5'-amine functional group at first, then it was covalent immobilized on carboxy-functionalized hydrophilic microfibers through the reactive carboxyl moieties via the EDC/NHS protocol. Under optimal conditions, the detection limit of the proposed method was 0.30 nM [73].

Recently, a three-dimensional-type SPME fiber modified with aptamer was developed to concentrate multiplex antibiotic residues from milk samples. Thiol-functionalized aptamers with high affinity for chloramphenicols was covalently immobilized on AuNPs, which electrodeposited on the gold wire around conductive indium tin oxide (ITO) glassy fiber. Coupled with high-performance liquid chromatography (HPLC) detection, this 3D aptamer-functionalized SPME platform exhibited much better enrichment performance than 2DApt@AuNPs-ITO fiber and 1D-Apt@Au wire-ITO fiber-based SPME platforms. In addition, the designed extraction fiber SPME method could be extended to selective concentrate other organic pollutant residues with the change of specific aptamers [36].

5.4.2 Aptamers Utilized in SBSE

SBSE was developed as a sample preparation technique in 1999 [74], and it shares a principle similar to SPME. However, different from the fiber utilized in SPME, the extraction phase (such as PDMS) is coated on the magnetic stir bars in SBSE

techniques. The direct SBSE is achieved when the coated stir bar is added to the sample mixtures directly for the purpose of extraction. Or the coated stir bar can also be exposed to the headspace until the equilibrium is reached. In addition, after the stir bar is removed from the aqueous sample, the absorbed compounds are desorbed or analyzed. To extract the ultra-trace level of targets in complicated samples, the selection of appropriate coatings on the SBSE fiber is vital.

In recent years, a great deal of attention has been paid to the increasing extraction efficiency of the SBSE technique [75–77]. For instance, aptamer-functionalized SBSE coupled with GC-MS was developed to enrich and determine PCBs from fish samples. The SBSE coating was prepared by immobilization of aptamers which could recognize PCBs on the MOF (MOF-5) substrate in one step and it showed higher selectivity and enrichment capacity than the commercial fiber [40].

5.4.3 Aptamers Utilized in Other Formats of SPME

As one kind of SPME, thin-film microextraction (TFME) was introduced by the Pawliszyn research group in 2003 [78]. The sorbent in TFME is composed of a thin and wide membrane. TFME exhibits the advantages of a large volume extraction phase and high surface-to-volume ratio. Hashemian et al. immobilized anticodine aptamers on Whatman cellulose paper through covalent connecting of the amino aptamers and aldehyde groups of the oxidized cellulose paper. Then the aptamer-modified paper was utilized for selective microextraction of codeine from urine samples; this strategy provided a good sensitivity with a detection limit of 3.4 ng ml^{-1} [79]. Later, they reported a similar aptamer-based TFME method. Unlike the previous work, the cellulose paper utilized played two important roles. One is served as an ionization source and the other could extract target analyte selectively with the aid of immobilized aptamers. This strategy integrated the sample preparation as well as the analyte ionization process in a Whatman paper [80].

5.5 Aptamers Utilized in Other Affinity Chromatography

Chromatography is particularly popular in separation and purification techniques [81, 82]. Affinity chromatography was introduced by Cuatrecasas [83, 84]. The mechanism for biomolecule separation and concentration is the reversible and specific binding reaction to the solid phase functionalized with certain ligands. One typical example of the affinity interaction is antibody-based affinity. It starts with an antibody-immobilized solid support. Then the target analytes will be retained and concentrated selectively by the effective and specific chemical binding process. However, the antibody needs to be purified at a high level before being utilized in sample separation methods. Otherwise, the impurities have adverse impacts on target isolation and purification. Besides, the denaturation susceptibility, high cost, and small batch production of antibodies

limit their further application in immunoaffinity chromatography. Compared with antibody-based affinity chromatography, aptamers offer several advantages and have emerged as a potential replacement for antibodies in the affinity chromatography field.

With extremely high affinity to their specific targets, the achievement of utilization aptamers as a stationary phase in affinity chromatography is expected. The general procedure of the aptamer-based chromatographic column is shown in Figure 5.4. Aptamers have long been investigated as an affinity ligand as well as a labeled probe to extract and concentrate target analytes in biological complexes. For instance, Connor and McGown designed a stationary phase by modifying thrombin-binding aptamers to the inner surface of a bare fused-silica glass capillary. After that, they were used to capture thrombin. It was a delight to see that approximately three times as much thrombin as the control columns was obtained by the designed aptamer stationary phase, indicating the promising potential of aptamers in affinity capillary chromatography [85]. A Concanavalin A (Con A)- specific aptamer-functionalized stationary phase was developed as affinity matrix to extract and purify Con A from other lectins. The Con A aptamer (a 41-nt ssDNA) was immobilized on the activated gel matrix site selectively with the help of amine moiety $[-H_2N-(CH_2)_6]$ functionalized on the terminal end. Meanwhile, a hexamer C6 linkage that existed at the end of the aptamer ensured maximal target binding. Owing to the high affinity and specificity of aptamers toward Con A, the aptamer-affinity chromatography showed exciting performance in purification and recovery [86]. Another aptamer-based stationary phase was synthesized by the specific covalent interaction between G-quartet structural DNA oligonucleotides and a fused-silica capillary; they were utilized as for separation of bovine milk proteins [87].

Aptamer-based affinity chromatography is utilized to isolate and purify proteins, as well as extract other biomolecules from complicated samples.

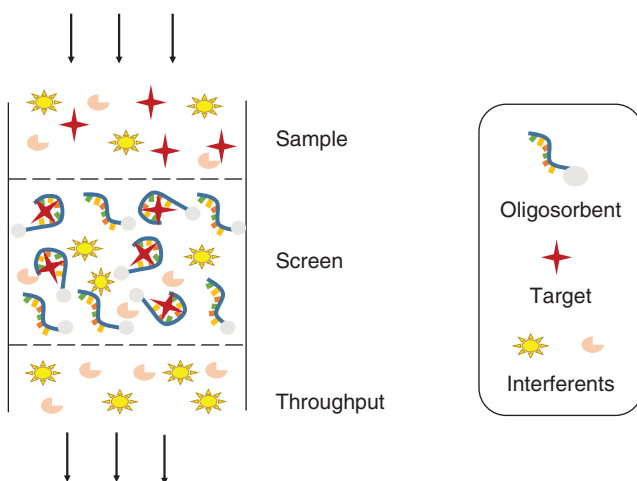


Figure 5.4 The general procedure of an oligosorbent chromatographic column for sample screening.

Deng et al. packed anti-adenosine aptamers into a capillary chromatography column to selective separate and preconcentrate adenosine from microdialysis samples. It was considerably simple, fast, and less costly [88]. Jiang et al. developed an aptamer-based organic-silica hybrid monolithic capillary column. In their proposal, a 5'-SH-modified aptamer specific to doxorubicin was chosen. Then with the aid of the sol-gel method combined with "thio-lene" click reaction, the aptamer was covalently immobilized in the hybrid silica monolithic column. With the developed aptamer-based affinity monolithic capillary liquid chromatography strategy, it could separate the enantiomers of doxorubicin and epirubicin easily [89].

Due to the properties of inherent high affinity and specificity, aptamer-based sorbents have been designed as target-specific chiral selectors. For instance, a chiral stationary phase was constructed by immobilization of L-RNA aptamers on a chromatographic support with the help of a biotin-streptavidin bridge. It could be used to distinguish racemates of both the target and various related compounds [90]. Michaud et al. designed a target-specific chiral selector; they immobilized D-vasopressin-specific DNA aptamers on a porous polystyrene-divinylbenzene support to construct a chromatographic column for HPLC. The specific chiral selector showed good enantioselectivity owing to the specific bonding of the stationary phase to the D-enantiomer [91].

5.6 Aptamers Utilized in Microfluidic Separation System

One important direction in microfluidics is integrating the sample preparation, multiple fluidic injection channel, and the analysis process on a single microchip. Benefits from the advantages of low-cost, rapid-separation and high-throughput, microfluidic devices have been successfully widening their application in separation and bioanalysis-related fields [92–94]. The solid structures of supports are quite important for the purpose of selective extraction and preconcentration of the target in the microfluidic-based separated system. Dziomba et al. have reviewed the latest achievements in sample processing techniques; they mainly focused on the application of solid supports for extraction and preconcentration of proteins and peptides with the aid of microfluidic devices. Different solid supports, such as microbeads, monolithic materials, and membranes have been discussed [95]. Other than that, aptamer-based microfluidic sample preparation techniques have also been applied to extract and purify minute amounts of target analytes from complex samples [96–98]. Figure 5.5 presents a schematic illustration of aptamer-functionalized microfluidic techniques. As is shown, a stationary phase can be obtained by packing the chamber with aptamer-modified microbeads inside the microfluidic devices. When the target molecules are transported to the assembled phase, they will be captured and concentrated on the basis of the specific affinity interaction between the aptamer and the target molecules. Moreover, the process of detection and analysis can also be accomplished in these developed microfluidic devices.

Aptamer-based microfluidics have attracted attention in designing diagnostic probes for various existing biomarkers, such as mRNAs, proteins, viruses,

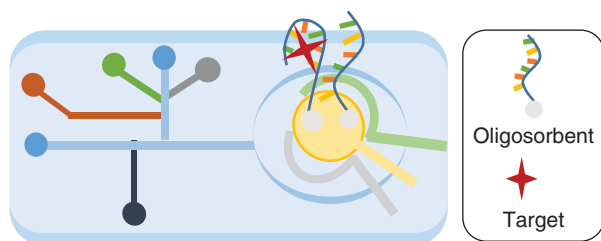


Figure 5.5 The schematic representation of the aptamer-based microfluidic technique.

and bacteria [99–102]. For example, an integrated microfluidic device using a single universal aptamer to detect multiple types of influenza viruses has been reported [103]. A cancer-cell-specific aptamer-based microfluidic device coupled with cell-affinity chromatography was developed, and it showed good enrichment efficiency and detection effect for multiple cancer cells in complex biological samples [99].

Aptamers have shown better stability compared with antibodies in synthesis application and storage. They can be an effective and economical alternative in designing new strategies. For instance, aptamers can replace one or both of the antibodies in a classical ELISA. Shin et al. reported an electrochemical biosensor integrated with a microfluidic platform. Instead of antibodies, aptamers were chosen as the antigen receptors for detection of secreted protein on-line [104]. Jolly et al. designed sandwich-based immunoassays in a microfluidic device using a DNA aptamer instead of a primary antibody. The integrated microfluidic device was finally used for detection of two kinds of free prostate-specific antigen (fPSA). The DNA aptamer exhibited good recognition capability for the antigens; and the detection limit for fPSA was 0.5 ng ml^{-1} , while it was 3 ng ml^{-1} for glycosylated fPSA. Both of them were in the clinical range [105].

Different from the one-aptamer-one-antibody assay mentioned, Li et al. developed a dual-aptamer-based microfluidic system for automatic glycosylated HbA1c measurement. At first, the target–aptamer–bead complexes were synthesized by conjugating HbA1c or hemoglobin (Hb)-specific aptamers on magnetic beads for the purpose of capturing target molecules in a closed chamber. After that, the complexes were collected with the help of an external magnetic field. Finally, sandwich-like structures with target–aptamer–bead complexes were obtained by incubating fluorescent dye-labeled second aptamers with the captured Hb or HbA1c proteins. The microfluidic system reduced reagent consumption of 75%. Besides, the analysis time was greatly shortened compared to previous bench-top manual assays [106]. Another interesting dual-aptamer assay was reported by Tseng et al. They designed an aptamer-virus-aptamer sandwich assay which automatically performed on an integrated, magnetic-bead-based microfluidic system. Due to the high affinity and specificity of the H1N1-specific aptamers, sensitive influenza H1N1 virus detection was achieved. Besides, the analysis time was also reduced largely compared with the conventional viral culture method [107]. Synergistic effect of two or more aptamers may enhance cell affinity; thus, multiple aptamers have also been investigated in an aptamer-capturing system.

For instance, a microfluidic system using aptamer cocktail to concentrate and capture circulating tumor cells from lung cancer patients has been designed. During which, the microfluidic chip was composed of a silicon nanowire substrate as well as a PDMS chaotic mixer. Then the multiple aptamers were modified on the silicon nanowire substrate. The cell capture affinity was improved obviously, owing to synergistic effects among individual aptamers [108].

Instead of utilizing aptamer-based microfluidic devices in bioanalysis-related applications, Fu et al. designed an aptamer-functionalized microfluidic device for 3,3',4,4'-tetrachlorobiphenyl (PCB77) detection based on surface-enhanced Raman scattering (SERS). Mercapto aptamers were covalently connected to the surface of Ag nanocrown array by thiol linkers primarily; then the SERS signal generated from Ag nanocrown array was utilized for sensitive PCB77 measurement [109].

5.7 Aptamers Utilized in Magnetic Separation System

Nowadays, magnetic nanocomposites have obtained heightened attention for bioactive molecule immobilization due to their unique advantages of easy control and simple separation [110, 111]. Besides the nanocomposites with the general formula MFe_2O_4 ($M = Fe, Co, Cu, Mn, \text{etc.}$), such as Fe_3O_4 , $\gamma\text{-}Fe_2O_3$, Co_3O_4 , there are many other magnetic carriers such as polymer-coated magnetic nanocomposites [112], mesoporous silica-coated magnetic nanocomposites [113], ionic liquid-coated magnetic nanocomposites [114], metal-nanoparticle-coated magnetic nanocomposites [115], and so on [116–118]. The basic principle of magnetic separation is illustrated in Figure 5.6. At first, magnetic carriers or magnetic particles are functionalized with certain materials, and then modified with the aptamers through chemical or physical interactions. Once exposed

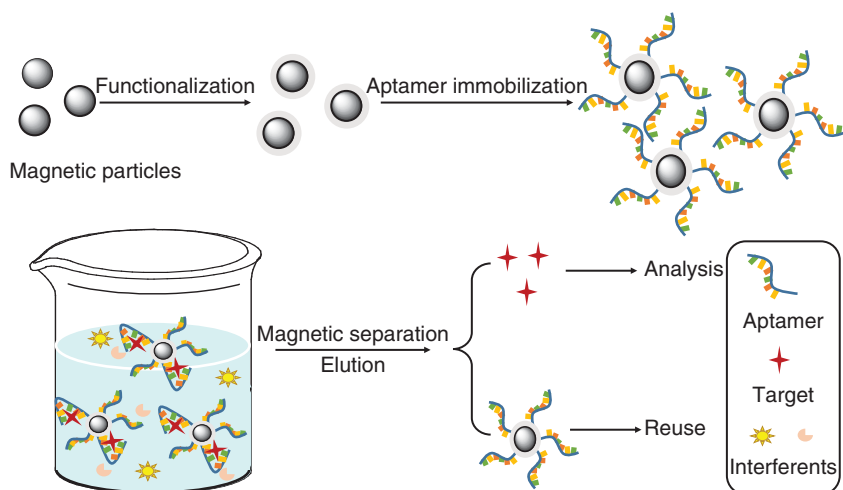


Figure 5.6 The general extraction procedure of an aptamer-based magnetic separation system.

to the complex sample solution, aptamers on the surface of magnetic particles instantly fold into unique structures, which can capture the target compound efficiently. After that, the whole magnetic complex can be easily selected from the complicated sample with the help of appropriate magnetic separators (strong permanent magnets in most cases). Finally, the isolated target compound can be eluted and utilized for further work after the washing treatment.

Magnetic separation techniques have several advantages, such as simple and integrated operation process, high magnetic separation efficiency, and nondestructive separation ways for biological analytes. Hence, magnetic separation techniques have been widely utilized in magnetic-particle-based immunoassay systems [119, 120] and magnetic-particle-based affinity systems [121, 122].

The approaches to immobilize aptamers on the surface of magnetic nanocomposites are diverse [123]. For example, magnetic nanocomposites previously modified with certain groups such as $-\text{COOH}$, $-\text{NH}_2$ can be functionalized with aptamers by the EDC/NHS protocol. Streptavidin-coated magnetic nanocomposites can conjugate with aptamers labeled with biotin. In addition, nanocomposites coated with AuNPs or Au shells can bind with thiolated aptamers through the formation of Au—S bond. After the aptamers are modified on the surface of nanocomposites, followed by incubating with the target molecule in the sample solution, the target molecule can be separated through affinity adsorption and magnetic separation under an external magnetic field.

5.7.1 Aptamers Utilized in Magnetic Solid-Phase Extraction (MSPE)

MSPE enables to preconcentrate and extract trace amounts of target analytes from complicated solutions or suspensions with the help of a magnetic-specific adsorbent. MSPE has certain advantages over other SPE techniques, such as shorter extraction time, higher adsorption capacity, and lower consumption of organic solvent. Moreover, it can extract target analytes from high-saline matrices [124]. However, magnetic nanocomposites are prone to aggregate and they are difficult to disperse in water samples; hence, functionalized magnetic sorbents were developed, such as CNTs filled with cobalt ferrite [125], multiwall carbon nanotubes (MWNTs) filled with $\gamma\text{-Fe}_2\text{O}_3$ nanoparticles [126], and so on. Aptamer-modified magnetic beads emerge as alternatives to antibodies in the enrichment techniques. For instance, Richards et al. immobilized biotinylated gonadotropin-releasing hormone (GnRH) aptamers on the magnetic beads and then utilized them in SPE for the enrichment of GnRH in equine urine. Combined with LC-MS/MS, GnRH were quantitative analyzed with detection limits of 1 pg ml^{-1} , which was more sensitive than the previous antibody-based enrichment methods (2.5 pg ml^{-1}) [127].

5.7.2 Aptamers Utilized in Other Magnetic Separation Formats

Aptamer-based magnetic separation techniques facilitate or accelerate the separation and purification procedures in biological analysis. A variety of aptamer-based magnetic separation researches have been reported [128–130]. For example, aptamer-conjugated upconversion nanoprobes isolated using

the magnetic separation technique was utilized for detection of circulating tumor cells [131]. Aptamer-functionalized magnetic beads were utilized in selective identification and separation of flame retardant chemicals [132]. Najafabadi et al. developed Fe_3O_4 MNPs conjugated with an aptamer for selective extraction of adenosine in urine samples [133]. Wang et al. designed aptamer-based sorbents by immobilizing aptamers on the surface of magnetic mesoporous TiO_2 (mTiO_2)-coated Fe_3O_4 nanoparticles ($\text{Fe}_3\text{O}_4@\text{mTiO}_2$ MNPs). The aptamer-based sorbents could selectively extract targets from complicated sample matrices and exhibited highly efficient target separation from aqueous solution [134].

Fischer et al. reported the first automated enrichment approach for antibiotics. They coated the MNPs with antibiotic sulfanilamide-specific aptamers. Then a magnetic-separator-enabled program-controlled automated catch and release of magnetic particles in a defined order was chosen to remove the aptamer-coated MNPs. Combined with fluorescence and LC-MS/MS techniques, the antibiotics in milk were determined and quantified. This aptamer-based automated magnetic separation strategy exhibited an increased reproducibility and a shrinking hands-on time. In addition, it was more stable compared to antibody analogs and exhibited lower variance compared to the manual approach [135].

Aptamer-based magnetic separation techniques have also been used for cell sorting assays. Guo et al. exploited a labeled aptamer to isolate adult mesenchymal stem cells from porcine bone marrow in a direct way, during which streptavidin-coated magnetic microbeads were utilized [136]. Nair et al. designed specific-target aptamer-conjugated superparamagnetic nanoparticles, and treated them as a nanosurgeon to target and remove cells. The synthesized aptamer-conjugated superparamagnetic nanoparticles were controlled by an externally applied 3D rotational magnetic field. When magnetic fields generated, adherent cells modified on the superparamagnetic nanoparticles would be pulled from the culture surface. This platform could be used for selective surgery and cell manipulation studies in the medical field [137].

5.8 Aptamers Utilized in CE

CE possesses various advantages in affinity studies such as low wastage, short analysis time, automated operation, and the possibility of monitoring interactions in the physiological environment. Most CE assays are combined with the laser-induced fluorescence (LIF) technique [138]. Aptamers provide a molecular basis for fluorescence labeling. When binding labeled aptamers with target analytes, structure switching occurs along with the changing of fluorescent signals [139]. Marechal et al. developed a composite capillary, which combined affinity preconcentration with electrophoretic separation. In their research, 5'-SH-modified oligonucleotide aptamers were immobilized on a fritless affinity monolithic, which acted as the preconcentration unit to enrich and separate OTA in standard solution [140]. In addition to the LIF technique, Zhou et al. utilized aptamer-functionalized GO for CEA detection, during which a capillary electrophoresis-chemiluminescence (CE-CL) system was adopted [141].

5.9 Aptamers Utilized in Other Sample Separation Methods

In addition to the aforementioned aptamer-based sample preparation techniques, there are many other well-established separation techniques, such as pipette-tip extraction, electrochemical methods, electromembrane extraction, single-drop microextraction, and protein precipitation, and so on [142–144]. For instance, protein precipitation is mainly utilized for antigen detection and purification in biological research. Kim et al. developed an aptamer-mediated magnetic protein precipitation strategy with the purpose of capturing and purifying target proteins. Aptamer-conjugated magnetic agarose beads as well as biotinylated aptamer-coated magnetic beads were synthesized. Benefiting from the high affinity of aptamers to the target analytes, endogenous proteins were enriched and protein–protein interaction was studied [145].

5.10 Conclusion and Outlook

Aptamers have been widely utilized in the sample preparation method in environmental science and the food and biomedicine industries. The aptamer-based systems such as sample preparation techniques and aptamer-based assays show great potential applications in the development of extraction devices. Although exciting progress has been achieved, the number of aptamer–target pairs is limited and needs to be further expanded. For the purpose of immobilization of aptamers, the development of new SPE supports is necessary with high chemical stability, excellent biocompatibility, as well as easy subsequent modification and low nonspecific adsorption. Moreover, the miniaturization of the high-throughput analytical device is still challenging, which can simultaneously realize extraction, separation, and purification of several target analytes from complex samples. The aptamer-based sample preparation techniques will be more broadly applied in SPE, affinity column, affinity chromatography, microfluidic separation systems, magnetic separation system, and CE.

References

- 1 Buszewski, B. and Szultka, M. (2012). Past, present, and future of solid phase extraction: a review. *Crit. Rev. Anal. Chem.* 42 (3): 198–213.
- 2 Augusto, F., Carasek, E., Silva, R.G. et al. (2010). New sorbents for extraction and microextraction techniques. *J. Chromatogr. A* 1217 (16): 2533–2542.
- 3 Baltussen, E., Cramers, C.A., and Sandra, P.J. (2002). Sorptive sample preparation – a review. *Anal. Bioanal. Chem.* 373 (1–2): 3–22.
- 4 Casado, N., Pérez-Quintanilla, D., Morante-Zarcelero, S., and Sierra, I. (2017). Current development and applications of ordered mesoporous silicas and other sol-gel silica-based materials in food sample preparation for xenobiotics analysis. *TrAC, Trends Anal. Chem.* 88: 167–184.

- 5 Ashley, J., Shahbazi, M.A., Kant, K. et al. (2017). Molecularly imprinted polymers for sample preparation and biosensing in food analysis: progress and perspectives. *Biosens. Bioelectron.* 91: 606–615.
- 6 Scorrano, S., Longo, L., and Vasapollo, G. (2010). Molecularly imprinted polymers for solid-phase extraction of 1-methyladenosine from human urine. *Anal. Chim. Acta* 659 (1–2): 167–171.
- 7 Machyňáková, A. and Hroboňová, K. (2017). Preparation and application of magnetic molecularly imprinted polymers for the selective extraction of coumarins from food and plant samples. *Anal. Methods* 9 (14): 2168–2176.
- 8 Wang, P., Zhao, X.Y., Luo, J. et al. (2017). Fluorescent, magnetic dual-responsive molecularly imprinted polymers for the selective detection of moxidectin in animal samples. *J. Iran. Chem. Soc.* 14 (4): 755–762.
- 9 De Faria, H.D., Abrão, L.C., Santos, M.G. et al. (2017). New advances in restricted access materials for sample preparation: a review. *Anal. Chim. Acta* 959: 43–65.
- 10 Yang, S.H., Fan, H., Classon, R.J., and Schug, K.A. (2013). Restricted access media as a streamlined approach toward on-line sample preparation: recent advancements and applications. *J. Sep. Sci.* 36 (17): 2922–2938.
- 11 Zhang, Z.W., Hu, X.F., Zhang, Q., and Li, P.W. (2016). Determination for multiple mycotoxins in agricultural products using hplc-ms/ms via a multiple antibody immunoaffinity column. *J. Chromatogr. B* 1021: 145–152.
- 12 Sintiprungrat, K., Chaisuriya, P., Watcharatanyatip, K., and Ratanabanangkoon, K. (2016). Immunoaffinity chromatography in anti-nomics studies: various parameters that can affect the results. *Toxicol.* 119 (1): 129–139.
- 13 Shimura, K. and Nagai, T. (2016). Capillary isoelectric focusing after sample enrichment with immunoaffinity chromatography in a single capillary. *Sci. Rep.* 6: 39221.
- 14 Tombelli, S., Minunni, M., and Mascini, M. (2005). Analytical applications of aptamers. *Biosens. Bioelectron.* 20 (12): 2424–2434.
- 15 Baumstummel, A., Lehmann, D., Janjic, N., and Ochsner, U.A. (2014). Specific capture and detection of *Staphylococcus aureus* with high-affinity modified aptamers to cell surface components. *Lett. Appl. Microbiol.* 59 (4): 422–431.
- 16 Shiratori, I., Akitomi, J., Boltz, D.A. et al. (2014). Selection of DNA aptamers that bind to influenza A viruses with high affinity and broad subtype specificity. *Biochem. Biophys. Res. Commun.* 443 (1): 37–41.
- 17 Weiss, T.C., Zhai, G.G., Bhatia, S.S., and Romaniuk, P.J. (2010). An RNA aptamer with high affinity and broad specificity for zinc finger proteins. *Biochemistry* 49 (112): 2732–2740.
- 18 Kim, Y.S. and Gu, M.B. (2013). Advances in aptamer screening and small molecule aptasensors. *Adv. Biochem. Eng./Biotechnol.* 140: 29–67.
- 19 Acquah, C., Danquah, M.K., Yon, J.L. et al. (2015). A review on immobilised aptamers for high throughput biomolecular detection and screening. *Anal. Chim. Acta* 888: 10–18.

- 20 Du, F.Y., Guo, L., Qin, Q. et al. (2015). Recent advances in aptamer-functionalized materials in sample preparation. *TrAC, Trends Anal. Chem.* 67: 134–146.
- 21 Pichon, V., Brothier, F., and Combes, A. (2015). Aptamer-based-sorbents for sample treatment-a review. *Anal. Bioanal. Chem.* 407 (3): 681–698.
- 22 Zhao, Y.J., Xu, D.K., and Tan, W.H. (2017). Aptamer-functionalized nano/micro-materials for clinical diagnosis: isolation, release and bioanalysis of circulating tumor cells. *Integr. Biol.* 9 (3): 188–205.
- 23 Liu, J. and Lu, Y. (2006). Preparation of aptamer-linked gold nanoparticle purple aggregates for colorimetric sensing of analytes. *Nat. Protoc.* 1 (1): 246–252.
- 24 Zhen, S.J., Chen, L.Q., Xiao, S.J. et al. (2010). Carbon nanotubes as a low background signal platform for a molecular aptamer beacon on the basis of long-range resonance energy transfer. *Anal. Chem.* 82 (20): 8432–8437.
- 25 Zhu, Z., Tang, Z.W., Phillips, J.A. et al. (2008). Regulation of singlet oxygen generation using single-walled carbon nanotubes. *J. Am. Chem. Soc.* 130 (33): 10856–10857.
- 26 Yang, R.H., Tang, Z.W., Yan, J.L. et al. (2008). Noncovalent assembly of carbon nanotubes and single-stranded DNA an effective sensing platform for probing biomolecular interactions. *Anal. Chem.* 80 (19): 7408–7413.
- 27 Gulbakan, B., Yasun, E., Shukoor, M.I. et al. (2010). A dual platform for selective analyte enrichment and ionization in mass spectrometry using aptamer-conjugated graphene oxide. *J. Am. Chem. Soc.* 132 (49): 17408–17410.
- 28 Hu, X.G., Mu, L., Wen, J.P., and Zhou, Q.X. (2012). Immobilized smart RNA on graphene oxide nanosheets to specifically recognize and adsorb trace peptide toxins in drinking water. *J. Hazard. Mater.* 213–214 (7): 387–392.
- 29 Zhang, X.R., Xu, Y.P., Yang, Y.Q. et al. (2012). A new signal - on photoelectrochemical biosensor based on a graphene/quantum - dot nanocomposite amplified by the dual - quenched effect of bipyridinium relay and aunps. *Chem. Eur. J.* 18 (51): 16411–16418.
- 30 Kawawaki, T., Takahashi, Y., and Tatsuma, T. (2013). Enhancement of dye - sensitized photocurrents by gold nanoparticles: effects of plasmon coupling. *J. Phys. Chem. C* 117 (11): 5901–5907.
- 31 Yan, Z.Y., Yang, M., Wang, Z.H. et al. (2015). A label - free immunosensor for detecting common acute lymphoblastic leukemia antigen (cd10) based on gold nanoparticles by quartz crystal microbalance. *Sens. Actuators, B* 210: 248–253.
- 32 Pons, T., Medintz, I.L., Sapsford, K.E. et al. (2007). On the quenching of semiconductor quantum dot photoluminescence by proximal gold nanoparticles. *Nano Lett.* 7 (10): 3157–3164.
- 33 Kim, D.K., Jeong, Y.Y., and Jon, S. (2010). A drug-loaded aptamer-gold nanoparticle bioconjugate for combined ct imaging and therapy of prostate cancer. *ACS Nano.* 4 (7): 3689–3696.

- 34 Yan, Z.Y., Wang, Z.H., Miao, Z., and Liu, Y. (2016). Dye-sensitized and localized surface plasmon resonance enhanced visible-light photoelectrochemical biosensors for highly sensitive analysis of protein kinase activity. *Anal. Chem.* 88 (1): 922–929.
- 35 Liu, Y.M., Cao, J.T., Liu, Y.Y. et al. (2015). Aptamer-based detection and quantitative analysis of human immunoglobulin E in capillary electrophoresis with chemiluminescence detection. *Electrophoresis* 36 (19): 2413–2418.
- 36 Liu, H.B., Gan, N., Chen, Y.J. et al. (2017). Three dimensional $m \times n$ type aptamer-functionalized solid-phase micro extraction fibers array for selectively sorptive extraction of multiple antibiotic residues in milk. *RSC Adv.* 7 (12): 6800–6808.
- 37 Ruta, J., Ravelet, C., Desire, J. et al. (2008). Covalently bonded DNA aptamer chiral stationary phase for the chromatographic resolution of adenosine. *Anal. Bioanal. Chem.* 390 (4): 1051–1057.
- 38 Liu, D.M., Lu, K., Poon, C., and Lin, W.B. (2014). Metal-organic frameworks as sensory materials and imaging agents. *Inorg. Chem.* 53 (4): 1916–1924.
- 39 Lin, S.C., Gan, N., Cao, Y.T. et al. (2016). Selective dispersive solid phase extraction-chromatography tandem mass spectrometry based on aptamer-functionalized UiO-66-NH₂ for determination of polychlorinated biphenyls. *J. Chromatogr. A* 1446: 34–40.
- 40 Lin, S.C., Gan, N., Zhang, J.B. et al. (2016). Aptamer-functionalized stir bar sorptive extraction coupled with gas chromatography-mass spectrometry for selective enrichment and determination of polychlorinated biphenyls in fish samples. *Talanta* 149: 266–274.
- 41 Yu, Y.B., Ren, Y.Q., Shen, W. et al. (2013). Applications of metal-organic frameworks as stationary phases in chromatography. *TrAC, Trends Anal. Chem.* 50: 33–41.
- 42 Wen, Y.Y., Chen, L., Li, J.H. et al. (2014). Recent advances in solid-phase sorbents for sample preparation prior to chromatographic analysis. *TrAC, Trends Anal. Chem.* 59 (4): 26–41.
- 43 Rocío-Bautista, P., Pacheco-Fernández, I., Pasán, J., and Pino, V. (2016). Are metal-organic frameworks able to provide a new generation of solid-phase microextraction coatings? –a review. *Anal. Chim. Acta* 939: 26–41.
- 44 Gu, Z.Y., Chen, Y.J., Jiang, J.Q., and Yan, X.P. (2011). Metal-organic frameworks for efficient enrichment of peptides with simultaneous exclusion of proteins from complex biological samples. *Chem. Commun.* 47 (16): 4787–4789.
- 45 Li, L.M., Wang, H.F., and Yan, X.P. (2012). Metal-organic framework ZIF-8 nanocrystals as pseudostationary phase for capillary electrokinetic chromatography. *Electrophoresis* 33 (18): 2896–2902.
- 46 Qi, F.F., Jian, N.G., Qian, L.L. et al. (2017). Development and optimization of a novel sample preparation method cored on functionalized nanofibers mat-solid-phase extraction for the simultaneous efficient extraction of illegal anionic and cationic dyes in foods. *Anal. Bioanal. Chem.* 409 (24): 1–13.

- 47 Zdravkovic, S.A. (2017). Solid-phase extraction for the preparation of aqueous sample matrices for gas chromatographic analysis in extractable/leachable studies. *Pharm. Technol.* 41 (5): 54–60.
- 48 Huertaspérez, J.F., Arroyomanzanas, N., Garcíacampaña, A.M., and Gámizgracia, L. (2017). Solid phase extraction as sample treatment for the determination of ochratoxin a in foods: a review. *Crit. Rev. Food Sci. Nutr.* 57 (16): 3405–3420.
- 49 Ambrosini, S., Shinde, S., De Lorenzi, E., and Sellergren, B. (2012). Glucuronide directed molecularly imprinted solid-phase extraction: isolation of testosterone glucuronide from its parent drug in urine. *Analyst* 137 (1): 249–254.
- 50 Pichon, V., Krasnova, A.I., and Hennion, M.C. (2004). Development and characterization of an immunoaffinity solid-phase-extraction sorbent for trace analysis of propanil and related phenylurea herbicides in environmental waters and in beverages. *Chromatographia* 60 (1): 221–226.
- 51 Boos, K.S. and Fleischer, C. (2001). Multidimensional on-line solid-phase extraction (spe) using restricted access materials (ram) in combination with molecular imprinted polymers (MIP). *Anal. Bioanal. Chem.* 371 (1): 16–20.
- 52 Wissiack, R., Rosenberg, E., and Grasserbauer, M. (2000). Comparison of different sorbent materials for on-line solid-phase extraction with liquid chromatography-atmospheric pressure chemical ionization mass spectrometry of phenols. *J. Chromatogr. A* 896 (1–2): 159–170.
- 53 Ibrahim, W.A., Nodeh, H.R., and Sanagi, M.M. (2016). Graphene-based materials as solid phase extraction sorbent for trace metal ions, organic compounds, and biological sample preparation. *Crit. Rev. Anal. Chem.* 46 (4): 267–283.
- 54 Płotka-Wasyłka, J., Szczepańska, N., Guardia, M.D.L., and Namieśnik, J. (2016). Modern trends in solid phase extraction: new sorbent media. *TrAC, Trends Anal. Chem.* 77: 23–43.
- 55 Qiang, H., Liang, Q.L., Zhang, X.Q. et al. (2016). Graphene aerogel based monolith for effective solid-phase extraction of trace environmental pollutants from water samples. *J. Chromatogr. A* 1447: 39–46.
- 56 De Girolamo, A., McKeague, M., Miller, J.D. et al. (2011). Determination of ochratoxin a in wheat after clean-up through a DNA aptamer-based solid phase extraction column. *Food Chem.* 127 (3): 1378–1384.
- 57 Zhao, Q., Li, X.F., and Le, X.C. (2008). Aptamer-modified monolithic capillary chromatography for protein separation and detection. *Anal. Chem.* 80 (10): 3915–3920.
- 58 Brothier, F. and Pichon, V. (2014). Miniaturized DNA aptamer-based monolithic sorbent for selective extraction of a target analyte coupled on-line to nanolc. *Anal. Bioanal. Chem.* 406 (30): 7875–7886.
- 59 Deng, N., Liang, Z., Liang, Y. et al. (2012). Aptamer modified organic–inorganic hybrid silica monolithic capillary columns for highly selective recognition of thrombin. *Anal. Chem.* 84 (23): 10186–10190.
- 60 Arthur, C.L. and Pawliszyn, J. (1990). Solid phase microextraction with thermal desorption using fused silica optical fibers. *Anal. Chem.* 62 (19): 2145–2148.

- 61 Tsai, S.-W. and Chang, T.-A. (2002). Time-weighted average sampling of airborne n-valeraldehyde by a solid-phase microextraction device. *J. Chromatogr. A* 954 (1–2): 191–198.
- 62 Demetrio, D.L.C.G., Reichenbacher, M., Danzer, K. et al. (2015). Investigations on wine bouquet components by solid-phase microextraction-capillary gas chromatography (SMPE-CGC) using different fibers. *J. Sep. Sci.* 20 (12): 665–668.
- 63 Cheng, W.H., Tsai, D.Y., Lu, J.Y., and Lee, J.W. (2017). Extracting emissions from air fresheners using solid phase microextraction devices. *Aerosol Air Qual. Res.* 16 (10): 2362–2367.
- 64 Canas, A. and Richter, P. (2012). Solid-phase microextraction using octadecyl-bonded silica immobilized on the surface of a rotating disk: determination of hexachlorobenzene in water. *Anal. Chim. Acta* 743: 75–79.
- 65 Chen, X.F., Zang, H., Wang, X. et al. (2012). Metal-organic framework MIL-53(Al) as a solid-phase microextraction adsorbent for the determination of 16 polycyclic aromatic hydrocarbons in water samples by gas chromatography-tandem mass spectrometry. *Analyst* 137 (22): 5411–5419.
- 66 Ho, T.D., William, H.Y., Cole, T.S., and Anderson, J.L. (2012). Ultraviolet (UV) photoinitiated on-fiber copolymerization of ionic liquid sorbent coatings for headspace and direct immersion solid-phase microextraction. *Anal. Chem.* 84 (21): 9520–9528.
- 67 Szultka, M., Kegler, R., Fuchs, P. et al. (2010). Polypyrrole solid phase microextraction: a new approach to rapid sample preparation for the monitoring of antibiotic drugs. *Anal. Chim. Acta* 667 (1-2): 77–82.
- 68 Wu, J.C., Mullett, W.M., and Janusz, P. (2002). Electrochemically controlled solid-phase microextraction based on conductive polypyrrole films. *Anal. Chem.* 74 (18): 4855–4859.
- 69 Wang, D., Wang, Q., Zhang, Z., and Chen, G. (2012). ZnO nanorod array polydimethylsiloxane composite solid phase micro-extraction fiber coating: fabrication and extraction capability. *Analyst* 137 (2): 476–480.
- 70 Zeng, J., Liu, H., Chen, J. et al. (2012). Octadecyltrimethoxysilane functionalized ZnO nanorods as a novel coating for solid-phase microextraction with strong hydrophobic surface. *Analyst* 137 (18): 4295–4301.
- 71 Hu, X.L., Zhang, M.Q., Ruan, W.H. et al. (2012). Determination of organophosphorus pesticides in ecological textiles by solid-phase microextraction with a siloxane-modified polyurethane acrylic resin fiber. *Anal. Chim. Acta* 736 (14): 62–68.
- 72 Kataoka, H. and Saito, K. (2011). Recent advances in spme techniques in biomedical analysis. *J. Pharm. Biomed. Anal.* 54 (5): 926–950.
- 73 Du, F., Alam, M.N., and Pawliszyn, J. (2014). Aptamer-functionalized solid phase microextraction-liquid chromatography/tandem mass spectrometry for selective enrichment and determination of thrombin. *Anal. Chim. Acta* 845 (5): 45–52.
- 74 Erik Baltussen, P.S., David, F., and Cramers, C. (1999). Stir bar sorptive extraction (SBSE), a novel extraction technique for aqueous samples theory and principles. *J. Microcolumn Sep.* 11: 737–747.

- 75 Nogueira, J.M. (2012). Novel sorption-based methodologies for static microextraction analysis: a review on sbse and related techniques. *Anal. Chim. Acta* 757 (23): 1–10.
- 76 Aparicio, I., Martín, J., Santos, J.L. et al. (2017). Stir bar sorptive extraction and liquid chromatography-tandem mass spectrometry determination of polar and non-polar emerging and priority pollutants in environmental waters. *J. Chromatogr. A* 1500 (2): 43–52.
- 77 Fan, W.Y., Mao, X.J., He, M. et al. (2014). Development of novel sol-gel coatings by chemically bonded ionic liquids for stir bar sorptive extraction-application for the determination of NSAIDs in real samples. *Anal. Bioanal. Chem.* 406 (28): 7261–7273.
- 78 Bruheim, I., Liu, X.C., and Pawliszyn, J. (2003). Thin-film microextraction. *Anal. Chem.* 75 (4): 1002–1010.
- 79 Hashemian, Z., Khayamian, T., and Saraji, M. (2015). Anticodine aptamer immobilized on a whatman cellulose paper for thin-film microextraction of codeine from urine followed by electrospray ionization ion mobility spectrometry. *Anal. Bioanal. Chem.* 407 (6): 1615–1623.
- 80 Zargar, T., Khayamian, T., and Jafari, M.T. (2017). Immobilized aptamer paper spray ionization source for ion mobility spectrometry. *J. Pharm. Biomed. Anal.* 132: 232–237.
- 81 Vetter, W., Hammann, S., Müller, M. et al. (2017). The use of counter-current chromatography in the separation of nonpolar lipid compounds. *J. Chromatogr. A* 1501 (9): 51–60.
- 82 Abe, R., Nagoshi, K., Arai, T. et al. (2017). Microscopic analyses of complexes formed in adsorbent for Mo and Zr separation chromatography. *Nucl. Instrum. Methods Phys. Res.* 404 (1): 173–178.
- 83 Cuatrecasas, P., Wilchek, M., and Anfinsen, C.B. (1968). Selective enzyme purification by affinity chromatography. *Proc. Natl. Acad. Sci. U.S.A.* 61 (2): 636–643.
- 84 Cuatrecasas, P. and Wilchek, M. (1968). Single-step purification of avidin from egg white by affinity chromatography on biocytin-sepharose columns. *Biochem. Biophys. Res. Commun.* 33 (2): 235–239.
- 85 Connor, A.C. and McGown, L.B. (2006). Aptamer stationary phase for protein capture in affinity capillary chromatography. *J. Chromatogr. A* 1111 (2): 115–119.
- 86 Ahirwar, R. and Nahar, P. (2015). Development of an aptamer-affinity chromatography for efficient single step purification of concanavalin a from canavalia ensiformis. *J. Chromatogr. B* 997: 105–109.
- 87 Rehder-Silinski, M.A. and McGown, L.B. (2003). Capillary electrochromatographic separation of bovine milk proteins using a g-quartet DNA stationary phase. *J. Chromatogr. A* 1008 (2): 233–245.
- 88 Deng, Q., Watson, C.J., and Kennedy, R.T. (2003). Aptamer affinity chromatography for rapid assay of adenosine in microdialysis samples collected in vivo. *J. Chromatogr. A* 1005 (1-2): 123–130.
- 89 Jiang, H.P., Zhu, J.X., Peng, C.Y. et al. (2014). Facile one-pot synthesis of a aptamer-based organic-silica hybrid monolithic capillary column by thiol-ene

- click chemistry for detection of enantiomers of chemotherapeutic anthracyclines. *Analyst* 139 (19): 4940–4946.
- 90 Ravelet, C., Boulkedid, R., Ravel, A. et al. (2005). A l-rna aptamer chiral stationary phase for the resolution of target and related compounds. *J. Chromatogr. A* 1076 (1-2): 62–70.
- 91 Michaud, M., Jourdan, E., Villet, A. et al. (2003). A DNA aptamer as a new target-specific chiral selector for HPLC. *J. Am. Chem. Soc.* 125 (28): 8672–8679.
- 92 Bandara, G.C., Heist, C.A., and Remcho, V.T. (2018). Chromatographic separation and visual detection on wicking microfluidic devices: quantitation of Cu^{2+} in surface, ground, and drinking water. *Anal. Chem.* 90 (4): 2594–2600.
- 93 Surawathanawises, K., Wiedorn, V., and Cheng, X. (2017). Micropatterned macroporous structures in microfluidic devices for viral separation from whole blood. *Analyst* 142 (12): 2220–2228.
- 94 Chen, X.M., Ren, Y.K., Liu, W.Y. et al. (2017). A simplified microfluidic device for particle separation with two consecutive steps: induced charge electroosmotic prefocusing and dielectrophoretic separation. *Anal. Chem.* 89 (17): 9583–9592.
- 95 Dziomba, S., Araya-Farias, M., Smadja, C. et al. (2017). Solid supports for extraction and preconcentration of proteins and peptides in microfluidic devices: a review. *Anal. Chim. Acta* 955 (22): 1–26.
- 96 Lou, B.H., Zhou, Z.X., Du, Y., and Dong, S.J. (2015). Resistance-based logic aptamer sensor for ccrf-cem and ramos cells integrated on microfluidic chip. *Electrochem. Commun.* 59: 64–67.
- 97 Sanghavi, B.J., Moore, J.A., Chavez, J.L. et al. (2016). Aptamer-functionalized nanoparticles for surface immobilization-free electrochemical detection of cortisol in a microfluidic device. *Biosens. Bioelectron.* 78: 244–252.
- 98 Gao, C.L., Sun, X.H., and Woolley, A.T. (2013). Fluorescent measurement of affinity binding between thrombin and its aptamers using on-chip affinity monoliths. *J. Chromatogr. A* 1291: 92–96.
- 99 Xu, Y., Phillips, J.A., Yan, J.L. et al. (2009). Aptamer-based microfluidic device for enrichment, sorting, and detection of multiple cancer cells. *Anal. Chem.* 81 (17): 7436–7442.
- 100 Jiang, Y.Q., Zou, S., and Cao, X.D. (2017). A simple dendrimer-aptamer based microfluidic platform for *E. coli* o157:H7 detection and signal intensification by rolling circle amplification. *Sens. Actuators, B* 251: 976–984.
- 101 Wang, L., Musile, G., and Mccord, B.R. (2017). An aptamer-based paper microfluidic device for the colorimetric determination of cocaine. *Electrophoresis* 4 (7): 1858–1863.
- 102 Weng, X. and Neethirajan, S. (2017). Aptamer-based fluorometric determination of norovirus using a paper-based microfluidic device. *Microchim. Acta.* 184 (11): 4545–4552.
- 103 Wang, C.H., Chang, C.P., and Lee, G.B. (2016). Integrated microfluidic device using a single universal aptamer to detect multiple types of influenza viruses. *Biosens. Bioelectron.* 86 (15): 247–254.

- 104 Shin, S.R., Zhang, Y.S., Kim, D.J. et al. (2016). Aptamer-based microfluidic electrochemical biosensor for monitoring cell-secreted trace cardiac biomarkers. *Anal. Chem.* 88 (20): 10019–10027.
- 105 Jolly, P., Damborsky, P., Madaboosi, N. et al. (2016). DNA aptamer-based sandwich microfluidic assays for dual quantification and multi-glycan profiling of cancer biomarkers. *Biosens. Bioelectron.* 79: 313–319.
- 106 Li, J., Chang, K.W., Wang, C.H. et al. (2016). On-chip, aptamer-based sandwich assay for detection of glycated hemoglobins via magnetic beads. *Biosens. Bioelectron.* 79: 887–893.
- 107 Tseng, Y.T., Wang, C.H., Chang, C.P., and Lee, G.B. (2016). Integrated microfluidic system for rapid detection of influenza H1N1 virus using a sandwich-based aptamer assay. *Biosens. Bioelectron.* 82: 105–111.
- 108 Zhao, L., Tang, C., Xu, L. et al. (2016). Enhanced and differential capture of circulating tumor cells from lung cancer patients by microfluidic assays using aptamer cocktail. *Small* 12 (8): 1072–1081.
- 109 Fu, C.C., Wang, Y., Chen, G. et al. (2015). Aptamer-based surface-enhanced raman scattering-microfluidic sensor for sensitive and selective polychlorinated biphenyls detection. *Anal. Chem.* 87 (19): 9555–9558.
- 110 Bruno, J.G., Phillips, T., Montez, T. et al. (2015). Development of a fluorescent enzyme-linked DNA aptamer-magnetic bead sandwich assay and portable fluorometer for sensitive and rapid listeria detection. *J. Fluoresc.* 25 (1): 173–183.
- 111 Bagheri, H., Afkhami, A., Saber-Tehrani, M., and Khoshshafar, H. (2012). Preparation and characterization of magnetic nanocomposite of schiff base/silica/magnetite as a preconcentration phase for the trace determination of heavy metal ions in water, food and biological samples using atomic absorption spectrometry. *Talanta* 97 (97): 87–95.
- 112 Burke, N.A.D., Stöver, H.D.H., and Dawson, F.P. (2002). Magnetic nanocomposites: preparation and characterization of polymer-coated iron nanoparticles. *Chem. Mater.* 14 (11): 4752–4761.
- 113 Fu, H., Chen, Y.Q., Zhang, H.Y. et al. (2017). Synthesis of mesoporous silica-coated magnetic nanocomposites using polyethylene glycol-poly(lactic acid) as a new template. *J. Nanosci. Nanotechnol.* 17 (5): 3077–3083.
- 114 Yang, Q., Wang, Y.Z., Zhang, H.M. et al. (2017). A novel dianionic amino acid ionic liquid-coated PEG 4000 modified Fe₃O₄ nanocomposite for the magnetic solid-phase extraction of trypsin. *Talanta* 174: 139–147.
- 115 Jiang, H.R., Zeng, X., He, N.Y. et al. (2013). Preparation and biomedical applications of gold-coated magnetic nanocomposites. *J. Nanosci. Nanotechnol.* 13 (3): 1617–1625.
- 116 Kim, E.J., Lee, C.S., Chang, Y.Y., and Chang, Y.S. (2013). Hierarchically structured manganese oxide-coated magnetic nanocomposites for the efficient removal of heavy metal ions from aqueous systems. *Appl. Mater. Interfaces* 5 (19): 9628–9634.
- 117 Molaei, K., Bagheri, H., Asgharinezhad, A.A. et al. (2017). SiO₂-coated magnetic graphene oxide modified with polypyrrole-polythiophene: a novel and efficient nanocomposite for solid phase extraction of trace amounts of heavy metals. *Talanta* 167 (15): 607–616.

- 118 Netzer, K., Jordakieva, G., Girard, A.M. et al. (2017). Next-generation magnetic nanocomposites: cytotoxic and genotoxic effects of coated and uncoated ferric cobalt boron (FeCoB) nanoparticles in vitro. *Basic Clin. Pharmacol. Toxicol.* 122 (3): 355–363.
- 119 Yan, C.H., Zhang, Y., Yang, H. et al. (2017). Combining phagomagnetic separation with immunoassay for specific, fast and sensitive detection of *Staphylococcus aureus*. *Talanta* 170: 291–297.
- 120 Wei, C., Zong, Y., Guo, Q.H. et al. (2017). Magnetic separation of clenbuterol based on competitive immunoassay and evaluation by surface-enhanced raman spectroscopy. *RSC Adv.* 7 (6): 3388–3397.
- 121 Tsai, H.Y., Hsu, F.H., Lin, Y.P., and Bor, F.C. (2006). Separation method based on affinity reaction between magnetic and nonmagnetic particles for the analysis of particles and biomolecules. *J. Chromatogr. A* 1130 (2): 227–231.
- 122 Kim, C. and Searson, P.C. (2017). Detection of plasmodium lactate dehydrogenase antigen in buffer using aptamer-modified magnetic microparticles for capture, oligonucleotide-modified quantum dots for detection, and oligonucleotide-modified gold nanoparticles for signal amplification. *Bioconjugate Chem.* 28 (9): 2230–2234.
- 123 He, J.C., Huang, M.Y., Wang, D.M. et al. (2014). Magnetic separation techniques in sample preparation for biological analysis: a review. *J. Pharm. Biomed. Anal.* 101: 84–101.
- 124 Tahmasebi, E., Yamini, Y., Moradi, M., and Esrafil, A. (2013). Polythiophene-coated Fe₃O₄ superparamagnetic nanocomposite: synthesis and application as a new sorbent for solid-phase extraction. *Anal. Chim. Acta* 770 (7): 68–74.
- 125 Du, Z., Liu, M., and Li, G.K. (2013). Novel magnetic SPE method based on carbon nanotubes filled with cobalt ferrite for the analysis of organochlorine pesticides in honey and tea. *J. Sep. Sci.* 36 (20): 3387–3394.
- 126 Qu, S., Huang, F., Yu, S. et al. (2008). Magnetic removal of dyes from aqueous solution using multi-walled carbon nanotubes filled with Fe₂O₃ particles. *J. Hazard. Mater.* 160 (2-3): 643–647.
- 127 Richards, S.L., Cawley, A.T., Cavicchioli, R. et al. (2016). Aptamer based peptide enrichment for quantitative analysis of gonadotropin-releasing hormone by LC-MS/MS. *Talanta* 150: 671–680.
- 128 Wang, Y.X., Ye, Z.Z., Ping, J.F. et al. (2014). Development of an aptamer-based impedimetric bioassay using microfluidic system and magnetic separation for protein detection. *Biosens. Bioelectron.* 59 (13): 106–111.
- 129 Ozalp, V.C., Bayramoglu, G., Kavruk, M. et al. (2014). Pathogen detection by core-shell type aptamer-magnetic preconcentration coupled to real-time PCR. *Anal. Biochem.* 447 (1): 119–125.
- 130 Xi, Z.J., Huang, R.R., Li, Z.Y. et al. (2015). Selection of hbsag-specific DNA aptamers based on carboxylated magnetic nanoparticles and their application in the rapid and simple detection of hepatitis B virus infection. *ACS Appl. Mater. Interfaces* 7 (21): 11215–11223.
- 131 Fang, S., Wang, C., Xiang, J. et al. (2014). Aptamer-conjugated upconversion nanoprobe assisted by magnetic separation for effective isolation and sensitive detection of circulating tumor cells. *Nano Res.* 7 (9): 1327–1336.

- 132 Kim, U.J. and Kim, B.C. (2016). DNA aptamers for selective identification and separation of flame retardant chemicals. *Anal. Chim. Acta* 936: 208–215.
- 133 Najafabadi, M.E., Khayamian, T., and Hashemian, Z. (2015). Aptamer-conjugated magnetic nanoparticles for extraction of adenosine from urine followed by electrospray ion mobility spectrometry. *J. Pharm. Biomed. Anal.* 107: 244–250.
- 134 Wang, J., Shen, H.J., Huang, C. et al. (2016). Highly efficient and multidimensional extraction of targets from complex matrices using aptamer-driven recognition. *Nano Res.* 10 (1): 145–156.
- 135 Fischer, C., Kallinich, C., Klockmann, S. et al. (2016). Automated enrichment of sulfanilamide in milk matrices by utilization of aptamer-linked magnetic particles. *J. Agric. Food Chem.* 64 (48): 9246–9252.
- 136 Guo, K.T., SchAfer, R., Paul, A. et al. (2006). A new technique for the isolation and surface immobilization of mesenchymal stem cells from whole bone marrow using high-specific DNA aptamers. *Stem Cells* 24 (10): 2220–2231.
- 137 Nair, B.G., Nagaoka, Y., Morimoto, H. et al. (2010). Aptamer conjugated magnetic nanoparticles as nanosurgeons. *Nanotechnology* 21 (45): 455102.
- 138 Iliuk, A.B., Hu, L., and Tao, W.A. (2011). Aptamer in bioanalytical applications. *Anal. Chem.* 83 (12): 4440–4452.
- 139 Zhu, Z., Ravelet, C., Perrier, S. et al. (2010). Multiplexed detection of small analytes by structure-switching aptamer-based capillary electrophoresis. *Anal. Chem.* 82 (11): 4613–4620.
- 140 Marechal, A., Jarrosson, F., Randon, J. et al. (2015). In-line coupling of an aptamer based miniaturized monolithic affinity preconcentration unit with capillary electrophoresis and laser induced fluorescence detection. *J. Chromatogr. A* 1406: 109–117.
- 141 Zhou, Z.M., Feng, Z., Zhou, J. et al. (2015). Capillary electrophoresis-chemiluminescence detection for carcino-embryonic antigen based on aptamer/graphene oxide structure. *Biosens. Bioelectron.* 64: 493–498.
- 142 Clark, S.L. and Remcho, V.T. (2003). Electrochromatographic retention studies on a flavin-binding RNA aptamer sorbent. *Anal. Chem.* 75 (21): 5692–5696.
- 143 Kolotov, V.P., Dogadkin, N.N., and Shkinev, V.M. (1994). Use of new chelating sorbents, membrane and electrochemical methods for metal preconcentration and separation in neutron activation analysis. *J. Anal. Chem.* 49 (1): 39–47.
- 144 Alhooshani, K., Basheer, C., Kaur, J. et al. (2011). Electromembrane extraction and hplc analysis of haloacetic acids and aromatic acetic acids in wastewater. *Talanta* 86: 109–113.
- 145 Kim, K., Lee, S., Ryu, S., and Han, D. (2014). Efficient isolation and elution of cellular proteins using aptamer-mediated protein precipitation assay. *Biochem. Biophys. Res. Commun.* 448 (1): 114–119.
- 146 Nguyen, T.H., Pei, R.J., Landry, D.W. et al. (2011). Microfluidic aptamer-icaffinity sensing of vasopressin for clinical diagnostic and therapeutic applications. *Sens. Actuators, B* 154 (1): 59–66.

- 147 Ali, W.H. and Pichon, V. (2014). Characterization of oligosorbents and application to the purification of ochratoxin a from wheat extracts. *Anal. Bioanal. Chem.* 406 (4): 1233–1240.
- 148 Aslipashaki, S.N., Khayamian, T., and Hashemian, Z. (2013). Aptamer based extraction followed by electrospray ionization-ion mobility spectrometry for analysis of tetracycline in biological fluids. *J. Chromatogr. B* 925 (8): 26–32.
- 149 Han, B., Zhao, C., Yin, J.F., and Wang, H.L. (2012). High performance aptamer affinity chromatography for single-step selective extraction and screening of basic protein lysozyme. *J. Chromatogr. B* 903 (903): 112–117.
- 150 Chang, K.W., Li, J.L., Yang, C.H. et al. (2015). An integrated microfluidic system for measurement of glycated hemoglobin levels by using an aptamer-antibody assay on magnetic beads. *Biosens. Bioelectron.* 68: 397–403.
- 151 Weng, X. and Neethirajan, S. (2016). A microfluidic biosensor using graphene oxide and aptamer-functionalized quantum dots for peanut allergen detection. *Biosens. Bioelectron.* 85: 649–656.
- 152 Rouah-Martin, E., Maho, W., Mehta, J. et al. (2014). Aptamer-based extraction of ergot alkaloids from ergot contaminated rye feed. *Adv. Biosci. Biotechnol.* 5: 692–698.
- 153 Shastri, A., McGregor, L.M., Liu, Y. et al. (2015). An aptamer-functionalized chemomechanically modulated biomolecule catch-and-release system. *Nat. Chem.* 7 (5): 447.
- 154 Ozalp, V.C., Bayramoglu, G., Erdem, Z., and Arica, M.Y. (2015). Pathogen detection in complex samples by quartz crystal microbalance sensor coupled to aptamer functionalized core-shell type magnetic separation. *Anal. Chim. Acta* 853 (1): 533–540.

6

Development of Aptamer-Based Colorimetric Analytical Methods

Subash C.B. Gopinath^{1,2}, Thangavel Lakshmipriya³, M.K. Md Arshad^{2,4}, and Chun Hong Voon²

¹Universiti Malaysia Perlis, School of Bioprocess Engineering, Kompleks Pusat Pengajian, Jejawi 3, Arau, Perlis 02600, Malaysia

²Universiti Malaysia Perlis, Institute of Nano Electronic Engineering, Jalan Kangar-Alor Setar, Seriab, Kangar, Perlis 01000, Malaysia

³Universiti Teknologi PETRONAS, Centre of Innovative Nanostructure and Nanodevices, Bandar Seri Iskandar, Perak Darul Ridzuan 32610, Malaysia

⁴Universiti Malaysia Perlis, School of Microelectronic Engineering, Pauh putra campus, 02600 Arau, Perlis, Malaysia

6.1 Introduction

Nanotechnology is the discipline that deals predominantly with material engineering at the nanoscale range. Nanotechnology has been used in fields such as physics, engineering, chemistry, and biology. The evaluation of metallic nanoparticles in the nanometer scale shows high impact in many biological fields such as biosensors, bioimaging, drug delivery, and purification due to their electrical and optical characteristics [1–3]. Among the different nanoparticles, gold nanoparticle (AuNP) shows excellent performance, due to its positive characteristics, such as easy dispersal, inertness, variation in sizes, and the ease for surface modifications [4–7]. Moreover, the plasmonic effect of AuNP helps in various optical-based applications [8, 9]. Under the optical scenario, AuNP adsorbs visible light at 520 nm (green region) due to the excitation of plasmons on the particle, and this wavelength can be adapted to reveal the optical properties.

In biosensing, AuNPs are used in different ways: as a probe, a quenching material, and for surface functionalization [10–12]. The immobilization of biomolecules on AuNPs is easier; and, in most cases, AuNPs with biomolecules have been used as the capture or detection probe. Biomolecules in the AuNP have been immobilized through electrostatic interaction and chemical or physical modification [13, 14]. Because of that, various sensors are utilizing AuNPs to improve the limit of detection in the methods, such as Raman spectroscopy [15], surface plasmon resonance (SPR) [16], waveguide mode sensor [6], ELISA [17], electrochemical sensor [18], impedance sensor [19], and colorimetric assay [7]. Using AuNPs, various biomolecules were detected in various ranges from the small molecule to the whole cell. Lakshmipriya et al. [4]

used a AuNP-conjugated antibody and AuNP-conjugated streptavidin for the detection of factor IX from human serum using the waveguide mode sensor and SPR [4, 20]. The AuNP-conjugated antibody has also been used to observe the presence of influenza viruses [21].

In the past, AuNP-conjugated DNA, protein, and antibody were used as the probe to improve detection of biomolecules with a lower level. Recently, aptamer-conjugated AuNP has attracted significant attention in the biological fields, including imaging and biosensing. The aptamer is an artificial antibody used in all fields to substitute the antibody. Since the aptamer has more advantages over antibodies, aptamers are used as the probe instead of antibodies in various sensors [4, 22]. In several instances, aptamers are found to show more sensitivity with the target molecule, and have improved the limit of detection compared to the antibody [23]. In the field of biosensing, the combination of aptamer and AuNP has shown excellent improvement. Many sensors have confirmed this combination. Among the several methods developed, aptamer-based colorimetric sensor (aptasensor) brought about easy naked-eye detection without involving any specific equipment [24–26]. In this chapter, we discuss the progress made in the aptamer-based colorimetric assay.

6.2 Aptamer Generation for Colorimetric Assay

The aptamer is an artificial nucleic acid, either DNA or RNA, generated from the randomized library of molecules by the SELEX (Systematic Evolution of Ligands by EXponential enrichment) method. The first aptamer was generated by two groups in 1990 (Ellington and Szostak [27]; Tuerk and Gold [28]). Aptamer generation involves three steps, which include binding, separation, and amplification. Figure 6.1 shows the schematic representation of the SELEX method. Using this concept, different SELEX methods were introduced, such as cell-SELEX, magnetic-bead-based SELEX, photo-SELEX, *in vivo* SELEX, and single-step SELEX. The microfluidic delivery system was also used in the SELEX method to find the specific aptamer [29]. Targets for aptamer generation can be anything from a small molecule to the whole cell. Various aptamers selected against a wide range of targets include influenza, human immunodeficiency virus (HIV), severe adult respiratory distress syndrome (SARS), adenosine triphosphate (ATP), clotting proteins, and metal ions [30–39]. The selected aptamers have a high binding affinity with their targets in the range of pico- to nanomolar order [35, 40] and are used for potential applications.

6.3 Aptasensor

Since aptamers show a high binding affinity with their target molecules, aptamer-based sensors (aptasensors) have been used to detect and screen for various diseases. Usually, only a few bases from the aptamer bind to the target; it makes aptamers more sensitive than other probes, yields a lower detection

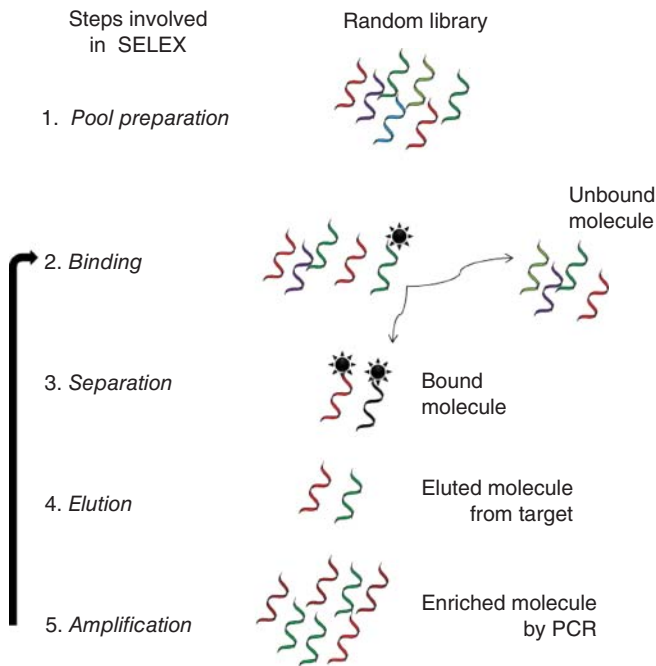


Figure 6.1 SELEX strategy. Five major steps involved are indicated. The critical steps are separation and amplification.

limit, and it can also discriminate closely related molecules. Gopinath et al. [41] discriminated closely related influenza viruses using aptamers, and the selected aptamers displayed a limit of detection lower than that by the antibody. Therefore, aptamers have been commonly used to develop aptasensors to substitute an immunosensor. In some cases, as in a sandwich assay, aptamers and antibodies are used as the capture and detection molecules; in that way, they complement each other [42]. Since the aptamer has a high binding affinity, it is used as the capture probe. In some other cases, two different aptamers for the same target were used in a sandwich assay as capture and detection molecules [43]. Due to its good stability and sensitivity, the aptasensor brings out the real interaction and detection of biomolecules and is useful in medical diagnosis.

6.4 Aptamer-AuNP-Based Colorimetric Assays

Aptamers and AuNPs have proved to be suitable candidates in the biosensor, and various sensors have used these two in order to improve the detection method. Among different sensing methods, the colorimetric assay shows easier detection of biomolecules without involving any specific equipment. The method has been proved to be low cost, easy to detect, besides being able to detect by consuming less [6, 44]. The unmodified AuNP that can be synthesized with citrate capping has been widely followed in this assay.

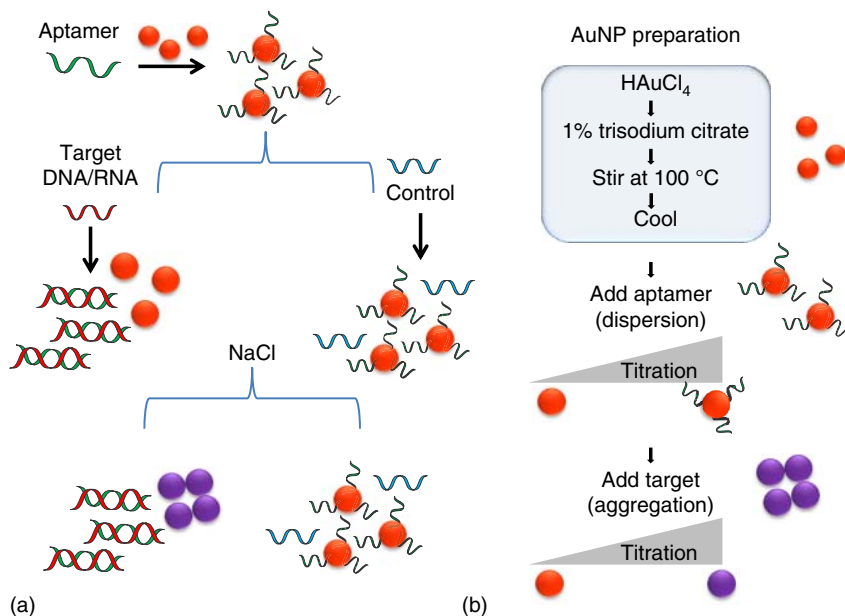


Figure 6.2 (a) Aptamer-mediated controlled assembly and disassembly of AuNP to detect oligonucleotide as the target. (b) Schematic representation of the method involved. This strategy is mainly due to the duplex formation between the nucleic acid strands. In the presence of aptamer and NaCl, the gold colloid shows the dispersion. In the presence of the target, it turns into the state of aggregation.

Different strategies with the colorimetric aptasensor were demonstrated for target detection. Figure 6.2 is the graphical representation of the common colorimetric assay that has been used involving aptamer and AuNP. As shown in the figure, initially the specific aptamer for the particular target was allowed to bind with the AuNP. AuNP can bind with the aptamer through hydrophobic adsorption, electrostatic interaction, and covalent binding [45, 46]. When the particular target was mixed with this complex solution followed by the addition of the suitable concentration of NaCl, the detection was made. In this assay, the strategy of balanced interparticle attractive or interparticle repulsive forces causes the aggregation or dispersion, due to gain or loss of surface charges. It was stated that the van der Waals attractive forces on the surface cause aggregation [46], and these two states are determined in the presence of metal ions dissolved in the gold colloidal solution. Because of the abovementioned mechanism, in the presence of salts, AuNPs can alter color between red and purple. With the aptamer-attached AuNP, in the presence of the target the color of the AuNP solution changes to purple; in the absence of the target, it retains the red color. Figure 6.3 shows the detection of a protein as the target using the colorimetric assay; the calibration versus target concentrations can be established proportionally for ultraviolet (UV) absorbance or absorbance ratio at two wavelengths to increase detection sensitivity.

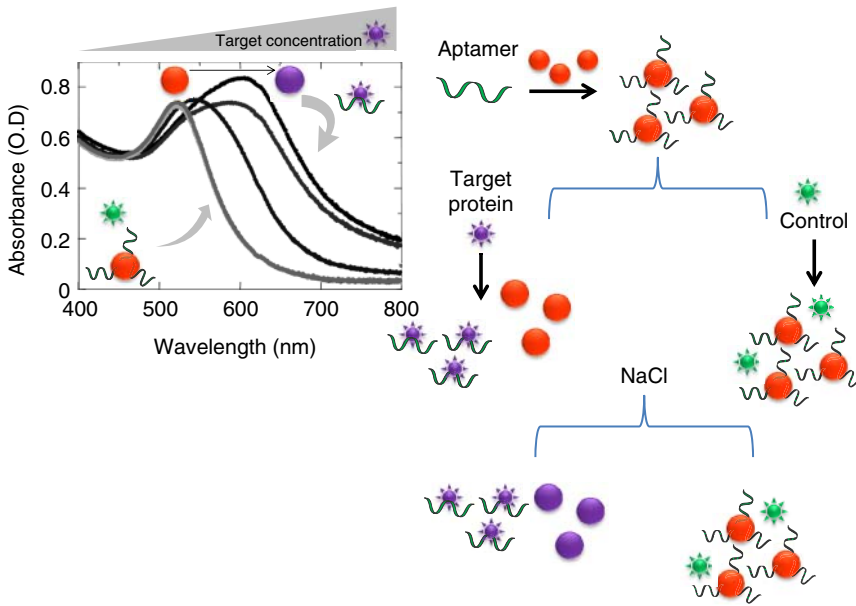


Figure 6.3 Aptamer-mediated controlled assembly and disassembly on AuNP to detect protein as the target. In the presence of aptamer and NaCl, the gold colloid shows the dispersion. In the presence of target, it turns into the state of aggregation. The spectrophotometric measurements display from red-shift to blue-shift with increasing target concentrations.

On addition of metallic salt caps, the repulsion among unmodified negatively charged AuNPs induces the aggregation and results in a purple solution. Usually, the as-received gold colloidal solution exhibits a strong absorbance at a visible wavelength (of 520 nm), due to the excitation [47–49]. When the color changes occur in the presence of salt or target with salt, the spectrum will move toward visible wavelengths (redshift).

The method shown in Figure 6.4 displays a different strategy from that used in the previous method. In this one, first the aptamer and the target (DNA or RNA) were allowed to bind. After that, AuNP was added to the solution and kept for a specified time, and then finally the suitable concentration of NaCl was added to check the color change. In the presence of the targets, the color of the solution will be purple; whereas it retains its red color in the absence of the target. A similar procedure is also followed to detect the protein by its aptamer (Figure 6.5).

Split aptamers have also been used for the development of colorimetric assay. As shown in Figure 6.6, first the aptamers are split and then mixed with the target protein, followed by the addition of AuNP, bringing about the color change. Finally, the AuNPs were added to detect the target protein. In the presence of the target protein, the split aptamers bind with the target and AuNP in the solution and changes the color to purple in the presence of NaCl. At the same time, in the control experiment, the split aptamers are attached on the AuNP and stabilized so that the color of the AuNP remains red even in the presence of NaCl [50].

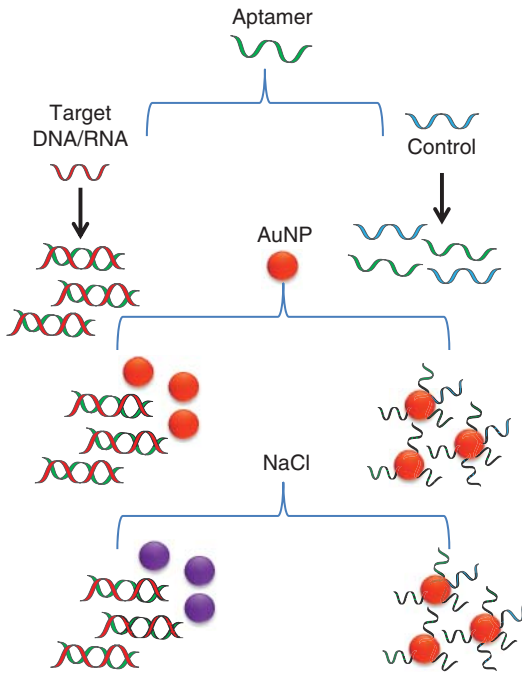


Figure 6.4 Aptamer-mediated controlled assembly and disassembly on AuNP to detect DNA as the target. This strategy is different from the abovementioned strategies, in which AuNP will be added after mixing the probe and the target.

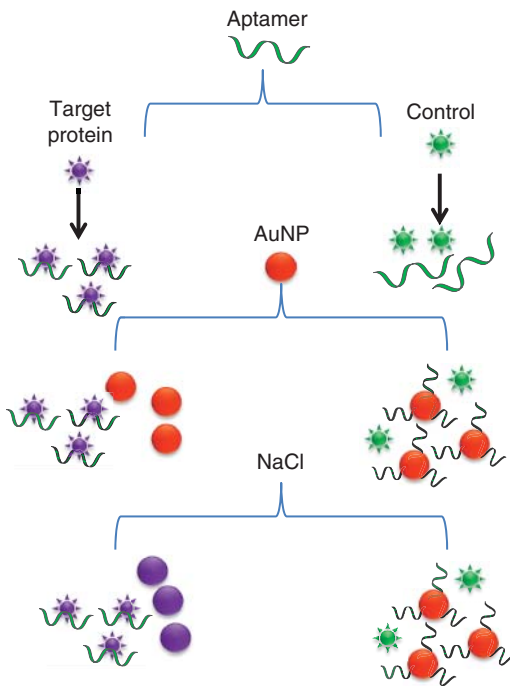
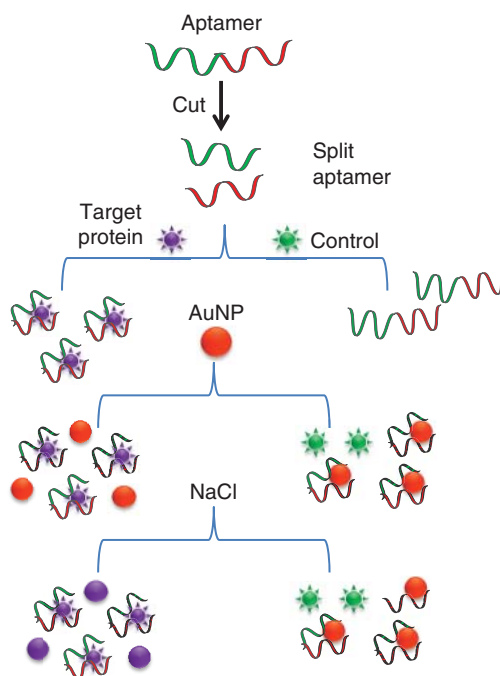


Figure 6.5 Aptamer-mediated controlled assembly and disassembly on AuNP to detect protein as the target. AuNP will be added after mixing the probe and the target.

Figure 6.6 Split aptamer-mediated controlled assembly and disassembly on AuNP. This strategy has a different approach, in which two pieces of aptamer are used.



6.5 Applications of AuNP-Aptamer-Based Colorimetric Assays

Using the AuNP-based colorimetric aptasensor, researchers detected various targets and disease biomarkers with different levels of sensitivities (Table 6.1). DNA or RNA is a well-suited probe in the biosensor field to detect various diseases. Recent sensors can even detect single mutations in DNA; they bring out the conditions that cause life-threatening diseases. Identifying and finding the mutation in the DNA sequence is mandatory in the field of medical diagnosis for accurate identification of diseases. Various sensors have been used to detect the nucleic acids (DNA or RNA). Among these, colorimetric sensors have proved capable of detecting DNAs easily and in the simplest way. Thiol-modified oligonucleotides were used for this method for easier modification on AuNP [24]. Zhao et al. [24] detected DNA by aptamer-based colorimetric assay, using the phenomenon of non-cross-linked AuNP aggregation induced by salt induction.

Metal ion detection is mandatory in the field of environment and food analyses. Metal ions are natural elements found in soils and water. Life-threatening metal ions such as lead, mercury, and arsenic are found in fish, rice, and in different food products [51]. Some plants adsorb the metal ions from the soil. High amounts of these metals cause various health problems to humans. Therefore, it is mandatory to check the level of metal ions in food products and plants. Several aptamers are synthesized against various metal ions such as lead, mercury, and arsenic. Using

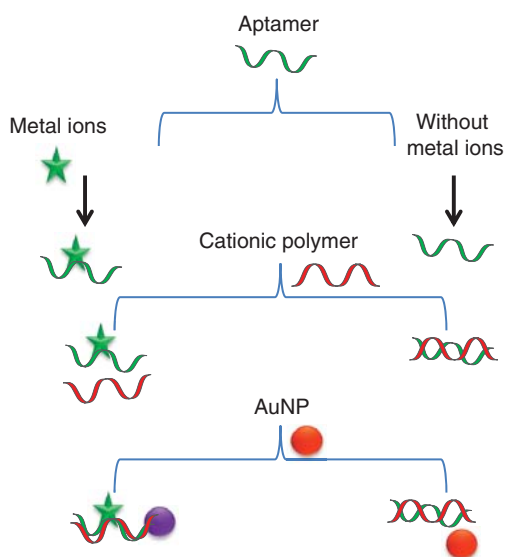
Table 6.1 Limit of detection of AuNP-based colorimetric aptasensors.

Target	Limit of detection	References
Adenosine	20 μM	[46]
Thrombin	20 nM	[56]
ATP	600 nM	[57]
Thrombin	830 pM	[58]
Cancerous cells	90 cells	[59]
Mercury	3 μM	[60]
Mercury	600 pM	[61]
Oxytetracycline	25 nM	[62]
Kanamycin	25 nM	[63]
Dopamine	360 nM	[64]
Platelet-derived growth factor	6 nM	[65]
Riboflavin	100 nM	[66]
Vitamin B ₁₂	0.1 $\mu\text{g ml}^{-1}$	[67]
Ampicillin	10 ng ml^{-1}	[68]
Thrombin	5 pM	[69]
Sulfadimethoxine	50 ng ml^{-1}	[70]
PDGF	25 nM	[71]
ATP	10 nM	[72]

these aptamers combined with AuNP helps detect these metal ions easily. Metal ions are small molecules suitable for the colorimetric assay, but several sensors struggle to detect metals.

Wu et al. [52] used an arsenic-specific aptamer and a water-soluble cationic polymer, poly(diallyldimethylammonium) (PDDA), specifically to detect arsenic ions (Figure 6.7). The binding of PDDA to the AuNP surface induces aggregation; and in the absence of arsenic ions, the aptamer forms a duplex structure with PDDA and prevents the binding to the AuNP. Thereby, the AuNPs remain stabilized and retain the original color (red) of the colloidal solution. However, in the presence of an arsenic ion, the aptamer makes a complex, leaving free PDDA molecules in the solution that bind to the AuNP, induces the aggregation of AuNPs, and changes the colors (red or purple) correspondingly. AuNP-functionalized amino acid, peptide moiety, and quaternary ammonium groups have been reported to efficiently detect mercury ions by inducing the aggregation of the functionalized AuNPs [53, 54]. The sensor was also used to monitor the chromium level in the blood of diabetic patients and for the detection of chromium ions in waste water samples [55].

Figure 6.7 Aptamer-mediated controlled assembly and disassembly on AuNP to detect metal ion as the target. The cationic polymer is also involved.



6.6 Conclusions

In this chapter, we have discussed the development of aptamer-mediated colorimetric assays. This assay is one of the least expensive and ideal sensing strategies in the field of biosensors. There are several colorimetric assays that have been formulated for the detection of a wide range of targets, from a small molecule to the whole cell. Among aptamer-based colorimetric assays, DNA aptamers have been involved predominantly in the development of this assay and proved with several targets. However, the limitation with this assay is that when preferring the protein as the target, it may tend to bind nonspecifically with the AuNP. Because of that, developing non-fouling-based colorimetric assays are highly appreciated. With this development, the strategies developed with colorimetric assays can be fine-tuned.

References

- 1 Perumal, V., Hashim, U., Gopinath, S.C.B. et al. (2015). A new nano-worm structure from gold-nanoparticle mediated random curving of zinc oxide nanorods. *Biosens. Bioelectron.* 78 (15): 14–22.
- 2 Boisselier, E. and Astruc, D. (2009). Gold nanoparticles in nanomedicine: preparations, imaging, diagnostics, therapies and toxicity. *Chem. Soc. Rev.* 38 (6): 1759–1782.
- 3 Soppimath, K.S., Aminabhavi, T.M., Kulkarni, A.R., and Rudzinski, W.E. (2001). Biodegradable polymeric nanoparticles as drug delivery devices. *J. Control. Release* 70 (1–2): 1–20.

- 4 LakshmiPriya, T., Horiguchi, Y., and Nagasaki, Y. (2014). Co-immobilized poly(ethylene glycol)-block-polyamines promote sensitivity and restrict bio-fouling on gold sensor surface for detecting factor IX in human plasma. *Analyst* 139 (16): 3977–3985.
- 5 Chen, C. (2014). Detection of mercury(II) ions using colorimetric gold nanoparticles on paper-based analytical devices. *Anal. Chem.* 86 (14): 6843–6849.
- 6 Gopinath, S.C.B., LakshmiPriya, T., and Awazu, K. (2014). Colorimetric detection of controlled assembly and disassembly of aptamers on unmodified gold nanoparticles. *Biosens. Bioelectron.* 51: 115–123.
- 7 Xiao, R.P., Wang, D.F., Lin, Z.Y. et al. (2015). Disassembly of gold nanoparticle dimers for colorimetric detection of ochratoxin A. *Anal. Methods* 7 (3): 842–845.
- 8 Daniel, M.C. and Astruc, D. (2004). Gold nanoparticles: assembly, supramolecular chemistry, quantum-size-related properties, and applications toward biology, catalysis, and nanotechnology. *Chem. Rev.* 104 (1): 293–346.
- 9 Li, Y., Schluesener, H.J., and Xu, S. (2010). Gold nanoparticle-based biosensors. *Gold Bull.* 43 (1): 29–41. doi: 10.1007/BF03214964.
- 10 Liu, D., Huang, X., Wang, Z. et al. (2013). Gold nanoparticle-based activatable probe for sensing ultralow levels of prostate-specific antigen. *ACS Nano.* 7 (6): 5568–5576.
- 11 Liu, J., Guan, Z., Lv, Z. et al. (2014). Improving sensitivity of gold nanoparticle-based fluorescence quenching and colorimetric aptasensor by using water resuspended gold nanoparticle. *Biosens. Bioelectron.* 52: 265–270.
- 12 Perrault, S.D. and Chan, W.C.W. (2009). Synthesis and surface modification of highly monodispersed, spherical gold nanoparticles of 50–200 nm. *J. Am. Chem. Soc.* 131 (47): 17042–17043.
- 13 Li, Z., Jin, R., Mirkin, C.a., and Letsinger, R.L. (2002). Multiple thiol-anchor capped DNA-gold nanoparticle conjugates. *Nucleic Acids Res.* 30 (7): 1558–1562.
- 14 Mao, S., Lu, G., Yu, K. et al. (2010). Specific protein detection using thermally reduced graphene oxide sheet decorated with gold nanoparticle-antibody conjugates. *Adv. Mater.* 22 (32): 3521–3526.
- 15 Assmus, T., Balasubramanian, K., Burghard, M. et al. (2007). Raman properties of gold nanoparticle-decorated individual carbon nanotubes. *Appl. Phys. Lett.* 90 (17).
- 16 Tu, M.H., Sun, T., and Grattan, K.T.V. (2012). Optimization of gold-nanoparticle-based optical fibre surface plasmon resonance (SPR)-based sensors. *Sensors Actuators, B Chem.* 164 (1): 43–53.
- 17 Ambrosi, A., Airò, F., and Merkoçi, A. (2010). Enhanced gold nanoparticle-based ELISA for a breast cancer biomarker. *Anal. Chem.* 82 (3): 1151–1156.
- 18 Yu, A., Liang, Z., Cho, J., and Caruso, F. (2003). Nanostructured electrochemical sensor based on dense gold nanoparticle films. *Nano Lett.* 3 (9): 1203–1207. doi: 10.1021/nl034363j.

- 19 Gopinath, S.C.B., Perumal, V., Kumaresan, R. et al. (2016). Nanogapped impedimetric immunosensor for the detection of 16 kDa heat shock protein against *Mycobacterium tuberculosis*. *Microchim. Acta.* 183 (10): 2697–2703.
- 20 LakshmiPriya, T., Fujimaki, M., Gopinath, S.C.B. et al. (2013). A high-performance waveguide-mode biosensor for detection of factor IX using PEG-based blocking agents to suppress non-specific binding and improve sensitivity. *Analyst* 138: 2863–2870.
- 21 Gopinath, S.C.B., Awazu, K., Fujimaki, M. et al. (2013). Observations of immuno-gold conjugates on influenza viruses using waveguide-mode sensors. *PLoS One* 8 (7): 1–10.
- 22 Gopinath, S.C.B., LakshmiPriya, T., Chen, Y. et al. (2016). Aptamer-based “point-of-care testing”. *Biotechnol. Adv.* 34 (3): 198–208.
- 23 LakshmiPriya, T., Fujimaki, M., Gopinath, S.C.B., and Awazu, K. (2013). Generation of anti-influenza aptamers using the systematic evolution of ligands by exponential enrichment for sensing applications. *Langmuir* 29 (48): 15107–15115.
- 24 Zhao, W., Chiuman, W., Brook, M.A., and Li, Y. (2007). Simple and rapid colorimetric biosensors based on DNA aptamer and noncrosslinking gold nanoparticle aggregation. *ChemBioChem* 8 (7): 727–731.
- 25 Smith, J.E., Griffin, D.K., Leny, J.K. et al. (2014). Colorimetric detection with aptamer-gold nanoparticle conjugates coupled to an android-based color analysis application for use in the field. *Talanta* 121: 247–255. doi: 10.1016/j.talanta.2013.12.062.
- 26 Liu, X., Zhou, Z., Zhang, L. et al. (2009). Colorimetric sensing of adenosine based on aptamer binding inducing gold nanoparticle aggregation. *Chin. J. Chem.* 27 (10): 1855–1859.
- 27 Ellington, A.D. and Szostak, J.W. (1990). In vitro selection of RNA molecules that bind specific ligands. *Nature* 346: 818–822. doi: 10.1038/346818a0.
- 28 Tuerk, C. and Gold, L. (1990). Systematic evolution of ligands by exponential enrichment: RNA ligands to bacteriophage T4 DNA polymerase. *Science* 249 (4968): 505–510.
- 29 Hybarger, G., Bynum, J., Williams, R.F. et al. (2006). A microfluidic SELEX prototype. *Anal. Bioanal. Chem.* 384 (1): 191–198.
- 30 Ye, B.-F., Zhao, Y.-J., Cheng, Y. et al. (2012). Colorimetric photonic hydrogel aptasensor for the screening of heavy metal ions. *Nanoscale* 4 (19): 5998–6003.
- 31 Neff, C.P., Zhou, J., Remling, L. et al. (2011). An aptamer-si RNA chimera suppresses HIV-1 viral loads and protects from helper CD4(+) T cell decline in humanized mice. *Sci. Transl. Med.* 3 (66): 66ra6.
- 32 Ahn, D.-G., Jeon, I.-J., Kim, J.D. et al. (2009). RNA aptamer-based sensitive detection of SARS coronavirus nucleocapsid protein. *Analyst* 134 (9): 1896–1901.
- 33 Gopinath, S.C.B., Misono, T.S., Kawasaki, K. et al. (2006). An RNA aptamer that distinguishes between closely related human influenza viruses and inhibits haemagglutinin-mediated membrane fusion. *J. Gen. Virol.* 87 (2006): 479–487.

- 34 Gopinath, S.C.B. and Kumar, P.K.R. (2013). Aptamers that bind to the hemagglutinin of the recent pandemic influenza virus H1N1 and efficiently inhibit agglutination. *Acta Biomater.* 9 (11): 8932–8941.
- 35 Gopinath, S.C.B., Sakamaki, Y., Kawasaki, K., and Kumar, P.K.R. (2006). An efficient RNA aptamer against human influenza B virus hemagglutinin. *J. Biochem.* 139 (5): 837–846. doi: 10.1093/jb/mvj095.
- 36 Webster, R.G., Bean, W.J., Gorman, O.T. et al. (1992). Evolution and ecology of influenza A viruses. *Microbiol. Mol. Biol. Rev.* 56 (1): 152–279.
- 37 Shigdar, S., Lin, J., Yu, Y. et al. (2011). RNA aptamer against a cancer stem cell marker epithelial cell adhesion molecule. *Cancer Sci.* 102 (5): 991–998.
- 38 Huizenga, D.E. and Szostak, J.W. (1995). A DNA aptamer that binds adenosine and ATP. *Biochemistry* 34 (2): 656–665. doi: 10.1021/bi00002a033.
- 39 Woo, H.-M., Kim, K.-S., Lee, J.-M. et al. (2013). Single-stranded DNA aptamer that specifically binds to the influenza virus NS1 protein suppresses interferon antagonism. *Antivir. Res.* 100 (2): 337–345.
- 40 Zeng, X., Zhang, X., Yang, W. et al. (2012). Fluorescence detection of adenosine triphosphate through an aptamer-molecular beacon multiple probe. *Anal. Biochem.* 424 (1): 8–11.
- 41 Gopinath, S.C.B., Misono, T.S., Kawasaki, K. et al. (2007). An RNA aptamer that distinguishes between closely related human influenza viruses and inhibits haemagglutinin-mediated membrane fusion. *J. Gen. Virol.* 87 (3): 479–487.
- 42 Kim, S., Lee, J., Lee, S.J., and Lee, H.J. (2010). Ultra-sensitive detection of IgE using biofunctionalized nanoparticle-enhanced SPR. *Talanta* 81 (4–5): 1755–1759.
- 43 Tennico, Y.H., Hutanu, D., Koesdjojo, M.T. et al. (2010). On-chip aptamer-based sandwich assay for thrombin detection employing magnetic beads and quantum dots. *Anal. Chem.* 82 (13): 5591–5597.
- 44 Zhang, L. and Li, L. (2016). Colorimetric thrombin assay using aptamer-functionalized gold nanoparticles acting as a peroxidase mimetic. *Microchim. Acta* 183 (1): 485–490.
- 45 Lou, S., Ye, J., Li, K., and Wu, A. (2012). A gold nanoparticle-based immunochromatographic assay: the influence of nanoparticulate size. *Analyst* 137 (5): 1174. doi: 10.1039/c2an15844b.
- 46 Zhao, W., Brook, M.A., and Li, Y. (2008). Design of gold nanoparticle-based colorimetric biosensing assays. *ChemBioChem.* 9 (15): 2363–2371.
- 47 Tinguely, J.C., Sow, I., Leiner, C. et al. (2011). Gold nanoparticles for plasmonic biosensing: the role of metal crystallinity and nanoscale roughness. *Bionanoscience* 1 (4): 128–135.
- 48 Nagel, J., Chunsod, P., Zimmerer, C. et al. (2011). Immobilization of gold nanoparticles on a polycarbonate surface layer during molding. *Mater. Chem. Phys.* 129 (1–2): 599–604. doi: 10.1016/j.matchemphys.2011.04.069.
- 49 Gopinath, S.C.B., Awazu, K., Fujimaki, M. et al. (2012). Surface functionalization chemistries on highly sensitive silica-based sensor chips. *Analyst* 137 (15): 3520.

- 50 Liu, J., Bai, W., Niu, S. et al. (2014). Highly sensitive colorimetric detection of 17beta-estradiol using split DNA aptamers immobilized on unmodified gold nanoparticles. *Sci. Rep.* 4: 7571.
- 51 Chibuike, G.U. and Obiora, S.C. (2014). Heavy metal polluted soils: effect on plants and bioremediation methods. *Appl. Environ. Soil Sci.* 2014: 752708.
- 52 Wu, Y., Zhan, S., Wang, F. et al. (2012). Cationic polymers and aptamers mediated aggregation of gold nanoparticles for the colorimetric detection of arsenic(III) in aqueous solution. *Chem. Commun.* 48 (37): 4459.
- 53 Yu, C.J. and Tseng, W.L. (2008). Colorimetric detection of mercury(II) in a high-salinity solution using gold nanoparticles capped with 3-mercaptopropionate acid and adenosine monophosphate. *Langmuir* 24 (21): 12717–12722. doi: 10.1021/la802105b.
- 54 Si, S., Kotal, A., and Mandal, T.K. (2007). One-dimensional assembly of peptide-functionalized gold nanoparticles: an approach toward mercury ion sensing. *J. Phys. Chem. C* 111 (3): 1248–1255.
- 55 Zhao, L., Jin, Y., Yan, Z. et al. (2012). Novel, highly selective detection of Cr(III) in aqueous solution based on a gold nanoparticles colorimetric assay and its application for determining Cr(VI). *Anal. Chim. Acta* 731: 75–81.
- 56 Pavlov, V., Xiao, Y., Shlyahovsky, B., and Willner, I. (2004). Aptamer-functionalized Au nanoparticles for the amplified optical detection of thrombin. *J. Am. Chem. Soc.* 126 (38): 11768–11769.
- 57 Wang, J., Wang, L., Liu, X. et al. (2007). A gold nanoparticle-based aptamer target binding readout for ATP assay. *Adv. Mater.* 19 (22): 3943–3946.
- 58 Wei, H., Li, B., Li, J. et al. (2007). Simple and sensitive aptamer-based colorimetric sensing of protein using unmodified gold nanoparticle probes. *Chem. Commun.* 2007 (0): 3735–3737. doi: 10.1039/b707642h.
- 59 Medley, C.D., Smith, J.E., Tang, Z. et al. (2008). Gold nanoparticle-based colorimetric assay for the direct detection of cancerous cells. *Anal. Chem.* 80 (4): 1067–1072.
- 60 Xue, X., Wang, F., and Liu, X. (2008). One-step, room temperature, colorimetric detection of mercury (Hg 2+) using DNA/nanoparticle conjugates. *J. Am. Chem. Soc.* 130 (11): 3244–3245. doi: 10.1021/ja076716c.
- 61 Li, L., Li, B., Qi, Y., and Jin, Y. (2009). Label-free aptamer-based colorimetric detection of mercury ions in aqueous media using unmodified gold nanoparticles as colorimetric probe. *Anal. Bioanal. Chem.* 393 (8): 2051–2057.
- 62 Kim, Y.S., Kim, J.H., Kim, I.A. et al. (2010). A novel colorimetric aptasensor using gold nanoparticle for a highly sensitive and specific detection of oxytetracycline. *Biosens. Bioelectron.* 26 (4): 1644–1649.
- 63 Song, K.M., Cho, M., Jo, H. et al. (2011). Gold nanoparticle-based colorimetric detection of kanamycin using a DNA aptamer. *Anal. Biochem.* 415 (2): 175–181.
- 64 Zheng, Y., Wang, Y., and Yang, X. (2011). Aptamer-based colorimetric biosensing of dopamine using unmodified gold nanoparticles. *Sensors Actuators, B Chem.* 156 (1): 95–99.

- 65 Chang, C.C., Lin, S., Lee, C.H. et al. (2012). Amplified surface plasmon resonance immunosensor for interferon-gamma based on a streptavidin-incorporated aptamer. *Biosens. Bioelectron.* 37 (1): 68–74. doi: 10.1016/j.bios.2012.04.038.
- 66 Chávez, J.L., MacCuspie, R.I., Stone, M.O., and Kelley-Loughnane, N. (2012). Colorimetric detection with aptamer-gold nanoparticle conjugates: effect of aptamer length on response. *J. Nanopart. Res.* 14 (10): 1166.
- 67 Selvakumar, L.S. and Thakur, M.S. (2012). Nano RNA aptamer wire for analysis of vitamin B12. *Anal. Biochem.* 427 (2): 151–157.
- 68 Song, K.M., Jeong, E., Jeon, W. et al. (2012). Aptasensor for ampicillin using gold nanoparticle based dual fluorescence-colorimetric methods. *Anal. Bioanal. Chem.* 402 (6): 2153–2161.
- 69 Peng, Y., Li, L., Mu, X., and Guo, L. (2013). Aptamer-gold nanoparticle-based colorimetric assay for the sensitive detection of thrombin. *Sensors Actuators, B Chem.* 177: 818–825.
- 70 Chen, A., Jiang, X., Zhang, W. et al. (2013). High sensitive rapid visual detection of sulfadimethoxine by label-free aptasensor. *Biosens Bioelectron.* 42 (1): 419–425.
- 71 Huang, C.-C., Huang, Y.-F., Cao, Z. et al. (2005). Aptamer-modified gold nanoparticles for colorimetric determination of platelet-derived growth factors and their receptors. *Anal. Chem.* 77 (17): 5735–5741.
- 72 Chen, S.J., Huang, Y.F., Huang, C.C. et al. (2008). Colorimetric determination of urinary adenosine using aptamer-modified gold nanoparticles. *Biosens. Bioelectron.* 23 (11): 1749–1753.

7

Enzyme-Linked Aptamer Assay (ELAA)

Yiyang Dong¹ and Sai Wang²

¹Beijing University of Chemical Technology, College of Life Science and Technology, Beijing, 100029, PR China

²Ocean University of China, College of Food Science and Engineering, Qingdao, 266003, PR China

7.1 Introduction

In recent years, derived from the well-established enzyme-linked immunosorbent assay (ELISA) using aptamer in place of antibody as schematically illustrated in Figure 7.1, the enzyme-linked aptamer assay (ELAA), or the enzyme-linked oligonucleotide assay (ELONA) has emerged as a potential analytical method. To better understand the scheme, a retrospective concise review of ELISA, the analytical merits of aptamer, and test modes of ELAA, are systematically summarized in this chapter.

7.2 Enzyme-Linked Immunosorbent Assay

ELISA, the most important immunoassay scheme with comparable sensitivity/selectivity and no radiation risk of radioimmunoassay, is widely utilized for various analytical and bioanalytical applications such as *in vitro* diagnosis, medical study, veterinary investigation, and food safety analysis. The scheme uses an immobilized antibody to specifically bind/capture an analyte or antigen in a sample. Then an antibody–antigen conjugate is coupled to an enzyme (such as horseradish peroxidase (HRP) or alkaline phosphatase), and the nonradioactive signal of color change when the enzyme reacts with a suitable substrate (such as ABTS or TMB) can be used for precise and high-throughput analyte quantification on a microtiter plate with multiple wells.

In 1971, two research groups, i.e. Peter Perlmann and Eva Engvall at Stockholm University, Sweden, and Anton Schuurs and Bauke van Weemen at the Research Laboratories of NV Organon, Oss, the Netherlands, independently developed the ELISA scheme and executed experiments to measure IgG in rabbit serum and human chorionic gonadotropin in urine to successfully demonstrate ELISA functionality, respectively. They were honored for their inventions when they received the German scientific award of the “Biochemische Analytik” in 1976 [1].

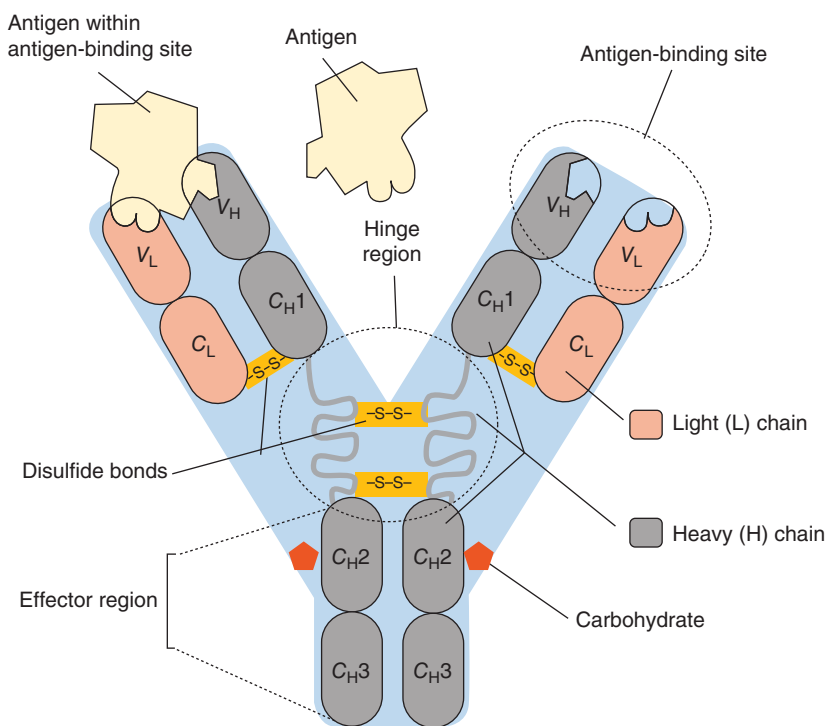


Figure 7.1 The four-chain structure of an antibody, or immunoglobulin, molecule. The basic unit is composed of two identical light (L) chains and two identical heavy (H) chains, which are held together by disulfide bonds to form a flexible Y shape. Each chain is composed of a variable (V) region and a constant (C) region.

Various ELISA kits are widely available commercially, as shown in Figure 7.2. Experimentally, depending on the resources available, ELISA can run in both direct and indirect modes. The steps of a direct ELISA follow the typical protocols given here:

- A buffered solution of the analyte is added to each polystyrene microtiter plate well; and after incubation, the analyte is immobilized onto the surface of the well.
- A solution of nonreacting protein, such as bovine serum albumin or casein, is added to the microtiter plate wells to block the nonspecific sites uncoated by the analyte.
- The antibody with a conjugated enzyme is added, and binds specifically to the analyte immobilized on the wells.
- A substrate for this enzyme is added after washing the plate thoroughly. This substrate reacts and changes color with the enzyme until the reaction is stopped for quantification.
- The color changes in accordance with the concentration of the analyte, and a microtiter spectrometer and precise calibration are needed to give quantitative analyte values.

by exponential enrichment protocol (SELEX). In contrast to the antibody, the aptamer produced by such an *in vitro* combinatorial chemistry process is more advantageous in terms of production ease, conformational adaptability, target affinity, analytical selectivity, structural tenability, and storage stability.

The aptamer is *in vitro* selected from an ssDNA/RNA library via various SELEX protocols, the process is faster than the time-consuming generation of monoclonal antibodies, and does not require the use of animals as is required to generate antibodies. An aptamer with a definite sequence can easily be synthesized in many laboratories and, unlike antibodies, will have uniform binding properties for analytical applications.

Theoretically, aptamers can be generated against any target; for small molecular hapten with little or no immunogenicity, no conjugation with a large molecule to trigger animal immunity is needed. For complicated targets, such as various cells or cell lysates, aptamers can be selected for cellular diagnosis or therapy. What is more, for chemicals with acute toxicity or some natural toxins, antibodies cannot be easily acquired because of the intolerance of animals.

An aptamer typically has a mass 10- to 15-fold less than an IgG antibody, so it is physically small and far less immunogenic than an antibody inherently. Due to the smaller size compared to antibodies, aptamers are expected to be effective in intracellular labeling or staining, i.e. aptamers can be used in detecting the expression of target molecules at the cellular level.

Aptamers may be utilized for the binding of a target compound with better affinity and selectivity than antibodies because of conformational adaptability or molecular flexibility. Aptamers with picomolar dissociation, or one methyl group discriminative recognition capability, are successfully reported, accordingly. In 2013, Michiko Kimoto proved that incorporation up to three unnatural Ds nucleotides in a random sequence library can yield aptamers with greatly augmented affinities; their selection experiments against two human target proteins, vascular endothelial growth factor-165 (VEGF-165) and interferon- γ (IFN- γ), yielded DNA aptamers that bind with K_d values of 0.65 and 38 pM, respectively, affinities that are >100-fold improved over those of aptamers containing only natural bases [2]. In 1994, species of RNA that bind with high affinity and specificity to the bronchodilator theophylline were identified by Jenison et al. via selection from an oligonucleotide library. One RNA aptamer binds to theophylline with a dissociation constant K_d of 0.1 μ M. This binding affinity is 10,000-fold greater than the RNA aptamer's affinity for caffeine, which differs from theophylline only by a methyl group at nitrogen atom N-7. These results demonstrate the ability of RNA aptamers to exhibit an extremely high degree of ligand recognition and discrimination [3].

While antibodies generally have multiple binding sites, most aptamers have limited specific binding sites. Thus, there is potentially far less nonspecific binding of nontarget compounds when aptamers are utilized in immunoassays as antibody alternatives. This necessitates a minimum blocking strategy and provides a more reliable detection signal for the presence of the target compound.

Furthermore, aptamers can be easily modified to incorporate not only biotins for immobilization but also other labeling moieties such as fluorochromes, radioisotopes such as phosphorus 32, and steroids such as digoxigenin and

peptides. The various modifications allow the ease of the choice of a reporter system for determination. In fact, it is facile to covalently or even non-covalently link the aptamer directly to a reporter enzyme such as HRP or alkaline phosphatase for further analysis.

7.4 Enzyme-Linked Aptamer Assay (ELAA)

ELAA originated from the ELONA developed by Drolet and his colleagues in 1996 [4]. They used a fluorescein-tagged nuclease resistant oligonucleotide ligand NX-244 derived through the SELEX process and a monoclonal human vascular endothelial growth factor (hVEGF) capture antibody 26503.11 to detect hVEGF, a potent endothelial cell mitogen, and angiogenic factor levels in human sera. Signal was collected for calibration (Figure 7.3) and subsequent quantitation using a chemiluminescent alkaline phosphatase detection system after final incubation with alkaline-phosphatase-conjugated anti-fluorescein Fab fragments. Error analyses as well as precision, accuracy, interference, and specificity analyses show equivalence to a conventional sandwich ELISA assay, demonstrating that ELONA represents a viable alternative to ELISA in clinical and research assays.

Similarly, ELAA or ELONA can operate in both direct and indirect modes. To detect the tetracycline residue in honey, the chapter authors successfully developed ELAA using a biotin-streptavidin (SA)-mediated system based on indirect and straightforward competition schemes in 2014 and 2015, respectively.

As shown in Figure 7.4, an indirect competitive enzyme-linked aptamer assay (*ic*-ELAA) based on a 76-mer-ssDNA aptamer with good K_d (63.6 nM) and

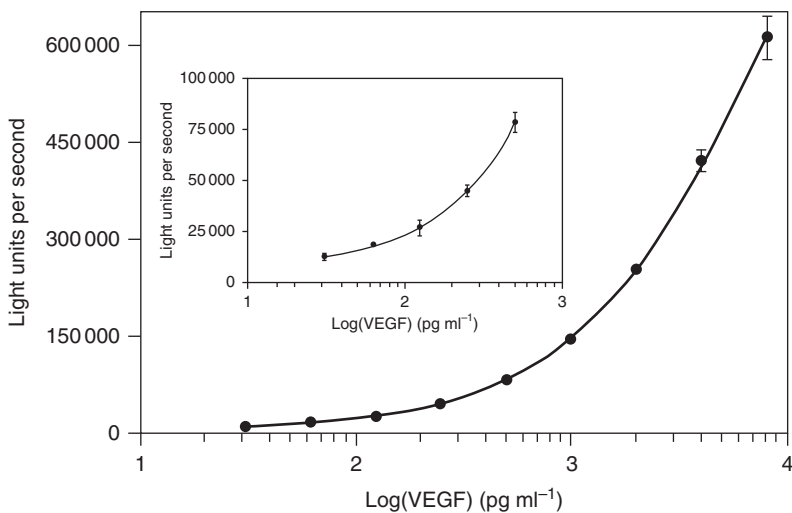


Figure 7.3 Typical calibration curve for the hVEGF ELONA; the bottom portion of the curve was expanded in the inset to better display the error. The range of the assay was from 31.25 to 8000 pg ml⁻¹. Source: Drolet et al. 1996 [4]. Reprinted with permission of Springer Nature.

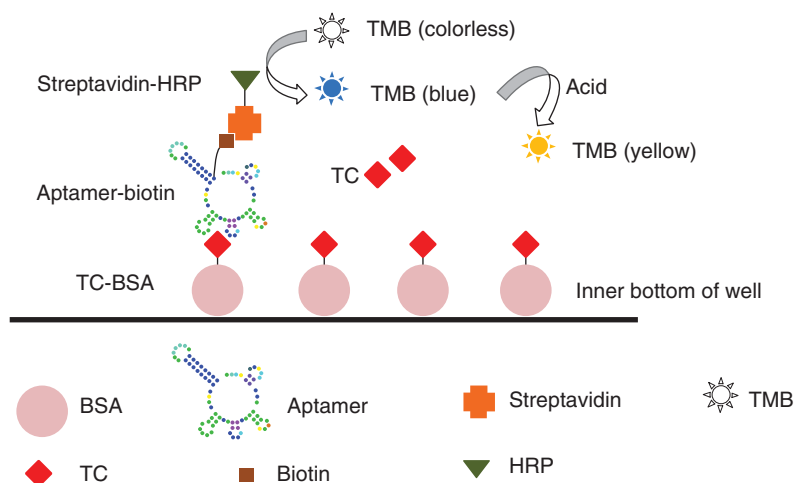


Figure 7.4 Schematic illustration of the aptasensor based on indirect competitive ELAA for TC detection. Source: Wang et al. 2014 [5]. Reprinted with permission of Elsevier.

bad cross-reactivity with oxytetracycline and doxycycline for the determination of TC in honey was developed. The microtiter plates were firstly coated with TC-BSA conjugate as competitor antigen and incubated overnight at 4 °C, the wells were washed three times with washing buffer to remove unbound TC-BSA. The plates were then blocked with Hammerstein bovine casein. Subsequently, biotinylated aptamer and various TC calibrators were added and the binding was allowed for 75 minutes with mild shaking at room temperature. After washing, SA-HRP was added to the plates to incubate 45 minutes at 37 °C. Finally, TMB solution was added and incubated for 20 minutes at 37 °C until the color of the solution changed to blue. Then the color reaction was stopped by adding H₂SO₄ and the color turned to yellow. The absorbance was measured immediately at 450 nm, with 630 nm as the reference wavelength. With each step protected from light, the final absorbance of the competition system, denoted by B , was consistent with the result of absorbance at 450 nm minus absorbance at 630 nm. B_0 means the absorbance value of the negative control. The absorbance values were converted into their corresponding test inhibition values (B/B_0). After systematic optimization toward concentrations of TC-BSA coating conjugate, biotinylated aptamer, SA-HRP, and types of coating buffer, blocking agent and binding buffer, this ELAA offers excellent sensitivity (the limit of detection, LOD = 9.6×10^{-3} ng ml⁻¹) with a wide linear range (0.01–100 ng ml⁻¹) and a mean recovery rate of 93.23% in TC-spiked honey samples [5].

To further investigate the versatility of ELAA, the chapter authors developed a direct competitive enzyme-linked aptamer assay (*dc*-ELAA) strategy to detect residual TC in honey sample using the same biotinylated 76-mer-ssDNA aptamer. As shown in Figure 7.5, the microtitre plates were firstly coated with SA at 4 °C for 16 hours, and the wells were washed three times with washing buffer to remove unbound SA. The plates were then blocked with 1% Casein or 2% BSA at 37 °C with mild shaking. Subsequently, biotinylated aptamer and

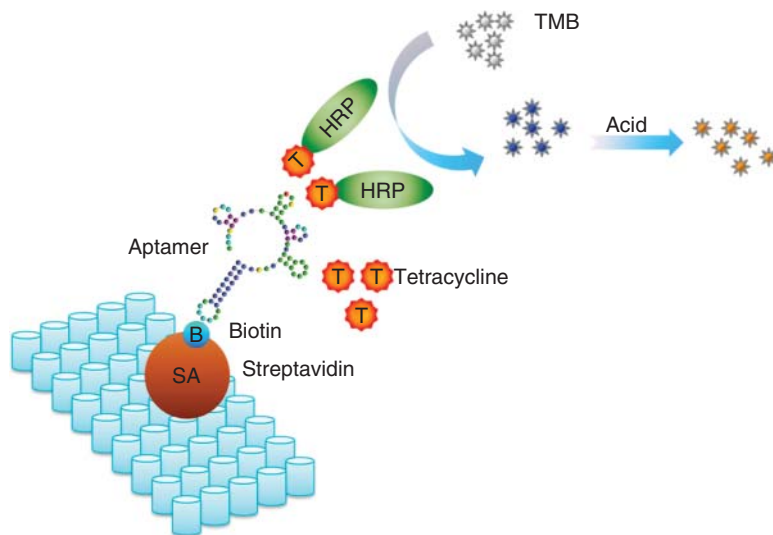


Figure 7.5 Schematic illustration of the aptasensor based on direct competitive ELAA for TC detection. Source: Wang et al. 2015 [6]. Reprinted with permission of Elsevier.

various TC calibrators were added and the binding was allowed for 45 minutes with mild shaking at 25 °C. After washing, TC–HRP as competitor antigen was added to the plates to incubate for 20 minutes at 37 °C. Finally, TMB solution was added and incubated for 20 minutes at 37 °C until the color of the solution changed to blue. Then the color reaction was stopped by adding H₂SO₄ and the color turned to yellow. The absorbance was measured immediately at 450 nm with 630 nm as the reference wavelength. Each step was protected from light with silver paper, the optical density of each well, denoted by B , was consistent with the result of absorbance at 450 nm minus absorbance at 630 nm. B_0 means the optical density value of the noncompetitive control (with no TC). B_{blank} means the optical density value of the blank control (with no aptamer or TC). To reflect the actual competitive effect and improve the sensitivity, the absorbance of the competitive system is defined by A , namely B minus B_{blank} . The final absorbance values were converted into their corresponding test inhibition values A/A_0 . After systematic optimization toward concentrations of SA, biotinylated aptamer, TC–HRP, types of blocking agents, and aptamer with or without a thermal treatment before immobilization, this ELAA offers a good sensitivity (the limit of detection, LOD = 0.0978 ng ml⁻¹) with a wide linear range (0.1–1000 ng ml⁻¹) and good recovery rates from 92.09% to 109.7% in TC-spiked honey samples [6].

7.5 Comparison of Direct-Competitive ELAA (*dc*-ELAA), Indirect-Competitive ELAA (*ic*-ELAA), and ELISA

As the sandwich assay scheme is not available with TC detection owing to its small size (Mw444.4), detection approaches based on competitive formats are

Table 7.1 Detection by *dc*-ELAA, *ic*-ELAA, and ELISA.

Honeys	Measured concentration (ng ml ⁻¹ , mean ± SD)		
	<i>dc</i> -ELAA	<i>ic</i> -ELAA	ELISA
Acacia honey	0.1782 ± 0.001604	0.1067 ± 0.07422	0.1239 ± 0.01808
Pipa honey	1.594 ± 0.07190	1.583 ± 0.1416	1.931 ± 0.04943
Jujube honey	1.157 ± 0.07660	1.683 ± 0.1445	1.629 ± 0.1448
Polyfloral honey	1.745 ± 0.1063	1.65 ± 0.02065	2.119 ± 0.1576

SD: standard deviation ($n = 7$).

Source: Wang et al. 2015 [6]. Adapted with permission of Elsevier.

preferred, performed directly or indirectly. An aptasensor based on the *ic*-ELAA scheme was developed in our previous study [5]. The analysis time of the two competitive methods was similar. The *dc*-ELAA in this study with a wider linear range can be used to detect higher concentration of TC in honey, thus applicable for countries with maximum residue limit (MRL) more than 100 ng ml⁻¹, and is more practical for on-site detection. The *ic*-ELAA provided slightly higher sensitivity than the *dc*-ELAA in terms of LOD (0.0096 ng ml⁻¹ in *ic*-ELAA) partly owing to the signal amplification of the indirect competition based on the highly specific biotin–SA combination. In the indirect competitive aptasensor, SA–HRP (horse-radish peroxidase labeled streptavidin) was introduced to amplify the signal after the competition of TC, TC–BSA for aptamer–biotin. And in the present study, SA–biotin was used to immobilize the aptamer on the microtiter plates, TC–HRP was employed as competitor and enzyme tracer, while there is no other amplification of competition. In short, the direct and indirect competitive aptasensors have their own merits, and they can both be employed to detect TC in honey.

In addition, the *dc*-ELAA was applied to quantify the TC residue in several collected honey samples (from white to dark, monofloral, and polyfloral), as well as the *ic*-ELAA and a standard ELISA (A/A_0 (%) = $-39.45 \times \text{Log}(\text{TC}) + 53.58$, $R^2 = 0.9905$). The results showed good proximity of the three methods (Table 7.1).

This case-dependent comparison is rather preliminary; more investigations will be needed in the near future to unveil possible inherent coincidence of *dc*-ELAA, *ic*-ELAA, and ELISA.

7.6 Conclusion

In summary, both the direct and indirect ELAA method with an expandable 96× high-throughput analytical capability can be utilized in food analysis or medical diagnosis nowadays, with analytical merits of aptamers, rich and diverse conjugation/labeling strategies, and various luminescence/color generating materials or reactions, ELAA is deemed as a promising derivative of ELISA with aptamer in place of antibody, many successful applications in medical or health science research will be safely envisaged in the next few decades. However, a better

understanding of aptamer–analyte interaction and a deliberate optimization for operational parameters, are always crucial for a successful ELAA.

References

- 1 Lequin, R.M. (2005). Enzyme immunoassay (EIA)/enzyme-linked Immunosorbent assay (ELISA). *Clin. Chem.* 51 (12): 2415–2418.
- 2 Kimoto, M., Yamashige, R., Matsunaga, K.-i. et al. (2013). Generation of high-affinity DNA aptamers using an expanded genetic alphabet. *Nat. Biotechnol.* 31: 453–457.
- 3 Jenison, R.D., Gill, S.C., Pardi, A., and Polisky, B. (1994). High-resolution molecular discrimination by RNA. *Science* 263 (5152): 1425–1429.
- 4 Drolet, D.W., Moon-McDermott, L., and Romig, T.S. (1996). An enzyme-linked oligonucleotide assay. *Nat. Biotechnol.* 14: 1021–1025.
- 5 Wang, S., Yong, W., Liu, J. et al. (2014). Development of an indirect competitive assay-based aptasensor for highly sensitive detection of tetracycline residue in honey. *Biosens. Bioelectron.* 57: 192–198.
- 6 Wang, S., Liu, J., Yong, W. et al. (2015). A direct competitive assay-based aptasensor for sensitive determination of tetracycline residue in honey. *Talanta* 131: 562–569.

8

Development of Aptamer-Based Fluorescence Sensors

Seyed M. Taghdisi^{1,2}, Rezvan Yazdian-Robati², Mona Alibolandi³, Mohammad Ramezani³, and Khalil Abnous^{3,4}

¹ Mashhad University of Medical Sciences, Pharmaceutical Technology Institute, Targeted Drug Delivery Research Center, Mashhad, Iran

² Mashhad University of Medical Sciences, School of Pharmacy, Department of Pharmaceutical Biotechnology, Mashhad, Iran

³ Mashhad University of Medical Sciences, Pharmaceutical Technology Institute, Pharmaceutical Research Center, Mashhad, Iran

⁴ Mashhad University of Medical Sciences, School of Pharmacy, Department of Medicinal Chemistry, Mashhad, Iran

8.1 Introduction

Aptamers are artificial single-stranded DNA (ssDNA) or RNA oligonucleotides that emerge from large combinatorial nucleic acid libraries (containing 10^{13} – 10^{16} random nucleic acid sequences), through the SELEX (Systematic Evolution of Ligands by EXponential enrichment) process which involves some repeated rounds of binding, partition, and amplification [1, 2]. These selected aptamers are able to bind to their definite target ranging from small molecules to proteins and even whole cells with high affinity and specificity, due to their well-defined three-dimensional structures, offering the design of aptamer-based biosensors (aptasensors) for a wide range of targets [3, 4]. Compared to antibodies, aptamers have some unique advantages, including low molecular weight and low toxicity, a quite thermal and chemical stability, fast tissue penetration (due to its small size), and easy labeling with various tags and functional groups. These promising features introduce aptamers as a novel and powerful class of ligands with various applications, such as biomedical diagnostics, environmental monitoring, and identifying pathogenic factors in the food chain [5, 6]. Moreover, aptamers are easily produced with a DNA synthesizer with extreme accuracy and reproducibility without relying on induction of an animal immune system [7]. Aptasensors have been introduced in recent years and based on their signal-harvesting method are classified into electrochemical, optical, and mass-sensitive assays [4].

Physically, fluorescence occurs when an orbital electron of a molecule, atom, or nanostructure, relaxes to its ground state by emitting a photon from an excited singlet state. In analytical chemistry, fluorescence is one of the most popular optical techniques widely utilized in aptasensor design because of its unique characteristics, including high sensitivity, high specificity, high efficiency, and simple operation. So far, several strategies have been developed for the design of fluorescent aptasensors [5]. This chapter is focused on understanding the principles and unique features of these fluorescent aptasensors.

8.2 Fluorescent-Dye-Based Aptasensors

Recently, label-free fluorescent aptasensors have attracted growing attention and several label-free fluorescence aptasensors with detection limit as low as subpicomolar levels were reported. Labeling is a time-consuming and tedious process and fluorescently labeled aptamers are expensive; and, moreover, it may affect the binding affinity and selectivity of aptamers [8]. A homogeneous label-free aptasensor for the determination of potassium ion was achieved through measuring the fluorescence intensity of crystal violet as the reporter element and the thrombin binding aptamer as the sensing element. Upon binding to ssDNA, the fluorescence of crystal violet increases several fold, while the free crystal violet shows a weak fluorescence. In the absence of a target, the structure of the thrombin-binding aptamer was intact. When crystal violet was added, it could be conjugated to the thrombin-binding aptamer via electrostatic interaction between the negatively charged aptamer and positively charged crystal violet, leading to the enhancement of fluorescence intensity. In the presence of potassium ions, a G-quadruplex structure, with less negative charge, is formed. Thus, less amounts of crystal violet could be attached to the aptamer, resulting in less fluorescence intensity. The designed method showed a detection limit of $6\ \mu\text{M}$ [9]. Another label-free fluorescent aptasensor for selective and sensitive detection of streptomycin (STR) was introduced by our group. This aptasensor was based on exonuclease III (Exo III), SYBR Gold dye, and aptamer complementary strand (CS). In this target-recycling-oriented amplification method, Exo III was used as a sequence-independent nuclease enzyme which does not require a specific recognition site and preferably digest the 3'-end of dsDNA instead of ssDNA. In this work, SYBR Gold was used as the fluorescent dye, due to its high sensitivity and selectivity for oligonucleotides and good stability [10, 11]. In the absence of STR, the aptamer binds to its CS and is subjected to digestion by Exo III. So, weak fluorescence intensity was detected. Upon the addition of STR to the sample, the aptamer binds to its target, inducing the release of CS from the aptamer and thereby the protection of oligonucleotides against the Exo III function. Following the addition of SYBR Gold, a strong fluorescence intensity was attained, due to its binding to CS and aptamer/STR complex (Figure 8.1). This aptasensor showed a high selectivity toward STR with a limit of detection (LOD) as low as $54.5\ \text{nM}$ [12]. One of the disadvantages of this sensor was the application of Exo III, which makes the detection process more time-consuming.

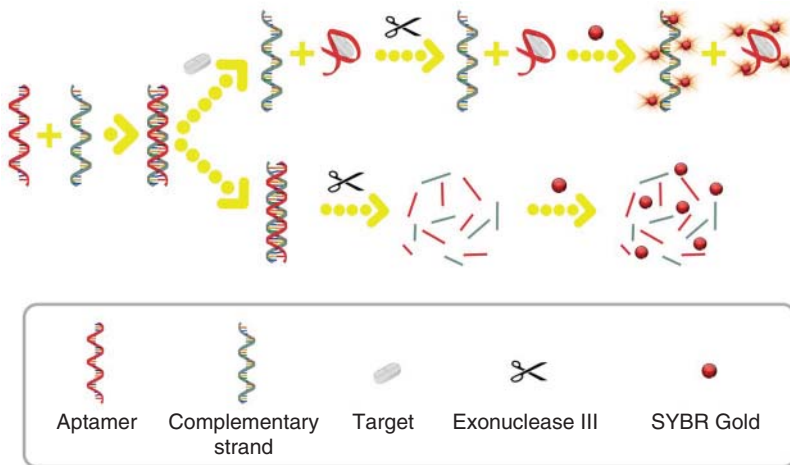


Figure 8.1 Detection of STR using SYBR Gold and Exo III. In the absence of a target, the aptamer bound to its CS and formed a dsDNA. The formed dsDNA was digested by Exo III. So, a low fluorescence intensity was detected. Upon addition of a target, the aptamer bound to STR, the complementary strand was released from the aptamer, and more protection against Exo III was obtained. Upon addition of SYBR Gold, a strong fluorescence intensity was observed. Source: Taghdisi et al. 2016 [12]. Reproduced with permission of Elsevier.

8.3 Nanoparticle-Based Aptasensors

8.3.1 Fluorescent Aptasensors Based on Gold Nanoparticles

Gold nanoparticles (AuNPs), also known as gold colloid or colloidal gold with 1–100 nm size, are extensively used in a wide range of bioanalytical and biomedical applications, including early diagnosis and drug delivery. Simple synthesis, large surface area, chemical stability, biocompatibility, low toxicity, excellent quenching of fluorophore, and ready interaction with labeled biomaterials including aptamers, antibodies, and biomarkers form the most important features of these nanoparticles [13, 14]. Moreover, using standard gold–thiol chemistry, AuNPs can be easily modified with nucleic acids [15]. Considering the fact that AuNPs can quench the fluorescence of a variety of dyes with high efficiency, aptamer–AuNPs become an excellent fluorescence sensing platform [13].

A fluorescence quenching aptasensor based on double-stranded DNA (dsDNA) and AuNPs was presented for the sensitive and simple detection of STR in blood serum and milk. In the absence of STR, dsDNA including carboxyfluorescein (FAM)-labeled CS and the STR aptamer remained intact without binding to AuNPs. Therefore, a strong fluorescence was detected. It has been shown that dsDNA could not bind to AuNPs because of its rigid structure and negative charge [16, 17]. In the presence of a target, STR aptamer bound to STR due to higher affinity of the aptamer to its target compared to its CS [18, 19]. So, the released FAM-labeled CS was adsorbed on the surface of AuNPs and the fluorescence of FAM-labeled CS was efficiently quenched by

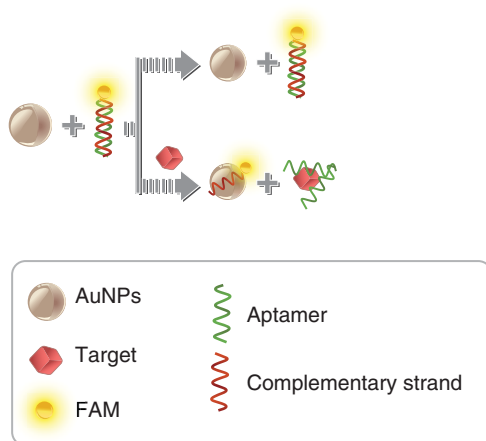


Figure 8.2 AuNPs and FAM-labeled CS were used to design a fluorescent aptasensor for STR detection. In the absence of STR, aptamer/FAM-labeled complementary strand (dsDNA) was stable, resulting in the strong emission of fluorescence. By addition of a target, the aptamer bound to its target and FAM-labeled CS was adsorbed on the surface of AuNPs and the fluorescence of FAM-labeled CS was efficiently quenched by AuNPs. Source: Emrani et al. 2016 [20]. Reproduced with permission of Elsevier.

AuNPs (Figure 8.2). This fluorescent aptasensor showed LOD as low as 47.6 nM [20]. Usually, exposure of AuNPs to blood serum leads to adsorption of plasma proteins (especially albumin) on the surfaces of these nanoparticles, which is called corona shield. Corona shield is a major problem because the interaction of proteins with AuNPs may affect the mobility and dispersity of AuNPs in blood [21]. Also, the corona shield could cover the target ligands on the surfaces of AuNPs, leading to disorganization of the function of AuNP-based sensors. In this study to solve the problem, the serum samples were diluted. However, this work led to a decrease in the sensitivity of the presented aptasensor [20].

As dsDNA cannot interact with the surface of AuNPs, we designed an amplified fluorescent aptasensor based on catalytic recycling activity of Exo III for the detection of kanamycin [22]. Without a target, the aptamer bound to its FAM-labeled CS and made a dsDNA; the formed dsDNA left the surface of AuNPs, because of its rigid structure. Upon addition of Exo III, the FAM-labeled CS was digested and the aptamer with a 3'-end overhang was recycled from dsDNA; and the cycle goes on, causing a very strong fluorescence emission. In the presence of kanamycin, an aptamer/target complex was formed and FAM-labeled CS remained on the surface of AuNPs and the fluorescence was quenched by AuNPs as a strong quencher (Figure 8.3). This aptasensor was effectively utilized to detect kanamycin in both milk and serum with LODs of 476 pM ($0.275 \mu\text{g l}^{-1}$) and 569 pM ($0.329 \mu\text{g l}^{-1}$), respectively. The obtained LODs were much lower than the maximum acceptable level of kanamycin in milk ($150 \mu\text{g l}^{-1}$) and toxicity level in blood ($25\text{--}30 \text{ mg l}^{-1}$) [22].

Benefiting from the excellent quenching nature of AuNPs, an aptasensor for detection of digoxin with a LOD as low as 392 pM was developed (Figure 8.4) [23].

AuNPs and ATTO 647N (dye)-labeled aptamer were also applied for the construction of a NSET (nanomaterial surface energy transfer)-based aptasensor for the determination of digoxin (LOD 392 pM) [23]. NSET is a technique capable of measuring distances nearly twice as far as FRET (fluorescence resonance energy transfer) in which energy transfer from a donor molecule to a nanoparticle surface follows a predictable distance dependence [24]. In the absence of digoxin,

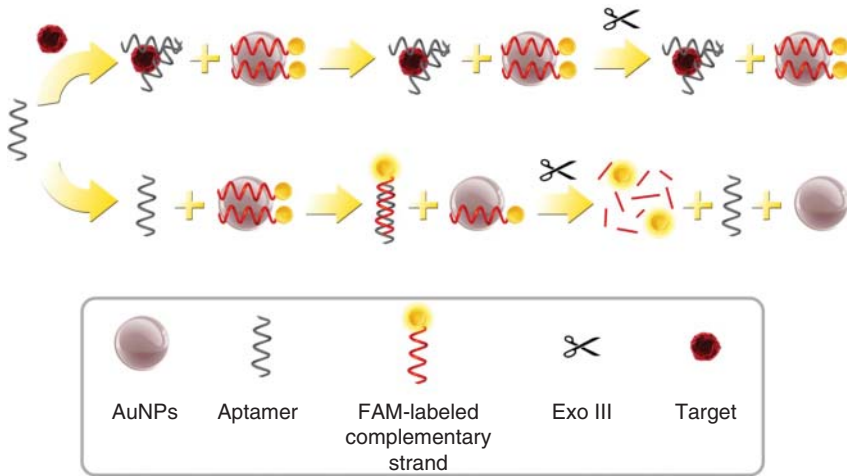


Figure 8.3 Fluorescent aptasensor to detect kanamycin based on exonuclease III activity (Exo III), gold nanoparticles (AuNPs), and FAM-labeled CS. In the absence of kanamycin, the aptamer and its CS formed a dsDNA and left the surface of AuNPs. Using Exo III, the aptamer was recycled from dsDNA and the cycle continued, resulting in a very strong fluorescence emission. Addition of kanamycin caused the aptamer to bind to its target and CSs remained on the surface of AuNPs, resulting in a weak fluorescence emission. Source: Ramezani et al. [22]. Reproduced with permission of Elsevier.

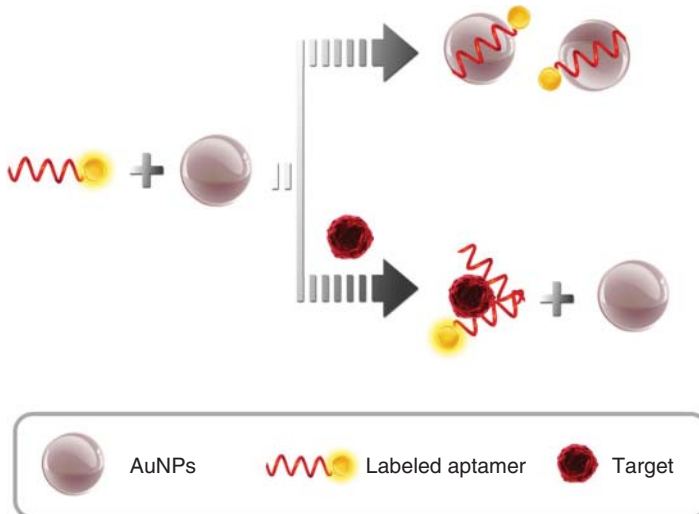


Figure 8.4 Detection of digoxin based on rapid fluorescence quenching. In the absence of digoxin, aptamers were adsorbed on the surfaces of AuNPs. Therefore, the fluorescence of the labeled aptamer was efficiently quenched by AuNPs. In the presence of digoxin, aptamers bound to digoxin, leading to the turning on of the fluorescence emission. Source: Emrani et al. 2015 [23]. Reproduced with permission of Royal Society of Chemistry.

ATTO 647N-labeled aptamer was adsorbed on the surface of AuNPs via van der Waals forces between the bases of ATTO 647N-labeled aptamer and AuNPs [25]. Therefore, a weak fluorescence intensity was recorded. In the presence of digoxin, an aptamer/digoxin complex was formed, which could not bind to AuNPs. Thus, a strong fluorescence intensity was measured.

Using the same mechanism, Chen et al. developed a fluorescent aptasensor for the detection of kanamycin A (LOD 0.3 nM) using FAM-labeled aptamer and AuNPs [26]. Also, a fluorescent aptasensor for the detection of lead ions, LOD of 10 nM, was designed by this strategy [27].

Duan et al. presented a fluorescent aptasensor based on target-induced release of CS from aptamer and AuNPs for detection of ochratoxin A. Thiol-modified aptamers were bound to AuNPs through S—Au bond. When ochratoxin A was added, the aptamer interacted with its target and the FAM-labeled CS left the aptamer and AuNPs, leading to the increase in fluorescence intensity. The detection limit for this sensor was $2 \times 10^{-12} \text{ g ml}^{-1}$ [28].

In another work, a fluorescence sensing method was fabricated on the basis of the aptamer-induced conformational change of FAM-labeled CS and AuNPs for the determination of organophosphorus pesticides. In the absence of a target, the aptamer was hybridized with its FAM-labeled CS on the surface of the electrode, leading to the disruption of the hairpin structure of the CS. So, the fluorophore and AuNPs were staying away from each other and the fluorescence signal was weak. In the presence of organophosphorus pesticides, the aptamer binds to its target and does not hybridize with its CS. Therefore, the hairpin structure of CS remains intact and the FAM comes in close proximity to the surface of AuNPs and the fluorescence signal was weak. This sensor exhibited a detection limit of 0.035 μM for isocarbophos, 0.134 μM for profenofos, 0.384 μM for phorate, and 2.35 μM for omethoate, respectively [29].

However, all of these aptasensors would suffer from corona shield because of the presence of unmodified AuNPs [21]. To surpass this problem, the AuNPs can be modified by substances like polyethylene glycol (PEG) [26–28, 30, 31].

8.3.2 Fluorescent Aptasensors Based on Carbon Nanomaterials

Graphene, a new class of two-dimensional carbon nanomaterials with one-atom thickness, exhibits properties clearly different from that of carbon, such as high planar surface, excellent mechanical strength, unparalleled thermal conductivity, and extraordinary electronic properties [32]. Moreover, compared with organic quenchers, graphene can quench efficiently a wider range of organic dyes and quantum dots (QDs) with low background and high signal-to-noise ratio [33]. Compared to carbon nanotubes (CNTs), graphene has several advantages like high thermal and electrical conductivity because of small thickness and large surface area [34]. Thus, graphene-based nanomaterials have found several applications in biosensing design. A highly sensitive and selective fluorescent graphene oxide (GO)-based aptasensor for mucin 1 (MUC1), a well-known tumor biomarker, was designed with a detection limit of 28 nM and a wide linear range of 0.04–10 mM. In the absence of MUC1, CY5-labeled aptamer non-covalently bound to GO through π – π stacking interactions and

its fluorescence was quenched. Upon addition of MUC1, the conformation of the aptamer was switched from a random coil to the aptamer/MUC1 complex, leading to release of the aptamer/MUC1 complex from the surface of the GO. Thus, the fluorophore stayed away from the GO and the fluorescence intensity was turned on [35]. On the basis of this sensing strategy, an aptasensor was designed for the detection of chloramphenicol using QDs and GO [36]. QDs present several advantages over common fluorophores, including photobleaching resistance, narrow emission spectra, high fluorescence efficiency, long fluorescence lifetimes, and large excitation spectra [37, 38]. The combination of QDs and GO led to a detection limit as low as 98 pM [36].

CNTs are molecular-scale tubes of graphitic carbon which act as excellent nanoquenchers for the fluorophores. Moreover, they can protect aptamers against nuclease digestion in real samples and *in vivo* [39]. CNTs are divided into two leading categories, including single-walled carbon nanotubes (SWNTs) and multiwalled carbon nanotubes (MWNTs) based on the number of layers of the graphene sheets [40]. Compared to GO, application of SWNTs in the construction of sensors can increase the selectivity and sensitivity because unlike the flat surface area of GO, the SWNTs have curved surfaces which can reduce the unspecific adsorption [41]. A simple and sensitive fluorescent sensor was designed using ATTO 647N (dye)-labeled aptamer–SWNT complex for the detection of lead (Pb^{2+}) in tap water and serum samples with LODs of 1.98 and 4.2 nM, respectively. In this sensor, labeled aptamer non-covalently bound to SWNT through π – π stacking interaction and its fluorescence was efficiently quenched. In the presence of Pb^{2+} , the aptamer left the surface of the quencher (SWNTs) in favor of binding to its target and formation of a G-quadruplex/ Pb^{2+} complex, leading to an increase in fluorescence intensity (Figure 8.5) [42].

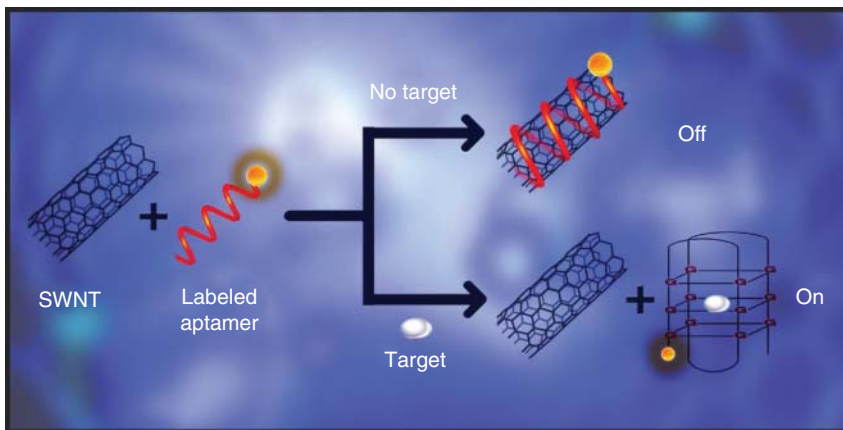


Figure 8.5 Super quenching capability of SWNTs and a labeled aptamer were used for design of this sensor. In the absence of Pb^{2+} , the fluorescence of labeled aptamer was quenched by SWNTs. Upon addition of Pb^{2+} , G-quadruplex/ Pb^{2+} complex was formed and ATTO 647 N-aptamer started fluorescence emission. Source: Taghdisi et al. 2014 [42]. Reproduced with permission of Elsevier.

8.3.3 Fluorescent Aptasensors Based on Silica Nanoparticles

Silica nanoparticles (SNPs) have been extensively used for biomedical and bioanalysis purposes, because of their attractive features such as high density, easy separation, protection of DNA from nuclease cleavage, low-cost production, biocompatibility, high hydrophilicity, and being strong fluorescence enhancers [43, 44]. Using SNPs, a sensitive and selective fluorescent aptasensor was introduced for recognition of digoxin (a useful drug in the treatment of heart failure) in serum based on target-induced release of FAM-labeled CS. In this sensor, a dsDNA structure including the biotinylated aptamer for digoxin and FAM-labeled CS were immobilized on the surface of SNPs coated with streptavidin (SNPs-streptavidin) via the strong interaction of SNPs-streptavidin with biotin-labeled aptamer with a dissociation constant (K_d) of about 10^{-14} M. In the absence of digoxin, the FAM-labeled CS remained in close proximity to the surface of the SNPs. Therefore, a strong fluorescence was detected. Upon the addition of digoxin, the aptamer bound to its target, leading to release of the FAM-labeled CS from the dsDNA and SNPs surface and thereby reducing the fluorescence intensity. The aptamer interacts with its target with a better binding constant relative to its CS [18, 19]. A detection limit as low as 566 pM was calculated for digoxin using this method [45]. A similar analytical assay was applied for the sensitive detection of kanamycin in serum with a LOD of 453 pM (Figure 8.6) [46].

In another assay, an amplified fluorescent aptasensor for ultrasensitive detection of myoglobin was designed on the basis of SNPs-streptavidin, CS,

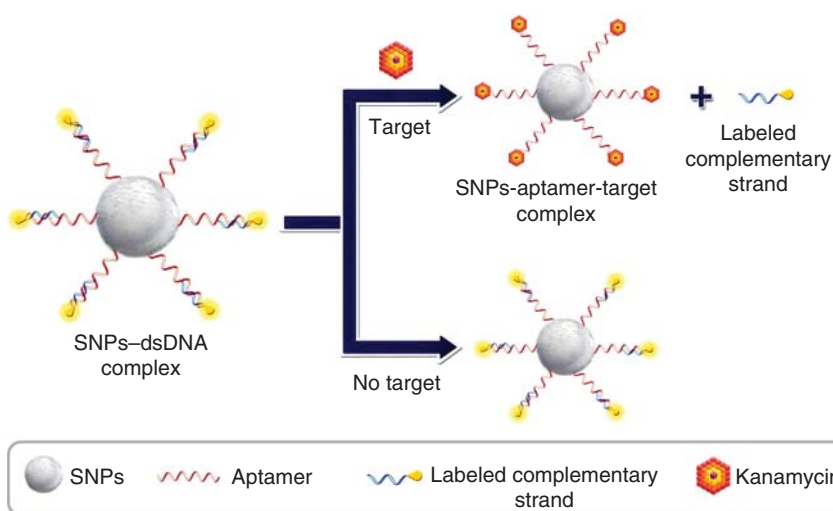


Figure 8.6 Kanamycin aptamer as the molecular recognition probe was immobilized on the surface of the SNPs. In the absence of a target, the SNPs-dsDNA complex was intact and the strong fluorescence emission was obtained. In the presence of kanamycin, the aptamer bound to its target and labeled CS was released from the aptamer and SNPs, so the fluorescence intensity was reduced. Source: Khabbaz et al. 2015 [46]. Reproduced with permission of Royal Society of Chemistry.

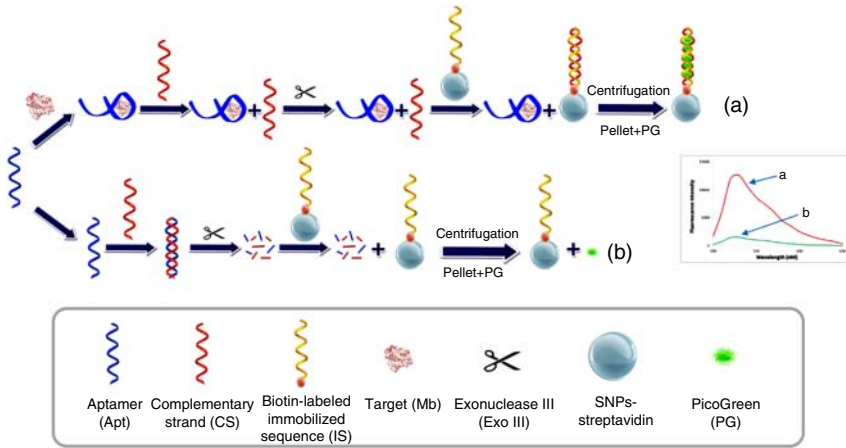


Figure 8.7 Biotin-labeled immobilized sequence (IS) as the complementary strand (CS) was attached on the surface of SNPs. In the absence of Mb, Apt/CS conjugate (dsDNA) was digested by Exo III. In the presence of a target, the aptamer bound to its target and free CS bound to IS. So, upon addition of PG, a very strong fluorescence emission was detected. Source: Abnous et al. 2016 [47]. Reproduced with permission of Elsevier.

PicoGreen (PG) dye, and Exo III. In this sensing platform, PG acted as a signal probe as its fluorescence could be enhanced by more than 1000-fold upon its binding to dsDNA. Exo III was used as an enzyme for the digestion of dsDNA. SNPs-streptavidin was decorated with a biotin-labeled immobilized sequence (IS) which was the complementary strand of CS. Without a target, aptamer/CS conjugate (dsDNA) was formed and the dsDNA was digested by Exo III. So, no free CS remained in the environment of IS-modified SNPs-streptavidin, resulting in a weak fluorescence emission upon addition of PG. In the presence of myoglobin, aptamer bound to its target and no dsDNA was formed. The aptamer/myoglobin complex and the CS were protected against Exo III because of their ssDNA nature. The free CS could bind to biotin-labeled IS on the surface of SNPs-streptavidin. Thus, by addition of PG, a very strong fluorescence emission was observed because of its binding to CS-IS (dsDNA)-modified SNPs-streptavidin (Figure 8.7). Using this approach, the LOD for myoglobin was calculated as low as 52 pM [47].

Taking advantage of the DNA-protection property of SNPs, Cai et al. constructed a fluorescent aptasensor for ATP detection in biological samples. The offered sensing platform was based on target-induced release of aptamer from its CS and hoechst33258 as a signal reporter, the fluorescence of which increases when it intercalates into ssDNA and dsDNA. In the first step, the aptamer/CS conjugate (dsDNA) was fixed on the carboxyl-modified SNPs. Upon addition of ATP, the number of aptamer/CS conjugate on the surface of SNPs was reduced owing to the switching of aptamer structure from aptamer/CS conjugate to aptamer/ATP complex. So, weak fluorescence intensity was detected when the hoechst33258 was added. However, in the absence of ATP, huge amounts of aptamer/CS conjugate was on the surface of SNPs, resulting in a strong fluorescence intensity. This fluorescent sensor exhibited a detection limit of $\sim 20 \mu\text{M}$

for ATP [48]. Using the advantages of the fluorescence quenching characteristic of AuNPs and fluorescence enhancing feature of SNPs-streptavidin, a novel fluorescent aptasensor was developed for ultrasensitive detection of ochratoxin A. Utilizing these two types of nanoparticles with opposite results on fluorophore (FAM), a very significant difference in the fluorescence intensity of the designed aptasensor in the presence and absence of ochratoxin A was observed, resulting in a very low detection limit. Thiol-modified aptamer was immobilized on the surface of AuNPs via Au—S bond. Then, FAM and biotin-labeled CS were hybridized with the aptamer on the surface of AuNPs. Without ochratoxin A, the structure of the dsDNA (aptamer/CS conjugate) remained intact on the surface of AuNPs. All dsDNA-modified AuNPs were sedimented following the mixture centrifugation, and so no CS was in the supernatant. Therefore, no fluorescence was observed following the addition of SNPs-streptavidin to the supernatant. In the presence of ochratoxin A, FAM and biotin-labeled CS were released from the aptamer-modified AuNPs and aptamer/Ochratoxin A complex was formed on the surface of AuNPs. When the mixture was centrifuged, the functionalized AuNPs were precipitated and CS remained in the supernatant. When SNPs-streptavidin was added to the supernatant, these nanomaterials bound to FAM and biotin-modified CS via the strong interaction of biotin with streptavidin, and SNPs-streptavidin-CS complex was formed. Since the FAM and biotin-labeled CS were in close proximity to the surface of SNPs, its fluorescence intensity significantly increased because SNPs were strong fluorescence amplifiers. A LOD as low as 0.098 nM was reported for this aptasensor [49].

Also, an amplified fluorescent aptasensor was designed for the sensitive and specific detection of cocaine, based on the hairpin structure of CS of aptamer, AuNPs, and SNPs-streptavidin. Besides high sensitivity, because of the presence of both AuNPs and SNPs-streptavidin (as mentioned), the hairpin structure of CS on the surface of SNPs-streptavidin guaranteed there was no binding of AuNPs to the surface of SNPs-streptavidin in the presence of cocaine, leading to higher sensitivity. In the absence of cocaine, no change happened to the structure of aptamer-modified AuNPs/CS-SNPs-streptavidin complex, leading to a weak fluorescence emission because the fluorophore (FAM) was far away from the surface of SNPs-streptavidin and in close proximity to the surface of AuNPs. In the presence of cocaine, FAM and biotin-labeled CS were released from the aptamer-modified AuNPs and the fluorophore was brought in close proximity to the surface of SNPs-streptavidin, due to the formation of the hairpin structure of CS, leading to a very strong fluorescence emission (Figure 8.8). This aptasensor detected cocaine in serum with a LOD as low as 293 pM [50].

8.3.4 Fluorescent Aptasensors Based on Silver Nanoparticles

Silver nanoparticles have been broadly utilized in various analytical assays due to their predominant characteristics, including long-term stability, high extinction coefficients, excellent electron transfer rates, and distance-dependent optical properties [51–53]. An aptamer-based fluorescence biosensor for sensitive and selective detection of H5N1 influenza virus was developed on the basis of silica-shell-coated silver nanoparticles (Ag@SiO₂) as metal-enhanced

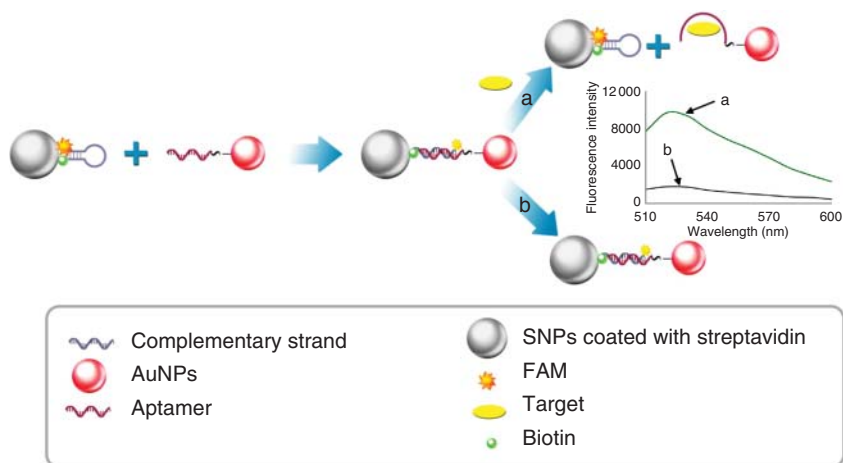


Figure 8.8 Cocaine detection based on fluorescent assay. In the presence of a target, a very strong fluorescence signal was detected due to the formation of the hairpin structure of CS. In the absence of a target, aptamer-modified AuNPs/CS-SNPs-streptavidin complex remained intact, resulting in a weak fluorescence emission. Source: Emrani et al. 2016 [50]. Reproduced with permission of Elsevier.

fluorescence detection substrate, a guanine-rich aptamer for the recombinant hemagglutinin protein of the virus (rHA), and thiazole orange as a specific dye for G-quadruplex structure. In the absence of rHA, the thiazole orange was free in the sample. So, no fluorescence emission was detected because the free thiazole orange had no fluorescence. Upon addition of rHA, the conformational structure of the aptamer changed from a random coil to a G-quadruplex sequence. So, when the thiazole orange was added to the sample, it was inserted into the G-quadruplex strand and the fluorescence intensity was significantly enhanced. A detection limit of 3.5 ng ml^{-1} for rHA protein was determined with an assay time of ~ 30 minutes in human serum [54]. However, as mentioned for the AuNPs, the corona shield is a big shortcoming for silver nanoparticles as well. This drawback can decrease and disorganize the function of these nanoparticles in sensing platforms and in medicinal applications [55, 56].

8.3.5 Fluorescent Aptasensors Based on DNA Structures

8.3.5.1 Fluorescent Aptasensors Based on DNA Nanostructures

Sensors based on DNA nanostructures are promising candidates for the detection of different materials due to their advantages, including rapid response, ease of application, and low cost [57]. A new fluorescent aptasensor for the detection of ochratoxin A, based on DNA pyramid nanostructure and PG dye, was designed [58]. The designed DNA pyramid nanostructure was composed of dsDNA building blocks and the ochratoxin A aptamer was a part of these dsDNA building blocks. The fluorescence feature of PG enhances more than 1000-fold when it binds to dsDNA, while the free PG shows no fluorescence emission [59, 60]. The offered DNA pyramid nanostructure had outstanding

characteristics, including high capacity for DNA pyramid nanostructure, high stability in biological samples, and monodispersity. By addition of ochratoxin A, the aptamer left its CS and aptamer/ochratoxin A was formed and the pyramid structure of the DNA nanostructure was disassembled. Thus, following the addition of PG, due to less dsDNA building blocks, a weak fluorescence emission was recorded. In the absence of a target, the pyramid structure of the DNA nanostructure remained intact. Therefore, by addition of PG a very strong fluorescence emission was obtained [58]. While the presented DNA pyramid nanostructure showed good sensitivity toward ochratoxin A (LOD = 0.135 nM), the design of the DNA nanostructures is really complicated [50, 58].

8.3.5.2 Fluorescent Aptasensors Based on Triple-Helix Molecular Switch (THMS)

A triple-helix molecular switch (THMS) system generally contains a target-specific hairpin-shaped aptamer with two arm segments and a dual-labeled oligonucleotide as signal transduction probe (STP) [61]. THMS has unique features over common double-helix DNA molecular switches and molecular beacon-based signaling aptamers, such as high sensitivity and stability as well as preserving the selectivity and sensitivity of the original aptamer [62]. Because of these outstanding features, THMS has been used in the design of several aptasensors. Two fluorescent THMS-based aptasensors were designed by our group. In one of them, an aptamer-based fluorescent sensing platform using THMS was developed for the detection of tetracycline in tap water and rat serum. Black hole quencher 1 (BHQ1) and FAM were attached to the 3'- and 5'-ends of the STP as an acceptor and a donor of light, respectively. The two arm segments of the aptamer were hybridized with the loop sequence of the STP using Watson–Crick and Hoogsteen base pairings, leading to the formation of a THMS structure. In this new structure, the STP showed an open conformation and the FAM (fluorophore) was away from the BHQ1 (quencher), resulting in the increase of fluorescence emission (Figure 8.9). Upon the addition of tetracycline, the aptamer bound to tetracycline, the THMS system was disassembled, and the released STP was folded into the original closed hairpin structure via intramolecular DNA hybridization, leading to FRET and fluorescence quenching. In FRET technology, the nonradiative transfer of energy from a donor fluorophore to an acceptor fluorophore occurs. The efficiency of energy transfer in this system is mainly dependent on interfluorophore distance and orientation. This sensor showed a high selectivity toward tetracycline with a LOD as low as 2.09 nM [63].

Optimizations of pH and the length of two arm segments of the aptamer are necessary for the efficient function of THMS-based aptasensors. This sensing strategy was also used for the detection of a pesticide, acetamiprid, with a LOD of 9.12 nM [64]. Also, this sensing platform was employed again for the easy, sensitive, and quick detection of insulin in biological samples by our group. The LODs of this fluorescence-based sensor were 13.47 and 18.08 nM in urine and serum samples, respectively [65].

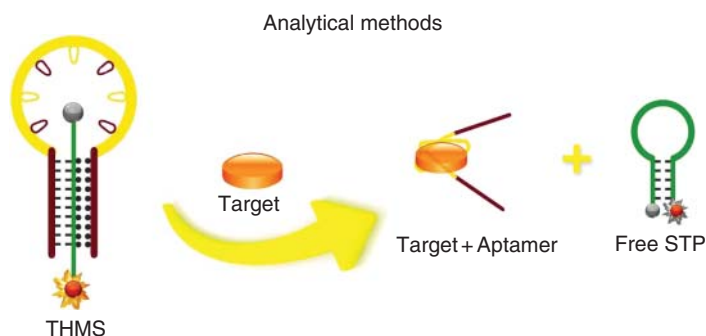


Figure 8.9 In the presence of tetracycline, the aptamer bound to its target and the THMS complex was disassembled. So, the free STP was folded into a stem-loop structure, and the fluorescence was quenched. In the absence of a target, the fluorescence was on. Source: Jalalian et al. 2015 [63]. Reproduced with permission of Royal Society of Chemistry.

8.4 Conclusion

In conclusion, in this chapter the recent advantages and properties of different fluorescent aptasensors were reported through descriptions of several research projects. Fluorescence as one of the most common signal transduction modes is applied in the design of several aptasensors due to rapid response, high sensitivity, and high efficiency. Each mentioned work possessed unique characteristics and challenges and we tried to address both challenges and unique properties for every designed fluorescent aptasensor. Labeling of aptamers with fluorescent dyes is laborious, expensive, and can reduce the binding properties of aptamers toward their targets. Amplification of the fluorescence signal could be achieved using nanoparticles such as SNPs as strong fluorescence enhancers or AuNPs as excellent quenchers of fluorophores. However, these nanoparticles have some disadvantages like the formation of corona for AuNPs and silver nanoparticles. This drawback can reduce and disorganize the function of these nanoparticles in sensing platforms, especially for real sample analysis. DNA origamis are promising candidates for the construction of fluorescent aptasensors because of their advantages like high stability, but the design of DNA nanostructures is complicated. To solve these shortcomings, researchers are attempting to develop fluorescent aptasensors which offer low cost, rapid detection, and need for less modification and sample preparation.

Acknowledgment

The authors are thankful to the Royal Society of Chemistry for Figures 8.4, 8.6, and 8.9 reproduced in this chapter.

Suggested Websites

Dr. Khalil Abnous

- 1 <http://pharmacy.mums.ac.ir/index.php/component/content/article/43-persian-category/1190-drabnousevcen>.
- 2 https://www.researchgate.net/profile/Khalil_Abnous.
- 3 <http://www.scopus.com/authid/detail.uri?origin=AuthorProfile&authorId=22937196500&zone>.

Dr. Seyed Mohammad Taghdis

- 1 <http://pharmacy.mums.ac.ir/index.php/component/content/article/43-persian-category/1179-drtaghdisicv>.
- 2 https://www.researchgate.net/profile/Seyed_Mohammad_Taghdisi.
- 3 <https://www.scopus.com/authid/detail.uri?origin=AuthorProfile&authorId=15726955700&zone>.

References

- 1 Deng, B., Lin, Y., Wang, C. et al. (2014). Aptamer binding assays for proteins: the thrombin example—a review. *Anal. Chim. Acta* 837: 1–15.
- 2 Wu, X., Chen, J., Wu, M., and Zhao, J. X. (2015). Aptamers: active targeting ligands for cancer diagnosis and therapy. *Theranostics* 5: 322–344.
- 3 McKeague, M. and DeRosa, M. C. (2012). Challenges and opportunities for small molecule aptamer development. *J. Nucleic Acids* 2012: 1–20.
- 4 Song, S., Wang, L., Li, J. et al. (2008). Aptamer-based biosensors. *TrAC, Trends Anal. Chem.* 27: 108–117.
- 5 Robati, R. Y., Arab, A., Ramezani, M. et al. (2016). Aptasensors for quantitative detection of kanamycin. *Biosens. Bioelectron.* 82: 162–172.
- 6 Duan, N., Wu, S., Dai, S. et al. (2016). Advances in aptasensors for the detection of food contaminants. *Analyst* 141: 3942–3961.
- 7 Jayasena, S. D. (1999). Aptamers: an emerging class of molecules that rival antibodies in diagnostics. *Clin. Chem.* 45: 1628–1650.
- 8 Feng, C., Dai, S., and Wang, L. (2014). Optical aptasensors for quantitative detection of small biomolecules: a review. *Biosens. Bioelectron.* 59: 64–74.
- 9 Zheng, B., Cheng, S., Dong, H. et al. (2014). Label free determination of potassium ions using crystal violet and thrombin-binding aptamer. *Anal. Lett.* 47: 1726–1736.
- 10 Rogers, S. G. and Weiss, B. (1980). Exonuclease III of *Escherichia coli* K-12, an AP endonuclease. *Methods Enzymol.* 65: 201–211.
- 11 Chen, F., Lu, J.-R., Binder, B. J. et al. (2001). Application of digital image analysis and flow cytometry to enumerate marine viruses stained with SYBR gold. *Appl. Environ. Microbiol.* 67: 539–545.
- 12 Taghdisi, S. M., Danesh, N. M., Nameghi, M. A. et al. (2016). A label-free fluorescent aptasensor for selective and sensitive detection of streptomycin in milk and blood serum. *Food Chem.* 203: 145–149.

- 13 Zhang, J., Liu, B., Liu, H. et al. (2013). Aptamer-conjugated gold nanoparticles for bioanalysis. *Nanomedicine* 8: 983–993.
- 14 Iliuk, A. B., Hu, L., and Tao, W. A. (2011). Aptamer in bioanalytical applications. *Anal. Chem.* 83: 4440–4452.
- 15 Liu, J. and Lu, Y. (2006). Fast colorimetric sensing of adenosine and cocaine based on a general sensor design involving aptamers and nanoparticles. *Angew. Chem.* 118: 96–100.
- 16 Gopinath, S. C., Lakshmipriya, T., and Awazu, K. (2014). Colorimetric detection of controlled assembly and disassembly of aptamers on unmodified gold nanoparticles. *Biosens. Bioelectron.* 51: 115–123.
- 17 Smith, J. E., Griffin, D. K., Leny, J. K. et al. (2014). Colorimetric detection with aptamer-gold nanoparticle conjugates coupled to an android-based color analysis application for use in the field. *Talanta* 121: 247–255.
- 18 Chen, L., Wen, F., Li, M. et al. (2017). A simple aptamer-based fluorescent assay for the detection of aflatoxin B1 in infant rice cereal. *Food Chem.* 215: 377–382.
- 19 Li, H., Zhao, Y., Chen, Z., and Xu, D. (2017). Silver enhanced ratiometric nanosensor based on two adjustable fluorescence resonance energy transfer modes for quantitative protein sensing. *Biosens. Bioelectron.* 87: 428–432.
- 20 Emrani, A. S., Danesh, N. M., Lavaee, P. et al. (2016). Colorimetric and fluorescence quenching aptasensors for detection of streptomycin in blood serum and milk based on double-stranded DNA and gold nanoparticles. *Food Chem.* 190: 115–121.
- 21 Dominguez-Medina, S., Blankenburg, J., Olson, J. et al. (2013). Adsorption of a protein monolayer via hydrophobic interactions prevents nanoparticle aggregation under harsh environmental conditions. *ACS Sustainable Chem. Eng.* 1: 833–842.
- 22 Ramezani, M., Danesh, N. M., Lavaee, P. et al. (2016). A selective and sensitive fluorescent aptasensor for detection of kanamycin based on catalytic recycling activity of exonuclease III and gold nanoparticles. *Sens. Actuators, B* 222: 1–7.
- 23 Emrani, A., Mohammadá Danesh, N., Hamidá Jalalian, S., and Mohammadá Taghdisi, S. (2015). Sensitive and selective detection of digoxin based on fluorescence quenching and colorimetric aptasensors. *Anal. Methods* 7: 3419–3424.
- 24 Darbha, G. K., Ray, A., and Ray, P. C. (2007). Gold nanoparticle-based miniaturized nanomaterial surface energy transfer probe for rapid and ultrasensitive detection of mercury in soil, water, and fish. *ACS Nano* 1: 208–214.
- 25 Li, H. and Rothberg, L. (2004). Colorimetric detection of DNA sequences based on electrostatic interactions with unmodified gold nanoparticles. *Proc. Natl. Acad. Sci. U.S.A.* 101: 14036–14039.
- 26 Chen, J., Li, Z., Ge, J. et al. (2015). An aptamer-based signal-on bio-assay for sensitive and selective detection of Kanamycin A by using gold nanoparticles. *Talanta* 139: 226–232.
- 27 Chun, L. and Huang, C.-Z. (2014). Detection of lead ions in water based on the surface energy transfer between gold nanoparticles and fluorescent dyes. *Chin. J. Anal. Chem.* 42: 1195–1198.

- 28 Duan, N., Wu, S., Ma, X. et al. (2012). Gold nanoparticle-based fluorescence resonance energy transfer aptasensor for ochratoxin A detection. *Anal. Lett.* 45: 714–723.
- 29 Dou, X., Chu, X., Kong, W. et al. (2015). A gold-based nanobeacon probe for fluorescence sensing of organophosphorus pesticides. *Anal. Chim. Acta* 891: 291–297.
- 30 Melaine, F., Coilhac, C., Roupioz, Y., and Buhot, A. (2016). A nanoparticle-based thermo-dynamic aptasensor for small molecule detection. *Nanoscale* 8: 16947–16954.
- 31 Wang, G., Lu, Y., Yan, C., and Lu, Y. (2015). DNA-functionalization gold nanoparticles based fluorescence sensor for sensitive detection of Hg²⁺ in aqueous solution. *Sens. Actuators, B* 211: 1–6.
- 32 Wang, Y., Li, Z., Wang, J. et al. (2011). Graphene and graphene oxide: bio-functionalization and applications in biotechnology. *Trends Biotechnol.* 29: 205–212.
- 33 Tang, Z., Wu, H., Cort, J. R. et al. (2010). Constraint of DNA on functionalized graphene improves its biostability and specificity. *Small* 6: 1205–1209.
- 34 Hernandez, F. J. and Ozalp, V. C. (2012). Graphene and other nanomaterial-based electrochemical aptasensors. *Biosensors* 2: 1–14.
- 35 He, Y., Lin, Y., Tang, H., and Pang, D. (2012). A graphene oxide-based fluorescent aptasensor for the turn-on detection of epithelial tumor marker mucin 1. *Nanoscale* 4: 2054–2059.
- 36 Alibolandi, M., Hadizadeh, F., Vajhedini, F. et al. (2015). Design and fabrication of an aptasensor for chloramphenicol based on energy transfer of CdTe quantum dots to graphene oxide sheet. *Mater. Sci. Eng., C* 48: 611–619.
- 37 Liu, Z. and Su, X. (2017). A novel fluorescent DNA sensor for ultrasensitive detection of *Helicobacter pylori*. *Biosens. Bioelectron.* 87: 66–72.
- 38 Liang, L., Su, M., Li, L. et al. (2016). Aptamer-based fluorescent and visual biosensor for multiplexed monitoring of cancer cells in microfluidic paper-based analytical devices. *Sens. Actuators, B* 229: 347–354.
- 39 Zhen, S. J., Chen, L. Q., Xiao, S. J. et al. (2010). Carbon nanotubes as a low background signal platform for a molecular aptamer beacon on the basis of long-range resonance energy transfer. *Anal. Chem.* 82: 8432–8437.
- 40 Jain, A., Homayoun, A., Bannister, C. W., and Yum, K. (2015). Single-walled carbon nanotubes as near-infrared optical biosensors for life sciences and biomedicine. *Biotechnol. J.* 10: 447–459.
- 41 Guo, Z., Ren, J., Wang, J., and Wang, E. (2011). Single-walled carbon nanotubes based quenching of free FAM-aptamer for selective determination of ochratoxin A. *Talanta* 85: 2517–2521.
- 42 Taghdisi, S. M., Emrani, S. S., Tabrizian, K. et al. (2014). Ultrasensitive detection of lead (II) based on fluorescent aptamer-functionalized carbon nanotubes. *Environ. Toxicol. Pharmacol.* 37: 1236–1242.
- 43 He, X., Wang, K., Tan, W. et al. (2003). *J. Am. Chem. Soc.* 125: 7168.
- 44 Tamba, B., Dondas, A., Leon, M. et al. (2015). Silica nanoparticles: preparation, characterization and in vitro/in vivo biodistribution studies. *Eur. J. Pharm. Sci.* 71: 46–55.

- 45 Emrani, A. S., Taghdisi, S. M., Danesh, N. M. et al. (2015). A novel fluorescent aptasensor for selective and sensitive detection of digoxin based on silica nanoparticles. *Anal. Methods* 7: 3814–3818.
- 46 Khabbaz, L. S., Hassanzadeh-Khayyat, M., Zaree, P. et al. (2015). Detection of kanamycin by using an aptamer-based biosensor using silica nanoparticles. *Anal. Methods* 7: 8611–8616.
- 47 Abnous, K., Danesh, N. M., Emrani, A. S. et al. (2016). A novel fluorescent aptasensor based on silica nanoparticles, PicoGreen and exonuclease III as a signal amplification method for ultrasensitive detection of myoglobin. *Anal. Chim. Acta* 917: 71–78.
- 48 Cai, L., Chen, Z. Z., Dong, X. M. et al. (2011). Silica nanoparticles based label-free aptamer hybridization for ATP detection using hoechst33258 as the signal reporter. *Biosens. Bioelectron.* 29: 46–52.
- 49 Taghdisi, S. M., Danesh, N. M., Beheshti, H. R. et al. (2016). A novel fluorescent aptasensor based on gold and silica nanoparticles for the ultrasensitive detection of ochratoxin A. *Nanoscale* 8: 3439–3446.
- 50 Emrani, A. S., Danesh, N. M., Ramezani, M. et al. (2016). A novel fluorescent aptasensor based on hairpin structure of complementary strand of aptamer and nanoparticles as a signal amplification approach for ultrasensitive detection of cocaine. *Biosens. Bioelectron.* 79: 288–293.
- 51 Wang, H., Wang, H., Li, T. et al. (2017). Silver nanoparticles selectively deposited on graphene-colloidal carbon sphere composites and their application for hydrogen peroxide sensing. *Sens. Actuators, B* 239: 1205–1212.
- 52 Nsengiyuma, G., Hu, R., Li, J. et al. (2016). Self-assembly of 1, 3-alternate calix [4] arene carboxyl acids-modified silver nanoparticles for colorimetric Cu^{2+} sensing. *Sens. Actuators, B* 236: 675–681.
- 53 Huang, J., Xie, Z., Xie, Z. et al. (2016). Silver nanoparticles coated graphene electrochemical sensor for the ultrasensitive analysis of avian influenza virus H7. *Anal. Chim. Acta* 913: 121–127.
- 54 Pang, Y., Rong, Z., Wang, J. et al. (2015). A fluorescent aptasensor for H5N1 influenza virus detection based-on the core-shell nanoparticles metal-enhanced fluorescence (MEF). *Biosens. Bioelectron.* 66: 527–532.
- 55 Ding, F., Radic, S., Chen, R. et al. (2013). Direct observation of a single nanoparticle–ubiquitin corona formation. *Nanoscale* 5: 9162–9169.
- 56 Drescher, D., Guttmann, P., Büchner, T. et al. (2013). Specific biomolecule corona is associated with ring-shaped organization of silver nanoparticles in cells. *Nanoscale* 5: 9193–9198.
- 57 Lin, M., Wen, Y., Li, L. et al. (2014). Target-responsive, DNA nanostructure-based E-DNA sensor for microRNA analysis. *Anal. Chem.* 86: 2285–2288.
- 58 Nameghi, M. A., Danesh, N. M., Ramezani, M. et al. (2016). A fluorescent aptasensor based on a DNA pyramid nanostructure for ultrasensitive detection of ochratoxin A. *Anal. Bioanal.Chem.* 408: 5811–5818.
- 59 Song, Q., Peng, M., Wang, L. et al. (2016). A fluorescent aptasensor for amplified label-free detection of adenosine triphosphate based on core-shell $\text{Ag}@ \text{SiO}_2$ nanoparticles. *Biosens. Bioelectron.* 77: 237–241.

- 60 Chen, Z., Tan, L., Hu, L., and Luan, Y. (2015). Superior fluorescent probe for detection of potassium ion. *Talanta* 144: 247–251.
- 61 Zheng, J., Li, J., Jiang, Y. et al. (2011). Design of aptamer-based sensing platform using triple-helix molecular switch. *Anal. Chem.* 83: 6586–6592.
- 62 Ramezani, M., Danesh, N. M., Lavaee, P. et al. (2015). A novel colorimetric triple-helix molecular switch aptasensor for ultrasensitive detection of tetracycline. *Biosens. Bioelectron.* 70: 181–187.
- 63 Jalalian, S. H., Taghdisi, S. M., Danesh, N. M. et al. (2015). Sensitive and fast detection of tetracycline using an aptasensor. *Anal. Methods* 7: 2523–2528.
- 64 Liu, X., Li, Y., Liang, J. et al. (2016). Aptamer contained triple-helix molecular switch for rapid fluorescent sensing of acetamiprid. *Talanta* 160: 99–105.
- 65 Taghdisi, S. M., Danesh, N. M., Lavaee, P. et al. (2015). Aptamer biosensor for selective and rapid determination of insulin. *Anal. Lett.* 48: 672–681.

9

Development of Aptamer-Based Electrochemical Methods

Jian-guo Xu, Li Yao, Lin Cheng, Chao Yan, and Wei Chen

Hefei University of Technology, School of Food Science and Engineering, No. 193 Tunxi Road, Hefei Anhui 230009, PR China

9.1 Introduction

Aptamers are essentially short and single-stranded oligonucleotide strands (DNA or RNA) that usually consist of 20–80 nucleotides with molecular weight of 6–30 kDa [1]. The word “aptamer” was meaningfully coined from the Latin *aptus* (“fit”) and Greek *meros* (“part”), and the first aptamer was screened by two research groups independently [2–4]. On the basis of the technique of systematic evolution of ligands by exponential enrichment (SELEX), aptamers can be currently screened against a broad range of target analytes, including small molecules, peptides, proteins, and even whole cells by adopting appropriate three-dimensional stem and loop structures. The binding mechanisms are van der Waals forces, hydrogen bonding, electrostatic interactions, stacking of flat moieties, and shape complementarity [5], which are similar to antibody–antigen recognition. Consequently, aptamers are referred to as “chemical antibodies”.

Generally, electrochemical signals take the form of current, potential, or impedance. According to the changes in electrochemical signals, it can be used to qualitatively identify the presence or quantitatively determine the concentration level of target analytes. Electrochemical sensors are analytical devices that can convert biological or chemical signals into straightforward electrical responses in terms of transducer principles. The electrochemical aptasensor is one of the electrochemical sensors first proposed by Ikebukuro’s group in 2004 using aptamer as the recognition element to characterize the thrombin level.

9.2 Classification of Electrochemical Aptasensors

By coupling the technique of electrochemistry and aptamers, electrochemical aptasensors have been widely developed over the past two decades, and these can be clearly divided into different categories on the basis of different classification criteria, as follows.

From the point of signal recognition, electrochemical aptasensors can be divided into labeled and label-free types. The former involves either covalent or non-covalent binding, while the latter refers to the use of non-labeled aptamers.

In accordance with the changes in electrochemical signals, electrochemical aptasensors can be divided into “signal-on” and “signal-off” models. Concretely speaking, the signal-on electrochemical aptasensor exhibits a monotonously increased signal with the increasing of target concentrations; while for “signal-off” electrochemical aptasensor, the electrochemical signal is inversely proportional to the target concentration.

In addition, electrochemical aptasensors can be generally divided into three types according to the output electronic signals including current, potential, and impedance. Presently, employment of amperometric, potentiometric, or impedimetric aptasensors, other than electrochemiluminescence (ECL) aptasensors for analytical investigation, is more extensive.

9.3 Amperometric Aptasensors

Covalent labeled, non-covalent-labeled and label-free amperometric aptasensors are completely summarized herein.

9.3.1 Covalent Labels

To the best of our knowledge, redox labels are required to be covalently linked to the terminal groups of aptamers. However, the labeling sites should be carefully selected so as not to interfere with the folding ability and essential binding positions of aptamers.

9.3.1.1 Enzyme Labels

Enzyme-labeled amperometric aptasensors consist of two types: one is the sandwich structure and the other is labeled aptamer displacement.

Amplified detection systems based on a sandwich configuration and enzyme-labeled signaling aptamers have been described. Sandwich assays are only available for the target with multiple aptamer binding sites. Zhao et al. reported a sandwich-based aptasensor using horseradish peroxidase (HRP) as an enzyme label for ultrasensitive electrochemical determination of thrombin [6] (Figure 9.1). Aptamer1 (Apt1) of thrombin was immobilized on core/shell-structured $\text{Fe}_3\text{O}_4/\text{Au}$ magnetic nanoparticles (Au/MNPs) and served as the capture probe. Aptamer2 (Apt2) of thrombin dually labeled with AuNPs and HRP was used as the detection probe. In the presence of thrombin, the sandwich structure of Au/MNPs–Apt1/thrombin/Apt2–AuNPs–HRP was formed, achieving a linear response to thrombin concentration ranging from 0.1 to 60 pM and a lower detection limit down to 30 fM ($S/N = 3$). Xu and Yuan's group developed a sandwich-based aptasensor using DNAzyme, hemin/G-quadruplex, as an enzyme label for thrombin analysis [7] (Figure 9.2).

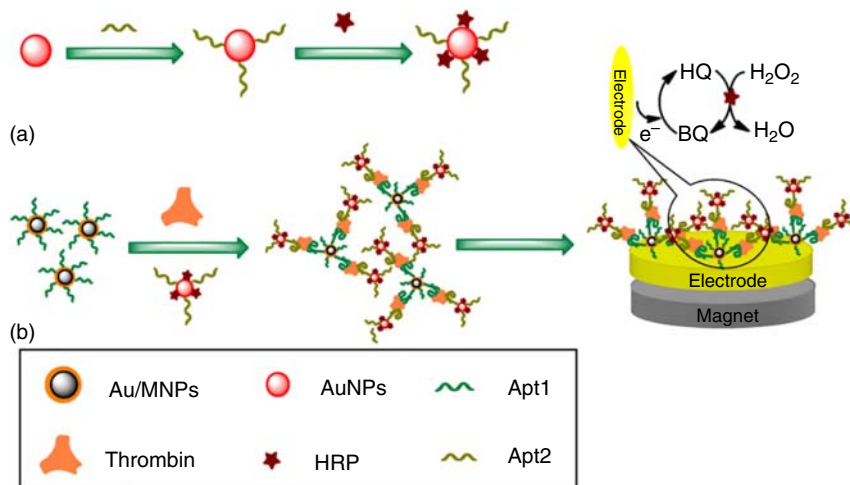


Figure 9.1 Sketch of (a) the preparation of Apt2–AuNPs–HRP conjugates and (b) the formation of AuMNPs–Apt1/thrombin/Apt2–AuNPs–HRP. Source: Zhao et al. 2011 [6]. Reprinted with permission of Elsevier.

The amplified electrochemical signal was achieved by the co-catalysis effect of alcohol dehydrogenase-graphene sheets (ADH-GSs) bionanocomposite and hemin/G-quadruplex, which was able to act as nicotinamide adenine dinucleotide (NADH) oxidase and HRP-mimicking DNAzyme, simultaneously. Through “sandwich” reaction, hemin/G-quadruplex-labeled gold nanoparticle-ADH-GSs bionanocomposite (AuNPs-ADH-GSs) was captured on an electrode surface and thus the electrochemical signal was obtained. After addition of ethanol into the electrolytic cell, ADH available catalyzed the oxidation of ethanol, resulting in the reduction of NAD^+ to NADH. Then, hemin/G-quadruplex functions as NADH oxidase to catalyze the oxidation of NADH, generating the H_2O_2 for hemin/G-quadruplex complex (DNAzyme) reduction. Such a catalysis strategy would greatly promote the electron transfer ability of hemin and lead to the electrochemical signal being significantly enhanced. The proposed thrombin aptasensor achieved a linear range of 1 pM–50 nM with a detection limit of 0.3 pM (defined as $S/N = 3$).

For the electrochemical aptasensor based on labeled aptamer displacement, it is applicable even in the case of a target with only one aptamer binding site. Shen et al. employed a thiolated single-stranded DNA (ssDNA) as the capture probe and assembled it on the surface of a gold electrode. Then the conjugate of Ap/Pd–AuNPs/HRP was attached via the hybridization of the capture probe with thrombin aptamer. The presence of thrombin would drive the Ap/Pd–AuNPs/HRP conjugate to dissociate from the electrode surface due to the formation of a tertiary target–aptamer complex, giving rise to a reduced amount of HRP responsible for a decreased electrochemical signal. In this

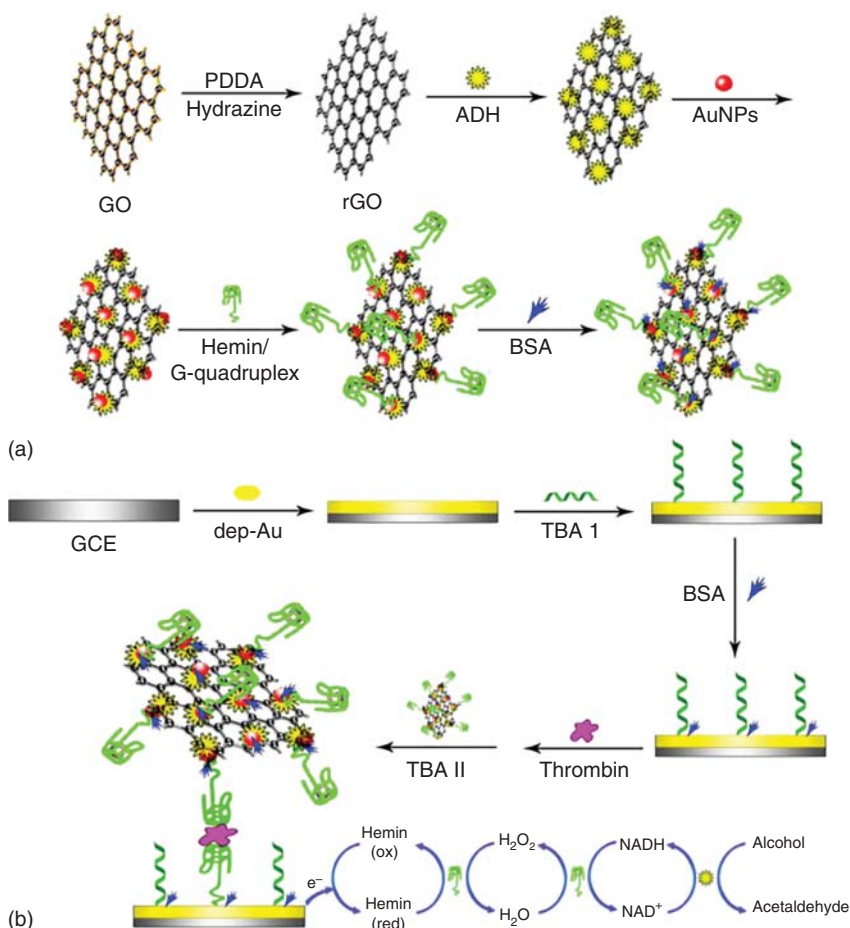


Figure 9.2 Preparation of (a) the second thrombin aptamer and (b) the sandwich-type electrochemical aptasensor. Source: Yi et al. 2014 [7]. Reprinted with permission of Elsevier.

condition, thrombin was detected within the range from 0.05 to 50 nM with a detection limit of 3 pM based on $S/N = 3$ [8] (Figure 9.3).

9.3.1.2 Other Covalently Linked Redox Species

Other redox-labeled amperometric aptasensors based on methylene blue (MB), ferrocene (Fc), or anthraquinone are intensively reported.

“Signal-off” and “signal-on” aptasensors have been described. However, the “signal-off” model, by measuring a decreased voltammetric signal, represents a disadvantage as it is a negative readout signal, while the “signal-on” model with a positive amperometric readout signal is generally preferred.

Different “signal-off” aptasensors based on conformational change of labeled aptamers or labeled strand displacement have been reported. Wu et al. reported a one-step electrochemical aptasensor using the thiol- and MB-dual-labeled aptamer-modified gold electrode for determination of ochratoxin A (OTA) [9]

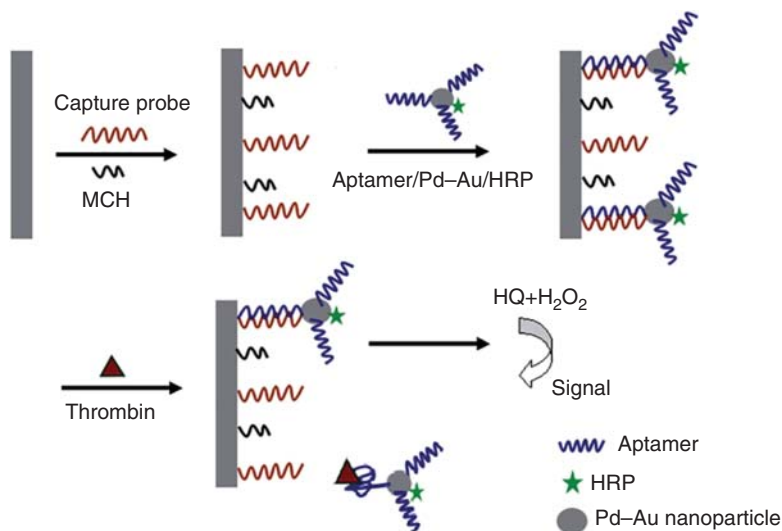


Figure 9.3 Schematic representation of the enzyme-labeled electrochemical aptasensors based on labeled aptamer displacement for thrombin detection. Source: Shen et al. 2016 [8]. Reprinted with permission of Royal Society of Chemistry.

(Figure 9.4). The aptamer against OTA was covalently immobilized on the surface of the electrode by the self-assembly effect and used as recognition probes for OTA detection by the binding-induced folding of the aptamer. OTA measurements were conducted using square wave voltammetry (SWV), which was performed using a potential window from -0.2 to -0.4 V (vs Ag/AgCl), a potential step of 0.001 V, amplitude of 0.05 V, and a frequency of 60 Hz. All measurements were carried out in 10 -mM phosphate-buffered saline (PBS; pH 7.4) with $MgCl_2$ at a concentration of 20 mM. Under all optimized conditions, the peak current decreased linearly with the increased OTA concentration in the range from 0.1 $\mu\text{g ml}^{-1}$ (ppt) to 1000 $\mu\text{g ml}^{-1}$ (ppt) with the R^2 of 0.9952 . As a consequence of binding of OTA to the aptamer immobilized on the electrode, the transfer of electrons was hindered. The limit of detection (LOD) was calculated to be 0.095 $\mu\text{g ml}^{-1}$ ($S/N = 3$). Jia et al. designed a novel method for adenosine triphosphate (ATP) detection based on the insertion approach and dual-hairpin structure as a signal amplifier for the improvement of repeatability and sensitivity, respectively [10] (Figure 9.5). For aptasensor preparation, the moiety and MB-labeled aptamer probe was inserted into a loosely packed cyclic-dithiothreitol (DTT) monolayer, and the MB-labeled adjunct probe could hybridize with the aptamer probe to form a dual-hairpin structure on the electrode. Without the target, the stable dual-hairpin conformation enabled the MB to stay close to the electrode surface, thereby generating a strong current signal. However, when the target was introduced, the high affinity binding of aptamer/target complex kept the MB of the aptamer probe distanced from the electrode surface and forced the adjunct probe to dissociate from the modified electrode, decreasing the current signal obviously. The current intensity was inversely proportional to the concentration of ATP in the range

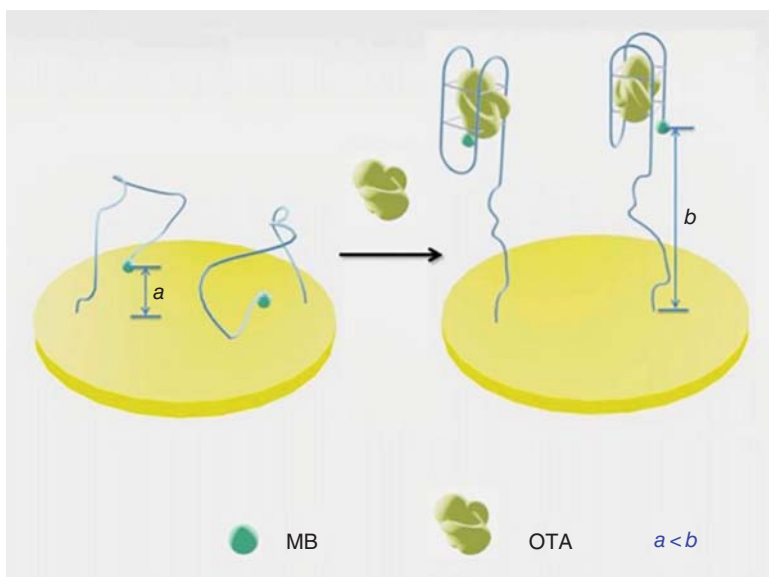


Figure 9.4 Scheme of one-step electrochemical aptasensor using the thiol- and methylene blue (MB)-dual-labeled aptamer-modified gold electrode for determination of ochratoxin A. Source: Wu et al. 2012 [9]. Reprinted with permission of Elsevier.

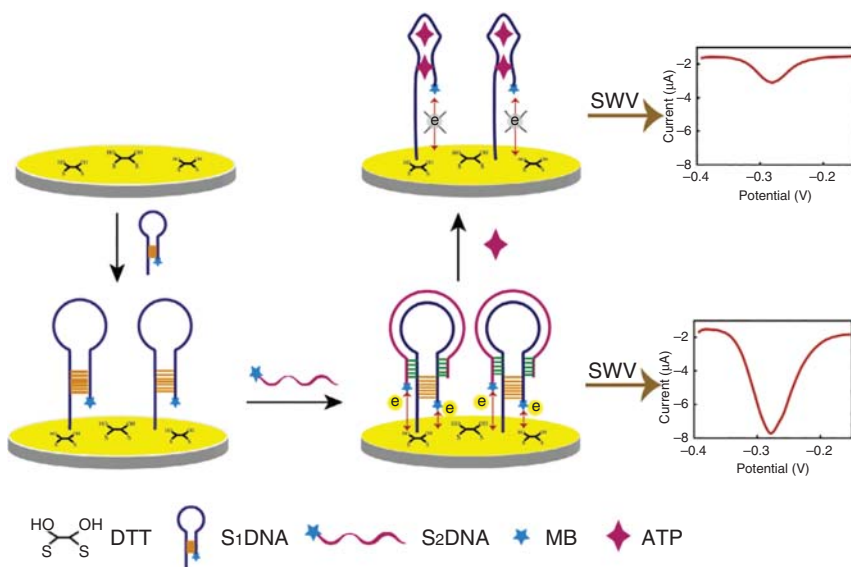


Figure 9.5 Schematic illustration of the detection of ATP based on electrochemical signal amplification by dual-hairpin DNA structure in combination with the insertion approach. Source: Jia et al. 2015 [10]. Reprinted with permission of Elsevier.

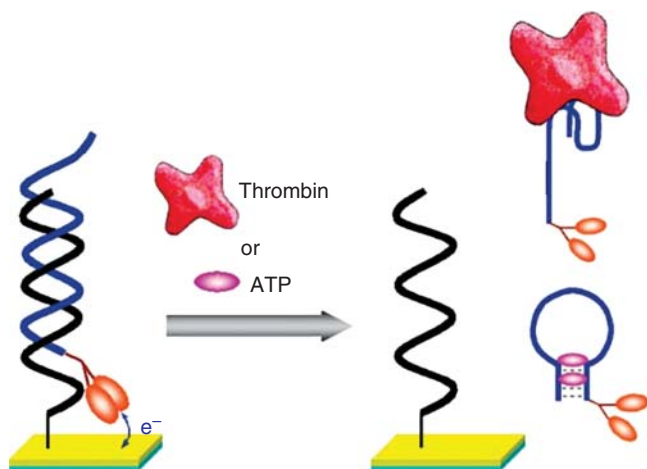


Figure 9.6 Schematic representation of the TISR E-AB sensor. Source: Yoshizumi et al. 2008 [11]. Reprinted with permission of Royal Society of Chemistry.

of 5 nM to 1 M, with a detection limit of 1.4 nM. Using target-induced strand release of a redox-modified aptamer from the aptamer–DNA duplex, Yamana’s group fabricated “signal-off” electrochemical aptasensors for the detection of a large protein-like thrombin and a small molecule-like ATP. In the initial aptamer–DNA duplex, the redox tag is appended onto the aptamer near the electrode surface, thereby giving an intense electrochemical signal in the absence of the target. With the addition of the target, via an aptamer structural switch, the redox-tagged aptamer strand is released from the surface and diffuses into the solution, resulting in a significant reduction of the signal [11] (Figure 9.6).

A variety of “signal-on” aptasensors based on conformational change of labeled aptamers or non-labeled aptamer displacements have been reported as well. The exemplified method is based on target-binding-induced folding of redox-labeled immobilized aptamers so that the redox labels would be in close proximity to the electrode surface. The first “signal-on” aptasensor for potassium ion detection was reported by Radi and O’Sullivan [12] (Figure 9.7). An Fc-labeled DNA aptamer containing multiple guanine-rich segments was self-assembled on a gold electrode by Au–S bond, which could be converted from a random-coil structure to a compact G-quadruplex structure by potassium-specific binding, associated with the Fc molecules in close proximity to the electrode surface. The Fc oxidation peak current was then measured by SWV, and its value was linearly related to the potassium ion concentration in a range varying from 0.1 to 0.8 mM. Plaxco’s group reported a reusable “signal-on” aptasensor based on cocaine-binding-induced conformational change of immobilized MB-labeled aptamers [13] (Figure 9.8). The aptasensor was fabricated by self-assembly of the relevant MB-tagged aptamer on a $\sim 1 \text{ mm}^2$ gold electrode via an alkanethiol group. In the absence of a target, the aptamer was thought to remain partially unfolded, with only one of its three double-stranded stems intact. In the presence of a target, the aptamer presumably folded into the cocaine-binding three-way

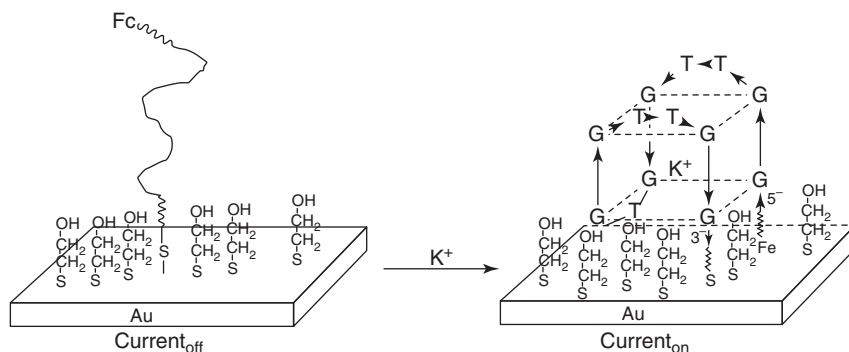


Figure 9.7 Mechanism of the structural transition of a G-rich aptamer from random coil to G-quadruplex induced by K^+ . Source: Radi and O'Sullivan 2006 [12]. Reprinted with permission of Royal Society of Chemistry.

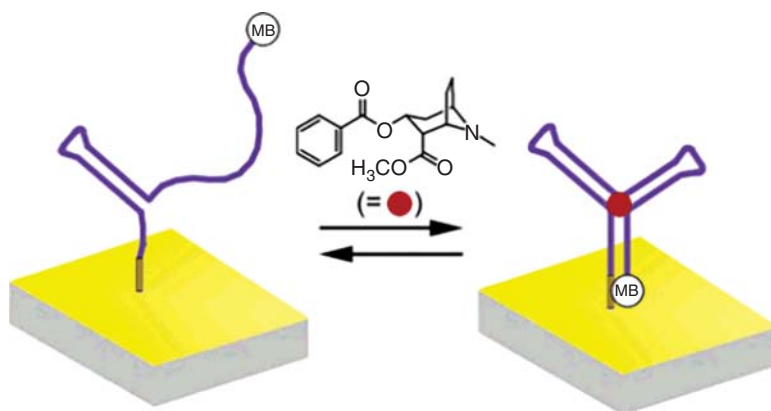


Figure 9.8 Mechanism of a reusable "signal-on" aptasensor based on cocaine-binding-induced conformational change of immobilized MB-labeled aptamers. Source: Baker et al. 2006 [13]. Copyright © 2006, with permission from American Chemical Society.

junction, altering electron transfer to increase the observed reduction peak and responding rapidly and specifically to the micromolar target in blood serum, saliva, and adulterated samples. Moreover, the sensing system requires only expensive and off-the-shelf electronics, which could be regenerated via a brief and room temperature wash.

In addition, a certain number of amperometric aptasensors by coupling "signal-on" with "signal-off" elements have also been constructed. Relying on the novel dual-signaling amplification strategy, an electrochemical "signal-on/off" aptasensor has been proposed by Chen's group [14] (Figure 9.9). The Fc-labeled aptamer probe (Fc-P) was designed to hybridize with thiolated MB-modified DNA probe (MB-P) on a gold electrode to form a rigid duplex DNA. In the presence of ATP, the interaction between ATP and the aptamer led to the dissociation of the duplex DNA structure and thereby the release of the Fc-P

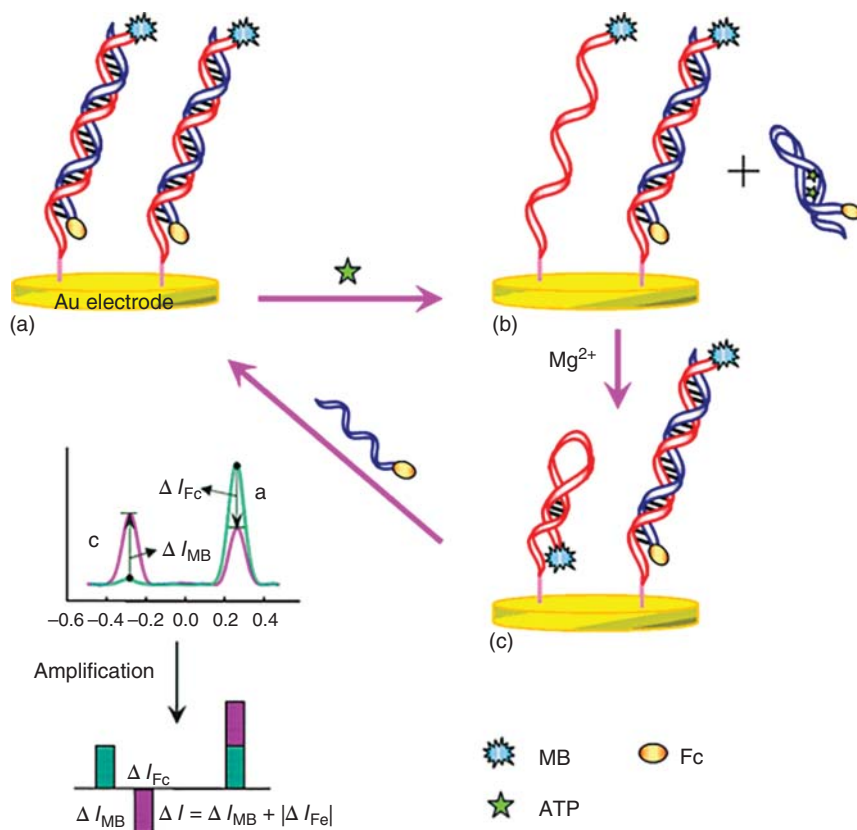


Figure 9.9 Schematic illustration of the dual-signaling E-AB biosensor for ATP analysis. Source: Wu et al. 2013 [14]. Reprinted with permission of American Chemical Society.

from the sensing interface. The single-stranded MB-P could thus tend to form a hairpin structure through the self-recognition of the complementary sequences at its two ends. Such conformational changes resulted in the oxidation peak current of Fc decreasing and that of MB increasing, and the changes of dual signals were linear with the concentration of ATP. The detection limit (1.9 nM) was much lower than that using either MB-P or Fc-P alone. Similarly, Cao et al. developed a new dual-signaling electrochemical aptasensor on the basis of “signal-on/signal-off” and “labeling/label-free” strategies [15] (Figure 9.10). Fc, being labeled on ssDNA as one signal indicator, could provide a “turn on” signal through the DNA conformational changes that resulted from target binding with the aptamer. $[\text{Ru}(\text{NH}_3)_6]^{3+}$ (RuHex), as another signal indicator, could provide a “turn off” signal through the electrostatic interaction between the anionic DNA phosphate backbones and the cationic RuHex, which was a label-free signal. Cyclic voltammetry (CV) and electrochemical impedance spectrum (EIS) were employed for monitoring the stepwise fabrication process of the biosensor. Under the optimized conditions, the dual signal changes were quantified using

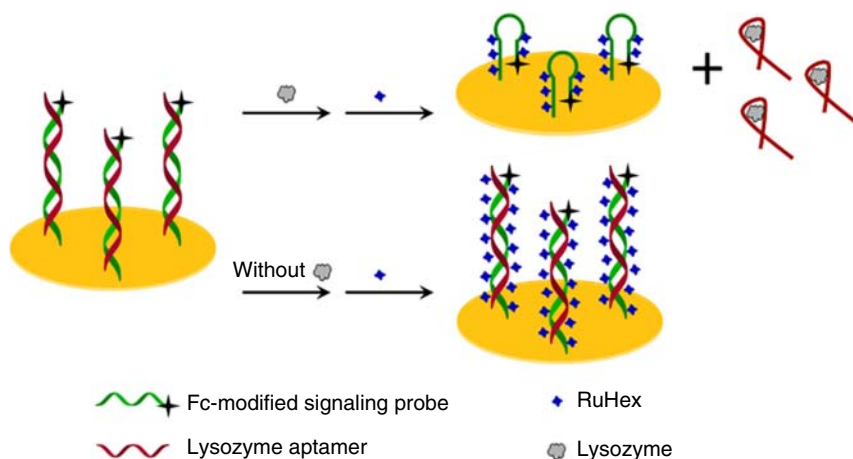


Figure 9.10 Schematic diagram for the fabrication of the dual-signaling electrochemical aptasensor. Source: Cao et al. 2016 [15]. Reprinted with permission of Elsevier.

SWV. The results indicated that lysozyme could be detected in a wide linear range (1.0×10^{-11} – 1.0×10^{-7} M) with a low detection limit down to 0.8 pM.

9.3.2 Non-covalent Labels

Electrochemical aptasensors using labels that are non-covalently bound to aptamers have also been studied for quite a long run time. Redox species can directly intercalate into the aptamer strands or interact with aptamers via electrostatic adhesion.

9.3.2.1 Intercalated Redox Species

Some amperometric aptasensors using intercalated labels have been reported. For example, Hianik et al. developed an electrochemical aptasensor based on the interaction of MB with the aptamer thrombin complex [16] (Figure 9.11). Chronologically, it was the second example of an electrochemical aptasensor. A biotinylated DNA aptamer was immobilized on a gold electrode via avidin–biotin interactions. In the presence of MB and thrombin, a significant change of charge transfer measured by differential pulse voltammetry (DPV) was obtained for 10 nM of thrombin (detection limit). The same sensitivity was also obtained by fluorescence detection, but amperometric detection appears an easier method than fluorescence detection since it does not need additional aptamer modification by quencher as that required for fluorescence detection. Kim's group reported an amperometric aptasensor based on MB intercalation into a beacon aptamer sequence [17] (Figure 9.12). Gold surface was modified with a beacon aptamer covalently linked at the 5'-terminus with a linker containing a primary aliphatic amine. MB was intercalated into the beacon sequence, and used as an electrochemical marker. When the beacon aptamer immobilized on the gold surface encountered thrombin, the hairpin-forming beacon aptamer was conformationally changed to release the intercalated MB, resulting in a

Figure 9.11 Schematic representation of biotinylated aptamers immobilized on a gold electrode through avidin and the charge transfer from the electrode to the electrochemical indicator methylene blue (MB). Source: Hianik et al. 2005 [16]. Reprinted with permission of Elsevier.

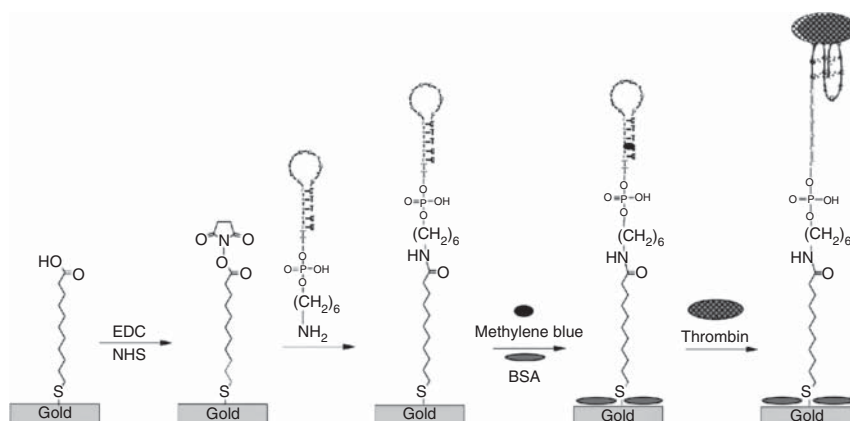
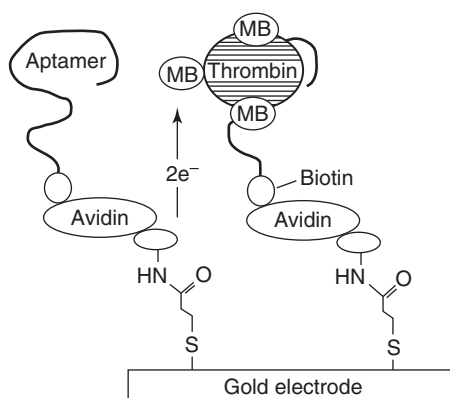


Figure 9.12 Schematic representation of the immobilization of beacon aptamer and detection of its target protein. Source: Bang et al. 2005 [17]. Reprinted with permission of Elsevier.

decrease in electrical current intensity in voltammogram. The peak signal of the MB was clearly decreased by the binding of thrombin onto the beacon aptamer. The linear range of the signal was observed between 0 and 50.8 nM of thrombin with 0.999 correlation factor. This method was able to linearly and selectively detect thrombin with a detection limit of 11 nM.

A rapid and ultrasensitive electrochemical aptasensor for bisphenol A (BPA) detection has been reported [18] (Figure 9.13). In this work, a specific aptamer against BPA and its complementary DNA probe were immobilized on the surface of a gold electrode via self-assembly and hybridization, respectively. The detection of BPA was mainly based on the competitive recognition of BPA by the immobilized aptamer on the surface of the electrode. The electrochemical aptasensor enabled BPA to be detected in drinking water with a LOD as low as 0.284 pg ml^{-1} in less than 30 minutes.

Chen's group reported a signal-amplified electrochemical aptasensor for ultrasensitive and reliable detection of OTA [19] (Figure 9.14). The primer for rolling chain amplification (RCA) was designed to compose a two-part

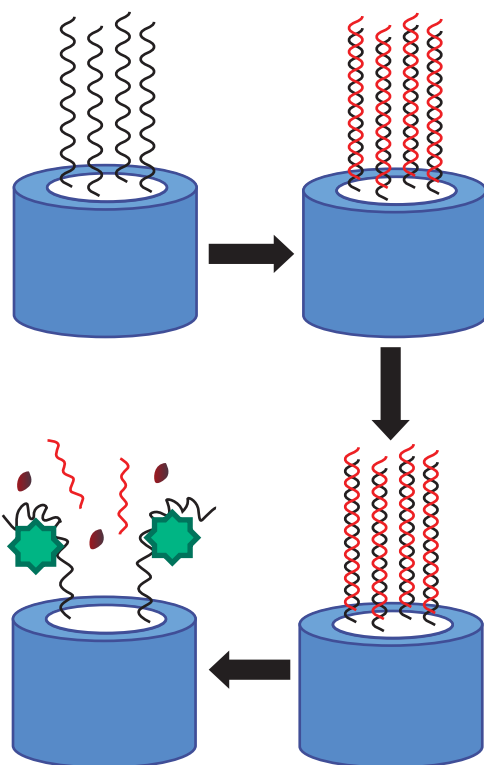


Figure 9.13 Schematic representation of the rapid and ultrasensitive electrochemical aptasensor for bisphenol A (BPA) determination. Source: Xue et al. 2013 [18]. Reprinted with permission of Springer Nature.

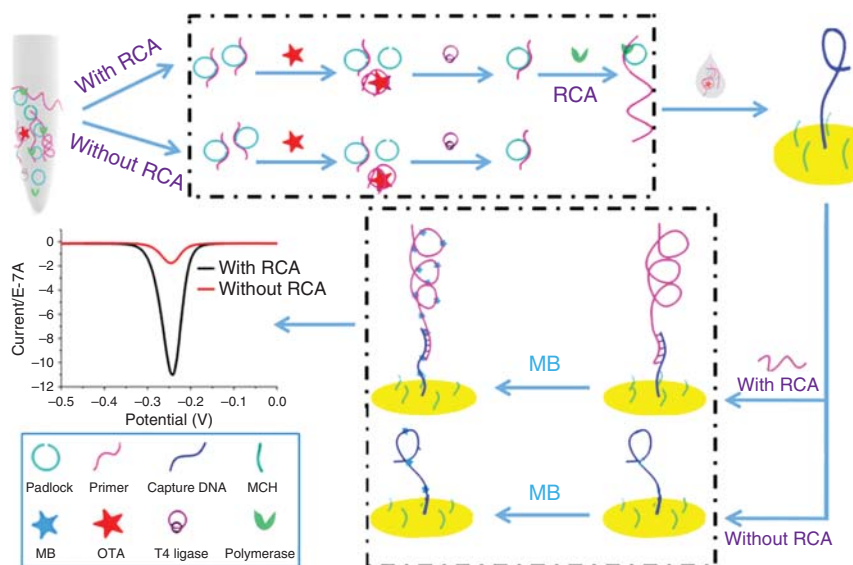


Figure 9.14 Schematic diagram of the RCA-based signal-amplification electrochemical aptasensor for detection of OTA. Source: Huang et al. 2013 [19]. Reprinted with permission of American Chemical Society.

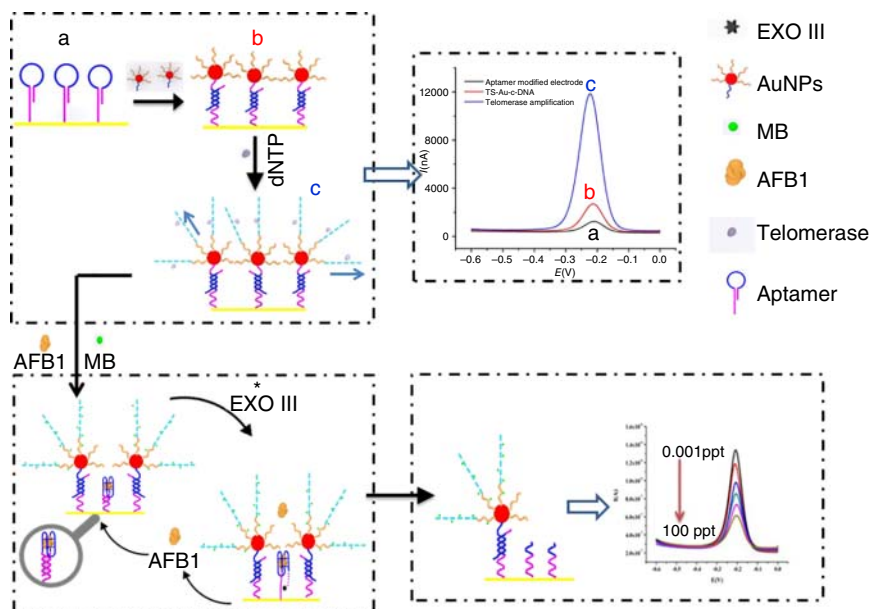


Figure 9.15 The schematic process of signal-amplified electrochemical aptasensor for AFB1 detection: (a) formation of stem-loop structure of the immobilized probe; (b) immobilization of TS-primer-AuNP-cDNA onto the sensing interface; and (c) telomerase-based first-round amplification. Source: Zheng et al. 2016 [20]. Reprinted with permission of Elsevier.

sequence, one part of the aptamer sequence directed against OTA while the other part was complementary to the capture probe on the electrode surface. In the presence of target OTA, the primer, originally hybridized with the RCA padlock, was replaced to combine with OTA. This induced the inhibition of RCA and decreased the OTA sensing signal obtained with the electrochemical aptasensor. Under the optimized conditions, ultrasensitive detection of OTA was achieved with a LOD of 0.065 ppt (pg ml^{-1}), which is much lower than previously reported. The same group has also reported an electrochemical aptasensor for trace detection of aflatoxin B1 (AFB1) using an aptamer as the recognition unit while adopting the telomerase and Exo III-based two-round signal amplification strategy as signal enhancement units [20] (Figure 9.15). The telomerase amplification was used to elongate the ssDNA probes on the surface of gold nanoparticles, by which the signal response range of the signal-off model electrochemical aptasensor could be correspondingly enlarged. Then, the Exo III amplification was used to hydrolyze the 3'-end of the double-stranded DNA (dsDNA) after the recognition of target AFB1, which caused the release of bounded AFB1 into the sensing system, where it participated in the next recognition-sensing cycle. With this two-round signal-amplified electrochemical aptasensor, target AFB1 was successfully measured at trace concentrations with an excellent detection limit of 0.6×10^4 ppt and satisfied specificity due to the excellent affinity of the aptamer against AFB1.

9.3.2.2 Cationic Redox Species

Some electrochemical aptasensors using cationic labels have been reported. Yu presented a “signal-off” aptasensor using $[\text{Ru}(\text{NH}_3)_6]^{3+}$ as a redox marker on the electrode surface for lysozyme analysis [21] (Figure 9.16). The anti-lysozyme DNA aptamer was immobilized on gold surfaces by means of self-assembly, for which the surface density of aptamers was determined by CV studies of redox cations (e.g. $[\text{Ru}(\text{NH}_3)_6]^{3+}$) bound to the surface via electrostatic interaction with the DNA phosphate backbone. Upon incubation of the electrode with a solution containing lysozyme, the CV response of surface-bound $[\text{Ru}(\text{NH}_3)_6]^{3+}$ changed substantially, and the relative decrease in the integrated charge of the reduction peak can be tabulated as a quantitative measure of the protein concentration. In this condition, lysozyme could be detected at physiological concentrations in the range from 0.5 to 50 mg ml^{-1} .

A “signal-off” aptasensor based on modified aptamer and DNA release has also been reported [22] (Figure 9.17). The half-duplex aptamer can be easily immobilized on a gold electrode and can change its conformation to bind its target, with the short complementary oligonucleoside acid being released. The chronocoulometric technique was first employed in this type of electrochemical aptasensor for detecting the changes in the surface charges via RuHex redox in solution. With such a “signal-off” aptasensor, a moderate sensitivity was obtained with a linear range extending from 0.1 to 1 mM AMP.

A novel electrochemical aptasensor for interferon gamma (IFN- γ) detection based on the exonuclease-catalyzed target recycling and the terminal deoxynucleotidyl transferase (TdT)-mediated cascade signal amplification has been reported [23] (Figure 9.18). To construct the aptasensor, a previously hybridized dsDNA (capture probe hybridization with a complementary IFN- γ

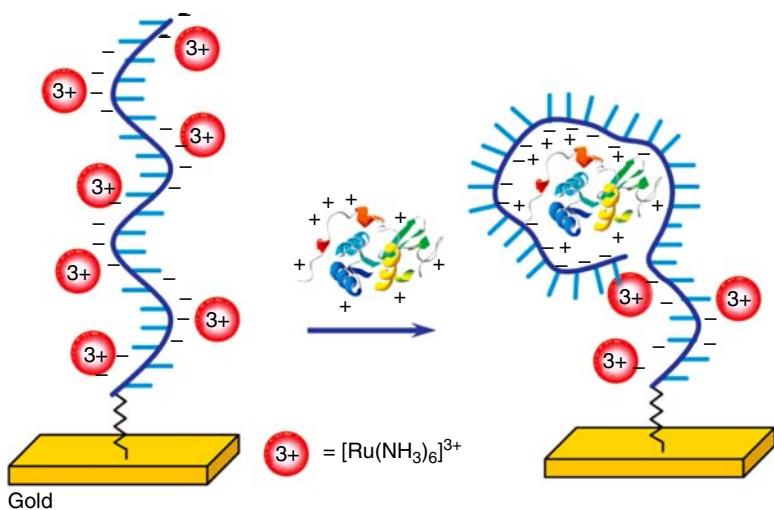


Figure 9.16 Schematic representation of the overall detection scheme of lysozyme with anti-lysozyme aptamers immobilized on gold electrodes via self-assembly. Source: Cheng et al. 2007 [21]. Reprinted with permission of American Chemical Society.

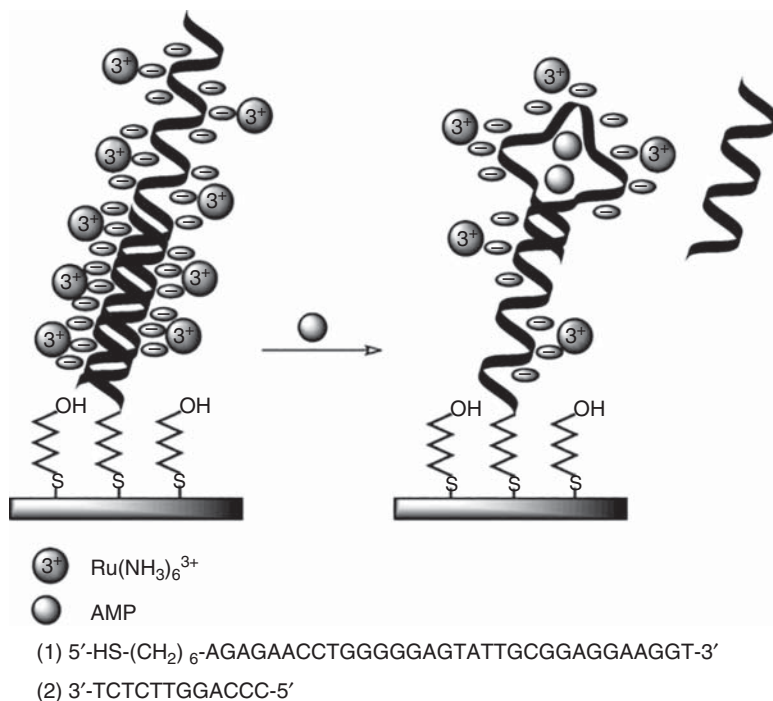


Figure 9.17 Schematic representation of the chronocoulometric aptamer sensor for AMP. Source: Shen et al. 2015 [22]. Reprinted with permission of Royal Society of Chemistry.

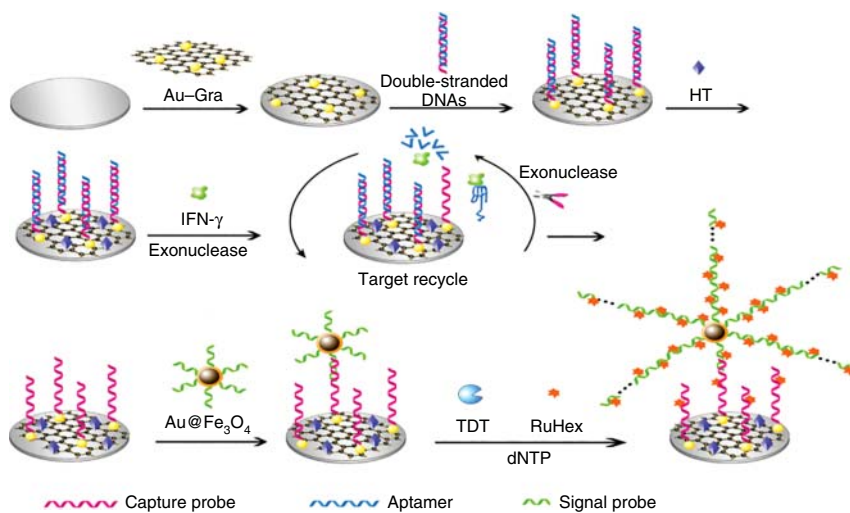


Figure 9.18 Schematic illustration of the stepwise aptasensor fabrication based on exonuclease-catalyzed target recycling and surface-initiated enzymatic polymerization for amplification. Source: Liu et al. 2015 [23]. Reprinted with permission of Royal Society of Chemistry.

binding aptamer) was immobilized on a gold nanoparticle–graphene (Au–Gra) nano hybrid–film–modified electrode. In the presence of IFN- γ , the formation of aptamer–IFN- γ complex led to the liberation of the aptamer from the dsDNA. Using exonuclease, the aptamer was selectively digested, and IFN- γ was released for the target recycling. As a result, substantial single-stranded capture probes were exposed to facilitate hybridization with signal-probe-labeled Au@Fe₃O₄. Then, the labeled signal probe sequences were catalyzed at the 3'-OH group by TdT to form a long ssDNA structure. As a result, the electron mediator hexaammineruthenium(III) chloride ([Ru(NH₃)₆]³⁺) electrostatically adsorbed onto DNA, producing a strong electrochemical signal which can be used to quantitatively measure the IFN- γ levels. This proposed aptasensor displayed a broad linearity with a low detection limit of 0.003 ng ml⁻¹.

A universal and sensitive “signal-on” electrochemical aptasensor platform based on a triple-helix molecular switch (THMS)-induced hybridization chain reaction (HCR) amplification has been reported [24] (Figure 9.19). This aptasensor platform system consisted of a THMS-based molecular recognition process in a homogeneous solution and HCR amplification on a gold electrode. In the absence of a target, the aptamer sequence was flanked by two arm segments (APT) and the triplex-forming oligonucleotide (TFO), forming a rigid THMS. It is in the electron transfer off state. However, upon the introduction of a target, the interaction between the target and the APT led to the dissociation of the THMS and thereby liberated the TFO, allowing the TFO to hybridize with the capture probe DNA and trigger the formation of dsDNA polymers through in

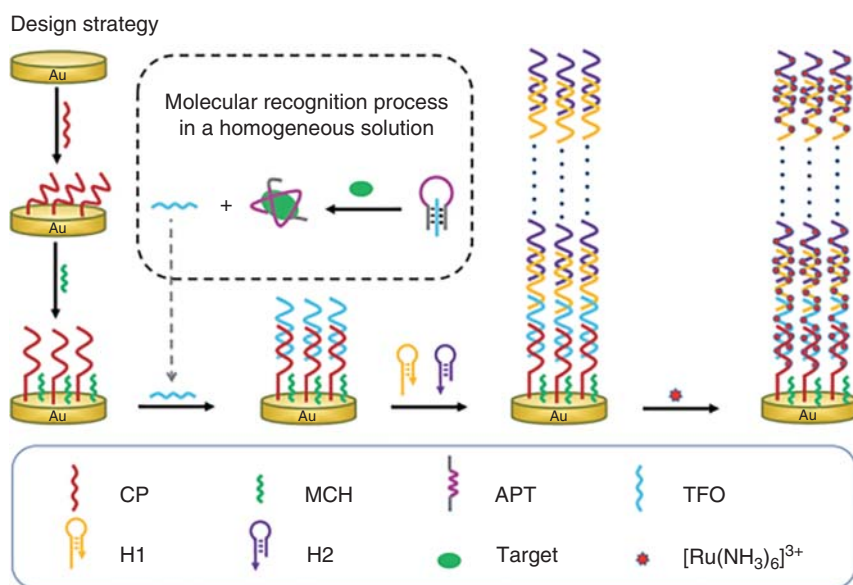


Figure 9.19 Schematic illustration of triple-helix molecular-switch-induced hybridization chain reaction amplification for developing a universal and sensitive electrochemical aptasensor. Source: Liu et al. 2016 [24]. Reprinted with permission of Royal Society of Chemistry.

situ HCR amplification. The dsDNA polymers caused the electrostatic attraction of numerous electroactive indicators $[\text{Ru}(\text{NH}_3)_6]^{3+}$, resulting in significantly amplified electrochemical signal output. Using this approach to detect adenosine and human α -thrombin (Tmb), it achieved lowest LOD values of 0.6 nM and 70.9 pM, respectively.

9.3.3 Label-Free Aptasensors

Although label-free devices eliminate the extra aptamer labeling procedure, they are still in need of other labeled molecules for electrochemical signal responses. Several representative sensing systems with certain complexities are presented in detail subsequently.

Label-free aptasensors that need the involvement of a redox probe such as $[\text{Fe}(\text{CN})_6]^{3-/4-}$ in solution are conventional methods. For instance, Wang and his colleagues proposed a label-free electrochemical (EC) aptasensor for ultrasensitive detection of ractopamine (RAC) [25] (Figure 9.20). A special immobilization media consisting of gold nanoparticles/poly dimethyl diallyl ammonium chloride–graphene composite (AuNPs/PDDA-GN) was utilized to improve the conductivity and performance of the biosensor followed by attachment of the RAC aptamer on AuNPs of the composite membrane via Au–S bond. Experimental results revealed that the peak currents obtained by DPV decreased linearly when the RAC concentrations were increased and the sensor responded approximately logarithmically over a wide dynamic range of RAC concentrations from 1.0×10^{-12} to $1.0 \times 10^8 \text{ mol l}^{-1}$. The linear correlation coefficient of the developed aptasensor was calculated to be 0.998, and the LOD

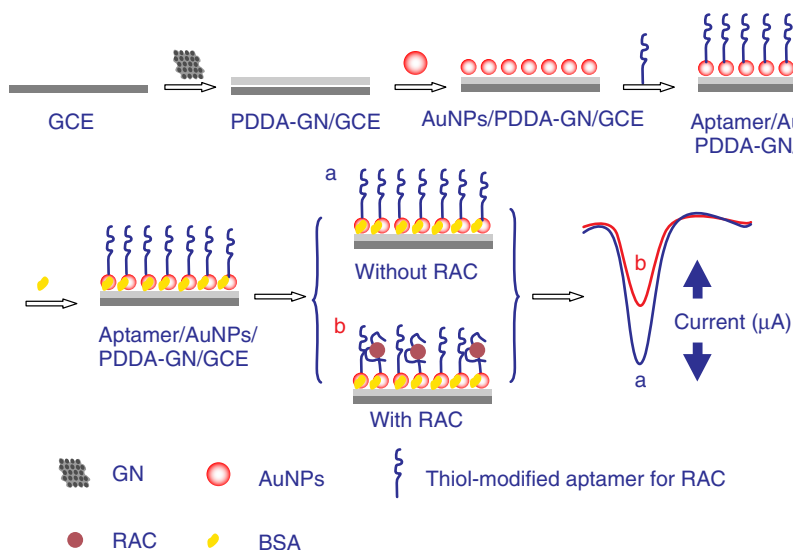


Figure 9.20 Schematic illustration of the label-free electrochemical (EC) aptasensor for ultrasensitive detection of ractopamine (RAC). Source: Yang et al. 2016 [25]. Reprinted with permission of Elsevier.

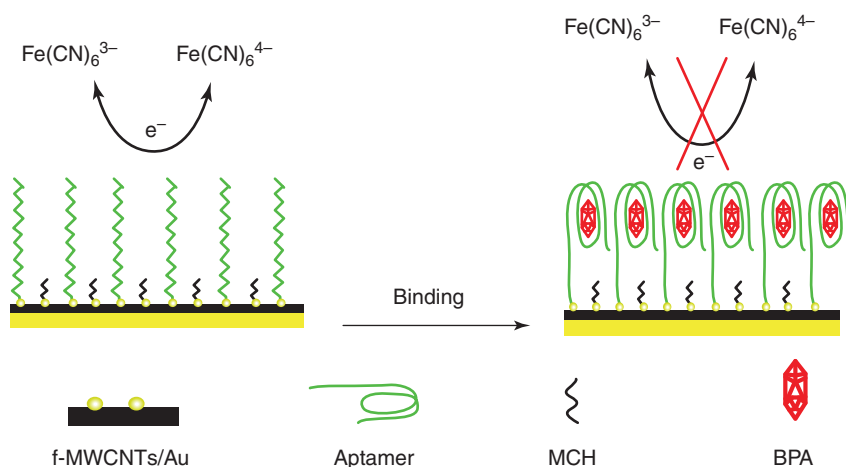


Figure 9.21 Schematic illustration of the label-free electrochemical aptasensor based on functionalized multiwall carbon nanotube/gold nanoparticle (f-MWCNT/AuNP) nanocomposite-film-modified gold electrode. Source: Deiminiat et al. 2016 [26]. Reprinted with permission of Elsevier.

was $5.0 \times 10^{-13} \text{ mol l}^{-1}$. Deiminiat et al. developed a label-free electrochemical aptasensor for BPA detection based on functionalized multiwalled carbon nanotube/gold nanoparticle (f-MWCNT/AuNP) nanocomposite-film-modified gold electrode [26] (Figure 9.21). The aptamer molecules that were directly immobilized on the surface of f-MWCNT/AuNP nanocomposite-modified gold electrode act as a gate of the long tunnels from which the redox probe $[\text{Fe}(\text{CN})_6]^{3-/4-}$ can reach the electrode surface. In the absence of BPA molecules, the aptamer molecules remained unfolded and the gate remained open, resulting in the passage of the electrons to the electrode surface. After exposure of the fabricated electrode to BPA molecules, the conformation of the aptamer was changed, which limited the chance for the electron transfer of the $[\text{Fe}(\text{CN})_6]^{3-/4-}$ redox probe on the electrode surface. In addition, the binding of BPA molecules with the aptamer exposed the negatively charged backbone of the aptamer to the redox probe, which led to a further increase in the repulsion toward the electron transfer. The SWV was applied as a sensitive analytical method for determination of BPA in solutions, and a good linear relationship was observed between the BPA concentration and the peak current within the range of 0.1–10 nM, with a detection limit of 0.05 nM.

Except for the label-free aptasensors, reagentless biosensing platforms have also been proposed in recent years. Suprun et al. described a label-free and reagentless aptasensor allowing direct detection of thrombin without using an additional electroactive label and based on gold nanoparticle redox properties [27] (Figure 9.22). The aptamer was immobilized on a screen-printed electrode modified with gold nanoparticles by avidin–biotin technology. The oxidation of the gold surface (resulting in gold oxide formation) upon polarization served as the basis for an analytical response. Cathodic peak area was found proportional to the thrombin quantity specifically adsorbed onto electrode surface.

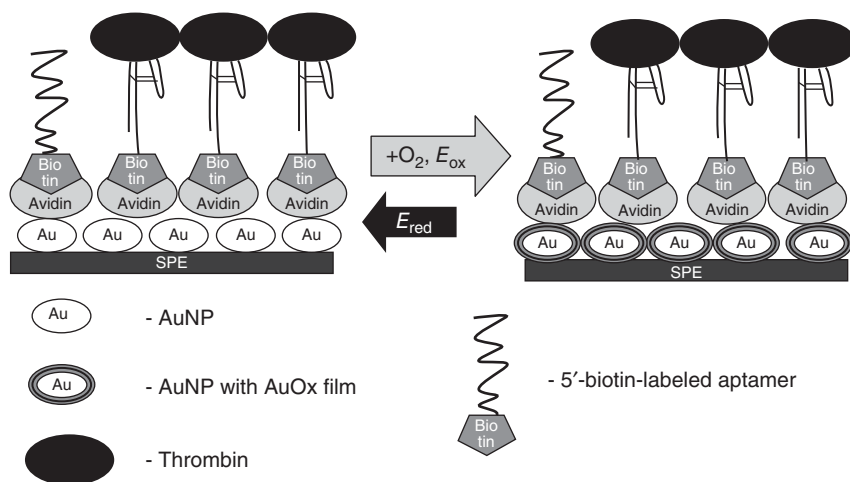


Figure 9.22 Schematic representation of the label-free and reagentless aptasensor allowing direct detection of thrombin without using additional electroactive label and based on gold NP redox properties. Source: Suprun et al. 2008 [27]. Reprinted with permission of Elsevier.

A sigmoid calibration curve, as is typical for immunoassay, was obtained, with a thrombin detection limit of 10^{-9} M. Linear range corresponds from 10^{-8} to 10^{-5} M thrombin concentration or 2×10^{-14} to 2×10^{-11} mol/electrode ($R = 0.996$).

9.4 Potentiometric Aptasensors

Majdidi et al. reported a reusable potentiometric screen-printed sensor and label-free aptasensor with pseudo-reference electrode for determination of tryptophan in the presence of tyrosine [28] (Figure 9.23). A gold screen-printed

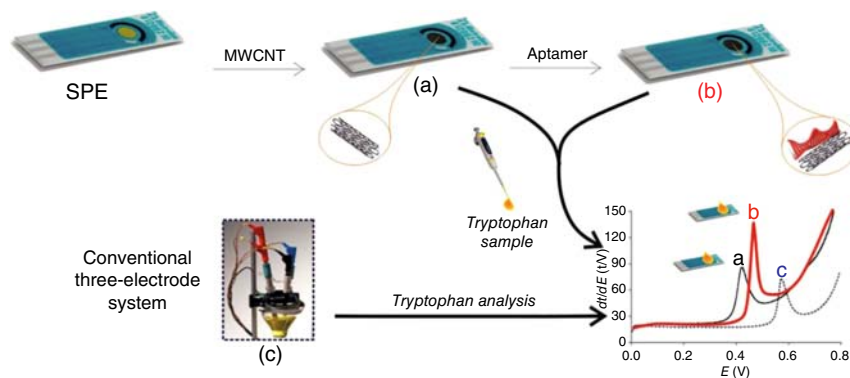


Figure 9.23 Schematic representation of the reusable potentiometric screen-printed sensor and label-free aptasensor with pseudo-reference electrode. Source: Majidi et al. 2016 [28]. Reprinted with permission of Elsevier.

electrode (SPE) was first modified with MWCNT-AuSPE and then armed with L-tryptophan aptamer molecules (Apt-MWCNT-AuSPE). The prepared sensors were characterized using constant current-potentiometric stripping analysis (CC-PSA) and EIS. The MWCNT-AuSPE and Apt-MWCNT-AuSPE were compared with respect to the linear detection range, LOD, accuracy, precision, and repeatability. MWCNT-AuSPE and Apt-MWCNT-AuSPE demonstrate a fast near-Nernstian response for PSA of Trp over the concentration ranging from 1.0×10^9 to 2.0×10^4 and 1.0×10^{11} to 1.0×10^4 mol $^{-1}$, with detection limits of 3.6×10^{10} and 4.9×10^{12} mol $^{-1}$, respectively.

9.5 Impedimetric Aptasensors

A highly sensitive and attractive antifouling impedimetric aptasensor for the determination of thrombin in undiluted serum sample has been reported by a coassembling thiol-modified anti-thrombin-binding aptamer, DTT, and mercaptohexanol on the surface of a gold electrode [29] (Figure 9.24). The performance of the aptasensor was characterized by atomic force microscopy, contact angle, and EIS. In the measurement of thrombin, the change in interfacial electron transfer resistance of the aptasensor was monitored using a redox couple of $[\text{Fe}(\text{CN})_6]^{3-/4-}$. The increase in the electron transfer resistance was linearly proportional to the concentration of thrombin in the range from 1.0 to 20 ng ml $^{-1}$, and a detection limit of 0.3 ng ml $^{-1}$ thrombin was achieved. The

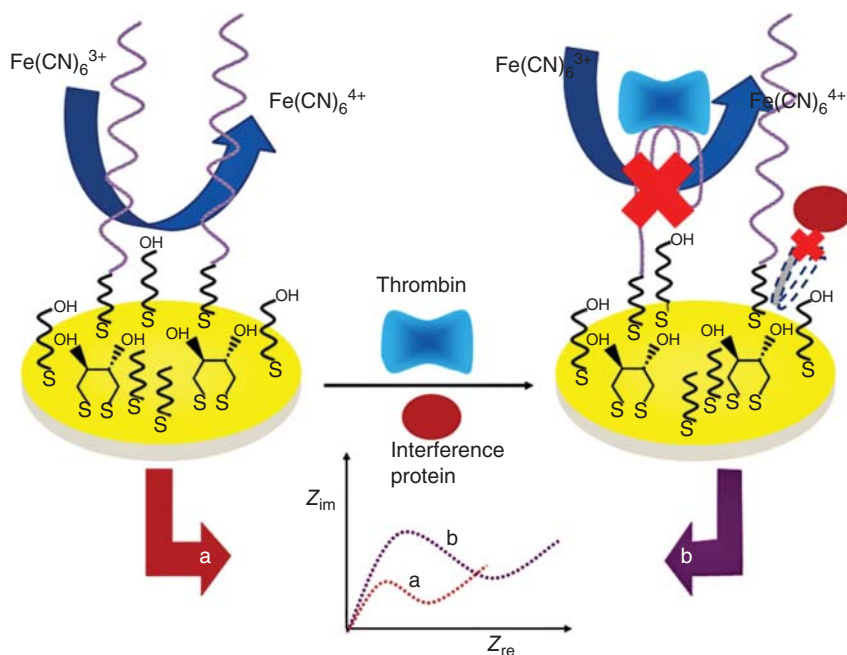


Figure 9.24 Schematic of the antifouling impedimetric aptasensor for the determination of thrombin. Source: Qi et al. 2013 [29]. Reprinted with permission of Elsevier.

fabricated aptasensor displayed attractive antifouling properties and allowed direct quantification of extrinsic thrombin down to 0.08 ng ml^{-1} in an undiluted serum sample.

Using bimetallic AgPt nanoparticle-decorated carbon nanotubes as highly conductive film surface, Shiravand and Azadbakht successfully developed an ultrasensitive impedimetric biosensor for the quantitative detection of diclofenac (DCF) based on a novel signal amplification strategy [30] (Figure 9.25). As a transducer material, acid-oxidized carbon nanotubes (CNT-COOH) and Pt and Ag nanoparticles (PtAgNPs) were used for promoting electron transfer between the electroactive probe and electrode. Aminated capture probe (ssDNA1) and DCF aptamer (ssDNA2) as a detection probe were attached at the surface of a modified electrode via the formation of covalent amide bond and hybridization, respectively. The change of interfacial charge transfer resistance (R_{ct}) recorded

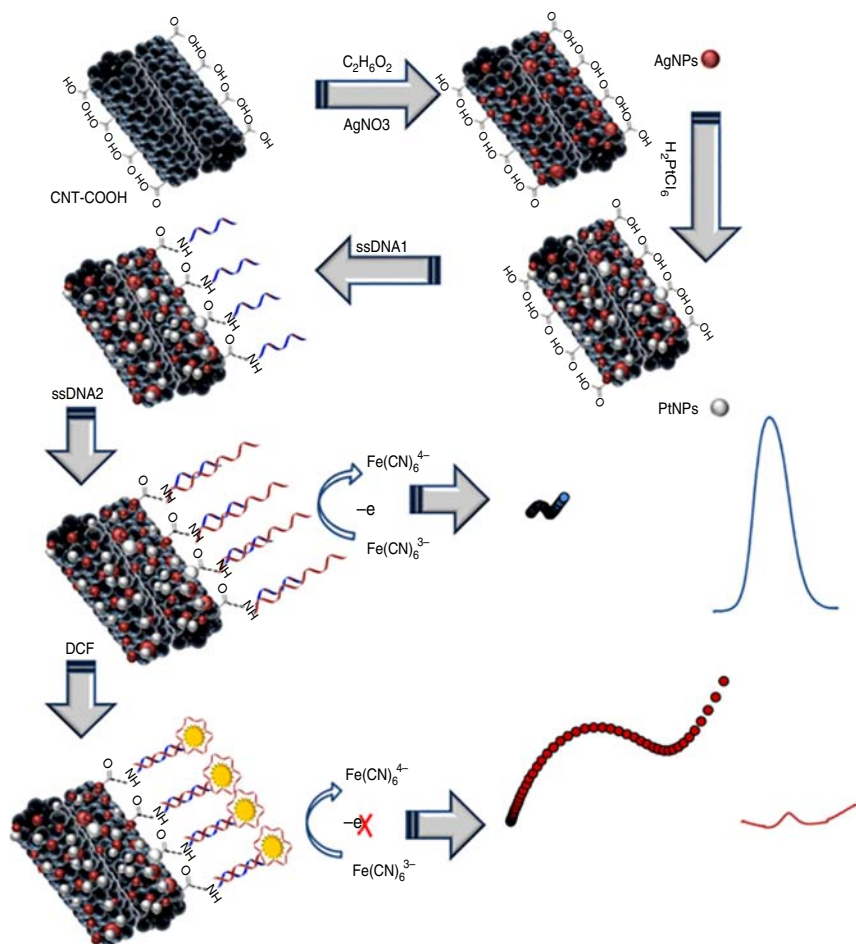


Figure 9.25 Schematic representation of the impedimetric biosensor based on bimetallic AgPt nanoparticle-decorated carbon nanotubes. Source: Shiravand and Azadbakht 2017 [30]. Reprinted with permission of Springer Nature.

by $[\text{Fe}(\text{CN})_6]^{3-/4-}$ as a redox probe was monitored for sensitive quantitative detection of DCF. Addition of DCF resulted in the increase in the value of R_{ct} due to suppression of the electron exchange between $[\text{Fe}(\text{CN})_6]^{3-/4-}$ in the surface layer. This aptasensor showed good detection range from 10 pM to 800 nM with an unprecedented detection limit of 2.8 pM.

9.6 Electrochemiluminescence Aptasensors

Zhao et al. firstly constructed a gold nanoparticle (AuNP)-driven ECL aptasensor for the sensitive detection of fumonisins B1 (FB1) [31] (Figure 9.26). Carboxyl-functionalized ionic $[(\text{ppy})_2\text{-Ir}(\text{dcbpy})]\text{PF}_6^-$ was synthesized and covered on the surface of AuNPs through mercaptoethylamine. The combination of AuNP- $[(\text{ppy})_2\text{-Ir}(\text{dcbpy})]\text{PF}_6^-$ complex increased the ECL intensity and accelerated the electron transfer, and further enhanced the ECL performance of aptasensors. The complementary strand immobilized on the surface of electrode first. In the absence of FB1, the aptamer-AuNP- $[(\text{ppy})_2\text{-Ir}(\text{dcbpy})]\text{PF}_6^-$ complex would bind with the strand on the surface. In the presence of FB1, the complex was bound to target to decrease the intensity, achieving a LOD as 0.27 ng ml^{-1} .

9.7 Conclusion

In summary, the emergence of aptamers has appeared as promising molecular recognition tools for electrochemical biosensor fabrication. Compared with

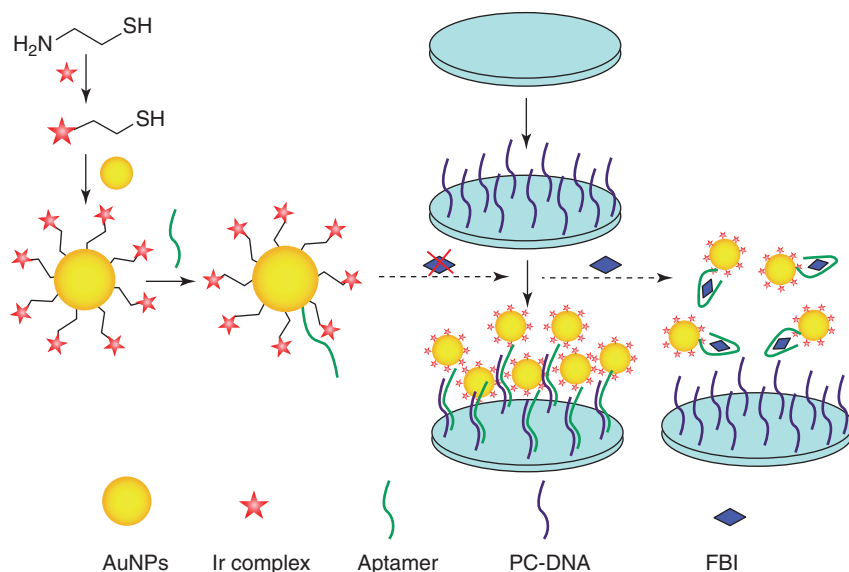


Figure 9.26 Schematic illustration of AuNP-driven ECL aptasensors for FB1 detection. Source: Zhao et al. 2014 [31]. Reprinted with permission of Royal Society of Chemistry.

other bio-recognition events that are based on enzymes or antibodies, the aptamers could be easily synthesized, functionalized, and modified. Moreover, development of biosensors with the characteristics of miniaturization, integration, and automation for more convenient applications are easier to realize using aptamers as the recognition probes. However, the exploitation and utilization of aptamers in electrochemical biosensing are still at an early stage, where several issues should be addressed to meet public requirements. For example, the biostability of aptamers against the serum degradation effect is relatively poor. Further improvement of the biostability by modifying the strand with protecting moieties is expected to benefit the on-site analysis and detection of target analytes in complex samples. It should be also mentioned that currently only approximately 250 kinds of aptamer toward different targets are available, which is much less than the number of antibodies. We are therefore encouraged to screen new aptamers for widespread usage. Actually, the relatively weak commercial areas of aptamer-based kits in contrast to the continuous growth of immune test kits are also attributed to the limited kinds of aptamer at present in the market. Overall, given the rapid progress of aptamers in the field of electrochemical analysis, the development of easy, simple, and rapid electrochemical aptasensors that advance sensitivity, specificity, reliability, and practicability provide a promising platform for researchers to continue pushing this field further.

References

- 1 Saberian-Borujeni, M., Johari-Ahar, M., Hamzeiy, H. et al. (2014). Nanoscaled aptasensors for multi-analyte sensing. *Bioimpacts* 4 (4): 205–215.
- 2 Ellington, A.D. and Szostak, J.W. (1990). In vitro selection of RNA molecules that bind specific ligands. *Nature* 346 (6287): 818–822.
- 3 Robertson, D.L. and Joyce, G.F. (1990). Selection in vitro of an RNA enzyme that specifically cleaves single-stranded DNA. *Nature* 344 (6265): 467–468.
- 4 Tuerk, C., Eddy, S., Parma, D. et al. (1990). Autogenous translational operator recognized by bacteriophage T4 DNA polymerase. *J. Mol. Biol.* 213 (4): 749–761.
- 5 Hermann, T. and Patel, D.J. (2000). Adaptive recognition by nucleic acid aptamers. *Science* 287 (5454): 820.
- 6 Zhao, J., Zhang, Y., Li, H. et al. (2011). Ultrasensitive electrochemical aptasensor for thrombin based on the amplification of aptamer–AuNPs–HRP conjugates. *Biosens. Bioelectron.* 6 (5): 2297–2303.
- 7 Yi, H., Xu, W., Yuan, Y. et al. (2014). A pseudo triple-enzyme cascade amplified aptasensor for thrombin detection based on hemin/G-quadruplex as signal label. *Biosens. Bioelectron.* 54 (12): 415–420.
- 8 Shen, G., Zhang, S., Shen, G. et al. (2016). Development of an electrochemical aptasensor for thrombin based on the aptamer/Pd–AuNPs/HRP conjugates. *Anal. Methods* 8 (10): 2150–2155.

- 9 Wu, J., Chu, H., Mei, Z. et al. (2012). Ultrasensitive one-step rapid detection of ochratoxin A by the folding-based electrochemical aptasensor. *Anal. Chim. Acta* 753 (21): 27–31.
- 10 Jia, J., Feng, J., Chen, H.G. et al. (2015). A simple electrochemical method for the detection of ATP using target-induced conformational change of dual-hairpin DNA structure. *Sens. Actuators, B* 222: 1090–1095.
- 11 Yoshizumi, J., Kumamoto, S., Nakamura, M. et al. (2008). Target-induced strand release (TISR) from aptamer-DNA duplex: a general strategy for electronic detection of biomolecules ranging from a small molecule to a large protein. *Analyst* 133 (3): 323.
- 12 Radi, A.E. and O’Sullivan, C.K. (2006). Aptamer conformational switch as sensitive electrochemical biosensor for potassium ion recognition. *Chem. Commun.* 32 (32): 3432–3434.
- 13 Baker, B.R., Lai, R.Y., Wood, M.S. et al. (2006). An electronic, aptamer-based small-molecule sensor for the rapid, label-free detection of cocaine in adulterated samples and biological fluids. *J. Am. Chem. Soc.* 128 (10): 3138–3139.
- 14 Wu, L., Zhang, X., Liu, W. et al. (2013). Sensitive electrochemical aptasensor by coupling “signal-on” and “signal-off” strategies. *Anal. Chem.* 85 (17): 8397–8402.
- 15 Cao, X., Xia, J., Liu, H. et al. (2016). A new dual-signalling electrochemical aptasensor with the integration of “signal on/off” and “labeling/label-free” strategies. *Sens. Actuators, B* 239: 166–171.
- 16 Hianik, T., Ostatná, V., Zajacová, Z. et al. (2005). Detection of aptamer–protein interactions using QCM and electrochemical indicator methods. *Bioorg. Med. Chem. Lett.* 15 (2): 291.
- 17 Bang, G.S., Cho, S., and Kim, B.G. (2005). A novel electrochemical detection method for aptamer biosensors. *Biosens. Bioelectron.* 21 (6): 863.
- 18 Xue, F., Wu, J., Chu, H. et al. (2013). Electrochemical aptasensor for the determination of bisphenol A in drinking water. *Microchim. Acta* 180 (1): 109–115.
- 19 Huang, L., Wu, J., Zheng, L. et al. (2013). Rolling chain amplification based signal-enhanced electrochemical aptasensor for ultrasensitive detection of ochratoxin A. *Anal. Chem.* 85 (22): 10842.
- 20 Zheng, W., Teng, J., Cheng, L. et al. (2016). Hetero-enzyme-based two-round signal amplification strategy for trace detection of aflatoxin B1 using an electrochemical aptasensor. *Biosens. Bioelectron.* 80: 574.
- 21 Cheng, A.K., Ge, B., and Yu, H.Z. (2007). Aptamer-based biosensors for label-free voltammetric detection of lysozyme. *Anal. Chem.* 79 (14): 5158–5164.
- 22 Shen, L., Chen, Z., Li, Y. et al. (2015). A chronocoulometric aptamer sensor for adenosine monophosphate. *Chem. Commun.* 21 (21): 2169.
- 23 Liu, C., Xiang, G., Jiang, D. et al. (2015). An electrochemical aptasensor for detection of IFN- γ using graphene and a dual signal amplification strategy based on the exonuclease-mediated surface-initiated enzymatic polymerization. *Analyst* 140 (22): 7784–7791.

- 24 Liu, Q., Liu, J., He, D. et al. (2016). Triple-helix molecular switch-induced hybridization chain reaction amplification for developing a universal and sensitive electrochemical aptasensor. *RSC Adv.* 6 (93): 90310–90317.
- 25 Yang, F., Wang, P., Wang, R. et al. (2016). Label free electrochemical aptasensor for ultrasensitive detection of ractopamine. *Biosens. Bioelectron.* 77: 347–352.
- 26 Deiminiat, B., Rounaghi, G.H., Arbab-Zavar, M.H. et al. (2016). A novel electrochemical aptasensor based on f-MWCNTs/AuNPs nanocomposite for label-free detection of bisphenol A. *Sens. Actuators, B* 242: 158–166.
- 27 Suprun, E., Shumyantseva, V., Bulko, T. et al. (2008). Au-nanoparticles as an electrochemical sensing platform for aptamer-thrombin interaction. *Biosens. Bioelectron.* 24 (4): 831–836.
- 28 Majidi, M.R., Omid, Y., Karami, P. et al. (2016). Reusable potentiometric screen-printed sensor and label-free aptasensor with pseudo-reference electrode for determination of tryptophan in the presence of tyrosine. *Talanta* 150: 425.
- 29 Qi, H., Shangguan, L., Li, C. et al. (2013). Sensitive and antifouling impedimetric aptasensor for the determination of thrombin in undiluted serum sample. *Biosens. Bioelectron.* 39 (1): 324.
- 30 Shiravand, T. and Azadbakht, A. (2017). Impedimetric biosensor based on bimetallic AgPt nanoparticle-decorated carbon nanotubes as highly conductive film surface. *J. Solid State Electrochem.* 21: 1–13.
- 31 Zhao, Y., Luo, Y., Li, T. et al. (2014). Au NPs driven electrochemiluminescence aptasensors for sensitive detection of fumonisin B1. *RSC Adv.* 4 (101): 57709–57714.

10

Development of Aptamer-Based Lateral Flow Assay Methods

Miriam Jauset-Rubio¹, Mohammad S. El-Shahawi², Abdulaziz S. Bashammakh², Abdulrahman O. Alyoubi², and Ciara K. O'Sullivan^{1,3}

¹Universitat Rovira I Virgili, INTERFIBIO Consolidated Research Group, Department of Chemical Engineering, Avinguda Països Catalans, 26, 43007 Tarragona, Spain

²King Abdulaziz University, Faculty of Science, Department of Chemistry, P.O. Box 80203, Jeddah 21589, Kingdom of Saudi Arabia

³Institució Catalana de Recerca i Estudis Avançats (ICREA), Passeig Lluís Companys, 23, 08010 Barcelona, Spain

10.1 Introduction

Aptamers are nucleic acids that can bind to a wide range of diverse targets, ranging from small molecules to larger proteins and cells [1–7]. Aptamers offer a variety of advantages over antibodies, including the use of an *in vitro* generation process, thus avoiding the need for an animal host, and also allowing the selection of aptamers against toxic and non-immunogenic molecules. Aptamers can thus be selected against specific regions of targets, which is sometimes difficult for antibodies, since the animal immune system is inherently generated toward specific epitopes on target molecules. In addition, aptamers, much more than antibodies over long storage periods and under extreme storage conditions, are easily regenerated; and once selected aptamers can be produced at a fraction of the cost of antibodies. Aptamers can also be easily modified and or immobilized and synthesized with high reproducibility and purity; besides, they are chemically stable. Furthermore, aptamers, taking advantage of their inherent nucleic acid nature, are far more flexible than antibodies and can be used in displacement formats, in molecular aptamer beacons, and can also exploit a combination of aptamer–target interaction and nucleic acid amplification to achieve ultrasensitive detection limits. Aptamers, in general, possess excellent selectivity and affinity toward their targets, binding with dissociation constants (K_d) ranging from picomolar to nanomolar levels [8, 9], and can discriminate closely related chemical structures by factors as high as 4 orders of magnitude, as demonstrated with the aptamers for theophylline and L-arginine [10, 11].

These attractive features have positioned aptamers as ideal recognition elements for analytical tools, such as biosensors [12–19], colorimetric assays [20, 21], surface plasmon resonance assays [22–24], and their use in combination with amplification [25–27]. However, all these methods require skilled personnel and laboratory-based instrumentation, thus limiting their application at point-of-need settings.

Lateral flow assays (LFAs) are paper-based platforms that provide rapid and reliable results, with the only required end-user intervention being sample addition. Due to their simplicity, LFAs have been widely exploited in different fields including biomedicine, quality control, product safety in food production, and environmental health and safety [28]; and they can be applied to a variety of biological samples including urine [29], saliva [30], sweat [31], serum [32], plasma, and blood [33].

The technical basis for the LFA format was derived from the latex agglutination assay in 1956 [34]; and in 1984, Unipath launched the first urine-based pregnancy test [35]. Hundreds of LFAs have been reported and commercialized to date. The concept of LFA is based on affinity interactions, where a visible line is observed on a membrane when a liquid sample containing a particular analyte of interest is applied. It is made up of different components including a sample pad, conjugate pad, nitrocellulose membrane, and a wicking or an absorbent pad, all of which are assembled on a plastic backing pad that provides mechanical support. The sample pad transports the sample to other components of the lateral flow strip. The conjugate pad contains labeled biomolecules, which are released upon contact with the liquid sample as it is wicked along the membrane by capillary action. Test and control lines are spotted on the membrane, and the absorbent pad provides the capillary-based driving force, maintaining the flow rate of the sample over the membrane and preventing backflow [36].

To date, sandwich and competitive assays have been reported using aptamers as the bioaffinity agent. A sandwich assay is used for larger molecules, while the competitive format is preferred for low-molecular-weight targets, targets with a single specific aptatope, or when only one single aptamer is available. In the sandwich format, a labeled reporter molecule reacts with the analyte of interest; and this complex is then captured on the test line by an immobilized capture molecule, which can be either an antibody or an aptamer. The excess of reporter molecules are then captured at the control line. In the competitive format, the target analyte competes with the same target immobilized on the test line, for binding to the labeled reporter molecule [37], with reporter labels such as gold nanoparticles, latex spheres, and quantum dots (QDs) used.

In this chapter, we explain the concept of LFAs and provide an overview of the lateral flow aptamer assays reported to date. While aptamer-based LFAs share the advantages of lateral flow immunoassays (LFIA), they offer several advantages including considerably lower cost, enhanced stability over time, and, at extreme storage conditions, facile preparations of aptamer–label bioconjugates, as well as their use in formats not achievable using antibodies.

10.2 Development of Aptamer-Based Lateral Flow Assay – Strategy

10.2.1 Analogies and Differences Compared to Lateral flow Immunoassays (LFIAs)

Aptamer-based LFAs and LFIAs share the same general architecture. Both consist of several areas constituted by individual segments of different materials, which overlap each other, facilitating transversal of sample across the strip. When a test is carried out, a sample is added to the sample pad and then migrates to the conjugate pad, which contains the absorbed labeled reporter molecule, a bioconjugate of aptamer/antibody/nucleic acid with gold nanoparticles/latex spheres/fluorophores/QDs, depending on the assay format. The sample interacts with these conjugates and both migrate to the nitrocellulose membrane, where specific biocomponents (proteins, antibodies, antigens, or aptamers) are immobilized, with the function of capturing the target and the bioconjugate on the control and test lines, with everything else flowing to the wicking/absorbent pad. Results are interpreted via the presence or absence of lines in the capturing areas and can be read by the naked eye, a strip reader, or a smartphone [35, 38] (Figure 10.1).

Compared to antibodies, aptamers offer several advantages [37, 39–41]. For instance, LFIAs require controlled temperature for storage, incurring high costs as well as considerable limitation for application in the developing world. In contrast, aptamers are stable over a wide temperature range, allowing their use in low-resource settings. The preferred LFA is the sandwich format, and different strategies for selecting aptamers against different aptatopes have been reported [42–53]. Alternatively, an aptamer can be divided into two pieces, which can then bind to the same target in a sandwich format avoiding the need for a pair of aptamers, as well as being applicable to the detection of small molecules where only one aptatope is available, e.g. adenosine triphosphate (ATP) highlighting the unique properties of aptamers not achievable with antibodies [54]. Furthermore, aptamers are much smaller than antibodies, permitting higher immobilization levels on reporter labels and the test/control lines. Aptamers are easily modified and orientation can be controlled. Finally, aptamers can be selected against toxic,

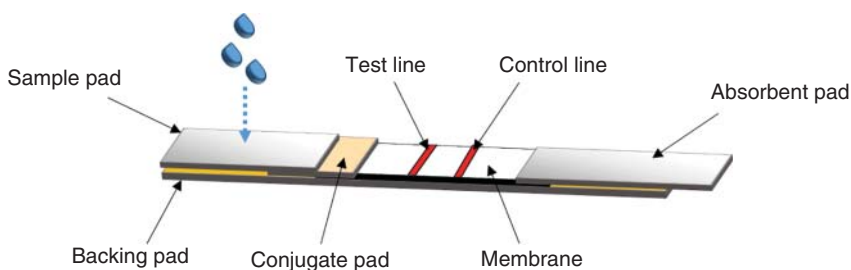


Figure 10.1 Schematic representation of the architecture of lateral flow assays.

as well as small or non-immunogenic molecules, including metal ions, expanding the potential applications of lateral flow aptamer assays [55].

In addition to these advantages of aptamers over antibodies, due to the inherent nucleic acid nature of aptamers, they can also be exploited in diverse displacement assay formats, where aptamers partially hybridized to complementary DNA can be displaced by their aptameric cognate target, or, alternatively, aptamer bound to its cognate target can be displaced by a fully complementary sequence [56].

10.2.2 Fundamental Assay Considerations

Summarizing the conclusions of O'Farrell [35, 57, 58], Koczula and Gallota [28], Sajid et al. [59], Ahmed et al. [60], Quesada-Gonzalez [61], and Bahadir and Sezginürk [62], regarding the factors critical for successful lateral flow development, herein we describe the essential components that must be taken into account, since some problems can be caused by material incompatibility, imperfections in the connection of overlapping elements, or incorrect material characteristics.

The membrane: It is the most critical element in LFA, and nitrocellulose is the material most commonly used. Other materials used include nylon or polyvinylidene fluoride (PVDF) membranes, but they have had limited success due to cost, limited utility, combined with new chemistry and processing requirements [63]. Nitrocellulose offers some advantages such as low cost, true capillary flow characteristics, high protein-binding capacity, relative ease of handling, and a wide variety of available products with varying wicking rates and surfactants. However, these kinds of membranes suffer from some drawbacks, such as imperfect batch-to-batch reproducibility, stability issues, and variable characteristics due to environmental conditions (i.e. relative humidity). To address these drawbacks, a careful control of dispensing, dipping, and drying processes as well as the chemical and biological treatment of the membrane is critical. The dispensing method used for the test and control lines must be as quantitative as possible and should not vary with material hydration or absorption characteristics. Two types are available: contact and noncontact dispensing methods; with the latter, the best solution is to quantitatively dispense proteins onto nitrocellulose. Blocking of nitrocellulose membranes is essential to prevent the binding of proteins and labeled conjugates to the membrane at areas other than the test and control lines. Blocking also serves other functions, including maintenance of hydration of membranes, modification of wicking rates, and stabilization of test and control line proteins. Drying is subsequently performed by a combination of blotting to remove surface fluids and air at elevated temperatures [58].

Flow rate: Another important issue is the flow rate. Nitrocellulose is a hydrophobic material, but is made hydrophilic by the addition of moisturizing agents during the membrane production. These agents are surfactants and they differ from manufacturer to manufacturer; and multiple membrane types should be evaluated during development. The velocity of the sample movement across

the membrane directly affects assay sensitivity, where a rapid flow rate can result in insufficient time for the reaction of the sample with the affinity molecules, while a low flow rate resulting in extended incubation times can produce false-positive results [62].

Conjugate pad: The materials typically used in the conjugate pad are glass fibers, polyesters, or rayons. They should be hydrophilic to allow rapid release rates of the bioconjugates, as this can affect the sensitivity.

Sample pad: The materials used for the sample pad depend on the requirements of the application. There are applications where sample pretreatment is required to filter out particles or red blood cells, or change the pH of the sample, or bind with sample components that can interfere with the assay or to disrupt matrix components. The most commonly used materials are cellulose, glass fiber, rayon, and other filtration media. The sample pad should be treated with assay buffer containing surfactants, blocking agents, additives, and other reagents to increase the sensitivity of the assay, and it is then dried before use.

Absorbent pad: The material is usually high-density cellulose, and it is chosen on the basis of its absorptive capacity. The main role of this element is to draw and wick all of the fluid across the membrane and to hold it for the duration of the assay, avoiding fluid backflow.

Backing pad: The materials are usually polystyrene or other plastic materials coated with a medium-to-high tack adhesive. The most important issue is to choose adhesives that are compatible with proteins during storage of the LFAs.

Labels for detection: Various types of reporter labels can be used for the visualization of a signal. The most commonly used materials are latex beads and colloidal gold nanoparticles. Other reporter labels include enzyme conjugates, colloidal metals, fluorescent particles, QDs, and magnetic particles. The size and shape of the particles can lead to differences in sensitivity and specificity [61].

Running buffer: The buffer used during the test should also be optimized, so that it does not affect the characteristics of the membrane (i.e. the flow rate, non-specific binding of the target in other regions that are not the capture areas) and should maintain the structural stability and reactivity of the target. Some of the parameters that should be optimized are the pH, the solubility of the target, salts, ions, and the molarity of the buffer.

10.2.3 Fundamental Analytical Considerations

LFAs are designed to be qualitative devices for a rapid screening of the absence or presence of a specific analyte. The main drawback of these assays is that the threshold is interpreted by the naked eye, which can be highly subjective. Commercially available reader systems have been developed to address this issue, the majority being automated, which reduces the chance of human error. Numerous companies commercialize these readers for use in lateral flow applications and these can be grouped into fluorescence, chemiluminescence, magnetic particles, and colorimetric readers [35].

In many cases, charge-coupled device (CCD)-based image systems and scanning systems are utilized in these readers:

- *CCD imaging systems*: Based on the production of a full picture record of the readout area containing the test and control lines. One advantage is that there are no moving parts, but the illumination and lens effects must be taken into account because a band may appear distorted if the illumination is not uniform. In addition, the number of data points that need to be recorded in CCD-based imaging systems is very high and this can limit the internal memory. A computer is always required and the first versions were not very suitable for point-of-need applications as they were large, heavy, and expensive [35]. Recently, pocket PCs and more portable systems have been launched, such as the AX-2X Visual and Fluorescence Lateral Flow Instrument from Axxin Inc. (<http://www.axxin.com/Immunoassay-AX-2X.php>).
- *Scanning systems*: The main advantage with this technique is that the scans are performed very rapidly, including data evaluation. The memory size can be smaller and more scans can be stored directly in the device. No computer is required, which is reflected in the lower price. The main drawback is that no image of the test strip is available and the data looks different from the images that the consumer is used to seeing from visual readout [35].

The strip reader application is practical in the developed world, as it is robust, of relatively low cost, and having supporting infrastructure for calibration, maintenance, and operation. However, for the developing world, these readers are too complex and expensive, requiring infrastructure and power supply.

An alternative approach is the use of a smartphone camera with the capacity to transform analog results into a digital format. Although still in its infancy, the past years have seen a considerable increase in the number of publications detailing smartphone-based analysis [64–71]. This kind of reader takes advantage of its high portability, low cost, and ease of use, making them more suitable for both the developed and the developing world.

10.3 Lateral Flow Aptamer Assays

10.3.1 Sandwich Assay

The sandwich assay format is the most commonly used for testing large analytes, which have multiple aptatope binding sites. In a typical format, a reporter-labeled coated antibody or aptamer bioconjugate is absorbed at the conjugate pad. A primary antibody or aptamer against the target analyte is immobilized on the test line and a secondary antibody or probe against the labeled bioconjugate is immobilized on the control line. When the analyte is applied to the sample pad, it migrates to the other parts of the lateral flow arriving at the conjugate pad, where the target analyte binds to the labeled bioconjugate. This complex passes across the membrane via capillary movement and is wicked to the test line, where it is captured. The excess of labeled bioconjugate is captured at the control line. The appearance of both lines, test line and control line, is interpreted as a positive

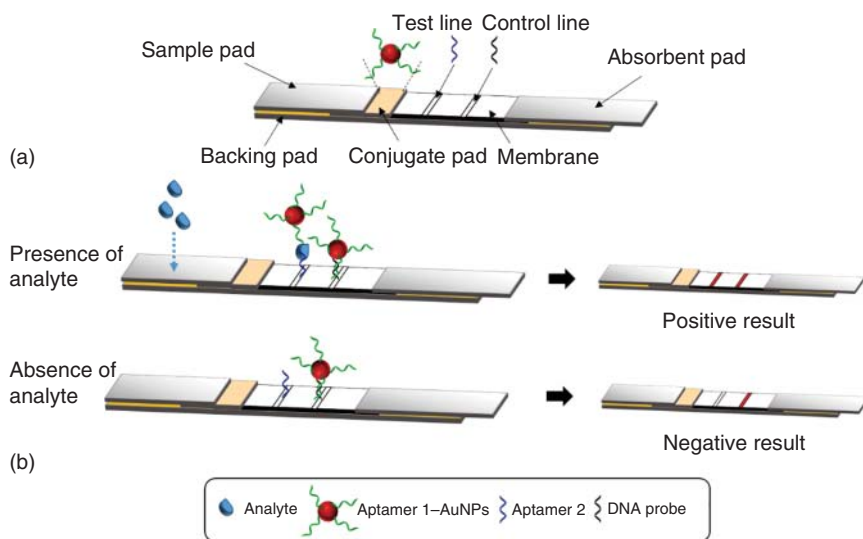


Figure 10.2 Schematic representation of a sandwich assay based on a pair of aptamers. (a) Configuration of lateral flow strip; (b) the principle of visual detection in the presence and absence of analyte.

result, with only color in the control line translating to a negative result, while confirming that the assay is working properly. The use of dual aptamers has also been reported for several analytes, following the architecture of the LFA outlined in Figure 10.2.

The first report of dual aptamers used in lateral flow was in 2009 [72], for the detection of thrombin. Both the test and the control lines were functionalized with streptavidin, while gold nanoparticles linked to a thiolated 15-mer thrombin aptamer with a 20-T linker were used as the labeled reporter. Biotinylated 29-mer aptamer was immobilized on the test line, with a biotinylated poly A oligoprobe immobilized on the control line. In the presence of thrombin, an aptacomplex between the target and aptamer-AuNPs was captured by the aptamer immobilized on the test line and a characteristic red band was observed. The excess bioconjugate was captured at the control line via the interaction between the poly A probe and the poly T linker of the aptamer/AuNP bioconjugate, resulting in a second red band. A limit of detection (LOD) of 2.5 nM was achieved using a portable strip reader in just 10 minutes. The specificity of the assay was evaluated using IgG, IgM, human serum albumin (HSA), and casein; and no cross-reactivity was observed. The LFA was tested in spiked human plasma samples, achieving a LOD of 0.6 pmol.

With the principle of the assay being the same as that described earlier, Liu et al. [73] also reported an LFA using a pair of aptamers selected against Ramos cells. In this assay, the control line was an oligo complementary to a part of the aptamer bioconjugate. Detection limits of 4000 and 800 Ramos cells were achieved by visual detection and a portable strip reader, respectively, with a 15-minute assay time, and the assay was tested in real blood samples.

Another example of a sandwich assay using dual aptamers is that reported for the detection of Vaspin [74], with the only difference being the control line, where an oligoprobe sequence fully complementary to the aptamer was immobilized. A LOD of 5 nM was achieved by naked eye and of 0.137 and 0.105 nM in buffer and spiked human serum, respectively, using Image J software analysis.

Other molecules tested in sandwich assay lateral flows include the chikungunya virus and the tick-borne encephalitis virus (TBEV) [75], with the assay architectures using aptamer bound to gold nanoparticles via biotin–streptavidin interactions. ChE 20R was used as the capture aptamer and ChE 17R as the reporter aptamer for chikungunya detection, while 8R was used as capture aptamer and 2F as the reporter aptamer for TBEV.

LFAs have also been reported using a combination of antibodies and aptamers that bind to different sites on the target, including the detection of salivary α -amylase (sAA), where AMYm1 aptamer was modified with biotin and linked to streptavidin–AuNPs. Anti-sAA antibody was immobilized on the test line and sAA protein was immobilized on the control line. The LFA was verified using 0.1% (v/v) human saliva [76] (Figure 10.3).

Finally, the detection of small molecules using split aptamer fragments in a sandwich-type format has been reported [54], consisting of two DNA probes that only assemble in the presence of the target, ATP. One part of the split aptamer was thiolated and chemisorbed onto AuNPs, while the other part was labeled with biotin and immobilized at the test line by streptavidin–biotin interactions. At the control line, a DNA probe complementary to the split aptamer–AuNPs was immobilized (Figure 10.4). In the presence of ATP, a complex between AuNP–aptamer/ATP/aptamer–biotin was formed at the test line. The remaining AuNP–aptamer conjugate bound to its complementary

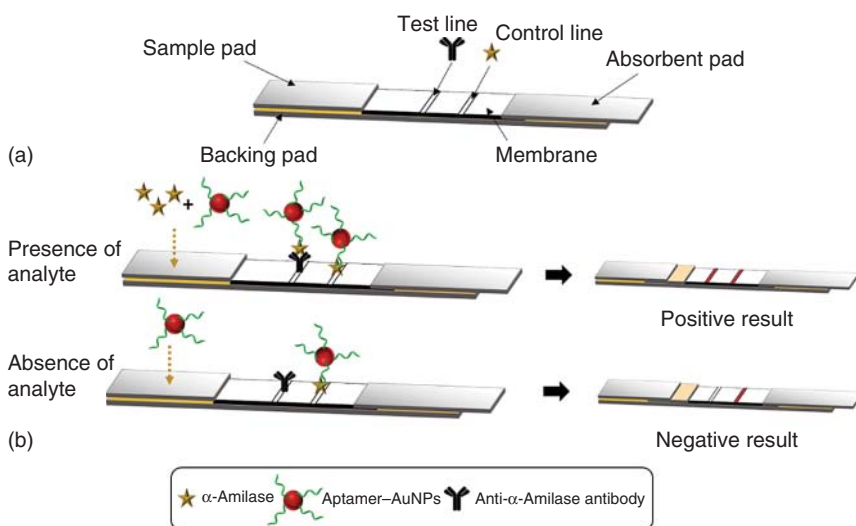


Figure 10.3 Schematic representation of LFA for salivary α -amylase. (a) Configuration of lateral flow strip; (b) the principle of visual detection in the presence and absence of analyte. Source: Adapted from Minagawa et al. 2017 [76].

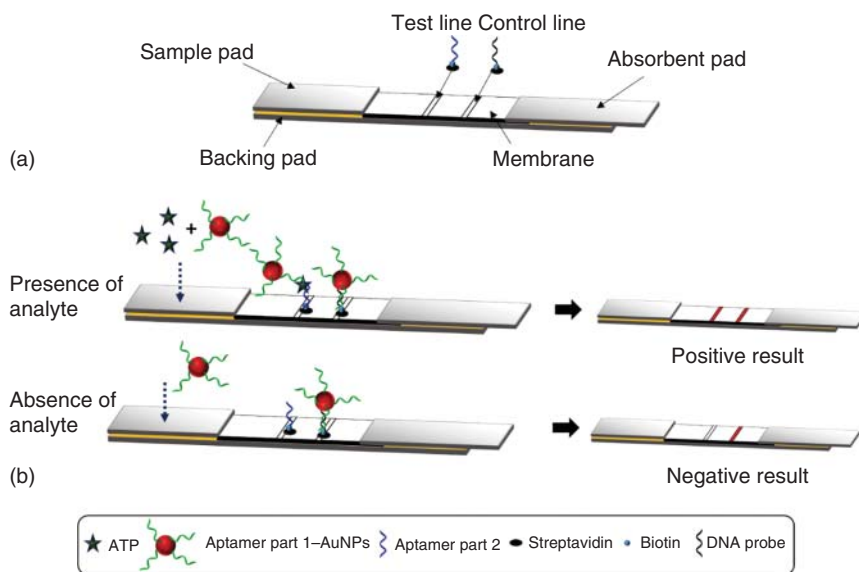


Figure 10.4 Schematic representation of ATP detection by split aptamers. (a) Configuration of lateral flow strip; (b) the principle of visual detection in the presence and absence of analyte. Source: Adapted from Zhu et al. 2016 [54].

DNA sequence at the control line. This assay was tested in real urine samples, achieving a LOD of $0.5 \mu\text{M}$ with high specificity against uridine triphosphate (UTP), cytidine triphosphate (CTP), and guanosine triphosphate (GTP).

10.3.2 Competitive Assay

Competitive assays are usually used for low-molecular-weight compounds where only one aptatope may be available, or, alternatively, where only one aptamer is available and two formats have been exploited, either exploiting competition between the target analyte in solution to be tested and the same target analyte immobilized on the test line, or, in an alternative approach, exploiting competition between immobilized DNA complementary to the aptamer–gold nanoparticle conjugate and the target analyte.

Jauset-Rubio et al. reported β -conglutin detection based on the competition between target in solution and target immobilized on the membrane [77]. The configuration of the strip was based on chemisorption of thiolated aptamer on in-house-prepared AuNPs using an optimized surface chemistry with immobilization of β -conglutin and a full complementary aptamer sequence on the test line and control line, respectively. With increasing concentrations of β -conglutin in solution, less aptamer was free to bind to the immobilized β -conglutin on the membrane. An alternative approach for generating signal at the control line was developed, exploiting the inherent properties of the nucleic acid nature of aptamers, using a full-length 94-mer oligo, 100% complementary to the β -conglutin aptamer. Following competition at the test line, either the unbound aptamer–AuNP or β -conglutin–aptamer–AuNP complex, or a combination of

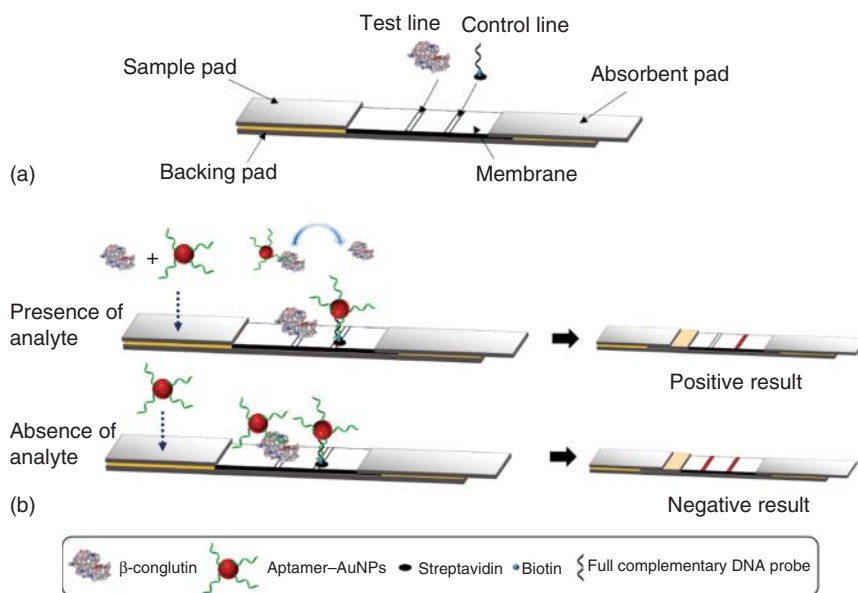


Figure 10.5 Schematic representation of β -conglutinin detection by competitive assay. (a) Configuration of lateral flow strip; (b) the principle of visual detection in the presence and absence of analyte. Source: Adapted from Jauset-Rubio et al. 2016 [77].

both, transverse to the control line. The aptamer has much greater affinity for its complementary DNA than for the β -conglutinin, which is thus displaced from the complex, liberating the aptamer to hybridize to its complementary sequence at the control line (Figure 10.5). The specificity of the assay against two nonspecific proteins (streptavidin and bovine serum albumin) was also tested. The LOD was 5.5×10^{-11} M, with the entire assay completed in just five minutes.

An LFA exploiting fluorescent detection of ochratoxin A (OTA) using a QD-labeled aptamer, incorporating a poly A linker has been described. The LFA is based on competition between an oligoprobe sequence with complementarity to the aptamer immobilized at the test line, and the OTA, for binding to the AuNP-labeled aptamer. Any unbound AuNP-labeled aptamer migrates to the control line where a poly T oligoprobe binds to the poly A linker. [78]. The LOD achieved was 1.9 ng ml^{-1} , which is comparable to ELISA and fluorescence polarization immunoassay methods [13].

In 2011, the same group reported a similar assay [79], but replacing the QDs with AuNPs, improving the LOD to 0.18 ng ml^{-1} with an optical strip reader (Figure 10.6). In addition, the assay was applied to real red wine samples. Cross-reactivity studies were not observed with other toxins, including zearalenone, fumonisin B1, deoxynivalenol, and microcystin-LR.

A similar LFA for the detection of OTA in *Astragalus membranaceus* was also reported [80], achieving a LOD of 1 ng ml^{-1} , and the assay was applied to nine contaminated *A. membranaceus* samples.

The LFA detection of aflatoxin B1 (AFB1) using aptamers has also been reported, exploiting a competition between the AFB1 and a cy5-modified

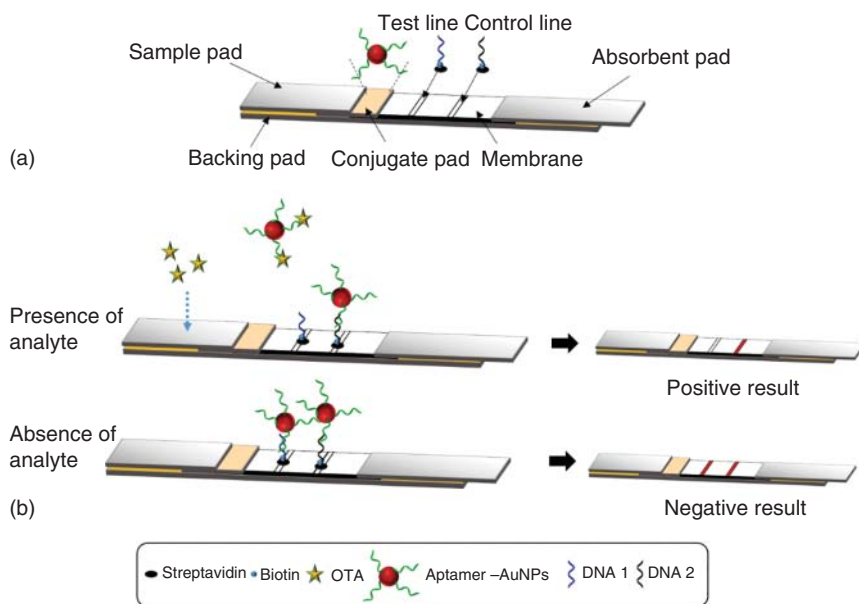


Figure 10.6 Schematic representation of OTA detection by competitive assay. (a) Configuration of lateral flow strip; (b) the principle of visual detection in the presence and absence of analyte. Source: Adapted from Wang et al. 2011 [79].

oligoprobe complementary to biotinylated aptamer. Streptavidin and anti-cy5 antibody were immobilized on the test and control line, respectively. The aptamer, a dilution range of AFB1 and DNA probe, was sequentially added into the wells of a microplate, incubated for 20 minutes, and the dipstick was then placed into the wells. In the presence of AFB1, the biotinylated aptamer first binds to the AFB1, preventing hybridization of the cy5-DNA probe with the aptamer. The biotin-aptamer-AFB1 complex is wicked to the test line, captured by immobilized streptavidin, and the remaining free cy5-modified DNA probe migrates to the control line where it is captured by the anti-cy5 antibody, with fluorescent signal observed at both the control and test spots, with less signal observed at the test line with increasing target concentration. In the absence of a target, strong fluorescent signals are observed at both the control and test spots [81] (Figure 10.7).

10.3.3 Signal Amplification

While LFAs are highly exploited for qualitative yes/no tests, their use for quantitative detection is not as widespread, particularly when lower detection limits are required [82], and there have been a number of reports of different methodologies to improve the sensitivity of LFAs. In one such approach, the use of AuNPs was compared with that of QD bioconjugates [83] for the detection of three different bacteria: *Escherichia coli*, *Listeria monocytogenes*, and *Salmonella enterica*. In this LFA, the reporter aptamer is modified on one end with biotin to link to streptavidin-modified AuNPs or QDs and on the other end with digoxigenin, for

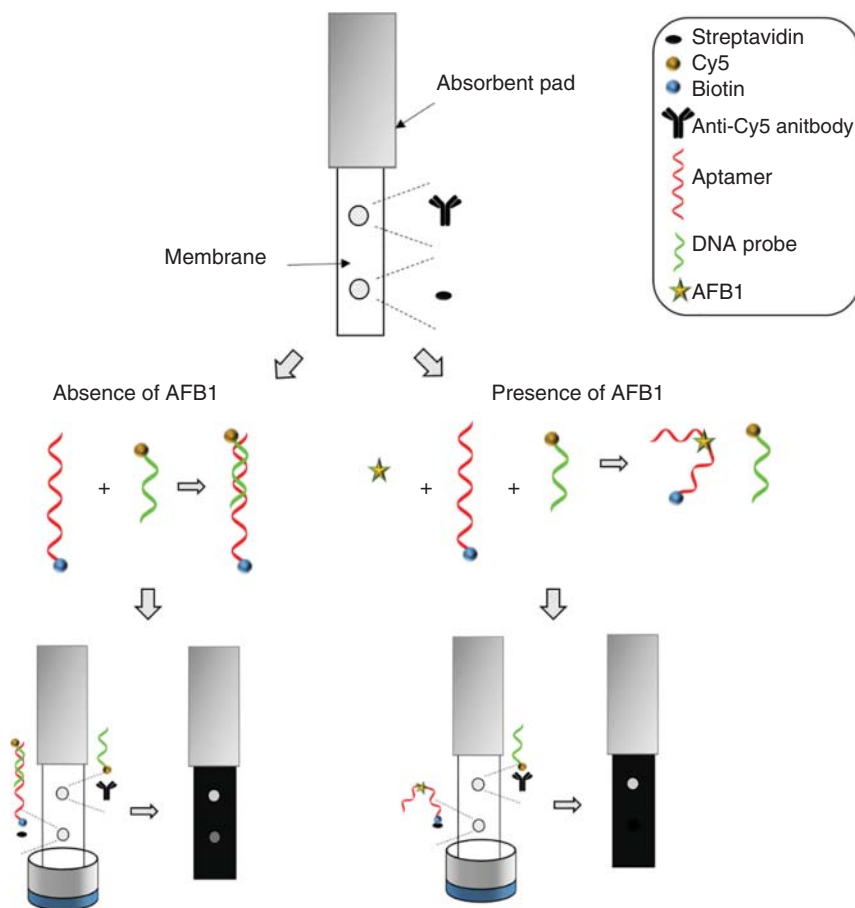


Figure 10.7 Schematic representation of aflatoxin B1 competitive assay dipstick detection. Source: Adapted from Shim et al. 2014 [81].

binding to anti-digoxigenin antibody immobilized on the control line. Capture aptamer is immobilized via an amino group and UV cross-linking at the test line, and in the presence of the specific bacterium, the target is sandwiched on the test line, with the digoxigenin of the aptamer being captured on the control line (Figure 10.8). This approach was demonstrated to produce a strong control line as compared to previous reports as the same bioconjugate binds at both lines. When no target is present, the bioconjugate only binds at the control line. The LOD of *E. coli* was around 3000 live *E. coli* 8739 cells and 6000 live *E. coli* O157:H7 cells by detection using the naked eye, with the LOD improving 10-fold using QDs and UV excitation.

An alternative approach for signal enhancement for the detection of adenosine and cocaine in serum using two types of bioconjugates and a dipstick test was reported [84]. AuNPs were functionalized with thiolated oligonucleotide complementary to a linker sequence linked to the aptamer in one bioconjugate. AuNPs functionalized with a thiolated oligonucleotide complementary to

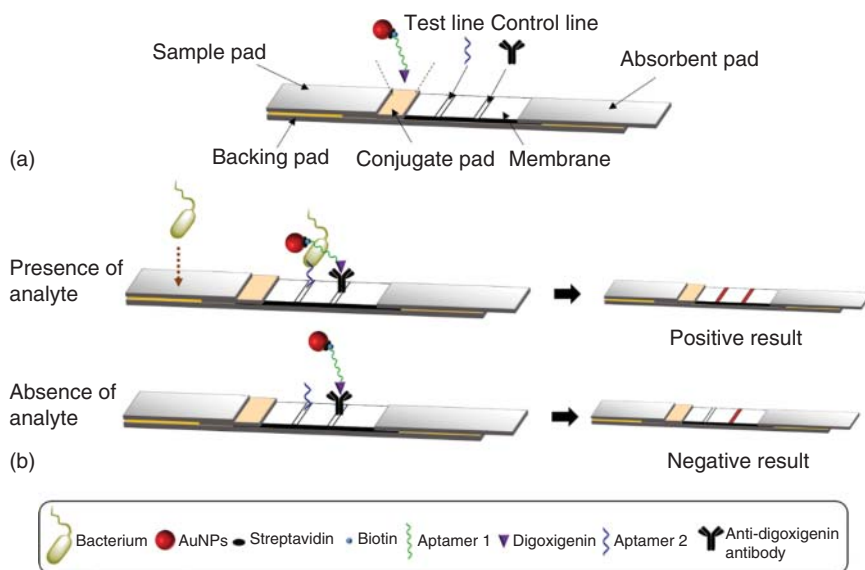


Figure 10.8 Schematic representation of bacteria detection with digoxigenin-5'-reporter aptamer-3'-biotin-streptavidin-AuNP conjugates. (a) Configuration of lateral flow strip; (b) the principle of visual detection in the presence and absence of analyte. Source: Adapted from Bruno 2014 [83].

another part of the aptamer was used in the second bioconjugate, which either did or did not contain a biotin functionality. Both functionalized nanoparticles mixed with the aptamer-created nanoparticle aggregates that were spotted on the conjugate pad. In the absence of adenosine, the aggregates are rehydrated by the sample solution and migrate but are stopped from further passage through the membrane due to their large size. However, in the presence of adenosine, due to the adenosine–aptamer interaction, the aggregate is dispersed, allowing further passage of the adenosine–aptamer complex along the membrane (Figure 10.9), resulting in a LOD of 20 μM . Finally, ribonucleosides were tested and no cross-reactivity was observed, with the LFA being successfully applied to spiked serum samples.

In a different approach, two conjugate pads were used [85], where DNA probe 1 coated on AuNPs was absorbed on the first conjugate pad, while on the second pad a complex between DNA probe 2, AuNPs, and aptamer was absorbed. At the test line anti-thrombin antibody was immobilized, and at the control line biotinylated DNA probe (poly A) complementary to a poly T sequence which had been incorporated into the aptamer–AuNP bioconjugate was immobilized. AuNP–DNA1 bioconjugate was designed to bind to the second AuNP–DNA 2–aptamer through hybridisation between DNA1 and DNA2, whilst AuNP–DNA2–aptamer was also designed to bind specifically to thrombin. When thrombin was added to the strip, the solution migrated until the first conjugate pad and the conjugate was then wicked to the second conjugate pad, where the aptamer reacts with thrombin and simultaneously the hybridization between DNA1 and DNA2 takes place. Consequently, a complex of

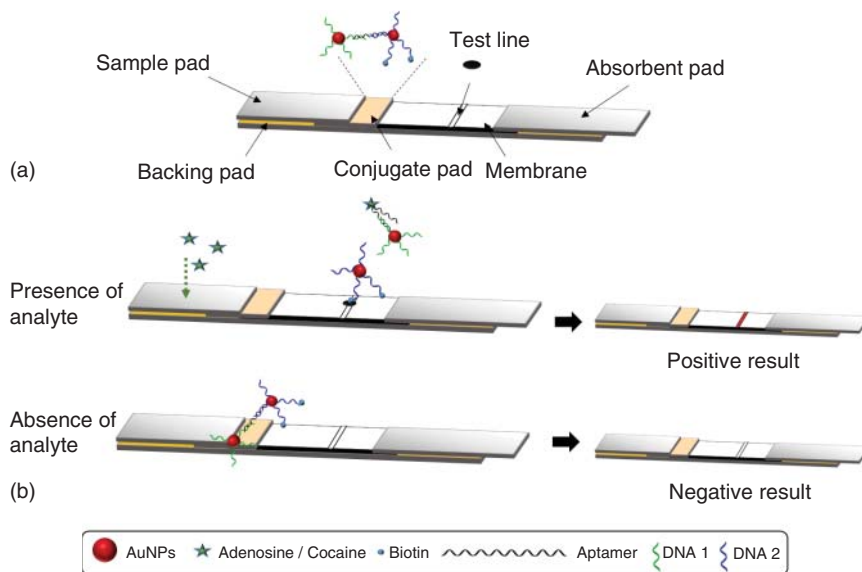


Figure 10.9 Schematic representation of adenosine–cocaine detection. (a) Configuration of lateral flow strip; (b) the principle of visual detection in the presence and absence of analyte. Source: Adapted from Liu et al. 2006 [84].

the AuNP–DNA1/AuNP–DNA2/aptamer/thrombin was formed and migrated to the test line, where it was captured by the immobilized antibodies. The excess of the AuNP–DNA1/AuNP–DNA2/aptamer was captured at the control line by the immobilized DNA3 probe (Figure 10.10). Quantitative analysis was realized using a portable strip reader, with a LOD of 0.25 nM, a 10-fold improvement as compared to the use of only one nanoparticle bioconjugate [72]. Furthermore, specificity was confirmed using other proteins, including prothrombin, casein, IgG, and HSA.

An aptamer-cleavage reaction was combined with an enzyme catalytic amplification system for the detection of thrombin, achieving a LOD of 4.9 pM with a strip reader [86] 3 orders of magnitude lower than that previously achieved with the AuNP-labeled aptamer [72] and 2 orders of magnitude lower than using two different nanoparticle bioconjugates [85]. In the latter approach, one AuNP bioconjugate with a DNA sequence was composed of a poly T and a few bases complementary to the 15-mer thrombin aptamer (DNA1) and a second AuNP bioconjugate with another DNA sequence with a few bases complementary to the aptamer and also bearing both biotin and horseradish peroxidase (HRP) moieties (DNA2). The strip consisted of three components, namely, a sample pad, a nitrocellulose membrane, and an absorbent pad. Streptavidin and cDNA1–streptavidin (poly A complementary to DNA1 via the incorporated poly T) were spotted on the test line and the control line, respectively. The particles were mixed and aptamer was added to form aggregates. In the presence of thrombin, there is a disaggregation due to the interaction between the aptamer and thrombin, and the biotinylated particles bind to streptavidin on the test line

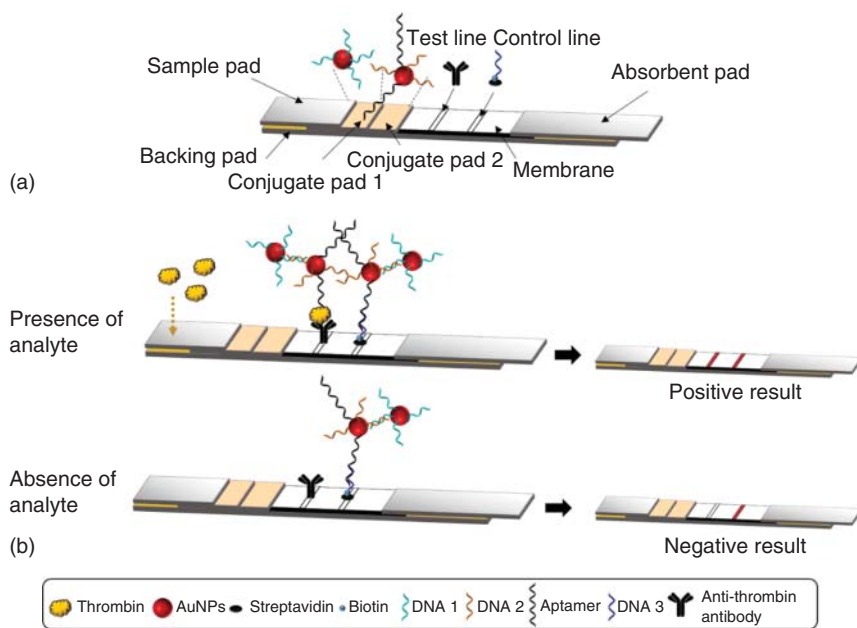


Figure 10.10 Schematic illustration of thrombin detection using two kinds of gold nanoparticles conjugates. (a) Configuration of lateral flow strip; (b) the principle of visual detection in the presence and absence of analyte. Source: Adapted from Shen et al. 2013 [85].

to form a red band. Any excess complex moves to the control line where cDNA1 captures DNA1– AuNP, producing a second red band. The authors then added 3-amino-9-ethyl carbazole (AEC) and H_2O_2 to produce more intense red bands (Figure 10.11).

In another interesting approach to achieve signal amplification, bacteriophage particles with aptamers as reporters were used for the detection of IgE in an LFA [87]. A M13 phage display AviTag peptide was biotinylated using biotin ligase, and covalently modified with HRP on the major coat protein pVIII, and the complex then linked to neutravidin, and subsequently to biotinylated IgE aptamer. A sandwich assay was performed on the LFA via immobilization of anti-IgE antibody at the test line and anti-M13 antibody at the control line. IgE added in the sample pad binds with the aptamer–phage conjugate, which is then captured on the test line by the anti-IgE antibody, with the excess conjugate being captured on the control line by the anti-M13 antibody (Figure 10.12). The LOD of the assay was 0.13 ng ml^{-1} , achieving better sensitivity than the ImmunoCAP Rapid test.

The use of aptamer-gated silica nanoparticles to facilitate the sensitive detection of small molecules has also been demonstrated [88], using ATP to demonstrate the proof of concept. To obtain an ATP aptamer molecular gate, the aptamer sequence was engineered into a hairpin via a short-stem DNA complementary to one end of the sequence. This hairpin was immobilized on the surface of rhodamine B encapsulating silica nanoparticles, and this complex was tethered on the test line of the membrane. At the control line, a mutated form of the aptamer sequence acted as a gating molecule. Upon addition of ATP, the

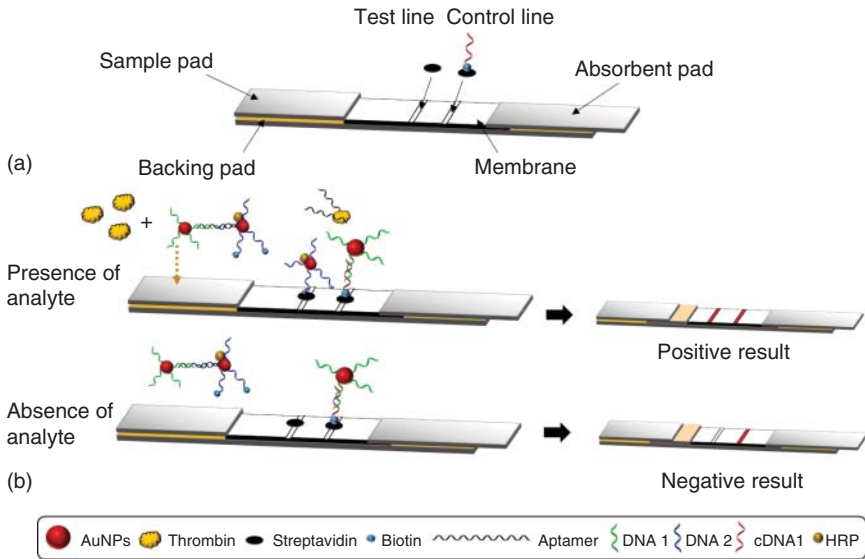


Figure 10.11 Schematic representation of thrombin detection based on aptamer-cleavage reaction. (a) Configuration of lateral flow strip; (b) the principle of visual detection in the presence and absence of analyte. Source: Adapted from Qin et al. 2015 [86].

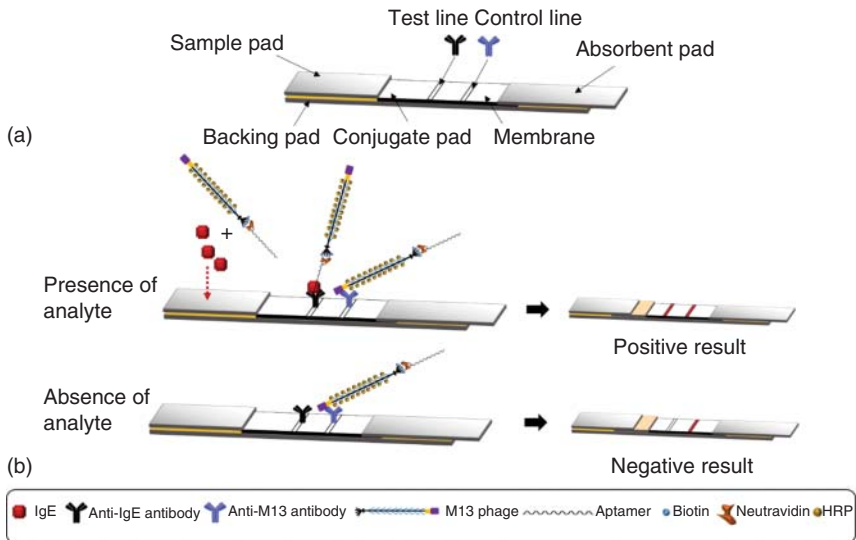


Figure 10.12 Schematic representation of IgE detection based on aptamer-phage reporters. (a) Configuration of lateral flow assay; (b) the principle of visual detection in the presence and absence of analyte. Source: Adapted from Adhikari et al. 2015 [87].

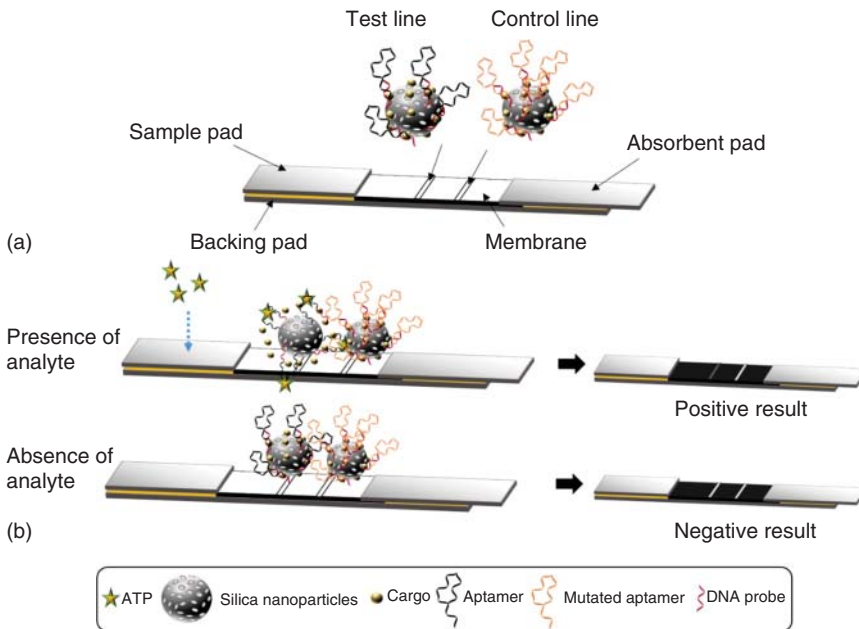


Figure 10.13 Schematic representation of ATP detection based on aptamer-gated silica nanoparticles. (a) Configuration of lateral flow strip; (b) the principle of visual detection in the presence and absence of analyte. Source: Adapted from Ozalp et al. 2016 [88].

hairpin was disrupted resulting in a release of the encapsulated fluorophores, producing a decrease in the fluorescence intensity at the test line. However, at the control line, no conformational change took place and the fluorescence intensity remained unaltered (Figure 10.13). The LOD was determined to be $69 \mu\text{M}$.

A straightforward and sensitive LFA for the detection of *Salmonella enteritidis* using a dual aptamer and isothermal strand displacement assay (SDA) was also developed for ultrasensitive detection [89]. One aptamer specific for the out membrane of *S. enteritidis* was linked to magnetic beads for enrichment, while the second was used as a reporter. Subsequent to formation of the sandwich complex, this second aptamer was amplified using SDA and detected by LFA (Figure 10.14). The specificity of this assay was evaluated using other pathogens including *S. typhimurium*, *E. coli*, *Pseudomonas aeruginosa*, and *Citrobacter freundii*, and no cross-reactivity was observed. The assay was also tested in spiked milk samples achieving a LOD of 10 CFU ml^{-1} . The same group subsequently demonstrated that this method can also be applied to other bacterium such as *E. coli* O157:H7 [90], again achieving a LOD of 10 CFU ml^{-1} , and this assay was tested in real samples, including milk, water, and apple juice.

Jauset-Rubio et al. described an alternative method for the detection of the anaphylactic allergen β -conglutinin via LFA, combining aptamer-based detection

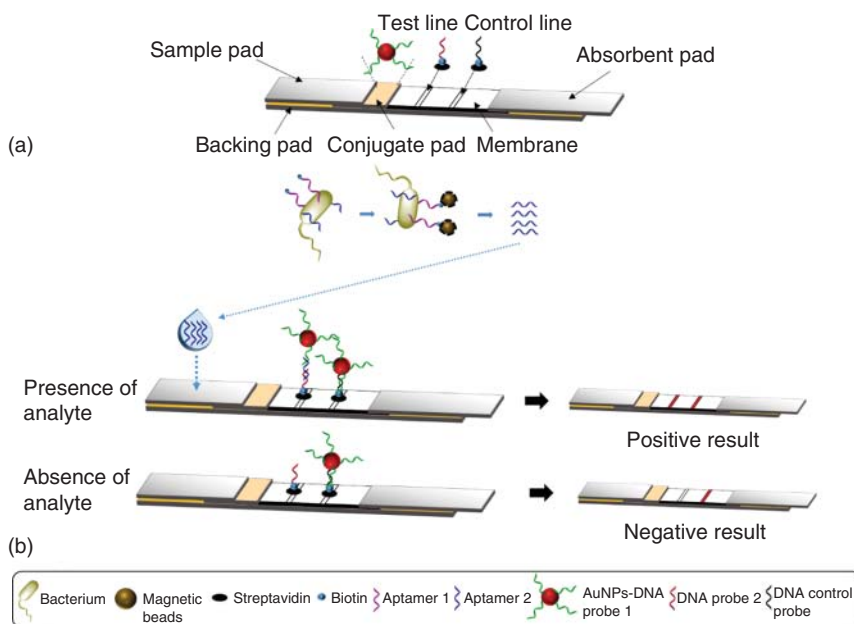


Figure 10.14 Schematic representation of bacterium detection based on aptamer-mediated strand displacement amplification. (a) Configuration of lateral flow assay; (b) Principle of visual detection in the presence and absence of analyte. Source: Adapted from Fang et al. 2014 [89].

with isothermal recombinase polymerase amplification (RPA) [77]. The assay was based on competition between target in solution and target immobilized on the surface of magnetic beads to bind to the aptamer. Following competition, the aptamer bound to the immobilized target on the beads was eluted and used as a template for amplification by RPA. The primers used for the amplification were designed with sequences specific to bind to extremes of eluted aptamer and flanked by single-stranded tails, designed to be complementary to the capture and reporter probes on the lateral flow strip. These primers are referred to as tailed primers, and result in amplicons of double-stranded DNA with a single-stranded DNA tail at each end, which is achieved by the use of a stopper, C3, located between the primer binding site and the single-stranded tail. The RPA product was mixed with the AuNP-linked reporter probe and added to the LFA, where two biotinylated capture probes, premixed with streptavidin, were used for the test line and the control line. At the test line, the probe was complementary to the tail 5'-region of the amplified aptamer, while on the control line, the probe was complementary to the AuNP-linked reporter probe. The reporter probe conjugated to AuNPs was also complementary to the other tail at the 3'-end of the amplified aptamer and thus will bind to the amplified aptamer forming a sandwich on the test line and with the capture probe on the control line, generating a red band in both cases. The LOD of the assay was 9×10^{-15} M, with the complete assay being completed in 22 minutes (Figure 10.15).

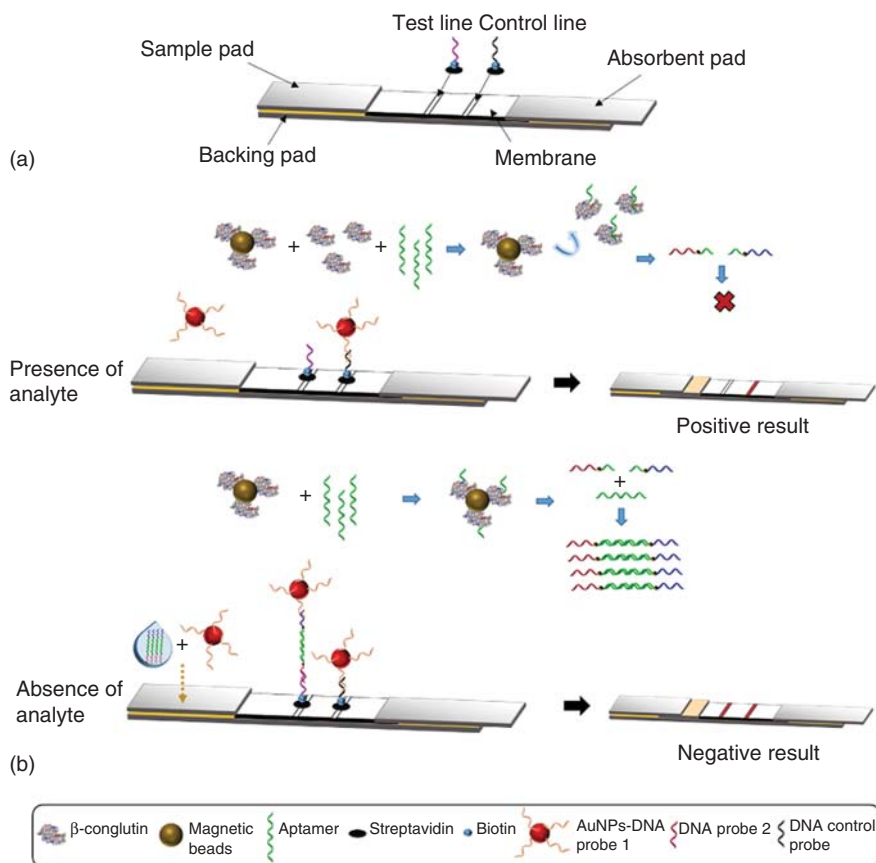


Figure 10.15 Schematic representation of β -conglutinin detection combining competitive assay with recombinase polymerase amplification and lateral flow. (a) Configuration of lateral flow strip; (b) Principle of visual detection in the presence and absence of analyte. Source: Adapted from Jauset-Rubio et al. 2016 [77].

10.4 Summary and Perspectives

LFA based on aptamers have demonstrated to be affordable and portable tools to detect a wide variety of targets in a few minutes (5–30 minutes) and allowing point-of-care testing (Table 10.1). They are ideal for qualitative analysis, where the presence or absence of an analyte is essential for a rapid diagnostic. However, some drawbacks have been reported for its quantitative detection when a low LOD is needed. Therefore, it is essential to take into account the different materials that compose the strip and choose their optimal characteristics depending on the design. In addition, different strategies have been reported here in order to enhance the signal such as the use of two gold nanoparticles, enzymatic reactions, different labels, and amplification techniques in order to have more copies of the detected aptamer to improve the LOD. Another promising issue is the growing interest of using smartphones as strip readers, to decrease the costs and because

Table 10.1 Aptamers in lateral flow assays.

Format	Target	Test line	Control line	Conjugate	LOD	References
Sandwich assay (pair of aptamers)	Thrombin	SA-biotin-aptamer	SA-biotin-DNA complementary primary aptamer	AuNPs-primary aptamer	2.5 nM	[72]
Sandwich assay (pair of aptamers)	Ramos cells	SA-biotin-TE02 aptamer	SA-biotin-control DNA	AuNPs-aptamer	4000 Ramos cells visual and 800 Ramos cells in strip	[73]
Sandwich assay (pair of aptamers)	Vaspin	SA-biotin-aptamer	SA-biotin-DNA complementary aptamer	AuNPs-aptamer	0.137 nM	[74]
Sandwich assay (pair of aptamers)	Arbovirus (Chikungunya virus and TBEV)	SA-biotin-aptamer	—	AuNPs-SA-biotin-DNA complementary	—	[75]
Sandwich assay (antibody/aptamer pair)	Salivary α -amylase (sAA)	Anti-sAA antibody	sAA protein	AuNPs-SA-biotin-aptamer	—	[76]
Sandwich assay (split aptamer)	ATP	SA-biotin-split aptamer 2	SA-biotin DNA probe	AuNPs-split aptamer 1	0.5 μ M	[54]
Competitive assay	β -Conglutin	β -Conglutin	SA-biotin full DNA complementary aptamer	AuNPs-aptamer	55 pM	[77]
Competitive assay	Ochratoxin A (OTA)	SA-biotin-cDNA	SA-biotin-poly T	QD-aptamer	1.9 ng ml ⁻¹	[78]
Competitive assay	Ochratoxin A (OTA)	SA-biotin-cDNA	SA-biotin-poly T	AuNPs-aptamer	1 ng m ⁻¹ ; 0.18 ng ml ⁻¹ (strip reader)	[79]
Competitive assay	Ochratoxin A (OTA) in <i>Astragalus membranaceus</i>	SA-biotin-cDNA	SA-biotin-poly A	AuNPs-aptamer	1 ng ml ⁻¹	[80]

Competitive assay	Aflatoxin B1 (AFB1)	SA	Anti-cy5 antibody	—	0.1 ng ml ⁻¹	[81]
Sandwich assay	Foodborne pathogens (<i>E. coli</i> , <i>L. monocytogenes</i> , <i>S. enterica</i>)	NH2-aptamer	Anti-digoxigenin antibody	AuNPs-aptamer-digoxigenin/QD-aptamer-digoxigenin	3000–6000 <i>E. coli</i> cells; 300–600 <i>E. coli</i> cells (QD)	[83]
Direct assay (2AuNP-conjugates)	Adenosine/cocaine	SA	—	AuNPs-DNA1 + biotin-DNA2-AuNPs-DNA2 + aptamer	20 μM adenosine 10 μM cocaine	[84]
Sandwich assay (2 AuNPs-conjugates)	Thrombin	Anti-thrombin antibody	SA-biotin-poly A	AuNPs-DNA1/DNA2-AuNPs-aptamer	0.25 nM	[85]
Aptamer-cleavage + enzymatic reaction	Thrombin	SA	SA-biotin-cDNA1	AuNPs-DNA1/biotin-DNA2-AuNPs-HRP	6.4 pM visual; 4.9 pM strip reader	[86]
Sandwich assay	IgE	Anti-IgE antibody	Anti-M13 antibody	Aptamer-phage	0.13 ng ml ⁻¹	[87]
Competition assay	ATP	Aptamer gated silica nanoparticles loaded rhodamine B dye	Mutated aptamer gated nanoparticles loaded rhodamine B dye	—	69 μM	[88]
Strand displacement amplification assay	<i>Salmonella enteritidis</i>	SA-biotin-DNA probe	SA-biotin-DNA probe	AuNPs-DNA probe	10 ⁵ CFU ml ⁻¹	[89]
Strand displacement amplification assay	<i>E. coli</i> O157:H7	SA-biotin-DNA probe	SA-biotin-DNA probe	AuNPs-DNA probe	10 CFU ml ⁻¹	[90]
Competitive assay + recombinase polymerase amplification	β-Conglutin	SA-biotin-DNA probe	SA-biotin-DNA probe	AuNPs-DNA probe	9 fM	[77]
SELEX	Recombinant human cellular prion protein (PrP ^C)	rhuPrPc23-231	—	—	—	[91]

they are more portable and accessible for point of care, for example, in developing countries.

Although aptamers have been shown to have advantages over antibodies in easier use in biosensors, due to their versatile and effective characteristics as molecular probes, few publications using them are reported until date. However, we speculate that this will change in the future since it is extremely challenging to develop antibodies against small molecular or no immunogenic targets. Moreover, the larger size, reduced flexibility, and higher cost of antibodies make aptamers a more interesting choice for use in LFAs, and an increasing number of reports of lateral flow aptamer assays can be expected.

References

- 1 Conrad, R.C., Giver, L., Tian, Y., and Ellington, A.D. (1996). In vitro selection of nucleic acid aptamers that bind proteins. *Methods Enzymol.* 267: 336–367.
- 2 Tuerk, C. and Gold, L. (1990). Systematic evolution of ligands by exponential enrichment: RNA ligands to bacteriophage T4 DNA polymerase. *Science* 249 (4968): 505–510.
- 3 Huizenga, D.E. and Szostak, J.W. (1995). A DNA aptamer that binds adenosine and ATP. *Biochemistry* 34 (2): 656–665.
- 4 McKeague, M. and Derosa, M.C. (2012). Challenges and opportunities for small molecule aptamer development. *J. Nucleic Acids* 2012: 1–20, 748913.
- 5 Sassanfar, M. and Szostak, J.W. (1993). An RNA motif that binds ATP. *Nature* 364 (6437): 550–553.
- 6 Famulok, M. (1994). Molecular recognition of amino acids by RNA-aptamers: an L-citrulline binding RNA motif and its evolution into an L-arginine binder. *J. Am. Chem. Soc.* 116 (9): 1698–1706.
- 7 Shangguan, D., Li, Y., Tang, Z. et al. (2006). Aptamers evolved from live cells as effective molecular probes for cancer study. *Proc. Natl. Acad. Sci. U. S. A.* 103 (32): 11838–11843.
- 8 Song, K.M., Lee, S., and Ban, C. (2012). Aptamers and their biological applications. *Sensors* 12 (1): 612–631.
- 9 Tombelli, S., Minunni, M., and Mascini, M. (2005). Analytical applications of aptamers. *Biosens. Bioelectron.* 20 (12): 2424–2434.
- 10 Geiger, A., Burgstaller, P., von der Eltz, H. et al. (1996). RNA aptamers that bind L-arginine with sub-micromolar dissociation constants and high enantioselectivity. *Nucleic Acids Res.* 24 (6): 1029–1036.
- 11 Jenison, R.D., Gill, S.C., Pardi, A., and Polisky, B. (1994). High-resolution molecular discrimination by RNA. *Science* 263 (5152): 1425–1429.
- 12 Mairal, T., Nadal, P., Svobodova, M., and O’Sullivan, C.K. (2014). FRET-based dimeric aptamer probe for selective and sensitive Lup an 1 allergen detection. *Biosens. Bioelectron.* 54: 207–210.
- 13 Cruz-Aguado, J.A. and Penner, G. (2008). Fluorescence polarization based displacement assay for the determination of small molecules with aptamers. *Anal. Chem.* 80 (22): 8853–8855.

- 14 Wu, C., Yan, L., Wang, C. et al. (2010). A general excimer signaling approach for aptamer sensors. *Biosens. Bioelectron.* 25 (10): 2232–2237.
- 15 Yamamoto, R., Baba, T., and Kumar, P.K. (2000). Molecular beacon aptamer fluoresces in the presence of Tat protein of HIV-1. *Genes Cells* 5 (5): 389–396.
- 16 Kim, Y.S., Niazi, J.H., and Gu, M.B. (2009). Specific detection of oxytetracycline using DNA aptamer-immobilized interdigitated array electrode chip. *Anal. Chim. Acta* 634 (2): 250–254.
- 17 Baker, B.R., Lai, R.Y., Wood, M.S. et al. (2006). An electronic, aptamer-based small-molecule sensor for the rapid, label-free detection of cocaine in adulterated samples and biological fluids. *J. Am. Chem. Soc.* 128 (10): 3138–3139.
- 18 Ferapontova, E.E., Olsen, E.M., and Gothelf, K.V. (2008). An RNA aptamer-based electrochemical biosensor for detection of theophylline in serum. *J. Am. Chem. Soc.* 130 (13): 4256–4258.
- 19 Du, Y., Li, B., Wei, H. et al. (2008). Multifunctional label-free electrochemical biosensor based on an integrated aptamer. *Anal. Chem.* 80 (13): 5110–5117.
- 20 Huang, C.C., Huang, Y.F., Cao, Z. et al. (2005). Aptamer-modified gold nanoparticles for colorimetric determination of platelet-derived growth factors and their receptors. *Anal. Chem.* 77 (17): 5735–5741.
- 21 Liu, J. and Lu, Y. (2006). Preparation of aptamer-linked gold nanoparticle purple aggregates for colorimetric sensing of analytes. *Nat. Protoc.* 1 (1): 246–252.
- 22 Fukusaki, E., Hasunuma, T., Kajiyama, S. et al. (2001). SELEX for tubulin affords specific T-rich DNA aptamers. Systematic evolution of ligands by exponential enrichment. *Bioorg. Med. Chem. Lett.* 11 (22): 2927–2930.
- 23 Tombelli, S., Minunni, M., Luzi, E., and Mascini, M. (2005). Aptamer-based biosensors for the detection of HIV-1 Tat protein. *Bioelectrochemistry* 67 (2): 135–141.
- 24 Bini, A., Centi, S., Tombelli, S. et al. (2008). Development of an optical RNA-based aptasensor for C-reactive protein. *Anal. Bioanal. Chem.* 390 (4): 1077–1086.
- 25 Fischer, N.O., Tarasow, T.M., and Tok, J.B.-H. (2008). Protein detection via direct enzymatic amplification of short DNA aptamers. *Anal. Biochem.* 373 (1): 121–128.
- 26 Svobodova, M., Mairal, T., Nadal, P. et al. (2014). Ultrasensitive aptamer based detection of β -conglutinin food allergen. *Food Chem.* 165: 419–423.
- 27 Jauset-Rubio, M., Sabaté del Río, J., Mairal, T. et al. (2017). Ultrasensitive and rapid detection of β -conglutinin combining aptamers and isothermal recombinase polymerase amplification. *Anal. Bioanal. Chem.* 409 (1): 143–149.
- 28 Koczula, K.M. and Gallotta, A. (2016). Lateral flow assays. *Essays Biochem.* 60 (1): 111–120.
- 29 Gina, P., Randall, P.J., Muchinga, T.E. et al. (2017). Early morning urine collection to improve urinary lateral flow LAM assay sensitivity in hospitalised patients with HIV-TB co-infection. *BMC Infect. Dis.* 17 (1): 339.
- 30 Johnson, N., Ebersole, J.L., Kryscio, R.J. et al. (2016). Rapid assessment of salivary MMP-8 and periodontal disease using lateral flow immunoassay. *Oral Dis.* 22 (7): 681–687.

- 31 De Giovanni, N. and Fucci, N. (2013). The current status of sweat testing for drugs of abuse: a review. *Curr. Med. Chem.* 20 (4): 545–561.
- 32 Yang, X., Liu, L., Hao, Q. et al. (2017). Development and evaluation of up-converting phosphor technology-based lateral flow assay for quantitative detection of NT-proBNP in blood. *PLoS One* 12 (2): e0171376.
- 33 Phan, J.C., Pettitt, J., George, J.S. et al. (2016). Lateral flow immunoassays for Ebola virus disease detection in liberia. *J. Infect. Dis.* 214 (suppl 3): S222–S228.
- 34 Plotz, C.M. and Singer, J.M. (1956). The latex fixation test. I. Application to the serologic diagnosis of rheumatoid arthritis. *Am. J. Med.* 21: 888–892.
- 35 O'Farrell, B. (2013). Lateral flow immunoassay systems: evolution from the current state of the art to the next generation of highly sensitive, quantitative rapid assays. In: *The Immunoassay Handbook*, 4e (ed. D. Wild), 89–107. Oxford: Elsevier Ltd.
- 36 Millipore (2017). Rapid lateral flow test strips: consideration for product development. <http://www.millipore.com/techpublications/tech1/tb500en500> (16 May 2017).
- 37 Chen, A. and Yang, S. (2015). Replacing antibodies with aptamers in lateral flow immunoassay. *Biosens. Bioelectron.* 71: 230–242.
- 38 O'Farrell, B. (2015). Lateral flow technology for field-based applications-basics and advanced developments. *Top. Companion Anim. Med.* 30 (4): 139–147.
- 39 Fischer, C., Wessels, H., Paschke-Kratzin, A., and Fischer, M. (2017). Aptamers: universal capture units for lateral flow applications. *Anal. Biochem.* 522: 53–60.
- 40 Zhou, W., Huang, P.-J.J., Ding, J., and Liu, J. (2014). Aptamer-based biosensors for biomedical diagnostics. *Analyst* 139 (11): 2627–2640.
- 41 Dhiman, A., Kalra, P., Bansal, V. et al. (2017). Aptamer-based point-of-care diagnostic platforms. *Sens. Actuators, B* 246: 535–553.
- 42 Tasset, D.M., Kubik, M.F., and Steiner, W. (1997). Oligonucleotide inhibitors of human thrombin that bind distinct epitopes. *J. Mol. Biol.* 272 (5): 688–698.
- 43 Wang, Q., Zhou, C., Yang, X. et al. (2014). Probing interactions between human lung adenocarcinoma A549 cell and its aptamers at single-molecule resolution. *J. Mol. Recognit.* 27 (11): 676–682.
- 44 Min, K., Jo, H., Song, K. et al. (2011). Dual-aptamer-based delivery vehicle of doxorubicin to both PSMA (+) and PSMA (–) prostate cancers. *Biomaterials* 32 (8): 2124–2132.
- 45 Jo, H., Youn, H., Lee, S., and Ban, C. (2014). Ultra-effective photothermal therapy for prostate cancer cells using dual aptamer-modified gold nanostars. *J. Mater. Chem. B* 2 (30): 4862–4867.
- 46 Fang, L.-X., Huang, K.-J., and Liu, Y. (2015). Novel electrochemical dual-aptamer-based sandwich biosensor using molybdenum disulfide/carbon aerogel composites and Au nanoparticles for signal amplification. *Biosens. Bioelectron.* 71: 171–178.
- 47 Ruslinda, A.R., Penmatsa, V., Ishii, Y. et al. (2012). Highly sensitive detection of platelet-derived growth factor on a functionalized diamond surface using aptamer sandwich design. *Analyst* 137 (7): 1692–1697.

- 48 Abbaspour, A., Norouz-Sarvestani, F., Noori, A., and Soltani, N. (2015). Aptamer-conjugated silver nanoparticles for electrochemical dual-aptamer-based sandwich detection of staphylococcus aureus. *Biosens. Bioelectron.* 68: 149–155.
- 49 Hu, P.P., Liu, H., Zhan, L. et al. (2015). Coomassie brilliant blue R-250 as a new surface-enhanced Raman scattering probe for prion protein through a dual-aptamer mechanism. *Talanta* 139: 35–39.
- 50 Ahmad Raston, N.H. and Gu, M.B. (2015). Highly amplified detection of visceral adipose tissue-derived serpin (vaspin) using a cognate aptamer duo. *Biosens. Bioelectron.* 70: 261–267.
- 51 Jauset Rubio, M., Svobodová, M., Mairal, T. et al. (2016). β -Conglutin dual aptamers binding distinct aptatopes. *Anal. Bioanal. Chem.* 408 (3): 875–884.
- 52 Jauset Rubio, M., Svobodova, M., Mairal, T., and O’Sullivan, C.K. (2016). Surface plasmon resonance imaging (SPRi) for analysis of DNA aptamer: β -conglutin interactions. *Methods* 97: 20–26.
- 53 Rinker, S., Ke, Y., Liu, Y. et al. (2008). Self-assembled DNA nanostructures for distance-dependent multivalent ligand-protein binding. *Nat. Nanotechnol.* 3 (7): 418–422.
- 54 Zhu, C., Zhao, Y., Yan, M. et al. (2016). A sandwich dipstick assay for ATP detection based on split aptamer fragments. *Anal. Bioanal. Chem.* 408 (15): 4151–4158.
- 55 Ye, B.F., Zhao, Y.J., Cheng, Y. et al. (2012). Colorimetric photonic hydrogel aptasensor for the screening of heavy metal ions. *Nanoscale* 4 (19): 5998–6003.
- 56 Lv, Z., Chen, A., Liu, J. et al. (2014). A simple and sensitive approach for ochratoxin A detection using a label-free fluorescent aptasensor. *PLoS One* 9 (1): e85968.
- 57 O’Farrell, B. and Bauer, J. (2006). Developing highly sensitive, more reproducible lateral flow assays. Part 1: New approaches to old problems. *IVD Technol.* 10 (6): 11–15.
- 58 O’Farrell, B. (2009). Evolution in lateral flow-based immunoassay systems. In: *Lateral Flow Immunoassay* (ed. R. Wong and H. Tse), 1–33. Totowa, NJ: Humana Press.
- 59 Sajid, M., Kawde, A.N., and Daud, M. (2015). Designs, formats and applications of lateral flow assay: a literature review. *J. Saudi Chem. Soc.* 19 (6): 689–705.
- 60 Ahmed, S., Bui, M.-P.N., and Abbas, A. (2016). Paper-based chemical and biological sensors: engineering aspects. *Biosens. Bioelectron.* 77: 249–263.
- 61 Quesada-Gonzalez, D. and Merkoci, A. (2015). Nanoparticle-based lateral flow biosensors. *Biosens. Bioelectron.* 73: 47–63.
- 62 Bahadır, E.B. and Sezgentürk, M.K. (2016). Lateral flow assays: principles, designs and labels. *TrAC Trends Anal. Chem.* 82: 286–306.
- 63 Tong, Y., Lemieux, B., and Kong, H. (2011). Multiple strategies to improve sensitivity, speed and robustness of isothermal nucleic acid amplification for rapid pathogen detection. *BMC Biotech.* 11 (1): 50.

- 64 Yeo, S.J., Choi, K., Cuc, B.T. et al. (2016). Smartphone-based fluorescent diagnostic system for highly pathogenic H5N1 viruses. *Theranostics* 6 (2): 231–242.
- 65 Carrio, A., Sampedro, C., Sanchez-Lopez, J.L. et al. (2015). Automated low-cost smartphone-based lateral flow saliva test reader for drugs-of-abuse detection. *Sensors (Basel)* 15 (11): 29569–29593.
- 66 Vashist, S.K., Schneider, E.M., and Luong, J.H.T. (2014). Commercial smartphone-based devices and smart applications for personalized healthcare monitoring and management. *Diagnostics* 4 (3): 104–128.
- 67 Dong, M., Wu, J., Ma, Z. et al. (2017). Rapid and low-cost CRP measurement by integrating a paper-based microfluidic immunoassay with smartphone (CRP-chip). *Sensors (Basel)* 17 (4), pii: E684.
- 68 Hou, Y., Wang, K., Xiao, K. et al. (2017). Smartphone-based dual-modality imaging system for quantitative detection of color or fluorescent lateral flow immunochromatographic strips. *Nanoscale Res. Lett.* 12: 291.
- 69 Lee, S., Kim, G., and Moon, J. (2013). Performance improvement of the one-dot lateral flow immunoassay for Aflatoxin B1 by using a smartphone-based reading system. *Sensors (Basel)* 13 (4): 5109–5116.
- 70 Lee, L.G., Nordman, E.S., Johnson, M.D., and Oldham, M.F. (2013). A low-cost, high-performance system for fluorescence lateral flow assays. *Biosensors* 3 (4): 360–373.
- 71 Rasooly, R., Bruck, H.A., Balsam, J. et al. (2016). Improving the sensitivity and functionality of mobile webcam-based fluorescence detectors for point-of-care diagnostics in global health. *Diagnostics* 6 (2), pii: E19.
- 72 Xu, H., Mao, X., Zeng, Q. et al. (2009). Aptamer-functionalized gold nanoparticles as probes in a dry-reagent strip biosensor for protein analysis. *Anal. Chem.* 81 (2): 669–675.
- 73 Liu, G., Mao, X., Phillips, J.A. et al. (2009). Aptamer-nanoparticle strip biosensor for sensitive detection of cancer cells. *Anal. Chem.* 81 (24): 10013–10018.
- 74 Ahmad Raston, N.H., Nguyen, V.-T., and Gu, M.B. (2017). A new lateral flow strip assay (LFSA) using a pair of aptamers for the detection of Vaspin. *Biosens. Bioelectron.* 93: 21–25.
- 75 Bruno, J.G., Carrillo, M.P., Richarte, A.M. et al. (2012). Development, screening, and analysis of DNA aptamer libraries potentially useful for diagnosis and passive immunity of arboviruses. *BMC Res. Notes* 5 (1): 633.
- 76 Minagawa, H., Onodera, K., Fujita, H. et al. (2017). Selection, characterization and application of artificial DNA aptamer containing appended bases with sub-nanomolar affinity for a salivary biomarker. *Sci. Rep.* 7: 42716.
- 77 Jauset-Rubio, M., Svobodova, M., Mairal, T. et al. (2016). Aptamer lateral flow assays for ultrasensitive detection of beta-conglutin combining recombinase polymerase amplification and tailed primers. *Anal. Chem.* 88 (21): 10701–10709.
- 78 Wang, L., Chen, W., Ma, W. et al. (2011). Fluorescent strip sensor for rapid determination of toxins. *Chem. Commun.* 47 (5): 1574–1576.

- 79 Wang, L., Ma, W., Chen, W. et al. (2011). An aptamer-based chromatographic strip assay for sensitive toxin semi-quantitative detection. *Biosens. Bioelectron.* 26 (6): 3059–3062.
- 80 Zhou, W., Kong, W., Dou, X. et al. (2016). An aptamer based lateral flow strip for on-site rapid detection of ochratoxin A in *Astragalus membranaceus*. *J. Chromatogr. B, Anal. Technol. Biomed. life Sci.* 1022: 102–108.
- 81 Shim, W.B., Kim, M.J., Mun, H., and Kim, M.G. (2014). An aptamer-based dipstick assay for the rapid and simple detection of aflatoxin B1. *Biosens. Bioelectron.* 62: 288–294.
- 82 Cheung, S.F., Cheng, S.K.L., and Kamei, D.T. (2015). Paper-based systems for point-of-care biosensing. *J. Lab. Autom.* 20 (4): 316–333.
- 83 Bruno, J.G. (2014). Application of DNA aptamers and quantum dots to lateral flow test strips for detection of foodborne pathogens with improved sensitivity versus colloidal gold. *Pathogens (Basel, Switzerland)* 3 (2): 341–355.
- 84 Liu, J., Mazumdar, D., and Lu, Y. (2006). A simple and sensitive “dipstick” test in serum based on lateral flow separation of aptamer-linked nanostructures. *Angew. Chem. Int. Ed. Engl.* 45 (47): 7955–7959.
- 85 Shen, G., Zhang, S., and Hu, X. (2013). Signal enhancement in a lateral flow immunoassay based on dual gold nanoparticle conjugates. *Clin. Biochem.* 46 (16–17): 1734–1738.
- 86 Qin, C., Wen, W., Zhang, X. et al. (2015). Visual detection of thrombin using a strip biosensor through aptamer-cleavage reaction with enzyme catalytic amplification. *Analyst* 140 (22): 7710–7717.
- 87 Adhikari, M., Strych, U., Kim, J. et al. (2015). Aptamer-phage reporters for ultrasensitive lateral flow assays. *Anal. Chem.* 87 (23): 11660–11665.
- 88 Ozalp, V.C., Cam, D., Hernandez, F.J. et al. (2016). Small molecule detection by lateral flow strips via aptamer-gated silica nanoprobe. *Analyst* 141 (8): 2595–2599.
- 89 Fang, Z., Wu, W., Lu, X., and Zeng, L. (2014). Lateral flow biosensor for DNA extraction-free detection of salmonella based on aptamer mediated strand displacement amplification. *Biosens. Bioelectron.* 56: 192–197.
- 90 Wu, W., Zhao, S., Mao, Y. et al. (2015). A sensitive lateral flow biosensor for *Escherichia coli* O157:H7 detection based on aptamer mediated strand displacement amplification. *Anal. Chim. Acta* 861: 62–68.
- 91 Takemura, K., Wang, P., Vorberg, I. et al. (2006). DNA aptamers that bind to PrP(C) and not PrP(Sc) show sequence and structure specificity. *Exp. Biol. Med. (Maywood)* 231 (2): 204–214.

11

Development of Aptamer-Based Non-labeling Methods

Huajie Gu, Liling Hao, and Zhouping Wang

Jiangnan University, School of Food Science and Technology, No. 1800 Lihu Avenue, Wuxi 214122, PR China

11.1 Introduction

According to whether the signal labels are introduced or not, detection methods can be divided into two types. One type is the labeling method, such as enzyme-linked assay, fluorescent assay, chemiluminescent assay, and so on. Another type is the non-labeling method, such as surface plasmon resonance (SPR) method, quartz crystal microbalance (QCM) method, isothermal titration calorimetry (ITC) method, and so on. These non-labeling methods have been widely used to determine molecular interactions. Therefore, they were originally employed to measure the binding affinity between aptamers and targets. Recently, more and more researchers have applied these methods for quantitative detection of analytes due to their properties of non-labeling and high sensitivity. The greatest advantage of the non-labeling method is that there is no need to label the aptamer, and thus it can avoid making any change of the aptamer. As is known, compared with only the aptamer itself, the change of aptamer may cause some variations in its secondary or tertiary structure. And some of the variations may have a serious effect on the affinity and specificity of the aptamer. In addition, some large-molecule labeling, like enzyme labeling, may induce steric-hindrance effect which will influence the recognition or association between target and aptamer. So the non-labeling methods have shown great prospect in the detection. The biggest challenge of these non-labeling methods was the requirement of more complex or special instruments. But once suitable non-labeling detection instruments, even handheld equipment, are developed, the non-labeling method will be more suitable for real-time monitoring.

Herein, we focus on these mainstream non-labeling methods, including SPR, QCM, ITC, and another frontier technique, MicroScale Thermophoresis (MST). Their principles and applications in analytical detection and binding affinity are introduced in this chapter.

11.2 Surface Plasmon Resonance (SPR)-Based Aptasensor

11.2.1 Introduction

SPR-based sensors have been commercialized due to their fast label-free detection with minimum requirement of analyte medium for sensing. The SPR technique utilizes evanescent waves generated at the core–metal interface to excite surface plasmons at the metal–dielectric (sensing medium) interface. The ability to immobilize bioreceptors easily and with much better stability over metal film facilitates its application in the biomedical field. The sensitivity of SPR-based fiberoptic sensors can be improved by modifications in their geometry, doping in layers, and addition of high index layers [1–3].

When p-polarized light, under conditions of total internal reflection (TIR), strikes an electrically conducting gold layer at the interface between two media with different refractive indices (RIs), e.g. the glass of a sensor surface (high RI) and a buffer (low RI), SPR occurs. The phenomenon of SPR was first observed by Wood [4] in 1902. After that, the development of SPR was stagnant until Kretschmann put forward the Kretschmann–Reather configuration in 1968 [5, 6].

11.2.2 The Principle of SPR Technique

The principle of SPR sensing can be described by the Kretschmann–Reather configuration, which is most commonly adopted. In this SPR system, an excitation light source, a prism, and a metallic film (~50 nm) coated on the prism or glass are the main components. The terms “surface plasmons” and “polaritons” are assigned to some quasi-particles exhibiting wave–particle duality (as the photons and the phonons), which primarily exist on the surface of substances containing abundant free electrons, or metals [7]. Plasmon refers to the oscillation of free electron density with respect to the fixed positive ions in a metal. The term “surface plasmon” designates the charge density wave propagating along the metal’s surface [8]. The interaction of photons hitting the metal surface with the surface plasmons yields the so-called surface plasmon polaritons (SPPs), which are entangled quasi-particles composed of both surface plasmons and photons [9].

When an incident light of p-polarization is shined from an optically denser medium (glass) onto an optically thinner medium (gas or water), total reflection will occur with the incident angle exceeding a critical value. The incident light produces an evanescent wave that penetrates into the thinner medium with a depth of approximately half of the wavelength, and then returns to the denser medium [8]. So the changes of RI of the sensing medium can cause SPR signal changes. In an actual instrument, a thin film of metal was used instead of some cladding of the fiber, and the sensing medium is kept around the metal layer. The changes in the sensing medium can affect the properties of the light transmitting through one end of the fiber. And the change in intensity or spectrum can be measured and then the changes in sensing medium can be determined [10].

Localized surface plasmon resonance (LSPR) is created when incident wavelength matches with the collective oscillations of the electron excited by the incident light in noble metal nanostructures [11]. The resonance generates sharp peaks in the extinction spectrum that are sensitive to the dielectric of the medium on the surface of the nanostructure. Thus, LSPR can recognize and characterize macromolecules without prism configuration. Different from the conventional SPR, long-range surface plasmon resonance (LRSPR) is generated when a buffer medium is introduced between the prism and the metallic layer, and in which the RI is similar to the analyte. Compared to conventional SPR, LRSPR sensors have significantly improved sensitivity and applicability due to their sharper angular resonance curve, deeper depth of penetration (~ 1000 nm), and higher resolution of RI [10].

There is a specific angle at which SPPs can be excited and resonated (the SPR angle) for a given monochromatic light source. At settled optical and material conditions, the SPR angle relies only on the RI of the medium (or dielectric constant) [8, 12]. The RI of the contacting dielectric medium is one of the most sensitive variables correlated with near-field phenomena, such as transport, temperature variation, evaporation, chemical reactions, or ligand–receptor binding [9, 13, 14]. For an SPR sensor, the sensitivity is defined by the ratio of the change in sensor output to the change in the quantity to be measured (the RI), while the resolution defines the smallest change in the RI that produces a detectable change in the sensor output.

11.2.3 The Classification of SPR Biosensors

There are four main modulations in SPR sensors including angle modulation, wavelength modulation, amplitude modulation, and phase modulation [15, 16], and the principle is illustrated in Figure 11.1.

11.2.3.1 SPR Biosensors Based on Angular Modulation

Angular modulation is the most commonly used mode, and its principle can be described as follows. When SPR occurs, there is an SPR angle and the identification of the angle is characteristic of the prism configuration. The metallic film

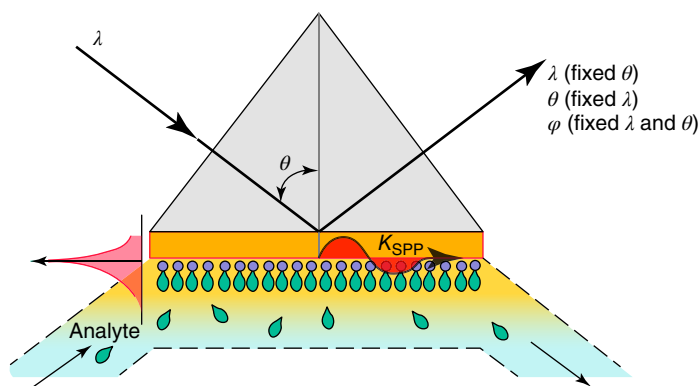


Figure 11.1 Interrogation modes for commercial surface plasmon resonance (SPR) instruments. Source: Kabashin et al. 2009 [17]. Reprinted with permission of OSA Publishing.

surface is irradiated with monochromatic light and scanned for a certain range angle. There the angular scanning is achieved (i) using a scanning source and (ii) using a rotating light source or prism with a light at a specific angle. For a fixed source, the beam of light has a divergent angle [18, 19].

11.2.3.2 SPR Biosensors Based on Wavelength Modulation

In the wavelength modulation mode, the angle of the incident light is fixed at a certain value and the wavelength of reflected light is modulated. The resonant condition is achieved in a prism configuration through attenuated total reflection (ATR). The reflected intensity dip is measured vs the change in the RI over a range of incident wavelengths [20].

11.2.3.3 SPR Biosensors Based on Amplitude Modulation

In the amplitude modulation mode, incidence angle and wavelength are fixed, and the changes in the resonance intensity can cause the RI variation, which can be detected. The drawback of this approach is given by the low sensitivity and resolution, because the output noise and resolution increase with the noise generated by the light source [19]. In the surface plasmon resonance imaging (SPRI) system, this mode is usually used; the reflectivity of monochromatic incident p-polarized light at a fixed angle is determined, unlike the scanning angle SPR or scanning wavelength SPR (traditionally termed “SPR spectroscopy”) [21].

11.2.3.4 SPR Biosensors Based on Phase Modulation

Under SPR, the phase of light can cause a sharp dip in the angular dependence of the phase on the p-polarized light. The “probe” beam and the “reference” beam are introduced in this mode [17]. The phase shifts, $\Delta\varphi$, due to interference are observed through spatial displacement of the light beam. The phase shift under SPR conditions, $\Delta\varphi_{\max}$, produces a change in the RI (n) of the medium, so that the phase derivative, $\Delta\varphi/\Delta n$, can be measured [22]. Maximal phase variations occur in the very dip of the SPR curve, where the vector of the “probe” electric field is maximal, whereas maximal amplitude changes are observed on the resonance slopes; thus, the sensitivity of the phase to RI variations is at least 10 times larger than the sensitivity of amplitude to RI changes [22, 23]. Phase noises are orders of magnitude lower compared to amplitude ones, providing a better signal-to-noise ratio [17]. The phase modulation can achieve a high sensitivity and is better fitted for SPRI and multiplex analysis with parallel detection of thousands of channels [24]. However, the phase modulation systems are more complex, and they are not amenable for point-of-care testing (POCT) platforms [19, 25].

11.2.4 The Application of Aptamer-Based SPR Technique

Due to the label-free analysis mode, the SPR system is real time, rapid, and sensitive, and it consumes minimal sample. The first application of an SPR-based sensor was used to monitor the biomolecular interaction [26]. With the development of the SPR technique, it has been widely used to determine the binding specificity between two molecules, the kinetic parameters of association and dissociation processes, cell adhesion and migration, and so on. In addition, as an advanced

and developed optical label-free biosensor, SPR has been used for powerful detection with vast applications in environmental protection, biotechnology, medical diagnostics, drug screening, food safety, and security. And in the application of binding aptamer with SPR technique, the binding affinity measurement as well as target analysis and detection are the most commonly used.

11.2.4.1 Determination of the Affinity of Aptamers

Characterization of aptamer binding properties including affinity, kinetics, specificity, ion dependence, and buffer sensitivity is critical for studying aptamer molecular recognition. As SPR strategy is label-free, it can determine the binding property of aptamer with targets avoiding the change of the aptamer–ligand binding interaction. For example, the affinity and selectivity of retinol-binding protein 4 (RBP4) with its aptamer were determined by SPR [27]. In this study, the aptamer was immobilized on a bare gold chip; after adding a series of concentrations of RBP4, the dissociation constant was determined via the response units (RUs) with RBP4 (0–2 μM). SPR-based biosensors can also monitor the interaction kinetics of aptamer with thrombin in order to detect a consistent response at a certain thrombin concentration for the aptamer [28]. And the thrombin-aptamer reaction ratio mode can also be forecast. In addition, SPR-based biosensors can determine the kinetics of the aptamer with almost all kinds of analytes including prostate-specific antigen [29], ochratoxin A (OTA) [30], calmodulin (CaM) [31], cancer antigen 125 (CA125) [32], and so on.

11.2.4.2 Detection Analyte Concentrations

The SPR technique provides the opportunity to develop an optimized protocol for single-stranded DNA (ssDNA) conjugation on SPR gold film by simple avidin–biotin basis. SPR promotes the adoption of aptamers as a versatile molecular probe for SPR biosensor generation and signal amplification development. Similarly, SPR-based detection methods can detect almost all kinds of analytes including bacteria, protein, viruses, and small molecules [33–36]. For example, Wang et al. [37] reported an SPR aptasensor to detect *Salmonella typhimurium* with a limit of detection (LOD) of 3×10^4 cfu ml⁻¹. In the report, the *S. typhimurium* aptamer was assembled on the surface of the SPR sensor film, and the interactions between the bacteria and the aptamers on the substrate were carefully investigated by both single-molecule atomic force microscopy (AFM) and SPR measurements. Mihai et al. [38] fabricated an aptasensor with SPR detection that allowed the determination of lysozyme, with high accuracy, good sensitivity, and a detection limit of 2.4 nM for spiked red and white wines. This aptasensor is useful to monitor the lysozyme levels during winemaking; the principle of the aptasensor is shown in Figure 11.2.

Zhu et al. [39] reported an SPR aptasensor for the detection of OTA using a direct binding assay by immobilizing anti-OTA aptamer on the sensor chip. In the report, streptavidin was first immobilized on the chip, and the biotin–aptamer was captured through streptavidin–biotin interaction. The biosensor exhibited a linear range from 0.094 to 10 ng ml⁻¹ of OTA with a lower detection limit of 0.005 ng ml⁻¹. Nguyen et al. [36] reported a sandwich-type SPR-based biosensor

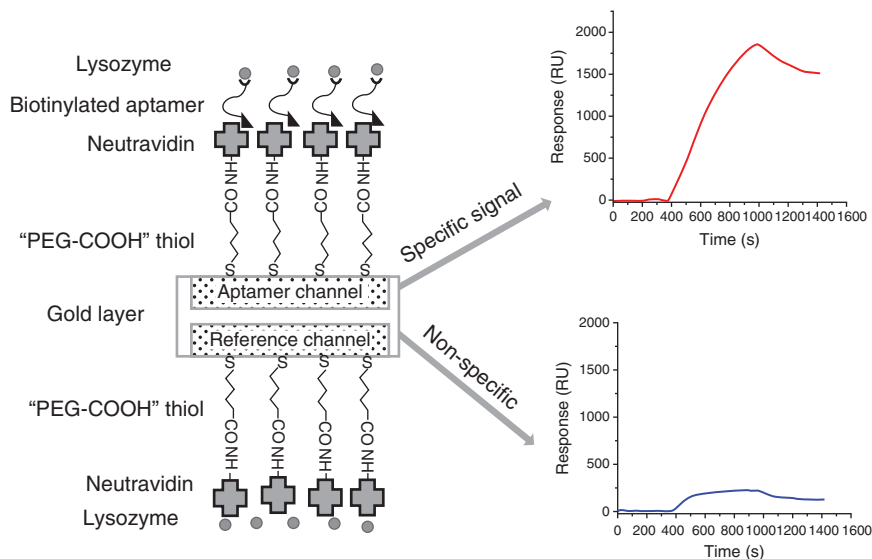


Figure 11.2 Design of the aptasensor for lysozyme detection in wines. Source: Mihai et al. 2015 [38]. Reprinted with permission of Elsevier.

for the detection of H₅Nx whole viruses (Figure 11.3). The authors first screened and characterized for whole avian influenza (AI) viruses, H₅Nx, by using the multi-graphene oxide-systemic evolution of ligands by exponential enrichment (GO-SELEX) method. Aptamers IF10 and IF22 were found to bind the H₅N₁ virus simultaneously and confirmed to bind the different sites of the same H₅N₁ whole virus. Therefore, this pair of aptamers, IF10 and IF22, was successfully applied to develop the sandwich-type SPR-based biosensor assay which is rapid and accurate for the detection of AI whole virus from H₅N₁-infected feces samples. The minimum detectable concentration of H₅N₁ whole virus was found to be 200 EID₅₀ m⁻¹.

In order to improve the sensitivity, signal amplification was usually introduced to the SPR detection system. The most primitive signal amplification mechanism is based on the specific combination of biotin and avidin. With the development of nanotechnology, the combination of some kinds of nanomaterials and SPR were also used. A new sandwich assay for tetracycline (TC) involving a DNA aptamer and antibody pair was demonstrated in conjunction with gold nanostar (GNS)-enhanced SPR to achieve detection in the low attomolar range [40]. GNS particles were covalently functionalized with the antibody probe (antiTC) and integrated into a surface sandwich assay in conjunction with an SPR gold chip modified with the TC-specific aptamer (Figure 11.4). After it was demonstrated that both affinity probes can bind simultaneously to TC, optimization of the assay was performed using either antiTC only or GNS-antiTC conjugates to interact with aptamer/TC complexes present on the chip surface. The LOD of TC was as low as 10 aM.

Besides, some molecular biology techniques, such as rolling circle amplification (RCA) and enzyme cycle amplification, were also usually used to amplify

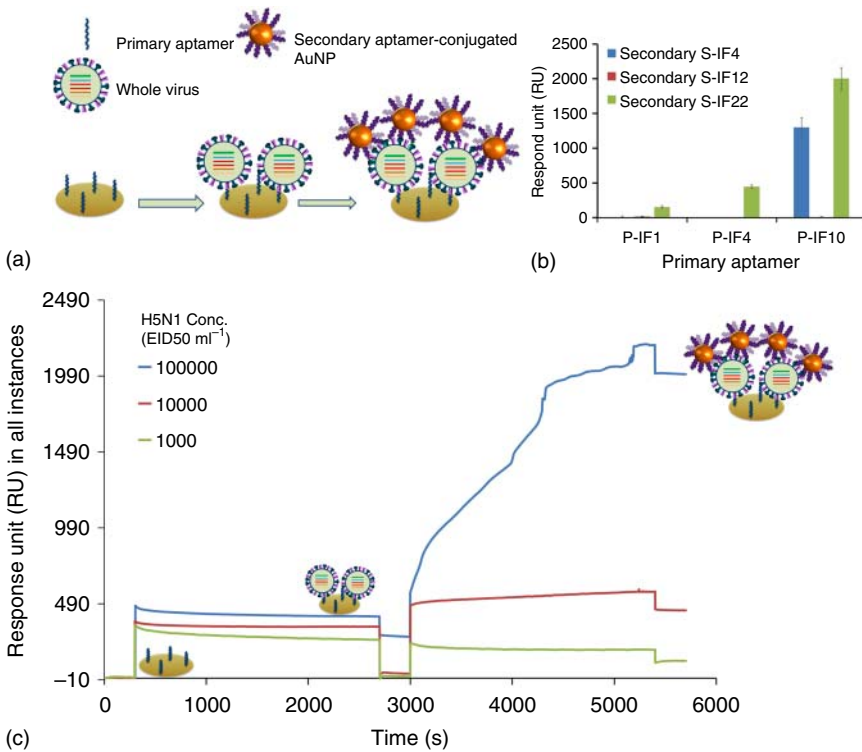


Figure 11.3 Dual aptamer using the combination of SPR assay and secondary aptamer-conjugated AuNP. (a) The scheme depicts the principal of SPR assay using secondary aptamer conjugated-AuNP. (b) The pair of aptamers IF1-IF12, IF4-IF22, IF10-IF12, and IF10-IF22 were rechecked using aptamer conjugated-AuNP. (c) The dose-dependent binding assays of the pair of aptamers IF10-IF22 using SPR-AuNP. Source: Nguyen et al. 2016 [36]. Reprinted with permission of Elsevier.

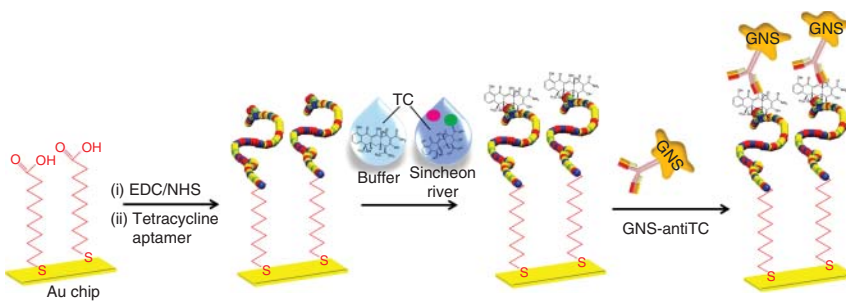


Figure 11.4 Schematic overview of strategy for TC detection. The TC aptamer was first immobilized on an SPR chip, followed by the covalent attachment of aptamer probes. TC binding was performed in both buffer and Sincheon river samples, followed by the subsequent binding of GNS-antiTC's for further SPR signal amplification. Source: Kim and Lee 2017 [40]. Reprinted with permission of American Chemical Society.

the signal [41–46]. Xiang et al. [45] developed an SPR DNA biosensor method using surface-anchored RCA and gold nanoparticle (AuNP)-modified probes to isothermally detect multiple point mutations associated with drug resistance in multidrug-resistant *Mycobacterium tuberculosis* (MDRTB) (Figure 11.5). A set of probes contains an allele-specific padlock probe (PLP), a capture probe, and an AuNP. The linear PLPs, circularized by ligation upon the recognition of the point mutation on DNA targets, hybridize to the capture probes via the specific tag/anti-tag recognition. Upon recognition, each point mutation is identified by locating into the corresponding channel on the chip. Then the immobilized primer (capture probe)–template (circular PLP) complex is amplified isothermally as RCA and further amplified by AuNPs. The RCA products immobilized on the chip surface cause great SPR angle changes consequently. The 5 pM of synthetic oligonucleotides and 8.2 pg ul⁻¹ of genomic DNA from clinical samples can be detected by the method.

Yao et al. [47] combined the advantage of the aptamer technique with the amplifying effect of enzyme-free signal amplification and AuNPs to design a sensitive SPR aptasensor for detecting small molecules. This detection system consists of an aptamer, a detection probe (c-DNA1) partially hybridizing to the aptamer strand, an AuNP-linked hairpin DNA (Au-H-DNA1), and a thiolated hairpin DNA (H-DNA2) previously immobilized on an SPR gold chip (Figure 11.6). In the absence of a target, the H-DNA1 possessing a hairpin structure cannot hybridize with H-DNA2 and thereby AuNPs will not be captured on the SPR gold chip surface. In the presence of a target, the detection probe c-DNA1 is forced to dissociate from the c-DNA1/aptamer duplex by the specific recognition of the target to its aptamer. The released c-DNA1 hybridizes with Au-H-DNA1 and opens the hairpin structure, which accelerates the hybridization between Au-H-DNA1 and H-DNA2, leading to the displacement of the c-DNA1 through a branch migration process. The released c-DNA1 then hybridizes with another Au-H-DNA1 probe, and the cycle starts anew, resulting in the continuous immobilization of Au-H-DNA1 probes on the SPR chip. This generates a significant change in SPR signal due to the electronic coupling interaction between the localized surface plasma of the AuNPs and the surface plasma wave. With the use of adenosine as a proof-of-principle analyte, this sensing platform can detect adenosine specifically with a detection limit as low as 0.21 pM.

Standard SPR biosensor instrumentation with 3–4 flow cells on a single sensor chip can be used in high-throughput screening (HTS) and multiplex analyses. Very recently, a modified version of the SPR design, called SPRI, was developed to simultaneously process hundreds or thousands of samples. SPRI systems showed great prospect in the HTS of drugs and biomarkers, as well as in multiplex analyses which represents an important step forward in SPR analysis. In an SPRI system, a coherent polarized light beam is used instead of polychromatic light. The reflected light is captured by a charge-coupled device (CCD) camera for further imaging analysis (Figure 11.7) [48]. The high-resolution CCD camera provides images across the array format in real time with up to hundreds of active spots. Unlike conventional SPR, the measurement conducted by SPRI is stringently performed at a constant wavelength and a constant angle [49]. Thus,

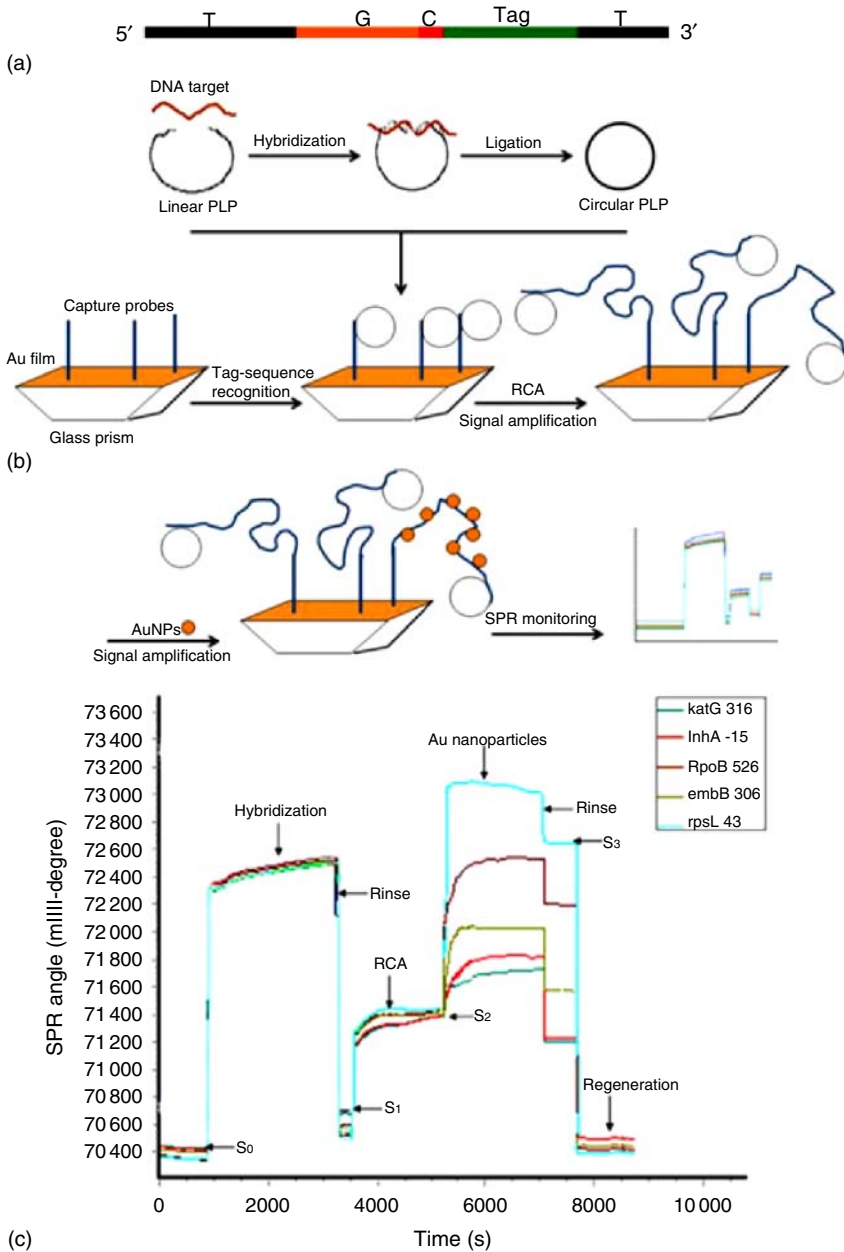


Figure 11.5 (a) PLP design. The PLP contains target-complementary sequence (T), general sequence (G), and tag sequence (Tag). Tag sequence is unique for each PLP and complementary to the capture probe immobilized on the chip surface. The general sequence provides the repeats on the RCA products for AuNP binding. "C" means the cutting site recognized by restriction endonuclease to remove the RCA products from the chip surface after the detection is completed. (b) Schematic representation of the proposed detection strategy. (c) Real-time detection of multiple point mutations by the SPR sensor. Source: Xiang et al. 2013 [45]. Reprinted with permission of Elsevier.

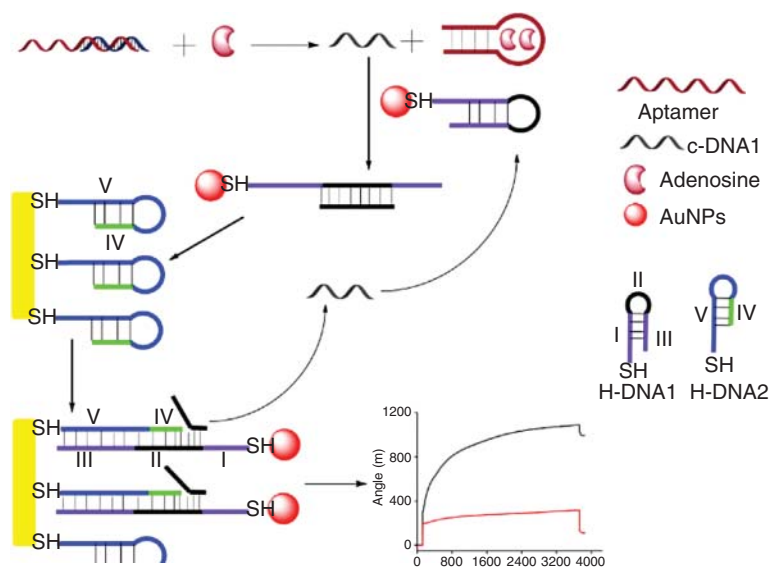


Figure 11.6 Schematic illustration of AuNPs and strand displacement cycle signal amplification-based SPR assay for the detection of adenosine. Source: Yao et al. 2015 [47]. Reprinted with permission of Elsevier.

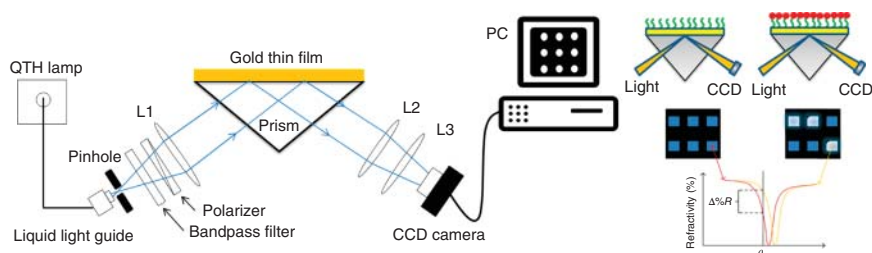


Figure 11.7 General principle of SPR imaging [48].

changes in reflected light intensity are proportional to any variation in the RI near the metal surface [50]. Abadian et al. [51] applied SPRI for the first time to image the processes of *Escherichia coli* and *Pseudomonas aeruginosa* cellular movement, attachment, and growth across a large surface. This approach offers important implications for monitoring macromolecular adsorption, microbial cell adhesion and movement, and biofilm formation.

11.2.5 Summary and Prospects of SPR Aptasensors

The SPR technique has been proved to be one of the most versatile frameworks for aptasensor applications in medical, biology, environment, and food safety areas. SPR aptasensors provide excellent analytical performance in terms of high sensitivity, short time consumed, and good reproducibility with its label-free approach. However, one challenge for SPR technology is that point-of-care

(POC) diagnostics has not been completely realized [52]. And, current SPR instruments are still bulky and costly, which remains an obstacle to the commercialization of SPR technology. In the next few years, more research on the development of innovative chip chemistry in combination with amplification schemes and miniaturization are needed to make SPR an irreplaceable tool for routine clinical analysis and POC diagnostics.

11.3 Quartz Crystal Microbalance (QCM)-Based Aptasensor

11.3.1 Introduction

QCM is a simple, cost-effective, high-resolution mass sensing technique based on the piezoelectric effect. The advantages of QCM-based biosensors are as follows: first, QCM biosensors rely on the varieties of mass and thus can realize non-labeling. Second, different from optical non-labeling biosensors, QCM can be used in any solution such as optically opaque solution media via the piezoelectric mechanism. Third, the technique is capable of detecting subtle changes in the solution–surface interface that can be due to density–viscosity changes in the solution, viscoelastic changes in the bound interfacial material, and changes in the surface free energy, to name a few. Fourth, the QCM technique can combine well with other techniques such as the electrochemical technique to form electrochemical quartz crystal microbalance (EQCM) to make the analysis more convenient.

The signal transduction mechanism of the QCM technique relies on the piezoelectric effect in quartz crystals, first discovered in 1880 by the Curie brothers, via a pressure effect on quartz [53]. A change in inertia of a vibrating crystal was then shown by Lord Rayleigh to alter its resonant frequency [54]. Important subsequent developments were good crystal stability through the use of electric resonators [55] and room-temperature-stable AT-cut crystals [56]. In 1959, the QCM was first used in a sensing mode when Sauerbray reported a linear relationship between the f decrease of an oscillating quartz crystal and the bound elastic mass of deposited metal [57]. In the 1980s, solution-based QCM developed as the new oscillator technology advanced to measure changes in frequency that could be related to changes in viscosity and density in highly damping liquid media [58, 59]. The recent success of the QCM technique is due to its ability to sensitively measure mass changes associated with liquid–solid interfacial phenomena, as well as to characterize energy dissipative or viscoelastic behavior of the mass deposited upon the metal electrode surface of the quartz crystal.

11.3.2 The Principle of QCM Technique

For the situation of pure elastic mass added to the surface, the well-known linear Sauerbray equation was first observed [57] and used to precisely quantify, with nanogram sensitivity, the quantity of elastic mass added to the surface:

$$\Delta f = -2\Delta m f^2 / A(\mu\rho_q)^{0.5} = -C_f \Delta m$$

where C_f is the measured resonant frequency decrease (Hz), f is the intrinsic crystal frequency, Δm is the elastic mass change (g), A is the electrode area (0.196 cm^2 in many applications), ρ_q is the density of quartz (2.65 g cm^{-3}), and μ is the shear modulus ($2.95 \times 10^{11} \text{ dyn cm}^{-2}$). This results in C_f , the integrated QCM sensitivity, having a value of 0.903 Hz ng^{-1} for a $\sim 9 \text{ MHz}$ crystal. From the Sauerbrey equation, one may see that an increase in mass bound elastically to the electrode surface results in a linear decrease in the oscillation frequency of the quartz crystal. It is important to note that the change in mass, Δm , is the most significant term in the Sauerbrey equation affecting the measured change in resonant frequency of the crystal, Δf . Given this integrated sensitivity level, nearly 1000 times greater than an electronic mass balance with a sensitivity of $0.1 \mu\text{g}$, this mass sensing technique has sometimes been termed the quartz crystal nanobalance.

Rodahl et al. [60] developed and commercialized quartz crystal microbalance with dissipation (QCM-D) monitoring technique, which is a connecting link between simple frequency determination and complex network analysis, and allows the simultaneous monitoring of the resonance frequency and the dissipation factor. In this technique, a frequency generator is used to excite a quartz plate. Then the source is switched off and the free decay of the quartz oscillation is recorded. This operation mode is repeated each second.

When QCM is used to monitor mass changes at electrode surfaces, it is frequently referred to as the EQCM. Briefly, the EQCM employs one of the excitation electrodes, which faces the solution, as a working electrode in a conventional electrochemical cell to study electron transfer processes in real time [61]. An important attribute of the EQCM is its ability to provide correlations between electrochemically induced mass changes at the electrode surface and the charge consumed in the process. Such measurements contribute to determine the deposit composition, its stoichiometry, and the optimization of the charge consumed.

11.3.3 The Application of Aptamer-Based QCM Technique

The QCM chip surface was easy to be modified by aptamers, which is convenient for the development of QCM aptasensors. QCM-based aptasensors can determine the affinity of aptamers with the targets as well as detecting the concentration of analytes. In particular, the label-free QCM technique is a powerful tool in biological binding phenomena with advantages, including high sensitivity and real-time measurement. The QCM has also been used as an active mode sensor for the direct detection of molecular interactions by oscillating the sensor surface and monitoring the acoustic emission produced by bond rupture [62].

11.3.3.1 Determination of the Affinity of Aptamers

Hianik et al. [63] developed a QCM method for detection of thrombin–aptamer interactions. Results showed that the aptamer configuration as well as variation in ionic strength and pH will affect the binding of thrombin to the aptamer. And the immobilization of aptamer by means of avidin–biotin technology revealed best results in sensitivity in comparison with immobilization utilizing dendrimers of the first generation and in comparison with chemisorption of aptamer to a

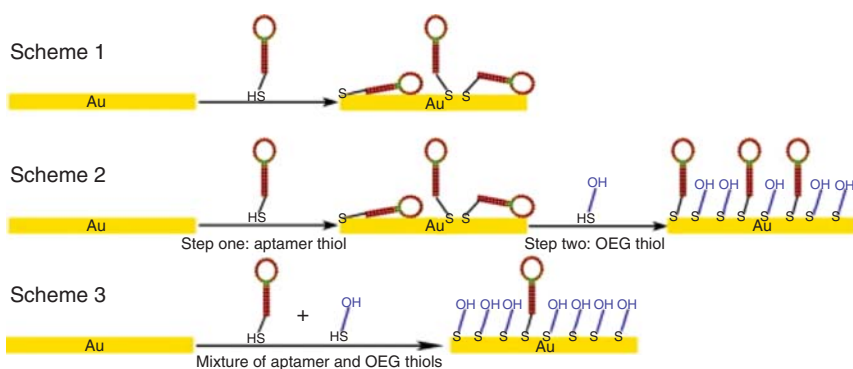


Figure 11.8 Schematic of different sensor configurations investigated. Source: Zhang et al. 2011 [64]. Reprinted with permission of Elsevier.

gold surface. Zhang and Yadavalli [64] reported on QCM measurements and AFM-based force spectroscopy studies to evaluate aptasensors fabricated by different modification strategies (Figure 11.8). Gold surfaces were modified with mixed self-assembled monolayers (SAMs) of aptamer and oligoethylene glycol (OEG) thiols ($\text{HS-C}_{11}(\text{EG})_n\text{-OH}$, $n = 3$ or 6) to impart resistance to nonspecific protein adsorption. By affinity analysis, we show that short OEG thiols have less impact on aptamer accessibility than longer chain thiols.

In addition, Wang et al. [65] used QCM to select aptamers against *S. typhimurium*, and determined the binding affinity of the candidates of aptamers (Figure 11.9). The advantage of QCM-based aptamer selection was that QCM can monitor the process of selection effectively.

11.3.3.2 Detection of Analyte Concentrations

QCM can detect almost all kinds of analytes, such as small molecules, metal ions, bacteria, cells, viruses, and so on. Because mass is the most obvious factor affecting the f of an oscillating crystal, many investigators design their systems in order to maximize the bound mass change to be detected. Often, the strategy will be to design a mass amplification feature into the signal to be transduced by the crystal. For example, if one is studying an enzyme biosensor immobilized on the QCM surface, an optimal sensitivity approach may be to use a substrate that, when catalytically converted to product by a high turnover number enzyme, forms an insoluble precipitated mass on the QCM surface, decreasing f significantly [66].

Yao et al. [67] developed a rapid method to measure immunoglobulin E (IgE) in human serum by use of a direct aptamer-based biosensor based on a QCM. An avidin monolayer was applied to immobilize aptamers specific for IgE on the gold surface of a quartz crystal. The frequency shifts (FSs) of the QCM were measured and related to IgE concentrations. The detection method demonstrated that aptamers were able to detect IgE with high specificity and sensitivity in 15 min. With the development of nanotechnology, nanoparticles with unique properties can be combined with QCM to make the detection method simple. A novel method for selective collection and detection of human acute leukemia cells was proposed using aptamer-conjugated magnetic beads

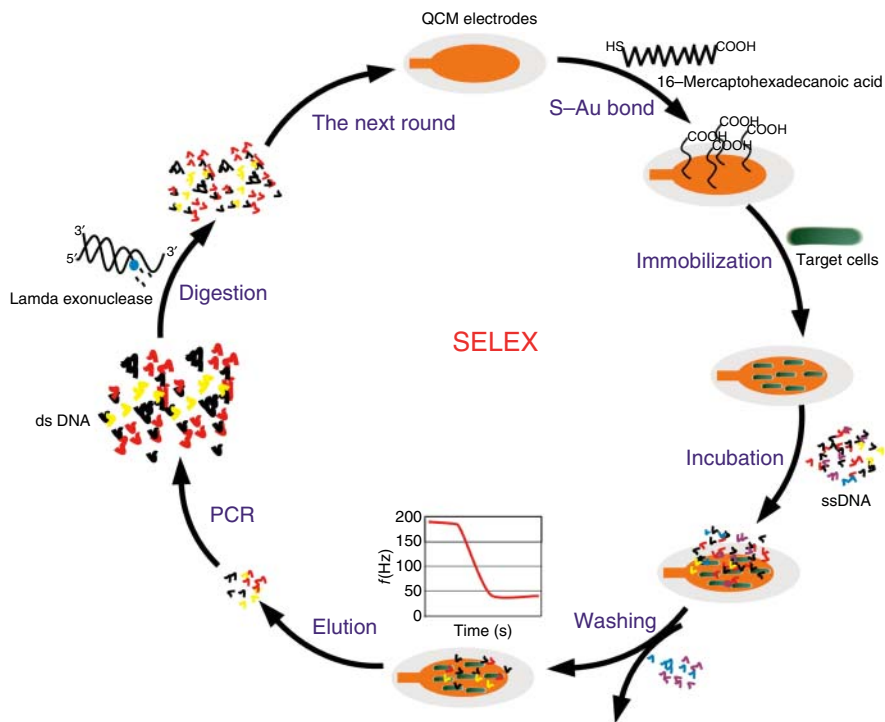
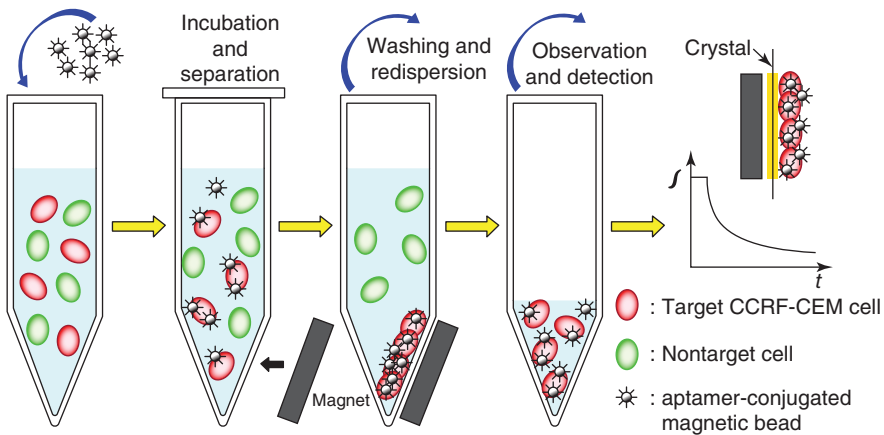


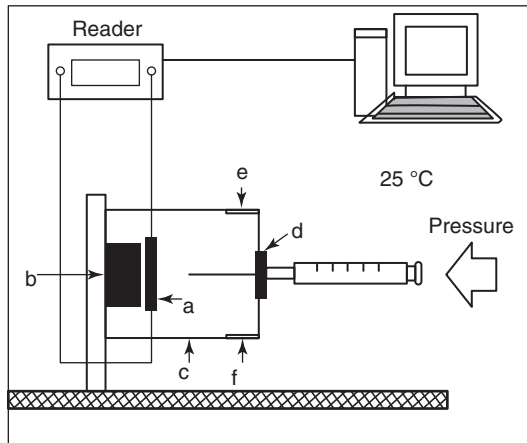
Figure 11.9 The selection process of DNA aptamers against *S. typhimurium* using the QCM-based SELEX. Source: Wang et al. 2017 [65]. Reprinted with permission of Elsevier.

and a magnet-QCM system [68] (Figure 11.10). The *sgc8c* aptamer-conjugated magnetic beads specifically binding to CCRF-CEM cells were used for target cell extraction from complex matrixes, and the magnet-QCM system was successfully applied for quantitative cell detection, requiring no further labeling of cells. The accumulation of magnetic beads-conjugated CCRF-CEM cells on a quartz crystal gold electrode surface under a magnetic field resulted in decreased resonant frequency. A linear relationship between the FS and cell concentration over the range of 1×10^4 – 1.5×10^5 cells ml^{-1} was obtained, with a detection limit of 8×10^3 cells ml^{-1} .

Nanoparticles were also introduced to the QCM system to improve the sensitivity of the detection method. A highly sensitive QCM-D biosensor for human α -thrombin was developed using aptamer-functionalized gold nanoparticles (Apt-AuNPs) for amplification [69] (Figure 11.11). Captured by immobilized aptamers, thrombin was determined on-line using Apt-AuNPs to enhance both frequency and dissipation signals. The fabricated sandwich of aptamer/thrombin/Apt-AuNPs on chip surface was confirmed by AFM. Compared to direct assay, the detection limit for thrombin was down to 0.1 nM, yielding about two orders of magnitude improvement in sensitivity. Shan et al. [70] reported that a signal-amplified aptamer-based QCM biosensor was developed for the selective and sensitive detection of leukemia cells (Figure 11.12). In this strategy, aminophenyl boronic acid-modified



(a)



a : Quartz crystal

b : Permanent magnet

c : Buffer room

d : Seal

e : Inlet

f : Outlet

Figure 11.10 (a) Schematic representation of the selective collection and detection of target CCRF-CEM cells on the magnet-QCM system using aptamer-conjugated magnetic beads. (b) Schematic diagram of the apparatus for magnet-QCM experiments. Source: Pan et al. 2010 [68]. Reprinted with permission of Elsevier.

gold nanoparticles (APBA-AuNPs), which could bind to cell membrane, were used for the labeling of cells followed by silver enhancement, through which significant signal amplification was achieved. Both the QCM and fluorescence microscopy results manifested the selectivity of the sensor designed. A good linear relationship between the frequency response and cell concentration over the range of $2 \times 10^3 - 1 \times 10^5$ cells ml^{-1} was obtained, with a detection limit of 1160 cells ml^{-1} .

Similar to SPR-based aptasensor, molecular biology techniques, such as circular nucleic acid strand-displacement polymerization technique and RCA

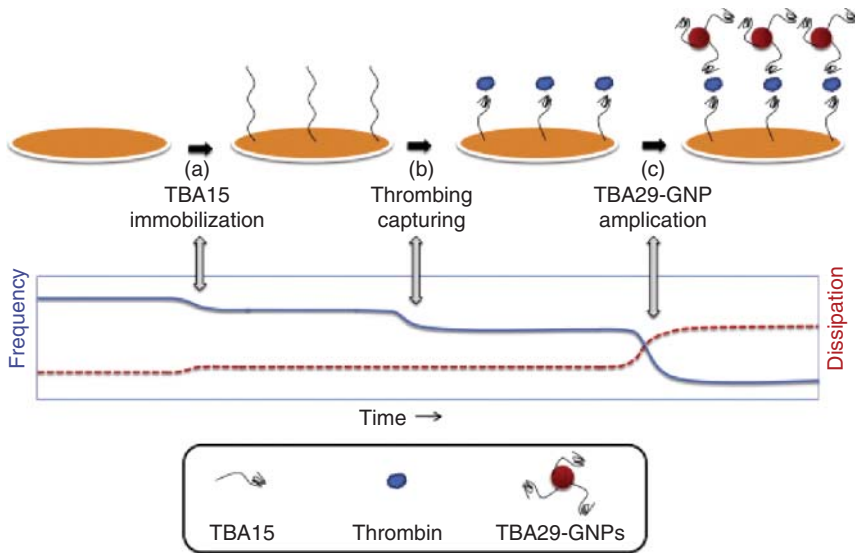


Figure 11.11 The schematic representation of the sandwich QCM-D biosensor for on-line detection of thrombin. The solid (dashed) curves show the corresponding frequency (dissipation) shift for the abovementioned three steps. Source: Chen et al. 2010 [69]. Reprinted with permission of Elsevier.

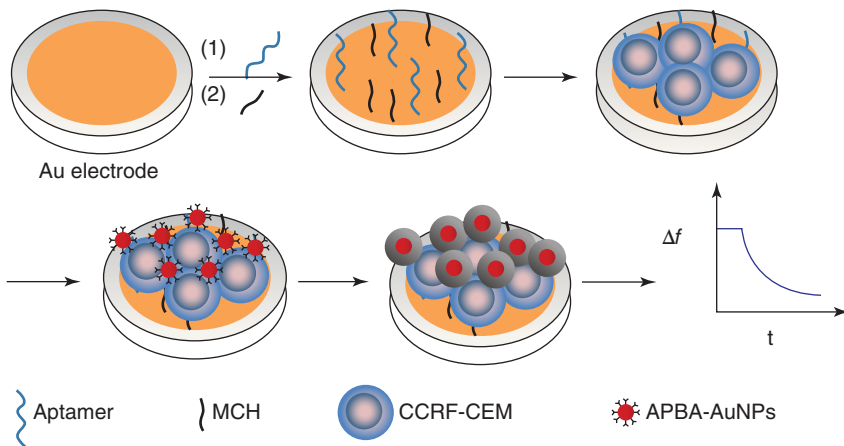


Figure 11.12 Schematic representation of the fabrication of the QCM biosensor for analysis of leukemia cells. Source: Shan et al. 2014 [70]. Reprinted with permission of Elsevier.

technique, were also introduced to QCM-based aptasensors. A simple and novel QCM assay is demonstrated to selectively and sensitively detect adenosine triphosphate (ATP) [71]. The amplification process consists of circular nucleic acid strand-displacement polymerization, aptamer recognition strategy, and nanoparticle signal amplification. With the involvement of an aptamer-based complex, two amplification reaction templates and AuNP-functionalized probes, the whole circle amplification process is triggered by the target recognition of ATP. As an efficient mass amplifier, AuNP-functionalized probes are introduced

to enhance the QCM signals. As a result of DNA multiple amplification, a large number of AuNP-functionalized probes are released and hybridized with the capture probes on the gold electrode. Therefore, the QCM signals are significantly enhanced, reaching a detection limit of ATP as low as 1.3 nM (Figure 11.13). He et al. [72] fabricated a QCM aptasensor combined with RCA and biobar-coded AuNP to detect the human thrombin, the linear relationship between the Δf and the logarithm of thrombin concentrations over a five-decade range from 1 aM to 0.1 pM was obtained, with the LOD of 0.8 aM.

In addition to the detection methods, some novel QCM instrumental approaches were also made to further improve the sensitivity of the detection. On the basis of the Sauerbrey equation [57], the straightforward route to improved sensitivity seems to be the use of high-frequency resonators, introduced first by Uttenthaler [73]. Such QCM resonators are based on a very thin (e.g. 8.3 μm for 200 MHz f_0) central part of the quartz disc surrounded by a thicker edge ring suitable for fixation in the flow cell. However, when operating in liquid, the theoretical gain in sensitivity is negatively influenced by the accompanying increase in noise due to the phase noise and less stable resonance at high frequencies. To solve this problem, a novel method based on phase shift at a fixed frequency near the resonance was developed by Montagnet

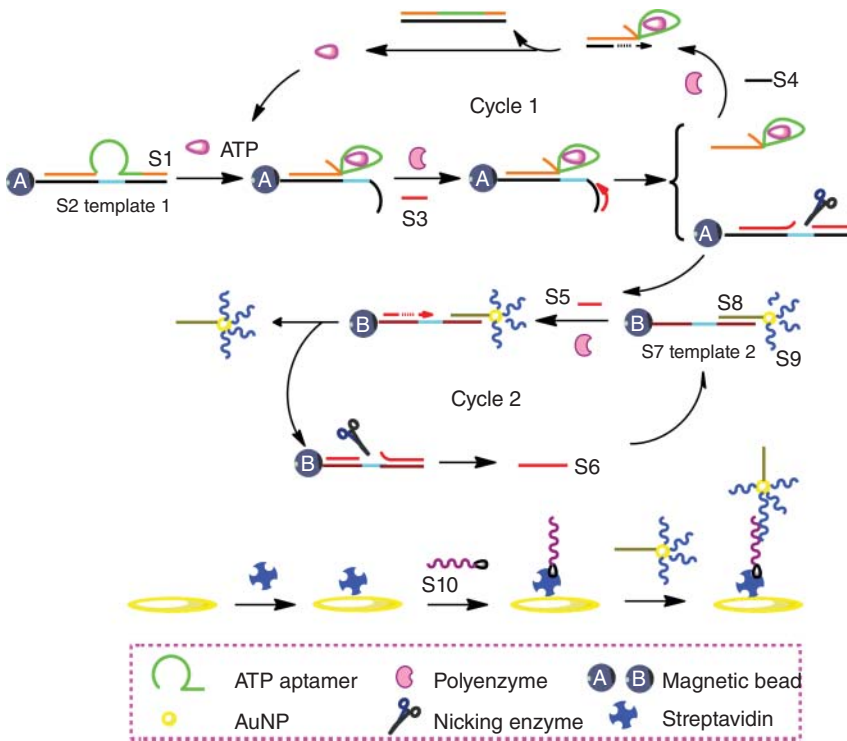


Figure 11.13 Schematic representation of ATP detection through DNAzyme-activated two-cycle amplification strategy based on the strand-displacement polymerization activity, which released AuNP-functionalized probes captured on the QCM biosensor. Source: Song et al. 2014 [71]. Reprinted with permission of Elsevier.

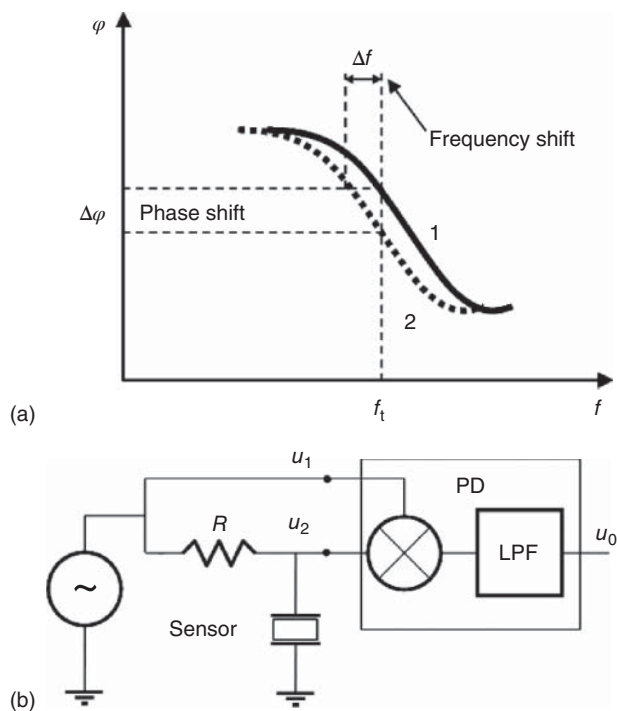


Figure 11.14 Concept of the novel QCM detector based on the phase shift measurements. The piezoelectric sensor is supplied with a constant frequency f_t within its resonant frequency band; the phase shifts resulting from surface interactions are then monitored using the circuit consisting of the highly stable source of interrogation voltage and mixer-based phase shift detector. Source: Montagut et al. 2011 [74]. Reprinted with permission of AIP Publishing LLC.

(Figure 11.14) [74]. This allowed improving the signal/noise ratio three times even for the common 10 MHz resonators. A more detailed comparison was realized for the piezoelectric immunosensor for the pesticide carbaryl. The achieved LODs for the phase shift method were 11 vs 0.14 ng ml⁻¹ when using 9 and 100 MHz resonators, respectively [75]. The electrothermal effect was employed to increase efficiency of affinity binding studies with QCM [76].

11.3.4 Summary and Prospect of QCM Aptasensors

The direct label-free and real-time monitoring of affinity interactions with piezosensors represents an economic alternative to the other often overpriced alternative systems. The valuable characteristics of binding reaction can be obtained easily and quickly. The piezoelectric system remains an open platform, and moderately skillful researchers can build the experimental devices themselves from components of the shell. This results in quite wide application fields. Furthermore, fruitful combination with other sensing technologies provides the route to innovative scientific achievements.

A high gain of sensitivity was achieved using the wireless electrodeless version of classic QCM [77]. Piezoelectric microelectromechanical resonators

are another promising system [78]. A “plastic” QCM alternative employed a polymer diaphragm polyvinylidene fluoride (PVDF) piezoelectric film sandwiched between gold electrodes; for detection of DNA, the mass sensitivity of $0.185 \text{ kHz } \mu\text{g}^{-1}$ was obtained (active area diameter of 5 mm, PVDF thickness 28 μm , resonance around 8.5 kHz) and the system operated in a flow-through mode [79]. Compared to classic quartz crystals, PVDF provides advantages such as low cost, light weight, simple fabrication, good stretch, and flexibility for operation in liquid.

To complete this technical part, one should perhaps mention the open QCM concept providing easily accessible and miniature piezoelectric detector based on the Arduino microcontroller platform well-known to hobbyists [80]. The very compact instrument is produced by the popular 3D printing process and perhaps opens a way to “home” piezoelectric biosensing compatible with the “point of-care” trends.

11.4 Isothermal Titration Calorimetry (ITC)

11.4.1 Introduction

ITC, which started around 25 years ago, is a classic biophysical technique used to determine reaction thermodynamic parameters of interactions quantitatively [81]. In 1990, Freire et al. published an article entitled “Isothermal titration calorimetry” and introduced this technique to researchers interested in studying binding interactions [82]. Since then, there has been an increasing number of research publications on ITC encouraged by the release of commercial instrumentation that made this method accessible to a wide population of scientists [83–85].

Compared with other methods that have been developed for analyzing molecular interaction, ITC is a unique approach because of its ability to provide quantitative thermodynamic information in a single experiment, including Gibbs free energy change (ΔG), enthalpy change (ΔH), entropy change (ΔS), binding constant (K), and so on. Because the heat exchange upon these interactions is a natural property, there is no requirement for modification of the molecules such as labeling or immobilization of the interacting molecules [86]. ITC relies only on detecting the heat involved during the molecular association [84]. So it is suitable for analyzing molecular interactions in a wide range of systems, such as protein–protein interactions [87], drug development [88], enzymatic kinetic studies [89], interactions between aptamers and targets [90], as well as many others.

11.4.2 The Principle of ITC Technique

A part of the beauty of ITC lies in its simplicity. The scheme of the standard ITC instrument is presented in Figure 11.15. A typical ITC instrument consists of two cells (sample cell and reference cell) placed inside an adiabatic jacket. The role of the reference cell is to follow heat changes produced by the buffer (solvent).

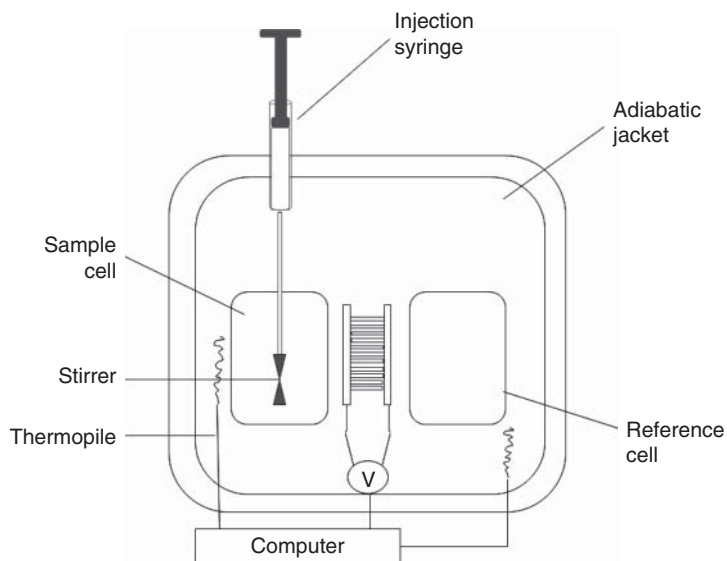


Figure 11.15 Schematic of the ITC instrument. Source: Kabiri and Unsworth 2014 [86]. Reprinted with permission of American Chemical Society.

A reactant is placed in a sample cell that is temperature controlled and coupled to a reference cell via a thermopile/thermocouple circuit. The solution of a ligand is then injected in small aliquots into the sample cell and the subsequent interaction between molecules will result in either heat emission (an exothermic reaction) or heat absorption (an endothermic reaction). The temperature difference between the sample and reference cells requires energy to maintain a constant temperature. This energy is then translated into heat change. The heat change will be measured with exquisite sensitivity (on the order of several hundred nanojoules) in a short time. The reaction heats tend to zero as the titration progresses, and the binding sites become saturated [81, 86]. Thermodynamic parameters which can be obtained with ITC are shown in Figure 11.16, including stoichiometry of the interaction (n), association constant (K_a)/dissociation constant (K_d), free energy (ΔG_b), enthalpy (ΔH_b), entropy (ΔS_b), and heat capacity of binding (ΔC_p). Average enthalpy and entropy of the ligand–reactant reactions can give an indication about the nature and type of the interaction. From the mentioned parameters, the Gibbs free energy of binding, ΔG , and the entropic contribution to the binding event ($-T\Delta S$) can be calculated [84, 91, 92].

11.4.3 Thermodynamic Parameters Obtained from ITC Experiment

K_a (K_d^{-1}) describes the ratio of concentration of a complex (R–L) at equilibrium for a reversible reaction between a free receptor (R) and a ligand (L), as shown in Eq. (11.1) [93]

$$K_a = \frac{[R-L]}{[R][L]} \quad (11.1)$$

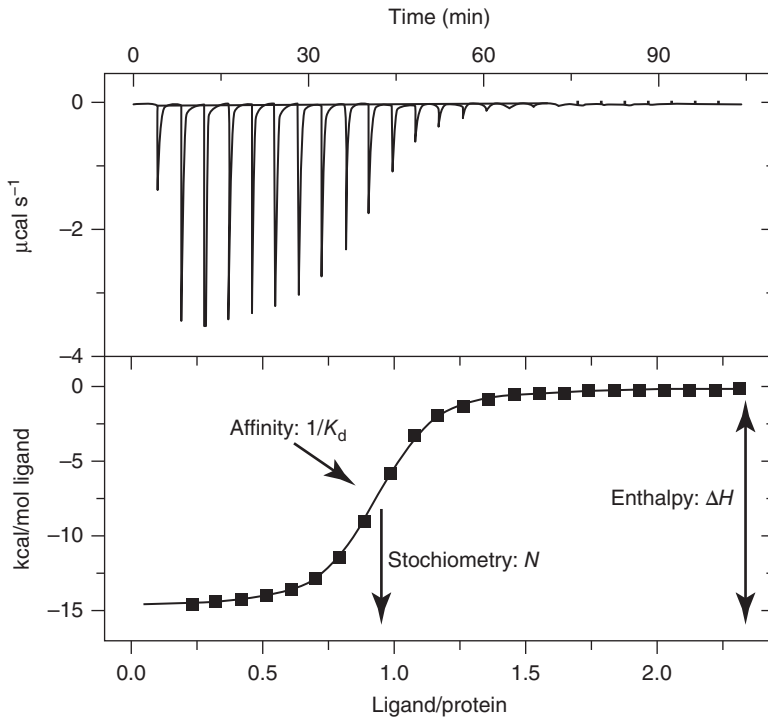


Figure 11.16 Raw data (upper panel) generated by an ITC experiment represent the heat released (or adsorbed) during titration ($\mu\text{cal s}^{-1}$). These raw data are converted into the binding isotherm (lower panel) by integration of each injection producing the thermal energy (ΔH) of each titration step. The signal is reduced until only the background heat of dilution remains. Corrections of such heat are necessary and are usually performed by control experiments. The change in enthalpy (ΔH), the stoichiometry (n), the dissociation constant (K_d), and affinity ($1/K_d$) can be derived from the binding isotherm. The change in enthalpy is presented by the distance of the two asymptotic lines corresponding to the minimal and maximal heat formation. Stoichiometry is molar ratio at the inflection point of the sigmoidal curve. The slope at the inflection point presents the association constant (affinity). Source: Omanovic Miklicanin et al. 2017 [81]. Reprinted with permission of Springer.

The change in the Gibbs free energy (ΔG) is linked with K_a , according to the van't Hoff relationship (11.2) [94]

$$\Delta G = -RT \ln K_a \quad (11.2)$$

in which R is the gas constant ($8.314 \text{ J K}^{-1} \text{ mol}^{-1}$) and T is the absolute temperature in Kelvin, the value of ΔG can be determined.

The entropic contribution to the binding event (ΔS) is related to the Gibbs free energy (ΔG) and the binding enthalpy (ΔH), and can be calculated from Eq. (11.3) [83]

$$\Delta G = \Delta H - T\Delta S \quad (11.3)$$

The binding enthalpy ΔH is temperature dependent, and measurement at different temperatures allows calculation of the binding heat capacity ΔC_p ,

according to Eq. (11.4) [84]

$$\Delta C_p = \delta\Delta H/\delta T \quad (11.4)$$

ΔC_p is increasingly employed in structure–thermodynamics correlation studies to probe the nature and extent of binding interfaces.

11.4.4 Application of ITC in Association Between Aptamer and Target

11.4.4.1 Interaction Between the Aptamer Domain of the Purine Riboswitch and Ligands

The Batey group from the University of Colorado investigated the basic thermodynamic and kinetic properties of ligand binding to a structurally characterized purine riboswitch [95]. A purine riboswitch consists of a regulatory switch coupled with a metabolite-responsive aptamer domain containing a pyrimidine residue (Y74) that forms a Watson–Crick base-pairing interaction with the bound purine nucleobase ligand that discriminates between adenine and guanine [96, 97]. In order to understand the structural basis of this specificity and the mechanism of ligand recognition and binding by the purine riboswitch, they presented the 2,6-diaminopurine-bound structure of a C74U mutant of the *xpt-pbuX* guanine riboswitch, along with a detailed thermodynamic and kinetic analysis of nucleobase recognition by both the native and mutant riboswitches. These studies demonstrated clearly that the pyrimidine at position 74 was the sole determinant of purine riboswitch specificity. The ability of the purine riboswitch to discriminate between guanine and adenine resided entirely within Y74 rather than structural differences outside this site. Using ITC, they found that the affinity of the ligand for riboswitch RNA was highly dependent on hydrogen bonding within the Watson–Crick face of the purine nucleobase. 2,6-diaminopurine bound the RNA with $\Delta H = -40.3 \text{ kcal mol}^{-1}$, $\Delta S = -97.6 \text{ cal mol}^{-1} \text{ K}^{-1}$, and $\Delta G = -10.73 \text{ kcal mol}^{-1}$. A kinetic analysis of binding revealed that the association of 2-aminopurine to the adenine-responsive mutant riboswitch ($0.15 \times 10^5 \text{ M}^{-1} \text{ s}^{-1}$) and the association of 7-deazaguanine to the guanine riboswitch ($2.1 \times 10^5 \text{ M}^{-1} \text{ s}^{-1}$) were both significantly slow. The slow rate proposed a mechanism for ligand recognition by the purine riboswitch. A conformationally dynamic unliganded state for the binding pocket was stabilized first by the Watson–Crick base pairing between the ligand and Y74, and by the subsequent ordering of the J2/3 loop, enclosing the ligand within the three-way junction. These experimental data demonstrated clearly that the purine riboswitch bound ligand via a multistep induced-fit mechanism (Figure 11.17).

In their second publication about the purine riboswitch, the Batey group undertook a detailed mutagenic survey of the purine riboswitch aptamer domain to ascertain the importance of conserved nucleotides to high-affinity ligand binding [98]. They introduced single-point mutations as well as base-pair substitutions and transversions into the terminal loops, the three-way junction, and the base pairs adjacent to the junction of a C74U adenine-responsive mutant of the *xpt-pbuX* guanine riboswitch from *Bacillus subtilis*. This research was based on a combination of crystallographic analysis and ITC, where the ITC was used to measure the varying ability of these mutants to bind ligand

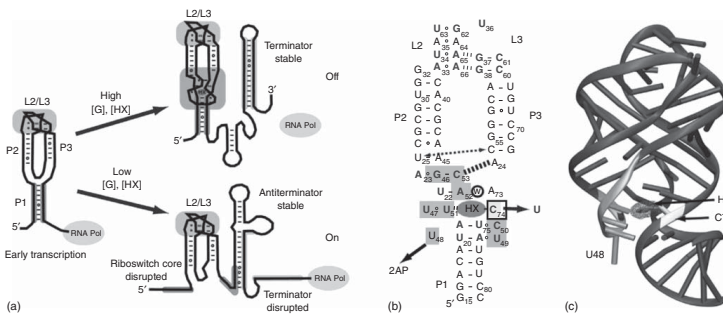


Figure 11.17 (a) A cartoon representation of the mechanism of genetic regulation by the guanine riboswitch. Early in transcription, the aptamer domain of the riboswitch forms, in which the terminal loops (L2/L3) form a tight interaction but the three-way junction is locally disordered. In the presence of high concentrations of guanine or hypoxanthine, ligand binding stabilizes the riboswitch core and the P1 helix, allowing the mRNA to form the terminator element. Without ligand binding, the 3'-side of the P1 helix and the 5'-side of the terminator are used to form an anti-terminator element, allowing transcription to continue. (b) Secondary structure representation of the aptamer domain, highlighting the ligand-binding pocket (nucleotides in light gray box in bold alphabet and C₆₁ in square box) in the presence of hypoxanthine (HX in highlighted oval box). Nucleotides highlighted in bold are at least 90% conserved across purine riboswitch phylogeny. (c) Global structure of the guanine riboswitch, with coloring consistent with the secondary structure. Source: Gilbert et al. 2006 [95]. Reprinted with permission of Elsevier.

(Figure 11.18). The results uncovered the conserved nucleotides, whose identity was required for purine binding. They also observed that certain conserved nucleotides within the three-way junction were not critical for formation of the ligand-bound complex but rather were essential for ensuring that the free state of the RNA was receptive to ligand.

Furthermore, to monitor the coupling of ligand binding and RNA folding within the aptamer domain of the purine riboswitch, the Batey group chemically probed the RNA with *N*-methylisatoic anhydride (NMIA) over a broad temperature range [99]. Analysis of the temperature-dependent reactivity of the RNA in the presence and absence of hypoxanthine revealed that a limited set of nucleotides within the binding pocket changed their conformation in response to ligand binding. The data demonstrated that a distal loop–loop interaction served to restrict the conformational freedom of a significant portion of the three-way junction, thereby promoting ligand binding under physiological conditions.

11.4.4.2 Interaction Between the Cocaine-Binding Aptamer and Quinine

The Johnson group of York University has used ITC to study the interaction of the cocaine-binding aptamer with quinine [100]. They quantified the quinine-binding affinity and thermodynamics of a set of cocaine-binding aptamer variants (Figure 11.19). The obtained affinity and thermodynamic parameters showed that the binding affinity of the aptamer variants for quinine was 30–40 times stronger than that for cocaine (Table 11.1). The ITC data also demonstrated that, for all aptamer variants, quinine binding was an enthalpically driven process with unfavorable binding entropy. Competitive-binding experiments demonstrated that both quinine and cocaine bind at the same site on the aptamer. The inability of cocaine to bind aptamer MN4 in the presence of quinine further confirmed the tighter bound with quinine by the cocaine-binding aptamer. They assumed that the observed increased affinity for quinine over cocaine may be due more to the presence of the large bicyclic aromatic ring on quinine which provides an increase in stacking interactions with the DNA bases in the aptamer than to the smaller monocyclic aromatic ring found in cocaine. The ITC experiments using two aptamers in the presence of Mg^{2+} showed that the addition of Mg^{2+} had a negligible effect on the affinity of these aptamers for quinine. The binding enthalpy in different buffers at a constant pH value was measured by the ITC method to detect changes in the protonation state of quinine during binding. The similarity of the binding enthalpies in different buffers indicated that little to no change in protonation state was taking place with quinine binding.

In order to understand better how the cocaine-binding aptamer interacts with quinine, the Johnson group used ITC-based binding experiments to study the interaction of the cocaine-binding aptamer to a series of structural analogs of quinine and a set of cocaine metabolites (Figure 11.20) [102]. They found that the bicyclic aromatic ring on quinine and a methoxy group at the six-position of the bicyclic ring played an important role in the tight binding between quinine and the cocaine-binding aptamer. But the aliphatic portion of quinine, represented by quinuclidine, and larger aromatic molecules that contain three fused rings were not bound by the aptamer. For all ligands that bind, association is driven by a negative enthalpy compensated for by an unfavorable binding entropy.

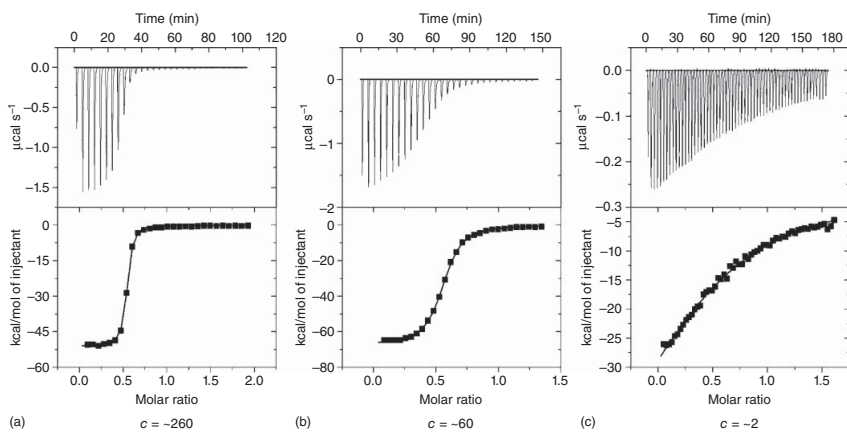


Figure 11.18 Representative data of 2,6-diaminopurine binding the (a) A35U, (b) C61U, and (c) G37A mutants of GRA RNA at 30 °C in a buffer containing 50 mM K^+ -HEPES, pH 7.5, 100 mM KCl, and 10 mM MgCl_2 . Source: Gilbert et al. 2007 [98]. Reprinted with permission of American Chemical Society.

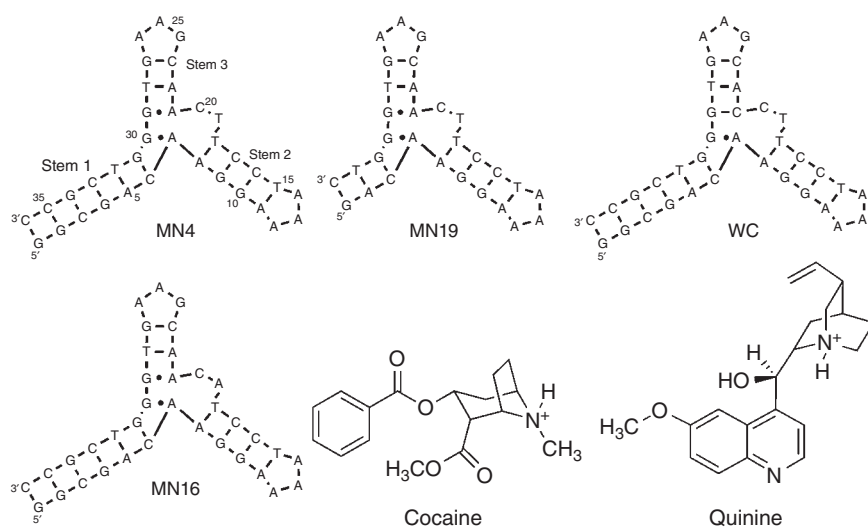


Figure 11.19 Sequence of the aptamer and chemical structure of ligands. Compared to MN4, aptamer MN19 has three base pairs removed from the end of stem 1. Aptamer WC contains a change at the three-way junction in which A21 has been replaced with a C, restoring the Watson–Crick base pair. MN16 is a weak-binding variant in which T19 has been swapped for an A. Dashes between nucleotides indicate Watson–Crick base pairs, and dots indicate non-Watson–Crick base pairs. Source: Reinstein et al. 2013 [100]. Reprinted with permission of American Chemical Society.

Table 11.1 Thermodynamic parameters for the Interaction between quinine and the aptamers^{a)}.

Aptamer	Quinine			Cocaine ^{b)} K_d (μM)
	K_d (μM)	ΔH (kcal mol^{-1})	$-T\Delta S$ (kcal mol^{-1}) ^{a)}	
MN4	0.23 ± 0.03	-14.5 ± 0.4	5.6 ± 0.4	7 ± 1
MN19	0.7 ± 0.2	-22.2 ± 0.4	14.0 ± 0.4	26.7 ± 0.7
WC	12 ± 4	-21 ± 4	15 ± 4	204 ± 6
MN16	51 ± 3	-6.9 ± 0.5	1.1 ± 0.4	vwb ^{c)}
MN4+Mg ²⁺	0.42 ± 0.02	-10.9 ± 0.7	2.4 ± 0.7	nd ^{c)}
MN19+Mg ²⁺	0.6 ± 0.4	-14.6 ± 1.6	6.4 ± 1.4	nd

a) Data acquired in a buffer of 20 mM Tris (pH 7.4), 140 mM NaCl, and 5 mM KCl. Data for WC, MN4, and MN16 were acquired at 20 °C; data for MN19 were acquired at 17.5 °C; data for MN4 and MN19 with Mg²⁺ were acquired at 15 °C. The values reported are averages of 2–5 individual experiments. The error range reported is one standard deviation.

b) The corresponding data for cocaine binding are included for the purpose of comparison [101].

c) vwb denotes that only very weak binding was observed; nd denotes not determined, the experiment was not performed.

Source: Reinstein et al. 2013 [100]. Reprinted with permission of American Chemical Society.

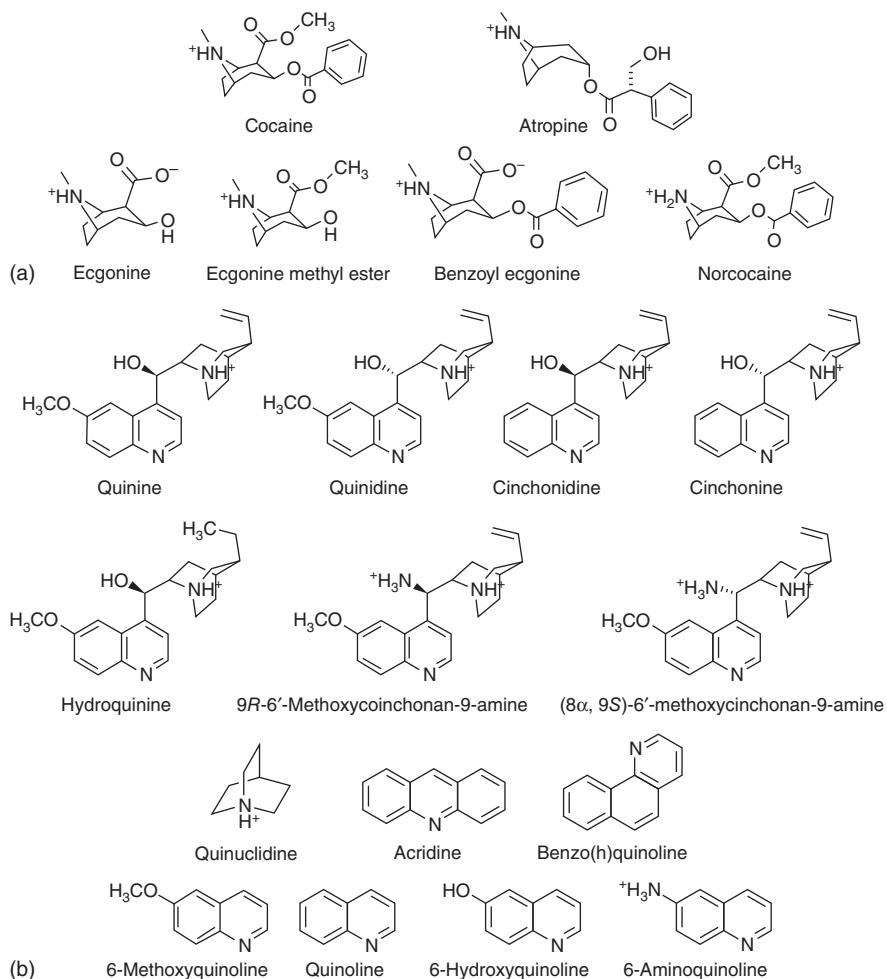


Figure 11.20 Structures of the molecules used in this study. In (a) are cocaine, atropine, and the cocaine metabolites investigated. In (b) are quinine and the different analogs of quinine studied. The chemical groups on quinine that are most important for aptamer binding are in bold and are drawn with thicker bonds. Source: Slavkovic et al. 2015 [102]. Reprinted with permission of Elsevier.

11.4.4.3 Affinity Test by ITC After Systemic Evolution of Ligands by Exponential Enrichment (SELEX)

Gu and coworkers have applied the GO-SELEX method to select aptamers which can bind to 25-hydroxy vitamin D₃ with high specificity and affinity [90]. By cloning and sequencing, 16 different sequences of aptamer candidates were obtained. After preliminarily estimating the affinity and specificity of all the aptamer candidates using the AuNP-based colorimetric assay, ITC was then applied to precisely measure the binding affinity of aptamer candidates with high specificity by calculating the dissociation constants (K_d). The aptamer VDBA14 showed the lowest K_d value of 11 nM, representing the highest affinity.

They further used the improved immobilization-free method, multi-GO-SELEX, to select aptamers against three different types of pesticides (tebuconazole, inabenfide, and mefenacet) [103]. The ITC assays were used to estimate the affinities and specificities of the aptamer candidates. The affinities of 10 different ssDNA aptamers successfully obtained for three pesticides were in the range of 10–100 nM. Besides a specific aptamer for each target, they found a couple of flexible multitarget aptamers, which can bind with two or three different molecules (Figure 11.21).

Sakyl et al. screened RNA aptamers specifically binding to mycolactone [104]. After seven rounds of selection and sequencing, nine aptamer candidates were selected and subjected to an enzyme-linked oligonucleotide assay to determine their affinity. Then, out of the nine candidates, five significantly bound sequences evaluated the binding kinetics by the ITC method to obtain the constant of dissociation (K_d) values. These aptamers showed K_d results in the lower micromolar ranging from 1.59 to 73.0 μM , indicating strong affinity to mycolactone.

Chen et al. used ITC to evaluate the affinity between the ssDNA and tetracycline [105], and obtained a DNA aptamer with high affinity to tetracycline. The dissociation constant (K_d) was calculated to be $5.18 \times 10^{-5} \text{ mol l}^{-1}$. The diagram of the ITC result showed that tetracycline binding with aptamer was an endothermic process. And the enthalpy change (ΔH) of $+1.30 \times 10^5 \text{ cal mol}^{-1}$

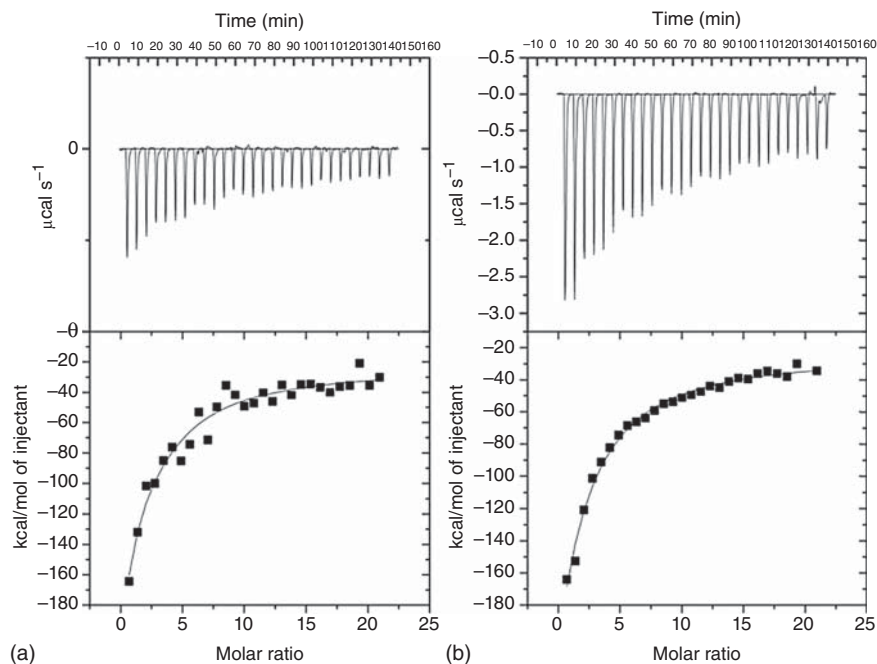


Figure 11.21 (a) Molecular interactions of the T2 aptamer and tebuconazole measured by ITC analysis with 50 mM tebuconazole titrated into 0.025 mM T2 aptamer. (b) Molecular interactions of the T2 aptamer and inabenfide measured by ITC analysis with 50 mM inabenfide titrated into 0.025 mM T2 aptamer. Source: Nguyen et al. 2014 [103]. Reprinted with permission of Royal Society of Chemistry.

suggested that tetracycline binding with aptamer broke some intramolecular hydrogen bonds. Then, they used the same method to screen a high-affinity aptamer against phenylethanolamine [106]. The affinity between the ssDNA and the target was analyzed by ITC and calculated to be $3.34 \times 10^{-5} \text{ mol}^{-1}$. Contrary to the tetracycline aptamer, according to the ITC diagram, aptamer binding with phenylethanolamine was an exothermic process. The enthalpy change (ΔH) was $-3.08 \times 10^6 \text{ cal mol}^{-1}$, suggesting that some intermolecular hydrogen bonds were formed when phenylethanolamine bound with aptamer.

Amano and coworkers selected an RNA aptamer against the Runt domain (RD), a DNA-binding domain of AML1 protein which is an essential transcription factor involved in the development of hematopoietic cells [107]. After the binding assay using SPR, a thermodynamic study using ITC was carried out. The thermodynamic study showed that the aptamer–RD interaction is driven by a large enthalpy change, and its unfavorable entropy change is compensated for by a favorable enthalpy change. Furthermore, the binding heat capacity change was identified from the ITC data at various salt concentrations. The aptamer binding showed a large negative heat capacity change, which suggests that a large apolar surface is buried upon such binding.

Ahirwar and coworkers screened an RNA aptamer to estrogen receptor alpha ($\text{ER}\alpha$) through a non-SELEX *in silico* method [108]. The *in silico* predictions were evaluated by measuring the binding affinities of all the probable aptamers with $\text{ER}\alpha$ using ITC. The majority of the selected RNAs showed a preferential binding to the ER with the values of binding constant (K_a) of an order of 10^7 M^{-1} . And ERaptR4 was found to be the most favored binding to $\text{ER}\alpha$ and selected as an RNA aptamer to $\text{ER}\alpha$ based on the obtained thermodynamic parameters (ΔH and ΔG).

11.4.5 Summary

In summary, ITC can provide quantitative and informative thermodynamic parameters without the requirement of chemical modification or labeling [109]. The information helps in uncovering the molecular mechanisms of an interaction. Thus, ITC can serve as a platform to better understand the chemistry and physics of how molecules respond to each other [84]. The use of ITC coupled with other characterization techniques to study the recognition of targets by aptamers is also an exciting area of development. We expect that ITC can be utilized to obtain more details of molecule interaction between aptamers and targets.

11.5 MicroScale Thermophoresis (MST)

11.5.1 Introduction

The innovative MST is a rapid, precise, and powerful immobilization-free technology to characterize molecule interactions in solution. The physical phenomenon “thermophoresis” describes the movement of molecules through temperature gradients. The thermophoretic movement of molecules depends on their size, charge, and hydration shell [110, 111]. Upon interaction of a ligand

to the target molecule, at least one of these parameters will be altered, resulting in a changed thermophoretic mobility of the molecule. Even ligands with small size will therefore alter the thermophoretic movement of the target molecule by changing the hydration shell and/or the charge [112].

The first merit of the MST method lies in its fast and flexible assay setup and optimization. Integrated quality controls (capillary scan and MST time traces) allow for detection of sticking and aggregation/precipitation effects in real time very early in the process. Upon detection of these effects, it is easy and rapid to optimize technical conditions and buffers to ensure optimal data quality [112]. The greatest advantage of the immobilization-free MST method is free choice of buffers, with measurements even in lysates and sera being possible [113, 114]. The dynamic affinity obtained from MST covers the range from picomolar to millimolar together with the low sample consumption [112]. Due to these advantages, MST has been successfully employed to analyze a variety of molecular interactions, including oligonucleotide interactions [115, 116], protein–DNA interactions [117, 118], protein–protein interactions [119], protein–small molecule interactions [120], and protein–liposome interactions [121].

11.5.2 The Principle of MST Technique

The MST records the thermophoretic movement of a target molecule in thin glass capillaries through temperature gradients in devices of the Monolith series from NanoTemper Technologies GmbH (e.g. in the Monolith NT.15, Figure 11.22a) [112, 122].

Figure 11.22b indicates the technical setup of an MST device. An infrared (IR) laser is focused through an observation window into the capillary to induce the microscopic temperature gradient with a diameter of $\sim 50\ \mu\text{m}$ and a temperature difference ΔT of $2\text{--}6\ ^\circ\text{C}$. Upon activation of the laser, thermophoretic depletion or accumulation of molecules can be detected in the region of elevated temperature, which is quantified by the Soret coefficient: $S_T: c_{\text{hot}}/c_{\text{cold}} = \exp(-S_T \Delta T)$ [112, 122].

Figure 11.22c represents a typical MST experiment. Initially, the fluorescence in the sample is measured without the temperature gradient to ensure homogeneity of the sample. After five seconds, the temperature gradient is established by activation of the IR laser. As a result of this, an initial steep drop of the fluorescence signal – the so-called temperature jump (T-jump) – reflecting the temperature dependence of the fluorophore quantum yield is observed. A slower thermophoresis-driven depletion of fluorophores follows the T-jump. Once the IR laser is deactivated, a reverse T-jump and concomitant back diffusion of fluorescent molecules can be observed [112, 122].

The binding of a ligand to the molecule will alter the thermophoretic behavior, which can be used to study equilibrium constants, such as the dissociation constant K_d . To obtain these important binding parameters, increasing concentrations of ligands are prepared, mixed with a constant concentration of fluorescent target molecule, loaded into multiple capillaries, and analyzed in the instrument by subsequent scanning of each capillary. The results of a typical binding experiment are illustrated in Figure 11.22d. Changes in thermophoresis

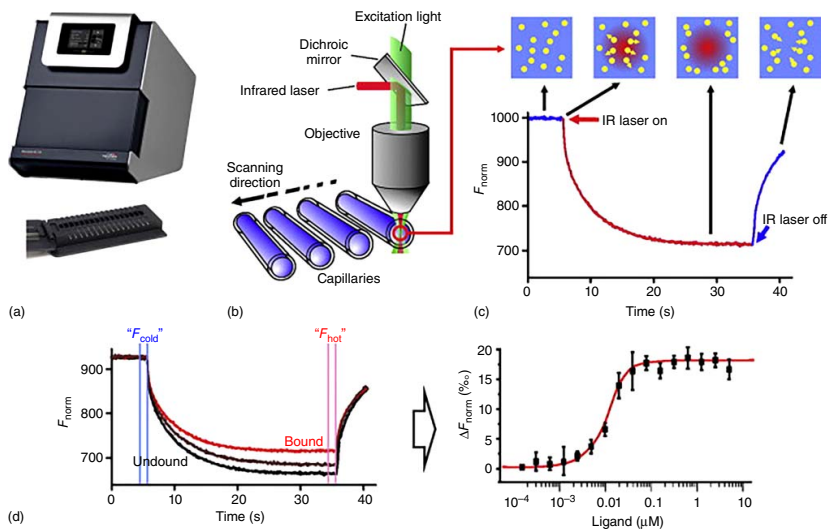


Figure 11.22 MST setup and experiments. Source: Entzian and Schubert 2016 [112] and Jerabek-Willemsen et al. 2014 [122]. Reprinted with permission of Elsevier.

of the fluorescent molecules due to binding to the ligand can then be used to calculate equilibrium binding constants [112, 122].

11.5.3 Application of MST in Association Between Aptamer and Target

11.5.3.1 Interaction Between Steroid Hormones and Aptamers

The Skouridou group from the Universitat Rovira i Virgili used a classic magnetic bead SELEX to select testosterone-binding aptamers [123]. Pools from different selection rounds were sequenced with next-generation sequencing and 10 aptamer candidates were selected for further characterization. A bead-based polymerase chain reaction (PCR) assay was used to perform apta-PCR affinity assay (APAA) and calculate dissociation constants. They selected the T5 aptamer candidate as the preferred candidate, with a high affinity calculated by APAA ($K_d = 4$ nM). MST was then applied to further confirm the affinity and specificity of the T5 candidate. The binding of the T5 candidate with three different steroids, testosterone, progesterone, and 17β -estradiol, was evaluated. A constant concentration (2.5 nM) of the 5'-Cy5-C6-labelled T5 aptamer in selection buffer and serial dilutions (60 μ M to 61 pM) of the native steroid of interest were used. A K_d of 5.7 nM was calculated for testosterone, confirming the high affinity suggested by the APAA assay. Weak binding of T5 to progesterone was indicated at high micromolar concentrations (>15 μ M), whereas no binding could be detected for 17β -estradiol (Figure 11.23).

The Skouridou group also characterized and compared all previously published 17β -estradiol aptamers in terms of affinity and specificity using three different techniques: MST (Table 11.2), SPR, and APAA [124]. In the most part, the obtained results using the three techniques were in agreement, indicating the suitability of the approaches for monitoring the interaction of aptamers with small molecules. Their results corroborated some of the findings reported

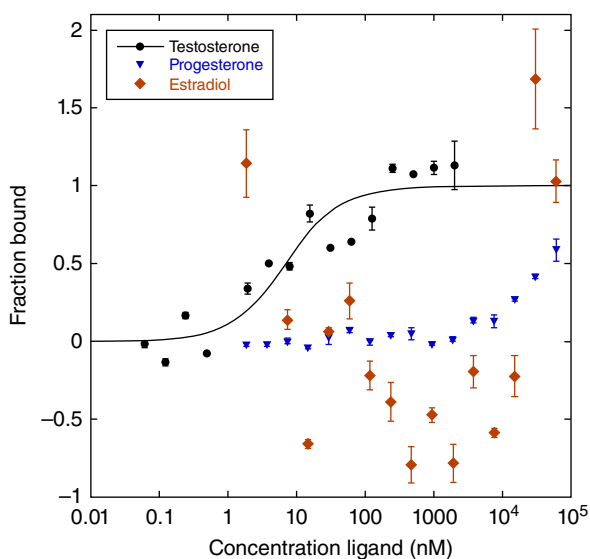


Figure 11.23 Affinity and specificity of T5 testosterone aptamer candidate studied by MST. Source: Skouridou et al. 2017 [123]. Reprinted with permission of Springer.

Table 11.2 17 β -Estradiol aptamer affinity dissociation constants for different steroids determined by MST.

Aptamer	Affinity dissociation constants K_d (nM)			
	17 β -Estradiol	Testosterone	Progesterone	Androstenedione
Kim	98 \pm 56	7316 \pm 2015	10348 \pm 3701	4807 \pm 1357
Alsager (75mer)	18 \pm 5	20726 \pm 11004	2767 \pm 1276	No binding
Alsager (35mer)	23 \pm 10	No binding	No binding	No binding
Alsager (22mer)	80 \pm 38	No binding	No binding	No binding
Akki	227 \pm 113	1751 \pm 748	113 \pm 41	1476 \pm 603
Vanschoenbeek 6a	5149 \pm 1290	1439 \pm 390	4396 \pm 1142	1041 \pm 453
Vanschoenbeek 1b	33464 \pm 11838	N.D.	N.D.	N.D.

N.D. not determined.

The errors correspond to the standard deviation from two technical repeats.

Source: Svobodova et al. 2017 [124]. Reprinted with permission of Elsevier.

initially by the authors and the differences observed might be attributed to the nature of the assays used for measuring binding affinities.

In another research referring to steroid hormone aptamer, the Skouridou group reported the mapping of the binding site of the progesterone aptamer, in an approach termed aptatope mapping [125]. They strategically selected a range of steroids based on their structural differences with progesterone at various positions on the cyclopentanoperhydrophenanthrene ring system, including 17 α -hydroxyprogesterone, testosterone, androstenedione, boldenone, 17 β -estradiol, and nandrolone. The interactions of the 5'-Cy5-labeled P4G13 progesterone aptamer with these steroids were monitored by MST. And the dissociation constants of the aptamer for each steroid were calculated. The obtained K_d value of 1 nM confirmed the high affinity of P4G13 for progesterone. By linking the affinity analysis to the structural differences on the ring structure of a range of steroids, they elucidated the moieties involved in aptamer-progesterone binding.

11.5.3.2 Affinity Test by MST After Systemic Evolution of Ligands by EXponential Enrichment (SELEX)

Zhu and coworkers performed a colorimetric detection of cholic acid (CA) based on an aptamer-adsorbed gold nanoprobe [126]. They first used MST technology to further verify the binding affinity between CA and the 48-nt aptamer. FAM-modified CA aptamers were used at a constant concentration of 0.1 μ M, judging from the 14 capillaries scan which was carried out before each MST measurement. Then, the interaction of aptamer with CA was tested. The binding curve was obtained (Figure 11.24a) and the shape of the MST curves for the FAM-labeled aptamer-CA interaction with a calculated K_d of 12.6 \pm 0.695 μ M (Figure 11.24b). Furthermore, no apparent interaction between CA and FAM was observed from the curve, which ensured that no FAM effects contributed to the binding processes.

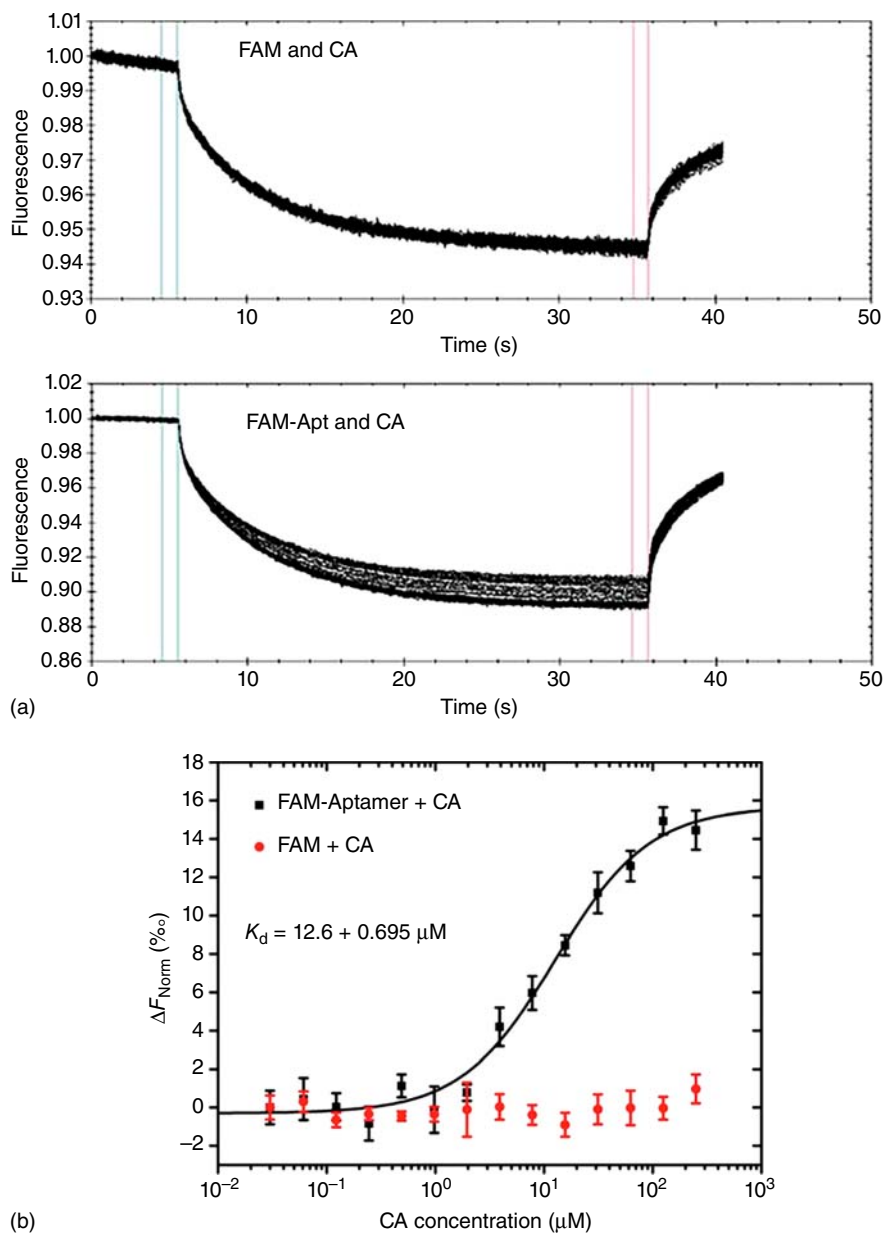


Figure 11.24 (a) The corresponding MST curves of CA solutions incubated with FAM and FAM-Apt, respectively. (b) Binding of CA to FAM-labeled aptamers and FAM. The concentration of the FAM-Apt was kept constant at $0.05 \mu\text{M}$, while the concentration of CA was varied from 0.03 to $250 \mu\text{M}$. Error bars indicate the SD of three independent experiments. Source: Zhu et al. 2017 [126]. Reprinted with permission of Royal Society of Chemistry.

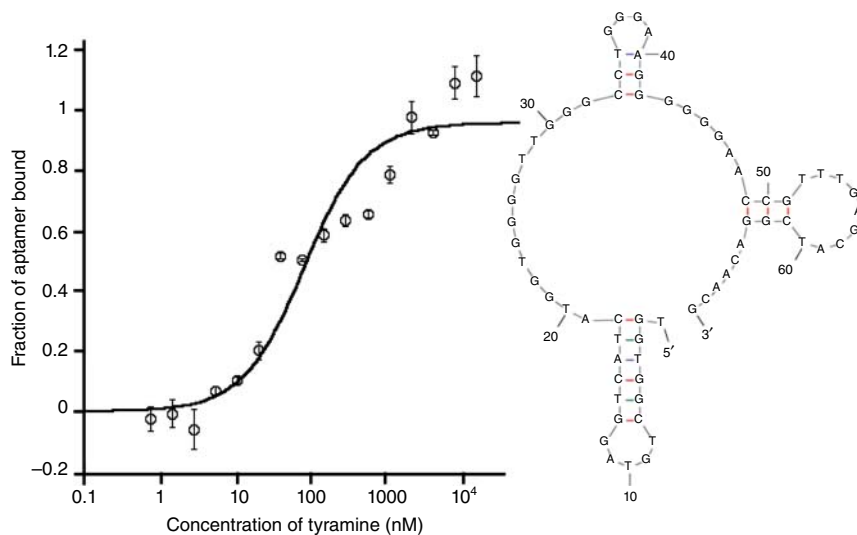


Figure 11.25 Full binding curve obtained with MST for aptamer Tyr₁₀ and its corresponding secondary structure predicted by Mfold software. Source: Valenzano et al. 2016 [127]. Reprinted with permission of American Chemical Society.

Valenzano and coworkers combined an immobilized SELEX with high-throughput sequencing to select DNA aptamers able to recognize the biogenic amine tyramine [127]. The 15 identified aptamer candidates were then screened for binding to tyramine using a one-point microequilibrium dialysis assay. Subsequently, the binding affinity of the most promising aptamers (Tyr₁₀ and Tyr₁₄) was investigated by MST. The K_d values calculated using this approach were $0.097 \pm 0.037 \mu\text{M}$ for Tyr₁₀ and $1.25 \pm 0.47 \mu\text{M}$ for Tyr₁₄, thus confirming the results obtained with the one-point microequilibrium dialysis assay and the high affinity of the aptamer Tyr₁₀ toward tyramine (Figure 11.25).

11.5.4 Summary

MST is a novel, powerful technology to identify and characterize molecular interactions of any kind. It is based on molecules moving through temperature gradients; and this movement depends on the size, charge, and hydration shell of the molecule. Upon the interaction between the target and the aptamer, the thermophoresis of an aptamer target complex differs significantly from that of an aptamer due to the changed parameters [128]. This technique offers free choice of buffers and is especially suited to small molecule–aptamer binding interactions [112].

References

- 1 Hernández, F.E. (2012). Optics and plasmonics: fundamental studies and applications. In: *Reviews in Plasmonics 2010*, 185–203. New York, NY: Springer New York.

- 2 Bhatia, P. and Gupta, B.D. (2013). Surface plasmon resonance based fiber optic refractive index sensor utilizing silicon layer: effect of doping. *Opt. Commun.* 286: 171–175.
- 3 Singh, S., Mishra, S.K., and Gupta, B.D. (2013). Sensitivity enhancement of a surface plasmon resonance based fibre optic refractive index sensor utilizing an additional layer of oxides. *Sens. Actuators A* 193: 136–140.
- 4 Wood, R.W. (1902). On a remarkable case of uneven distribution of light in a diffraction grating spectrum. *Philos. Mag. Ser. 6* 4 (21): 396–402.
- 5 Kretschmann, E. and Raether, H. (1968). Notizen: radiative decay of non radiative surface plasmons excited by light. *Z. für Naturforsch A* 2135.
- 6 Olaru, A., Bala, C., Jaffrezic-Renault, N., and Aboul-Enein, H.Y. (2015). Surface plasmon resonance (SPR) biosensors in pharmaceutical analysis. *Crit. Rev. Anal. Chem.* 45 (2): 97–105.
- 7 Kihm, K.D. (2010). Surface plasmon resonance reflectance imaging technique for near-field (~100 nm) fluidic characterization. *Exp. Fluids* 48 (4): 547–564.
- 8 Maier, S.A. (2007). *Plasmonics: Fundamentals and Applications[M]*. New York, NY: Springer.
- 9 Kihm, K.D., Cheon, S., Park, J.S. et al. (2012). Surface plasmon resonance (SPR) reflectance imaging: far-field recognition of near-field phenomena. *Opt. Lasers Eng.* 50 (1): 64–73.
- 10 Shi, H., Liu, Z., Wang, X. et al. (2013). A symmetrical optical waveguide based surface plasmon resonance biosensing system. *Sens. Actuators B* 185: 91–96.
- 11 Mayer, K.M. and Hafner, J.H. (2011). Localized surface plasmon resonance sensors. *Chem. Rev.* 111 (6): 3828–3857.
- 12 Dastmalchi, B., Tassin, P., Koschny, T., and Soukoulis, C.M. (2016). A new perspective on plasmonics: confinement and propagation length of surface plasmons for different materials and geometries. *Adv. Opt. Mater.* 4 (1): 177–184.
- 13 Erickson, D., Mandal, S., Yang, A.H.J., and Cordovez, B. (2008). Nanobiosensors: optofluidic, electrical and mechanical approaches to biomolecular detection at the nanoscale. *Microfluid. Nanofluid.* 4 (1-2): 33–52.
- 14 Hoang Hiep, N., Park, J., Kang, S., and Kim, M. (2015). Surface plasmon resonance: a versatile technique for biosensor applications. *Sensors* 15 (5): 10481–10510.
- 15 Peng, W., Liu, Y., Fang, P. et al. (2014). Compact surface plasmon resonance imaging sensing system based on general optoelectronic components. *Opt. Express* 22 (5): 6174–6185.
- 16 Couture, M., Zhao, S.S., and Masson, J.F. (2013). Modern surface plasmon resonance for bioanalytics and biophysics. *Phys. Chem. Chem. Phys.* 15 (27): 11190–11216.
- 17 Kabashin, A.V., Patskovsky, S., and Grigorenko, A.N. (2009). Phase and amplitude sensitivities in surface plasmon resonance bio and chemical sensing. *Opt. Express* 17 (23): 21191–21204.

- 18 Wang, X., Zhan, S., Huang, Z., and Hong, X. (2013). Review: advances and applications of surface plasmon resonance biosensing instrumentation. *Instrum Sci. Technol.* 41 (6): 574–607.
- 19 Homola, J. (2008). Surface plasmon resonance sensors for detection of chemical and biological species. *Chem. Rev.* 108 (2): 462–493.
- 20 Zhang, H., Song, D., Gao, S. et al. (2013). Enhanced wavelength modulation SPR biosensor based on gold nanorods for immunoglobulin detection. *Talanta* 115: 857–862.
- 21 Scarano, S., Mascini, M., Turner, A.P.F., and Minunni, M. (2010). Surface plasmon resonance imaging for affinity-based biosensors. *Biosens. Bioelectron.* 25 (5): 957–966.
- 22 Kashif, M., Bakar, A., Arsad, N., and Shaari, S. (2014). Development of phase detection schemes based on surface plasmon resonance using interferometry. *Sensors* 14 (9): 15914.
- 23 Kabashin, A.V., Evans, P., Pastkovsky, S. et al. (2009). Plasmonic nanorod metamaterials for biosensing. *Nat. Mater.* 8 (11): 867–871.
- 24 Su, Y.D., Chen, S.J., and Yeh, T.L. (2005). Common-path phase-shift interferometry surface plasmon resonance imaging system. *Opt. Lett.* 30 (12): 1488–1490.
- 25 Piliarik, M. and Homola, J. (2009). Surface plasmon resonance (SPR) sensors: approaching their limits? *Opt. Express* 17 (19): 16505–16517.
- 26 Chiang, H.P., Chen, C.W., Wu, J.J. et al. (2007). Effects of temperature on the surface plasmon resonance at a metal–semiconductor interface. *Thin Solid Films* 515 (17): 6953–6961.
- 27 Lee, S.J., Youn, B.S., Park, J.W. et al. (2008). ssDNA aptamer-based surface plasmon resonance biosensor for the detection of retinol binding protein 4 for the early diagnosis of type 2 diabetes. *Anal. Chem.* 80 (8): 2867–2873.
- 28 Trapaidze, A., Hérault, J.P., Herbert, J.M. et al. (2016). Investigation of the selectivity of thrombin-binding aptamers for thrombin titration in murine plasma. *Biosens. Bioelectron.* 78: 58–66.
- 29 Park, J.W., Lee, S.J., Ren, S. et al. (2016). Acousto-microfluidics for screening of ssDNA aptamer. *Sci. Rep.* 6 (27121).
- 30 Mejri Omrani, N., Miodek, A., Zribi, B. et al. (2016). Direct detection of OTA by impedimetric aptasensor based on modified polypyrrole-dendrimers. *Anal. Chim. Acta* 920: 37–46.
- 31 Manandhar, Y., Wang, W., Inoue, J. et al. (2017). Interactions of in vitro selected fluorogenic peptide aptamers with calmodulin. *Biotechnol. Lett.* 39 (3): 375–382.
- 32 Lamberti, I., Scarano, S., Esposito, C.L. et al. (2016). In vitro selection of RNA aptamers against CA125 tumor marker in ovarian cancer and its study by optical biosensing. *Methods* 97: 58–68.
- 33 Bianco, M., Sonato, A., De Girolamo, A. et al. (2017). An aptamer-based SPR-polarization platform for high sensitive OTA detection. *Sens. Actuators B* 241: 314–320.
- 34 Liu, R., Wang, Q., Li, Q. et al. (2017). Surface plasmon resonance biosensor for sensitive detection of microRNA and cancer cell using multiple signal amplification strategy. *Biosens. Bioelectron.* 87: 433–438.

- 35 Vasilescu, A., Purcarea, C., Popa, E. et al. (2016). Versatile SPR aptasensor for detection of lysozyme dimer in oligomeric and aggregated mixtures. *Biosens. Bioelectron.* 83: 353–360.
- 36 Nguyen, V.-T., Seo, H.B., Kim, B.C. et al. (2016). Highly sensitive sandwich-type SPR based detection of whole H5Nx viruses using a pair of aptamers. *Biosens. Bioelectron.* 86: 293–300.
- 37 Wang, B., Park, B., Xu, B., and Kwon, Y. (2017). Label-free biosensing of *Salmonella enterica* serovars at single-cell level. *J Nanobiotechnol* 15 (1): 40.
- 38 Mihai, I., Vezeanu, A., Polonschii, C. et al. (2015). Label-free detection of lysozyme in wines using an aptamer based biosensor and SPR detection. *Sens. Actuators B* 206: 198–204.
- 39 Zhu, Z., Feng, M., Zuo, L. et al. (2015). An aptamer based surface plasmon resonance biosensor for the detection of ochratoxin A in wine and peanut oil. *Biosens. Bioelectron.* 65: 320–326.
- 40 Kim, S. and Lee, H.J. (2017). Gold nanostar enhanced surface plasmon resonance detection of an antibiotic at attomolar concentrations via an aptamer-antibody sandwich assay. *Anal. Chem.* 89: 6630–6624.
- 41 Ding, X., Cheng, W., Li, Y. et al. (2017). An enzyme-free surface plasmon resonance biosensing strategy for detection of DNA and small molecule based on nonlinear hybridization chain reaction. *Biosens. Bioelectron.* 87: 345–351.
- 42 Li, X., Cheng, W., Li, D. et al. (2016). A novel surface plasmon resonance biosensor for enzyme-free and highly sensitive detection of microRNA based on multi component nucleic acid enzyme (MNAzyme)-mediated catalyzed hairpin assembly. *Biosens. Bioelectron.* 80: 98–104.
- 43 Xiang, Y., Zhu, X., Huang, Q. et al. (2015). Real-time monitoring of mycobacterium genomic DNA with target-primed rolling circle amplification by a Au nanoparticle-embedded SPR biosensor. *Biosens. Bioelectron.* 66: 512–519.
- 44 Chen, H., Hou, Y., Qi, F. et al. (2014). Detection of vascular endothelial growth factor based on rolling circle amplification as a means of signal enhancement in surface plasmon resonance. *Biosens. Bioelectron.* 61: 83–87.
- 45 Xiang, Y., Deng, K., Xia, H. et al. (2013). Isothermal detection of multiple point mutations by a surface plasmon resonance biosensor with Au nanoparticles enhanced surface-anchored rolling circle amplification. *Biosens. Bioelectron.* 49: 442–449.
- 46 Huang, Y.-Y., Hsu, H.-Y., and Huang, C.-J.C. (2007). A protein detection technique by using surface plasmon resonance (SPR) with rolling circle amplification (RCA) and nanogold-modified tags. *Biosens. Bioelectron.* 22 (6): 980–985.
- 47 Yao, G.-H., Liang, R.-P., Huang, C.-F. et al. (2015). Enzyme-free surface plasmon resonance aptasensor for amplified detection of adenosine via target-triggering strand displacement cycle and Au nanoparticles. *Anal. Chim. Acta* 871: 28–34.
- 48 Nguyen, H., Park, J., Kang, S., and Kim, M. (2015). Surface plasmon resonance: a versatile technique for biosensor applications. *Sensors* 15 (5): 10481.

- 49 Yu, X., Xu, D., and Cheng, Q. (2006). Label-free detection methods for protein microarrays. *Proteomics* 6 (20): 5493–5503.
- 50 Shumaker-Parry, J.S. and Campbell, C.T. (2004). Quantitative methods for spatially resolved adsorption/desorption measurements in real time by surface plasmon resonance microscopy. *Anal. Chem.* 76 (4): 907–917.
- 51 Abadian, P.N., Tandogan, N., Jamieson, J.J., and Goluch, E.D. (2014). Using surface plasmon resonance imaging to study bacterial biofilms. *Biomicrofluidics* 8 (2): 021804.
- 52 Schasfoort, R.B.M. and Schuck, P. (2008). Future Trends in SPR Technology. In: *Handbook of Surface Plasmon Resonance*, 354–394. The Royal Society of Chemistry.
- 53 Curie, J. and Curie, P. (1880). Piezoelectric and allied phenomena in Rochelle salt. *Comput. Rend. Acad. Sci. Paris* 91 (9): 294–297.
- 54 Rayleigh, L. On the free vibrations of an infinite plate of homogeneous isotropic elastic matter. *Proc. Lond. Math. Soc.* s1-20 (1): 520–527.
- 55 Cady, W.-G. (1922). The piezo-electric resonator. *Proc. Inst. Radio Eng.* 10 (2): 83–114.
- 56 Lack, F., Willard, G., and Fair, I. (1934). Some improvements in quartz crystal circuit elements. *Bell Syst. Tech. J.* 13 (3): 453–463.
- 57 Sauerbrey, G.Z. (1959). The use of quartz crystal oscillators for weighing thin layers and for microweighing. *Z. Phys.* 155: 206–222.
- 58 Nomura, T., Okuhara, M., Nomura, T., and Okuhara, M. (1982). Frequency shifts of piezoelectric quartz crystals immersed in organic liquids. *Anal. Chim. Acta* 142 (OCT): 281–284.
- 59 Kurosawa, S., Tawara, E., Kamo, N. et al. (1990). Oscillating frequency of piezoelectric quartz crystal in solutions. *Anal. Chim. Acta* 230 (1): 41–49.
- 60 Rodahl, M., Höök, F., Krozer, A. et al. (1995). Quartz crystal microbalance setup for frequency and Q-factor measurements in gaseous and liquid environments. *Rev. Sci. Instrum.* 66 (7): 3924–3930.
- 61 Ward, M.D. and Buttry, D.A. (1990). In situ interfacial mass detection with piezoelectric transducers. *Science* 249 (4972): 1000–1008.
- 62 Dultsev, F.N., Ostanin, V.P., and Klenerman, D. (2000). “Hearing” bond breakage. measurement of bond rupture forces using a quartz crystal microbalance. *Langmuir* 16 (11): 5036–5040.
- 63 Hianik, T., Ostatná, V., Sonlajtnerova, M., and Grman, I. (2007). Influence of ionic strength, pH and aptamer configuration for binding affinity to thrombin. *Bioelectrochemistry* 70 (1): 127–133.
- 64 Zhang, X. and Yadavalli, V.K. (2011). Surface immobilization of DNA aptamers for biosensing and protein interaction analysis. *Biosens. Bioelectron.* 26 (7): 3142–3147.
- 65 Wang, L., Wang, R., Chen, F. et al. (2017). QCM-based aptamer selection and detection of *Salmonella typhimurium*. *Food Chem.* 221: 776–782.
- 66 Reddy, S.M., Jones, J.P., Lewis, T.J., and Vadgama, P.M. (1998). Development of an oxidase-based glucose sensor using thickness-shear-mode quartz crystals. *Anal. Chim. Acta* 363 (2–3): 203–213.

- 67 Yao, C., Qi, Y., Zhao, Y. et al. (2009). Aptamer-based piezoelectric quartz crystal microbalance biosensor array for the quantification of IgE. *Biosens. Bioelectron.* 24 (8): 2499–2503.
- 68 Pan, Y., Guo, M., Nie, Z. et al. (2010). Selective collection and detection of leukemia cells on a magnet-quartz crystal microbalance system using aptamer-conjugated magnetic beads. *Biosens. Bioelectron.* 25 (7): 1609–1614.
- 69 Chen, Q., Tang, W., Wang, D. et al. (2010). Amplified QCM-D biosensor for protein based on aptamer-functionalized gold nanoparticles. *Biosens. Bioelectron.* 26 (2): 575–579.
- 70 Shan, W., Pan, Y., Fang, H. et al. (2014). An aptamer-based quartz crystal microbalance biosensor for sensitive and selective detection of leukemia cells using silver-enhanced gold nanoparticle label. *Talanta* 126: 130–135.
- 71 Song, W., Zhu, Z., Mao, Y., and Zhang, S. (2014). A sensitive quartz crystal microbalance assay of adenosine triphosphate via DNAzyme-activated and aptamer-based target-triggering circular amplification. *Biosens. Bioelectron.* 53: 288–294.
- 72 He, P., Liu, L., Qiao, W., and Zhang, S. (2014). Ultrasensitive detection of thrombin using surface plasmon resonance and quartz crystal microbalance sensors by aptamer-based rolling circle amplification and nanoparticle signal enhancement. *Chem. Commun.* 50 (12): 1481–1484.
- 73 Uttenthaler, E., Schraml, M., Mandel, J., and Drost, S. (2001). Ultrasensitive quartz crystal microbalance sensors for detection of M13-Phages in liquids. *Biosens. Bioelectron.* 16 (9-12): 735–743.
- 74 Montagut, Y., García, J., Jiménez, Y. et al. (2011). Frequency-shift vs phase-shift characterization of in-liquid quartz crystal microbalance applications. *Rev. Sci. Instrum.* 82 (6): 064702.
- 75 March, C., García, J.V., Sánchez, A. et al. (2015). High-frequency phase shift measurement greatly enhances the sensitivity of QCM immunosensors. *Biosens. Bioelectron.* 65: 1–8.
- 76 Huang, Y.H., Chang, J.S., Chao, S.D. et al. (2014). Improving the binding efficiency of quartz crystal microbalance biosensors by applying the electrothermal effect. *Biomicrofluidics* 8 (5): 116–123.
- 77 Hirotsugu, O. (2013). Wireless-electrodeless quartz-crystal-microbalance biosensors for studying interactions among biomolecules: a review. *Proc. Jpn Acad Series B* 89 (9): 401–417.
- 78 Pang, W., Zhao, H., Kim, E.S. et al. (2012). Piezoelectric microelectromechanical resonant sensors for chemical and biological detection. *Lab Chip* 12 (1): 29–44.
- 79 Zhao, B., Hu, J., Ren, W. et al. (2015). A new biosensor based on PVDF film for detection of nucleic acids. *Ceram. Int.* 41: S602–S606.
- 80 Skladal, P. (2016). Piezoelectric biosensors. *TrAC, Trends Anal. Chem.* 79: 127–133.
- 81 Omanovic Miklicanin, E., Manfield, I., and Wilkins, T. (2017). Application of isothermal titration calorimetry in evaluation of protein–nanoparticle interactions. *J. Therm. Anal. Calorim.* 127 (1): 605–613.
- 82 Freire, E., Mayorga, O.L., and Straume, M. (1990). Isothermal titration calorimetry. *Anal. Chem.* 62 (18): 950A–959A.

- 83 Falconer, R.J., Penkova, A., Jelesarov, I., and Collins, B.M. (2010). Survey of the year 2008: applications of isothermal titration calorimetry. *J. Mol. Recognit.* 23 (5): 395–413.
- 84 Ghai, R., Falconer, R.J., and Collins, B.M. (2012). Applications of isothermal titration calorimetry in pure and applied research--survey of the literature from 2010. *J. Mol. Recognit.* 25 (1): 32–52.
- 85 Falconer, R.J. (2016). Applications of isothermal titration calorimetry - the research and technical developments from 2011 to 2015. *J. Mol. Recognit.* 29 (10): 504–515.
- 86 Kabiri, M. and Unsworth, L.D. (2014). Application of isothermal titration calorimetry for characterizing thermodynamic parameters of biomolecular interactions: peptide self-assembly and protein adsorption case studies. *Biomacromolecules* 15 (10): 3463–3473.
- 87 Wu, J., Li, J., Li, G. et al. (1996). The receptor binding site for the methyltransferase of bacterial chemotaxis is distinct from the sites of methylation. *Biochemistry* 35 (15): 4984–4993.
- 88 Qu, X., Ren, J., Riccelli, P.V. et al. (2003). Enthalpy/entropy compensation: influence of DNA flanking sequence on the binding of 7-amino actinomycin D to its primary binding site in short DNA duplexes. *Biochemistry* 42 (41): 11960–11967.
- 89 Livingstone, J.R. (1996). Antibody characterization by isothermal titration calorimetry. *Nature* 384: 491–492.
- 90 Lee, B.H., Nguyen, V.T., and Gu, M.B. (2017). Highly sensitive detection of 25-HydroxyvitaminD3 by using a target-induced displacement of aptamer. *Biosens. Bioelectron.* 88: 174–180.
- 91 Leavitt, S. and Freire, E. (2001). Direct measurement of protein binding energetics by isothermal titration calorimetry. *Curr. Opin. Struct. Biol.* 11 (5): 560–566.
- 92 Velazquez-Campoy, A., Leavitt, S.A., and Freire, E. (2004). Characterization of protein–protein interactions by isothermal titration calorimetry. In: *Protein-Protein Interactions: Methods and Applications*, 35–54. Springer Nature.
- 93 Callies, O. and Hernandez Daranas, A. (2016). Application of isothermal titration calorimetry as a tool to study natural product interactions. *Nat. Prod. Rep.* 33 (7): 881–904.
- 94 Roselin, L.S., Lin, M.S., Lin, P.H. et al. (2010). Recent trends and some applications of isothermal titration calorimetry in biotechnology. *Biotechnol. J.* 5 (1): 85–98.
- 95 Gilbert, S.D., Stoddard, C.D., Wise, S.J., and Batey, R.T. (2006). Thermodynamic and kinetic characterization of ligand binding to the purine riboswitch aptamer domain. *J. Mol. Biol.* 359 (3): 754–768.
- 96 Ebbole, D.J. and Zalkin, H. (1987). Cloning and characterization of a 12-gene cluster from *Bacillus subtilis* encoding nine enzymes for de novo purine nucleotide synthesis. *J. Biol. Chem.* 262 (17): 8274–8287.
- 97 Mandal, M. and Breaker, R.R. (2004). Gene regulation by riboswitches. *Nat. Rev. Mol. Cell Biol.* 5 (6): 451–463.

- 98 Gilbert, S.D., Love, C.E., Edwards, A.L., and Batey, R.T. (2007). Mutational analysis of the purine riboswitch aptamer domain. *Biochemistry* 46 (46): 13297.
- 99 Stoddard, C.D., Gilbert, S.D., and Batey, R.T. (2008). Ligand-dependent folding of the three-way junction in the purine riboswitch. *RNA* 14 (4): 675–684.
- 100 Reinstein, O., Yoo, M., Han, C. et al. (2013). Quinine binding by the cocaine-binding aptamer. Thermodynamic and hydrodynamic analysis of high-affinity binding of an off-target ligand. *Biochemistry* 52 (48): 8652–8662.
- 101 Neves, M.a.D., Reinstein, O., Saad, M., and Johnson, P.E. (2010). Defining the secondary structural requirements of a cocaine-binding aptamer by a thermodynamic and mutation study. *Biophys. Chem.* 153 (1): 9–16.
- 102 Slavkovic, S., Altunisik, M., Reinstein, O., and Johnson, P.E. (2015). Structure-affinity relationship of the cocaine-binding aptamer with quinine derivatives. *Bioorg. Med. Chem.* 23 (10): 2593–2597.
- 103 Nguyen, V.T., Kwon, Y.S., Kim, J.H., and Gu, M.B. (2014). Multiple GO-SELEX for efficient screening of flexible aptamers. *Chem. Commun. (Camb.)* 50 (72): 10513–10516.
- 104 Sakyi, S.A., Aboagye, S.Y., Otchere, I.D. et al. (2016). RNA aptamer that specifically binds to mycolactone and serves as a diagnostic tool for diagnosis of buruli ulcer. *PLoS Negl. Trop. Dis.* 10 (10): e0004950.
- 105 Chen, D., Yao, D., Xie, C., and Liu, D. (2014). Development of an aptasensor for electrochemical detection of tetracycline. *Food Control* 42 (42): 109–115.
- 106 Chen, D., Yang, M., Zheng, N. et al. (2016). A novel aptasensor for electrochemical detection of ractopamine, clenbuterol, salbutamol, phenylethanolamine and procaterol. *Biosens. Bioelectron.* 80: 525–531.
- 107 Amano, R., Takada, K., Tanaka, Y. et al. (2016). Kinetic and thermodynamic analyses of interaction between a high-affinity RNA aptamer and its target protein. *Biochemistry* 55 (45): 6221–6229.
- 108 Ahirwar, R., Nahar, S., Aggarwal, S. et al. (2016). In silico selection of an aptamer to estrogen receptor alpha using computational docking employing estrogen response elements as aptamer-alike molecules. *Sci. Rep.* 6: 21285.
- 109 Huang, R. and Lau, B.L. (2016). Biomolecule-nanoparticle interactions: elucidation of the thermodynamics by isothermal titration calorimetry. *Biochim. Biophys. Acta* 1860 (5): 945–956.
- 110 Braun, D. and Libchaber, A. (2002). Trapping of DNA by thermophoretic depletion and convection. *Phys. Rev. Lett.* 89 (18): 188103.
- 111 Duhr, S. and Braun, D. (2006). Why molecules move along a temperature gradient. *Proc. Natl. Acad. Sci.* 103 (52): 19678–19682.
- 112 Entzian, C. and Schubert, T. (2016). Studying small molecule-aptamer interactions using MicroScale Thermophoresis (MST). *Methods* 97: 27–34.
- 113 Wienken, C.J., Baaske, P., Rothbauer, U. et al. (2010). Protein-binding assays in biological liquids using microscale thermophoresis. *Nat. commun.* 1: 100.
- 114 Seidel, S.A., Dijkman, P.M., Lea, W.A. et al. (2013). Microscale thermophoresis quantifies biomolecular interactions under previously challenging conditions. *Methods* 59 (3): 301–315.

- 115 Baaske, P., Wienken, C.J., Reineck, P. et al. (2010). Optical thermophoresis for quantifying the buffer dependence of aptamer binding. *Angew. Chem. Int. Ed.* 49 (12): 2238–2241.
- 116 Wienken, C.J., Baaske, P., Duhr, S., and Braun, D. (2011). Thermophoretic melting curves quantify the conformation and stability of RNA and DNA. *Nucleic Acids Res.* 39 (8): e52.
- 117 Martin, D., Charpilienne, A., Parent, A. et al. (2013). The rotavirus nonstructural protein NSP5 coordinates a [2Fe-2S] iron-sulfur cluster that modulates interaction to RNA. *FASEB J.* 27 (3): 1074–1083.
- 118 Zillner, K., Filarsky, M., Rachow, K. et al. (2013). Large-scale organization of ribosomal DNA chromatin is regulated by Tip5. *Nucleic Acids Res.* 41 (10): 5251–5262.
- 119 Xiong, X., Coombs, P.J., Martin, S.R. et al. (2013). Receptor binding by a ferret-transmissible H5 avian influenza virus. *Nature* 497 (7449): 392–396.
- 120 Shang, X., Marchioni, F., Evelyn, C.R. et al. (2013). Small-molecule inhibitors targeting G-protein-coupled Rho guanine nucleotide exchange factors. *Proc. Natl. Acad. Sci.* 110 (8): 3155–3160.
- 121 Van Den Bogaart, G., Thutupalli, S., Risselada, J.H. et al. (2011). Synaptotagmin-1 may be a distance regulator acting upstream of SNARE nucleation. *Nat. Struct. Mol. Biol.* 18 (7): 805–812.
- 122 Jerabek-Willemsen, M., André, T., Wanner, R. et al. (2014). MicroScale thermophoresis: interaction analysis and beyond. *J. Mol. Struct.* 1077: 101–113.
- 123 Skouridou, V., Jauset-Rubio, M., Ballester, P. et al. (2017). Selection and characterization of DNA aptamers against the steroid testosterone. *Microchim. Acta* 184 (6): 1631–1639.
- 124 Svobodova, M., Skouridou, V., Botero, M.L. et al. (2017). The characterization and validation of 17beta-estradiol binding aptamers. *J. Steroid Biochem. Mol. Biol.* 167: 14–22.
- 125 Skouridou, V., Schubert, T., Bashammakh, A.S. et al. (2017). Aptatope mapping of the binding site of a progesterone aptamer on the steroid ring structure. *Anal. Biochem.* 531: 8–11.
- 126 Zhu, Q., Li, T., Ma, Y. et al. (2017). Colorimetric detection of cholic acid based on an aptamer adsorbed gold nanoprobe. *RSC Adv.* 7 (31): 19250–19256.
- 127 Valenzano, S., De Girolamo, A., Derosa, M.C. et al. (2016). Screening and identification of DNA aptamers to tyramine using in vitro selection and high-throughput sequencing. *ACS Comb. Sci.* 18 (6): 302–313.
- 128 Stoltenburg, R., Schubert, T., and Strehlitz, B. (2015). In vitro selection and interaction studies of a DNA aptamer targeting protein A. *PLoS One* 10 (7): e0134403.

12

Challenges of SELEX and Demerits of Aptamer-Based Methods

Haiyun Liu and Jinghua Yu

University of Jinan, Institute for Advanced Interdisciplinary Research, No. 336, West Road of Nan Xinzhuang, Shandong 250022, PR China

12.1 Introduction

In 1990, within a short time interval, two different laboratories reported their results on the development of an *in vitro* selection and amplification technique for the isolation of specific nucleic acid sequences able to bind to target molecules with high affinity and specificity [1, 2]. The technique was coined as SELEX (Systematic Evolution of Ligands by EXponential enrichment) [1] and the resulting oligonucleotides were referred to as aptamers.

The SELEX process is also applicable under nonphysiological conditions. Selection of aptamers for toxic target molecules or for molecules with no or only low immunogenicity is possible. Various modifications can be introduced into the basic SELEX process to direct the selection to desired aptamer features or to intended applications of the aptamers. For example, chemical modifications at the nucleotide level or terminal capping can significantly improve the stability of aptamers [3–9]. The attached functional groups, reporter molecules, polyethylene glycol, cholesterol, or lipid tag modifications serve for the quantification and immobilization of aptamers. Increasing the pharmacokinetic half-life is useful in improving the bioavailability of potential therapeutic aptamers. Further optimizations of the selected aptamers are possible with regard to their affinities and specificities [10–13]. Variations in the selection conditions (buffer composition, temperature, binding time), the design of the randomized oligonucleotide library, or additional selection steps can strongly affect the specific affinity and selectivity binding features of aptamers. However, often-observed problems of aptamer selections are the enrichment of nonspecifically binding oligonucleotides or the repeated selection of already known aptamer sequences in different SELEX processes depending on target composition and SELEX conditions. Therefore, the selection conditions have to be adapted accurately to current requirements, and negative selection or subtractive steps are strongly recommended.

Despite many strategies about aptamers and the optimization of their selection, SELEX is still a relatively slow and complicated process. No standardized

SELEX protocol is applicable for any type of target. The selection conditions have to be adapted to the current circumstances (target, desired features of the aptamers, applications). The entire process to get high-affine and specific aptamers is very time consuming. Furthermore, automated SELEX protocols were described and established on the basis of a robotic workstation [14–17] or microfabricated chip-based SELEX platform [18] to make the aptamer selection process more accessible and more rapid.

The SELEX technology is applicable to a wide variety of targets. Besides defined single targets, complex target structures or mixtures without proper knowledge of their composition are suitable for successful aptamer selection. However, not all target molecules are suitable for an aptamer selection. Target features that facilitate successful aptamer selection are, for example, positively charged groups, the presence of hydrogen-bond donors and acceptors, and planarity [19, 20]. Defined single-target molecules should be available in sufficient amount and with high purity for the SELEX performance. Aptamer selection is more difficult for targets with a largely hydrophobic character and for negatively charged molecules. These target requirements are based on the fundamental principles of intermolecular interactions in an aptamer–target complex.

Aptamers are artificial specific oligonucleotides, DNA or RNA, with the ability to bind to non-nucleic acid target molecules by SELEX [19, 21–25], such as peptides, proteins, drugs, organic and inorganic molecules, or even whole cells, with high affinity, specificity, accuracy, and reproducibility [26–31]. The understanding of the nucleic acids in terms of their conformation and ligand binding properties has recently opened a new research area, where these two properties are exploited for the development of new analytical techniques. Aptamers are similar to monoclonal antibodies regarding their binding affinities, but they offer a number of advantages over the existing antibody-based detection methods, with K_d values in the picomolar range achieved [30, 32]. The binding specificities of the aptamers have been demonstrated to allow 10 000-fold to 12 000-fold [30, 33] discrimination of aptamers toward their target molecules even in the case of very closely related structures. Aptamers are often viewed as artificial antibodies and promise to replace real antibodies in future biomedical and analytical applications [3, 20, 34].

Aptamers are selected by an *in vitro* process independent of animals or cell lines. They can be delivered into cells or expressed within cells by transcription of expression cassettes. Aptamers could be used for intracellular detection of target molecules or could function as intracellular inhibitors due to their low immunogenicity [35, 36]. The affinity and specificity characteristics inherent to aptamers make their utilization very promising in analytical or clinical applications [28, 37, 38]. SELEX is carried out *in vitro*, avoiding the need for animals, and aptamers can also be selected against non-immunogenic and toxic targets, as the process does not rely on the induction of an animal immune system, as in the case of antibody generation. Moreover, SELEX can be manipulated to produce aptamers to a specific region of the target, a facet sometimes not possible with antibodies, as the animal immune system inherently hones the epitopes on the target molecule.

12.2 Challenges of SELEX

Only a few aptamer-based technologies are used today. Essentially, the major efforts have been focused on the known aptamers, such as the thrombin aptamer, for novel design strategies rather than expending the efforts and energies in isolating new aptamers for practical usage [39, 40]. Geoffrey Baird reports that the major issues in the aptamer field are described as the “thrombin problem” [39–41]. Other reasons that contribute to the problems in the aptamer field includes (i) the process of isolating new aptamers is currently repetitious, tedious, and time intensive because of suboptimal SELEX methods [42, 43], (ii) the high costs associated with SELEX [43], (iii) limited abilities of the polymerases to accommodate for modified and unnatural nucleic acids [42, 44, 45], and (iv) relatively short half-life *in vivo* due to nuclease degradation and renal clearance [46–49]. In an ideal SELEX scenario, each cycle should contain rapid positive and negative selection processes and efficient and precise partitioning of unbound from bound aptamers, as well as efficient separation of bound aptamers from their target molecules [50]. Amplification of remaining binding aptamers should be quick, followed by efficient purification of the amplified aptamer pool so that it may be fed back into the beginning of the system. Furthermore, SELEX should have the ability to select for aptamers with predefined binding specificity. Unfortunately, SELEX, like any other technique, is not without limitations.

Aptamers are extremely versatile molecules that have high applicable potentials. A potential trait of SELEX that makes it worthy of pursuing is that it enables the isolation of functional DNA and RNA molecule from enormous, randomized pools without any prior knowledge of target molecules or binding interaction with its ligand [51, 52]. Although many different types of aptamers have been identified via the variation of the SELEX technique [50], the aptamer field still contains many hurdles before it can be fully adapted in the scientific community and its potentials are recognized. Many researchers attempted to manipulate the selection scheme to improve the rate at which aptamers can be achieved as mentioned earlier.

12.2.1 Aptamer Degradation

The rapid degradation of aptamers (especially RNA aptamers) by nucleases is a serious problem. The average time of oligonucleotide decay in the blood and cell ranges from several minutes to several tens of minutes depending on the oligonucleotide concentration and conformational structure [47]. Several methods for protecting aptamers against degradation by nucleases have been developed. One of the conventional methods used to generate nuclease-resistant aptamers is by performing SELEX with oligonucleotide-containing modified nucleotides. Most aptamers in analytical studies are chemically modified by replacing the 2' position with a fluoro (F) [53, 54], amino (NH₂) [55, 56], *O*-methyl (OCH₃) group [57, 58], locked nucleic acids (LNA) [59, 60] and by capping the 3'-end with inverted thymidine to increase nuclease resistance while also enhancing binding affinity. Multiple modifications are sometimes applied in combination for optimal performance. As the affinity and/or specificity and function of an aptamer are sensitive

to its structure, post-SELEX modification may affect the inherent properties and folding structures of the original aptamers, thereby compromising binding affinity. Nevertheless, some modifications can increase aptamer resistance to nucleases without affecting their binding to target molecules. The most common and effective type of such aptamer improvements is the modification of 3'- and 5'-nucleotides [61]. Therefore, it is necessary to precisely tailor the modifications for the desired functions [62]. Unfortunately, universal rules are not available for all aptamers, and laborious evaluation and optimization are often needed [63].

12.2.2 Purification

Aptamer generation, in most cases, requires the availability of purified target molecules. The type of a target and its purity are also critical for aptamer selection. Usually, targets for SELEX are obtained by expression in prokaryotic or eukaryotic cells followed by chromatography purification. Sometimes, aptamers obtained against targets expressed in prokaryotic systems fail to bind to the same target expressed in eukaryotic cells. This may occur due to the lack of posttranslational modifications in the latter cells [64]. Protein target molecules are expressed in cell cultures and purified by affine chromatography. These procedures are time and labor consuming, thus delaying the production of corresponding aptamers. Moreover, some proteins are difficult to purify due to their chemical properties. Sometimes aptamers generated against target proteins expressed in prokaryotic cells do not interact with the same proteins expressed in eukaryotic cells due to posttranslational modifications. These modifications can make epitopes of eukaryotic proteins inaccessible to aptamers generated against the proteins expressed in prokaryotic cells [64]. Cell-SELEX technology enables selection of aptamers without knowledge about the target. But as in the case of other methods, cell-SELEX also has its pitfalls. For example, the presence of dead cells in a suspension used for aptamer generation led to nonspecific uptake or binding of oligonucleotides by these cells that had a negative impact on whole selection process [65]. Microbeads were a possible solution for dead cell removal. Such removal might help decrease the number of nonspecific aptamers obtained through cell-SELEX. Actually, introduction of a counterselection against dead cells might be another, maybe even more cost-effective, alternative to decrease the number of nonspecific aptamers generated by cell-SELEX.

12.2.3 Binding Affinity (K_d)

An important criterion of SELEX is the affinity of selected aptamers [66]. While new methods for the determination of binding affinity are constantly being developed [67–69], this is often the limiting factor in the rapid development and testing of aptamers. This is particularly true for small-molecule-binding aptamers. To measure K_d , a constant concentration of either the aptamer or target is titrated with an increasing concentration of the other component to yield a binding isotherm. Relatively few of these common K_d methods are effective for measuring aptamer binding to small molecules. Separation-based techniques

are among the most common approaches for determining binding affinity, and many of these are more challenging for small-molecule targets than for proteins. In particular, separation-based methods that rely on a dramatic change in the size of the aptamer–target complex upon target binding are of limited use when the target is much smaller than the aptamer. Other methods require that the target has some intrinsic fluorescence/absorbance, which is often not the case. For targets lacking these properties, an alternative is to label the target, which can affect the chemical properties of the small molecule and interfere with aptamer binding. Surface mass-sensitive detection methods such as quartz crystal microbalance (QCM) and surface plasmon resonance (SPR) are typically limited to large targets such as proteins [70]. These approaches generally require one binding partner to be tethered to the surface. In cases where the aptamer is surface bound, the sensitivity of the technique may be compromised by the small overall mass change caused by small molecule binding. As an alternative, the target could be attached to the surface, but once again this chemical modification of the target can negatively impact binding affinity. Other methods that detect a change in aptamer conformation upon binding to the target can be applicable to small-molecule aptamers, but measurable conformation change is not a universal property of all aptamers [71]. Some recent reports of approaches for determining aptamer binding affinity have recognized the unique challenges for small-molecule aptamers and attempted to address them using more innovative approaches such as automated microchip electrophoresis and atomic force spectroscopy, although no technique can be considered generally applicable to small-molecule aptamers at this stage [72, 73].

12.2.4 Target Immobilization

The separation of target-bound sequences from those with no affinity for the target is a critical step in the SELEX process [66]. For protein targets, partitioning can be achieved using a matrix that selectively adsorbs the target and any interacting aptamer sequences. For example, nitrocellulose filters are an inexpensive and convenient matrix for this purpose due to their nucleic acid permeability and their ability to retain proteins by hydrophobic adsorption. With cell targets, partitioning can be accomplished by centrifugation, fluorescence-activated cell sorting (FACS) [74], or by gentle washing of adherent cells [75]. In the case of both these target types, the selection can be accomplished without chemical modification of the target; this is ideal since it increases the likelihood of finding aptamers capable of binding the molecule in its unaltered form. This is typically not possible with small-molecule aptamer selections. Thus, the primary complication arises from the need to immobilize the target to a solid support matrix, for example, magnetic beads, acrylic beads, and agarose/sepharose, to facilitate the partitioning process. Earlier small-molecule aptamers were selected for targets for which premade agarose material was commercially available [76]. In the absence of commercially available material, there is a wide array of conjugation chemistries that are available for preparing these materials for SELEX experiments. However, these are all dependent on the presence of certain functional groups that allow for coupling, which are not always present

on the desired target. For cases where conjugation is possible, the proportionally large amount of column material, in comparison to the target, that is presented to the nucleic acid pool during each SELEX round can result in high nonspecific binding of the library. As chemical modification of the target is required to facilitate column immobilization, the library is exposed to a chemically modified target rather than the desired, unmodified target molecule, increasing the likelihood of selecting sequences that display binding properties toward the matrix, and/or the linker arm. Despite negative selection steps, carry-over of such sequences is difficult to avoid [59]. Many aptamer applications, particularly those *in vivo*, require the selected sequences to bind the target free in solution. Therefore, any aptamer affinity derived from partial binding to the matrix or from chemical modifications will reduce the functionality of the aptamer in the intended applications. For example, the published rhodamine aptamer displays a weaker binding to the target rhodamine when in solution compared to when it is immobilized on the matrix used in the selection [60]. Moreover, introduction of a counterselection step enables removal of nonspecific aptamers bound to the immobilization matrix. When performed with structurally similar molecules, counterselection helps minimize aptamer cross-reactivity [77, 78]

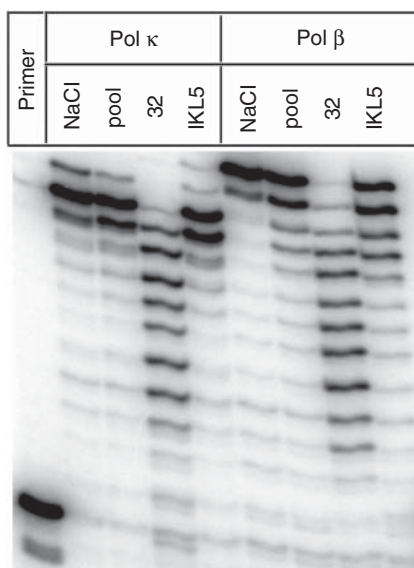
12.2.5 Cross-Reactivity

Aptamer cross-reactivity can be an obstacle to practical application because of the possible side effects caused by aptamer interaction with other proteins. Aptamers that recognize particular targets can also bind to molecules with a similar structure. Four generated aptamers against DNA polymerase β can also bind and inhibit DNA polymerase κ , which belongs to another DNA polymerase family [77]. However, this problem can be avoided by introducing a SELEX-negative selection step with structurally similar molecules. A more stringent SELEX protocol was used to produce a highly specific aptamer against DNA polymerase ι . This aptamer can bind neither to DNA polymerases κ nor to β , and DNA-polymerase activity of polymerases κ and β in the presence of aptamer IKL5 was shown in Figure 12.1 [78].

12.2.6 Time and Cost

The inefficiency of SELEX lies mainly with the high reagent consumption and time demands [42, 43]. Generation of aptamers seems to be a rather simple protocol, but in reality it is a time- and labor-consuming process. First of all, the cost of the aptamer selection process should be taken into consideration. Thus, to start a selection process, researchers have to synthesize a massive DNA oligonucleotide library consisting of at least 10^{15} sequences [79]. For this purpose, a laboratory has to be equipped with a robotic station for chemical synthesis; this greatly increases the cost of an aptamer selection. Often, RNA aptamers are preferred over DNA ones due to their ability to fold into more complex 3D structures. In this case, the initial DNA library should be converted into RNA by *in vitro* transcription, which increases not only the cost of production but also its length.

Figure 12.1 DNA-polymerase activity of Pol κ and Pol β in the presence of aptamer IKL5. Source: Lakhin et al. 2012 [78]. Reprinted with permission from Mary Ann Liebert.



To minimize the selection time of aptamers, several SELEX modifications have been developed, some of them even offering automatization of the SELEX process [14, 16, 43, 80]. One new method known as CE-SELEX (capillary electrophoresis SELEX) includes a modified stage of selection of target-bound oligonucleotides and allows to generate aptamers in one round. Nonequilibrium capillary electrophoresis of equilibrium mixtures (NECEEM) is used for aptamer fractioning. The entire selection procedure lasts one to two days and allows selecting aptamers with strictly specified binding parameters, K_d , K_{off} , and K_{on} [50, 81]. Automatization might provide significant advantages in aptamer selection, enabling the large-scale production of novel aptamers and decreasing the time of selection. But flexible devices that enable such automatic selection have not been produced commercially yet; thus, each research group has to fabricate such devices on their own, which is a laborious and expensive process. Besides, the cost of oligonucleotide modifications has to be reduced especially for large-scale manufacturing, enabling wider access to the end users.

12.2.7 Interaction of Aptamers with Intracellular Targets

Most aptamers were selected using molecules located on the cell surface or in the blood stream. This potentially makes their application rather easy, since all that is needed to trigger the therapeutic effect is to deliver the aptamers into the blood stream. However, some advances in the intracellular delivery of aptamers have recently been achieved. Special expression systems are able to generate aptamers inside cells and ensure their accumulation either in the nucleus or in the cytoplasm. For example, transfection of cells with a recombinant vector expressing the aptamer sequence under a U6 promoter allows specific inactivation of nuclear target proteins [82, 83], while aptamer expression under

a tRNA promoter ensures predominantly cytoplasmic localization of aptamers [84]. Cell-type-specific aptamer synthesis can be achieved using directional viral expression systems that deliver vectors to particular cells [85, 86]. The concentration of expressed aptamers can be increased not only using strong promoters that ensure a high level of expression but also by limiting the rate of aptamer degradation by nucleases through protection of the 3'- and 5'-termini with additional structures [82]. Another way of delivering aptamers to intracellular target molecules is by the transfer of aptamers from the bloodstream to cells through receptor-dependent endocytosis [87, 88]. For example, endocytosis of aptamer binding prostate-specific membrane antigen (PSMA) provides effective and specific delivery of conjugated drugs to cancer cells expressing this antigen on their surface [89, 90].

12.2.8 Bioinformatics Tools

Last but not least, there is an immense need for novel bioinformatics tools that are capable of processing the large-scale sequencing data along with the secondary structure predictions, in order to gain further insight into the correlation between the pool enrichment and the aptamer affinities [91, 92]. Although there is still a long way for the aptamers to go quickly from the laboratory benches to the markets, it is indeed a very interesting and promising field that is well worth the effort.

12.3 Demerits of Aptamer-Based Methods

It has been a quarter century since Andrew Ellington and Larry Gold revealed the aptamers as a new class of selected oligonucleotides rivaling antibodies. Since their inception, hundreds of aptamers have been selected from combinatorial oligonucleotide libraries, spanning a wide range of targets regardless of the size, surface charge, toxicity, and physical, chemical, or biological structure. Given their small size, *in vitro* screening capability, chemical and thermal stability, ease of labeling, and the productiveness in relation to the overall synthesis cost, aptamers have been employed in a number of different analytical methods including colorimetric, fluorescence, electrochemical, lateral flow assay, materials science, and non-labeling methods. However, in contrast to the rapid development and application of aptamers, there are still some demerits in various aptamer-based methods.

12.3.1 Sensitivity

The sensitivity required for any target analyte is based on its concentration in the detection medium. Despite the fact that electrochemical techniques have obtained huge success, particularly with aptamers that have shown increasing possibility and advantage in stability and affinity, these strategies suffer from low sensitivity. Usually, in cases of strategies employing aptamer hairpins, one end of

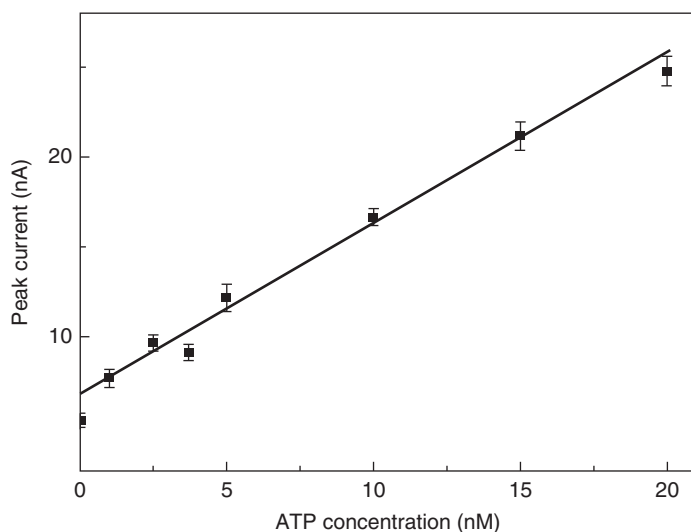


Figure 12.2 The detection limit of 1 nM could be readily achieved with the concentrations of ATP in the range from 1 to 20 nM. Source: Liu et al. 2013 [93]. Reprinted with permission of Royal Society of Chemistry.

the aptamer hairpin is linked to the redox moiety and the other end is attached to the electrode surface and the electrochemical signal is attributed depending on the proximity of the redox moiety and the conformational changes of the hairpin. This could lead to discrepancies in understanding the signal determined by the binding affinity of the target. In particular, the chances of signal arising is relatively limited to occur due to distance barriers between the redox species and the electrode surface. Therefore, this leads to false positives; and moreover the stem-loop stability due to the immobilization of any aptamer hairpin is subject to question. To increase sensitivity, an electrochemical aptamer-based adenosine triphosphate (ATP) assay using homogeneous solutions was reported by Liu et al., as shown in Figure 12.2 [93]; however, no trials have been conducted to fabricate aptamer-based biosensors using this strategy. Substantial progress was made using homogeneous solutions; however, studies have shown that low-affinity-binding constants of the target species to their specific aptamers were obtained, leading to lower sensitivities [93].

More recently, techniques such as electrochemical impedance spectroscopy (EIS), SPR, and fluorescence spectroscopy are based on TBA as their target analyte and much of the research is done using the sequence in aptamer-based assays, sensors, and biosensors. These methods have shown low sensitivity, poor detection limits, lengthy measurements, and long sample preparation. To improve sensitivity, a novel method using SERS with magnetic beads as supporting materials was reported with high sensitivity for the detection of the lung cancer marker antigen. Compared to previously reported surface-enhanced Raman spectroscopy (SERS) aptasensors, this sensor has several advantages in terms of sensitivity with linear response in the lower concentration range from 0.27 pM to 0.27 nM and in less time (less than 1.5 hours) [94]. Another work used

a polymer consisting of poly(*m*-phenylenediamine) (PMPD) rods as an effective sensing platform to create a novel fluorescent aptasensor. An extraordinarily high sensitivity with a detection limit as low as 100 pM was configured by this sensor [95].

12.3.2 Selectivity and Specificity

Several affinity-based biosensors with aptamers have been developed using biomolecules as target analyte. The reason for this is that these larger targets have more functional groups and structural ligands that could be captured via hydrogen bonds, electrostatic interactions, or hydrophobic bonds. Therefore, larger targets are in continuous demand, and there are many compelling reasons for limitations in pursuing the detection of small molecules. One of the reasons is their relatively low dissociation constants and poor detection limit. Some small molecules that are less often used for biosensing include cocaine, theophylline, kanamycin, growth factors, tobramycin, tetracycline, aflatoxin [96–101], which could be detrimental or beneficial in normal daily life. For this reason, simple direct binding procedures for developing aptamer-based assays are barely applicable as aptamers may not be able to bind directly to these targets and attempts to develop effective paths for improving sensitivity have been reported [102].

Selectivity issues have also led to the development of multianalyte detection aptasensors for proteins, small molecules, and other analytes. Recently, bifunctional aptamer binding to two different targets has been demonstrated, where a sensitive biosensor for adenosine and Lys using $[\text{Ru}(\text{NH}_3)_6]^{3+}$ as signal transducer and AuNP amplification was reported [103]. However, these sensors cannot detect multitargets in one sample and a versatile system is highly desired. More recently, one spot detection of adenosine and thrombin was demonstrated using voltammetry followed by similar work done using the ECL technique as a novel strategy [104]. Furthermore, a novel universal fluorescence aptasensor for detecting proteins, ions, and small molecules was designed and reported by Lv et al. [105].

One of the key parameters to evaluate selectivity is cross-reactivity, where aptamer could bind with more than one target analyte due to structural similarities, which leads to false positives. Cross-reactivity was observed when selectivity experiments were carried out between OTA and AFM1 (aflatoxin M1) having the same molecular weight, using $(\text{Fe}_3\text{O}_4/\text{PANi})$ integrated electrode aptasensor [106]. Zheng et al. have shown that in these kinds of situations, evaluation of the sensing system for selectivity should be done by detecting the signal changes induced by other mycotoxins [107]. Specificity and selectivity issues in the detection of pathogenic bacteria should be more precisely evaluated to discriminate the real signals from false-positive signals. In one of the embodiments, the specificity was demonstrated by a competitive inhibition assay. For this, different concentrations of phage were preincubated with a known concentration of *Staphylococcus aureus* for one hour to block the receptor sites from binding, and the solutions were introduced through the sensor [108]. Another phage-based incubation approach used 360-fold excess of bovine serum

albumin in a mixture with galactosidase and found only 2% reduction in the biosensor signal and excellent selectivity [109].

12.3.3 Reproducibility

One of the key problems associated with aptamer-based sensors is the reproducibility of certain results. The occurrence of error is based on the technique used and the detection range. For instance, SPR-based optical immunosensors are commonly reported with low detection levels and error deviations at 2–8% level. Therefore, these instruments are less commonly used than amperometric immunosensors. With much success ascribed to aptamers, aptasensors are not without similar disadvantages in terms of repeatability. For example, eight different samples of OTA with similar concentrations of 10 ng ml^{-1} were measured independently using eight different aptasensors and the relative standard deviation (RSD) was found to be 4.7%, which indicates an acceptable reproducibility. Similar RSD values were also obtained in other novel aptasensors employed for the detection of thrombin. Despite the novel improvements, the problem of uncertainty is consistently unavoidable, and always a great challenge.

12.3.4 Calibration and Uncertainty

Ideal sensor performance is assessed on the basis of a reliable calibration method. Much effort in sensor development frequently presumes calibrations performed under *in vitro* (buffer) conditions. Consequently, assumptions made with this method are not always true for detecting molecules residing in biological fluids under physiological conditions. In fact, this approach is complicated by a number of factors that can affect the concentrations of the target species that vary considerably. In addition, this could initiate further problems for the determination of concentrations of small molecules, ions, and enzyme activities as buffers are usually spiked with electrolyte ion (Na^+ , K^+) conditions for electrochemistry. One of the issues in electrochemical sensors is the need for repetitive calibration for every measurement. This could be avoided by simultaneous measurements conducted under similar conditions that mimic biological fluids or serum solutions [110–112]. Although most of the methods use serum solutions as a quick confirmation measurement, the standard calibration curve performed was not under similar conditions. To minimize the measurement uncertainty, it is crucial to use similar medium or matrix conditions for both standard calibrations as well as for the sample. Furthermore, it is also desirable to invent a favorable and reliable biosensor that can be used in complicated real samples.

12.3.5 Regeneration

Biosensor technology has advanced in developing smart and unique sensors, which unfortunately in the case of the affinity-based approach could be applicable only for one-time use. Therefore, several successful attempts have been made to regenerate the sensor usage for multiple times. However, despite novel strategies, these sensors not only have to survive but also have to show good

precision and sensitivity after reuse. For example, electrochemical aptasensors with surface-confined aptamer probes require large conformational changes induced by the target binding. These complex immobilization procedures suffer the problem of sensor regeneration due to the strong binding of the aptamers with the analytes [113]. In another study, although the sensor had high sensitivity and reproducibility, it was unable to exhibit satisfactory regeneration due to split up of thiol groups attached on the gold surface due to applied potential [114]. Moreover, the sensor does not always compromise sensitivity after recycling, leading to the use of multiple concentrations of the bioreceptor on the surface layer [115]. To avoid this limitation, more convenient and general covalent binding approaches are sought for.

12.3.6 Immobilization of Aptamers

The crucial step in electrochemical aptasensor development is the immobilization of aptamers to an electrode surface, and it is important to develop strategies for reliable immobilization of aptamers so that they retain their biophysical characteristics and binding abilities, as well as for minimizing nonspecific binding/adsorption events. In principle, these strategies are similar to those applied for the immobilization of single- or double-stranded DNA in genosensors or DNA biosensors for detection of DNA damage [116]. The methods of immobilization based on physical adsorption of DNA by means of electrostatic interactions are, in general, not suitable due to low stability caused by aptamer desorption from the surface. The common pathways for immobilizing a stable, flexible, and repeatable aptamer layer surface are chemical covalent attachment, via avidin-to-biotin conjugation [117], and self-assembling the thiolated aptamer onto gold substrate using a thiol-alkane linked to the aptamer sequence [116]. Streptavidin-polymer-coated indium tin oxide electrodes for immobilizing a DNA aptamer against lysozyme have been also designed. In spite of these rapid advances, aptamer-based bioassays are still immature when compared to immunoassays, which, in a sense, reflects the limited availability of aptamer types and the relatively poor knowledge of surface-immobilization technologies for aptamers [118].

12.4 Summary and Perspectives

It has been more than two decades since the first aptamer molecule was discovered. Since then, aptamer molecules have gained a great deal of attention in the scientific field. Aptamers have been widely used in a variety of sensor applications, offering a variety of possibilities for aptamer-based sensors in analytical applications. Yet, despite the advances and the huge body of literature documenting the success of the technology, the selection and application of aptamer-based methods come with a unique set of challenges, unless aptamers offer verifiably significant improvements on current technologies. Overcoming these challenges and taking full advantage of the unique attributes of aptamers is vital for the future success of aptamers as analytical elements. Continued effort

in the development of aptamers for important small molecules is required in order for this field to realize its full potential. Efforts to mine this data to better tailor SELEX and binding affinity experiments for aptamer-based methods is currently under way. As more researchers devote themselves to rational aptamer development, next-generation analytical-based aptamers with superior biological functions is highly anticipated. The aptamer field has probably touched only the tip of the iceberg. Applications of aptamers in other burgeoning areas, such as metabolomics, drug discovery, and synthetic biology, could also soon see dramatic growth.

References

- 1 Tuerk, C. and Gold, L. (1990). Systematic evolution of ligands by exponential enrichment: RNA ligands to bacteriophage T4 DNA polymerase. *Science* 249 (4968): 505–510.
- 2 Ellington, A.D. and Szostak, J.W. (1990). In vitro selection of RNA molecules that bind specific ligands. *Nature* 346 (6287): 818–822.
- 3 Jayasena, S.D. (1999). Aptamers: an emerging class of molecules that rival antibodies in diagnostics. *Clin. Chem.* 45 (9): 1628–1650.
- 4 Andreola, M.L., Calmels, C., Michel, J. et al. (2000). Towards the selection of phosphorothioate aptamers optimizing in vitro selection steps with phosphorothioate nucleotides. *Eur. J. Biochem.* 267 (16): 5032–5040.
- 5 Dougan, H., Lyster, D.M., Vo, C.V. et al. (2000). Extending the lifetime of anticoagulant oligodeoxynucleotide aptamers in blood. *Nucl. Med. Biol.* 27 (3): 289–297.
- 6 Kopylov, A.M. and Spiridonova, V.A. (2000). Combinatorial chemistry of nucleic acids: SELEX. *Mol. Biol.* 34 (6): 940–954.
- 7 Kusser, W. (2000). Chemically modified nucleic acid aptamers for in vitro selections: evolving evolution. *J. Biotechnol.* 74 (1): 27–38.
- 8 Marro, M.L., Daniels, D.A., McNamee, A. et al. (2005). Identification of potent and selective RNA antagonists of the IFN-gamma-inducible CXCL10 chemokine. *Biochemistry* 44 (23): 8449–8460.
- 9 Klussmann, S. (2006). *The Aptamer Handbook: Functional Oligonucleotides and their Applications*. Weinheim: Wiley-VCH.
- 10 Pan, W., Craven, R.C., Qiu, Q. et al. (1995). Isolation of virus-neutralizing RNAs from a large pool of random sequences. *Proc. Natl. Acad. Sci. U. S. A.* 92 (25): 11509–11513.
- 11 Hwang, B. and Lee, S.W. (2002). Improvement of RNA aptamer activity against myasthenic autoantibodies by extended sequence selection. *Biochem. Biophys. Res. Commun.* 290 (2): 656–662.
- 12 Held, D.M., Greathouse, S.T., Agrawal, A., and Burke, D.H. (2003). Evolutionary landscapes for the acquisition of new ligand recognition by RNA aptamers. *J. Mol. Evol.* 57 (3): 299–308.
- 13 Bittker, J.A., Le, B.V., and Liu, D.R. (2002). Nucleic acid evolution and minimization by nonhomologous random recombination. *Nat. Biotechnol.* 20 (10): 1024–1029.

- 14 Cox, J.C. and Ellington, A.D. (2001). Automated selection of anti-protein aptamers. *Bioorg. Med. Chem.* 9 (10): 2525–2531.
- 15 Cox, J.C., Rajendran, M., Riedel, T. et al. (2002). Automated acquisition of aptamer sequences. *Comb. Chem. High Throughput Screen.* 5 (4): 289–299.
- 16 Eulberg, D., Buchner, K., Maasch, C., and Klussmann, S. (2005). Development of an automated in vitro selection protocol to obtain RNA-based aptamers: identification of a biostable substance P antagonist. *Nucleic Acids Res.* 33 (4): e45.
- 17 Nitsche, A., Kurth, A., Dunkhorst, A. et al. (2007). One-step selection of Vaccinia virus-binding DNA aptamers by MonoLEX. *BMC Biotech.* 7: 48.
- 18 Hybarger, G., Bynum, J., Williams, R.F. et al. (2006). A microfluidic SELEX prototype. *Anal. Bioanal. Chem.* 384 (1): 191–198.
- 19 Wilson, D.S. and Szostak, J.W. (1999). In vitro selection of functional nucleic acids. *Annu. Rev. Biochem.* 68: 611–647.
- 20 Rimmele, M. (2003). Nucleic acid aptamers as tools and drugs: recent developments. *ChemBioChem* 4 (10): 963–971.
- 21 Famulok, M. (1994). Molecular recognition of amino acids by RNA-aptamers: an L-citrulline binding RNA motif and its evolution into an L-arginine binder. *J. Am. Chem. Soc.* 116 (5): 1698–1706.
- 22 Burke, J.M. and Berzal-Herranz, A. (1993). In vitro selection and evolution of RNA: applications for catalytic RNA, molecular recognition, and drug discovery. *FASEB J.* 7 (1): 106–112.
- 23 Conrad, R.C., Baskerville, S., and Ellington, A.D. (1995). In vitro selection methodologies to probe RNA function and structure. *Mol. Diversity* 1 (1): 69–78.
- 24 Uphoff, K.W., Bell, S.D., and Ellington, A.D. (1996). In vitro selection of aptamers: the dearth of pure reason. *Curr. Opin. Struct. Biol.* 6 (3): 281–288.
- 25 Nieuwlandt, D. (2000). In vitro selection of functional nucleic acid sequences. *Curr. Issues Mol. Biol.* 2 (1): 9–16.
- 26 Patel, D.J., Suri, A.K., Jiang, F. et al. (1997). Structure, recognition and adaptive binding in RNA aptamer complexes. *J. Mol. Biol.* 272 (5): 645–664.
- 27 Clark, S.L. and Remcho, V.T. (2002). Aptamers as analytical reagents. *Electrophoresis* 23 (9): 1335–1340.
- 28 Luzi, E., Minunni, M., Tombelli, S., and Mascini, M. (2003). New trends in affinity sensing. *TrAC, Trends Anal. Chem.* 22 (11): 810–818.
- 29 You, K.M., Lee, S.H., Im, A., and Lee, S.B. (2003). Aptamers as functional nucleic acids: in vitro selection and biotechnological applications. *Biotechnol. Bioprocess Eng.* 8 (2): 64–75.
- 30 Jenison, R.D., Gill, S.C., Pardi, A., and Polisky, B. (1994). High-resolution molecular discrimination by RNA. *Science* 263 (5152): 1425–1429.
- 31 Famulok, M., Mayer, G., and Blind, M. (2000). Nucleic acid aptamers—from selection in vitro to applications in vivo. *Acc. Chem. Res.* 33 (9): 591–599.
- 32 Win, M.N., Klein, J.S., and Smolke, C.D. (2006). Codeine-binding RNA aptamers and rapid determination of their binding constants using a direct coupling surface plasmon resonance assay. *Nucleic Acids Res.* 34 (19): 5670–5682.

- 33 Geiger, A., Burgstaller, P., von der Eltz, H. et al. (1996). RNA aptamers that bind L-arginine with sub-micromolar dissociation constants and high enantioselectivity. *Nucleic Acids Res.* 24 (6): 1029–1036.
- 34 Rusconi, C.P., Scardino, E., Layzer, J. et al. (2002). RNA aptamers as reversible antagonists of coagulation factor IXa. *Nature* 419 (6902): 90–94.
- 35 Burgstaller, P., Girod, A., and Blind, M. (2002). Aptamers as tools for target prioritization and lead identification. *Drug Discovery Today* 7 (24): 1221–1228.
- 36 Nimjee, S.M., Rusconi, C.P., and Sullenger, B.A. (2005). Aptamers: an emerging class of therapeutics. *Annu. Rev. Med.* 56: 555–583.
- 37 Baldrich Rubio, E., Homs, M.C.I., and O’Sullivan, C.K. (2005). Aptamers: powerful molecular tools for therapeutics and diagnostics. In: *Molecular Analysis and Genome Discovery* (ed. R. Rapley and S. Harbron), 191–215. Chichester: Wiley.
- 38 Deisingh, A.K. (2006). Aptamer-based biosensors: biomedical applications. In: *RNA Towards Medicine* (ed. V. Erdmann, J. Barciszewski and J. Brosius), 341–357. Berlin, Heidelberg: Springer.
- 39 Lin, H., Zhang, W., Jia, S. et al. (2014). Microfluidic approaches to rapid and efficient aptamer selection. *Biomicrofluidics* 8 (4): 041501.
- 40 Baird, G.S. (2010). Where are all the aptamers? *Am. J. Clin. Pathol.* 134 (4): 529–531.
- 41 Breaker, R.R. (2009). *Aptamers in Bioanalysis*. Chichester: Wiley.
- 42 Bowser, M.T. (2005). SELEX: just another separation? *Analyst* 130 (2): 128–130.
- 43 Lou, X., Qian, J., Xiao, Y. et al. (2009). Micromagnetic selection of aptamers in microfluidic channels. *Proc. Natl. Acad. Sci. U. S. A.* 106 (9): 2989–2994.
- 44 Klussmann, S., Nolte, A., Bald, R. et al. (1996). Mirror-image RNA that binds D-adenosine. *Nat. Biotechnol.* 14 (9): 1112–1115.
- 45 Nolte, A., Klussmann, S., Bald, R. et al. (1996). Mirror-design of L-oligonucleotide ligands binding to L-arginine. *Nat. Biotechnol.* 14 (9): 1116–1119.
- 46 Pieken, W.A., Olsen, D.B., Benseler, F. et al. (1991). Kinetic characterization of ribonuclease-resistant 2'-modified hammerhead ribozymes. *Science* 253 (5017): 314–317.
- 47 Healy, J.M., Lewis, S.D., Kurz, M. et al. (2004). Pharmacokinetics and biodistribution of novel aptamer compositions. *Pharm. Res.* 21 (12): 2234–2246.
- 48 Ng, E.W., Shima, D.T., Calias, P. et al. (2006). Pegaptanib, a targeted anti-VEGF aptamer for ocular vascular disease. *Nat. Rev. Drug Discov.* 5 (2): 123–132.
- 49 Griffin, L.C., Tidmarsh, G.F., Bock, L.C. et al. (1993). In vivo anticoagulant properties of a novel nucleotide-based thrombin inhibitor and demonstration of regional anticoagulation in extracorporeal circuits. *Blood* 81 (12): 3271–3276.
- 50 Berezovski, M., Drabovich, A., Krylova, S.M. et al. (2005). Nonequilibrium capillary electrophoresis of equilibrium mixtures: a universal tool for development of aptamers. *J. Am. Chem. Soc.* 127 (9): 3165–3171.

- 51 Ali, M.M., Aguirre, S.D., Lazim, H., and Li, P.Y. (2011). Fluorogenic DNzyme probes as bacterial indicators. *Angew. Chem. Int. Ed.* 50 (16): 3751–3754.
- 52 Klug, S.J. and Famulok, M. (1994). All you wanted to know about SELEX. *Mol. Biol. Rep.* 20 (2): 97–107.
- 53 Li, N., Nguyen, H.H., Byrom, M., and Ellington, A.D. (2011). Inhibition of cell proliferation by an anti-EGFR aptamer. *PLoS One* 6 (6): e20299.
- 54 Derbyshire, N., White, S.J., Bunka, D.H. et al. (2012). Toggled RNA aptamers against aminoglycosides allowing facile detection of antibiotics using gold nanoparticle assays. *Anal. Chem.* 84 (15): 6595–6602.
- 55 Yan, X., Gao, X., and Zhang, Z. (2004). Isolation and characterization of 2'-amino-modified RNA aptamers for human TNFalpha. *Genom. Proteom. Bioinform.* 2 (1): 32–42.
- 56 Kuwahara, M. and Sugimoto, N. (2010). Molecular evolution of functional nucleic acids with chemical modifications. *Molecules* 15 (8): 5423–5444.
- 57 Lebars, I., Richard, T., Di Primo, C., and Toulme, J.J. (2007). LNA derivatives of a kissing aptamer targeted to the trans-activating responsive RNA element of HIV-1. *Blood Cells Mol. Dis.* 38 (3): 204–209.
- 58 Hernandez, F.J., Stockdale, K.R., Huang, L. et al. (2012). Degradation of nuclease-stabilized RNA oligonucleotides in mycoplasma-contaminated cell culture media. *Nucleic Acid Ther.* 22 (1): 58–68.
- 59 Kuwahara, M. and Obika, S. (2013). In vitro selection of BNA (LNA) aptamers. *Artif. DNA PNA XNA* 4 (2): 39–48.
- 60 Veedu, R.N. and Wengel, J. (2009). Locked nucleic acid nucleoside triphosphates and polymerases: on the way towards evolution of LNA aptamers. *Mol. Biosyst.* 5 (8): 787–792.
- 61 Mayer, G. (2009). The chemical biology of aptamers. *Angew. Chem. Int. Ed.* 48 (15): 2672–2689.
- 62 Lee, Y., Urban, J.H., Xu, L. et al. (2016). 2'Fluoro modification differentially modulates the ability of RNAs to activate pattern recognition receptors. *Nucleic Acid Ther.* 26 (3): 173–182.
- 63 Aaldering, L.J., Tayeb, H., Krishnan, S. et al. (2015). Smart functional nucleic acid chimeras: enabling tissue specific RNA targeting therapy. *RNA Biol.* 12 (4): 412–425.
- 64 Liu, Y., Kuan, C.T., Mi, J. et al. (2009). Aptamers selected against the unglycosylated EGFRvIII ectodomain and delivered intracellularly reduce membrane-bound EGFRvIII and induce apoptosis. *Biol. Chem.* 390 (2): 137–144.
- 65 Avci-Adali, M., Paul, A., Wilhelm, N. et al. (2010). Upgrading SELEX technology by using lambda exonuclease digestion for single-stranded DNA generation. *Molecules* 15 (1): 1–11.
- 66 Mckeague, M. and Derosa, M.C. (2012). Challenges and opportunities for small molecule aptamer development. *J. Nucleic Acids* 2012 (4968): 748913.
- 67 Elshafey, R., Sijaj, M., and Zourob, M. (2014). In vitro selection, characterization, and biosensing application of high-affinity cylindrospermopsin-targeting aptamers. *Anal. Chem.* 86 (18): 9196–9203.

- 68 Kim, Y.S. and Gu, M.B. (2014). Advances in aptamer screening and small molecule aptasensors. *Adv. Biochem. Eng. Biotechnol.* 140: 29–67.
- 69 Lin, H.I., Wu, C.C., Yang, C.H. et al. (2015). Selection of aptamers specific for glycated hemoglobin and total hemoglobin using on-chip SELEX. *Lab Chip* 15 (2): 486–494.
- 70 Yao, C., Qi, Y., Zhao, Y. et al. (2009). Aptamer-based piezoelectric quartz crystal microbalance biosensor array for the quantification of IgE. *Biosens. Bioelectron.* 24 (8): 2499–2503.
- 71 White, R.J., Rowe, A.A., and Plaxco, K.W. (2010). Re-engineering aptamers to support reagentless, self-reporting electrochemical sensors. *Analyst* 135 (3): 589–594.
- 72 Hu, J. and Easley, C.J. (2011). A simple and rapid approach for measurement of dissociation constants of DNA aptamers against proteins and small molecules via automated microchip electrophoresis. *Analyst* 136 (17): 3461–3468.
- 73 Nguyen, T.H., Steinbock, L.J., Butt, H.J. et al. (2011). Measuring single small molecule binding via rupture forces of a split aptamer. *J. Am. Chem. Soc.* 133 (7): 2025–2027.
- 74 Mayer, G., Ahmed, M.-S.L., Dolf, A. et al. (2010). Fluorescence-activated cell sorting for aptamer SELEX with cell mixtures. *Nat. Protoc.* 5 (12): 1993–2004.
- 75 Sefah, K., Shangguan, D., Xiong, X. et al. (2010). Development of DNA aptamers using cell-SELEX. *Nat. Protoc.* 5 (6): 1169–1185.
- 76 Jhaveri, S. and Ellington, A. (2002). In vitro selection of RNA aptamers to a small molecule target. *Curr. Protoc. Nucleic Acid Chem.* 8 (1): 9.5.1–9.5.14.
- 77 Gening, L.V., Klincheva, S.A., Reshetnjak, A. et al. (2006). RNA aptamers selected against DNA polymerase beta inhibit the polymerase activities of DNA polymerases beta and kappa. *Nucleic Acids Res.* 34 (9): 2579–2586.
- 78 Lakhin, A.V., Kazakov, A.A., Makarova, A.V. et al. (2012). Isolation and characterization of high affinity aptamers against DNA polymerase iota. *Nucleic Acid Ther.* 22 (1): 49–57.
- 79 Shaw, R.A. and Mantsch, H.H. (2008). Infrared spectroscopy in clinical and diagnostic analysis. *Encycl. Anal. Chem.* 964 (s1–3): 1–4.
- 80 Oh, S.S., Qian, J., Lou, X. et al. (2009). Generation of highly specific aptamers via micromagnetic selection. *Anal. Chem.* 81 (13): 5490–5495.
- 81 Drabovich, A.P., Berezovski, M., Okhonin, V., and Krylov, S.N. (2006). Selection of smart aptamers by methods of kinetic capillary electrophoresis. *Anal. Chem.* 78 (9): 3171–3178.
- 82 Good, P.D., Krikos, A.J., Li, S.X. et al. (1997). Expression of small, therapeutic RNAs in human cell nuclei. *Gene Ther.* 4 (1): 45–54.
- 83 Auslander, D., Wieland, M., Auslander, S. et al. (2011). Rational design of a small molecule-responsive intramer controlling transgene expression in mammalian cells. *Nucleic Acids Res.* 39 (22): e155.
- 84 Chaloin, L., Lehmann, M.J., Sczakiel, G., and Restle, T. (2002). Endogenous expression of a high-affinity pseudoknot RNA aptamer suppresses replication of HIV-1. *Nucleic Acids Res.* 30 (18): 4001–4008.

- 85 Mi, J., Zhang, X., Rabbani, Z.N. et al. (2006). H1 RNA polymerase III promoter-driven expression of an RNA aptamer leads to high-level inhibition of intracellular protein activity. *Nucleic Acids Res.* 34 (12): 3577–3584.
- 86 Mayer, G., Blind, M., Nagel, W. et al. (2001). Controlling small guanine-nucleotide-exchange factor function through cytoplasmic RNA intramers. *Proc. Natl. Acad. Sci. U. S. A.* 98 (9): 4961–4965.
- 87 Davydova, A.S., Vorobjeva, M.A., and Venyaminova, A.G. (2011). Escort aptamers: new tools for the targeted delivery of therapeutics into cells. *Acta Naturae* 3 (4): 12–29.
- 88 Meyer, C., Eydeler, K., Magbanua, E. et al. (2012). Interleukin-6 receptor specific RNA aptamers for cargo delivery into target cells. *RNA Biol.* 9 (1): 67–80.
- 89 Zhao, Y., Duan, S., Zeng, X. et al. (2012). Prodrug strategy for PSMA-targeted delivery of TGX-221 to prostate cancer cells. *Mol. Pharmaceutics* 9 (6): 1705–1716.
- 90 Min, K., Jo, H., Song, K. et al. (2011). Dual-aptamer-based delivery vehicle of doxorubicin to both PSMA (+) and PSMA (–) prostate cancers. *Biomaterials* 32 (8): 2124–2132.
- 91 Hoon, S., Zhou, B., Janda, K.D. et al. (2011). Aptamer selection by high-throughput sequencing and informatic analysis. *BioTechniques* 51 (6): 413–416.
- 92 Hoinka, J., Zotenko, E., Friedman, A. et al. (2012). Identification of sequence-structure RNA binding motifs for SELEX-derived aptamers. *Bioinformatics* 28 (12): i215–i223.
- 93 Liu, S., Wang, Y., Zhang, C. et al. (2013). Homogeneous electrochemical aptamer-based ATP assay with signal amplification by exonuclease III assisted target recycling. *Chem. Commun.* 49 (23): 2335–2337.
- 94 Yoon, J., Choi, N., Ko, J. et al. (2013). Highly sensitive detection of thrombin using SERS-based magnetic aptasensors. *Biosens. Bioelectron.* 47: 62–67.
- 95 Zhang, Y. and Sun, X. (2011). A novel fluorescent aptasensor for thrombin detection: using poly(m-phenylenediamine) rods as an effective sensing platform. *Chem. Commun.* 47 (13): 3927–3929.
- 96 Kim, Y.J., Kim, Y.S., Niazi, J.H., and Gu, M.B. (2010). Electrochemical aptasensor for tetracycline detection. *Bioprocess. Biosyst. Eng.* 33 (1): 31–37.
- 97 Velasco, M. and Missailidis, S. (2009). New trends in aptamer-based electrochemical biosensor. *Gene Ther. Mol. Biol.* 13 (1): 1–9.
- 98 Famulok, M. and Mayer, G. (2014). Aptamers and SELEX in chemistry & biology. *Chem. Biol.* 21 (9): 1055–1058.
- 99 Zhou, J. and Rossi, J. (2017). Aptamers as targeted therapeutics: current potential and challenges. *Nat. Rev. Drug Discov.* 16 (3): 181–202.
- 100 Tan, W., Donovan, M.J., and Jiang, J. (2013). Aptamers from cell-based selection for bioanalytical applications. *Chem. Rev.* 113 (4): 2842–2862.

- 101 Ma, H., Liu, J., Ali, M.M. et al. (2015). Nucleic acid aptamers in cancer research, diagnosis and therapy. *Chem. Soc. Rev.* 44 (5): 1240–1256.
- 102 Li, W., Nie, Z., Xu, X. et al. (2009). A sensitive, label free electrochemical aptasensor for ATP detection. *Talanta* 78 (3): 954–958.
- 103 Deng, C., Chen, J., Nie, L. et al. (2009). Sensitive bifunctional aptamer-based electrochemical biosensor for small molecules and protein. *Anal. Chem.* 81 (24): 9972–9978.
- 104 Chai, Y., Tian, D., and Cui, H. (2012). Electrochemiluminescence biosensor for the assay of small molecule and protein based on bifunctional aptamer and chemiluminescent functionalized gold nanoparticles. *Anal. Chim. Acta* 715: 86–92.
- 105 Lv, Z., Liu, J., Zhou, Y. et al. (2013). Highly sensitive fluorescent detection of small molecules, ions, and proteins using a universal label-free aptasensor. *Chem. Commun.* 49 (48): 5465–5467.
- 106 Nguyen, B.H., Tran, L.D., Do, Q.P. et al. (2013). Label-free detection of aflatoxin M1 with electrochemical Fe₃O₄/polyaniline-based aptasensor. *Mater. Sci. Eng. C Mater. Biol. Appl.* 33 (4): 2229–2234.
- 107 Chen, J., Fang, Z., Liu, J., and Zeng, L. (2012). A simple and rapid biosensor for ochratoxin A based on a structure-switching signaling aptamer. *Food Control* 25 (2): 555–560.
- 108 Balasubramanian, S., Sorokulova, I.B., Vodyanoy, V.J., and Simonian, A.L. (2007). Lytic phage as a specific and selective probe for detection of *Staphylococcus aureus* – a surface plasmon resonance spectroscopic study. *Biosens. Bioelectron.* 22 (6): 948–955.
- 109 Nanduri, V., Sorokulova, I.B., Samoylov, A.M. et al. (2007). Phage as a molecular recognition element in biosensors immobilized by physical adsorption. *Biosens. Bioelectron.* 22 (6): 986–992.
- 110 Deng, K., Xiang, Y., Zhang, L. et al. (2013). An aptamer-based biosensing platform for highly sensitive detection of platelet-derived growth factor via enzyme-mediated direct electrochemistry. *Anal. Chim. Acta* 759: 61–65.
- 111 Xiao, Y., Lou, X., Uzawa, T. et al. (2009). An electrochemical sensor for single nucleotide polymorphism detection in serum based on a triple-stem DNA probe. *J. Am. Chem. Soc.* 131 (42): 15311–15316.
- 112 Shahdost-fard, F., Salimi, A., Sharifi, E., and Korani, A. (2013). Fabrication of a highly sensitive adenosine aptasensor based on covalent attachment of aptamer onto chitosan-carbon nanotubes-ionic liquid nanocomposite. *Biosens. Bioelectron.* 48: 100–107.
- 113 Xia, Y., Gan, S., Xu, Q. et al. (2013). A three-way junction aptasensor for lysozyme detection. *Biosens. Bioelectron.* 39 (1): 250–254.
- 114 Li, F. and Cui, H. (2013). A label-free electrochemiluminescence aptasensor for thrombin based on novel assembly strategy of oligonucleotide and luminol functionalized gold nanoparticles. *Biosens. Bioelectron.* 39 (1): 261–267.
- 115 Liu, Y., Tuleouva, N., Ramanculov, E., and Revzin, A. (2010). Aptamer-based electrochemical biosensor for interferon gamma detection. *Anal. Chem.* 82 (19): 8131–8136.

- 116 Pividori, M.I., Merkoci, A., and Alegret, S. (2000). Electrochemical genosensor design: immobilisation of oligonucleotides onto transducer surfaces and detection methods. *Biosens. Bioelectron.* 15 (5–6): 291–303.
- 117 Rodriguez, M.C., Kawde, A.N., and Wang, J. (2005). Aptamer biosensor for label-free impedance spectroscopy detection of proteins based on recognition-induced switching of the surface charge. *Chem. Commun.* 0 (34): 4267–4269.
- 118 Song, S., Wang, L., Li, J. et al. (2008). Aptamer-based biosensors. *TrAC, Trends Anal. Chem.* 27 (2): 108–117.

13

State of the Art and Emerging Applications*Lin-Chi Chen, Jui-Hong Weng, and Pei-Wei Lee*

National Taiwan University, College of Bioresources and Agriculture, Department of Bio-industrial Mechatronics Engineering, No.1, Sec. 4, Roosevelt Road, Taipei, 10617, Taiwan

13.1 Introduction

While it is about time to celebrate the 30th anniversary of the advent of SELEX (Systematic Evolution of Ligands by EXponential Enrichment) and aptamers, aptamer-based analysis is still a young and rapidly growing field as compared to the maturity of antibody immunoassays. According to PubMed's statistics, the numbers of papers published per year with the key phrase "aptamer assay" are 16, 115, and 420 in 1997, 2007, and 2017, respectively. By contrast, the numbers for "antibody assay" in the corresponding years are 18 021, 17 184, and 14 714, showing a declining trend. Also, it is worthwhile to note that the current total paper number of "antibody assay" is almost 200 times that of "aptamer assay." Instead of considering the aptamer assay a premature technology, this comparison tells us how great are the opportunities that await aptamers in analytical applications. Before stating the cutting-edge aspects of aptamer-based analysis, let us rethink what aptamers are and why aptamers have been reshaping analytical technologies. By definition, aptamers are synthetic short DNA or RNA ligands that are obtained from *in vitro* selection and resemble monoclonal antibodies in function. (*Note:* there are also peptide aptamers, but they are out of the scope of this book.) With this understanding, it is not difficult to name several advantages of aptamers over antibodies in *in vitro* diagnostics (IVD), sensors, and general analytical applications. Moreover, the three-dimensional features of aptamers – (i) *resulted from directed molecular evolution*, (ii) *composed of four-letter synthetic oligonucleotides*, and (iii) *working like monoclonal antibodies* – have provided various interdisciplinary chances for sensing tech innovations. For example, an aptamer microarray [1] is a DNA microarray intrinsically. However, the aptamer probes are generated from SELEX instead of the cDNA library or GenBank[®], and such a DNA microarray is used to profile protein signatures like an antibody microarray instead of gene expression measurements. From this example, we see how aptamers can and have redefined the modern DNA chip development from their unique features. Hence, aptamer technology is not only young enough to talk about the state of the art and

the emerging applications but also with a cross-border nature for constant evolution.

Looking back at the three decades of aptamer development especially for analytical applications, most of the research innovations rely on constructing a rapid SELEX platform, selecting new aptamers for emerging targets, designing high-affinity and high-specificity aptamer probes, and devising high-sensitivity and label-free aptamer assays, sensors, or biochips. With the success of pioneer SELEX and aptamer studies in the 1990s (e.g. the discovery of two aptamers that bind distinct epitopes of human α -thrombin) and later triumph breakthroughs of fluorescence techniques (e.g. fluorescence resonance energy transfer (FRET), black-hole quenchers, and molecular beacons), nanomaterials (e.g. carbon nanotubes (CNTs), gold/silver nanoparticles, quantum dots (QDs), and graphene), biosensors (e.g. label-free surface plasmon resonance (SPR), electrochemical sensors, and nanowire field-effect transistor (FET) sensors) and biochips (e.g. microarrays and microfluidic chips), aptamer-based analysis has been explored in many frontiers of analytical applications along with either proof-of-concept studies using anti-thrombin aptamers or conjugating a newly discovered aptamer to a known or innovative biosensing approach. An emerging analytical field of “aptamer diagnostics” [2] has formed and has attracted the attention of applied scientists and industrial researchers since the 2000s. After 2010, aptamer diagnostics development has further fueled up and accelerated with commercial interests, unmet clinical and environmental monitoring needs, and cutting-edge technologies. Together with the application domains of aptamer therapeutics, the number of aptamer-related publications in the recent years is soaring high. Searching the keyword “aptamer” results in 7495 paper records from PubMed till the end of 2017. In addition, the related topics are favored in first-line, esteemed scientific journals and conferences, and there have been a number of thematic review articles available reflecting expanding diagnostic niches [2–4].

An overview of the field reveals three innovation models (Figure 13.1) for recent aptamer diagnostics. (i) *Exploration of the limit of sensing capability*. Aptamer affinity and specificity are optimized during or after SELEX. Aptamer sequences are reengineered and modified to render target-binding flexibility and multivalent avidity. Surface and anti-fouling chemistry are developed to lower the background signal or to reduce the interferences from a complex nontarget



Figure 13.1 Overview of the features and innovation models for aptamer diagnostics. Source: The computer figure is obtained from open-source website and modified by Lin-Chi Chen. Copyright © 2018, with permission from Prof. Lin-Chi Chen.

matrix (e.g. serum total protein). Nanomaterials, micro-fabricated biochips, and sensor array design are carried out to receive highly responsive signals, to reduce the sample volume and to perform parallel detection of a panel of analytes, respectively. All of these efforts together push the limits of aptamer-based sensing toward single-molecule specificity, μM -to-nM detection for metal ions and small molecules, and pM-to-fM detection for protein biomarkers, which rival existing ligand and antibody assays. (ii) *Cross-development with another emerging technology*. It is easy to acquire state-of-the-art aptamer research ideas and papers by Google search of “aptamer + X,” where X is an emerging term or hot topic of today’s science and technology. For instance, aptamers have recently been demonstrated as promising partners for collaborating with several cutting-edge technologies ranging from gene technology (e.g. next-generation sequencing (NGS), clustered regularly interspaced short palindromic repeats (CRISPR)/Cas9, and small interfering RNA (siRNA)), biotechnology (e.g. organ-on-a-chip, stem cells, and cancer cell theranostics), information technology (e.g. 3D DNA/RNA structure prediction, protein–DNA docking, *in silico* selection, and machine learning), and smart-sensing technology (e.g. smartphone point-of-care and wearable sensors). This innovation model is particularly exciting, as it attracts more interdisciplinary researchers to work on aptamers and discover more unthought-of, innovative applications of aptamer diagnostics. (iii) *Translation of laboratory research into real applications*. Several aptamer biotechnology companies are working to take a significant portion of the global market share of monoclonal antibodies and immunoassays, which compose of the major part of the IVD business. Custom aptamer selection and assay kits are now available. With the advantages of *in vitro* selection, ease of synthesis and modification, small size and high chemical stability, more and more patents of aptamer assays for detection of biomarkers associated with disease diagnosis and prognosis have been filed and issued. Searching the keyword “aptamer” results in 7563 patent records from the United States Patent and Trademark Office (USPTO) in early March of 2018, and most of them are related to analytical assays. Aptamer sensor (abbreviated as “aptasensor”) prototypes in response to the urgent needs of growing and aging world population – monitoring water/soil pollution, food safety, and infectious disease in addition to rapid diagnosis of cancer and heart and other chronic diseases have been widely investigated recently. Use of aptamers as a molecular tool for high-throughput biomarker discovery and therapeutic model assessment is also of great translational potential. The three innovation models are complementary and beneficial to each other. They interest academic scientists, engineers, industrial researchers, and investors; and all together serve as the driving forces to propel the advance of aptamer diagnostics.

This chapter is provided to complete the scope of “aptamers for analytical applications” by describing and discussing the cutting-edge developments of “analytical aptamers” and “aptasensing” – the two main pillars of aptamer diagnostics. We aim to help readers quickly understand how innovations of aptamer diagnostics have been planned and realized. Through the proof of concepts and examples in the text, we hope to inspire more creative endeavors to make aptamer diagnostics more appealing and mature to benefit human health

and well-being. But it should be noted that this chapter reflects the authors' personal viewpoints of aptasensing R&D trends and perspectives of possible new directions. Thus, this chapter serves as a general guide article for the readers to appreciate the advances of novel aptamer research rather than an up-to-date review article. For the details of each sub-field's development, the readers are recommended to refer to the related review papers or directly browse specific papers in Web of Science or PubMed.

13.2 Frontiers of Analytical Aptamer Selection and Probe Design

Recalling the first glance at manual SELEX experiments in the early 2000s, the first author still remembers how he considered his postdoctoral project as a daunting task – since he was told that a SELEX job against a single-protein target required 15 rounds to complete, in which every round spent two working days including a tedious step of denatured polyacrylamide gel electrophoresis (PAGE) purification of the PCR amplicons with accurate size for ssDNA ligand isolation, not counting the time required in subsequent cloning, sequencing, K_d characterization, aptamer identification, sequence optimization, and so on. Thinking that there was plenty of room in improving the SELEX speed, the first author investigated in-round PCR size control (Figure 13.2a) and K_d monitoring to avoid overamplification and PCR parasites for aptamer evolution, respectively. With the attempts, the speed of SELEX was advanced to two rounds per day from two days per round. Aptamers were identified in earlier SELEX rounds (e.g. 4–8 rounds) and could be selected in an automated format with a programmable liquid handling system (Figure 13.2b).

Then, a shotgun SELEX against *Escherichia coli* total protein was demonstrated with the potential to generate a multitude of DNA aptamer probes for microarray-based differential protein expression profiling. It happened 15 years ago, while SomaLogic's photoaptamer microarray [5] and Ellington group's automated SELEX [6] demonstrated the appealing niches of aptamer biochip and instrument-based SELEX. Compared to today's bead-based aptamer selection in conjugation with quantitative polymerase chain reaction (qPCR) monitoring [7] that spends only a few days to obtain the selected aptamer pool, the abovementioned history contrasts the trends and advantages of next-generation aptamer selection.

13.2.1 Biochip-Based Aptamer Selection

A common practice to start a protein-based SELEX is to anchor the target protein on magnetic beads through either covalent attachment (e.g. Schiff base reaction) or strong non-covalent interaction (e.g. biotin–streptavidin interaction) and then to “fish,” “collect,” and “amplify” the ssDNA or RNA ligands specifically bound to the target protein on the beads from a pool of the 10^{15} randomized ligand library. In response to the need for expanding the list of analytical aptamers, SELEX itself has been evolved toward an easier (less tedious),

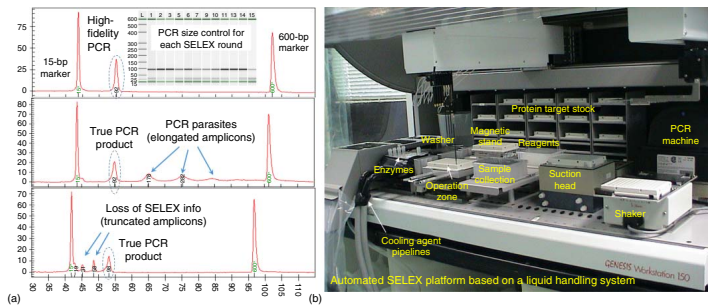


Figure 13.2 (a) In-round size control with Bioanalyzer[®] for ligand pool amplification to avoid elongated and truncated PCR parasites. (b) An automated SELEX platform. Source: Copyright © 2018, with permission from Prof. Lin-Chi Chen.

faster (less time-consuming), more reliable (less experience-dependent), more sensitive (less target or sample required), more informative (able to do real-time monitoring), and high-throughput (multiplex) aptamer selection process. And biochips have been proved as ideal platforms to meet these trends for next-generation SELEX. Biochip-based aptamer selection refers to any miniaturized SELEX platform developed with the aid of a biosensor (e.g. SPR) [8], a microarray chip (either DNA or protein microarray) [9], a microfluidic chip (lab chip) [10], or an integrated biochip system (e.g. microfluidics integrated with a microarray) [11]. It is developed for *in situ* monitoring of the evolution of high-affinity aptamer ligands during SELEX rounds or to increase the throughput of aptamer generation. Here we elaborate on the concepts of biochip-based selection with some recent SELEX advances using microfluidics and microarrays. A “lab-on-a-chip” system aiming to shrink and integrate sample preparation, purification, mixing or reaction, and analysis steps in a single tiny device drives the modern microfluidics development. Microfluidics employs a semiconductor-manufacturing-like process to fabricate customized and versatile patterns of microscale flow channels, reactors, and detecting zones for microliter-scale liquid handling, sample preparation, and analysis, respectively. Hence, microfluidics has recently been demonstrated as a promising platform for aptamer selection [12, 13]. Microfluidics selection (Figure 13.3a) is typically carried out by assaying a DNA library with the immobilized target proteins or cells, followed by separation and collection of the specifically bound ligands with various microfluidic operations with the aid of applied flow field, magnetic field, or electric field. It combines the featured advantages of capillary electrophoresis SELEX (CE-SELEX, capable of high efficiency of bound and unbound ligand separation) [14], SPR SELEX (capable of real-time monitoring k_{on} and k_{off} of label-free ligand–target binding) [15], and flow cytometry SELEX (capable of performing cell-SELEX) [16]. In addition, it reduces the need for input amount of precious protein targets for selection, enhances the nucleic

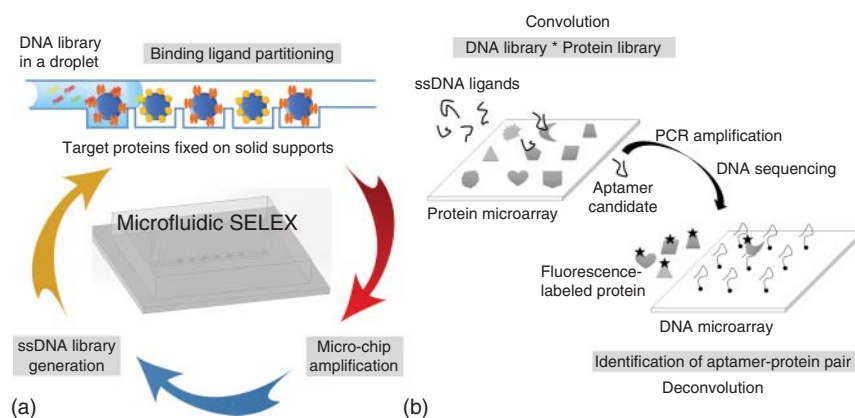


Figure 13.3 (a) Microfluidic and (b) microarray SELEX with an advantage for parallel examination of ligand pool specificity against target and nontarget proteins in selection. Source: Copyright © 2018, with permission from Jui-Hong Weng from Prof. Chen’s lab.

acid ligand–protein binding kinetics, allows programmable washing, selection, counterselection, selected ligand recovery, and even *in situ* PCR amplification and parallel multiplex selection. Yet, “SELEX-on-a-chip” is still a goal with a distance, since most microfluidic aptamer selection works to only deal with bound/unbound ligand separation and ligand–target binding monitoring of a SELEX round. Integration with *in situ* PCR purification modules for amplification of winning ligands and subsequent ssDNA or RNA ligand isolation requires further research input. Other challenging factors such as reduced diversity of input-randomized ssDNA or RNA library, addressable immobilization of the selection targets (e.g. proteins), performing the iterative SELEX rounds and even cloning/sequencing the selected aptamers, particularly when nanofluidic [17], and multiplex selection are investigated.

In situ synthesis or printing hundreds to tens of thousands of different DNA or protein probes based on one-probe-per-spot format on a cm^2 -size glass slide for analyzing a large scale of DNA–RNA, DNA–DNA, protein–protein, or protein–DNA interactions in parallel are the central concept of microarray chips. It was once the most exciting and the only promising technology for high-throughput differential gene expression profiling, genotyping, and chip-based sequencing; and it promoted the development of bioinformatics and systems biology in its gold decade since 1995. Although the crowds in the microarray fields have headed toward NGS, the maturity of DNA and protein microarray technology can contribute to the innovation of SELEX. From the perspectives of engineering and matrix mathematics, SELEX is a “convolutional” process between a multitude of ssDNA (or RNA) ligands and a list of protein targets (when more than one protein target is selected at the same time) to result in an array of aptamer–protein pairs. To identify each selected aptamer for every protein, a “deconvolution process” is required [18]. With this viewpoint, we can understand that a protein microarray [19] is an ideal device for convolution-wise parallel selection of distinct ssDNA ligands for multiple protein targets (Figure 13.3b). With spatial resolution, the bound ssDNA ligands on each protein spot can be taken out and transferred for subsequent PCR amplification and selected ssDNA pool preparation to call a round of SELEX. After SELEX rounds and sequencing the winning ssDNA ligand pools, a corresponding DNA microarray composed of the selected aptamer candidates can be fabricated to assay with fluorescently labeled protein targets of significance to deconvolute and identify the specific aptamer–protein binding pair. Thus, microarray chips can help achieve the throughput and correctness of aptamer generation along with the reduction in protein consumption during SELEX, but without sacrificing the initial ssDNA library diversity. When the protein microarray is composed of a family of disease-associated proteins or protein isoforms, specificity and cross-reactivity can be monitored during selection. Also, for secondary aptamer selection with a given aptamer sequence motif information (e.g. *de novo* selection or with computer-aided aptamer probe design) [20] or post-SELEX optimization [21], high-density DNA microarray can be harnessed for direct identification of aptamers through assays with proteins. Yet, the concern will be the fluorescent labeling bias, so label-free aptamer microarray assays such as surface plasmon resonance imaging (SPRI) [22] technique or sandwich detection [23] have been

reported. In addition, despite with reduced throughput, microarray designs can be combined with microfluidics to accelerate the development of multiplex SELEX [11].

13.2.2 SELEX with Next-Generation Sequencing (NGS)

The final SELEX round results in an enriched pool of high-affinity and high-specificity ssDNA or RNA ligands as well as aptamer candidates. The ordinary steps following the SELEX rounds are cloning and sequencing for the final pool of selected ligands. Typically, PCR or real-time polymerase chain reaction (RT-PCR) amplification of the final pool is carried out to prepare double-stranded amplicons (copies) of the selected ligand sequences. The amplicons are cloned to sequencing vectors (e.g. T–A cloning vectors) to form recombinant plasmids, which are then transformed to *E. coli* competent cells for growing bacterial colonies containing aptamer sequence information. For Sanger dideoxy sequencing (using CE sequencers), tens to hundreds of cloned aptamer sequences are determined to name the high-frequency winning sequences as aptamers (the survival of the fittest) for further conformation, K_d , and specificity characterization. These are the typical post-SELEX steps which are classical and reliable but also have several unavoidable disadvantages to consider, like PCR bias, parasite sequence contamination, low throughput, and potential loss of sequence information (Figure 13.2a). To cope with the issues, NGS and digital PCR offer promising opportunities in next-generation SELEX.

NGS represents a novel class of high-throughput DNA sequencing techniques that are considerably faster and cheaper than 384-channel capillary sequencing. Integrating shot-gun fragment sequencing with microarray, bead array, microfluidics, and large-scale bioinformatics computation, NGS instruments (second-generation NGS is referred to here, e.g. Roche 454[®] or Illumina HiSeq[®] system) are generating more and more user-affordable genome-wide sequence data (e.g. RNA-seq.) for both fundamental studies and personalized diagnostics. Such high-throughput NGS techniques have been recently applied in SELEX [24]. NGS in SELEX shows a promising niche for round-to-round ligand sequence evolution monitoring and large-scale aptamer candidate sequence analysis. NGS, therefore, identifies potential aptamers in earlier rounds of SELEX through statistical analysis and prevents over-selection. It also allows analyzing and comparing the selected ligand pools of serial (with different libraries) or parallel (with different protein targets) SELEX experiments in one shot, as long as the primer (or tag) sequences are distinguishable for each single SELEX experiment. NGS is also potential in generating a draft pool of aptamer candidates from single-round selection for preparing a high-density DNA microarray for direct aptamer identification.

Being a complementary technique to NGS, digital PCR that allows precise clonal amplification of a random DNA library has also been investigated for SELEX in recent years. Different from ordinary PCR carried out in a single tube, digital PCR utilizing compartmentalized microenvironment, such as emulsion polymerase chain reaction (ePCR), droplet digital polymerase chain reaction (ddPCR), and micro/nanowell PCR, to amplify every single DNA in a confined

space allows homogeneous amplification of a randomized DNA pool, which is not only well suited for NGS applications but also advantageous for SELEX purposes. Recent papers [25, 26] have shown that digital PCR or ePCR can perform high-fidelity clonal amplification of either initial library or selected ligand pool and thus greatly reduce the problems of PCR artifact and parasite in classical SELEX. Hence, it is an important update in SELEX to use the digital PCR technique for high-fidelity amplification of selected sequences in each round, which is followed by deciphering the complete sequence information of the selected pool(s) with NGS.

13.2.3 Aptamer Optimization and Specialized Selection

As-selected aptamers from SELEX require further optimization and modification to produce aptamer probes that exhibit high affinity, high specificity, minimal size, and high stability for real applications. The approaches of aptamer probe design can be described from the following two aspects – working with as-selected aptamers vs specialized aptamer selection. Working with as-selected aptamers (from either new selection or reported sequences) relies on investigating how sequence engineering affects the aptamer structure and sensing performance [27]. The structure–performance relationship can be assessed with circular dichroism (CD, to check duplex and quadruplex conformation and melting temperature), qPCR-HRM (high-resolution melting; to check melting temperature), enzyme-linked aptamer assay (ELAA; aptamer version of enzyme-linked immunosorbent assay (ELISA), to check affinity and specificity) and SPR (with function similar to ELAA). Here we describe five methods (Table 13.1) frequently used for optimization of an as-selected aptamer. (i) *Trimming non-requiring bases* [28–30]. This is similar to the splicing of a premature messenger RNA (mRNA) to a mature one, while a full-length as-selected aptamer contains two priming sequences at both ends in order to flank the randomized evolutionary domain (e.g. N30 or N40) for SELEX’s PCR amplification. These priming bases, in principle, are not responsible for target recognition and can thus be trimmed away or truncated along with other bases outside the so-called aptamer core. The aptamer core in an as-selected, full-length sequence can be forecasted using a computational 2° structure prediction server (e.g. mfold or RNA structure) that plots the sequence with

Table 13.1 Summary of post-SELEX optimization methods for as-selected aptamers.

Method	Principle	Result
Base trimming	Size minimization	Improved K_d and specificity
Sequence mutation	Secondary selection	Improved K_d and specificity
Multimeric construct	Structural enhancement	Improved K_d and maximum binding
Bivalent avidity	Distinct epitope binding	Improving K_d and specificity
Spacer/base incorporation	Structural flexibility	Rapid beacon response

Source: Copyright © 2018, with permission from Prof. Lin-Chi Chen.

folding motifs [30] or a high-density aptamer microarray experiment that assays a complete coverage of the sequence domains of an as-selected aptamer [21]. This process results in the minimal size of an aptamer. (ii) *Editing or mutation of the aptamer sequence*. It is reasonable to assume that to edit or mutate a few bases of an as-selected sequence is likely to yield an enhanced aptamer with improved targeting performance [25]. This is because that SELEX only selects the fittest sequences from the library, not from all the possibilities. Therefore, an as-selected aptamer is more like a selected sequence pattern rather than an absolutely best ligand. (iii) *Synthesis of multimeric aptamers*. Resembling IgM and hemoglobin structures, a synthetic multimeric aptamer probe [31] that possesses multiple aptamer core sequences in tandem with base linkers shows enhanced active conformation characteristics (which can be evident from CD) and collaborative binding property with improved K_d [32]. (iv) *Bivalent or binary aptamer construction*. Demonstrated with thrombin-binding aptamers, either connecting or directly using two distinct epitope-binding aptamers as a probe would greatly enhance the protein detection sensitivity and specificity owing to the avidity effect [33]. Other examples also confirm the existence of bi-specific aptamer avidity and encouraging the recent trend of aptamer pair selection, which is described later. In addition, a split aptamer [34] is also an interesting sequence design, which uses two (or more) DNA sequences to assemble into a target-binding aptamer construct. (v) *Addition of poly T (or A) spacers or incorporation of additional bases*. This alters the structure of an aptamer and results in an aptamer beacon or molecular switch [27], which increases the signal change and response speed for dynamic aptasensing.

Specialized aptamer selection refers to the new or *de novo* SELEX with specially designed libraries, targets, or evolution strategies for a specific purpose and generates aptamers with “active” functions that are more than simple target binding. Here we describe four examples of specialized selection (Table 13.2). (i) *Slow off-rate-modified aptamer (SOMAmer) selection* [35]. The dissociation constant, K_d , a standard measure of binding affinity, is determined as the ratio of the de-binding rate constant (k_{off}) to the binding rate constant (k_{on}) for an aptamer–target binding event. A small K_d value (high affinity) can be resulted from either a small “off” rate or a large “on” rate. For aptamer diagnostics with wash steps to remove nonspecific binding interferences (e.g. ELAAs, microarray assays, SPR, and quartz crystal microbalance (QCM) and aptamer therapeutics as well, a slow off-rate characteristic is a more precise

Table 13.2 Summary of specialized aptamer selection designs.

Method	Principle	Result
SOMAmer selection	Chemical diversity	Slow off-rate aptamer
Aptamer pair selection	Bivalent avidity	Distinct-epitope aptamer duo
Epitope-specific SELEX	Epitope targeting	Antagonistic aptamer
Capture SELEX	Strand displacement	Small-molecule apta-beacon

Source: Copyright © 2018, with permission from Prof. Lin-Chi Chen.

and important factor than small K_d to name a “good” aptamer. Unlike typical aptamers composed of natural bases, SOMAMers bearing dU residues are functionalized at the 5-position with moieties (e.g. benzyl, 2-naphthyl, or 3-indolyl-carboxamide) to enhance both structural diversity and binding capability. Similarly, X-aptamers are proposed for greatly improving affinity and specificity via adding drug-like molecules to 5-positions of certain uridines on a complete monothiophosphate-backbone-substituted oligonucleotide aptamer [36]. These examples address the advantages of chemically modified bases in expanding the library diversity for SELEX, enhancing binding affinity, and endowing nuclease resistance. (ii) *Aptamer pair or duo selection*. Aptamers are oligonucleotide ligands and are relatively small as compared to antibodies; thus, there are chances for selection of a pair (even a set) of aptamers binding to distinct epitopes of a protein target. Inspired by the works of the NeXstar (now Gilead Sciences) team in 1997 (discovery of another aptamer binding to a distinct epitope of thrombin – exosite II) [29] and related bivalent-avidity aptasensing effects, there has been an increasing number of SELEX works devoted to generate an aptamer pair or aptamer duo [37, 38]. For example, enzyme-linked oligonucleotide assay (ELONA), microarray, and SPR were investigated as the duo selection platforms, recently, for the abovementioned platforms’ capabilities to report enhanced binding responses reflecting sandwich target recognition by two distinct aptamers, while the NeXstar work suggested that an aptamer pair would be selected from two distinct libraries and independent SELEX experiments. With more aptamer pairs reported, extra experiments, however, should be performed to call two aptamers a real pair. It is because two different oligonucleotides might hybridize with each other through base pairing without sandwiching the target and cause a false-positive signal. Moreover, to take a rigorous viewpoint, an aptamer pair should have clear, different, and well-determined binding epitopes, which is still a cost-intensive task but can be indirectly proved if epitope-specific ligands or antibodies exist and are available for validation. (iii) *Epitope-specific SELEX* [33, 39–41]. For protein, virus, or cell aptasensing, isoform discrimination and receptor targeting are important topics. In such a case, the aptamers generated from typical protein-binding SELEX may not be qualified for applications due to lack of epitope specificity, and thus epitope-specific SELEX is preferred. In general, epitope-specific SELEX can be designed by modification of original SELEX rounds with one of the following methods: (i) carrying out counterselection against a recombinant protein isoform or transformed cell without the target epitope or receptor [40], (ii) selection against a synthetic peptide fragment representing the epitope or receptor [39], and (iii) use of known epitope-specific ligands [33] or receptor-specific antibodies [41] to compete off (or elute) the bound ssDNA or RNA ligands on the native proteins or cells, which is also termed ligand-guided selection (LIGS). Each approach is compatible with currently existing SELEX platforms, while flow cytometry or microfluidic SELEX is considered particularly promising for selection of receptor-specific aptamers for cell surface targeting. (iv) *Capture SELEX* [42]. It is difficult to directly apply a typical SELEX method to select aptamers targeting a small-molecule analyte (e.g. mycotoxin or pesticide). In most cases, it needs to covalently attach the

small-molecule analyte to an inert protein (e.g. bovine serum albumin (BSA)) to construct a complete antigen unit (like a hapten–protein carrier assembly) and to treat the attached analyte as the epitope for specific aptamer selection. By contrast, it has been a common practice to use capture SELEX that uses a ligand library based on two or multistranded oligonucleotide nano-assemblies and selects analyte-displaced sequences as the capture aptamers. The aptamers selected in this way usually have a flexible structure and can serve as sensing beacons for small-molecule analytes.

13.2.4 *In Silico* Aptamer Design

Selection of one or a few target-specific aptamers from a 10^{15} randomized sequence library requires efficient enrichment of winning ligand pools that are mainly determined by the efficiency of bound-to-unbound ligand partition, PCR amplification of the selected ligands, and single-stranded ligand isolation from the amplicons. Enriching the ligand pool by a factor of 10^{13} – 10^{14} is both a time- and labor-consuming process in practice and comes with a risk of over-selection or parasite sequence contamination. Semi-empirical or knowledge-based computer-aided selection can help reduce the initial library size from a huge size of 10^{15} to a single-round selection-compatible size of 10^5 – 10^3 and be realized by the following rational library designs: (i) *eliminating thermodynamically non-favored sequences* (for those that lack the potentials of secondary structure folding or quadruplex formation), (ii) *discarding the ligands with sequence similarity and redundancy*, and (iii) *choosing sequence patterns or motifs from the known aptamer databases for a given target* (i.e. *de novo* selection). With *in silico* rational library design, it is not only possible to identify aptamers (or aptamer candidates) from a single-round selection experiment but also likely to directly determine the minimized aptamer sequences with a synthetic high-density DNA microarray (10^3 – 10^5) that completely gets rid of the influences of additional priming sites on aptamer recognition.

Computer-aided SELEX or *in silico* aptamer selection (Figure 13.4) similar to molecular dynamics software that is used to design small-molecule drug leads has been attempted and proven viable in recent years [43, 44]. In practice, sequence alignment tools (e.g. BLAST or TreeView X), melting temperature/guanine–cytosine (GC) content prediction tools, and secondary structure formation prediction websites (e.g. mfold and RNA structure) have been used to assist the analysis of the sequencing results of the selected ligand pool and determination of highly potential aptamer candidates for costly K_d and specificity assessment for years. Recently, tertiary structure prediction software or servers (Figure 13.4a) for a given ssDNA or RNA sequence (converting 1D sequence to 2D structure and then to a 3D motif) and corresponding protein–DNA docking tools are available (e.g. RNAComposer and iFoldRNA), which allows *in silico* assays of many given aptamer or ligand sequences with respect to a protein target having a known 3D structure from the protein data bank (PDB; Figure 13.4b). Thus, high-throughput *in silico* aptamer selection is possible since large-scale and rapid calculation is readily available (typically for bioinformatics experts). However, it should be noted that most currently

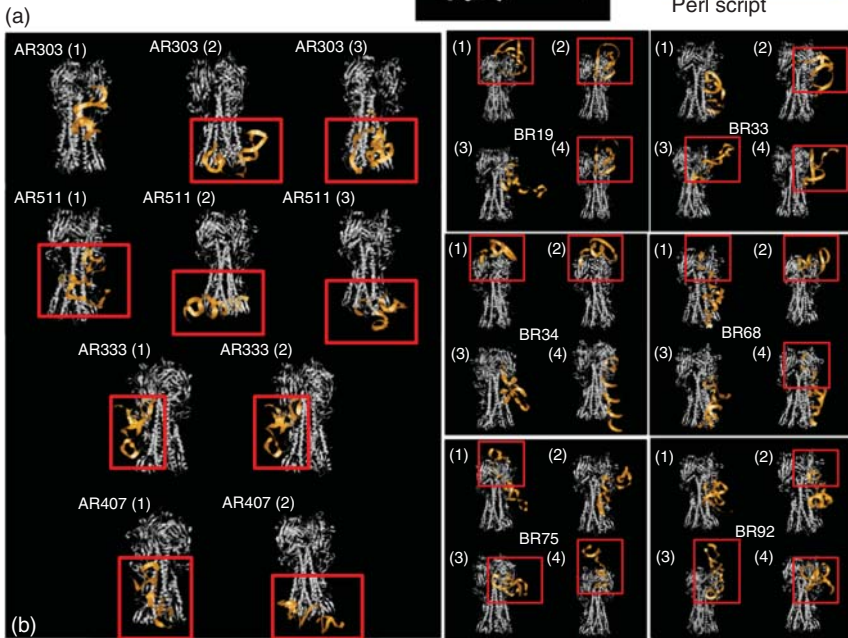
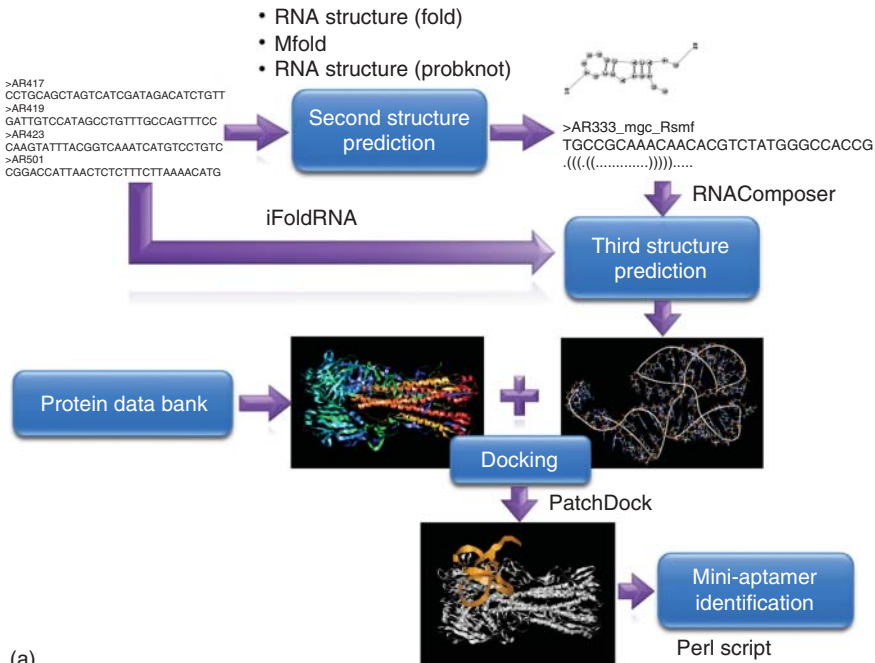


Figure 13.4 (a) A pipeline of *in silico* 3D structure prediction for an aptamer sequence. (b) *In silico* aptamer-hemagglutinin protein (H1) docking simulation experiments. Source: Copyright © 2018, with permission from Hui-Yu Chiang from Prof. Chen's Lab.

available DNA–protein interaction prediction tools are evolved by “machine learning” with the prior structural knowledge and known dsDNA–transcription factor interaction databases, which have been well established since the initiatives of genomics and proteomics studies. Thus, a DNA–protein docking tool like UCSF Chimera can precisely predict the binding results of mutated double-stranded decoy DNAs toward an oncogenic transcription factor [45]. In comparison, machine learning for artificial intelligence of *in silico* aptamer design still needs more established ssDNA or RNA–protein binding data and sequence-to-2D/3D structure knowledge. This field has a promising future as the progress of information technology is speeding faster than ever.

13.3 Novel Aptasensing Platforms – From Assays and Sensors to Instrumental Analyses

The word “aptasensing” has been coined to describe a sensing event or analytical application that harnesses aptamers. From the perspective of etymology, “apt” means “to fit” in Greek, while the present-day concept of “sensing” means to perceive a fact or situation by detecting a change in physical quantity or detecting a chemical component with a device, particularly in terms of digital electronics. Knowing this, we can understand that aptasensing provides a distinguished feature – it allows sensor developers to generate their own recognition elements by selecting aptamers with SELEX for a specific sensing task. Custom design of an aptamer probe to fit sensor application is not difficult, as compared to the related issues in classical chemical sensors (e.g. ion-selective electrodes) or biosensors (e.g. enzyme electrodes or immunological test strips). Hence, aptasensing can lower the barriers for new assay and biosensor inventions. In addition, bearing the properties of nucleic acids and the function of monoclonal antibodies, aptamers have been taking advantage of both DNA sensing breakthroughs and immunoassay platforms for diagnostic innovations in recent years along with new nanosensing materials and biosensing devices.

13.3.1 Aptamer Assays

Aptamer assays aim at easy and rapid on-site analyte tests using aptamer-based reagents, and the test results can be judged by the naked eye or a simple device (e.g. a smartphone or a simple fluorometer; Table 13.3). There are two major types of aptamer assays – aptamer beacons and aptamer-based immunoassays. Aptamer beacons are molecular switches made of a single structurally active aptamer or an aptamer probe with its partner oligonucleotide(s). They act like or can be viewed as molecular beacons which give an “on/off” response change when recognizing the analyte. In the early 2000s, aptamer beacons were proposed and proven with thrombin sensing [27]. Researchers observed that a 3D-folded quadruplex aptamer probe could form a 2D hairpin conformation by attaching extra bases at one aptamer terminal to yield a duplex stem and further found that the 2D-to-3D structure folding could be induced by target recognition. As a

Table 13.3 Emerging aptamer assay applications.

Assay format	Advantage(s)
<i>Beacon reagents</i>	
Fluorescent beacon ^{a)}	Rapid and sensitive on/off signal response to target analyte
QD beacon/nano-flare ^{a)}	Improved fluorescent properties; intracellular aptasensing
Au nanoparticles/LSPR ^{a)}	Colorimetric detection
<i>Immunoassay mimics</i>	
Lateral-flow assay ^{a)}	Quick on-site strip test
ELAA (ELISA-mimic)	Semi-quantitative K_d and specificity evaluation; multiplex
Immuno-PCR	Ultrasensitive binding assay

a) With the potential for on-site or smartphone-integrated rapid diagnostics.

Source: Copyright © 2018, with permission from Prof. Lin-Chi Chen.

consequence, engineering an aptamer probe to possess a hairpin-to-non-hairpin switch property with FRET labeling resulted in the first generation of aptamer beacons. DNA-binding dyes were subsequently introduced to form a complex with aptamer probes to result in the second generation of aptamer beacons, which eliminated the costly synthesis of a fluorophore/quencher dual-labeled aptamer [46]. Such an aptamer beacon requires only an unmodified aptamer probe showing affinity difference for the binding dye upon analyte change, since it works according to competitive aptamer binding between the dye and analyte. Analyte binding induces dye displacement off the aptamer probe and thus results in a change in the dye binding signal (e.g. fluorescence intensity). With advantages of flexible surface chemistry, broadband UV excitation, and free of photobleaching, QDs have also been used and studied in aptamer beacon study later [47]. The roles of QDs for aptamer beacon design are twofold. One is used as the nano-solid-support for anchoring aptamer probe(s) (labeled with a reporter dye or to be interacted with dye); the other is to serve as the donor fluorophore for the reporter dye (acceptor) in FRET sensing. Aptamer probes with both hairpin-opening and dye-displacement properties have been demonstrated to be well suited for forming molecular beacons with QDs. Recently, a rather simple class of competitive aptamer beacons, also termed “aptamer nano-flares,” using nano-quenchers [48, 49] (e.g. gold nanoparticles, carbon nanotubes, graphene, and 2D metal–organic framework nanosheets) have been intensively studied. The turn-on type sensing is achieved through analyte competitive binding to a preadsorbed fluorescence-labeled aptamer on a nano-quencher. When analyte binding, the labeled aptamer/nano-quencher complex dissociates and the fluorescent label shines. The emission signal is proportional to the analyte concentration. Parallel detection of two analytes is also possible for a nano-quencher-based aptamer beacon. Along with fluorescent aptamer beacons, there are also some aptamer assays reporting colorimetric signals that are easier to be observed – such as gold nanoparticle assays [50] and other assays based on localized surface plasmon resonance (LSPR) [51].

All of these are suitable to be developed as a rapid test reagent, and precise reading of the assay result can be achieved with smartphone's image sensor applications [52].

In contrast to aptamer beacons or nanoassays, the immunoassays (e.g. ELISA, lateral flow immunochromatographic assay, and Western blot assay) that use aptamers to replace antibodies promise enormous commercial opportunities in clinical and point-of-care applications, since all ordinary laboratory instruments (e.g. 96- or 384-well ELISA readers and lateral flow assay strip fabrication tools) can serve aptamer-based immunoassays as well. ELISAs have been adapted for detecting oligonucleotide hybridization as ELONAs for eliminating the tedious steps in Southern or Northern blot. Combining the features of ELISA and ELONA, the ELAA [7] has also been demonstrated as a reliable and simple technique to determine the aptamer–protein binding specificity and affinity. For detection of small-molecule analytes and protein isoforms, competitive, sandwich, direct, and indirect ELAAs have all been proved effective. Sensitivity can be further improved to pM or fM detection using a chemiluminescent, fluorescent, or gold nanoparticle substrate to replace a colorimetric one. Micro-ELAA can be a trend to reduce the reagent consumption cost for ELAA. While ELISA has been a common practice in clinical and research laboratories, lateral flow assays using wash-free affinity separation and colorimetric labels have been ideal rapid strip tests for on-site applications. The most known example is the beta-hCG (beta-human chorionic gonadotropin) test strip, by which the appearance of two lines in response to a urine sample indicates pregnancy. This lateral flow assay is typically achieved by antibody sandwich detection, in which one antibody (capturing antibody) is preimmobilized in the detection zone and the other antibody (reporting antibody) conjugated with a gold nanoparticle or colorimetric label is flowed through the paper channel with the sample. Aptamers have been proved as ideal antibody surrogates for lateral flow assays [53] attributed to the flexibility of oligonucleotide synthesis and modification and conjugation chemistry; and applications to biomarker and virus detection have been demonstrated and commercialized. In addition to ELAA and aptamer lateral flow assays, paper-based assays, aptamer-based Western blots, aptamer-based immunohistochemistry (IHC), aptamer-based immuno-PCR [54], and aptamer rolling circle amplification [55] have emerged as new aptamer assays that can compete or collaborate with ordinary antibody-based immunoassays.

13.3.2 Aptasensors

Aptasensors that integrate aptamers with physical or chemical sensors to detect one or a set of meaningful analytes are the most promising analytical application for aptamers when we consider the facts of (i) convenience of blood sugar monitoring brought by modern glucose sensors, (ii) smartphone as a miniaturized personal computer and sensor interface [56], and (iii) need for informative biological data for smart personalized health managing system development. Sensing a range of analytes with aptamers in a similar way like operating a glucose sensor means direct test of samples without purification, labeling, and adding reagents and wash steps, plus the user-friendly features such as small size,

simple operation, rapid and accurate response, and easy (digital or graphical) reading. This is the goal to be achieved for future aptasensor development. Here we focus on the design and fabrication of aptamer-based sensor strips or chips, which not only require immobilizing aptamers on sensor surfaces but also involve optical or electrochemical sensing events with label-free, reagent-less, and even wash-free characteristics.

Label-free aptasensing has been achieved with SPR, QCM, electrochemical impedance spectroscopy (EIS), differential pulse voltammetry (DPV), and FET techniques. Nowadays, the binding affinity and specificity between an aptamer and its target are usually characterized by a label-free SPR instrument, which has replaced traditional radiolabeled filter binding assays. Aptamer-binding and de-binding sensorgrams as well as k_{on} and k_{off} kinetic constants are recorded similar to the SPR analysis of the interaction between an antibody–antigen pair. Miniaturization of SPR instrumentation [57] and CCD-array-based SPRI systems [58] are currently being developed for flexible aptasensor applications. QCM sensing works on reporting a mass gain from affinity binding on the quartz crystal chip in terms of a frequency decrease [59]. Thus, QCM aptasensing is highly similar to SPR aptasensing. Both are label-free, real-time, and flow detection-based. The only difference from SPR detection is that QCM generates an electronic signal read by an impedance analyzer, which thus can be better coupled with electrochemical detection. Electrochemical label-free aptasensing [60] is the most desired, since the successful homecare glucose sensor is an electrochemical sensor as well. A straightforward thought to attain electrochemical label-free aptasensing is to measure the changes in charge-transfer resistance and double-layer capacitance before and after analyte binding to an aptamer-immobilized electrode. This can be carried out by the EIS method. To date, there have been a number of successful EIS label-free aptasensing works reported. Yet, in most cases, EIS label-free aptasensing not only requires a gold electrode to immobilize an aptamer probe but also needs a redox indicator (e.g. ferric cyanide or ferrocene) to work with. Such EIS detection is label-free but not reagent-less. To this end, sophisticated electrochemical (or redox) aptamer beacon designs [61, 62] have been proposed for achieving label-free and reagent-less electrochemical aptasensing with DPV. To construct an electrochemical aptamer beacon, a dual-labeled aptamer probe, of which one end is labeled with a redox reporter (e.g. methylene blue) and the other end is labeled with a linker for electrode immobilization, is used. The probe has an analyte-binding-induced folding property, so the distance between the redox reporter and the electrode surface changes while the aptamer probe binds to the analyte. By this means, the DPV response can correlate with the analyte concentration, and label-free, reagent-less detection is attained. Recently, we proved that affinity HbA1c sensing can be carried out in the form of label-free and reagent-less amperometric detection using an ion-dependent redox polymer electrode [63]. This work suggests that a chemically modified electrode can serve as both the electrode surface for aptamer immobilization and the redox indicator for label-free and reagent-less purposes. In such a case, a gold electrode and an additional ferric cyanide reagent are no longer needed for electrochemical aptasensing. In addition to these methods, label-free aptasensing can also be

Table 13.4 Partial list of emerging aptasensing modes.

Mode	Sensor surface	Signal	Niche(s)
SPR	Au film/glass	Resonance unit	Standard k_{on} , k_{off} , and K_{d} measurement
SPRI	Au film/glass	CCD image	Multiplex, microarray-like detection
QCM	Au film/quartz	Frequency (ω)	SPR-mimic label-free detection
EIS	Au or SPCE ^{a)}	Impedance (Z)	Ultrasensitive; microfluidics-compatible
DPV	Au or SPCE ^{a)}	Current (I)	Well-suited for electronic aptamer beacon
FET	Gate electrode	V_{G} or I_{SD}	Aptasensor miniaturization

a) Carbon electrode can be applied when modified w/a layer for aptamer immobilization.

Source: Copyright © 2018, with permission from Prof. Lin-Chi Chen.

done with FET-based sensing as long as the analyte binding leads to a detectable change in electrical charge on the aptamer gate electrode [64]. These aptasensing modes are summarized in Table 13.4.

For aptasensor fabrication, anchoring an aptamer probe on a gold or modified gold electrode is the most studied topic and has become a common practice. For example, different surface chemistries have been developed for immobilizing aptamers on SPR gold chips, including self-assembled monolayer (SAM) and biotin–streptavidin chemistry. Also, a method to determine immobilized aptamer probe density on a gold electrode has been developed [62]. By contrast, for emerging aptasensor fabrication tasks, generating a range of surface functionalities with cost-effective electrodes, chemically modified electrodes, transparent substrates, and semiconductors and nanomaterials for aptamer immobilization has been an important practical topic for aptasensor researchers [65]. This not only brings in the opportunities for manufacturing low-cost aptasensors with screen-printed carbon electrodes (SPCEs) but also allows for new label-free and reagent-less electrochemical aptasensing design. Moreover, a high-quality surface chemistry can help result in a low interference background and improve aptasensing sensitivity and specificity while coping with protein-rich samples like serum and urine [66]. As the probability for commercialization of an aptasensor is increasing, wash-free electrochemical aptasensing like what people experience in blood sugar detection is less discussed. Washes are typically required for removing nonspecific binding events in immunoassays, but they can cause sensing biases for non-trained users. To cope with this issue, anti-fouling or anti-adsorption coating on an aptamer electrode might help attain a wash-free aptasensor. Another possible approach is to conjugate a later flow immunochromatographic channel or microfluidic channel to separate analyte from the interfering species before detection with an electrochemical aptasensor.

13.3.3 Aptamer Chips

Aptamer chips can be categorized into aptamer microarrays and aptamer microfluidic devices. Their applications in aptamer selection and post-SELEX

optimization have been discussed in Section 13.2.1. Here we focus on the analytical applications. Aptamer microarrays immobilize a multitude or an array of different aptamer probes on a cm^2 -size glass slide for multiplex protein detection. The type, number, and density of immobilized probes determine what application of an aptamer microarray is. High-density aptamer microarrays can be custom fabricated by DNA microarray providers or with addressable solid-phase oligonucleotide synthesis technique [67]. They are promising alternatives to antibody microarrays for differential protein expression profiling [1] and biomarker discovery [68] (Figure 13.5). The corresponding large-scale aptamer probes can be obtained from complex SELEX (e.g. proteomic SELEX), ligand pools of earlier SELEX rounds, and mutation of selected aptamers. By contrast, low-density aptamer microarrays are often homemade by contact printing [69] or *in situ* synthesizing [70] a meaningful combination of aptamer probes that allow precise diagnosis or monitoring the progress of a specific disease through simultaneous detection of a set of protein biomarkers or protein–protein interaction study [71]. Since the number of reported anti-biomarker aptamers is increasing, fabricating aptasensors in the form of arrays for parallel biomarker detection is also a promising and viable direction.

Microfluidic lab chips have been developed to manipulate a tiny amount of sample and to carry out sample preparation, treatment, and detection on a single small-sized device since the 1990s. Advanced microfluidics technologies have shown great niches in reshaping immunoassays for their reagent-saving nature, automation of liquid handling, and compatibility with sensor integration. Compared to antibodies, aptamers are more suitable for being employed in a microfluidic immunoassay for their higher tolerance to device bonding conditions and flexibility of immobilization chemistry. Although most recent interests of microfluidic applications for aptamers focus on SELEX (see Section 13.2.1), successful examples of integration with an electrochemical sensor array [72] or bead array sensor [73] have demonstrated the advantage of microfluidics in multiplex aptamer detection. Regeneration for repeated impedance-based aptasensing is another advantage of microfluidic detection [74], which also shows the great niches for real-time, simultaneous electrochemical affinity

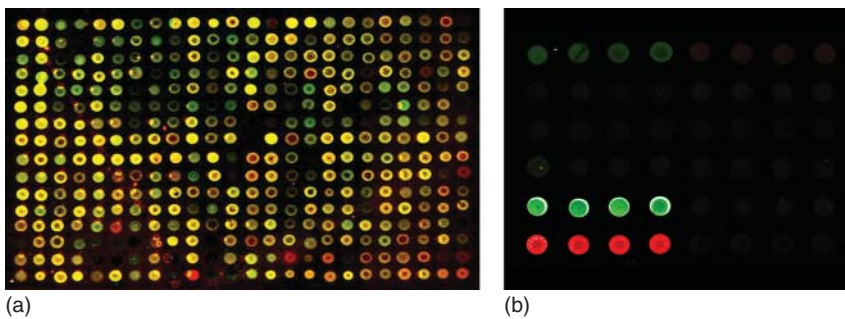


Figure 13.5 (a) Bacterial protein expression profiling on an aptamer microarray with fluorescent labels. (b) Simultaneous detection of an *E. coli* protein (light gray spots, Cy3 signal) and thrombin (dark gray spots, Cy5 signal) on an aptamer microarray. Source: Reprinted from Ref. [69]. Copyright © 2018, with permission from Prof. Lin-Chi Chen.

measurement [75] similar to the functions of SPR and bio-layer interferometry (BLI). For further reducing sample and reagent volumes and higher level integration, single-droplet manipulation (like digital microfluidics [76]), nanoslits technique [77], and nanofluidics [78] are being studied and can be applied to future aptamer diagnostics.

13.3.4 Cell-Based Aptasensing

Instrumental cell analysis like confocal microscopy or flow cytometry plays a pivotal role in biomedical research for precision diagnostics and therapeutics development. Antibodies usually serve as the highly specific and sensitive probes to label the targeted cell surface proteins or intracellular proteins in the abovementioned applications. In the past decade, analysis of a single cell with an aptamer probe defines the emerging cell-based aptasensing field. Similar to antibodies, aptamers have been selected and studied for specifically targeting cell surface receptors and have the potential to compete with antibodies in cell analysis. The applications are attractive and range from cell isolation [79], cell-based diagnostics, and drug delivery to antagonistic therapeutics [80]. Cell-surface-targeted aptamers are obtained from SELEX against receptor proteins (e.g. prostate-specific membrane antigen (PSMA) and mucin 1 (MUC1)) or direct SELEX against target cells called cell-SELEX. Cell-SELEX is usually performed by flow cytometry with the aid of a cell sorter that collects the cells bound with selected aptamer ligands [16]. Counterselection against nontarget cells (e.g. receptor-deficient cells or normal cells) can help improve selectivity. Recently, microfluidic chips have also been investigated for cell-SELEX [81], and the results are promising due to the selection efficiency and significant reduction of the instrumental cost. Cell-surface-targeted aptamers have been investigated for differential flow cytometry analysis of the cells with and without surface markers. Recently, aptamers have been applied for capturing circulating tumor cells (CTCs) and for precious cell isolation [82]. Some of the works are carried out with microfluidic chips. In addition, cell-surface-targeted aptamers have been studied for both cell-based sensing and drug (e.g. doxorubicin) delivery applications (Figure 13.6a).

Intracellular sensing is another interesting direction for cell-based aptasensing [48, 49]. Being both an inspiring and intriguing topic, targeting intracellular molecules or proteins with aptamers has resulted in a great deal of hope and many tasks for both diagnostics and therapeutics. After all, it is considerably easier to deliver or present an aptamer to or inside a cell than doing the same for antibodies. In addition, many gene vectors and/or siRNA presenting tools are ready for delivering an aptamer once the aptamer is advantageous as compared to current probes or anti-sense molecules. In fact, SELEX has been applied to select aptamers against intracellular targets like viral replicase [83]. Recently, we also selected aptamers against AMACR (alpha-methylacyl-CoA racemase), which is a fatty acid metabolism enzyme residing in the cell [7]. Yet, intracellular aptasensing has been relatively less discussed as compared to aptasensors, and several papers showed the interest and niche areas for this application. For instance, intracellular ATP sensing using an aptamer has been successfully

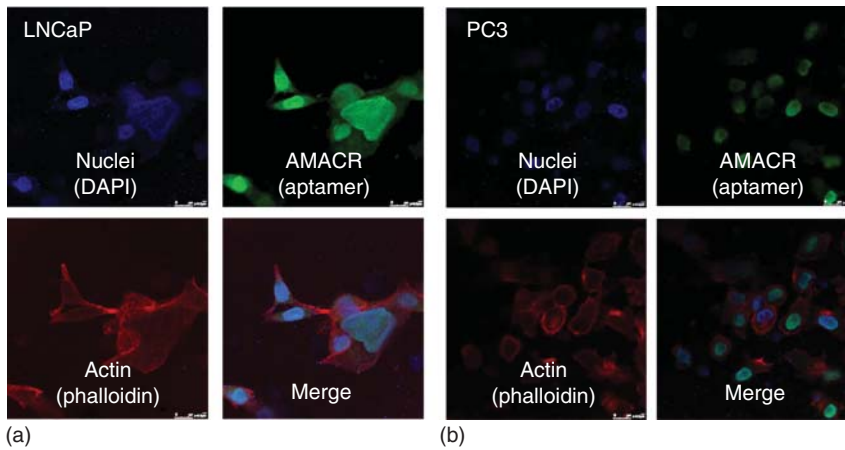


Figure 13.6 (a) Cancer cell surface recognition and fluorescent Dox drug delivery by an aptamer for cancer cell theranostics. (b) Decoy oligodeoxynucleotide (dODN) as an intracellular aptamer targeting an oncogenic transcription factor for cancer inhibition. Source: Copyright © 2018, with permission from Wan-Ju Chen from Prof. Chen's Lab.

demonstrated with the aid of confocal microscopy [48, 84]. It helps researchers probe the health status of a single cell. Other aptamer beacons are potential for intracellular protein or molecule tracking as well. The challenges are twofold: (i) *an aptamer might not fold properly inside the cell as it is selected in the binding buffer* and (ii) *an aptamer would need a transfection agent to deliver it into the cell if it is a DNA ligand*. For the latter challenge, liposome vectors like Lipofectamine[®] reagents can be applied for aptamer delivery for research and laboratory purposes. For the former challenge, it requires a custom design or extra care of the SELEX protocol to consider the difference between the binding conditions, especially the temperature and ionic composition, in the selection buffer and cytoplasm. In addition to aptamers, synthetic double-stranded or hairpin promoter sequence elements called decoy oligonucleotides (DONs) that selectively bind to (oncogenic) transcription factors can be viewed as intracellular aptamers. They can also be applied to probe an intracellular transcription factor inside a cell and exert an anti-sense-like effect for gene knockdown by inhibition of the transcription factor [85]. Then such an intracellular aptasensing event will be not only of diagnostic interest but also have targeted treatment potential (Figure 13.6b).

13.4 Emerging Applications of Aptamer Diagnostics

The rapid growth of IVD and the precision medicine market is in response to the quick growth of both global and aging population. More affordable immunoassays and kits are required to help prevent and combat the infectious diseases in developing countries, while developed countries are seeking advanced molecular tools to tackle life-style-dependent chronic diseases, genetic

diseases, and cancers. Furthermore, immunodetection also becomes popular in water, food, and agricultural and environmental surveillance in addition to the increasing need in pet and vet medicine. Consequently, we have seen an expanding market and end applications of monoclonal antibodies or their rivals such as aptamers. Being proven working for specific binding to a wide spectrum of targets ranging from ions, small molecules, nucleic acids, and proteins to cells, aptamers have great potential in all the aforementioned application domains because of their cost and structural advantages. Apart from replacing antibodies in immunoassays, the nature and design concept of aptamers are also promising in immunotherapy, targeted gene silencing, and guided gene editing, which can also be viewed as an extension of intracellular aptasensing with a meaning highly similar to precision medicine. Here we provide a brief of the emerging applications of aptamer diagnostics in the fields of human disease diagnosis, food/environmental monitoring, therapeutic drug assessment, and new molecular biology applications to depict the picture of the continued growing, prosperous future for analytical aptamers.

13.4.1 Human Disease Diagnosis

For human disease diagnosis and prognosis, the market and future are highly dependent on the significance of the analyte. Taking diabetes monitoring as an example, glucose sensing alone holds a considerable market share of the global IVD business. Thus, whether an analytical aptamer will have a prominent role in human disease diagnosis depends on whether its detection target is a well-proven disease biomarker and whether the assay is frequently prescribed or ordered by clinical physicians. To this end, a list of analytical aptamers have been selected and processed as assay kits or sensors for the interest in clinical monitoring of a number of diseases [3]. For example, glycosylated hemoglobin (HbA1c)-specific aptamers [86] are useful for long-term blood sugar level surveillance, and the corresponding HbA1c aptasensor can be integrated with glucose sensors for achieving better diabetes health care. Specific aptamers against thrombin, C-reactive protein (CRP) [87], and troponin I [88] have been selected, respectively, and have been developed as quick assays or sensors for help in acute cardiovascular disease diagnosis. Aptasensing for a range of cancer biomarkers such as PSA (prostate-specific antigen) [89], CEA (carcinoembryonic antigen) [90] and AMACR [7, 66] has also been demonstrated for potential applications in routine health checks and cancer treatment monitoring. In addition, infectious diseases such as AIDS, influenza infection, and bacterial infection can be diagnosed with aptamers [91, 92]. These examples have not only all been proved in research papers but also have been patented and even commercialized into products for some of them. For sure, the unmet medical needs and smartphone-based homecare will together drive the further development. Non- or least-invasive sample analysis (such as painless blood sampling and urine, saliva, sweat, or tear test) will be favored, while this also brings challenges for aptamer diagnostics in the aspects of sensitivity and interference issues.

13.4.2 Food/Environmental Monitoring – Mycotoxins, Pesticides, Heavy Metal Ions

Food safety and environmental monitoring have become more and more important issues in recent years for globalization of crop production, food supply chains, and industrial manufacturing. There is an increasing need to detect infectious bacteria, mycotoxins, pesticides, and heavy metals on sites to keep the foods and living environments safe for people. This opens up opportunities for aptamers, too. Aptamers have been selected and studied for detecting pathogenic microorganisms by specific recognition of cell surface markers [93], which can be applied to prevent bacterial contamination during food packaging and transportation. Mycotoxin detection with aptamers has attracted much attention recently, which is an important topic for safe consumption of corn products, coffee, and seafood [94]. Aptamer-based pesticide detection has been studied as well [95]. It helps check the pesticide residue for crop and fruit production. Heavy metal ion contamination in water [96] and active component in herbal medicine [97] can also be monitored by aptasensing technology, as recent papers show the possibility. Except for bacterial sensing, all other applications involve small-molecule- or ion-based aptasensing, in which aptamers are typically selected by capture SELEX [42] and exert sensing performance through an analyte-induced conformational change mechanism similar to that of a molecular beacon assay. For these applications, the cost per assay should be as low as possible and the assay would be better on-site and quick, and it should be noticed that some analytes are hydrophobic molecules and have low solubility in water.

13.4.3 Therapeutic Drug Assessment – Organ-on-a-Chip

Aptamer therapeutics [80] comprises the drug carriers based on aptamers and antagonistic aptamers (aptamer drugs). It belongs to one of the three main branches of aptamer applications (the other two are aptamer diagnostics and aptamer-based purification). Inspired by a drug (Macugen[®]) once approved by the U.S. Food and Drug Administration (FDA) for age-related macular degeneration (AMD) and many others being tested in different phases of clinical trials, therapeutic aptamers have attracted a lot of academic and company researchers to invest their time and budget to study them. Despite having different end applications, aptamers for therapeutics act according to the same specific-binding principle as analytical aptamers. Thus, there is sometimes only a fine line between diagnostic and therapeutic aptamer research, especially when emerging cell-specific aptamers and intracellular aptamer are discussed. This class of aptamers can be called “theranostic” ones, as they have the potential to serve as the nano-cargoes to carry high-contrast medical image agents and/or cancer-killing chemical drugs. Such theranostic aptamers can thus be deemed a unique class of analytical aptamers, as they help therapeutic assessment in laboratory benches before translation. While more experimental animals are demanded for proving preclinical trials, a novel lab chip concept called “organ-on-a-chip” [98] based on 3D tissue cultures with extracellular matrices

that mimic a real tissue or a microscale functional organ has emerged as a promising drug test platform. It can not only reduce the sacrifice of experimental animals but also increase the throughput of preclinical drug assessments. Besides, microfluidics-based organ-on-a-chip is also an ideal platform to critically examine the selectivity of a cell-specific aptamer for targeted therapy optimization. For example, nuclease-resistance modification and PEGylation to reduce the degradation and renal filtration effects and oligonucleotide penetration to solid tumor tissues for therapeutic aptamers can all be better assessed with such a platform. Moreover, it can be a powerful tool for rapid selection of tissue-specific aptamers without *in vivo* SELEX that requires consumption of experimental animals, many laboratory efforts, and much time.

13.4.4 New Molecular Biology Applications – CRISPR/Cas9, Stem Cells, IHC

From the discussions till now, we know that aptamers are a promising class of molecular tools with a variety of applications. For the same reason, we have no doubt that they are also well suited for conjugation with new molecular biology applications for laboratory purposes. The most emerging topic in the field of biotechnology of the very recent years is the CRISPR/Cas9 technique, which makes gene editing easier and shows prominent potential for a wide range of biotech applications. Since aptamers and guided strands have similar functions, they have shown potential to work with a CRISPR/Cas9 system for precise molecular diagnostics [99]. The possibility to work with Ago protein can be expected as well. In the meantime, aptamers have also been studied for stem cells [81, 100], which might be applied to enrichment of induced pluripotent stem (iPS) cells. Rivaling antibodies, aptamers have also been studied for immunocytochemistry (Figure 13.7) or IHC applications [101]. To sum up, being novel laboratory molecular tools is as promising as being analytical antibody surrogates for aptamers.

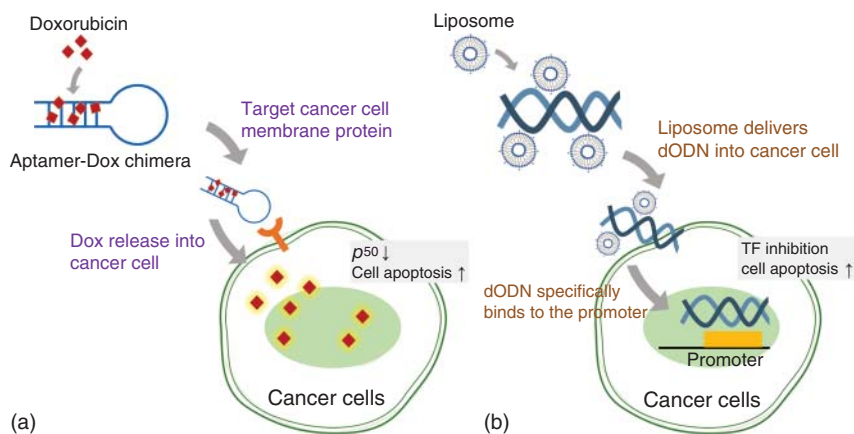


Figure 13.7 Immunocytochemistry with aptamers: prostate cancer cell lines (a) LNCaP (AMACR(+)) and (b) PC3 (AMACR(-)) stained with Cy3-labeled AMACR aptamer. Source: Copyright © 2018, with permission from Yu-En Lee from Prof. Chen's Lab.

13.5 Concluding Remarks – Frontiers of Frontiers

In the beginning of this chapter, we pointed out the three unique features of aptamers: (i) resulted from molecular evolution, (ii) composed of four-letter synthetic oligonucleotides, and (iii) working like monoclonal antibodies. From that viewpoint, we also conclude three innovation models for aptamer diagnostics: (i) improving the selection rate and detection limit, (ii) cross-developing with a new field, and (iii) translation of fundamental research into real applications. These concepts have been elaborated with the examples described in Sections 13.2–13.4. Looking into the future, we may anticipate that the following frontiers of frontiers for aptamer technology will be investigated and realized step by step according to the trends and the state-of-the-art developments described earlier. First, we may see that the speed and throughput of aptamer discovery and generation will be faster than it is. NGS allows determining a multitude of aptamer sequences from parallel SELEX experiments. High-throughput microarrays and bio-interaction analysis (e.g. SPRI arrays and BLI) can speed up the affinity and specificity evaluations for selected aptamers. Second, while more and more information about aptamer–sequence–protein interaction is reported, machine learning is being studied in accelerated aptamer selection. Deep learning can be applied to develop a reduced-size ligand library or even a precise pool of aptamer leads, by which SELEX may be no longer needed to generate aptamers. Researchers can directly test the reduced library or aptamer leads by high-to-middle density DNA microarrays with the protein targets for direct aptamer identification. In such a case, priming regions of an aptamer sequence are no longer needed, either. Minimal aptamers will be picked out in one shot. Third, direct identification of an aptamer sequence will also probably be achieved while the third generation of DNA sequencing is more ready for bench users. The aptamer sequence bound to a single-molecule protein may be directly read by the nanopore sequencing. Fourth, the size of global aptamer database (both published and private) will be expanded faster. Finding one or two aptamers against each protein in human proteome seems more possible with the abovementioned high-throughput selection development. Human “apt-omics” may be developed one day and provides a list of molecular strategies for precision diagnostics and therapeutics. Finally, the aptamer selection concept can be applied to any evolutionary ligand that specifically fits to recognize a target, as long as the ligands can be replicated easily. After all, “aptamer” is a conceptual idea rather than a well-defined material. With encouraging and ever-lasting evolution, aptamers may change to a new form but stay young and energetic in the visible future. For sure, the most practical aspects for aptamer diagnostics will always be the specificity and affinity, no matter what cutting-edge techniques are blended in for the innovation.

Acknowledgments

The authors thank Wan-Ju Chen, Jou-Hsuan Chu, Chih-Yu Lai, and Wei-Cheng Huang for their help in literature survey and discussion. Figures 13.4 and 13.7 are provided by Ms. Hui-Yu Chiang and Ms. Yu-En Lee from our group,

respectively; other experimental data were from the first author during his postdoctoral research under Dr. Konan Peck's laboratory at Academia Sinica. The writing is supported by an Academia Sinica Thematic Research Project under grant number AS-106-TP-A03.

References

- 1 Bock, C., Coleman, M., Collins, B. et al. (2004). Photoaptamer arrays applied to multiplexed proteomic analysis. *Proteomics* 4 (3): 609–618.
- 2 Zhou, W., Huang, P.J.J., Ding, J., and Liu, J. (2014). Aptamer-based biosensors for biomedical diagnostics. *Analyst* 139 (11): 2627–2640.
- 3 Meirinho, S.G., Dias, L.G., Peres, A.M., and Rodrigues, L.R. (2016). Voltammetric aptasensors for protein disease biomarkers detection: a review. *Biotechnol. Adv.* 34 (5): 941–953.
- 4 Sun, H., Tan, W., and Zu, Y. (2016). Aptamers: versatile molecular recognition probes for cancer detection. *Analyst* 141 (2): 403–415.
- 5 Petach, H. and Gold, L. (2002). Dimensionality is the issue: use of photoaptamers in protein microarrays. *Curr. Opin. Biotechnol.* 13 (4): 309–314.
- 6 Cox, J.C. and Ellington, A.D. (2001). Automated selection of anti-protein aptamers. *Bioorg. Med. Chem.* 9 (10): 2525–2531.
- 7 Yang, D.K., Chen, L.C., Lee, M.Y. et al. (2014). Selection of aptamers for fluorescent detection of alpha-methylacyl-CoA racemase by single-bead SELEX. *Biosens. Bioelectron.* 62: 106–112.
- 8 Dausse, E., Barré, A., Aimé, A. et al. (2016). Aptamer selection by direct microfluidic recovery and surface plasmon resonance evaluation. *Biosens. Bioelectron.* 80: 418–425.
- 9 Jolma, A., Kivioja, T., Toivonen, J. et al. (2010). Multiplexed massively parallel SELEX for characterization of human transcription factor binding specificities. *Genome Res.* 20 (6): 861–873.
- 10 Huang, C.J., Lin, H.I., Shiesh, S.C., and Lee, G.B. (2012). An integrated microfluidic system for rapid screening of alpha-fetoprotein-specific aptamers. *Biosens. Bioelectron.* 35 (1): 50–55.
- 11 Liu, X., Li, H., Jia, W. et al. (2017). Selection of aptamers based on a protein microarray integrated with a microfluidic chip. *Lab Chip* 17 (1): 178–185.
- 12 Cho, M., Xiao, Y., Nie, J. et al. (2010). Quantitative selection of DNA aptamers through microfluidic selection and high-throughput sequencing. *P. Natl. Acad. Sci.* 107 (35): 15373–15378.
- 13 Hung, L.Y., Wang, C.H., Hsu, K.F. et al. (2014). An on-chip Cell-SELEX process for automatic selection of high-affinity aptamers specific to different histologically classified ovarian cancer cells. *Lab Chip* 14 (20): 4017–4028.
- 14 Mosing, R.K., Mendonsa, S.D., and Bowser, M.T. (2005). Capillary electrophoresis-SELEX selection of aptamers with affinity for HIV-1 reverse transcriptase. *Anal. Chem.* 77 (19): 6107–6112.
- 15 Misono, T.S. and Kumar, P.K. (2005). Selection of RNA aptamers against human influenza virus hemagglutinin using surface plasmon resonance. *Anal. Biochem.* 342 (2): 312–317.

- 16 Tang, Z., Shangguan, D., Wang, K. et al. (2007). Selection of aptamers for molecular recognition and characterization of cancer cells. *Anal. Chem.* 79 (13): 4900–4907.
- 17 Weerakoon-Ratnayake, K.M., O’Neil, C.E., Uba, F.I., and Soper, S.A. (2017). Thermoplastic nanofluidic devices for biomedical applications. *Lab Chip* 17: 362–381.
- 18 Fitter, S. and James, R. (2005). Deconvolution of a complex target using DNA aptamers. *J. Biolumin. Chemilumin.* 280 (40): 34193–34201.
- 19 Moore, C.D., Ajala, O.Z., and Zhu, H. (2016). Applications in high-content functional protein microarrays. *Curr. Opin. Chem. Bio.* 30: 21–27.
- 20 Kinghorn, A.B., Dirkwager, R.M., Liang, S. et al. (2016). Aptamer affinity maturation by resampling and microarray selection. *Anal. Chem.* 88 (14): 6981–6985.
- 21 Chang, Y.C., Kao, W.C., Wang, W.Y. et al. (2009). Identification and characterization of oligonucleotides that inhibit Toll-like receptor 2-associated immune responses. *FASEB J.* 23 (9): 3078–3088.
- 22 Li, Y., Lee, H.J., and Corn, R.M. (2006). Fabrication and characterization of RNA aptamer microarrays for the study of protein–aptamer interactions with SPR imaging. *Nucleic Acids Res.* 34 (22): 6416–6424.
- 23 Susic, A., Meneghello, A., Antognoli, A. et al. (2013). Development of a multiplex sandwich aptamer microarray for the detection of VEGF165 and thrombin. *Sensors* 13 (10): 13425–13438.
- 24 Schütze, T., Wilhelm, B., Greiner, N. et al. (2011). Probing the SELEX process with next-generation sequencing. *PLoS One* 6 (12): 1–10.
- 25 Levay, A., Brenneman, R., Hoinka, J. et al. (2015). Identifying high-affinity aptamer ligands with defined cross-reactivity using high-throughput guided systematic evolution of ligands by exponential enrichment. *Nucleic Acids Res.* 43 (12): 1–10.
- 26 Ouellet, E., Foley, J.H., Conway, E.M., and Haynes, C. (2015). Hi-Fi SELEX: a high-fidelity digital-PCR based therapeutic aptamer discovery platform. *Biotechnol. Bioeng.* 112 (8): 1506–1522.
- 27 Hamaguchi, N., Ellington, A., and Stanton, M. (2001). Aptamer beacons for the direct detection of proteins. *Anal. Biochem.* 294 (2): 126–131.
- 28 Bock, L.C. and Griffin, L.C. (1992). Selection of single-stranded DNA molecules that bind and inhibit human thrombin. *Nature* 355 (6360): 564–566.
- 29 Tasset, D.M., Kubik, M.F., and Steiner, W. (1997). Oligonucleotide inhibitors of human thrombin that bind distinct epitopes. *J. Mol. Biol.* 272 (5): 688–698.
- 30 Kaur, H. and Yung, L.Y.L. (2012). Probing high affinity sequences of DNA aptamer against VEGF 165. *PLoS One* 7 (2): 1–9.
- 31 Mallikaratchy, P.R., Ruggiero, A., Gardner, J.R. et al. (2011). A multivalent DNA aptamer specific for the B-cell receptor on human lymphoma and leukemia. *Nucleic Acids Res.* 39 (6): 2458–2469.
- 32 Yang, D.K., Kuo, C.J., and Chen, L.C. (2015). Synthetic multivalent DNazymes for enhanced hydrogen peroxide catalysis and sensitive colorimetric glucose detection. *Anal. Chim. Acta* 856: 96–102.

- 33 Lao, Y.H., Chiang, H.Y., Yang, D.K. et al. (2014). Selection of aptamers targeting the sialic acid receptor of hemagglutinin by epitope-specific SELEX. *Chem. Commun.* 50 (63): 8719–8722.
- 34 Sharma, A.K., Kent, A.D., and Heemstra, J.M. (2012). Enzyme-linked small-molecule detection using split aptamer ligation. *Anal. Chem.* 84 (14): 6104–6109.
- 35 Kraemer, S., Vaught, J.D., Bock, C. et al. (2011). From SOMAmer-based biomarker discovery to diagnostic and clinical applications: a SOMAmer-based, streamlined multiplex proteomic assay. *PLoS One* 6 (10): 1–13.
- 36 He, W., Elizondo Riojas, M.A., Li, X. et al. (2012). X-aptamers: a bead-based selection method for random incorporation of druglike moieties onto next-generation aptamers for enhanced binding. *Biochemistry* 51 (42): 8321–8323.
- 37 Cho, M., Oh, S.S., Nie, J. et al. (2014). Array-based discovery of aptamer pairs. *Anal. Chem.* 87 (1): 821–828.
- 38 Lee, K.A., Ahn, J.Y., Lee, S.H. et al. (2015). Aptamer-based sandwich assay and its clinical outlooks for detecting lipocalin-2 in hepatocellular carcinoma (HCC). *Sci. Rep.* 5: 1–13.
- 39 Ferreira, C., Matthews, C., and Missailidis, S. (2006). DNA aptamers that bind to MUC1 tumour marker: design and characterization of MUC1-binding single-stranded DNA aptamers. *Tumor Bio.* 27 (6): 289–301.
- 40 Stoltenburg, R., Schubert, T., and Strehlitz, B. (2015). In vitro selection and interaction studies of a DNA aptamer targeting protein A. *PLoS One* 10 (7): 1–23.
- 41 Zumrut, H.E., Ara, M.N., Maio, G.E. et al. (2016). Ligand-guided selection of aptamers against T-cell receptor-cluster of differentiation 3 (TCR-CD3) expressed on Jurkat. E6 cells. *Anal. Biochem.* 512: 1–7.
- 42 Spiga, F.M., Maietta, P., and Guiducci, C. (2015). More DNA-aptamers for small drugs: a capture-SELEX coupled with surface plasmon resonance and high-throughput sequencing. *ACS Comb. Sci.* 17 (5): 326–333.
- 43 Bini, A., Mascini, M., Mascini, M., and Turner, A.P. (2011). Selection of thrombin-binding aptamers by using computational approach for aptasensor application. *Biosens. Bioelectron.* 26 (11): 4411–4416.
- 44 Nonaka, Y., Yoshida, W., Abe, K. et al. (2012). Affinity improvement of a VEGF aptamer by in silico maturation for a sensitive VEGF-detection system. *Anal. Chem.* 85 (2): 1132–1137.
- 45 Souissi, I., Ladam, P., Cognet, J.A. et al. (2012). A STAT3-inhibitory hairpin decoy oligodeoxynucleotide discriminates between STAT1 and STAT3 and induces death in a human colon carcinoma cell line. *Mol. Cancer* 11 (1): 1–12.
- 46 Jiang, Y., Fang, X., and Bai, C. (2004). Signaling aptamer/protein binding by a molecular light switch complex. *Anal. Chem.* 76 (17): 5230–5235.
- 47 Chi, C.W., Lao, Y.H., Li, Y.S., and Chen, L.C. (2011). A quantum dot-aptamer beacon using a DNA intercalating dye as the FRET reporter: application to label-free thrombin detection. *Biosens. Bioelectron.* 26 (7): 3346–3352.

- 48 Zheng, D., Seferos, D.S., Giljohann, D.A. et al. (2009). Aptamer nano-flares for molecular detection in living cells. *Nano Lett.* 9 (9): 3258–3261.
- 49 Wang, H.S., Li, J., Li, J.Y. et al. (2017). Lanthanide-based metal-organic framework nanosheets with unique fluorescence quenching properties for two-color intracellular adenosine imaging in living cells. *NPG Asia Mater.* 9 (3): 1–9.
- 50 Liu, J., Bai, W., Niu, S. et al. (2014). Highly sensitive colorimetric detection of 17 β -estradiol using split DNA aptamers immobilized on unmodified gold nanoparticles. *Sci. Rep.* 4: 1–6.
- 51 Xie, L., Yan, X., and Du, Y. (2014). An aptamer based wall-less LSPR array chip for label-free and high throughput detection of biomolecules. *Biosens. Bioelectron.* 53: 58–64.
- 52 Wei, Q., Nagi, R., Sadeghi, K. et al. (2014). Detection and spatial mapping of mercury contamination in water samples using a smart-phone. *ACS Nano* 8 (2): 1121–1129.
- 53 Chen, A. and Yang, S. (2015). Replacing antibodies with aptamers in lateral flow immunoassay. *Biosens. Bioelectron.* 71: 230–242.
- 54 Yoshida, Y., Horii, K., Sakai, N. et al. (2009). Antibody-specific aptamer-based PCR analysis for sensitive protein detection. *Anal. Bioanal. Chem.* 395 (4): 1089–1096.
- 55 Zhou, L., Ou, L.J., Chu, X. et al. (2007). Aptamer-based rolling circle amplification: a platform for electrochemical detection of protein. *Anal. Chem.* 79 (19): 7492–7500.
- 56 Roda, A., Michelini, E., Zangheri, M. et al. (2016). Smartphone-based biosensors: a critical review and perspectives. *TrAC Trends Anal. Chem.* 79: 317–325.
- 57 Cennamo, N., Pesavento, M., Lunelli, L. et al. (2015). An easy way to realize SPR aptasensor: a multimode plastic optical fiber platform for cancer biomarkers detection. *Talanta* 140: 88–95.
- 58 Zeidan, E., Shivaji, R., Henrich, V.C., and Sandros, M.G. (2016). Nano-SPRi aptasensor for the detection of progesterone in buffer. *Sci. Rep.* 6: 1–8.
- 59 Wang, R. and Li, Y. (2013). Hydrogel based QCM aptasensor for detection of avian influenza virus. *Biosens. Bioelectron.* 42: 148–155.
- 60 Hianik, T. and Wang, J. (2009). Electrochemical aptasensors – recent achievements and perspectives. *Electroanalysis* 21 (11): 1223–1235.
- 61 Radi, A.E., Acero Sánchez, J.L., Baldrich, E., and O’Sullivan, C.K. (2006). Reagentless, reusable, ultrasensitive electrochemical molecular beacon aptasensor. *J. Am. Chem. Soc.* 128 (1): 117–124.
- 62 White, R.J., Phares, N., Lubin, A.A. et al. (2008). Optimization of electrochemical aptamer-based sensors via optimization of probe packing density and surface chemistry. *Langmuir* 24 (18): 10513–10518.
- 63 Wang, J.Y., Chou, T.C., Chen, L.C., and Ho, K.C. (2015). Using poly (3-aminophenylboronic acid) thin film with binding-induced ion flux blocking for amperometric detection of hemoglobin A1c. *Biosens. Bioelectron.* 63: 317–324.
- 64 Wang, C., Cui, X., Li, Y. et al. (2016). A label-free and portable graphene FET aptasensor for children blood lead detection. *Sci. Rep.* 6: 1–8.

- 65 Balamurugan, S., Obubuafo, A., Soper, S.A., and Spivak, D.A. (2008). Surface immobilization methods for aptamer diagnostic applications. *Anal. Bioanal. Chem.* 390 (4): 1009–1021.
- 66 Jolly, P., Miodek, A., Yang, D.K. et al. (2016). Electro-engineered polymeric films for the development of sensitive aptasensors for prostate cancer marker detection. *ACS Sensors* 1 (11): 1308–1314.
- 67 Deyholos, M.K. and Galbraith, D.W. (2001). High-density microarrays for gene expression analysis. *Cytom. Part A* 43 (4): 229–238.
- 68 Gold, L., Ayers, D., Bertino, J. et al. (2010). Aptamer-based multiplexed proteomic technology for biomarker discovery. *PLoS One* 5 (12): 1–17.
- 69 Sathish, S., Ricoult, S.G., Toda-Peters, K., and Shen, A.Q. (2017). Microcontact printing with aminosilanes: creating biomolecule micro- and nanoarrays for multiplexed microfluidic bioassays. *Analyst* 142 (10): 1772–1781.
- 70 Franssen-van Hal, N.L., van der Putte, P., Hellmuth, K. et al. (2013). Optimized light-directed synthesis of aptamer microarrays. *Anal. Chem.* 85 (12): 5950–5957.
- 71 Chen, L.C., Tzeng, S.C., and Peck, K. (2013). Aptamer microarray as a novel bioassay for protein–protein interaction discovery and analysis. *Biosens. Bioelectron.* 42: 248–255.
- 72 Du, Y., Chen, C., Zhou, M. et al. (2011). Microfluidic electrochemical aptameric assay integrated on-chip: a potentially convenient sensing platform for the amplified and multiplex analysis of small molecules. *Anal. Chem.* 83 (5): 1523–1529.
- 73 Zhang, H., Hu, X., and Fu, X. (2014). Aptamer-based microfluidic beads array sensor for simultaneous detection of multiple analytes employing multienzyme-linked nanoparticle amplification and quantum dots labels. *Biosens. Bioelectron.* 57: 22–29.
- 74 Jin, S., Ye, Z., Wang, Y., and Ying, Y. (2017). A novel impedimetric microfluidic analysis system for transgenic protein Cry1Ab detection. *Sci. Rep.* 7: 1–8.
- 75 Capaldo, P., Alfarano, S.R., Ianeselli, L. et al. (2016). Circulating disease biomarker detection in complex matrices: real-time, in situ measurements of DNA/miRNA hybridization via electrochemical impedance spectroscopy. *ACS Sensors* 1 (8): 1003–1010.
- 76 Choi, K., Ng, A.H., Fobel, R., and Wheeler, A.R. (2012). Digital microfluidics. *Annu. Rev. Anal. Chem.* 5: 413–440.
- 77 Sanghavi, B.J., Moore, J.A., Chávez, J.L. et al. (2016). Aptamer-functionalized nanoparticles for surface immobilization-free electrochemical detection of cortisol in a microfluidic device. *Biosens. Bioelectron.* 78: 244–252.
- 78 Sang, J., Du, H., Wang, W. et al. (2013). Protein sensing by nanofluidic crystal and its signal enhancement. *Biomicrofluidics* 7 (2): 1–10.
- 79 Yoon, J.W., Jang, I.H., Heo, S.C. et al. (2015). Isolation of foreign material-free endothelial progenitor cells using CD31 aptamer and therapeutic application for ischemic injury. *PLoS One* 10 (7): 1–19.
- 80 Zhou, J. and Rossi, J. (2016). Aptamers as targeted therapeutics: Current potential and challenges. *Nat. Rev. Drug Discovery* 16: 181–202.

- 81 Hung, L.Y., Wang, C.H., Che, Y.J. et al. (2015). Screening of aptamers specific to colorectal cancer cells and stem cells by utilizing on-chip cell-SELEX. *Sci. Rep.* 5: 1–12.
- 82 Dickey, D.D. and Giangrande, P.H. (2016). Oligonucleotide aptamers: a next-generation technology for the capture and detection of circulating tumor cells. *Methods* 97: 94–103.
- 83 Lee, C.H., Lee, Y.J., Kim, J.H. et al. (2013). Inhibition of hepatitis C virus (HCV) replication by specific RNA aptamers against HCV NS5B RNA replicase. *J. Virol.* 87 (12): 7064–7074.
- 84 Wang, Y., Tang, L., Li, Z. et al. (2014). In situ simultaneous monitoring of ATP and GTP using a graphene oxide nanosheet–based sensing platform in living cells. *Nat. Protoc.* 9 (8): 1944–1955.
- 85 Wang, S.J., Hou, Y.T., and Chen, L.C. (2015). A selective decoy–doxorubicin complex for targeted co-delivery, STAT3 probing and synergistic anti-cancer effect. *Chem. Commun.* 51 (68): 13309–13312.
- 86 Lin, H.I., Wu, C.C., Yang, C.H. et al. (2015). Selection of aptamers specific for glycosylated hemoglobin and total hemoglobin using on-chip SELEX. *Lab Chip* 15 (2): 486–494.
- 87 Yang, X., Wang, Y., Wang, K. et al. (2014). DNA aptamer-based surface plasmon resonance sensing of human C-reactive protein. *RSC Adv.* 4 (58): 30934–30937.
- 88 Jo, H., Gu, H., Jeon, W. et al. (2015). Electrochemical aptasensor of cardiac troponin I for the early diagnosis of acute myocardial infarction. *Anal. Chem.* 87 (19): 9869–9875.
- 89 Chen, Z., Lei, Y., Chen, X. et al. (2012). An aptamer based resonance light scattering assay of prostate specific antigen. *Biosens. Bioelectron.* 36 (1): 35–40.
- 90 Lee, Y.J., Han, S.R., Kim, N.Y. et al. (2012). An RNA aptamer that binds carcinoembryonic antigen inhibits hepatic metastasis of colon cancer cells in mice. *Gastroenterology* 143 (1): 155–165.
- 91 Wandtke, T., Woźniak, J., and Kopyński, P. (2015). Aptamers in diagnostics and treatment of viral infections. *Viruses* 7 (2): 751–780.
- 92 Davydova, A., Vorobjeva, M., Pyshnyi, D. et al. (2016). Aptamers against pathogenic microorganisms. *Crit. Rev. Microbiol.* 42 (6): 847–865.
- 93 Chang, Y.C., Yang, C.Y., Sun, R.L. et al. (2013). Rapid single cell detection of *Staphylococcus aureus* by aptamer-conjugated gold nanoparticles. *Sci. Rep.* 3 (1863): 1–7.
- 94 Rhouati, A., Yang, C., Hayat, A., and Marty, J.L. (2013). Aptamers: a promising tool for ochratoxin A detection in food analysis. *Toxins* 5 (11): 1988–2008.
- 95 Sassolas, A., Prieto Simón, B., and Marty, J.L. (2012). Biosensors for pesticide detection: new trends. *American J. Anal. Chem.* 3 (3): 210–232.
- 96 Zhu, G. and Zhang, C.Y. (2014). Functional nucleic acid-based sensors for heavy metal ion assays. *Analyst* 139 (24): 6326–6342.
- 97 Zhang, A., Chang, D., Zhang, Z. et al. (2017). In Vitro selection of DNA aptamers that binds geniposide. *Molecules* 22 (383): 1–12.

- 98 Bhise, N.S., Ribas, J., Manoharan, V. et al. (2014). Organ-on-a-chip platforms for studying drug delivery systems. *J. Controlled Release* 190: 82–93.
- 99 Wang, S., Su, J.H., Zhang, F., and Zhuang, X. (2016). An RNA-aptamer-based two-color CRISPR labeling system. *Sci. Rep.* 6 (26857): 1–7.
- 100 Guo, K.T., Schäfer, R., Paul, A. et al. (2006). A new technique for the isolation and surface immobilization of mesenchymal stem cells from whole bone marrow using high-specific DNA aptamers. *Stem Cells* 24 (10): 2220–2231.
- 101 Won, J.Y., Choi, J.W., and Min, J. (2013). Micro-fluidic chip platform for the characterization of breast cancer cells using aptamer-assisted immunohistochemistry. *Biosens. Bioelectron.* 40 (1): 161–166.

Index

- a**
- acousto-microfluidic SELEX method 9
 - activated ester method 92
 - adenosine/cocaine detection 286
 - AEGIS-Cell-SELEX 50
 - affinity capillary electrophoresis (ACE) 136, 137
 - aflatoxin B1 (AFB1) 112, 259, 282, 284
 - allele-specific padlock probe (PLP) 308
 - 3-amino-9-ethyl carbazole (AEC) 287
 - aminophenyl boronic acid-modified gold nanoparticles (APBA-AuNPs) 315
 - amperometric aptasensors
 - cationic redox species 260–263
 - enzyme labels 248–250
 - intercalated redox species 256–259
 - label-free aptasensors 263–265
 - redox-labeled 250–256
 - analytical aptamers 15, 367, 368, 386, 387
 - selection and probe design
 - aptamer optimization and specialized selection 373–376
 - biochip-based aptamer selection 368–372
 - in-round PCR size control 368, 369
 - SELEX with next-generation sequencing 372–373
 - in silico* aptamer design 376–378
 - SomaLogic's photoaptamer microarray 368
 - angular modulation 303
 - 1,5 anhydrohexitol nucleic acids (HNA) 39
 - antibody assay 188, 365, 367
 - antifouling impedimetric aptasensor 266
 - anti-lysozyme DNA aptamer 260
 - anti-sAA antibody 280, 292
 - aptamer-based lateral flow assays
 - absorbent pad 277
 - backing pad 277
 - buffer 277
 - CCD-imaging systems 278
 - competitive assays 281–283
 - conjugate pad 277
 - flow rate 276
 - labels for detection 277
 - vs. lateral flow immunoassays 275
 - membrane 276
 - sample pad 277
 - sandwich assay 278–281
 - scanning systems 278
 - signal amplification 283–291
 - aptamer-based methods
 - calibration and uncertainty 355
 - immobilization of aptamers 356
 - regeneration 355–356
 - reproducibility 355
 - selectivity and specificity 354–355
 - sensitivity 352–354
 - aptamer-based pesticide detection 387
 - aptamer-based quartz crystal microbalance (QCM) biosensor 312–318
 - aptamer-conjugated magnetic beads 313–315

- aptamer-functionalized gold
 - nanoparticles (Apt-AuNPs) 314
 - aptamer-gated silica nanoparticles
 - 287, 289
 - aptamer-ligand complexes
 - kinetic characterization 146–162
 - thermodynamics 128–146
 - aptamer microarray 21, 365, 368, 371, 374, 382, 383
 - aptamers 86, 247, 273
 - amperometric aptasensors 248
 - vs. antibody 221–223
 - assays 365, 378–380
 - binding mechanisms 247
 - biostability 269
 - chips 382–384
 - cross-reactivity 350
 - degradation 347
 - diagnostics 366
 - CRISPR/Cas9, stem cells, IHC 388
 - food/environmental monitoring 387
 - human disease diagnosis 386
 - therapeutic drug assessment 387–388
 - DNA and RNA 32
 - electrochemical aptasensors 247
 - electrochemiluminescence aptasensor 268
 - GACTZP 48–50
 - hydrophobic fifth base 50–51
 - impedimetric aptasensors 266–268
 - nano-flares 379
 - non-enzymatic selection 45
 - optimization and specialized selection 373
 - phosphorothioate 36
 - potentiometric aptasensors 265
 - SELEX optimization 30
 - sequences 366
 - SOMAmers 46
 - systematic evolution of ligands by exponential enrichment 247
 - TNA 39
 - XNA 38
 - aptamer-target interactions 85, 129, 273
 - Apta-PCR affinity assay (APAA) 332
 - aptasensing 116, 367, 368, 374, 375, 378–385
 - aptasensors 85–87, 92, 95, 101, 109, 112, 206, 207, 212, 226, 229–241, 247–268, 310–319, 367, 380
 - Apt2–AuNPs–HRP conjugates 249
 - arabinonucleic acids (ANA) 39
 - artificially expanded six-letter genetic information system (AEGIS) 15
 - AuMnPs–Apt1/thrombin/Apt2–AuNPs–HRP 249
 - AuNP-DNA1/AuNP-DNA2/aptamer/thrombin 286
 - AuNPs driven ECL aptasensors 268
 - automated SELEX process 17
 - avidin-biotin binding 100–101
 - avidin-biotin technology 264, 312
- b**
- backbone alterations 29, 47
 - backbone modifications, nucleotides
 - 2'-OH modifications 36
 - phosphodiester bond modifications 36
 - XNA 38
 - beacon aptamer 256, 257
 - β -conglutin 282, 291
 - β -conglutin detection 281
 - β -Estradiol 221
 - 17 β -Estradiol aptamers 333
 - bifunctional aptamer 354
 - bimetallic AgPt nanoparticle-decorated carbon nanotubes 267
 - binding affinity 14, 42, 51, 130, 131, 133, 142, 146, 147, 150, 174, 206, 207, 222, 230, 301, 305, 313, 324, 327, 333, 335, 347–349, 353, 357, 374, 375, 381
 - bioaffinity agent 274
 - Bioanalyzer[®] 369
 - Biochemische Analytik 219
 - biochip-based aptamer selection 368–372

- biochips 366, 367, 370
 bioinformatics tools 352
 biosensors 85, 95, 109, 176, 205, 213,
 229, 269, 274, 294, 303–305, 311,
 353, 354, 356, 366, 378
 biotin-avidin 100, 175
 biotin-labeled immobilized sequence
 237
 biotinylated aptamers 100, 113, 192,
 224, 225, 236, 257, 283
 biotinylated 29-mer aptamer 279
 bisphenol A (BPA) 257, 258
 bivalent/binary aptamer construction
 374
 black hole quencher 1 (BHQ1) 240
 bridged/locked nucleic acid (BNA/LNA)
 14, 39, 347
 bromodeoxyuridine (BrdU)
 photoaptamers 19
- C**
- calmodulin (CaM) 305
 Cancer Antigen 125 (CA125) 305
 cancer-related biomarkers 11
 capillary electrophoresis (CE) 3, 39,
 136, 157–159, 175, 191, 351
 capillary electrophoresis (CE)-SELEX
 6, 370
 capture SELEX 374, 375, 376, 387
 carbodiimide method 92
 carbon nanomaterials 176, 234–235
 carbon nanotubes (CNTs) 95, 116,
 124, 175, 234, 366, 379
 carbonyldiimidazole (CDI) 95, 96
 cationic redox species 260–263
 CCRF-CEM cells 11, 314, 315
 cell-based aptasensing 384–385
 cell-SELEX 3, 4, 10–11, 20, 44, 50, 206,
 348, 370, 384
 cell surface-targeted aptamers 384
 cell-type-specific aptamer 352
 charge-coupled device (CCD)-based
 image system 278
 chemical antibodies 247
 chronocoulometric aptamer sensor
 261
- Click-SELEX 45, 46
 cocaine-binding aptamer with quinine
 324–327
 colorimetric analytical methods
 aptamer generation 206
 aptasensor 206–207
 AuNP 207–211
 competitive assays 274, 281–283
 complementary strand (CS) 151,
 230–232, 237, 268
 Concanavalin A (Con A) 186
 covalent immobilization
 activated aptamer, surface 88–95
 electrografting 97–98
 entrapment 95–97
 modified aptamers, activated surfaces
 92–95
 CRISPR/Cas9 technique 388
 cyclohexenyl nucleic acids (CeNA) 39
 5'-Cy5 labeled P4G13 progesterone
 aptamer 333
- d**
- decoy oligodeoxynucleotide (dODN)
 385
 decoy oligonucleotides (DONs) 385
 dendrimers 97, 312
 dendron-modified substrate 97
 2'-deoxy-2'-fluoroarabinonucleotides
 (FANA) 39
 diclofenac (DCF) 267
 digoxigenin-5'-reporter aptamer-
 3'-biotin-streptavidin-AuNP
 conjugates 285
 direct competitive ELAA (*dc*-ELAA)
 224–226
 direct methods for thermodynamic
 fluorescence-based methods
 140–146
 ITC 138–140
 microScale thermophoresis 141,
 142–146
 dispersive SPE (dSPE) 182
 DNA microarray 117, 365, 371, 372,
 376, 383, 389
 DNA nanostructures 239–241

- double-stranded DNA (dsDNA) 231,
232, 259, 290, 356
polymers 263
- droplet digital polymerase chain
reaction (ddPCR) 372
- dual aptamer 188, 279, 280, 289,
307
- dual-hairpin DNA structure 252
- dual-signaling E-AB biosensor 255
- dual-signaling electrochemical
aptasensor 255, 256
- e**
- electrochemical aptamer-based ATP
assay 353
- electrochemical aptasensors 95,
247–253, 255–260, 262, 264, 269,
356, 382
- electrochemical impedance
spectroscopy (EIS) 109, 148,
152–154, 353, 381
- electrochemical label-free aptasensing
381
- electrochemical quartz crystal micro-
balance (EQCM) 311, 312
- electrochemical sensors 205, 247, 355,
361, 366, 381, 383
- electrochemiluminescence aptasensor
268
- electrophoresis 3, 39, 51, 136–137,
157–159, 175, 191, 349, 351, 368,
370
- electrospray ionization-ion mobility
spectrometry (ESI-IMS) 115
- emulsion polymerase chain reaction
(ePCR) 372
- enzyme cycle amplification 306
- enzyme-labeled amperometric
aptasensors 248–250
- enzyme-labeled electrochemical
aptasensors 251
- enzyme-linked aptamer assay (ELAA)
380
direct competitive 224–226
hVEGF ELONA 223
indirect competitive 223, 226
- enzyme-linked immunosorbent assays
(ELISA) 219–221, 226, 380
- enzyme-linked oligonucleotide assays
(ELONA) 223, 380
- epitope-specific SELEX 375
- equilibrium dialysis 133–135
- 5'-ethynyl(deoxy)uridine triphosphate
(EdU) 45
- exonuclease III (EXO III) 230, 233
- ExSELEX 51
- f**
- ferrocene (Fc)-labeled DNA aptamer
253
- fiber SPME 183–184
- field-effect transistor (FET)-based
sensing 382
- flat gold substrate
electrochemical detection 109, 111
SPR detection 109, 110
- fluorescence-activated cell sorting
(FACS) 349
- fluorescence-based methods
anisotropy/polarization 141–142
MST technique 144, 145
- fluorescence polarization (FP) 86,
141–143, 282
- fluorescent aptasensors 354
carbon nanomaterials 234–235
DNA nanostructures 239–240
gold nanoparticles 231–234
silver nanoparticles 238–239
SNPs 236–238
THMS 240–241
- fluorescent dyes-based aptasensors
230–231
- fumonisin B1 268, 282
- functionalized multiwall carbon
nanotubes/gold nanoparticle
(f-MWCNTs/AuNP)
nanocomposite film modified
gold electrode 264
- g**
- GACTZP aptamers 48–50
- GenBank[®] 365

- genomic SELEX 3, 18–19
 Glypican 3 (GPC3) 15, 50
 gold nanoparticle (AuNP)-aptamer
 based colorimetric assays
 applications 211–213
 biomolecules 205
 biosensing 205
 characteristics 205
 conjugated antibody 206
 detect DNA 210
 detect protein 209, 210
 oligonucleotide 208
 plasmonic effect of 205
 split aptamers 209
 gold nanoparticles (AuNPs) 86, 116,
 175, 176, 231, 259, 263, 264, 274,
 275, 277, 279, 280, 287, 291, 314,
 379
 gold screen-printed electrode (SPE)
 265–266
 G-riched aptamer 254
 guanine nucleobase 62
- h**
- half-duplex aptamer 260
 hepatocellular carcinoma (HCC) 15,
 113
 heterogeneous methods
 EIS 152–154
 SPR spectroscopy 148–152
 high-density aptamer microarrays 383
 highly sensitive QCM-D biosensor 314
 homogeneous methods
 capillary electrophoresis 157–159
 nanopore-based studies 159–162
 rotating droplet electrochemistry
 154–157
 human “apt-omics” 389
 hydrophobic fifth base, aptamers
 50–51
- i**
- Illumina HiSeq® 372
 immobilization of aptamer
 advantages and challenges 87
 aptasensor 85, 86
 avidin-biotin binding 100
 covalent binding 88–92
 definition 85, 87
 electrochemical adsorption 101
 flat gold substrate 102–104
 future perspectives 116, 118
 hybridization 101–102
 nanomaterials surface 107, 115
 physical adsorption 87–88
 sample clean-up 114
 SAMs 98–100
 sensing surface 87
 sensor surface 87, 88
 solid phase substrates 105, 106,
 111
 immobilization of aptamers 178, 356
 CNTs 175
 gold nanomaterials (AuNPs) 175,
 176
 graphene oxide (GO) 175, 176
 MOFs 177
 silicon nanomaterials 175, 176
 immobilized MB-labeled aptamers
 253, 254
 impedance-based aptasensing 383
 impedimetric aptasensors 248,
 266–268
 impedimetric biosensor 267
in chemico-SELEX 3, 14–17
 indirect competitive enzyme-linked
 aptamer assay (*ic*-ELAA)
 223–226
in silico aptamer design 376–378
in silico aptamer-hemagglutinin protein
 377
in silico-SELEX 3, 12–14
 integrin alfa V (ITGAV) 4
 intercalated redox species 256–259
 intracellular sensing 384
 isogenic cell-SELEX procedure 4
 isothermal titration calorimetry (ITC)
 12, 138
 affinity test 327
 interaction between the aptamer
 domain of the purine riboswitch
 and ligands 322–324

- isothermal titration calorimetry (ITC) (*contd.*)
 interaction between the cocaine-binding aptamer and quinine 324–327
 principle 319–320
 quantitative thermodynamic information 319
 thermodynamic parameters 320
- k**
- Kallikreine-related peptidase 6 (KLK6) 5
- kanamycin aptamer 236
- kinetic capillary electrophoresis (KCE) 157
- kinetic characterization
 heterogeneous methods 148–154
 homogeneous methods 154–162
- kinetic methods 137, 140, 154–156
- l**
- label-free aptasensing 381
- label-free aptasensors 230, 263–265
- label-free fluorescent aptasensors 230
- lateral flow assays (LFA) 112, 274–276, 279, 280, 282, 283, 285, 287, 289, 290, 380
- latex agglutination assay 274
- liquid chromatography 50, 135–136, 184, 187
- localized SPR (LSPR) 303, 379
- locked nucleic acids (LNA) 14, 39–40, 347
- m**
- Macugen® 387
- magnetic nanoparticles (MNPs) 175, 191, 248
- magnetic separation techniques
 advantages 190
 cell sorting assays 191
 MSPE 190
- magnetic solid phase extraction (MSPE) 190
- metal-organic frameworks (MOFs) 175, 177, 182, 183, 379
- methylene blue (MB) labeled aptamer probe 251
- microbeads 187, 191, 348
- micro-ELAA 380
- microfluidic-SELEX 3, 8
- micro/nanowell PCR 372
- MicroScale thermophoresis (MST) 142
 advantage 330
 affinity test 333
 interaction between steroid hormones and aptamers 332–333
 molecular interactions 330
 principle 330
 technique 144
 thermophoresis 329
- monothiophosphate-backbone substituted oligonucleotide aptamer 375
- multianalyte detection aptasensors 354
- multimeric aptamers 374
- multi-walled carbon nanotubes (MWCNT) 95, 235
- n**
- nanomaterials 87, 102, 115–116, 142, 175, 176, 234–235, 238, 306, 366, 382
- nanomaterial surface energy transfer (NSET) 232
- nanoparticles-based aptasensors
 carbon nanomaterials 234–235
 gold 231–234
 silver 238–239
 SNPs 236–238
- nanopore-based studies 148, 159–162
- nanotechnology 115, 205, 306, 313
- NeXstar 375
- next-generation sequencing (NGS) 9, 21, 29, 332, 367, 372–373
- N*-hydroxysuccinimide (NHS) 92, 176
- nitrocellulose 112, 135, 274–276, 286, 349
- N*-methylisatoic anhydride (NMIA) 324

- non-equilibrium capillary
 - electrophoresis of equilibrium mixtures (NECEEM) 157–159, 351
- nuclease-resistant aptamers 347
- nucleic acids, aptamers 127
- nucleobase modifications
 - catalysts, protein-like sidechains 43–44
 - cationic moieties 42–43
 - Click-SELEX 45
 - glycans targeting, boronic acids 44–45
 - nucleobase-linked nucleobases 44
 - SOMAmers 46–48
 - sugar and phosphate moieties 40
 - X-aptamers 45–46
- nucleotides
 - aptamers 48
 - ATGC 27–29
 - backbone modifications 35
 - cytosine nucleobase 60
 - guanine nucleobase 62
 - in-line modifications 30–31
 - nucleobase modifications 40–48
 - polymerase-driven exponential amplification 31
 - polymerase-mediated reactions 31
 - polymeric structure of 35
 - post-SELEX optimization 30
 - scope of 29–30
 - SOMAmers 32, 33
 - triphosphates and phosphoramidites 34
- nucleotides thymine/uracil nucleobase 53
- nylonpolyvinylidene fluoride (PVDF) membranes 276
- O**
 - ochratoxin A (OTA) 86, 109, 115, 134, 146, 181, 234, 238–240, 250, 252, 282, 305
 - 2'-OH modifications 36
 - oligonucleotide synthesis 30, 87, 380, 383
 - Oncostatin M (OSM) 14
 - one-round SELEX 3, 5–6
 - one-step electrochemical aptasensor 250, 252
 - organ-on-a-chip 367, 387–388
- P**
 - phosphoramidite method 1
 - phosphor-carboxy anhydride 92
 - photo-SELEX 3, 19, 206
 - piezoelectric microelectromechanical resonators 318
 - poly(diallyldimethylammonium) (PDDA) 212
 - polypyrrole (Ppy) 95, 97
 - positioned aptamers 274
 - post-SELEX 3, 14–17, 30, 31, 36, 38, 40, 47, 51, 152, 348, 371–373, 382
 - potentiometric aptasensors 265–266
 - primer-free SELEX method 3, 17
 - prostate-specific antigen 9, 188, 305, 386
 - protein target molecules 348
 - proteomic SELEX 383
 - proximity ligation selection (PLS) 5, 6
- Q**
 - qPCR-SELEX 3, 19–20
 - quantum dots(QDs) 100, 116, 234, 235, 274, 275, 277, 282–284, 366, 379
 - bioconjugates 283
 - quartz crystal microbalance (QCM) based aptasensor
 - affinity determination 312–313
 - analyte concentrations 313–318
 - principle 311–312
 - signal transduction mechanism 311
 - biosensor 311, 314, 316, 317
 - sensing 381
 - quartz crystal microbalance with dissipation monitoring(QCM-D) technique 312, 314

r

ractopamine (RAC) 263
 RCA-based signal-amplification
 electrochemical aptasensor 258
 reactive anhydrides method 92
 reagentless aptasensor 264, 265
 redox-labeled amperometric
 aptasensors 248, 250
 retinol binding protein 4 (RBP4) 305
 reusable potentiometric screen-printed
 sensor 265
 RNA aptamers 1, 4, 12, 17, 32, 42, 85,
 152, 176, 187, 222, 329, 347, 350
 Roche 454[®] 372
 rolling circle amplification (RCA)
 257–259, 306, 308, 315, 317, 380
 rotating droplet electrochemistry 148,
 154–157

s

salivary α -amylase (sAA) 44, 280
 sample preparation methods, aptamers
 CE 191
 chromatography 185–187
 in magnetic separation system
 189–191
 in microfluidic separation system
 187, 188
 protein precipitation 192
 SPME 182–185
 substrate materials, immobilization
 175–177
 sandwich assay 5, 188, 207, 225, 248,
 274, 278–281, 287, 306
 sandwich-based aptasensor 248
 sandwich QCM-D biosensor 316
 sandwich-type electrochemical
 aptasensor 250
 screened RNA aptamer 328
 SELEX-on-a-chip 371
 self-assembled monolayers (SAMs)
 98–100, 151, 176, 313, 382
 semi-permeable membrane 133
 separation-based methods
 diafiltration 133, 134
 electrophoresis 136–137
 equilibrium dialysis 133–135
 liquid chromatography 135–136
 ultrafiltration 133, 134
 sgc8c aptamer-conjugated MBs 314
 signal amplification 226, 259, 260, 267,
 283–291, 305–308, 315, 316
 signal-off aptasensors 250
 signal-on aptasensors 250, 253
 signal transduction probe (STP) 240,
 241
 silica nanoparticles (SNPs) 236–238,
 287
 silicon nanomaterials 175, 176
 silver nanoparticles 238–239, 241, 366
 simple fluorometer 378
 single-cycle SELEX process 8
 single-stranded DNA (ssDNA) 41, 85,
 146, 174, 176, 229, 249, 290, 305
 single-walled carbon nanotubes
 (SWCNT) 95, 235
 slow off-rate modified aptamer
 (SOMAmer) selection 32, 113,
 147, 374
 solid-phase extraction (SPE) 114
 aptamer affinity based columns 181
 dSPE 182
 solid-phase microextraction (SPME)
 chemistry and physical properties
 182
 in fiber 183–184
 microextraction technique 182
 oligosorbent 183
 in SBSE 184–185
 TFME 185
 solid phase substrates
 optical detection 112–114
 SomaLogic's photoaptamer microarray
 368
 SomaLogic team 33, 35, 47
 SOMAscan platform 47, 113
 spiegelmers 40
 SPR-based optical immunosensors
 355
 SPR biosensors
 based on amplitude modulation 304

- based on angular modulation 303–304
 - based on phase modulation 304
 - based on wavelength modulation 304
 - standard SPR biosensor 308
 - stepwise aptasensor 261
 - stir-bar sorptive extraction (SBSE) 173, 184–185
 - streptavidin 9, 17, 100, 109, 112–114, 151, 175, 187, 190, 191, 206, 223, 226, 279, 282, 283, 286, 290, 305
 - streptavidin-AuNPs 280
 - surface-bound aptamer 86
 - surface plasmon polaritons (SPPs) 302
 - analyte concentrations 305–310
 - classification of SPR biosensors 303–304
 - determination of the affinity 305
 - fiber optic sensors 302
 - principle of 302–303
 - total internal reflection 302
 - surface plasmon resonance (SPR)
 - detection 109–111
 - spectroscopy 148
 - synthetic short DNA/RNA ligands 365
 - systematic evolution of ligands by exponential enrichment (SELEX) 247
 - aptamer cross-reactivity 350
 - aptamer degradation 347–348
 - aptazymes 32
 - automated process 17
 - binding affinities 346
 - binding affinity 348–349
 - bioinformatics tools 352
 - black box of 32
 - capillary electrophoresis 6
 - cell 10–11
 - in chemico*-SELEX 14–17
 - defined single target molecules 346
 - DNA and RNA aptamers 32
 - essential steps of 2
 - genomic 18–19
 - in vitro* screening protocol 3
 - in vitro* selection 12
 - interaction of aptamers with intracellular targets 351
 - intracellular detection of target molecules 346
 - microarray 21
 - microfluidic 8
 - microfluidic delivery system 206
 - negative selection 4
 - next-generation sequencing 21
 - nonphysiological conditions 345
 - one round 6
 - pharmacokinetic half-life 345
 - photo 19
 - polymerase-driven exponential amplification 31
 - post optimization 30
 - primer-free method 17
 - procedures 2
 - purification 348
 - qPCR 19–20
 - randomized oligonucleotide library 345
 - robotic workstation 346
 - SomaLogic research team 32
 - ssDNA library 1
 - ssDNA/RNA library 222
 - target immobilization 349–350
 - thrombin problem 347
 - time and cost 350–351
 - X-Aptamer Selection Kit 20
- t**
- target immobilization 349–350
 - TC aptamer 307
 - tetracycline-binding aptamers 115
 - Therminator DNA polymerase 39
 - thermodynamics
 - direct methods 137–146
 - principles of 128–133
 - separation-based methods 133–137
 - thermophoresis 86, 142–146, 329, 330, 335
 - thin-film microextraction (TFME) 185
 - thiol- and MB-dual-labeled aptamer 250

- thiol-and methylene blue
 - (MB)-dual-labeled aptamer
 - modified gold electrode 252
 - thiolated 15-mer thrombin aptamer 279
 - thiolated methylene blue (MB)-modified DNA probe (MB-P) 254
 - Thiol-modified oligonucleotide 211
 - 4'-thioribose 40
 - 3D-folded quadruplex aptamer probe 378
 - threose nucleic acid (TNA) 39
 - thrombin aptasensor 249
 - thrombin-binding aptamers (TBAs) 14, 186, 230, 266, 374
 - thymine/uracil nucleobase 53
 - TISR E-AB sensor 253
 - trifunctional cross-linkers 97
 - triple-helix molecular switch (THMS) 240–241, 262
 - triple-helix molecular switch (THMS)-induced hybridization chain reaction (HCR) amplification 262
 - triplex-forming oligonucleotide (TFO) 262
 - T5 testosterone aptamer 332
- u**
- ultrasensitive electrochemical aptasensor 257, 258
- universal fluorescence aptasensor 354
 - unnatural base pairs (UBPs) 29, 31, 48, 49
- v**
- vascular endothelial growth factor (VEGF) 11, 137
 - Vaspin 280
- w**
- Watson–Crick base pairs 29, 31, 40, 322, 326
 - Watson–Crick duplexes 38
- x**
- X-aptamers 20, 45–46, 375
 - xeno nucleic acids (XNA)
 - ANA 39–40
 - CeNA 39–40
 - FANA 39
 - HNA 39–40
 - LNA 39–40
 - (deoxy)ribose sugar moiety 38
 - spiegelmers 40
 - 4'-thioribose 40
 - TNA 39
- z**
- Zeolitic imidazolate framework-8 (ZIF-8) 177